THE INTERPLAY OF STRUCTURE AND REACTIVITY ON A RING CLOSING METATHESIS REACTION

Thesis submitted for the degree of Doctor of Philosophy at the University of Leicester

by

Lisa Mitchell
Department of Chemistry
University of Leicester

April 2008

ProQuest LLC
789 East Eisenhower Parkway
P.O. Box 1346
Ann Arbor, MI 48106-1346

Contents

Acknowledgements

I would like to thank, first of all, my PhD supervisor Professor Jonathan Percy for his encouragement, help and guidance during my research, and for giving me the opportunity to work in two different yet academically nurturing environments. I would also like to thank Dr John Parkinson of the Strathclyde University NMR service for his genuine interest and enthusiasm, help and patience during my final year; and Professor John Atherton from the University of Huddersfield for introducing me to Madonna. My thanks are also extended to Dr Gerry Griffiths, Dr Graham Eaton, Mick Lee and Dr Igor Efimov at the University of Leicester, and Pat Keating and Craig Irving at the University of Strathclyde for their time and assistance.

I am grateful to the Percy group, past and present, not only for their help, but also for shared jokes and amusement both in and out of the lab. I have also enjoyed the company of friends and colleagues outside of the Percy group at both Leicester and Strathclyde Universities and thank those who welcomed me and included me in many social activities, especially those who made the move to the University of Strathclyde such an easy one.

I would like to thank my parents and family in the UK, Germany and Japan for their love and support over the years, and for encouraging me to discover the correct path for me. A special mention goes to Anna who has proved to be an endless source of amusement, laughs and most importantly, a fellow cake enthusiast. I also thank all of my friends for their support, for lending an ear when it was necessary, and for the good times, of which I hope there are many more to come.

My final thanks go to Tatiana Tretyakova for her words of wisdom. She encouraged me as a disillusioned and confused 17 year old to pursue something I really enjoyed. Without her advice, I am not sure I would have chosen this path and so owe her my deepest gratitude.

This thesis is dedicated to the memory of Jack Mitchell

Abbreviations

ADMET	Acyclic diene metathesis
BuLi	Butyl lithium
CACPO	Citraconic anhydride chloroperoxidase
CI	Chemical ionisation
CM	Cross metathesis
COD	*cis,cis*-Cyclooctadiene
COSY	Correlation Spectroscopy
CPO	Chloroperoxidase
DAST	Diethylaminosulfur trifluoride
DCE	1,2-Dichloroethane
DCM	Dichloromethane
DEC	Diethylcarbamoyl
DEDAM	Diethyldiallyl malonate
DFT	Density functional theory
DIPA	Di*iso*propylamine
DMAP	4-Dimethylaminopyridine
DNA	Deoxyribonucleic Acid
EDTA	Ethylenediamine tetraacetate
EI	Electron impact
EM	Effective Molarity
ESMS	Electrospray Mass Spectrometry
eu	Entropy unit
EXAFS	Extended X-Ray Absorption Fine Structure
GC	Gas Chromatography
GC-MS	Gas Chromatography-Mass Spectrometry
GPC	Gel permeation chromatography
HMBC	Heteronuclear multi-bond correlation
HMQC	Heteronuclear Multiple Quantum Coherence
HPLC	High Performance Liquid Chromatography
HRMS	High resolution mass spectrometry
LDA	Lithium di*iso*propylamide
LRMS	Low resolution mass spectrometry

MACPO	Maleic anhydride chloroperoxidase
MALDI	Matrix Assisted Laser Desorption Ionisation
Mcb	Metallacyclobutane
m-CPBA	*meta*-Chloroperbenzoic acid
MEM	Methoxyethoxymethoxy
MM	Molecular mechanics
MOM	Methoxymethyl
NHC	N-Heterocyclic carbene
NMI	N-Methyl imidazole
O1p	Spectrum centering (for NMR)
OBn	Benzyl
OBz	Benzoate
OMe	Methoxy
OPiv	Pivaloate
OTf	Trifluoromethyl sulfonate
PACPO	Phthalic anhydride chloroperoxidase
PMB	*para*-methoxybenyl
PVP	Poly(4-vinylpyridine)
RCM	Ring closing metathesis
R_f	Relative front
ROMP	Ring-opening metathesis polymerisation
SEC	Size exclusion chromatography
SPE	Solid phase extraction
Sw	Sweep width
TBAF	Tetrabutylammonium fluoride
TBAHS	Tetrabutylammonium hydrogensulphate
TBAI	Tetrabutylammonium iodide
TBDPS	*t*-Butyldiphenylsilyl
TEA	Triethylamine
TFAA	Trifluoroacetic anhydride
THF	Tetrahydrofuran
TIBAL	Tri*iso*butyl aluminium
TLC	Thin layer chromatography
TON	Turnover number

TOR	*trans*-Polyoctenamer
T_r	Retention time
XRD	X-ray diffraction

Abstract

This Thesis describes investigations of how structure affects a cyclooctannulation of a difluorinated diene *via* ruthenium-catalysed ring closing metathesis (RCM). The study originated in attempts to optimise these reactions towards the synthesis of novel difluorinated analogues of sugars.

Eight-membered ring formation presents a challenge to synthetic chemists, and many literature syntheses use high dilutions or high temperatures and/or high catalyst loadings where appropriate over long reaction times, resulting in reactions which are difficult to scale up. There are conflicting accounts in the literature as to how diene structures affect the outcome of cyclisations *via* RCM, especially for medium rings, so precursor design is often a case of trial and error, rather than a more rational process.

A range of difluorinated dienes have been synthesised in order to study the effects of allylic protecting group on cyclisation efficiency, using the CF_2 group as a probe to of reaction outcomes *via* ^{19}F NMR. We identified a 10^2 fold difference in cyclisation efficiency depending on which allylic protecting group was used. However, kinetic studies have shown us that allylic protecting groups have only a moderate effect on cyclisation rate. Kinetic studies have also shown us that the cyclisation is affected by the presence of *gem*-dialkyl groups, which accelerate the rate – an effect which has not been quantified for the formation of medium rings by RCM previously.

^1H NMR kinetics has enabled the identification of the most significant catalytic species on the reaction timescale, including identification of catalytic decomposition products. This has led to the development of a kinetic model to which all kinetic data were fitted, using simulation software, and has allowed a deeper analysis and understanding of how olefin structure affects reactivity in RCM.

Based on the kinetic data, RCM substrates, which prolong catalytic lifetime and simplify reaction kinetics have been synthesised and examined. In addition to this,

the effects of reaction solvent, temperature, catalyst and catalyst loading on the cyclisation rate have been studied in order to identify the optimum conditions for synthesis of the desired difluorinated cyclooctenones.

1 Introduction

1.1 Development of a Route Towards Novel Difluorinated Analogues of Sugars

Recently, Percy *et al* developed a synthesis of *gem*-difluorinated cyclooctenones, with the aim of synthesising new conformationally-locked sugar analogues such as **1**.[1,2] The eight-membered ring **2** was synthesised using ring closing metathesis, much of which will be discussed in this thesis. The group developed a synthesis, using the building block approach to incorporate fluorine into the molecule, starting with trifluoroethanol. Retrosynthetically, the cyclooctenone species can be synthesised from a diene **4** *via* ring closing metathesis to give a cyclic alkene which can undergo epoxidation or dihydroxylation to give an oxidised species such as **3**. Diene **4** can undergo functional group interconversion from the ketone group to the MEM-protected enol **5** and this species can be obtained through [2,3]-Wittig rearrangement of difluoroallylic compounds **6.** The difluoroallylic species **7** can be synthesised from MEM-protected trifluoroethanol **8** and an aldehyde with LDA.

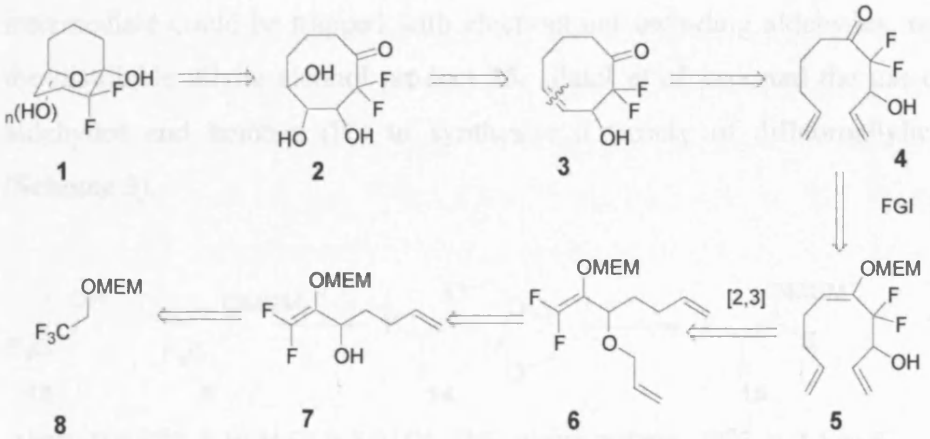

Scheme 1 Retrosynthetic analysis of conformationally-locked analogues of sugars

Patel *et al.* developed building block chemistry relevant to this synthesis. Difluoroallylic alcohols such as **7** can be made from the MEM-ether of commercially available trifluoroethanol **13**.[3] These difluorinated compounds can be used to synthesise highly functionalised difluorinated molecules **11** and **12** with a

mid-chain CF_2 group following [2,3]-Wittig rearrangement of difluoroallylic species **10** (**Scheme 2**).[4]

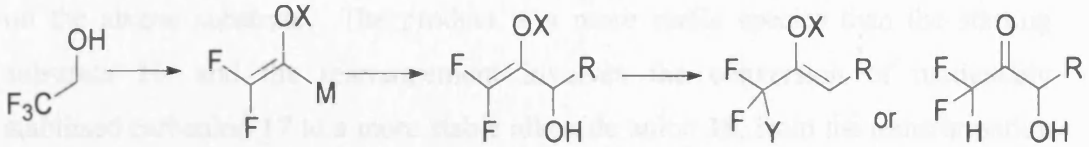

Scheme 2 Synthesis of allylic alcohol from trifluoroethanol, followed by [2,3]-Wittig rearrangement

The key intermediate in the difluoroallylic alcohol synthesis is the metallated difluoroenol derivative **9** which relies on the use of the MEM group. This chelates to the lithium cation and stabilises the intermediate, preventing lithium fluoride elimination. This ensures an adequate lifetime at -78°C and allows clean conversion to the desired product. Trifluoroethanol **13** was converted to the corresponding MEM ether **8** with MEM chloride *via* the sodium salt. The ether reacted with LDA to afford the metallated difluoroenol derivative **14**. This intermediate could be trapped with electrophiles including aldehydes, resulting in the distillable allylic alcohol product **15.** Patel *et al.* reported the use of various aldehydes and ketones (E^+) to synthesise a variety of difluoroallylic alcohols (**Scheme 3**).

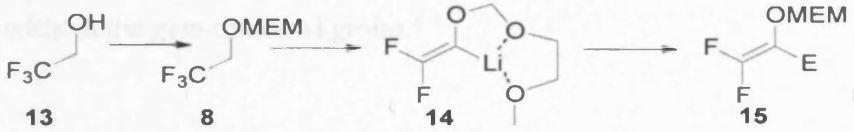

i: NaH, THF, 0°C; ii: MEM-Cl; iii: 2.0 LDA, THF, inverse addition, -78°C; iv: 1.1 eq E^+;
v: warm to -30°C then NH_4Cl/MeOH

Scheme 3 Allylic alcohol synthesis from trifluoroethanol

These allylic alcohols **15** were found to be useful substrates for further transposition, with a key step being rearrangement to a product with a mid-chain CF_2 functionality. Patel *et al.* reported the use of [2,3]-Wittig chemistry in the rearrangement of the difluoroalkene species **16** in the synthesis of species with a mid-chain CF_2 group **19** (**Scheme 4**).

The [2,3]-Wittig chemistry was used to synthesise a variety of midchain difluorinated species **19** and takes advantage of the properties conferred by fluorine on the alkene substrate. The product is a more stable species than the starting substrate **16**, and the rearrangement involves the conversion of moderately stabilised carbanion **17** to a more stable alkoxide anion **18**, from the transformation of an sp^2 hybridised CF_2 centre to an sp^3 hybridised CF_2 centre.

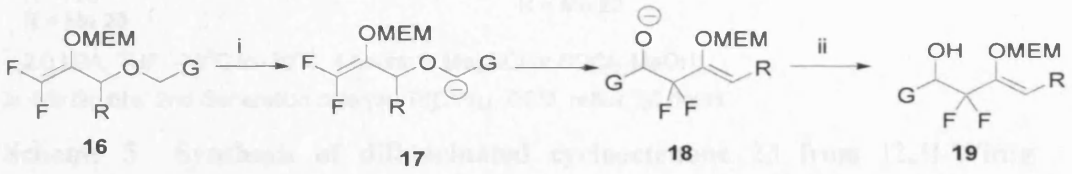

16 **17** **18** **19**

i: 2.0 LDA, THF, -78°C to -30°C, 4 hours; ii: NH_4Cl

Scheme 4 [2,3]-Wittig rearrangement

The CF_2 centre destabilises the alkene with the result that the transposition of the difluoroallylic system often occurs unusually easily.[5,6]

Kariuki *et al.* progressed the products of [2,3]-Wittig rearrangement **21** towards eight-membered ring **23** *via* RCM chemistry after unmasking the ketone functionality in **22**, using allylated rearrangement precursor **20** (**Scheme 5**), and showed that even highly functionalised species such as **23** undergo RCM successfully.[1] More recently the same synthetic procedure was adapted for **6-3** without the *gem*-dimethyl group.[3]

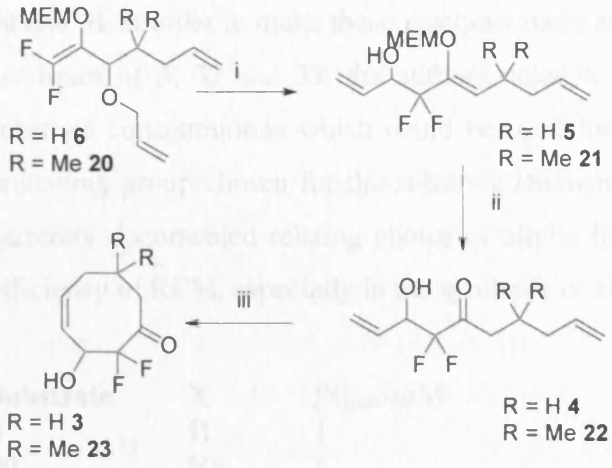

i: 2.0 LDA, THF, -78°C to -30°C, 4 hours; ii: Me_3SiCl or $SOCl_2$, MeOH;
iii: 5% Grubbs' 2nd Generation catalyst, $Ti(O^iPr)_4$, DCM, reflux, 36 hours

Scheme 5 Synthesis of difluorinated cyclooctenone 23 from [2,3]-Wittig product

This methodology employs the previously described building block approach to synthesise multigram yields of the eight-membered ring species and was adapted by Percy *et al.* in the synthesis of a variety of highly functionalised eight-membered rings **26** and **27** *via* RCM with good yields (**Scheme 6**) with both Grubbs' first and second generation catalysts **28** and **29**.[1]

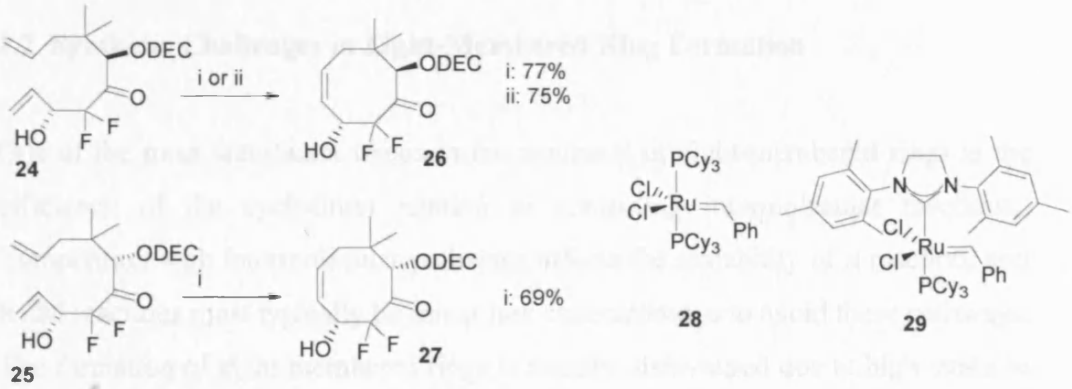

i: Grubbs' I, $Ti(O^iPr)_4$, DCM, reflux, 122 hrs
ii: Grubbs' 2, $Ti(O^iPr)_4$, DCM, reflux, 18 hours

Scheme 6 Synthesis of highly functionalised difluorinated cyclooctenones *via* ring closing metatheis

Eight-membered rings typically present a large challenge for synthetic chemists, and some of the work carried out by Percy attempted to optimise the syntheses of **4**,

30 and **31** in order to make these reactions more attractive for scale up. During the syntheses of **3**, **32** and **33**, the authors noted a large variation in the maximum substrate concentrations which could be used for RCM, dependent on the allylic protecting group chosen for the substrate (**Scheme 7** and **Table 1**). Very little is currently documented relating choice of allylic hydroxyl protection to rate and/or efficiency of RCM, especially in the synthesis of eight-membered rings.

Substrate	**X**	**$[S]_{max}$/mM**
4	H	1
30	Bn	5
31	Bz	20

Table 1 Concentration maxima $[S]_{max}$ for RCM reactions for 4, 30 and 31

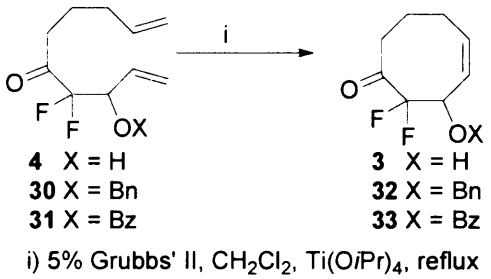

Scheme 7 Synthesis of cyclooctenones 3, 32 and 33 *via* RCM

1.2 Synthetic Challenges in Eight-Membered Ring Formation

One of the most significant issues in the synthesis of eight-membered rings is the efficiency of the cyclisation relative to competing intermolecular reactions.[7] Competition with intermolecular pathways affects the scalability of a reaction, and RCM reactions must typically be run at low concentrations to avoid these pathways. The formation of eight-membered rings is usually disfavoured due to high strain in the final products or the transition states which lead to them. Mandolini calculated the strain energies for the formation of 4-20 membered rings, and found that the strain energy for the formation of the eight-membered ring in this series was approximately 37.7 kJ mol^{-1}, second only to that of three and four-membered ring (115.1 and 109.2 kJ mol^{-1} respectively).[8] Bruice re-examined some of the lactonisation and ring size work carried out by Mandolini more recently, and concluded that lactonisation in 3-6-membered rings is enthalpy-limited, whereas

lactonisation of 8-membered rings upwards is entropy-limited, so different activation parameters control the reaction depending on the ring size.[9]

During the formation of the eight-ring product, the system must freeze a maximum of 7 rotors hence cyclisation has both an unfavourable, negative entropy of activation in addition to high enthalpy of activation. Through molecular mechanics combined with experimental work, De Tar and Luthra found that the entropic contribution of each frozen rotor is equal to 4.5 eu (or 18.8 J K^{-1} mol^{-1}).[10] In a fully flexible system of eight bonds, the entropic contribution attributed to freezing rotors is equal to 131.6 J K^{-1} mol^{-1}, which is a large entropic contribution to overcome. Under normal RCM conditions (refluxing dichloromethane), this would contribute -41.2 kJ to the calculation of $\Delta G^{\ddagger}$, which presents a large negative contribution to the calculation of the Gibbs free energy of activation.

The synthesis of eight-membered rings presents a large challenge to synthetic chemists due to unfavourable entropic and enthalpic contributions to $\Delta G^{\ddagger}$.[12] The structure of the ring to be formed also has an effect on the outcome of the cyclisation, as shown by Grubbs.[13] The rate of cyclisation depends on the structure of the uncyclised molecule's initial state, and also on the transition state resembling the final product.

The activation energy for a cyclisation reaction gives an indication as to the strain energy of the ring product and/or its transition states. The amount of strain is highly dependent on the ring size. There are three types of strain which must be considered: Pitzer strain refers to bond opposition forces arising due to imperfect angles in the product and/or transition states. Baeyer strain is caused by the deformation of the regular bonds angles in the ring.

Transannular strain is caused by atoms in the ring which are close in space, causing repulsion. Medium rings have bond angles greater than 109.5°, which causes strain in the product and transition state(s), and even in the most stable conformation (the boat-chair in the case of eight-membered rings), atoms within the cyclic molecule are close in space, which causes repulsion. Mandolini studied the formation of

cyclic lactones (**Scheme 8**) for 3-24 membered rings and plotted ring size *vs* $\Delta H^{\ddagger}$, $\Delta S^{\ddagger}$ and log k for all ring sizes (**Figures 1**, **2** and **3**).[8]

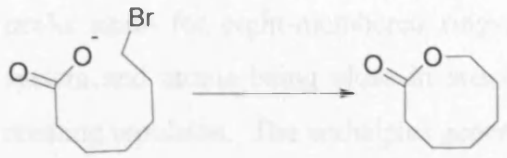

34 **35**

Scheme 8 Synthesis of an eight-membered ring lactone

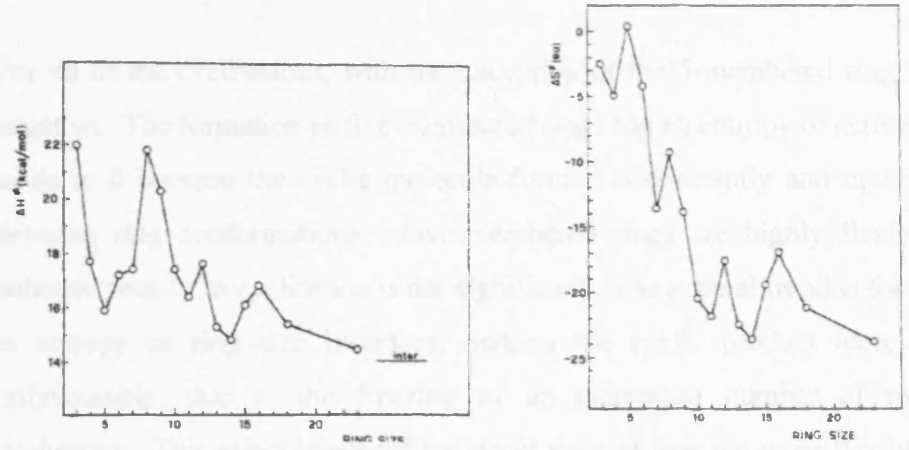

Figure 1 and 2 $\Delta H^{\ddagger}$ $\Delta S^{\ddagger}$ profiles for 3-24 membered ring lactone formation (from ref 8)

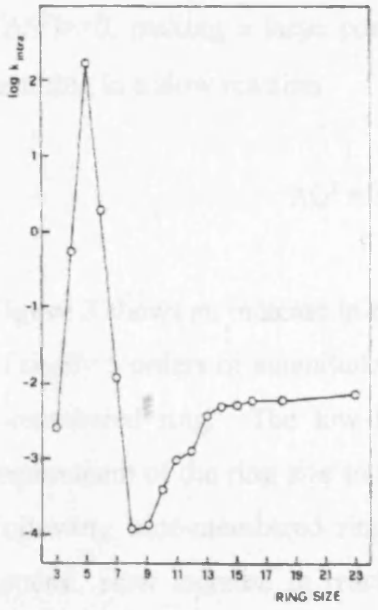

Figure 3 Ring size *vs* Reactivity Profile for Lactone Formation (from ref 8)

The ring size *vs* enthalpy plot shows that three and eight-membered rings are the least enthalpically favourable rings to synthesise. Three-membered rings have a

high enthalpy due to high strain in the system caused by small bond angles in the ring. The enthalpy for 5 and 6-membered rings is much lower because the bond angles in the ring are much less strained and are close to 109.5°. The enthalpy peaks again for eight-membered rings; this is due to transannular strain in the system and atoms being close in space in the cyclic product or transition state, creating repulsion. The enthalpies generally fall as ring size increases. Larger rings have more flexibility and bear closer resemblance to open chains than smaller ring species, and can avoid more of the strain-causing interactions.

For all of the cyclisations, with the exception of the 5-membered ring, entropy is negative. The formation of five-membered rings has an entropy of activation which tends to 0 because the cyclic molecule formed is constantly and rapidly flipping between ring conformations. Five-membered rings are highly flexible, so the entropic penalty in cyclisation is not significant. The general trend is for a decrease in entropy as ring size increases, making the cyclic product more and more unfavourable, due to the freezing of an increasing number of rotors upon cyclisation. This effect levels off for larger rings as they are more flexible. For the eight-membered rings, the entropy is against the general trend in increasing negativity of $\Delta S^{\ddagger}$ with increasing ring size, but is still negative. This means that $(-T\Delta S^{\ddagger}) >> 0$, making a large positive contribution to $\Delta G^{\ddagger}$ (**Equation 1**) and hence resulting in a slow reaction.

$$\Delta G^{\ddagger} = \Delta H^{\ddagger} - T\Delta S^{\ddagger} \qquad \textbf{Equation 1}$$

Figure 3 shows an increase in reactivity for the formation of 3 to 5-membered rings of nearly 5 orders of magnitude and then a linear decrease in reactivity down to the 8-membered ring. The low reactivity for the 8-membered ring is due to the requirement of the ring size to force the ester functionality into a *cis* conformation. Following nine-membered ring formation, which is also challenging, there is a general, slow increase in reactivity which levels off for the larger rings due to increased flexibility within the systems with increasing ring size.

1.3 Scope and Limitations of RCM

Recently, RCM has become a very powerful tool for the synthesis of cyclic molecules since the introduction of relatively stable catalysts which are able to tolerate a wide range of functionalities.[13, 14, 15] The RCM reaction converts a diene precursor into a cyclic alkene and a molecule of ethylene (in most cases), which provides some compensation for the negatively entropic formation of the cyclic product.

RCM provides access to a wide range of cyclic alkenes. The most common uses of RCM are for the syntheses of five and six-membered rings, but the highly active metathesis catalysts are also used for the syntheses of more challenging medium rings, and also for the syntheses of macrocycles.

Whereas the syntheses of many five and six-membered rings *via* RCM are relatively trivial, and require mild reaction conditions, short reaction times and low catalyst loadings (**Scheme 9**), the syntheses of medium rings present a larger challenge.

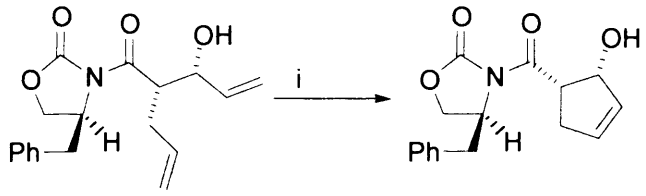

36 **37**

i) 1% Grubbs' I **28**, CH_2Cl_2, RT

Scheme 9 Synthesis of a carbocyclic nucleoside precursor *via* RCM

The synthesis of seven-membered rings by RCM is well documented, as these form fairly readily due to relatively low ring strain. Forbes synthesised seven-membered heterocycle **39** using Schrock's molybdenum alkylidene catalyst **40** in near-quantitative yield without the need for any solvent (**Scheme 10**).

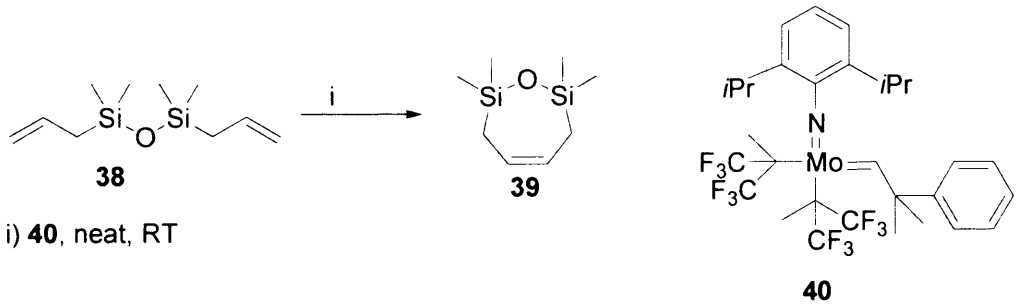

Scheme 10 Seven-memberered ring synthesis with Schrock catalyst 40

Strain in either (or both) the product or the transition states makes medium ring formation unfavourable, so in ring closing metathesis, high catalyst loadings and long reaction times are usually quoted in published syntheses.[16,17,18] Eight-membered ring syntheses are a particular challenge, since the resulting rings are good substrates for Ring-Opening Metathesis Polymerisation (ROMP), which is a strain relieving reaction, or Acyclic Diene Metathesis (ADMET), which run in competition with the cyclisation reaction. The balance by ROMP and RCM is affected by ring strain and so high dilution conditions are usually employed to reduce the likelihood of the competing polymerisation reaction.[19,20,21]

There are many recent accounts of eight-membered ring synthesis by RCM, with some of the earliest being by Grubbs. In the presence of first generation catalyst **28**, the fully flexible systems such as **41** and **42** could not be cyclised and even when reactions were performed at high dilution, or under syringe pump conditions only dimeric products were observed and identified by LC-MS (**Scheme 11**).[22]

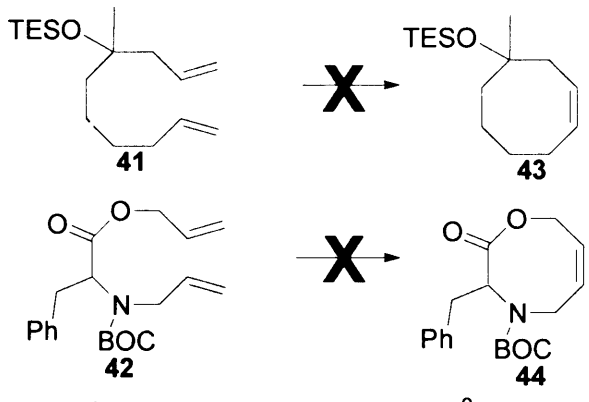

Scheme 11 Failed eight-membered ring syntheses

Access to eight-membered rings *via* RCM is important, as many cyclooctenes occur in natural products, so a relatively easy synthesis of these eight-membered rings could potentially reduce the number of steps in a natural product synthesis. Although eight-membered rings are less common in nature than smaller rings, they still occur widely in plants, marine organisms and fungi and are therefore of interest to chemists.[17] Furstner used the Neolyst metathesis catalyst **47** to synthesise eight-membered ring **46** as part of the ADE ring system of alkaloid Nakadomarin, which shows promising anticancer activity (**Scheme 12**).[23] Catalyst **47** is a first generation-type catalyst with two trisalkylphosphine ligands on the ruthenium centre, and a large stabilising alkylidene group.

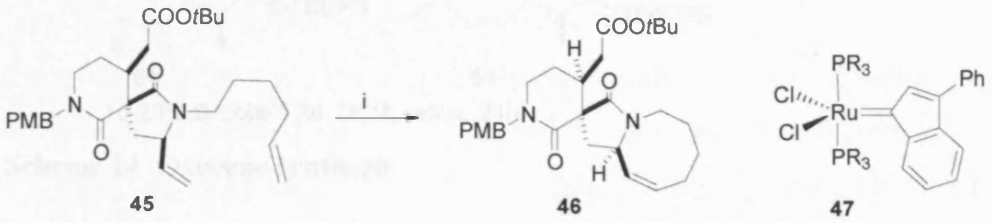

45 46 47

i) 5% **47**, 0.002 M CH_2Cl_2, reflux

Scheme 12 Synthesis of the ADE ring system of Nakadomarin *via* RCM

Prunet attempted the synthesis of eight-membered rings from diene **48** using Grubbs I **28** (**Scheme 13**) but found, surprisingly that only one diastereoisomer underwent cyclisation, resulting in formation of only the *trans*-cyclooctene **50**, which appears highly strained.[24] The authors suggested a specific complexation of the catalyst to the carbonyl functionality in the acyclic starting material **48**, preventing formation of the *cis*-cyclooctene **49** – something which did not occur in the case of the *trans*-isomer. This observation shows us that RCM can be used for the synthesis of even highly strained systems.

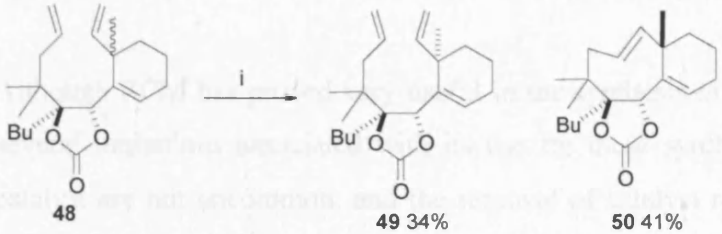

48 49 34% 50 41%

i) 10 mol % Grubbs' I **28**, 8 days

Scheme 13 Synthesis of *trans*-cyclooctene *via* RCM

Buszek synthesised natural compound Octalactin A using Grubbs' first generation catalyst **28** (**Scheme 14**).[25] Octalactin A is of interest for its toxicity against certain human colon cancer cell lines. A key segment was the synthesis of natural product oxocene **52**. However the loading of **28** is extremely high, making larger scale syntheses expensive, and the cyclic product **52** difficult to purify. There are no published attempts by Buszek to synthesise the same system with Grubbs' second generation catalyst **29**. The more active catalyst may be a more efficient choice for this synthesis.

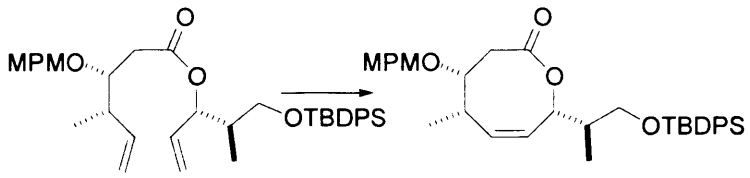

51 **52**

10-20% Grubbs' I **28**, DCM, reflux, 24hr

Scheme 14 Oxocene synthesis

The use of RCM for the synthesis of eight-membered rings does appear to present the biggest synthetic challenge. Nine-membered rings have proved more problematic, however nine-membered ring **54** was successful synthesised using RCM, using relatively mild conditions, although a long reaction time was required to effect complete conversion of **53** to **54** (**Scheme 15**).[26]

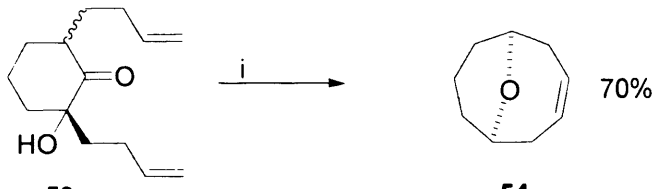

53 **54**

i) 5% Grubbs' II **29**, 0.005 M CH_2Cl_2, RT, 15 hours

Scheme 15 Synthesis of nine-membered ring carbocycle *via* RCM

Although RCM has proved very useful in the synthesis of medium rings, there are several limitations associated with its use for these syntheses. High loadings of catalyst are not uncommon, and the removal of catalyst residues from products is often not trivial. High dilutions are also required, meaning large volumes of solvent are required to synthesise relatively small amounts of cyclic product. High

dilutions make processes unattractive for larger scale synthesis, since the large solvent volumes become inhibitory for normal laboratory apparatus. Challenging systems may also require long reaction times and/or high reaction temperatures to force reactions to completion.

1.4 Kinetic *vs* Thermodynamic Products of RCM

For systems where competing acyclic diene metathesis (ADMET) oligomerisation pathways compete with the intramolecular cyclisation reaction, the ADMET oligomers are generally the thermodynamic product of the reaction, and the cyclic alkene the kinetic product. Control over the preference towards the formation of intra- over intermolecular products is maintained by using high dilution. Recently, Fogg claimed that the formation of thermodynamic ADMET oligomers can be exploited in the synthesis of the desired cyclic product, *via* the backbiting process.[21] The group argue that although high dilution favours direct cyclisation of the alkene, the low substrate concentration in solution slows down the rate of reaction between the alkene and catalyst. Using higher concentrations would speed up this bimolecular process, as well as favouring the formation of oligomeric products. Subsequent dilution, after the formation of oligomers resulted in back-biting to the desired cyclic product.

Fogg used this strategy in the syntheses of eight-membered rings **57** and **58** (**Scheme 16**, **Table 2**). Although the synthesis of eight-membered ring **57** was effected in 99% yield, this appears only to have been successful due to the high dilution (5 mM). After the initial equilibration period, no oligomer was identified within the reaction mixture, which suggests that the high yield of **57** was obtained through direct cyclisation, rather than *via* backbiting. When the same reaction was carried out at 100 mM, oligomers were identified after 45 minutes, but the yield of cyclic product at equilibrium was much lower, suggesting that although exploiting backbiting may be a more rapid way of synthesising medium ring targets, the products are unlikely to be synthesised cleanly. The attempted synthesis of **58** was carried out at high dilution (5 and 0.5 mM) but in both cases, although oligomer was identified after equilibration, no product was identified at equilibrium.

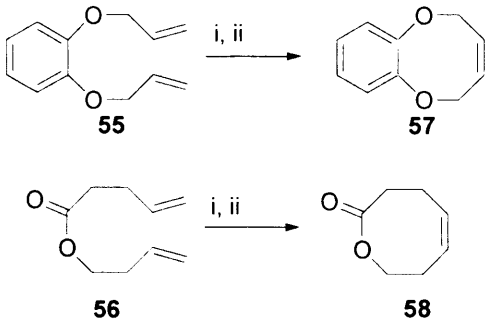

i) 5% Grubbs' II **29**, CH_2Cl_2, 22°C

ii) Reflux

Scheme 16 Synthesis of eight-membered rings *via* backbiting of oligomers

Substrate	[S]/mM	T_{equil}/min	% Oligomers (15 min)	% RCM
55	5	30	0	99
55	100	45	18	61
56	5	45	12	0
56	0.05	180	25	0

Table 2 Oligomerisation/RCM conditions used by Fogg

It is clear from these results that although direct cyclisation at lower concentration may retard the bimolecular reaction between alkene and catalyst, this gives the cleanest product. The synthesis of cyclic products *via* ADMET dimers is likely to lead to a mixture of products and although the initial oligomerisation reactions can be carried out at higher concentrations, large volumes of solvent are still required, since all reactions were diluted to allow backbiting to occur, so this method does not appear to offer any advantage over more conventional Ziegler methods.

1.5 Substituent Effects on Cyclisation *via* RCM

The syntheses of cyclooctenones **3, 30-31** by Percy were carried out on dienes with an allylic hydroxyl or protected allylic hydroxyl functionality. The are several published accounts of the effects of the presence of an allylic hydroxyl group, and of allylic hydroxyl protection, but these are generally contradictory, and therefore confusing for chemists attempting rational design of substrates based on their reactivity and likely outcome of the reaction.

The structure of the alkene molecule has an effect on its behaviour towards cross metathesis. Grubbs studied the link between precursor structure in relation to its likelihood to undergo cross-metathesis, and divided olefins into four groups as shown in **Table 3**.[27] The probability of cross metathesis of an olefin is dependent on substituents both on the double bond or on allylic substituents. The authors found that by changing the electronic properties of the double bond, they achieved improved product selectivity and stereoselectivity in cross metathesis. Examples of each of the types of double bonds for Grubbs' second generation catalyst **29** are shown in **Figure 4**. These findings have been useful for synthetic chemists to predict the susceptibility of their systems towards cross metathesis.

Type I	Rapid homodimerisation, homodimers consumable
Type II	Slow homodimerisation, homodimers sparingly consumable
Type III	No homodimerisation
Type IV	Olefins inert to cross metathesis but do not deactivate catalyst

Table 3

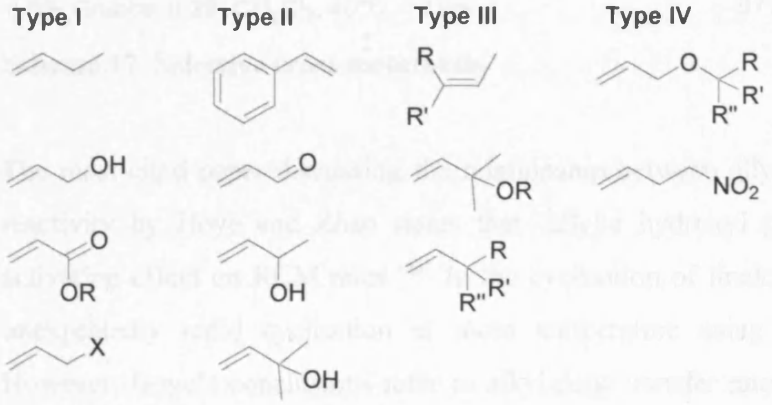

Figure 4 Examples of Type I-IV double bonds for Grubbs' second generation catalyst

Type I olefins include terminal olefins, primary allylic alcohols, esters and allyl halides. Type II olefins include styrenes, vinyl ketones, secondary and tertiary allylic alcohols; Type III olefins include 1,1-disubstituted olefins, protected tertiary allylic alcohols and quarternary allylic carbons; and Type IV olefins include trisubstituted protected allyl alcohols and vinyl nitro olefins (**Figure 4**). With these

properties in mind, chemists can predict the likelihood of cross metathesis in their substrates, both with cross metathesis and ring closing metathesis in mind.

Grubbs used this model to selectively synthesise alkenes **62** and **63** *via* cross metathesis (**Scheme 17**). Type I alkene **59** was reacted with Type III alkenes **60** or **61** with Grubbs' second generation catalyst **29**. Upon analysis, the cross metathesis product from reaction with tertiary alcohol **60** gave a reduced yield of product alkene **62**. The greater selectivity in the reaction between alkenes **59** and **61** was attributed to the steric bulk of the silyl protecting group, as cross metathesis between the product alkene **63** and further alkenes was avoided.

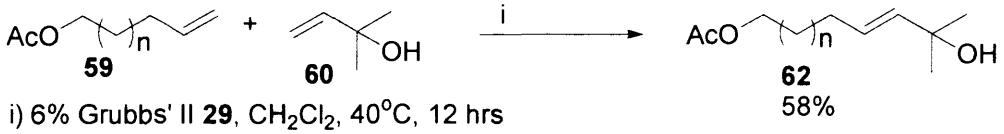

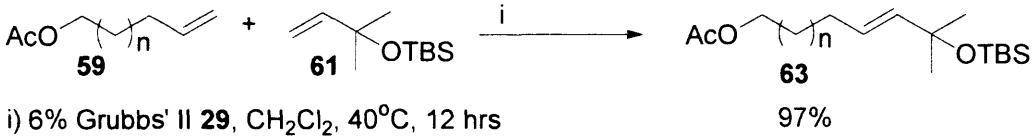

Scheme 17 Selective cross metathesis

The most cited paper discussing the relationship between allylic functionality and reactivity by Hoye and Zhao states that 'allylic hydroxyl groups exert a large activating effect on RCM rates.'[28] In the cyclisation of linalool **64** they found an unexpectedly rapid cyclisation at room temperature using 5% Grubbs' I **28**. However, Hoye's conclusions refer to alkylidene transfer rate by these substrates, and this is often misinterpreted or completely missed by groups citing this paper. Substrates with allylic protecting groups were then run in competition against the free alcohol in $CDCl_3$ at room temperature and reactions were monitored by ^1H NMR. Their results are shown in **Figure 5**.

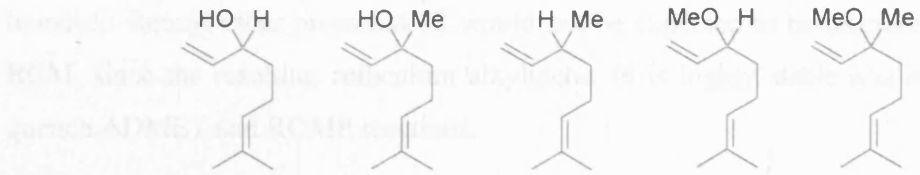

	64	65	66	67	68
approx relative reactivity	60	12	8	1	~0

Figure 5 Relative reactivies of Hoye's RCM substrates

Although the allylic hydroxyl groups are thought to exert an activating effect on the metathesis, this particular cyclisation is a challenging one since the most reactive double bond in these systems is that with the allylic hydroxyl or ether, rather than the dimethylated one, so the metathesis must start at the allylic end. In this particular instance, the substrate with the allylic hydroxyl group is the most reactive and substitution appears to deactivate the substrate towards metathesis. Hoye's observations suggest the ethers are less reactive towards alkylidene transfer due to inductive effects which reduce the electron density of the double bond and reduce the rate by nearly an order of magnitude. One omission in this range of substrates is one without an allylic double bond, as it is impossible to draw a definitive conclusion about the effect of the allylic hydroxyl group without this substrate.

However, most groups citing this paper do not take this fact into account. With their substrates, the metathesis would not be expected to start at the allylic double bond.

Maishal found that some allylic groups (acetonides and benzyl ethers) appear to deter RCM (**Figure 6**).[29] However, the group do not appear to have taken their choice of protecting groups into full consideration, as shown in **Figure 7**. The RCM of diol **69** proceeds, but due to the formation of the Ru-alkylidene **73**, isomerisation is likely to be an issue with Grubbs' first generation catalyst **28**. The RCM of acetonide-protected **70** does not proceed, although this is not due to the choice of protecting group, it is due to the cyclic nature of the acetonide, and the strained product **74** forming as a result of RCM (**Figure 8**). The RCM of **71** proceeds, but as discussed by Hoye, initial alkylidene formation takes place at the allylic double bond, and the effect of the allylic OH is on the rate of vinylidene

transfer. Benzyl ether protected **72** would not be expected to be reactive towards RCM, since the resulting ruthenium alkylidene **76** is highly stable and is used to quench ADMET and ROMP reactions.

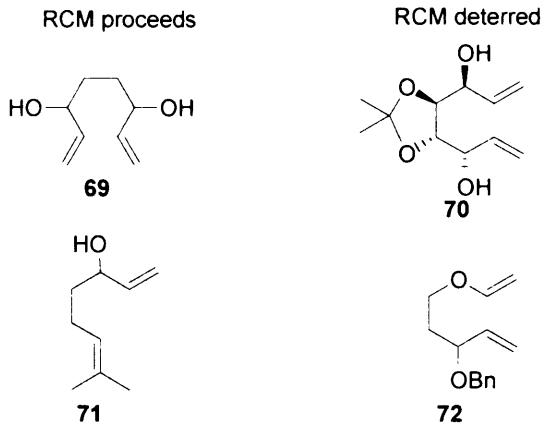

Figure 7 Differences in reactivity towards RCM dependent on hydroxyl protecting group

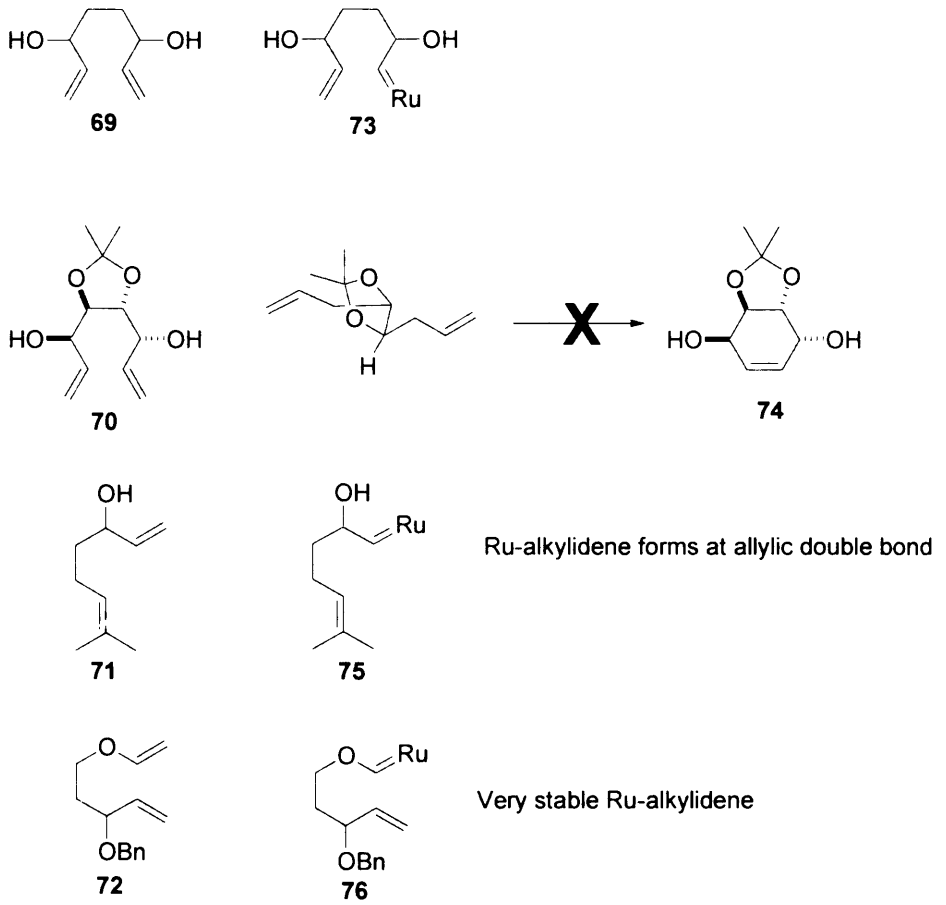

Figure 8

They also compared the activity of a free allylic hydroxyl in cyclisation with an allylic acetate (**Scheme 18**). Their studies found that the acetate protected hydroxyls cyclised more rapidly than the free hydroxyl systems.

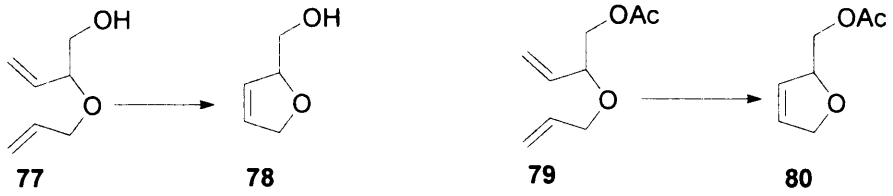

77 **78** **79** **80**

2.5% Grubbs' 1st Gen **28**, CH_2Cl_2, 2.5hr, RT, 79%

2.5% Grubbs' 1st Gen **28**, CH_2Cl, 5 min, RT, 98%

Scheme 18

However, the group do not appear to take into account the possibility of chain transfer in the ruthenium alkylidene **81**. If this occurs, the ruthenium is in close proximity to the hydroxyl group, which may result in the formation of a chelate between the oxygen of the hydroxyl group and the ruthenium of the catalyst (**Figure 9**). The chelate **82** forms a favourable five-membered ring and so would be expected to be stable and therefore slow down the overall conversion of **77** into cyclic **78**.

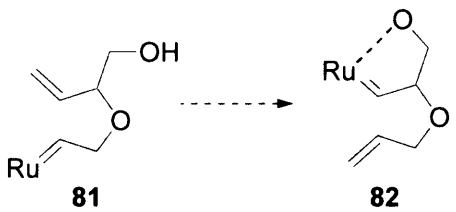

81 **82**

Figure 9 Formation of chelate during RCM of 77

Ghosh suggested that chelation between an allylic alcohol functionality and the ruthenium of the catalyst is also possible, and retards the RCM process. The group believed this was the reason that dienol **83** did not undergo RCM to give 5-membered ring **85**, as complexation of the hydroxyl group to the ruthenium was strong (**Scheme 19**).[30,31]

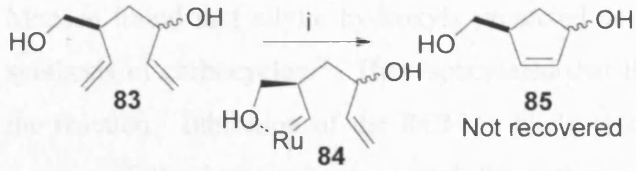

i) 6 mole % Grubbs' I **28**, CH_2Cl_2, RT, 24 hours

Scheme 19 Possible chelation by a hydroxyl group to Ru centre during RCM

Maishal's acetate-protected diene **79** underwent rapid RCM. Although it is still possible that **79** could form a chelate with the ruthenium, the resulting structure would be a less favoured seven-membered ring (**Figure 10**). Although chelate **86** appears less favourable, Mulzer suggested a seven-membered ring chelate was responsible for obstructing the synthesis of analogues of prostglandins *via* cross metathesis (**Scheme 20**), although this chelate may be more stable because of some restriction of rotation due to the fused ring. Chelation between acetate **79** and ruthenium is likely to occur much more slowly than in the case of alcohol **77**, so less catalyst is trapped in chelate form, allowing more rapid conversion of diene **79** into cyclic **80**.[32]

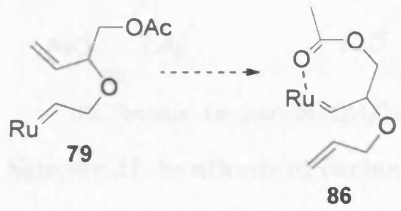

Figure 10 Chelate formation by acetate 79

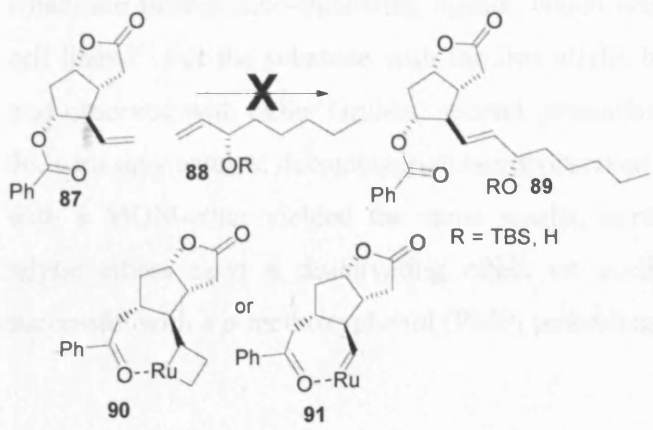

Scheme 20 Possible chelates formed by a benzoate protecting group in the failed formation of 89 by cross metathesis

Madsen found that allylic hydroxyls protected as acetates facilitated RCM in the synthesis of carbocycles.[33] They speculated that the hydroxyl groups may inhibit the reaction. Inhibition of the RCM is likely to occur *via* chelation between the oxygen of the hydroxyl group and the ruthenium centre, in a similar way to Maishal's system, and would explain the higher loading of catalyst required for alcohol **92** compared with acetate **94**, since some of the ruthenium is trapped in the chelate. Acetate **94** could also be expected to form a chelate in a similar way to **79**, but this would once again be a seven-membered ring, and so the formation of this chelated structure would be slower than the formation of the five-membered ring chelate between the free hydroxyl group and ruthenium.

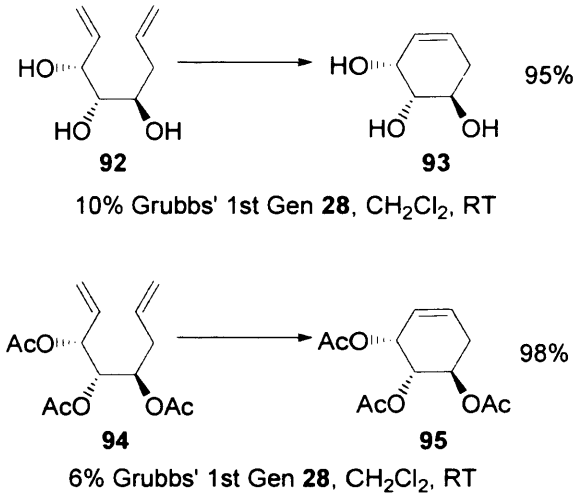

Scheme 21 Synthesis of carbocycles *via* RCM

Gennari synthesised a ten-membered ring in the synthesis of simplified eluethisides which are microtubule-stabilising agents, which are active against certain tumour cell lines.[34] For the substrate with the free allylic hydroxyl group **97**, no reaction was observed with either Grubbs' second generation catalyst **29** or Nolan catalyst **96**, with only catalyst decomposition being observed. Protection of the free alcohol with a MOM-ether yielded the same results, agreeing with Hoye's theory that allylic ethers exert a deactivating effect on cyclisation. The cyclisation was successful with a *p*-methoxyphenol (PMP) protecting group **99** (**Scheme 22**).

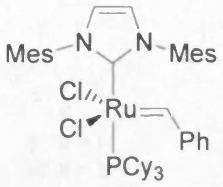

96

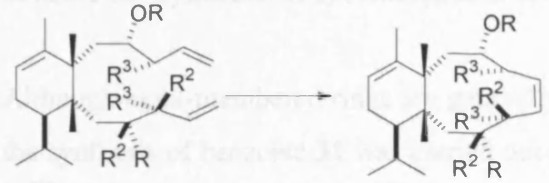

97 **98**

R = H, R^2 = H, R^3 = OMOM

Grubbs' II **29** or Nolan cat **96**

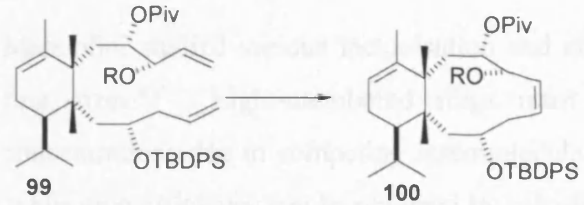

99 **100**

10% Grubbs' 2nd gen, 11mM, CH_2Cl_2, reflux

Scheme 22 Synthesis of simplified eleuthisides *via* RCM

All of the accounts explained in this section are purely qualitative and give no real understanding of allylic substitution or electronic effects on RCM. Therefore, substrate design at present is a matter of trial and error for many chemists, rather than a rational process, based on knowledge of structure-activity relationships.

From the synthesis of conformationally-locked analogues of sugars, Percy noted that the choice of allylic protecting group appears to affect the efficiency of the cyclisation reaction. Cyclooctenones **3, 32-33** could be synthesised at very different concentration maxima (**Table 5**, **Scheme 23**).[2]

Substrate	**X**	**$[S]_{max}$/mM**
3	H	1
30	Bn	5
31	Bz	20

Table 5 Concentration maxima for RCM reactions for 3, 30 and 31

3 X = H
30 X = Bn
31 X = Bz
i) 5% Grubbs' II, CH_2Cl_2, $Ti(O/Pr)_4$, reflux

Scheme 23 Synthesis of cyclooctenones 3, 32 and 33 *via* RCM

Although eight-membered rings are generally considered challenging to synthesise, the synthesis of benzoate **31** was carried out at a relatively high concentration of 20 mM, compared with alcohol **4** and benzyl ether **30**, which had much less efficient RCMs (syntheses were carried out at 1 mM and 5 mM respectively).

Mandolini studied various lactonisation and etherification reactions of a range of ring sizes.[8,35] Eight-membered rings must typically be synthesised at low concentrations due to competing intermolecular reaction pathways. A measure of cyclisation efficiency can be obtained by calculating the effective molarity (EM) for the reaction. The EM is a measure of the relative rates of intra and competing intermolecular reaction. For 8-membered rings, EM values reach a minimum (10^0 – 10^{-3} M), meaning that the cyclisation efficiency is very low and in order to avoid formation of intermolecular reaction products, the reactions must be carried out at high dilution, limiting their scaleability severely. Mandolini calculated several effective molarities (EMs) for eight-membered ring syntheses. Larger EM values were obtained for systems in which one or more rotors was already frozen, reducing the entropic penalty on the reaction (**Scheme 24**).

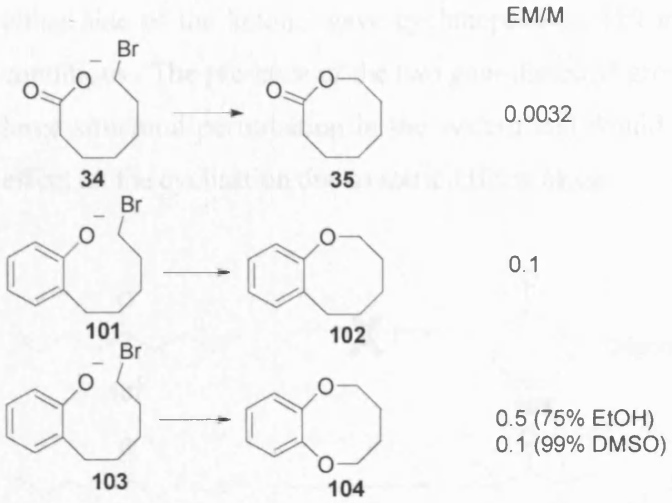

Scheme 24 EM values for eight-membered ring syntheses

There are relatively few accounts of substituent effects on reaction efficiency in RCM. Grubbs attempted one of the earliest eight-membered ring syntheses *via* ring closing metathesis and found that diene **42** did not form any isolable cyclic product with Grubbs' first generation catalyst **28**, even at high dilution.[22] However, diene **105**, with a fused aromatic ring, cyclised under the same conditions within three hours, at a substrate concentration of 15 mM (**Scheme 25**).

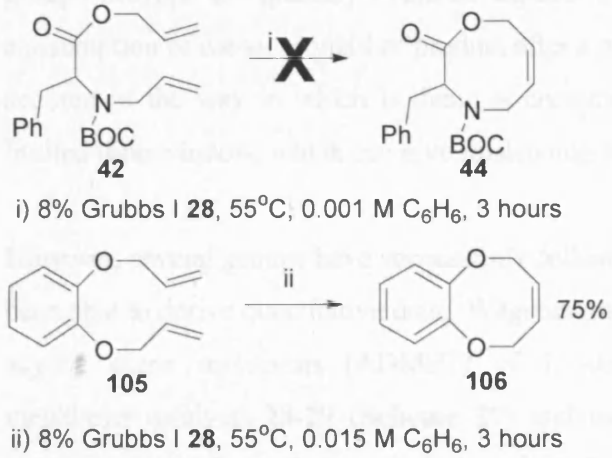

Scheme 25 Synthesis of eight-membered rings *via* RCM

Forbes attempted the synthesis of seven-membered ring **108** *via* RCM using Schrock's molybdenum catalyst **40** (**Scheme 26**).[36] The group observed that when the cyclisation was carried out neat with diene **107,** only oligomers were formed, rather than cyclic product **108**, whereas diene **109** with a *gem*-dimethyl group on

either side of the ketone, gave cycloheptenone **110** in 95% yield under the same conditions. The presence of the two *gem*-dimethyl groups, however is an extremely large structural perturbation in the system and would be expected to exert a large effect on the cyclisation due to steric effects alone.

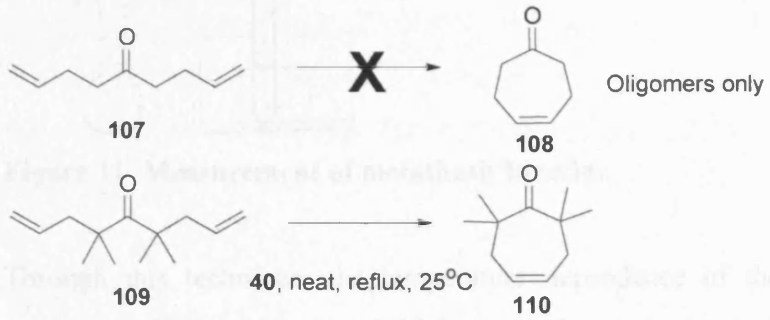

Scheme 26 Attempted syntheses of seven-membered rings *via* RCM

1.6 Study of Metathesis Kinetics

There are several published accounts of metathesis kinetics, with authors using various techniques to follow reactions. However, some are more accurate than others, and give a good insight into substrate reactivity and consumption. Several groups attempt to 'quantify' various aspects of RCM by examining only the consumption of diene, or yield of product after a given time. This does not give any account of the way in which is diene is consumed, and groups often use only a limited time window, which can give misleading results about reaction outcomes.

However, several groups have successfully followed metathesis reactions, and have been able to derive quantitative data. Wagener attempted to quantify the kinetics of acyclic diene metathesis (ADMET) of 1,9-decadiene by Grubbs' ruthenium metathesis catalysts **28-29 (Scheme 27)** and used apparatus which allowed the measurement of the evolution of ethylene from the reaction (**Figure 11**).[37]

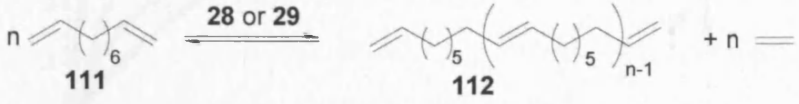

Scheme 27

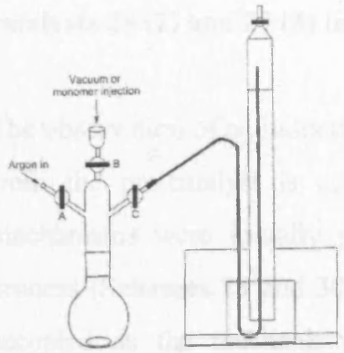

Figure 11 Measurement of metathesis kinetics

Through this technique, the temperature dependence of the reaction could be compared (**Figure 12**), and initial rates of metathesis could be calculated for comparison between the two catalysts at different temperatures. This technique also gave insight into slightly different behaviour between the first and second generation catalysts, in that Grubbs' second generation catalyst **29** appeared to show an induction period, which was defined as a period before the maximum rate of metathesis is reached. The induction period observed for catalyst **29** was attributed to the lower rate of phosphane dissociation relative to Grubbs' first generation catalyst **28**. However, the presence of the IMes ligand on Grubbs' second generation catalyst **29** stabilises the resulting 14 electron catalyst which results from phosphane dissociation.[38] Following the whole reaction in this way allowed for observations of differences in behaviour between the two catalysts, which is not possible by recording only reaction end points, half lives or yields after a given time.

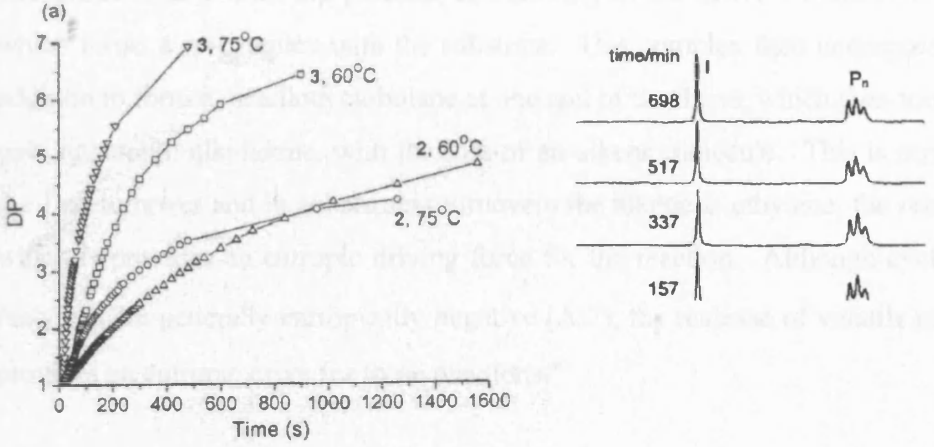

Figure 12 Temperature dependence of Grubbs' first and second generation catalysts 28 (2) and 29 (3) in the ADMET of 1,9-decadiene 111

The observation of an induction phase attributed to the loss of the phosphane ligand from the pre-catalyst is consistent with the mechanism of metathesis. Two mechanisms were initially proposed – the associative process and dissociative process (**Schemes 28** and **30**).[39] However, the dissociative process is now widely accepted as the mechanism for metathesis, meaning that dissociation of the phosphane ligand occurs before complexation of the alkene.

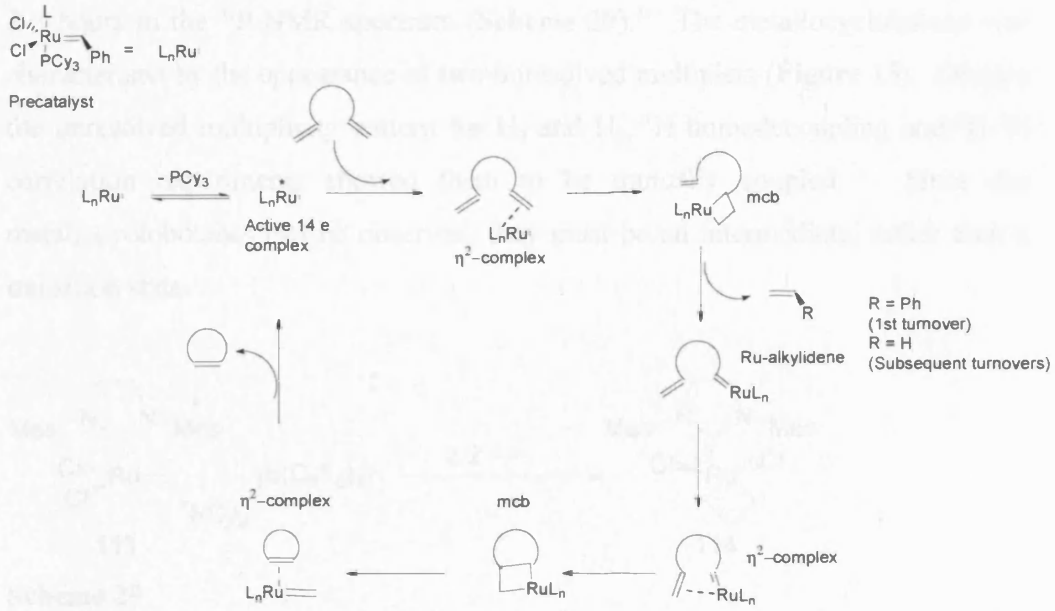

Scheme 28 The dissociative process in ring closing metathesis

The dissociative process (**Scheme 28**) involves the initial reversible loss of the phosphane ligand from the precatalyst, resulting in the active 14-electron species which forms a η^2-complex with the substrate. This complex then undergoes [2+2] addition to form a metallocyclobutane at one end of the diene, which then forms a new ruthenium alkylidene, with the loss of an alkene molecule. This is styrene in the first turnover and in subsequent turnovers the alkene is ethylene, the release of which is provides an entropic driving force for the reaction. Although cyclisation reactions are generally entropically negative ($\Delta S^{\ddagger}$), the realease of volatile ethylene provides an entropic drive for these reactions.[40]

The new ruthenium alkylidene then forms a new cyclic η^2-complex with the other end of the diene, followed by the cyclic metallocyclobutane. The final product η^2-complex breaks down to release the product and regenerate the propagating active catalyst, which goes on to turnover further substrate molecules.

The metallocyclobutane was the subject of much speculation until recently. It was not known if this species was a transition state or an intermediate. However, Piers was recently able to directly observe the 14-electron metallocyclobutane species using ^{1}H NMR at -50°C. An excess of ethylene was added to a solution of **113** in CD_2Cl_2 and quantitative generation of metallocyclobutane **114** was observed after 2-3 hours in the ^{31}P NMR spectrum (**Scheme 29**).[41] The metallocyclobutane was characterised by the appearance of two unresolved multiplets (**Figure 13**). Despite the unresolved multiplicity pattern for H_α and H_β, ^{1}H homodecoupling and ^{1}H-^{1}H correlation experiments showed them to be mutually coupled. Since the metallocyclobutanes can be observed, they must be an intermediate, rather than a transition state.

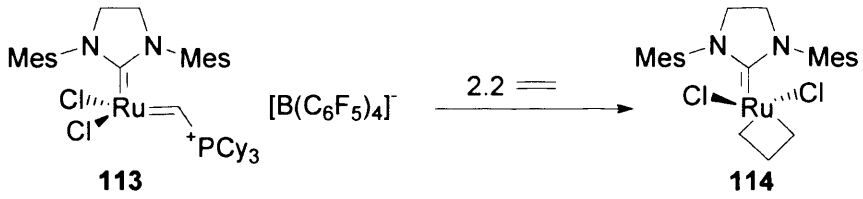

113 **114**

Scheme 29

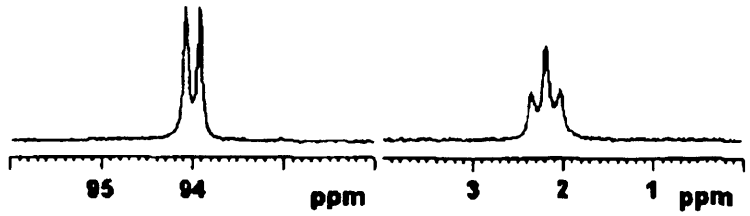

Figure 13 ^{13}C NMR resonances for a C_α (left) and C_β (right) in the ^{13}C enriched metallocyclobutane 114 (from ref 41)

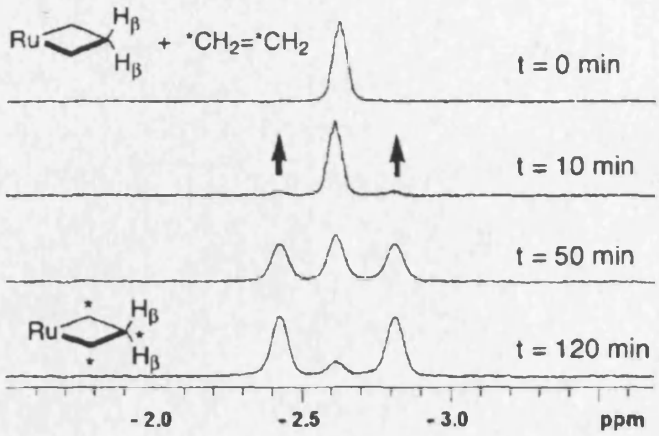

Figure 14 Low temperature ^{1}H NMR of H_β (from ref 41)

The associative mechanism (**Scheme 30**) was proposed along with the dissociative mechanism, where the substrate molecule binds to the ruthenium centre without loss of the phosphane ligand. This mechanism, however, is now no longer considered to be the major pathway for metathesis, since the active catalytic ruthenium species is believed to be a 14 electron one, rather than a 16 electron one, and also because the propagating methylidene is known to be inactive when phosphane-bound.[42]

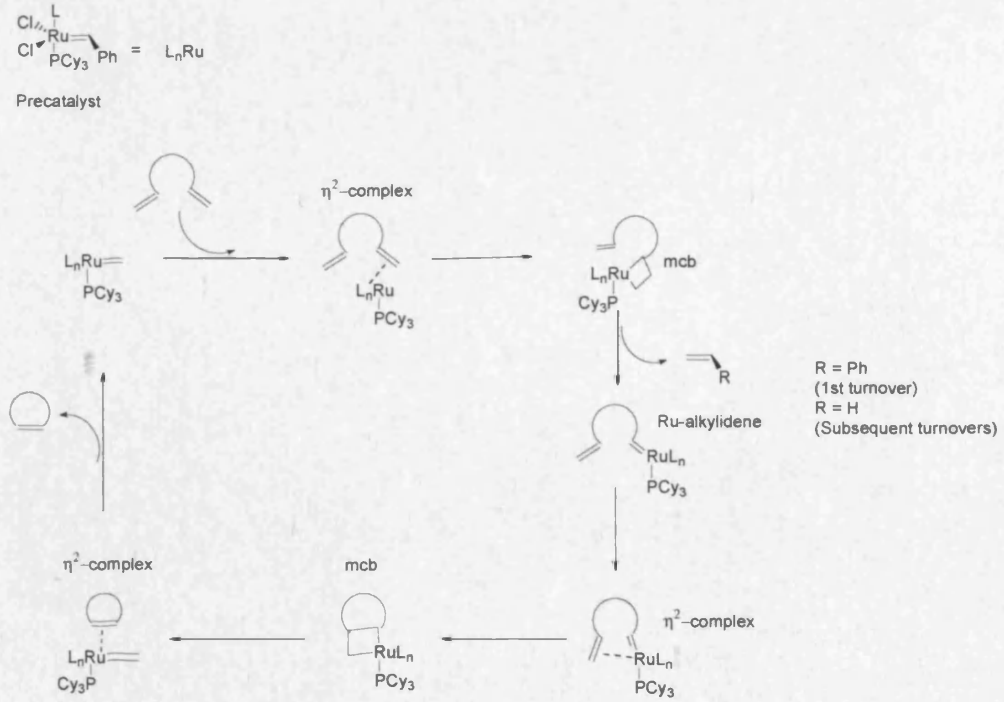

Scheme 30 The associative process in ring closing metathesis

NMR kinetics have been used to study and compare the lifetimes of ruthenium metathesis catalysts. Grubbs used ^{1}H NMR to monitor the lifetime of alkylidenes **28, 115-116** over several half lives and found vast differences in alkylidene stability depending on the nature of Ru=CHR (**Table 5**). Substituted carbenes were found to decompose *via* bimolecular pathways, whereas methylidene **116** was found to decompose unimolecularly following the recapture of free phosphine in solution.

Akylidene	$t_{1/2}$/hours
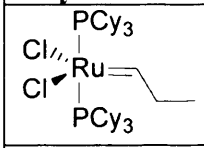 **115**	8
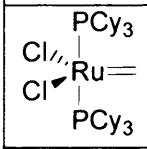 **116**	0.67
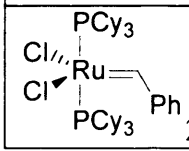 **28**	192

Table 5 Thermolytic half lives of alkylidenes 28, 115-116

The relatively short lifetime of methylidene **116** is significant, since this is the propagating species in the majority of metathesis reactions. This result has particular implications for difficult cyclisations, which, due to the unimolecular decomposition of methylidene **116**, require high catalyst loadings.[43]

Several have used NMR kinetics to quantify various aspects of metathesis. Grubbs followed the RCM of diethyl diallylmalonate **117** (DEDAM) with catalyst **119** using ^{1}H NMR at 20°C in order to quantify relative catalyst activities, and to compare the effects of different ligands on catalyst activity (**Scheme 31**). The disappearance of diene **117** was monitored by integrating the allylic methylene peaks and results such as those shown in **Figure 15** were typically obtained.

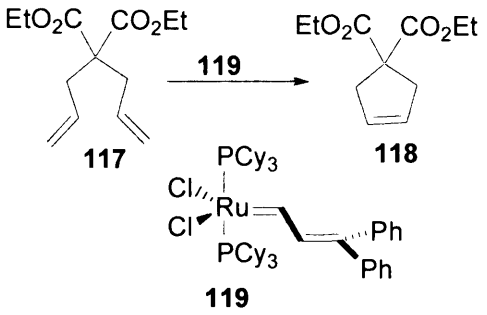

Scheme 31 RCM of DEDAM

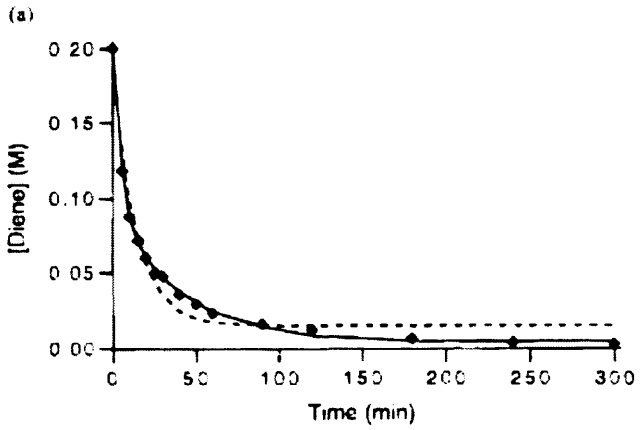

Figure 15 Grubbs' data from ^{1}H NMR kinetics of RCM of DEDAM with 119 (dotted line is double exponential expression fit)

Grubbs observed that the experimentally obtained data did not exhibit first order behaviour with respect to diene. However, the curves were fitted to a double exponential expression (**Equation 2**), which was believed to take into account the difference in kinetic behaviour between the initiating Ru-alkylidene and the propagating methylidene **120**.[44,45]

$$y = (k_1-k_2)/(k_1e^{-k_2t})-(k_2e^{-k_1t})$$

Equation 2

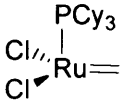

120

However, isolation of methylidene **120**, and subsequent study of its catalytic behaviour still revealed the same behaviour, and the same double exponential

expression was used to fit the data, which suggested that the differences between the two catalytic species were not responsible for the observed kinetic behaviour. Grubbs' kinetic studies showed that RCM kinetics are complex and do not follow simple first order kinetics.

The initiation kinetics of the ring-opening metathesis polymerisation (ROMP) of 7-oxanorbornene **121** by Grubbs' first generation catalyst **28** were followed by France using UV-vis spectroscopy, which enabled the calculation of activation parameters for the process (**Scheme 32**).[46] The initiation reaction was followed by tracking the change in the absorption at 335 nm (due to catalyst **28**) over time. This corresponds to phosphane dissociation from pre-catalyst **28**. NMR kinetics could not be used in this case because the initiation step for polymerisation was too rapid. The group also used ^{1}H and ^{31}P NMR to show that the pre-catalyst **28** was completely consumed during this time, liberating the propagating species **123** (**Scheme 33**). Under saturation conditions, phosphane dissociation is the rate-limiting step of the initiation process, and under these conditions, the rate of initiation was found to be independent of the concentration of **121**. This therefore suggests that the initiation process is a unimolecular one, involving only pre-catalyst **28**.

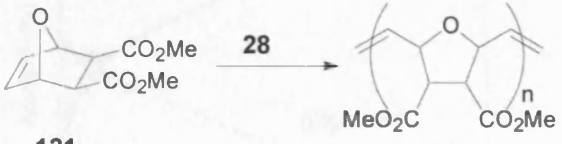

121 **122**

Scheme 32 ROMP of 7-oxanorbornene with Grubbs' first generation catalyst

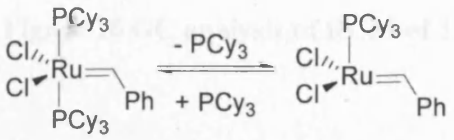

28 **123**

Scheme 33 Phosphane dissociation from catalyst 28

^{1}H NMR was then used to follow the propagation kinetics of the reaction in $CDCl_3$. The decrease in monomer concentration over time was followed by monitoring the disappearance of the *endo*-methine protons relative to a ferrocene internal standard.

Fogg recently used GC and MALDI-MS to follow the formation of cyclic alkenes *via* ADMET oligomers (**Scheme 34**).[21] In this case, the use of ^{1}H NMR to follow the reaction was not feasible, due to the spectra of ADMET oligomers closely resembling that of the starting diene. The use of GC allowed the formation and subsequent consumption of oligomers into cyclic alkene **125** to be tracked (**Figure 16**), and the use of MALDI-TOF mass spectrometry allowed the identification of non-volatile products present within the mixture after 15 minutes (**Figure 17**).

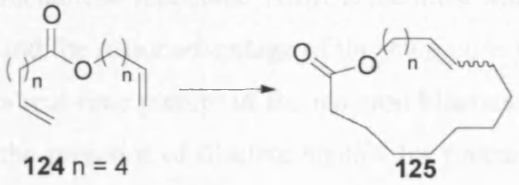

Scheme 34

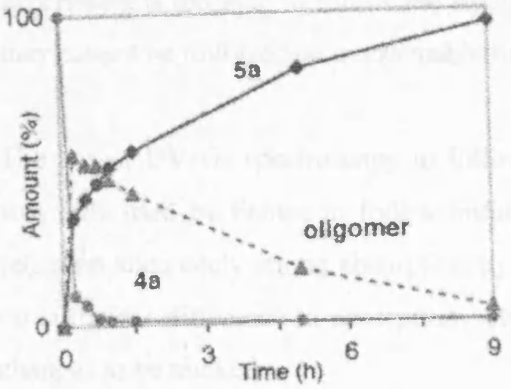

Figure 16 GC analysis of RCM of 124 *via* formation of ADMET oligomers

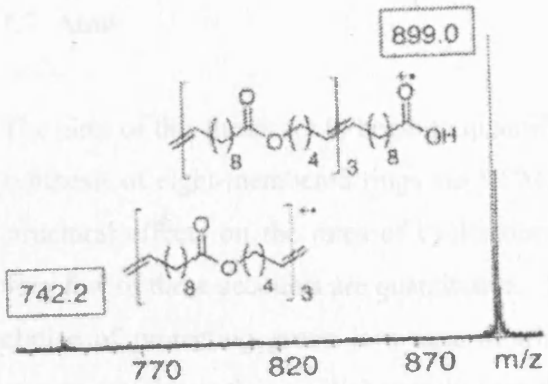

Figure 17 MALDI-TOF mass spectrum of involatile products isolated after 15 minutes

There are advantages and limitations to the different methods of following metathesis reactions. NMR is the most widely used method for following reactions, and the major advantage of this method is that reactions are followed *in situ*, giving a real-time picture of the reaction kinetics. The use of this technique is limited by the presence of discrete signals for precursor and product, and relies on reactions which can be followed at a concentration sufficient for adequate signal to noise. The use of NMR also requires that reactions are not so rapid that each NMR experiment is too long to follow the reaction, or that reactions are not so slow that they cannot be followed on a reasonable timescale.

The use of UV-vis spectroscopy to follow metathesis reactions is limited, and so was only used by France to follow initiation kinetics. The use of this technique relies on adequately strong absorption by the precursor or product, and also relies on sufficient difference in absorption between the precursor and product to allow changes to be tracked.

Fogg's use of GC relies on the volatility of the ADMET oligomers formed, although the use of MALDI-MS in conjunction with GC allowed for the identification of larger, non-volatile oligomers. However, the formation of ADMET oligomers appears to be very rapid, and much of the consumption of the starting diene was missed, and so a detailed picture of the reactivity behaviour of the starting diene cannot be obtained.

1.7 Aims

The aims of this thesis are to begin to quantify a number of important aspects of the synthesis of eight-membered rings *via* RCM. Current literature relating to various structural effects on the rates of cyclisation is limited and often conflicting, and very few of these accounts are quantitative. This therefore means that, for example, choice of protecting group is a case of trial and error. Quantitative studies of structure and reactivity will hopefully enable some degree of rational reactivity-based design of precursors.

Little is currently documented regarding the efficiency of eight-membered ring syntheses *via* RCM. Effective molarities have been calculated for various eight-membered ring lactonisations and etherifications, but none for RCM, so little is known about the efficiency or inefficiency of these processes. Groups which have reported the syntheses of eight-membered rings *via* RCM generally adopt high dilution conditions to avoid competing intermolecular reaction pathways, however, there are no attempts to quantify the relative rates of intra and intermolecular reaction. We aim to use the precursors synthesised *via* the route developed by Percy and exploit highly sensitive ^{19}F NMR to study the relative efficiencies of the cyclisation reaction and competing cross metathesis pathways, and also identify any products of cross metathesis.

Little is currently understood about the equilibria of eight-membered ring syntheses *via* RCM. Through the use of NMR kinetics, this thesis aims to explore the balance between the formation of thermodynamic (cyclic) product and kinetic (oligomeric) products; the stability of the cyclic product and its susceptibility to ring opening; and also the effect of volatile ethylene on the reaction equilibrium. All of these factors are likely to affect the balance of eight-membered ring formation and a comprehensive understanding of these is essential for rational experimental design and optimisation.

This thesis also aims to explore a range of variables affecting the rate of cyclisation, such as solvent, temperature dependence, choice of catalyst and co-catalyst using a

range of kinetic techniques, with a view to identifying the optimum reaction conditions.

Results and discussion

2.1 Optimisation of the Route Towards Conformationally-Locked Sugar Analogues

The route towards difluorinated conformationally-locked sugar analogues developed by Percy was optimised to ensure each step was high yielding, even in larger scale reactions.[2] The group showed that fluorinated acetal **8b** could be synthesised easily from commercially available trifluoroethanol **13** and MEM-chloride up to molar scale, and purified easily by reduced pressure distillation, resulting in material of good purity which could be stored for long periods of time.

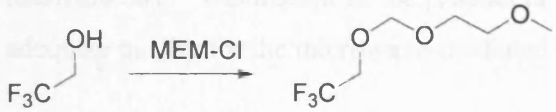

13 **8**

Scheme 35 Synthesis of MEM ether 8b from trifluoroethanol

When the synthetic route was first developed, commercially-available 4,4-dimethylpentenal **126** was used (**Scheme 36**). However, the resulting conformationally-locked sugar analogue **127** had the hydrophobic *gem*-dimethyl group on the already unnatural hydrophobic conformational-locking group, which was an undesirable structural feature of the molecule.

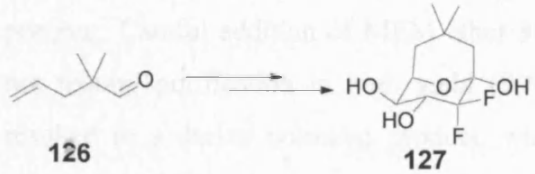

126 **127**

Scheme 36

The synthesis was modified to include pentenal **128**, rather than **126**, which was made *via* [3,3] rearrangement of commercially available allyl vinyl ether **129** (**Scheme 37**).[47] Small scale syntheses were carried out in the microwave over six hours and formed **128** in sufficient purity (by ^{1}H NMR) for use in the synthesis of allylic alcohol **7** without purification. Larger scale syntheses of **128** were carried

out in an Ace tube over 24 hours at 100°C. The resulting product was distilled carefully at atmospheric pressure to isolate the pentenal product from polymeric residues.

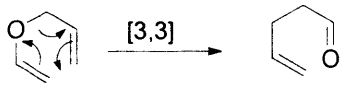

129 **128**

Scheme 37 Synthesis of pentenal 128 *via* [3,3] rearrangement of allyl vinyl ether 129

Allyl vinyl ether **129** could also be synthesised by refluxing allyl alcohol **130** and ethyl vinyl ether **131**, with a catalytic amount of mercury (II) trifluoroacetate (**Scheme 38**).[48] Distillation of the product at atmospheric pressure gave material of adequate quality for the microwave-mediated synthesis of the aldehyde.

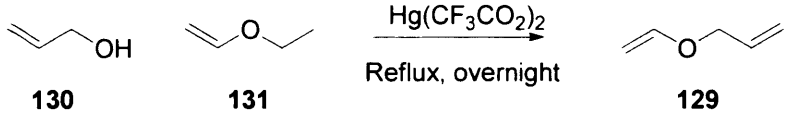

130 **131** **129**
51%

Scheme 38 Synthesis of allyl vinyl ether 129

The synthesis of allylic alcohol **7** could be carried out at up to a 0.1 M scale (**Scheme 39**). The synthesis was carried out low temperature (-78°C), using LDA formed *in situ* from *n*BuLi and DIPA. MEM ether **8** was added to the LDA at low temperature (-78°C) over one hour, and aldehyde **128** subsequently added in one portion. Careful addition of MEM ether **8** resulted in allylic alcohol **7** which did not require purification in high yield (90%). Rapid addition of MEM ether **8** resulted in a darker coloured product, which had to be distilled under reduced pressure, which resulted in lower yield (69%).

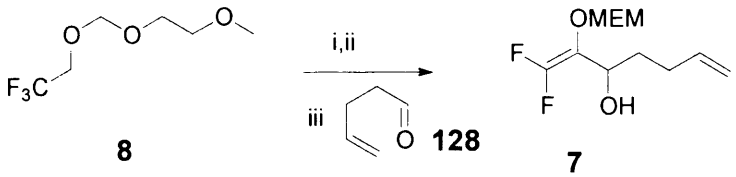

8 7

90% (69% after distillation)

i) *n*BuLi, DIPA, THF, -78°C to 0°C

ii) MEM ether, -78°C, 1 hour

iii) Pentenal, -78°C to -30°C, then NH_4Cl aq.

Scheme 39 Synthesis of allylic alcohol 7 from MEM ether 8 and pentenal 128

The next step in the synthesis was the formation of allyl ether **6** from allylic alcohol **7**, this was carried out under phase transfer conditions. The product obtained was of good purity by ^1H and ^{19}F NMR so did not require purification, and yields were near quantitative (**Scheme 40**).

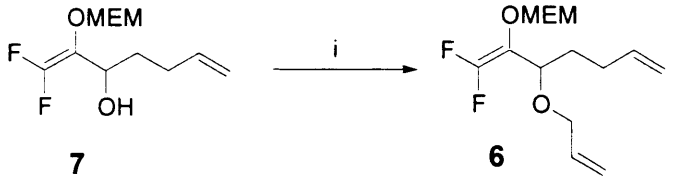

7 6

i) Allyl bromide, 50% NaOH aq, Bu_4NHSO_4, 0°C-RT overnight

Scheme 40 Allylation of allylic alcohol 7

A [2.3]-Wittig rearrangement was used to move the difluoro group midchain. *In situ* preparation of LDA followed by addition of ether **6** at -78°C and quenching at -30°C with aqueous ammonium chloride resulted in low recovery of **5**, and apparent decomposition due to competing *E2* elimination, resulting in vinylic product **132** (**Scheme 41**). *Des*-methyl substrate **6** is more reactive under the same conditions because there is another position at which deprotonation can occur, which is not possible in the case of the dimethyl substrate **20**. To improve the selectivity of deprotonation, the ether was added to the LDA at -100°C rather than -78°C, stirred at -70°C for two hours to allow the rearrangement to take place, and then quenched with aqueous ammonium chloride solution at -30°C (**Scheme 42**). Despite the brown colour of the product, the product was of good purity by ^1H and ^{19}F NMR and did not require purification.

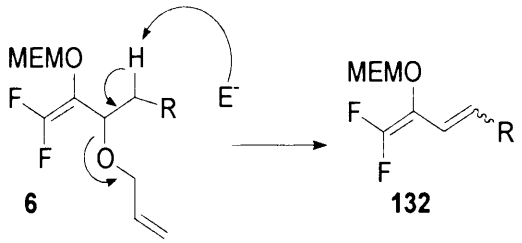

Scheme 41 Formation of undesired vinylic product 132 during [2,3]-Wittig rearrangement of 6

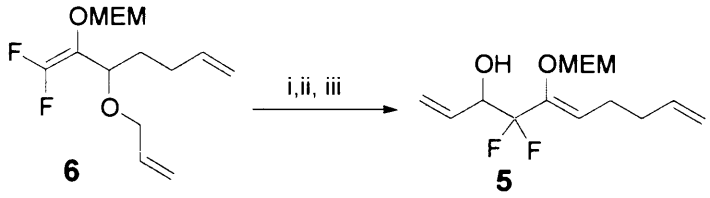

i) *n*BuLi, DIPA, THF, -78°C-0°C

ii) **6**, -100°C

iii) -70°C, 2 hours, then -30°C, NH_4Cl aq

Scheme 42 [2,3]-Wittig rearrangement of 6

With the *gem*-dimethyl series of compounds, the next synthetic step was cleavage of the MEM group under acidic conditions, to obtain difluoroketone **4**. However, in this synthetic series, early attempts at RCM on the ketone resulting from the acidic MEM cleavage suggested that the cyclisation was not working. Upon closer analysis, it appeared that the resulting eight-membered ring was volatile and therefore large volumes of solvent had to be carefully removed by distillation (**Scheme 43**).

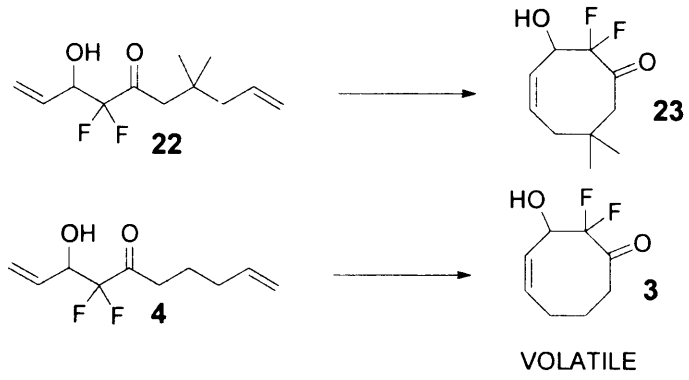

Scheme 43

Although this added an extra step to the synthesis, protecting group chemistry had to be used to protect the allylic hydroxyl group and ensure the eight-ring product of

RCM was not volatile. The allylic hydroxyl group on 2,3-Wittig product **5** was protected as a benzoate ester using benzoic anhydride, catalytic DMAP and a polymer-supported pyridine reagent (**Scheme 44**). The polymer supported reagent was easier to remove than liquid pyridine, so the resulting benzoate **133** was obtained in good yield and did not require purification. Washing the PVP with aqueous base also allowed it to be reused after drying.

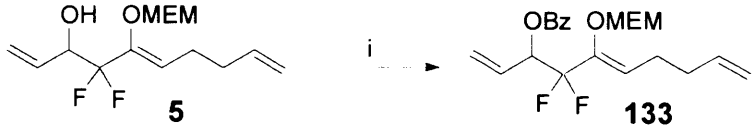

i) Bz_2O, 0.2 eq DMAP, PVP, CH_2Cl_2

Scheme 44 Synthesis of benzoate-protected 133

The MEM group was then cleaved using thionyl chloride in methanol, obtaining diene **31** in good yield (**Scheme 45**). Initially, diene **31** was purified by column chromatography but RCM proceeded with crude material, so the purification step was later omitted.

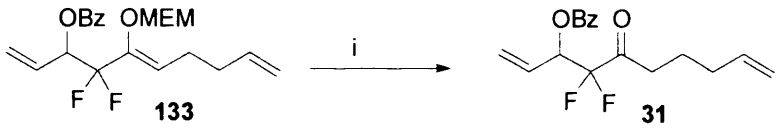

i) $SOCl_2$, MeOH, 0°C-RT, overnight

Scheme 45 MEM cleavage from benzoate 133

Benzoate **31** underwent RCM with Grubbs' second generation catalyst **29** (5 mole %), with titanium(IV) *iso*propoxide co-catalyst in refluxing dichloromethane (3 mM) overnight (**Scheme 46**). The resulting non volatile cyclooctenone **33** was purified by column chromatography, to obtain **33** as a white solid.

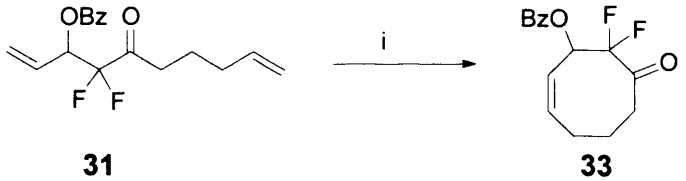

i) Grubbs' II **29** (5%), $Ti(OiPr)_4$ (30%), CH_2Cl_2 0.003 M, overnight

Scheme 46 Synthesis of cyclooctenone 33 *via* RCM

Benzoate **33** was much easier to handle due to its crystalline nature. A small amount of optimisation work was carried out to find the maximum possible running concentration for the cyclisation, before the appearance of competing cross metathesis products. Compared with the synthesis of volatile **3** which was carried out at 1 mM, benzoate **33** could be synthesised at 20 mM in refluxing CH_2Cl_2 before other products were observed in the ^{19}F NMR. These observations were investigated more fully and will be discussed in more detail in **3.1**.

Many groups have observed rearrangement or isomerisation in their syntheses of medium rings. Fogg recently observed that the common structural features of second generation metathesis catalysts are also common structural features of catalysts used for olefin hydrogenation.[20] A possible side-reaction resulting from this is olefin isomerisation, which can be particularly problematic for slow RCM reactions, such as the syntheses of medium rings. In this case, the terminal olefin is transformed into a less reactive internal olefin, which undergoes RCM more readily, due to the smaller ring size (since a seven-membered ring forms more readily than an eight-membered ring).

Isomerisation reactions are more common with NHC ligands, and appear to be worse in aromatic solvents. Some groups have taken advantage of this phenomenon, however, and use this isomerisation reaction to reach their target cyclic molecules. Van Otterlo exploited this occurrence in the synthesis of 6, 7 and 8-membered benzo-fused heterocycles (**Scheme 47**).[49] Benzo-fused heterocycles appear frequently in natural products, as well as in modern pharmaceuticals, so a convenient synthesis of these compounds is of high interest.

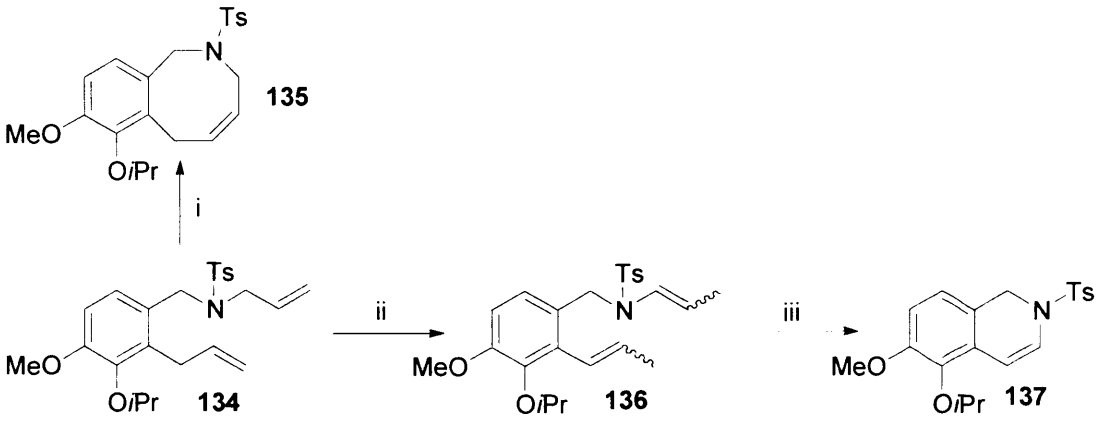

i) 5 % Grubbs' 2 **29**, toluene, 60°C, 60°C, 1 hr
ii) 0.5% xx, toluene, 110°C, 2 hr
iii) 5 % Grubbs' 2 **29**, toluene, 110°C, 3 hr

Scheme 47 Isomerisation behaviour of diene 134 under RCM conditions with 29

It is currently unclear whether the ruthenium alkylidene itself can induce isomerisation; catalyst decomposition to a ruthenium hydride species is widely regarded as the cause. However, recent findings suggest that the substrate itself can lead to the catalytic deactivation which causes isomerisation.[50] This will be discussed further in **4.1**.

Some groups have also observed double bond migration in their attempts at RCM. The migration products are often observed as mixtures with the expected ring closure product. This was observed by Schmidt in the synthesis of dihydrofurans **139** and **140** (**Scheme 48**) using Grubbs' first generation catalyst **28**.[51] However, double bond isomerisation is favourable in these systems due to conjugation with the lone pair of electrons on the oxygen atom within the ring.

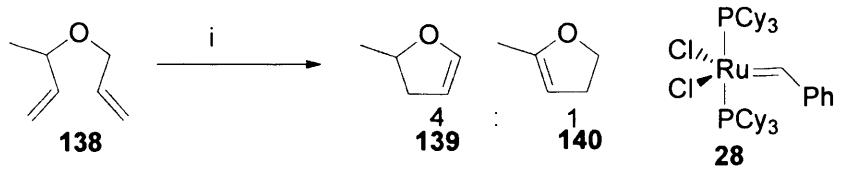

138 **139** : **140** **28**

i) 5% Grubbs I **28**, toluene, 25°C

Scheme 48 Isomerisation behaviour of 138 with Grubbs' I 28

This transformation is relatively rapid for five and six-membered ring formation, and slow for seven-membered ring formation. Fustero synthesised *gem*-difluorinated seven-membered ring lactams **142-143** and observed tandem metathesis-olefin isomerisation.[52] Through careful selection of solvent, the group were able to control the product formation. They claimed that the *gem*-difluoro group directs the isomerisation step, making the process a regioselective one.

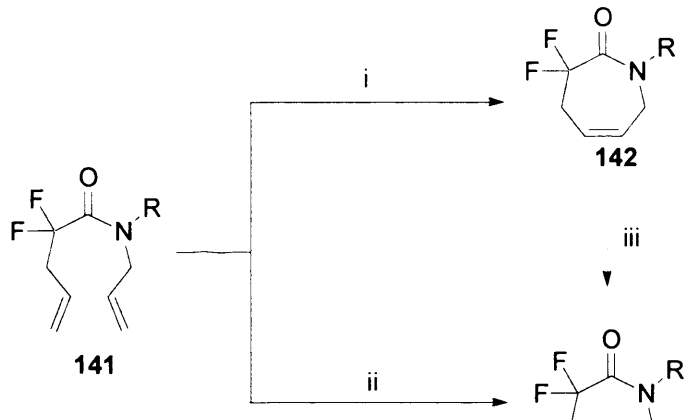

i) Grubbs I **28**, CH_2Cl_2 20 mM, 40°C, 2 hr
ii) Grubbs II **29**, Toluene 20 mM, 110°C, 2 hr
iii) Grubbs' II **29**, toluene 20 mM, 100°C, 2 hr

Scheme 49 Solvent effects on RCM behaviour

Generally, this isomerisation reaction is slow for medium rings and would not be expected in the synthesis of eight-membered rings. The clean conversation to only one product by ^{19}F NMR, and crystallographic data have confirmed that we do not observe any of these undesired side reactions in the synthesis of cyclooctenone **33**. To ensure that our observations were not due to solvent effect, since these isomerisations are more common in aromatic solvents, the RCM of **31** was run in toluene at 120°C at the same concentration, with the same catalyst loading (5%). The ^{19}F NMR spectrum (**Figure 17**) did not show any evidence of a different cyclic product under these conditions, and instead, showed clean conversion to cyclooctenone **33**.

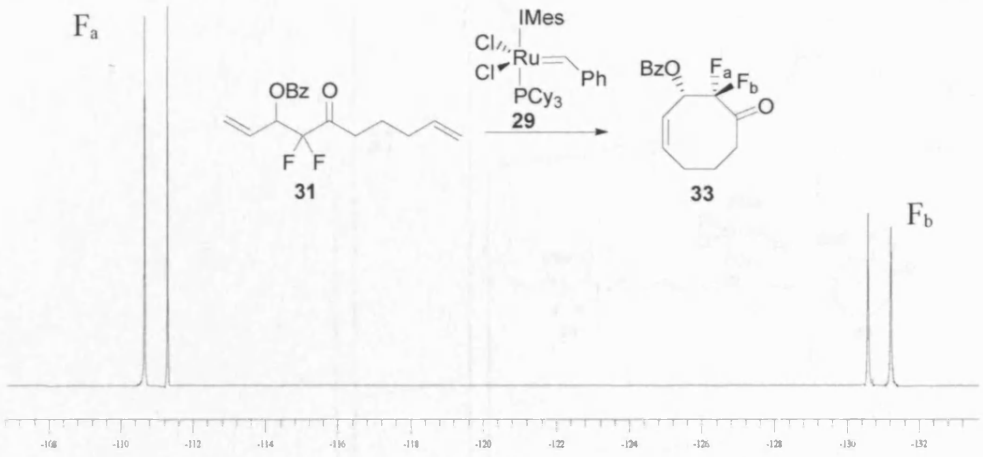

Figure 17 ^{19}F NMR obtained after RCM of benzoate 31 in toluene with 5% 29

It was possible that the Ti (IV) co-catalyst was blocking the formation of the rearrangement, product, or preventing the formation of a seven-membered ring, so the same reaction was run in toluene without the presence of titanium isopropoxide. The ^{19}F NMR did not show any evidence of smaller rings, or isomerisation products, but interesting, conversion to cyclooctenone **33** was only 20%, suggesting that the presence of the co-catalyst has a large effect on the conversion of diene **31** into eight-membered ring **33** (**Figure 18**). The same RCM was repeated, this time using 20% Grubb's second generation catalyst. All of the diene **31** was consumed, but under these conditions, eight-membered ring **33** made up **65%** of the product mixture, with cross metathesis products making up the rest of the product mixture. These results show us that the Ti (IV) co-catalyst has an important effect on the efficiency of the reaction, and also that the outcome of the reaction is affected by the presence of the co-catalyst. The presence of the co-catalyst under these conditions appears to block the cross metathesis pathway at 20 mM.

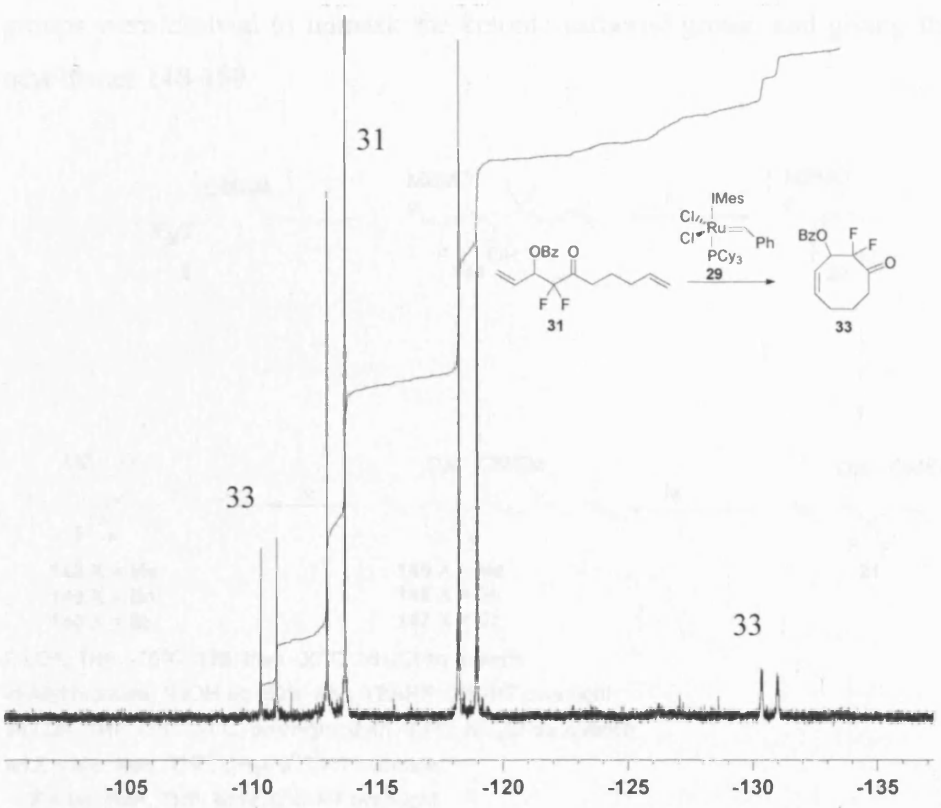

Figure 18 ^{19}F NMR obtained from RCM of benzoate 31 in toluene with 5% 29 in the absence of Ti(O*i*Pr)$_4$

2.2 Investigating Structural Effects on Cyclisation Rate

2.2.1 Synthesis of Substrates

For the purposes of studying the kinetics of the ring closing metathesis reactions, a series of *gem*-dimethylated substrates **148-150** were synthesised, using the methodology published by Percy.[1,2] The group had carried out the synthesis of alcohol **22**, starting from trifluoroethanol, and using commercially-available dimethylpentenal **126** as the aldehyde in the synthesis of the allylic alcohol **144** (**Scheme 50**). The allylation and 2,3-Wittig reactions were carried out according to the published procedure, and this was followed by addition of various protecting groups, giving access to new difluorinated RCM precursors.

Three new dienes were prepared, alongside alcohol **22** - benzyl ether **149**, benzoate **150** and methyl ether **148**. Following addition of the protecting groups, the MEM

groups were cleaved to unmask the ketonic carbonyl group, and giving the three new dienes **148-150**.

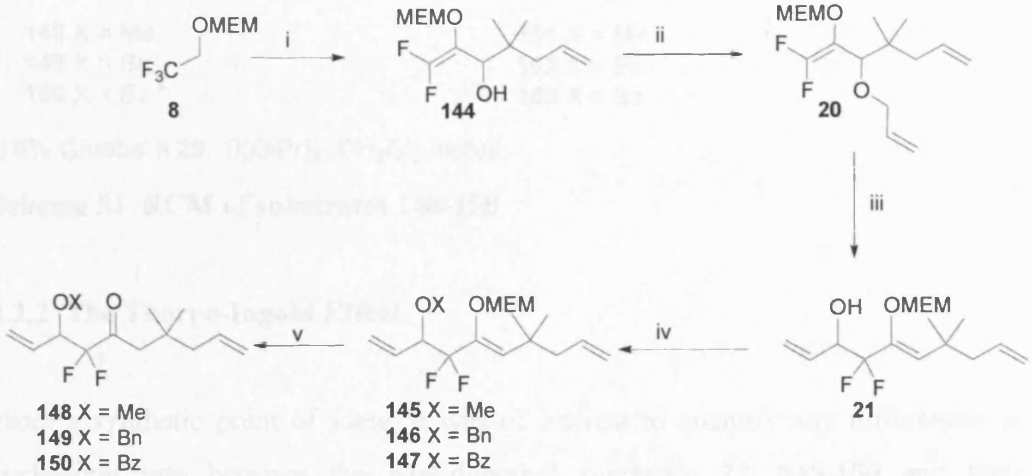

i) LDA, THF, -78°C, **126**, then -30°C, NH_4Cl aq quench

ii) Allyl bromide, NaOH aq (50% w/v), TBAHS, 0°C-RT overnight

iii) LDA, THF, -78- -70°C, overnight, then -30°C, NH_4Cl aq, quench

iv) X = Me: NaH, THF, CH_3I, 0°C-RT overnight

X = Bn: NaH, THF, BnBr, 0°C-RT overnight

X = Bz: Bz_2O, cat DMAP, PVP, CH_2Cl_2, RT, overnight

v) $SOCl_2$, MeOH, 0°C to RT, overnight

Scheme 50 Synthesis of *gem*-dimethyl series of RCM precursors 145-147

Purification was not necessary until the protection step of the sequence, and was only necessary for characterisation of methyl ether **145** and benzoate **147**. Pufication was necessary for **146** to remove residual benzyl bromide from the mixture. All substrates successfully underwent RCM in CH_2Cl_2 with 5% Grubbs' second generation catalyst **29** and 30% Ti (IV) co-catalyst (**Scheme 51**). All products were purified by column chromatography, and then passed through Polymer Labs MP-Thiol SPE tubes (eluting with methanol) to remove the last traces of catalyst residues, affording material of good quality, and in the case of benzoate **150**, a crystalline solid. The ^{19}F NMRs of these RCM products **151-153** were run at low temperature (212-128 K) due to the fluxional nature of the signals at ambient temperature. All products showed a major and minor conformer in both the ^{1}H and ^{19}F NMRs at low temperatures.

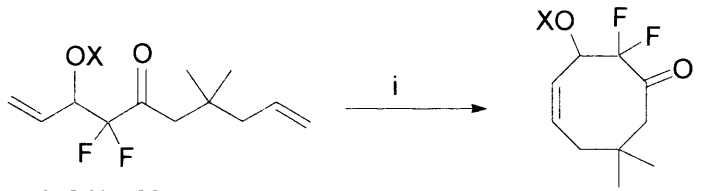

148 X = Me
149 X = Bn
150 X = Bz

151 X = Me
152 X = Bn
153 X = Bz

i) 5% Grubbs' II **29**, $Ti(OiPr)_4$, CH_2Cl_2, reflux

Scheme 51 RCM of substrates 148-150

2.2.2 The Thorpe-Ingold Effect

From a synthetic point of view, it was of interest to quantify any differences in cyclisation rate between the *gem*-dimethyl substrates **22, 148-150** and their corresponding CH_2 substrates because the CH_2 substrates were of greater interest for further chemistry. To our knowledge, this has not previously been quantified for the synthesis of medium rings by RCM. The *gem*-dimethyl group adds an extra steric and hydrophobic bulk to the already-unnatural, hydrophobic and bulky conformational locking group in the target sugar analogues. Although we knew that the RCMs of the CH_2 substrates were possible, since products had been isolated and characterised, the effect of removing the *gem*-dimethyl group from the precursors was unknown. A competition reaction was carried out to determine if the RCM was accelerated by *gem*-dimethyl substitution.

The Thorpe-Ingold effect was first proposed by Thorpe and Ingold, who suggested that cyclisation reactions are accelerated through the presence of a *gem*-dialkyl group on the chain.[53] Allinger and Zalkow considered the formation of six-membered rings in terms of enthalpy and entropy effects.[54] Ring closure for *gem*-dimethyl substituted substrates is favoured due to a change in the number of *gauche* interactions from the acyclic precursor to the cyclic product or transition state. However, the most important factor in the *gem*-dialkyl effect maybe that the rate of cyclisation generally increases because the alkyl groups repel each other, increasing the angle between them, β, and decreasing angle α, therefore increasing the probablility of ring closure (**Figure 19**).

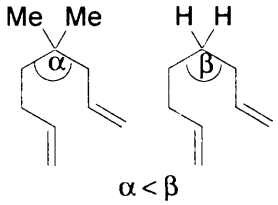

Figure 19

Gem-dialkyl groups are also believed to accelerate cyclisation reactions by lowering the energies of transition states, intermediates or products, and do this by providing some restriction of rotors in the linear chain. This lowers the entropy for the cyclisation reaction.

Benzyl ether **30** (prepared by J. Miles) and **149** were run in competition in the same reaction vessel.[55] The reaction was carried out at room temperature (25°C) in CH_2Cl_2 with 2 mole % catalyst **29** (**Scheme 52**) and 30 mole % Ti(IV) co-catalyst. The reaction was followed at room temperature since earlier attempts at quantifying this difference at reflux, with 5 mole % **29**, and using GC to analyse reaction aliquots (by E. Uneyama) showed that reactions were much too rapid to follow at this temperature, although this outcome may also have been due to experimental artefact, as will be discussed in this chapter.[56]

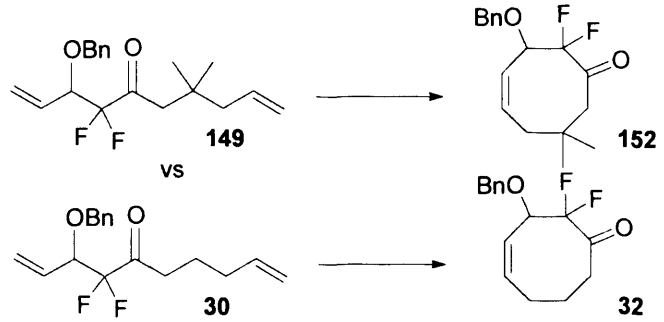

Scheme 52 RCM competition reaction between 30 and 149

Initial attempts at following the reactions did not prove successful since even with a lower catalyst loading and reaction temperature the results suggested that the cyclisation of **149** was almost complete by the time first aliquot was removed from the reaction. These results appeared unreliable and were not reproducible, as

several attempts gave differing results. **Figure 20** shows the results for **149**, which show an apparently extremely rapid cyclisation.

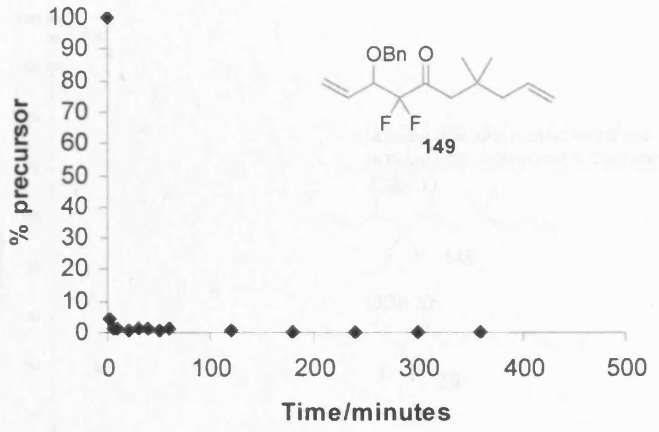

Figure 20 RCM of benzyl ether 149 with 2 mole % 29 at 25°C in CH_2Cl_2

Dienes **30** and **149** were run in competition within the same flask, in dichloromethane (0.01 M each), with 2% **29** and Ti (IV) co-catalyst. The reaction was run at 25°C in a jacketed flask connected to a water bath circulating at this temperature. A lower catalyst loading than was used for synthetic reaction was used (2% compared to 5%), and the reaction temperature was dropped to 25°C to allow the more rapid reaction to be followed more easily.

Even though all samples were diluted with wet dichloromethane, it appeared that the catalytic reaction was continuing in the GC vial, giving misleading results, and also showing a surprising tolerance of catalyst **29** for wet solvent.

To overcome this problem, a sample treatment procedure was developed, which allowed catalyst deactivation as close as possible to the time of sampling. A previous attempt to run the RCM of **31** in dry, degassed acetonitrile had recovered only unreacted starting material after overnight reflux with **29**, suggesting that the reaction cannot be run in this solvent. We also knew from the epoxidation reactions that the cyclooctenone products dissolved in this solvent. We used reverse phase (C-18) solid phase extraction tubes, pre-treated with 1 mL wet acetonitrile (20 % water), and passed each reaction aliquot through one of these tubes, eluting the sample with 1 mL acetonitrile. GC analysis yielded more encouraging results

(**Figure 22**), which were reproducible and enabled all of the kinetic studies detailed in this section.

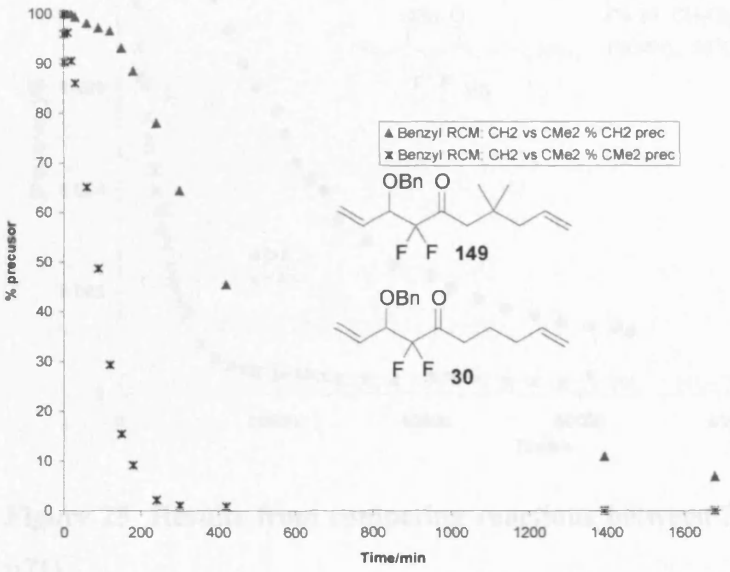

Figure 22 Initial competition reaction between benzyl ethers 30 and 149 using SPE sample treatment procedure (Section 10, p66)

The experiment was repeated, running **30** and **149** in competition, with 2% catalyst **29**, 30% Ti (IV) co-catalyst, 0.01 M in CH_2Cl_2, at 25°C. All samples were treated using the SPE methodlogy described above, and analysed by GC. Results are shown in **Figure 23**. The results show that the presence of the *gem*-dimethyl groups in the system accelerates the rate of cyclisation.

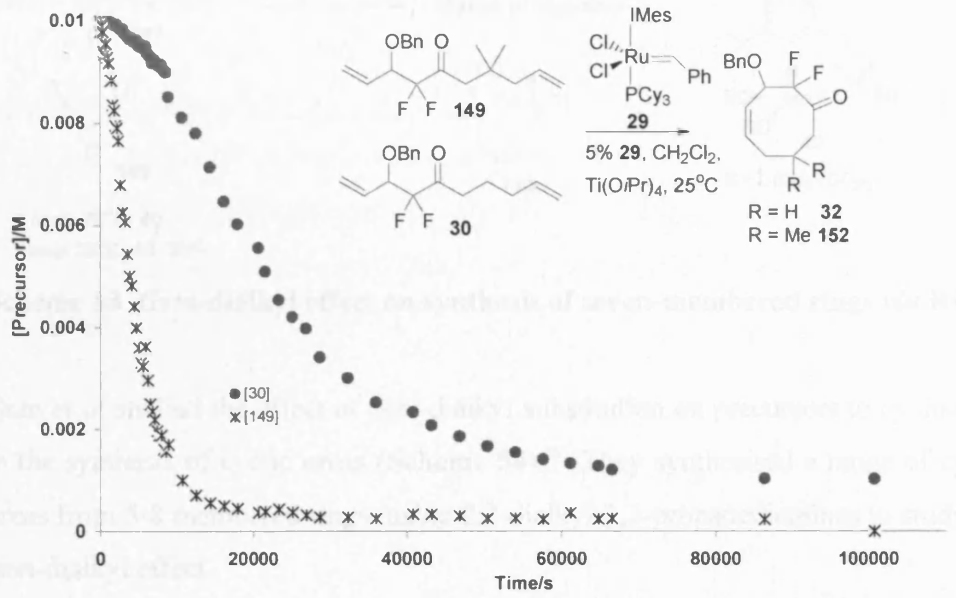

Figure 23 Results from competing reactions between 30 and 149 (Section 10, p71)

The approximate half lives of **149** and **30** are 3900 s and 21,600 s, a 5.5-fold difference. Jung studied the effect of *gem*-dialkyl groups on cyclisation and found that the typical rate increase was 5-10 fold.[57]

There are very few examples of the effect of *gem*-dialkyl substitution on medium ring synthesis, and even fewer relating to medium ring synthesis by RCM. One of the sole examples was by Forbes, in the synthesis of cyclooheptenone **108** using Schrock's molybdenum catalyst **40** (**Scheme 53**).[58] The group observed that when the cyclisation was carried out neat, diene **107** formed only oligomers, rather than cyclic product **108**, whereas diene **109** with a *gem*-dimethyl group on either side of the ketone, gave cycloheptenone **110** in 95% yield under the same conditions. The presence of the two *gem*-dimethyl groups, however, is an extremely large structural perturbation in the system and would be expected to exert a large effect on the cyclisation due to steric effects alone.

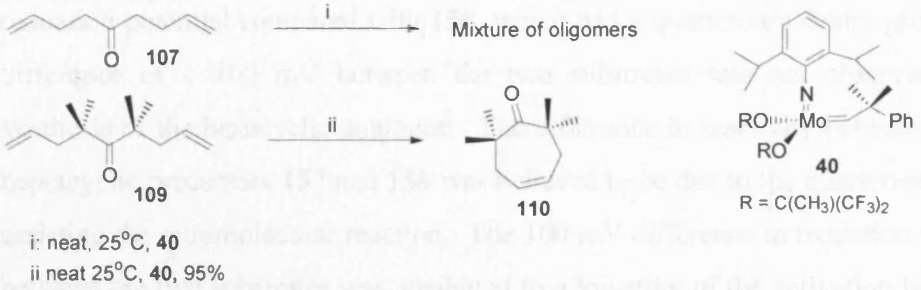

Scheme 53 *Gem*-dialkyl effect on synthesis of seven-membered rings *via* RCM

Qian *et al* studied the effect of *gem*-dialkyl substitution on precursors to cyclisation in the synthesis of cyclic ureas (**Scheme 54**).[59] They synthesised a range of cyclic ureas from 5-8 membered rings, using 2,2-dialkyl-1,3-propanediamines to study the *gem*-dialkyl effect.

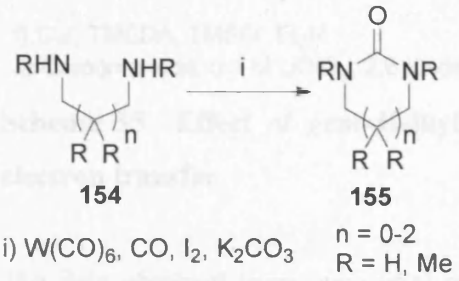

Scheme 54 Synthesis of cyclic ureas

In this case, the group observed two effects of the presence of the *gem*-dialkyl groups. The cyclisation reaction was facilitated, but the recovered yields of the 5,6 and 7-membered rings were lower than those of the unsubstituted substrates, suggesting that the *gem*-dimethyl group was causing steric hindrance around the amine groups. However, for the synthesis of the eight-membered ring, the group observed an increased in recovered yield (38%) for the dialkylated substrate, compared with only trace amounts for the non-alkylated substrated, concluding that *gem*-dialkylation is useful for eight-membered ring synthesis.

Wright observed that *gem*-dialkyl groups assisted the cyclisation of medium rings in an electron-transfer reaction, in the synthesis of small molecule inducers of nerve growth factors (**Scheme 55**).[60] In the case of the **157**, the group could not identify any traces of the desired seven-membered ring **159**, and also noted a much higher

oxidation potential compared with **158**, which had a quarternary centre group. The difference of ~ 100 mV between the two substrates was not observed in the synthesis of the hexacyclic analogue. The difference in reactivity between the two heptacyclic precursors **157** and **158** was believed to be due to the quarternary centre assisting the intramolecular reaction. The 100 mV difference in oxidation potential between the two substrates was attributed to a lowering of the activation barrier for the formation of the radical cation.

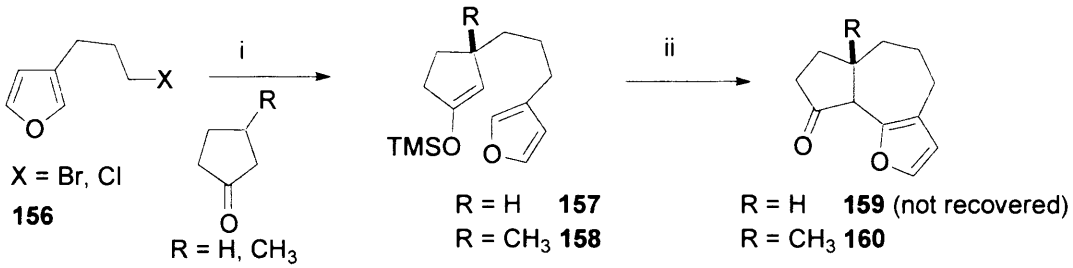

i) CuI, TMEDA, TMSCl, Et_2N
ii) Carbon anode, 0.1 M $LiClO_4$, 2,6-lutidine, CH_3CN, iPrOH

Scheme 55 Effect of *gem*-dialkyl groups on intramolecular cyclisation *via* electron transfer

The data obtained from our initial competition experiment are in agreement with these literature accounts, which all show that the presence of *gem*-dialkyl groups increases rates of cyclisation for the synthesis of medium rings. This effect appears to be much less, and sometimes even a negative one for the formation of 5 and 6-membered rings, where the rings may be too small to accommodate the perturbation in the structure, and the resulting steric hindrance.[61] However, none of these accounts are quantitative, and to our knowledge, this data is one of the only existing accounts of a quantified Thorpe-Ingold effect by RCM.

2.2.3 Analysis of *Gem*-Dialkyl Effect Data

The decay curves shown in **Figure 24** appear more complex than simple first order decay, and attempts at fitting an exponential curve to the data confirmed that the decay of the substrates was not first order.

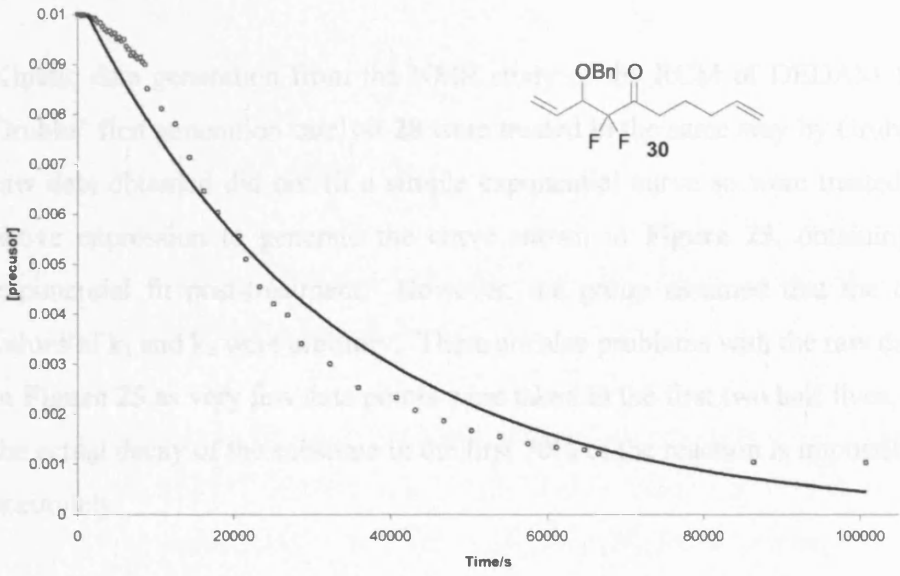

Figure 24 Exponential fit to experimental data obtained for RCM of 30

Figure 24 shows the decay curve of precursor **30**, and the best exponential fit possible. There is clearly an induction phase to the reaction, and this does not fit the exponential profile at all. This slower substrate, **30**, also fails to reach completion. This meant that the data needed to be treated with a more complex method of data analysis in order to understand the real effects of the *gem*-dimethyl group on the RCM.

The data were first treated using the assumption that two first order reactions are occurring, with the general equation:

$$A \xrightarrow{k_1} B \xrightarrow{k_2} C \qquad \textbf{Equation 3}$$

In this assumption, both reactions have separate rate constants. Data were treated using **Equation 2**, using the Solver tool in Excel to generate a simulation, using the same start and end points as obtained experimentally.

$$y = (k_1-k_2)/(k_1e^{-k_2t})-(k_2e^{-k_1t}) \qquad \textbf{Equation 2}$$

Kinetic data generation from the NMR study of the RCM of DEDAM **117** using Grubbs' first generation catalyst **28** were treated in the same way by Grubbs.[44] The raw data obtained did not fit a simple exponential curve so were treated with the above expression to generate the curve shown in **Figure 25**, obtaining a good exponential fit post-treatment. However, the group assumed that the calculated values of k_1 and k_2 were arbitrary. There are also problems with the raw data shown in **Figure 25** as very few data points were taken in the first two half lives, therefore the actual decay of the substrate in the first 70% of the reaction is impossible to plot accurately.

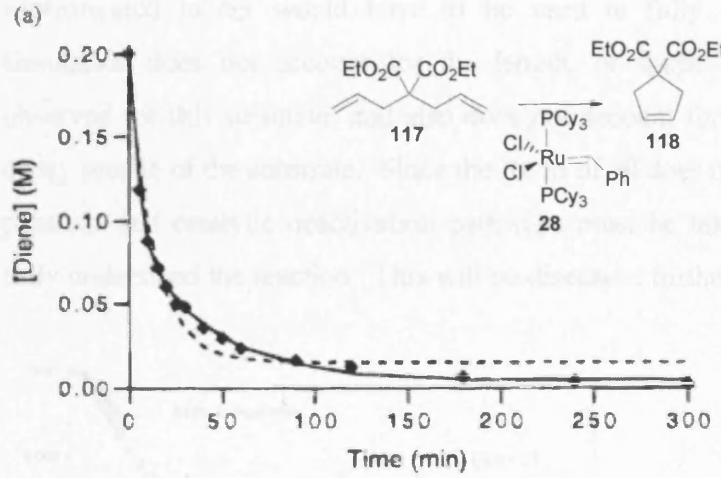

Figure 25 Grubbs' Experimental Data (filled points) and simulated data (dashed line)

First attempts at fitting the data using this expression appeared promising, as the simulation generated for **149** fit the initial 30% of the reaction well (**Figure 26**). However, the middle stages of the reaction did not give a good representation of the experimentally-obtained results, and the simulation for **30** gave an even worse fit.

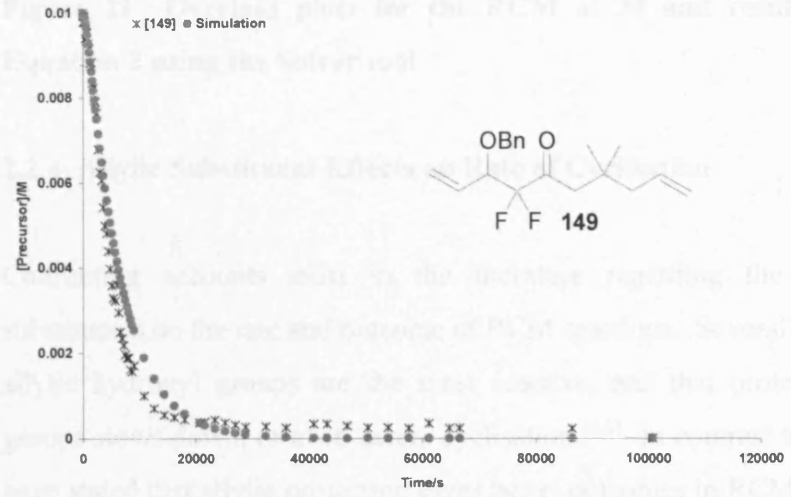

Figure 26 Overlaid plots for the RCM of 149 and results simulated with Equation 2 using the Solver tool

For slower substrate **30**, there was a large difference between the real and simulated data sets (**Figure 27**), leading us to believe that the multi-step mechanism of RCM could not be accounted for by two consecutive first order reactions, and a more sophisticated model would have to be used to fully analyse the data. The simulation does not account for the length, or shape of the induction period observed for this substrate, and also does not account for the overall shape of the decay profile of the substrate. Since the RCM of **30** does not reach completion, it is possible that catalytic deactivation pathways must be taken into consideration to truly understand the reaction. This will be discussed further in **Section 4.1.**

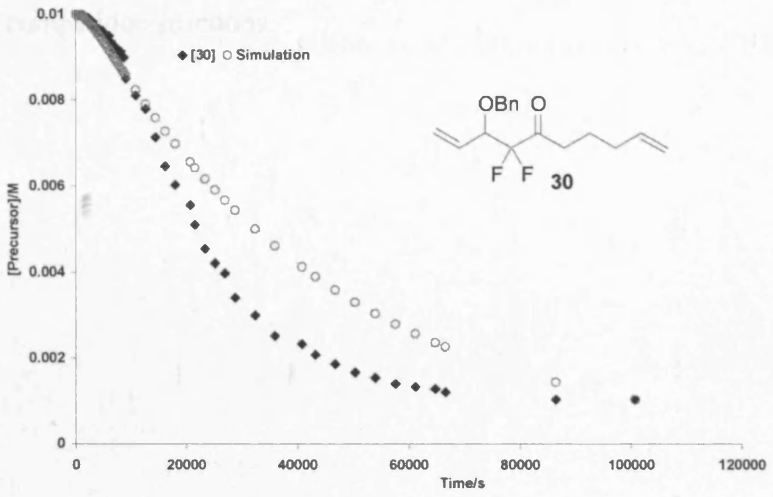

Figure 27 Overlaid plots for the RCM of 30 and results simulated with Equation 2 using the Solver tool

2.2.4 Allylic Substituent Effects on Rate of Cyclisation

Conflicting accounts exist in the literature regarding the effects of allylic substituents on the rate and outcome of RCM reactions. Several groups suggest that allylic hydroxyl groups are the most reactive, and that protecting the hydroxyl groups slows down, or even deters cyclisation.[33,34] In contrast to this, other groups have stated that allylic protection gives better outcomes in RCM reactions than free hydroxyl groups.[28] However none of these accounts is quantitative, all are qualitative, and most observations are based purely on recovered yield after a certain amount of time. This leads to some confusion for chemists hoping to use rational precursor design for RCM reactions, as it is not clear if allylic protection facilitates or hinders cyclisation. In an attempt to clarify this, we carried out competition reactions between substrates **22, 148-150**.

Initially competition reactions were carried out between one allylic protected substrate **148-150** and the free alcohol **22**, all with the *gem*-dimethyl group for a more convenient timescale for following the reaction. All competition reactions were run at 0.01 M in CH_2Cl_2 at 25°C, with mole % **29** and 30 mole % $Ti(O\textit{i}Pr)_4$. All samples were treated using the sample treatment procedure described in **2.2** to ensure catalyst deactivation. **Figures 28-30** show the results for the three competition reactions.

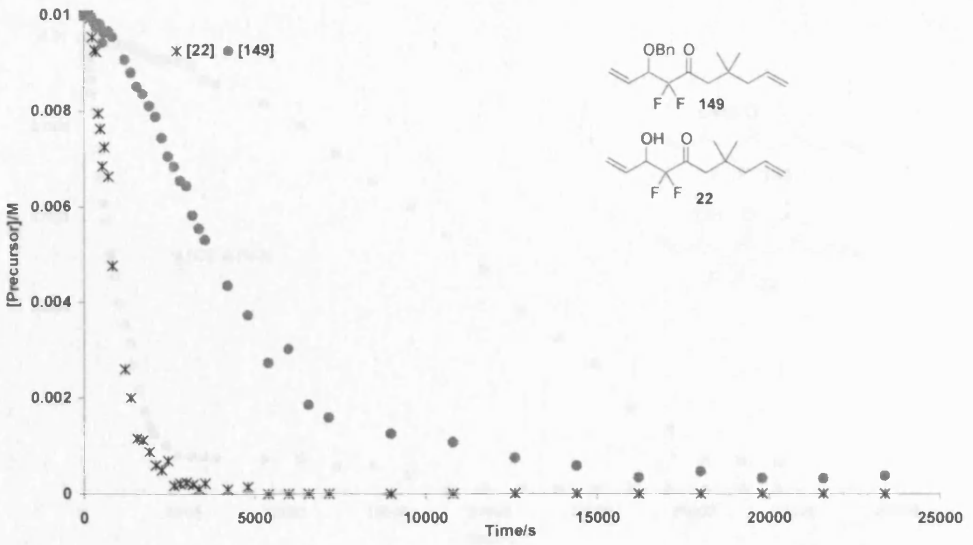

Figure 28 Competition reaction between benzyl ether 149 and alcohol 22

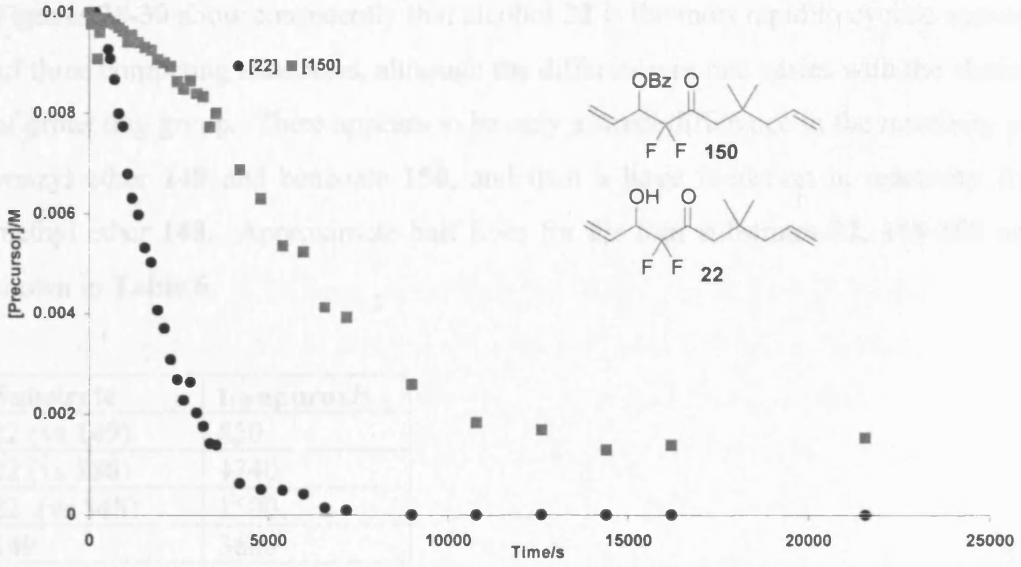

Figure 29 RCM competition reaction between benzoate 150 and alcohol 22

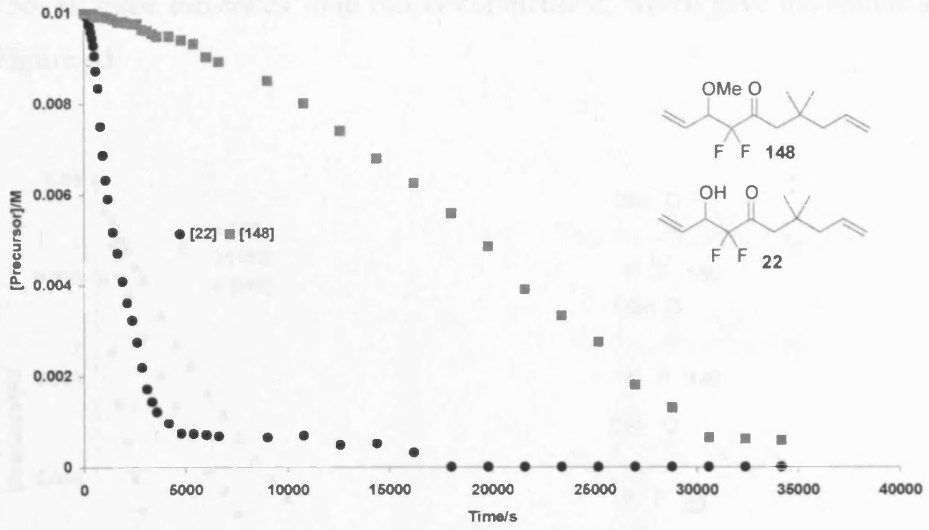

Figure 30 RCM competition reaction between methyl ether 148 and alcohol 22

Figures 28-30 show consistently that alcohol **22** is the most rapid to cyclise against all three competing substrates, although the difference in rate varies with the choice of protecting group. There appears to be only a small difference in the reactivity of benzyl ether **149** and benzoate **150**, and then a large reduction in reactivity for methyl ether **148.** Approximate half lives for the four substrates **22, 148-150** are shown in **Table 6**.

Substrate	$t_{1/2}$ approx/s
22 (vs **149**)	850
22 (vs **150**)	1740
22 (vs **148**)	1500
149	3600
150	6100
148	19300

Table 6 Table showing relative half lives for competition reaction substrates 22, 148-150

Table 6 shows a difference in cyclisation rate of 4-fold, 3.5-fold and 12.8-fold for **149**, **150** and **148** respectively. However, the differences in the half life for alcohol **22** between the three experiments were of concern. The difference was believed to be due to batch-to-batch variation in catalyst quality, so to remove this variable, and to determine the real difference in reactivity beween benzyl ether **149** and benzoate

150, all three substrates were run in competition, which gave the results shown in **Figure 31**.

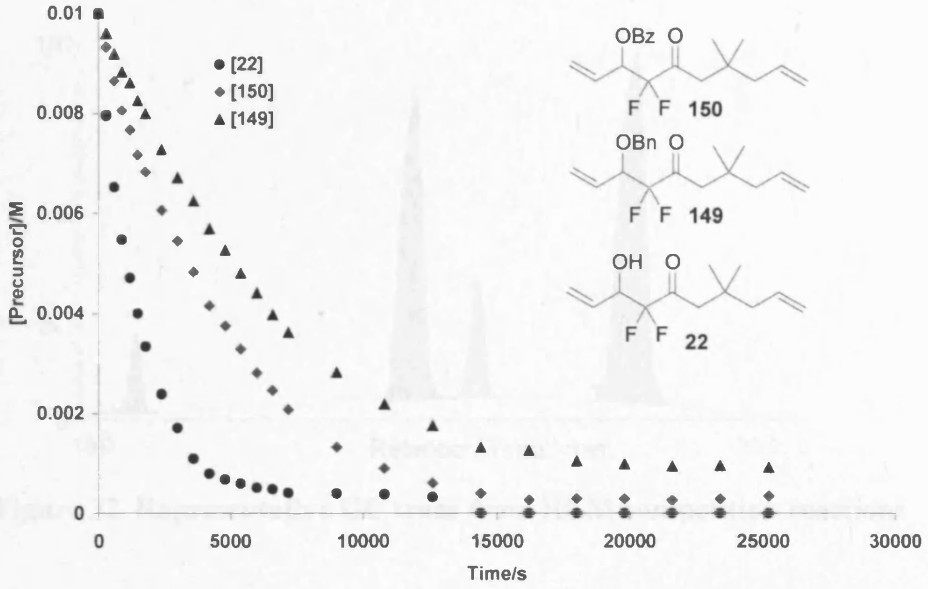

Figure 31 Three substrate RCM competition reaction between 22, 149 and 150 (Section 10, p68-69)

This results shows clearly and unambiguously that alcohol **22** cyclises more rapidly than both the benzoate **150** and benzyl ether **149**, with **149** being the slowest of the three substrates to cyclise. There is also a difference in the degree to which the precursors are consumed. Alcohol **22** is completely consumed, benzoate **150** appears very close to completion, and this is within the error limitations for the experiment, so can be assumed completed. Benzyl ether **149** does not reach completion, and consumption levels off, suggesting that even after a longer reaction time, this reaction would not complete. This appears once again to be due to the limited lifetime of the catalyst. The approximate half lives and relative reactivities are shown in **Table 7**. An example GC trace from a 2 substrate competition reaction is shown in **Figure 32**.

Substrate	Approx $t_{1/2}$/s	Relative reactivity
22	1050	1
150	3400	0.31
149	5100	0.21

Table 7 Table showing reaction half lives for three-fold competition reaction and relative reactivities

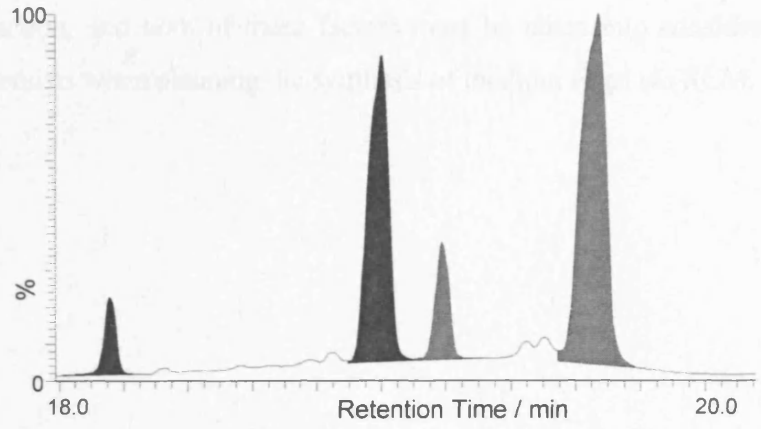

Figure 32 Representative GC trace from RCM competition reactions

Although there is a difference between the four substrates, the difference in cyclisation rates appears to be modest, with a maximum difference of 12.8-fold for the methyl ether, and from a synthetic point of view, with the CH_2 substrates, this protecting group would not be chosen, due to higher volatility of this ether over alcohol **22**, making synthesis and isolation of the corresponding eight-membered ring more difficult. The difference in half lives for benzoate **150** and benzyl ether **149** both less than 5-fold, therefore suggesting that allylic hydroxyl protection does not deter the metathesis, and only reduces the cyclisation rate modestly. The larger effect of the allylic protecting group appears to be on the efficiency of the reaction, which has much larger implications for large scale syntheses.

These results agree with literature accounts that precursors with allylic hydroxyl groups cyclise more rapidly than those with protected allylic hydroxyl groups, although the validity of these accounts is questionable since conclusions by the authors are often drawn from yields of cyclic product after a set amount of time. It is possible, especially for species protected by a methyl ether, that the reaction was not left for a sufficient period of time. In comparison with **22**, a very small amount of methyl ether **148** was turned over within the same timescale early on in the reaction.

The results from these competition reactions show that allylic protection exerts only a moderate effect on the rate of cyclisation. However, as results in **3.1** show, the effect of the allylic protection is much more significant for the efficiency of the reaction, and both of these factors must be taken into consideration by synthetic chemists when planning the synthesis of medium rings *via* RCM.

3.1 Effective Molarity and Scaleability of the RCM

In order to make the whole synthetic pathway more attractive, it was important to investigate the scaleability of the RCM and find a maximum concentration at which high yielding reactions could be carried out. A synthetic concentration of 0.01 M or higher would be minimal for scale up; at lower concentrations, the large volumes of solvent required become prohibitive for normal laboratory reaction vessels.

We synthesised three RCM precursors **4**, **30**, and **31** (**Scheme 56**), as well as **150** with a *gem*-dimethyl group (see **2.2.1**).[1,2] The first precursor **4** had an unprotected allylic hydroxyl group, but this compound cyclised to a volatile eight-membered ring product which was difficult to isolate. Protection of the free OH group in either benzoate ester **31** or benzyl ether **30** resulted in the formation of crystalline (and therefore more easily isolable) cyclooctenone products (**Scheme 56**). It was observed that the syntheses of eight-membered rings **3**, **32** and **33** could be carried out at different maximum concentrations before other products started to be visible in the ^{19}F NMR spectra of reaction products. Benzoate **33** could be synthesised cleanly at a substrate concentration of 20 mM, whereas ether **32** and alcohol **3** could only be cyclised cleanly at 2.5 mM and 1 mM respectively. We therefore investigated the effects of concentration on the RCMs of substrates **4**, **30** and **31** in order to identify the upper concentration limits of these reactions.

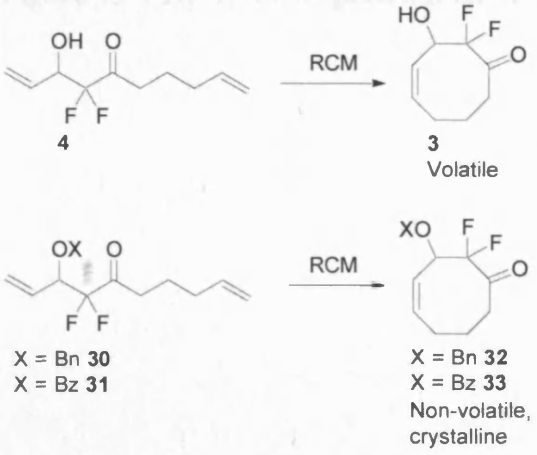

Scheme 56

The RCM of benzoate **31** was carried out varying the concentration from 20 mM to 200 mM in refluxing CH_2Cl_2 containing 5% Grubbs' second generation catalyst **29** and a titanium(IV) co-catalyst. At concentrations greater than 40 mM, other products became visible in the ^{19}F NMR spectra. The presence of the *gem*-difluoro group in the molecule allowed us to exploit the enhanced chemical shift range observed in ^{19}F NMR Spectra (at 376 MHz) by integrating discrete signals of new products forming at higher concentrations. $\{^1H\}^{19}F$ spectra were recorded to enhance the signal-to-noise ration. ^{19}F-^{19}F COSY spectra were also run on some samples, and used in conjunction with $^2J_{F\text{-}F}$ coupling constants to determine which sets of signals arose from the same cross metathesis (CM) products (**Figure 33**).

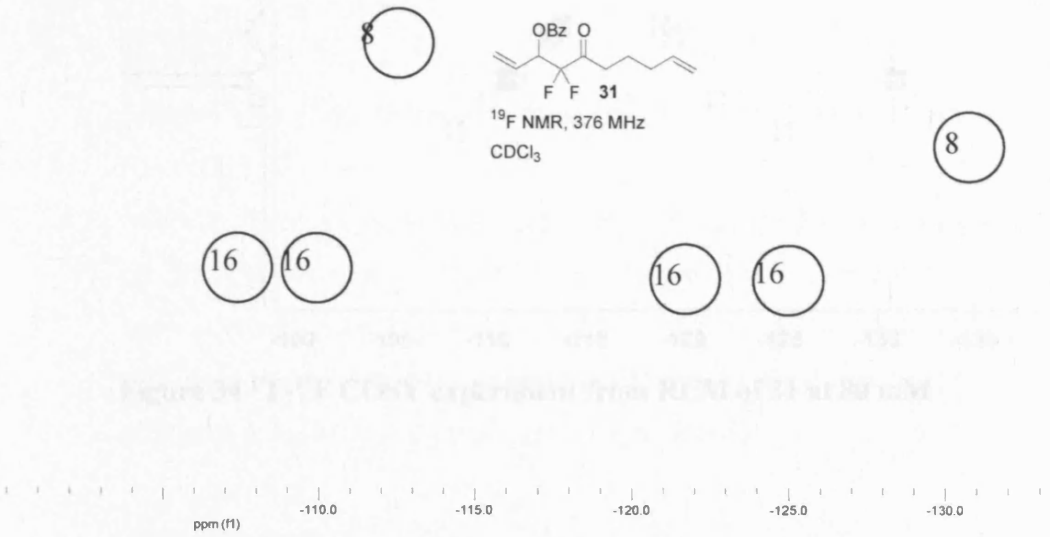

Figure 33 $\{^1H\}^{19}F$ NMR spectrum for RCM of 31 at 0.06 M

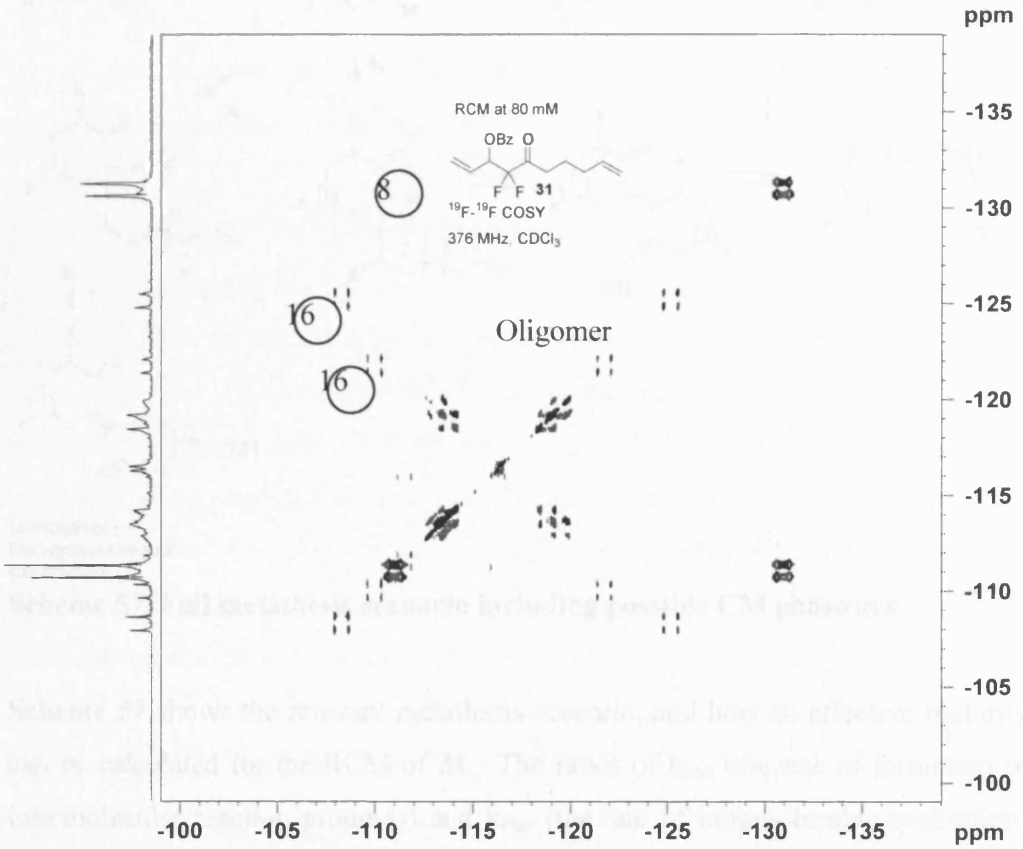

Figure 34 ^{19}F-^{19}F COSY experiment from RCM of 31 at 80 mM

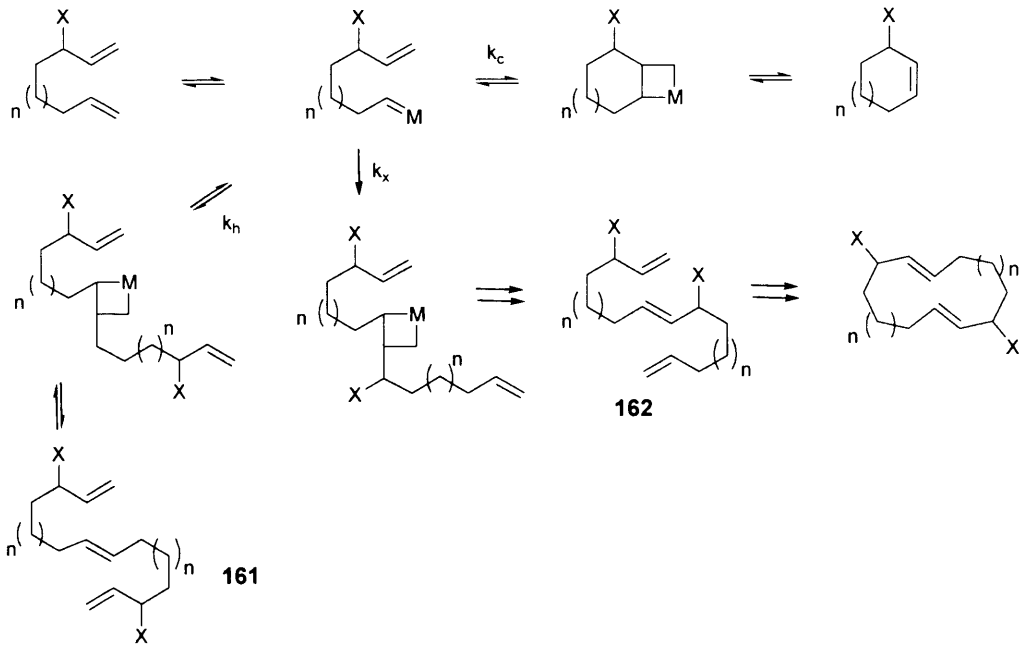

Scheme 57 Full metathesis scenario including possible CM pathways

Scheme 57 shows the relevant metathesis scenario, and how an effective molarity can be calculated for the RCM of **31**. The ratios of k_{inter} (the rate of formation of intermolecular reaction products) and k_{intra} (the rate of intramolecular cyclisation) give an effective molarity for this reaction and an indication of the cyclisation efficiency relative to cross metathesis (**Equation 4**).

$$\frac{\text{Mole fraction Intra}}{\text{Mole fraction Inter}} = \frac{k_{intra}}{k_{inter}} \times \frac{[B]}{[S][B]} = EM \times \frac{1}{[S]}$$

Equation 4

The desired pathway results in formation of the eight-membered ring, but at higher substrate concentrations, cross metathesis becomes a more competitive route. In the non-productive pathway, two type I double bonds are joined together, resulting in homodimer **161**. This pathway is considered likely to be fast and reversible because type I homodimers are formed rapidly and reversibly.[x] The productive cross metathesis pathway involves the formation of heterodimer **162**, where a type I and type II double bond are joined together, leaving a type I and type II double bond which can react further to form oligomers or cyclise to give a 16-membered ring via subsequent initiation on the Type I alkene terminus. Acyclic dimers and

larger species can also backbite to form the eight-membered ring product, although at higher concentrations this seems unlikely.[21] At higher concentrations it is also possible that the cyclooctenone **33** can ring open to form oligomeric products, though this depends on the rate of reaction between **33** and the active catalyst present in the reaction. This is discussed later in this chapter.

Effective molarities (EMs) are used to measure the efficiency of an intramolecular reaction. The rate of cyclisation is compared with competing intermolecular reactions. EMs are usually calculated from accurate k_{intra} rate constants, and the rate constant for the closest equivalent intermolecular process, under conditions which are as similar as possible. EMs have been calculated from product ratios in a few important cases, especially the study of macrocyclisation reactions published by Mandolini.[7,62] When the effective molarity for a reaction is low, competition between intra and intermolecular reactions of the same compound can be observed relatively easily, even at low concentration.

To determine if any of the peaks in the NMRs were not properly resolved due to inadequate relaxation time, T_1 values for all peaks identified in the spectra were determined and are shown in **Table 8**. This was an important analysis to carry out since there are many species of varying size in the mixtures at higher concentrations and these may be expected to have different relaxation times in NMR. More reliable spectra were then recorded using a delay time D_1 equal to 5 x T_1. This allow for complete relaxation of all species present in the product mixture on the timescale of the NMR experiment.

All $\{^1H\}^{19}F$ NMR spectra were re-recorded, setting D_1 = 5 seconds, since the slowest species to relax had a T_1 = 1 s. The species with the longest relaxation time was actually the smallest one, eight-membered ring **33**, rather than any larger products formed as a result of cross metathesis. The overall range of T_1's is modest.

Entry	Peak (ppm)	T_1/ms
1	-108.9	382.2
2	-109.9	464.9
3	-111.0	929.1
4	-111.3	950.1
5	-117.5	590.8
6	-118.5	547.0
7	-121.7	446.5
8	-125.0	435.0
9	-130.9	1080.0
10	-131.1	1110.01

Table 8 Determined T_1 Values for all species present in the $\{^1H\}^{19}F$ NMR Spectrum for RCM of 31 at 0.08 M

The integrations of the mole fractions of cyclooctenone and CM products were plotted against concentration (**Figure 35**). At higher concentrations we identified two main products increasing at the same rate as each other, as well as other products, assumed to be oligomers. The spectra run with $D_1 = 5$ were also integrated and results plotted alongside those with the default value of T_1.

The total integral was measured, and the mole fraction of eight-membered ring **33** calculated (**Section 10, p1**). It was assumed initially that everything else was oligomer, the mole fraction for which could not be accurately calculated because the number of nuclei was not known. Further analysis revealed that two sets of discrete peaks in the $\{^1H\}^{19}F$ NMR spectrum were due to two 16-membered rings. Since the integral is proportional to the number of nuclei present, this was taken into account for all EM calculations where 16-membered rings were present.

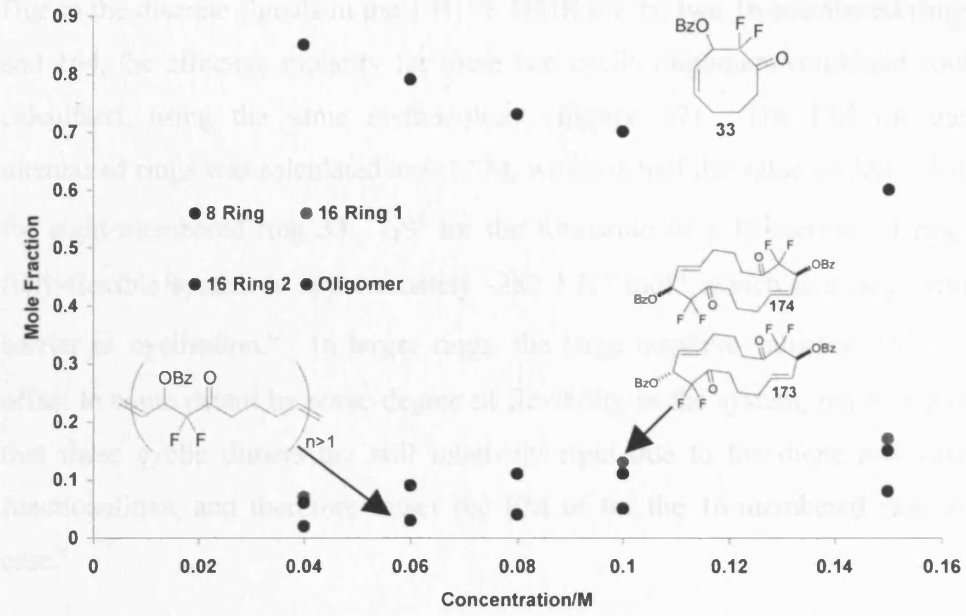

Figure 35 The effect of concentration of benzoate 31 on product formation by RCM

A plot of 1/[S] *vs* mole fraction cyclooctene/total intermolecular products fitted a straight line well (R^2 0.9981) (**Figure 36**). Based on the previous argument, the gradient of the plot is the effective molarity for the reaction and this gives an indication of the efficiency of the intramolecular reaction compared with the intermolecular reaction. **Figure 36** shows the EM for the cyclisation of **31** was calculated to be 0.23 M.

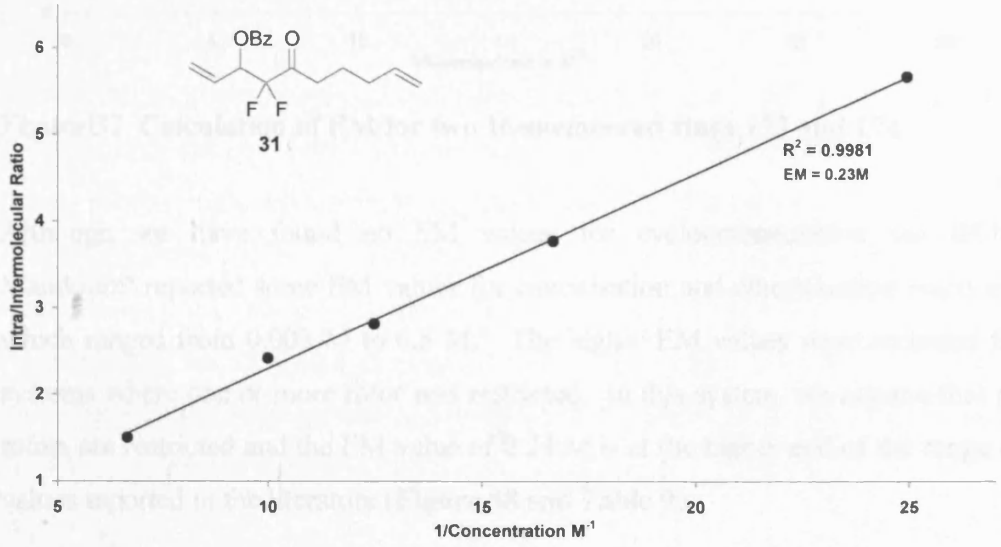

Figure 36 Effective Molarity for RCM of 31 (benzoate)

Due to the discrete signals in the $\{^1H\}^{19}F$ NMR for the two 16-membered rings **163** and **164**, the effective molarity for these two cyclic oligomers combined could be calculated, using the same methodology (**Figure 37**). The EM for the 16-membered rings was calculated as 0.12 M, which is half the value of that calculated for eight-membered ring **33**. $\Delta S^{\ddagger}$ for the formation of a 16-membered ring in a fully-flexible system is approximately -282 J K^{-1} mol^{-1}, which is a large entropic barrier to cyclisation.[62] In larger rings, the large negative value of $\Delta S^{\ddagger}$ is often offset to some extent by some degree of flexibility in the system, but it is possible that these cyclic dimers are still relatively rigid due to the diene and diketone functionalities, and therefore lower the EM of for the 16-membered ring in this case.[x]

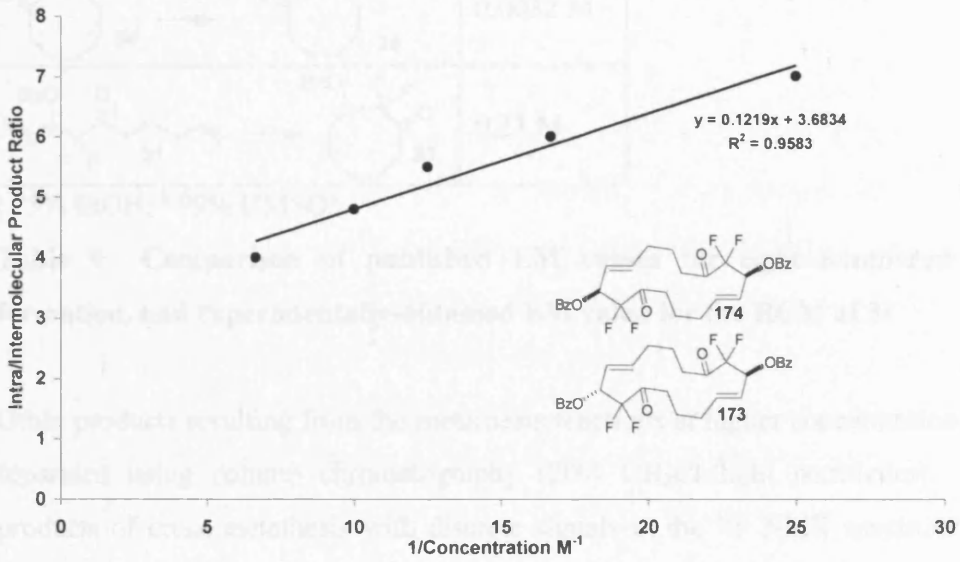

Figure 37 Calculation of EM for two 16-membered rings 173 and 174

Although we have found no EM values for cyclooctannulation *via* RCM, Mandolini[x] reported some EM values for lactonisation and etherification reactions, which ranged from 0.003 M to 0.5 M.[8] The higher EM values were recorded for systems where one or more rotor was restricted. In this system, we assume that no rotors are restricted and the EM value of 0.24 M is at the higher end of the range of values reported in the literature (**Figure 58** and **Table 9**).

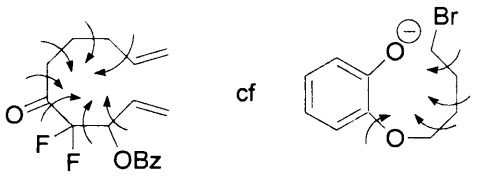

No rotors restricted,
EM 0.23 M

1 rotor restricted
EM 0.1 - 0.5 M (solvent dependent)

Figure 58

Cyclisation Reaction	EM/M
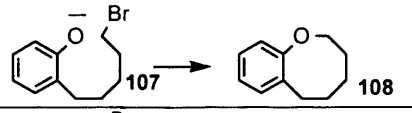	0.1 M
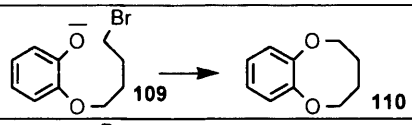	0.5 M[a] 0.1 M[b]
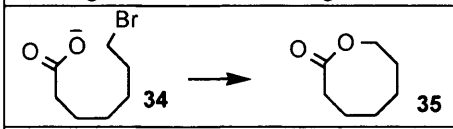	0.0032 M
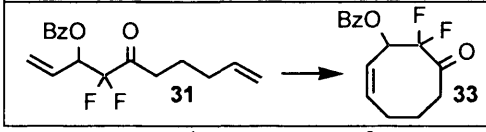	0.23 M

[a] 75% EtOH; [b] 99% DMSO[8]

Table 9 Comparison of published EM values for eight-membered ring formation, and experimentally-obtained EM value for the RCM of 31

Other products resulting from the metathesis reactions at higher concentration were separated using column chromatography (20% CH_2Cl_2/light petroleum). Two products of cross metathesis with discrete signals in the ^{19}F NMR spectrum were present in relatively large concentrations, along with acyclic oligomers. The products with discrete signals were isolated in small amounts and were identified as 16-membered rings, and the structures determined by X-ray crystallography. None of the oligomeric products could be isolated cleanly as discrete compounds, but their presence was assumed on the basis of their similar chemical shifts in the ^{19}F NMR spectra, which appear to show an increasingly wide distribution of products with increasing diene concentration, revealed by the presence of broad signals in the ^{19}F NMR spectra.

However, some smaller oligomeric products could be separated from the larger cyclic products as mixtures, using C_{18} solid phase extraction (SPE) tubes. Eluted fractions were analysed by ES-MS and gave some insight into the range of products and the size limits of the cross metathesis reactions under these conditions. Results are given in **Table 10**.

Elution Conditions	**Ions in ES-MS**
1 mL CH_2Cl_2	[8 ring + Na]$^+$, [16 ring + Na]$^+$, [24 ring + Na]$^+$, [32 ring + Na]$^+$
1 mL 1% MeOH/CH_2Cl_2	[Dimer + Na]$^+$, [Trimer + Na]$^+$, [Tetramer + Na]$^+$, [Pentamer + Na]$^+$
1 mL 10% MeOH/CH_2Cl_2	[Dimer + Na]$^+$, [Trimer + Na]$^+$, [Tetramer + Na]$^+$, [Pentamer + Na]$^+$

Table 10 Conditions for solid phase extraction separation of products formed in the RCM of 31 at 0.1 M

ES-MS of the cyclic product mixture revealed the presence of 8 up to 32-membered rings for benzoate **31**, and ES-MS of the acyclic product mixture revealed ions corresponding to dimers up to pentamers. No larger ions were observed using ES-MS, so the sample analyses were attempted by MALDI. Limited characterisation of acyclic oligomers was carried out by Fogg using MALDI, from a pyrene matrix.[21] However, we were unable to identify any ion corresponding to oligomeric series in the MALDI, despite the use of a range of acidic, basic and neutral matrices (**Table 11**), although a very limited series was visible when using anthrecenetriol as a matrix.

Matrix	Ion Mode	Visible Ion(s)
Anthrecenetriol[a]	Positive	24-ring, Trimer
Anthracenetriol[a]	Negative	16 ring, Dimer, 24-ring, Trimer
2-Aminohydroxypyridine[a]	Positive	-
2-Aminohydroxypyridine[a]	Negative	-
α-Cyano-4-hydroxycinnamic acid[a]	Positive	-
α-Cyano-4-hydroxycinnamic acid[a]	Negative	-
3,5-Dimethoxy-4-hydroycinnamic acid (Sinapinic acid)[b]	Positive	-
3,5-Dimethoxy-4-hydroycinnamic acid (Sinapinic acid)[b]	Negative	-
Pyrene[c]	Positive	-
Pyrene[c]	Negative	-

[a] Prepared 10 mg/mL CH_3CN/water, 0.1% TFA; [b] Prepared 20 mg/mL CH_3CN/water, 0.1% TFA; [c] Prepared 10 mg/mL CH_3CN/water.

Table 11 MALDI matrices used for analysis of samples from RCMs of 31 at high concentration

The oligomer mixture eluted with 10% MeOH/CH_2Cl_2 was separated by reverse phase HPLC using a C-18 column and a THF/water mobile phase with a solvent gradient (65% THF/water to 85% THF/water over 35 minutes). The best separation obtained did not give a good baseline, but suggested that an oligomeric series was present in the mixture. Each peak had a small peak at its shoulder, which suggested there may be more than one stereoisomer (**Figure 38, Section 10, p4**).

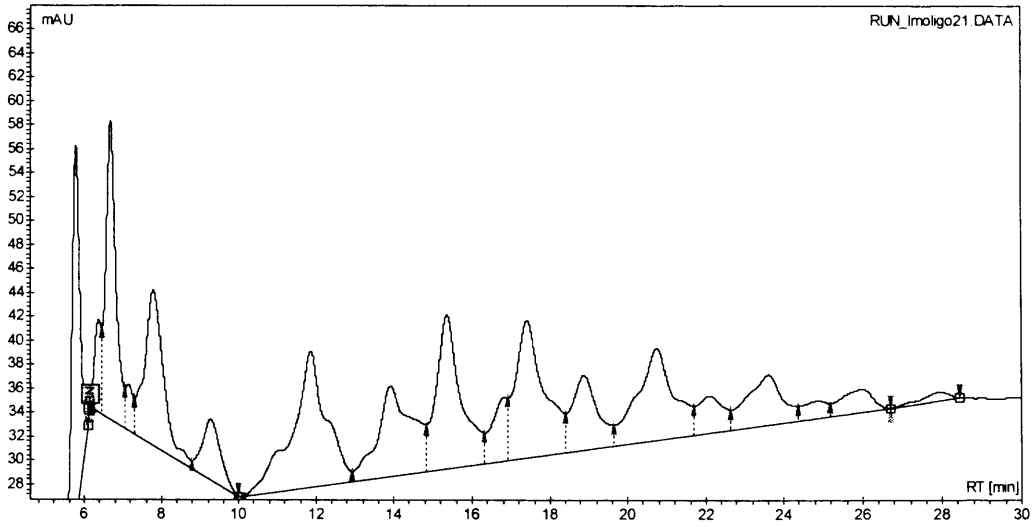

Figure 38 Reverse-phase HPLC trace for RCM of 31 at 0.08 M using a THF/water mobile phase

The same mixture was analysed using size exclusion methods (GPC) in THF. However, the results were inconclusive, and this was believed to be due to the presence of either the two stereoisomers of the oligomers, or of the presence of cyclic oligomers, which appeared to distort the results. The results appeared to show oligomers with mass of around 10^5-10^6. Although not completely unfeasible, reactions were carried out at relatively low concentration which would disfavour the formation of extremely large oligomers/polymers, and the size exclusion did not identify any oligomers of lower mass, as identified by mass spectrometry, which suggests that the product mixture cannot be successfully analysed in this way.

To our knowledge, currently only one study reports the products of cross metathesis during eight-membered ring formation. Creighton synthesised eight-membered cyclic peptidomimetic **166** *via* RCM with Grubbs' first generation catalyst **28** (**Scheme 59**), at a reaction concentration of 3 mM in CH_2Cl_2.[63] They carried out a limited concentration study varying the concentration between 12 mM and 100 mM. At 12 mM with first generation Grubbs' catalyst, uncyclised dimer **165** was indentified. With Grubbs' first generation catalyst **28** at 100 mM, uncyclised dimer was not the major product. Instead, 16-membered ring **168** was identified as the major product. However, the study did not examine enough sets of conditions to calculate an EM value for the reaction, and cross-metathesis products were identified solely from the electrospray mass spectra which cannot distinguish between homo and heterodimers.

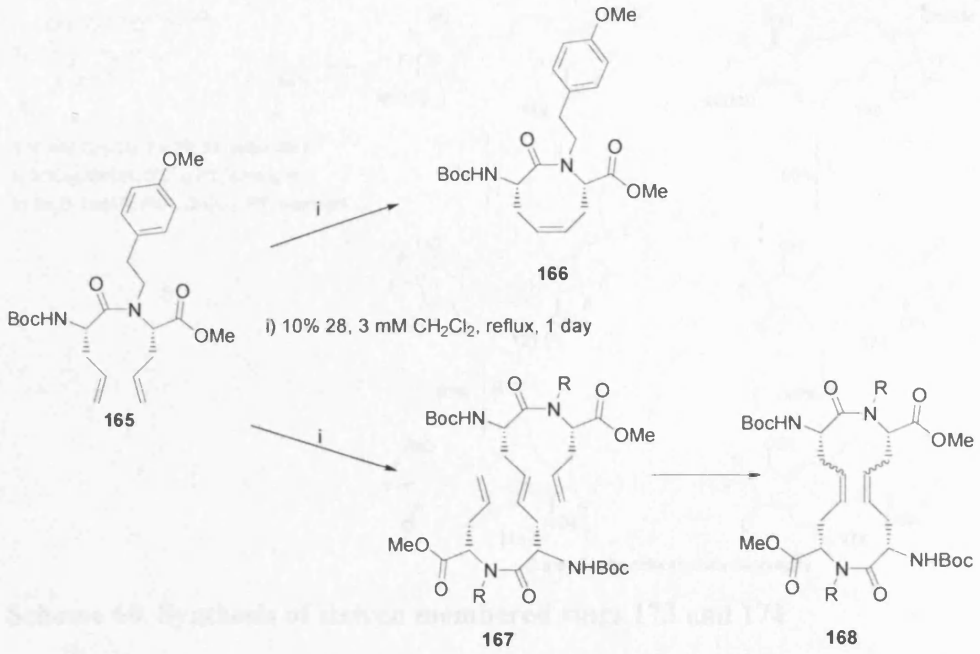

Scheme 59 Synthesis of cyclic peptidomimetic 166 by RCM

Two diastereoisomeric cyclic heterodimers **169** and **170** were synthesised on a larger scale by carrying out a dimerisation/RCM on the [2,3]-Wittig product **5**, adding 10% Grubbs' second generation catalyst **29** in two portions and refluxing over two nights. The products **169** and **170** were separated and used to synthesise benzoates **173** and **174**. The MEM groups could be cleaved off to yield the two 16-membered ring dione diols **171** and **172**, using the usual acidic conditions. Finally, the diols were benzoylated using benzoic anhydride and PVP in CH_2Cl_2 to yield two products **173** and **174** which had ^{19}F NMR chemical shifts identical to those of the two products appearing in the high concentration RCM reactions (**Scheme 60**).

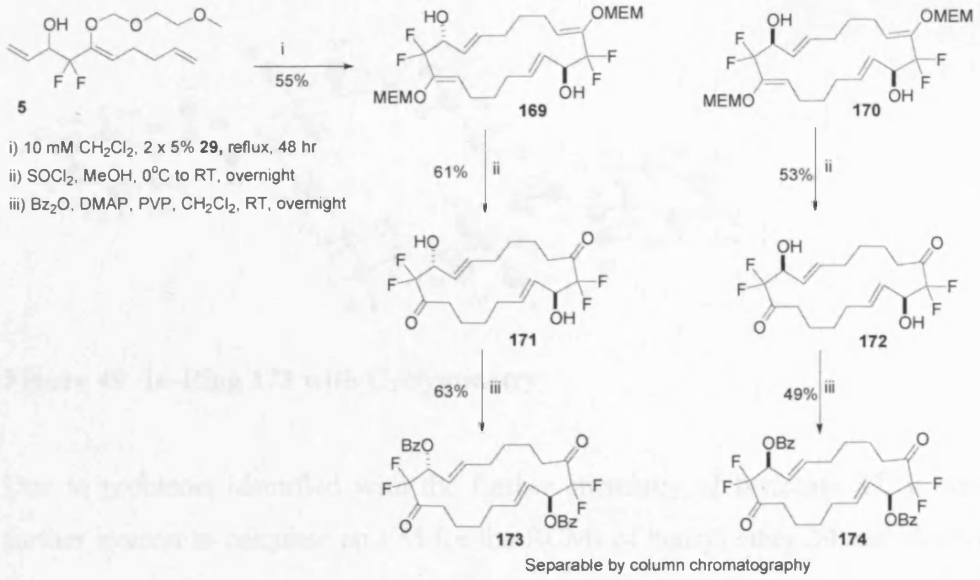

Scheme 60 Synthesis of sixteen membered rings 173 and 174

The two 16-membered rings both had distinctly different ^{19}F NMR spectra and could be separated from each other by column chromatography once benzoylated. Their diketone structures were proved by ^{13}C NMR which revealed peaks in the region characteristic of ketones (200.0 and 199.9), and by X-ray diffraction.

The two dibenzoylated 16-membered rings were separated by flash column chromatography (80% ethyl acetate/hexane) and both products were crystalline. One 16-membered ring had a centre of inversion (or was achiral and *meso*), while the other had C_2 symmetry (**Figures 39** and **40**).

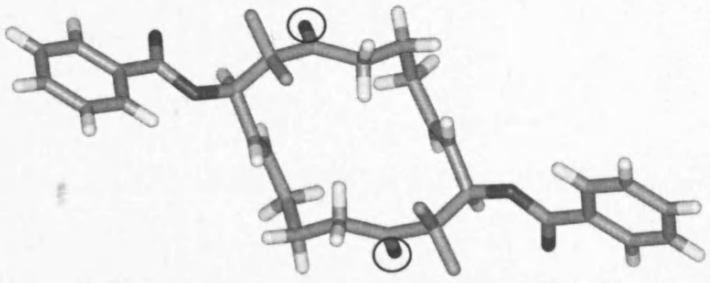

Figure 39 16-Ring 174 with a Centre of Inversion (NB purple atoms (circled) are deuterium atoms)

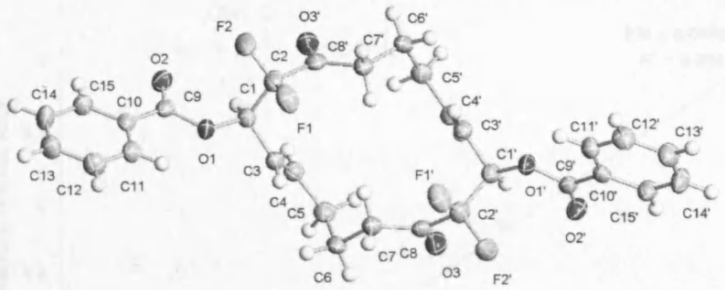

Figure 40 16-Ring 173 with C_2 Symmetry

Due to problems identified with the further chemistry of benzoate **33**, it was of further interest to calculate an EM for the RCMs of benzyl ether **30** and alcohol **4**. Reactions of both substrates formed oligomer at lower concentration so a lower EM was expected for both substrates. The RCMs of **30** and **4** were measured in CH_2Cl_2 in Carousel tubes, varying the substrate concentration between 2 mM and 12 mM for **4,** and 5 mM and 80 mM for **30**, using 5% catalyst **29** and 30% titanium co-catalyst. In the case of alcohol **4,** different methods of sample concentration were used to ensure that the calculation of the EM was accurate for this substrate. The solvent from some samples was carefully distilled off at reduced pressure, some samples were concentrated slowly by allowing the solvent to evaporate at atmospheric pressure, and reactions carried out at higher concentrations were analysed directly by $\{^1H\}^{19}F$ NMR. The resulting $\{^1H\}^{19}F$ NMR spectra were integrated in order to determine the ratio of cyclooctene and cross metathesis products. The results revealed a large difference in EM values between the three substrates (**Figures 41** and **42**).

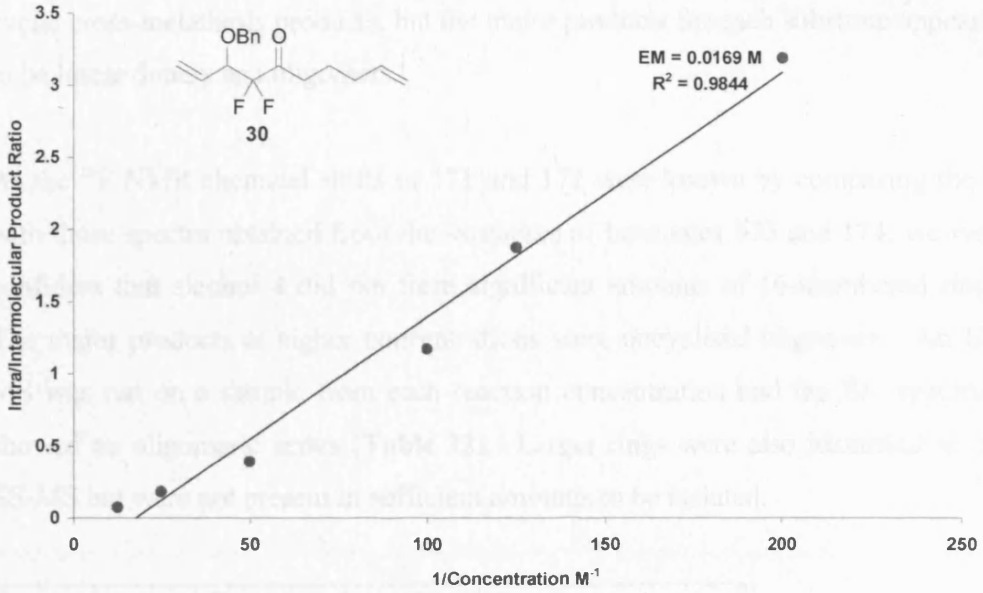

Figure 41 Effective Molarity determination for benzyl ether 30 (Section 10, p94)

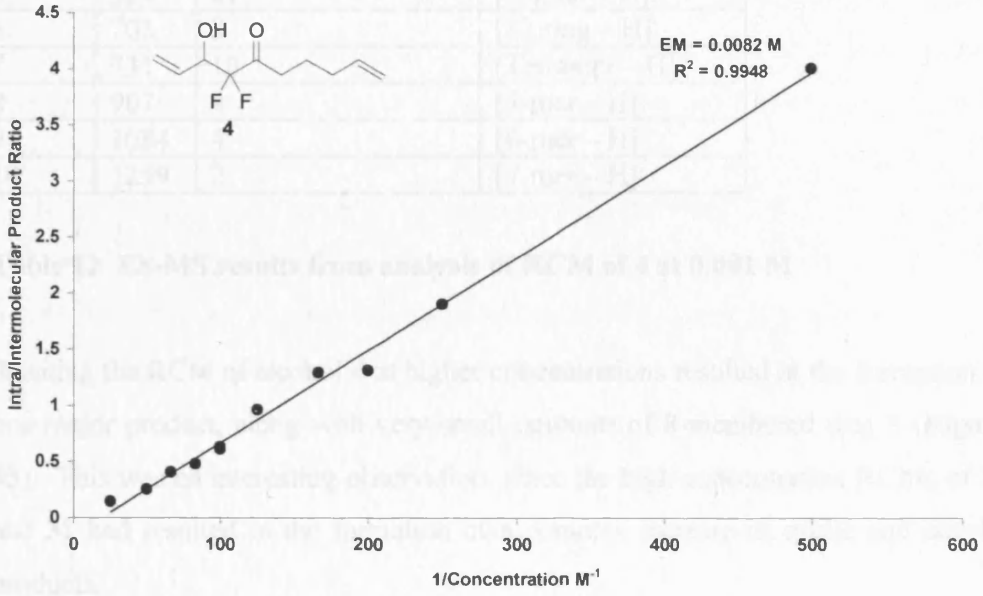

Figure 42 Effective Molarity determination for alcohol 4 (Section 10, p92)

These results show a 30-fold difference in EM between alcohol **4** and benzoate **31**. The large difference in EM is consistent with the observed difference in scaleability of the RCM and the efficiency of the cyclisation. However, the EMs for **4** and **30** differ only by a factor of two. In these cases we did not identify or isolate any

cyclic cross-metathesis products, but the major products for each substrate appeared to be linear dimers and oligomers.

As the ^{19}F NMR chemical shifts of **171** and **172** were known by comparing the δ_F with those spectra obtained from the syntheses of benzoates **173** and **174**, we were confident that alcohol **4** did not form significant amounts of 16-membered rings. The major products at higher concentrations were uncyclised oligomers. An ES-MS was run on a sample from each reaction concentration and the ES^- spectrum showed an oligomeric series (**Table 12**). Larger rings were also identified in the ES-MS but were not present in sufficient amounts to be isolated.

Entry	*m/z*	Rel Abundance %	Species
1	176	45	[8 ring – H]$^-$
2	351	23	[16 ring - H]$^-$
3	379	18	[Dimer – H]$^-$
4	527	100	[24 ring – H]$^-$
5	555	21	[Trimer – H]$^-$
6	703	8	[32 ring – H]$^-$
7	731	10	[Tetramer – H]$^-$
8	907	4	[5-mer – H]$^-$
9	1084	4	[6-mer – H]$^-$
10	1259	2	[7-mer – H]$^-$

Table 12 ES-MS results from analysis of RCM of 4 at 0.001 M

Running the RCM of alcohol **4** at higher concentrations resulted in the formation of one major product, along with very small amounts of 8-membered ring **3** (**Figure 43**). This was an interesting observation, since the high concentration RCMs of **30** and **31** had resulted in the formation of a complex mixture of cyclic and acyclic products.

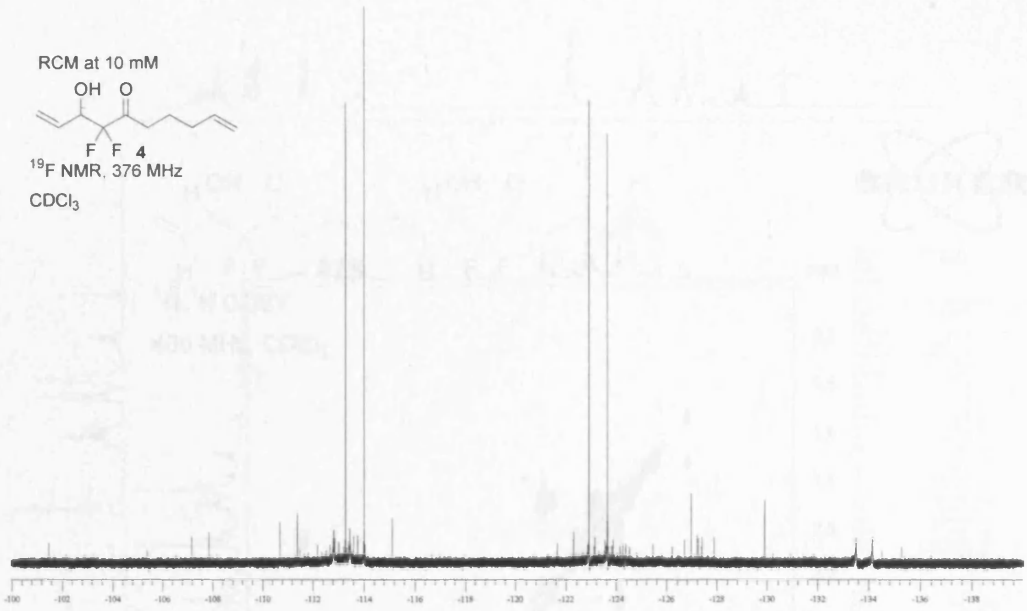

Figure 43 ^{19}F NMR after RCM of 4 at 10 mM

Figure 43 shows the $\{^1H\}^{19}F$ NMR spectrum of a product mixture obtained from the exposure of alcohol **4** to Grubbs' II **29** at 10 mM. The major product gives peaks at -113.8 and -123.4 ppm, these occur close to those observed for the acyclic monomer, suggesting that this is an acyclic oligomer. At higher concentrations, less variation in acyclic products was observed. ^1H NMR analysis suggested that the major product was acyclic **175**, which has two different CHOH protons, along with eight alkene environments. Forward projections and simulations were run on the ^1H-^1H COSY for the dimer (**Figures 44** and **45)** and revealed two stereoisomers. Evidence for this was supported by reverse phase HPLC (THF/water) which revealed two products in the mixture, one major and one minor, with similar retention times (**Figure 46**).

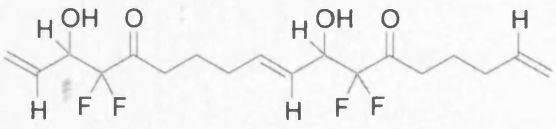

175

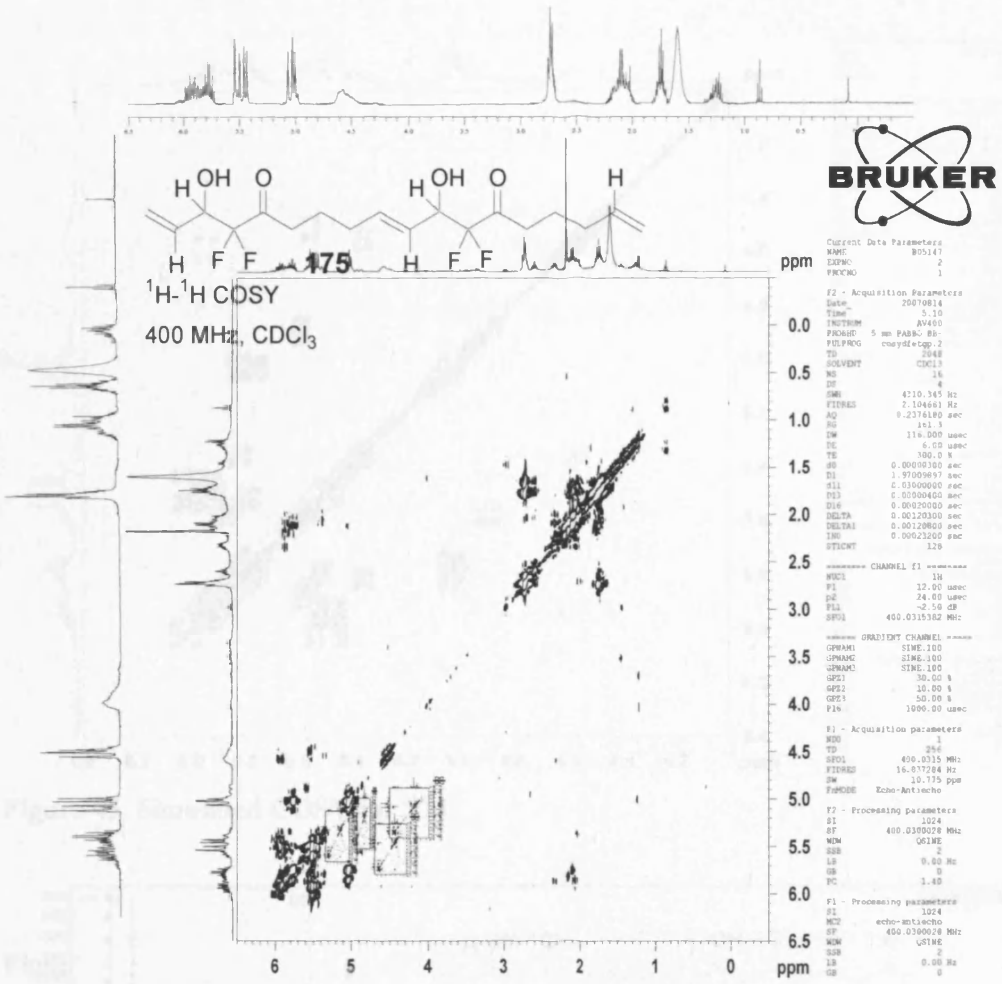

Figure 44 ^{1}H-^{1}H COSY of 175

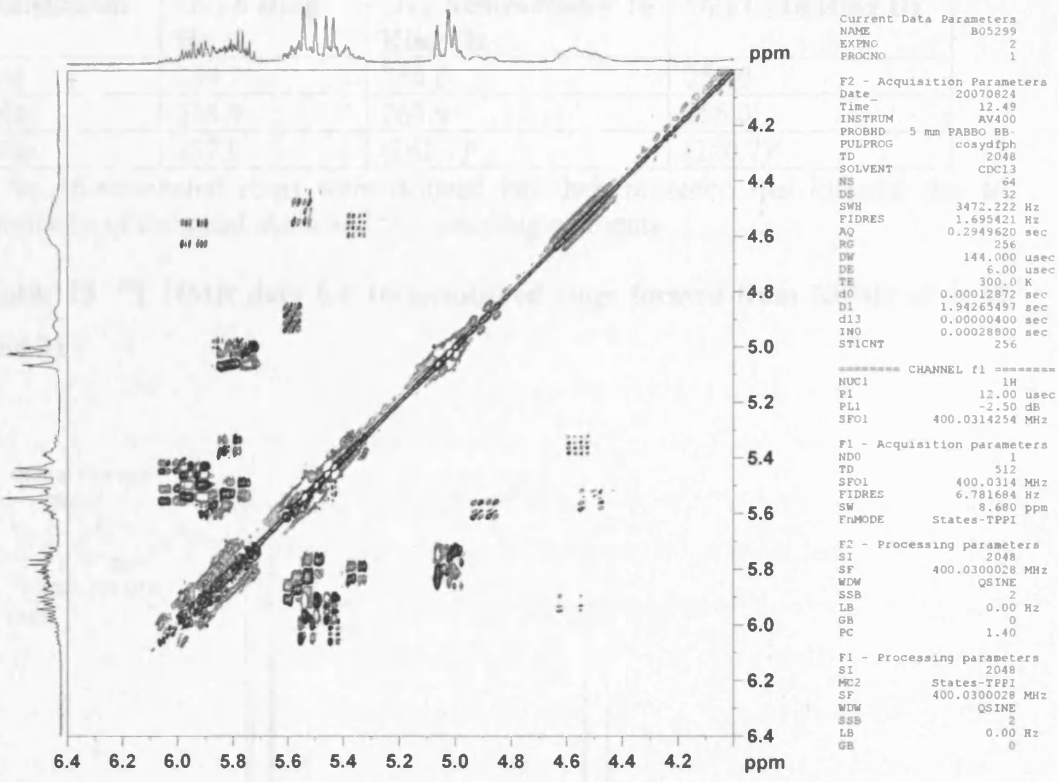

Figure 45 Simulated COSY for 175

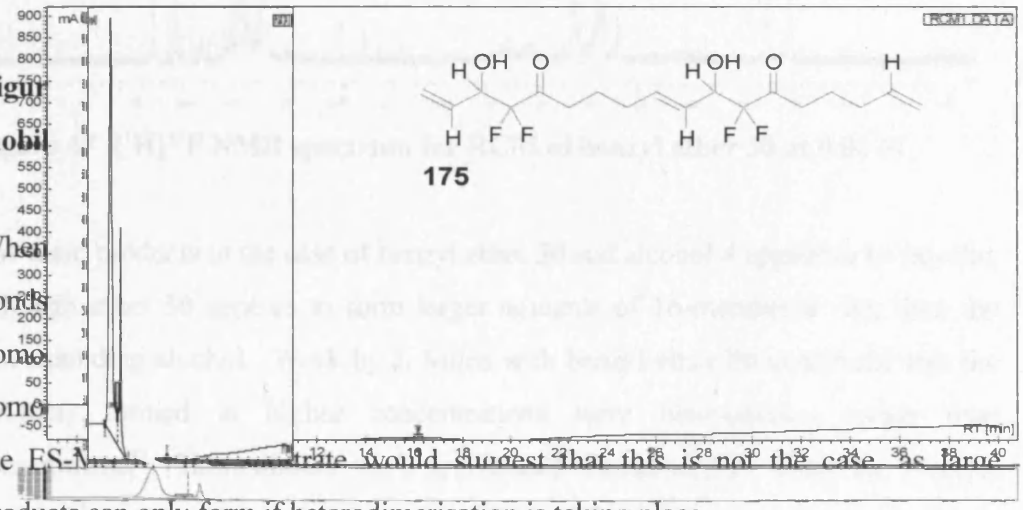

Figur
mobil

When
bonds
homo
home
the ES-M
products can only form if heterodimerisation is taking place.

Ether **30** formed small amounts of 16-membered rings, with similar chemical shifts to those of benzoates **173** and **174** but these were not isolated. **Table 13** shows a table of $^{2}J_{F\text{-}F}$ values for the 16-membered rings for all three substrates **4**, **30** and **31.** The ^{19}F NMR of the product mixture from **30** at 20 mM is shown in **Figure 47**.

Substituent	$^2J_{F-F}$ 8 Ring Hz	$^2J_{F-F}$ Achiral/*meso* 16 Ring Hz	$^2J_{F-F}$ C_2 16 Ring Hz
OH	234.1	265.0	253.0
OBz	239.9	264.9	255.0
OBn	237.9	(262.1)[a]	(250.7)[a]

[a] No 16-membered rings were isolated but their presence was inferred due to similarity of chemical shifts and $^2J_{F-F}$ coupling constants

Table 13 ^{19}F NMR data for 16-membered rings formed from RCMs of 4, 30 and 31

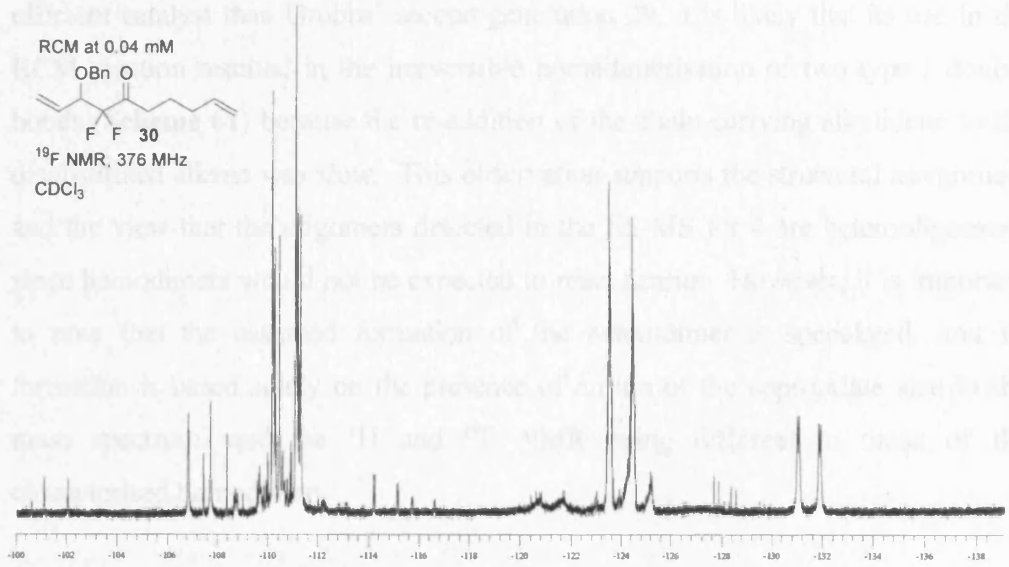

Figure 47 {^{1}H}^{19}F NMR spectrum for RCM of benzyl ether 30 at 0.04 M

The main products in the case of benzyl ether **30** and alcohol **4** appear to be acyclic, although ether **30** appears to form larger amounts of 16-membered ring than the corresponding alcohol. Work by J. Miles with benzyl ether **30** confirmed that the products formed at higher concentrations were heterodimers rather than homodimers.[55] Homodimers were synthesised independently using the Neolyst metathesis catalyst **47** and benzyl ether **30**. The reaction was run at 8 mM in CH_2Cl_2 with 10 mole % catalyst. The formation of homodimer **176** was confirmed by a ^{1}H COSY experiment. The peak corresponding to the proton highlighted in **176** was a triplet with splitting by the two neighbouring methylene protons. There was no coupling to the neighbouring alkene proton due to the symmetry in the molecule.

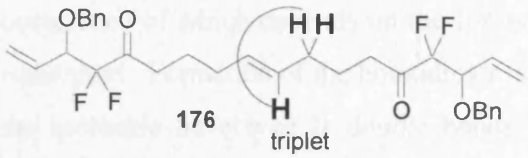

Miles exposed the same substrate **30**, to Grubbs' second generation catalyst **29** at high concentration (8 mM) and isolated a product with a different chemical shift in the ^{19}F NMR, which was identified as the heterodimer **177** from the *trans* alkene couplings in the ^{1}H NMR spectrum. Since Neolyst catalyst **47** appears to be a less efficient catalyst than Grubbs' second generation **29**, it is likely that its use in the RCM reaction resulted in the irreversible homodimerisation of two type I double bonds (**Scheme 61**) because the re-addition of the chain-carrying alkylidene to the disubstituted alkene was slow. This observation supports the structural assignment and the view that the oligomers detected in the ES-MS for **4** are heterooligomers, since homodimers would not be expected to react further. However, it is important to note that the assumed formation of the heterodimer is speculated, and its formation is based solely on the presence of an ion of the appropriate size in the mass spectrum, and the ^{1}H and ^{19}F NMR being different to those of the characterised homodimer.

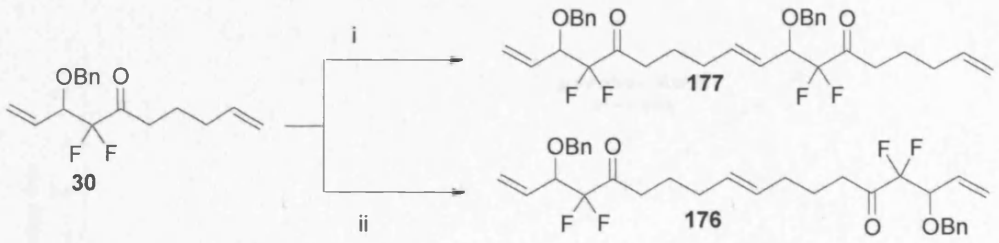

i) 5% Grubbs' II **29**, 0.005 M, CH_2Cl_2, reflux
ii) 5% Neolyst **47**, 0.005 M, CH_2Cl_2, reflux

Scheme 61 Dimerisation of benzyl ether 30 with different Ru-metathesis catalysts

In the presence of Grubbs' second generation catalyst **29** (10 mole %) in CH_2Cl_2 (2.5 mM), the homodimer slowly formed eight-membered ring **32**, which supports the structural assignment, the ^{19}F NMR spectrum confirmed 50% conversion of dimer to eight ring. Formation of the heterodimer is reversible by backbiting, the

occurrence of which depends on the formation of the substrate alkylidene with the ruthenium. Formation of the homodimer is considered reversible since both ends of the molecule have type II double bonds with allylic groups. Therefore, in the presence of a more reactive catalyst, eight-membered ring synthesis should be possible, as was proved (**Scheme 62**).

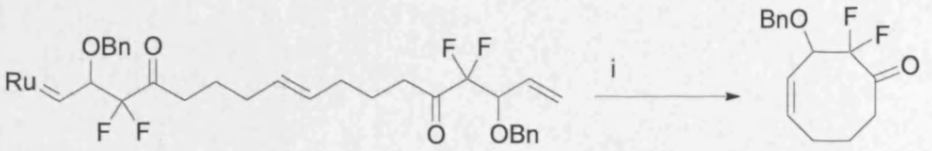

176 **32**

i) 5% Grubbs' II **29**, 0.005 M, CH_2Cl_2, reflux

Scheme 62 Formation of 32 from homodimer 176 with Grubbs' II

The EM of **31** was also calculated in the absence of the Ti(O*i*Pr)$_4$ co-catalyst, in order to determine whether the presence of the co-catalyst was having an effect on the reaction efficiency (**Section 10, p5**). The substrate concentration in dichloromethane was varied between 10-100 mM, using 5 mole % catalyst **29**. Solutions were refluxed overnight and concentrated before analysing by $\{^1H\}^{19}F$ NMR. Results showing the EM for this reaction are shown in **Figure 48**, and show a large (5-fold) effect on the EM by the Ti (IV) co-catalyst.

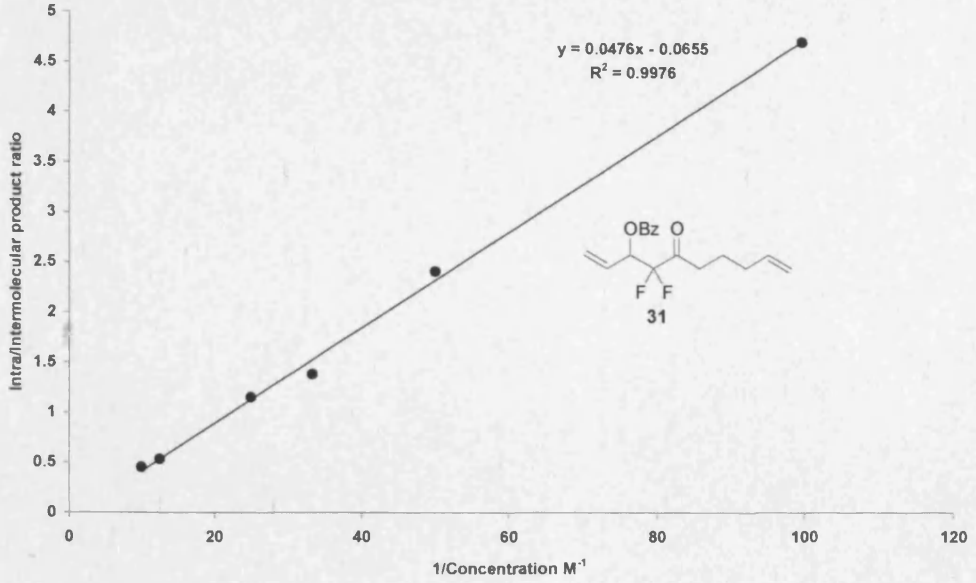

Figure 48 EM for RCM of 31 in the absence of Ti(O*i*Pr)$_4$

It is clear from **Figure 48** that the use of the co-catalyst in our RCM systems increases the cyclisation efficiency. It is possible that the presence of $Ti(OiPr)_4$ in these synthetic systems hinders the cross metathesis pathway in some way, or that it provides access to a more efficient cyclisation pathway. It is also possible that chelation is an issue in the absence of the co-catalyst. The Lewis acidic $Ti(OiPr)_4$ was initially employed to prevent chelation between the ketonic carbonyl and the ruthenium, so its absence from the system may lead to chelation.[64] The co-catalyst was also found to have an effect on the rate of cyclisation (section **4.1**) and this may also impact the EM if the CM pathway is more rapid under these conditions than cyclisation. This result therefore has implications for groups synthesising challenging cyclic systems by RCM, where high dilutions are required, the amount of solvent required can be reduced in the presence of $Ti(OiPr)_4$. Further investigations into the effects of the Ti (IV) co-catalyst on RCM, and more in-depth kinetic analyses are presented in **4.3**.

Ferland attempted to optimise a 15-membered ring formation by RCM in the synthesis of peptidomimetic inhibitors of the hepatitis C NS3 protease (**Scheme 63**).[65,66] Large scale synthesis of these macrocycles **183-186** was important if they were to be of use in the pharmaceutical industry to deliver sufficient quantity of a candidate for clinical trials, so minimum dilution and catalyst loadings were studied on four substrates.

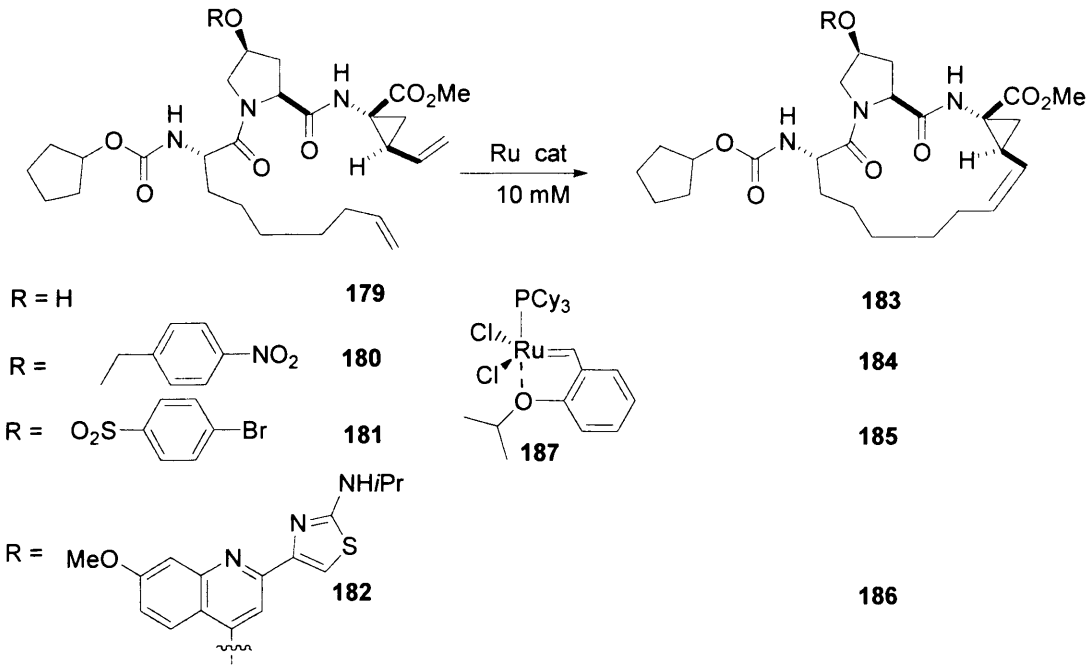

Scheme 63 Synthesis of 15-membered rings 183-186

These macrocycles could be synthesised at a maximum substrate concentration of 10 mM in a variety of solvents. (The solvents found to give the greatest efficiency, allowing the highest diene concentrations in solution, were THF and EtOAc but these resulted in slow cyclisation reactions so a mixture of PhMe and THF was used in the optimised reaction.) The authors comment on both the kinetic and thermodynamic EMs, since they observed an equilibrium after 5 minutes, at around 95% conversion of the diene and in the formation of dimer in 7% yield. However, no calculated EMs are given in paper, and the authors draw their conclusions on kinetic and thermodynamic EMs from the percentage yields of cyclic product and CM products after the reaction. However, cross metathesis products were not fully characterised, and were only identified by ions from LC-MS analysis. The equilibrium was reached only when ethylene *was not allowed to evaporate from the system.* Allowing ethylene to escape from the system resulted in the equilibrium shifting to the right, and in the formation of approximately 7% dimers (which were identified by LC-MS.) The dimer was the thermodynamic product and contributes to the thermodynamic EM. Kinetic control of the RCM was observed with Grubbs'-Hoveyda first generation catalyst **187** with **180**. With substrates **180** and **181**, the EMs were observed to be lower since higher percentages of dimer were formed under the same conditions. The group were unable to explain this

difference given that any substituent effects would be very long range. These results show that understanding the formation of cyclic products by RCM can be challenging, since many factors affect the efficiency and outcome of a reaction, and all of these factors need to be considered.

Some groups are able to exploit low effective molarities of RCM reactions, in order to synthesise larger products. Ghadiri used the low effective molarity of diene **188** to ultimately synthesise macrocycle **190** (**Scheme 64**).[67] The group attempted the RCM of **188** but after 2 days of reaction with Grubbs' second generation catalyst **29** over 48 hours, they identified, and separated what appeared to be dimers by RP-HPLC. They exploited this finding in the synthesis of macrocycle **190**, allowing the formation of dimer **189** under relatively dilute conditions due to the low EM, then finding the same conditions, dimer **189** underwent RCM with the same catalyst to form macrocycle **190**.

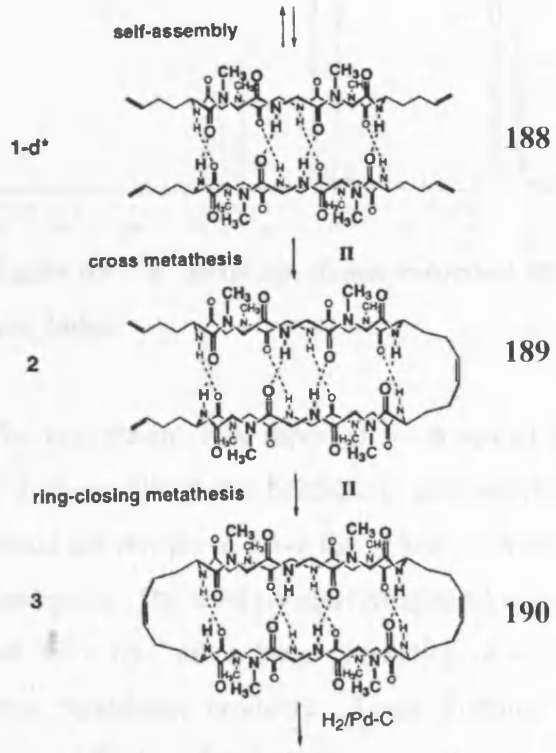

Scheme 64

In order to determine if the ethylene released had any effect on cyclisation, the RCM of **31** was carried out at 20 mM in CH_2Cl_2 in an Ace Tube. The solvent was sparged with ethylene prior to adding the substrate, co-catalyst and catalyst **29.** The

reaction was refluxed under a positive pressure of ethylene in the sealed Ace tube overnight. The resulting ^{19}F NMR spectrum was very different to that obtained from a normal synthetic reaction (**Figure 49**), showing only a small amount of cyclooctenone **33**, some oligomer, and unconverted starting diene. This experiment showed that low substrate conversion is achieved when ethylene cannot leave the system, and results in a different product distribution to that obtained under synthetic conditions, where ethylene is free the leave the system.

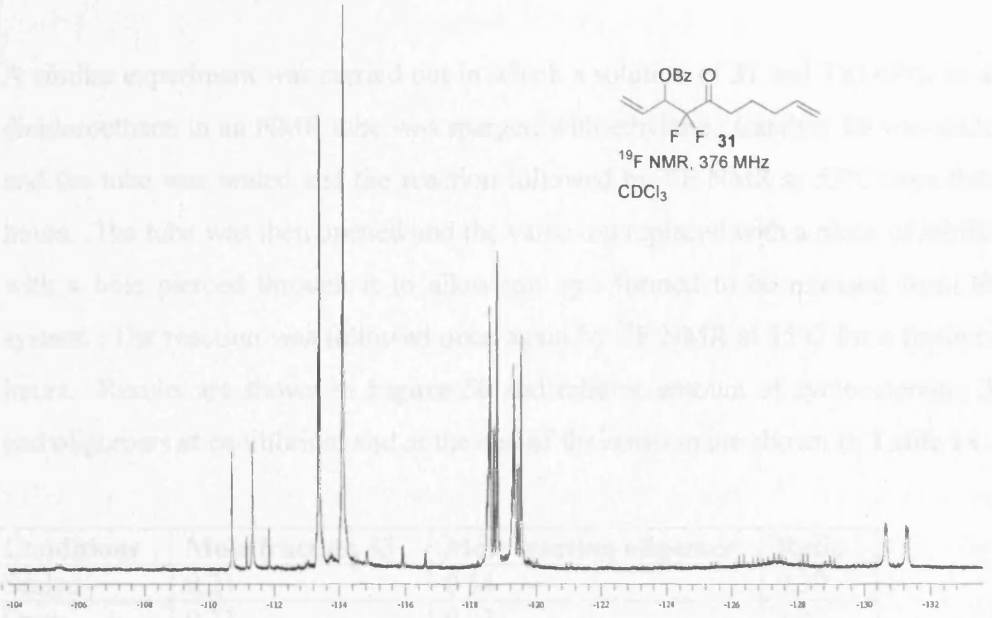

Figure 49 ^{19}F NMR spectrum recorded after RCM of benzoate 31 in a sealed Ace Tube

The experiment was repeated, in a sealed Ace Tube, but without sparging the system or filling the headspace with ethylene. However, any ethylene formed would not be able to leave the system, and would either remain in solution or in the headspace. The level of eight-membered ring formed appeared to be slightly higher but there was still a large proportion of unconverted starting material as well as cross metathesis products. These findings appear to contradict the findings of Farina, who found that allowing ethylene to escape from the system increased the % formation of cross metathesis products, and suggests that under normal synthetic conditions, our RCMs are under kinetic control, because the system can only form a thermodynamic product if reversible, and it can only be reversible if ethylene is not allowed to escape. In an experiment carried out by J. Miles, cyclooctenone **33** was

re-exposed to catalyst **29** (5 mole %) in refluxing dichloromethane and no ring opening was observed.[55] However, no ethylene was bubbled through the system and this may have effected ring opening. The ring opening of **33** with **29** was only achieved at higher concentrations (0.1 M). This is discussed further from p117 in this section. It appears from **Figure 49** that allowing ethylene release from the system results in a shift in the reaction equilibrium, and favours formation of the kinetic product, cyclooctenone **33** through kinetic trapping. This possibility was investigated further using ^{19}F NMR kinetics.

A similar experiment was carried out in which a solution of **31** and Ti(O*i*Pr)$_4$ in d_4-dichloroethane in an NMR tube was sparged with ethylene. Catalyst **29** was added and the tube was sealed and the reaction followed by ^{19}F NMR at 55°C over three hours. The tube was then opened and the valve top replaced with a piece of labfilm with a hole pierced through it to allow any gas formed to be released from the system. The reaction was followed once again by ^{19}F NMR at 55°C for a further 6 hours. Results are shown in **Figure 50** and relative amount of cyclooctenone **33** and oligomers at equilibrium and at the end of the reaction are shown in **Table 14**.

Conditions	Mole fraction 33	Mole fraction oligomer	Ratio
Sealed	0.21	0.54	0.39
Open	0.73	0.23	3.2

Table 14 Mole fractions of eight-membered ring and oligomer

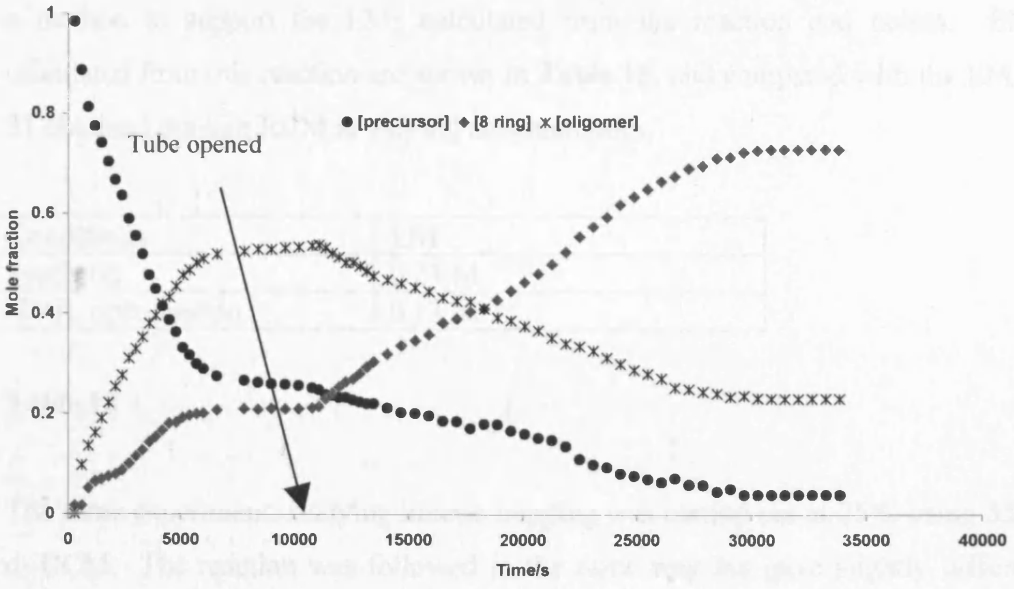

Figure 50 Plot showing metathesis of 31 in d_4-DCE at 55°C in a sealed NMR tube and subsequent tube opening (Section 10, p54)

The plot in **Figure 50** shows two distinct phases to the reaction. There is an initial, rapid formation of oligomer, as well as relatively slow formation of cyclooctenone **33** which appears to level off at around 5000 seconds. This is in the sealed system, from which ethylene was unable to escape, and appears to be due to the system reaching equilibrium under these conditions. Subsequent events show that active catalyst remains after this time has elapsed, at least until 30,000 s.

The second phase of the reaction begins after the NMR tube was opened. We observed a fall in the amount of oligomer, and increase in the amount of cyclooctenone **33**. The amounts of oligomer and eight-membered ring level off around at 22,000 s, which indicates an end point. The reaction was carried out over approximately 10 hours, and some degree of catalyst decomposition would be expected over this timescale, especially in the presence of ethylene, due to the initial sealed system. Metathesis of the metallocyclobutane with ethylene is known to be degenerate and lead to the formation of inactive species.[50,68] This is discussed further in **4.1**. The formation of the kinetic product, cyclooctenone **33** is favoured by the elevated temperature in this case, whereas the formation of the oligomer is favoured at lower temperatures.[19,69] The mole fractions of these species at equilibrium are an alternative way of calculating the EM for a substrate, and allows a method to support the EMs calculated from the reaction end points. EMs calculated from this reaction are shown in **Table 15**, and compared with the EM of **31** obtained through RCM at varying concentrations.

Conditions	**EM**
Synthetic	0.24 M
NMR, open system	0.13 M

Table 15

The same experiment, studying kinetic trapping was carried out at 25°C using **33** in d_2-DCM. The reaction was followed in the same way but gave slightly different

results (**Figure 51**). We still observe that the sealed system reaches equilibrium after approximately 4200 seconds, but with slower consumption of benzoate **31**, and almost equal rates of formation of cyclooctenone **33** and oligomer. However, since we do not know fully the size distribution of the oligomers, and therefore the number of fluorine nuclei accounted for by the peaks in the ^{19}F NMR spectra, true evaluation of these rates is difficult. Upon opening the system, the ratios of cyclooctenone **33** and oligomer become very different, which suggests that further consumption of diene **31** leads directly to formation of the eight-membered ring, rather than oligomers. The amount of oligomer in the system decreases slightly upon opening the system, but only from approximately 20% to 15% which suggests that under these conditions, there is very little backbiting to smaller products. Initially, this result was surprising, since the lower temperature would be expected to favour oligomerisation over cyclisation, but from the EM calculation for **31**, we observed that cyclooctenone **33** was still the major product at a substrate concentration of 0.04 M in the synthetic (open) system.

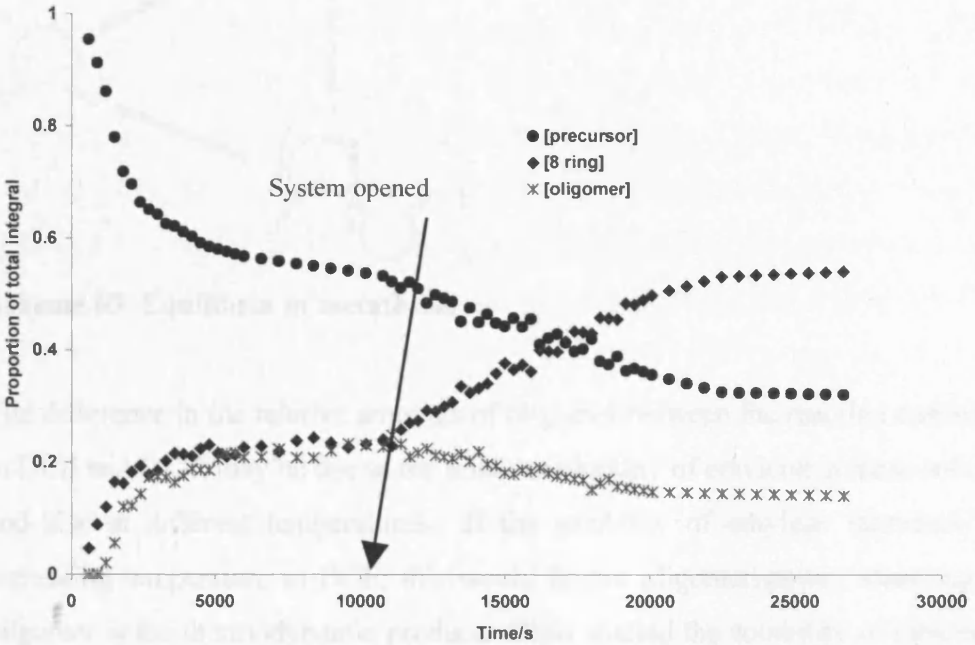

Figure 51 Plot showing metathesis of 31 in d_2-DCM at 25°C in a sealed NMR tube and subsequent tube opening (Section 10, p56)

Opening the system under these conditions does not change the distribution of oligomer and cyclooctenone **33** as significantly as in the d_4-DCE experiment,

although the ratio of cyclooctenone **33** to oligomer is similar to that obtained in the experiment carried out in DCE, suggesting that the EM for **33** is not affected by the change of solvent significantly or the 20°C temperature difference . The main difference between these two experiments is the reaction temperature, which is clearly affecting the rate of consumption of starting diene, and at 25°C in DCM, **31** is not completely consumed on the reaction timescale.

A general schematic for the reaction equilibrium is shown in **Scheme 65**. The equilibrium can be maintained despite continuing consumption of starting diene into either cyclic product, or oligomer *via* ring opening of the cyclic product to larger acyclic species, or *via* backbiting of oligomers to the cyclic product. Through the backbiting and ring opening processes, it is also possible to regenerate the starting diene, due to the presence of ethylene within the system.

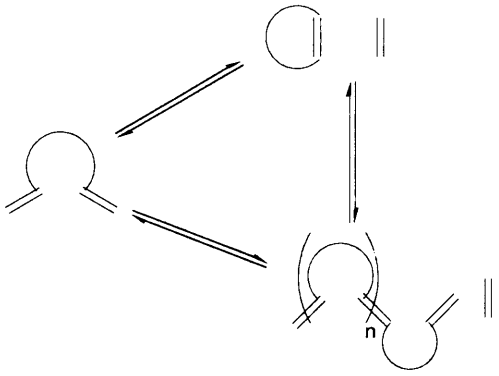

Scheme 65 Equilibria in metathesis

The difference in the relative amounts of oligomer between the reaction carried out in DCE and DCM may be due to the relative solubility of ethylene in these solvents, and also at different temperatures. If the solubility of ethylene increases with increasing temperature in DCE, this would favour oligomerisation, assuming that oligomer is the thermodynamic product. Chao studied the solubility of ethylene in three paraffins (*n*-eicosane, *n*-octacosane, *n*-hexatriacontane) and found that in all three cases, the solubility of ethylene decreased with increasing temperature, but increased with increasing pressure.[70] The reduced temperature in the reaction followed in DCM would therefore be expected to increase the level of ethylene in solution, which is inconsistent with the observed amount of oligomerisation.

However, extensive studies into ethylene solubility have not been published. The most extensive study of ethylene solubility was carried out by Sahgal, who studied solubility of the gas in a range of polar and non-polar solvents, and varying pressures and temperatures.[71] The general conclusion was that ethylene is more soluble in less polar solvents, and solubility decreases with increasing temperature. However, the authors only studied chlorobenzene and carbon tetrachloride as halogenated solvents, and no studies exist, to our knowledge of dichloromethane or dichloroethane. Hsu studied the solubility of ethylene in toluene at various temperatures and pressures and found that the solubility of ethylene increases with increasing pressure, but decreases with increasing temperature, which is in agreement with Chao's findings.[72] Few other studies have been carried out into the solubility of ethylene, so there is limited knowledge of the solubility of ethylene across a range of widely-used solvents. The existing data do not allow any estimate to be made of the likely quantity of ethylene in solution under the conditions of our experiments.

The effect of ethylene on the outcome of metathesis reactions has been relatively well-explored in a variety of systems. Weiler used RCM to synthesise a range of macrocyclic lactams and lactones (**Scheme 66**) using Grubbs' first generation catalyst **28** in dichloromethane.[73] The group synthesised a range of 14 membered rings **194-196**, and in general (with one exception), the *E*-macrocycle was obtained in higher yield than the *Z*-isomer. Since the *E*-cyclooalkene was therefore believed to be the more stable stereoisomer, the *Z*-macrocycles were re-exposed to catalyst **28** in CH_2Cl_2 under ethylene. The expected product from this reaction was the *E*-macrocycle, however, this was not observed, and instead the starting diene was recovered. This suggests that addition of ethylene along with **28** allows the thermodynamic product to form, which was the diene monomer in this case. This outcome may also suggest that Grubbs' I **28** does not react with the cyclic product under these conditions, or that the catalyst decomposes rapidly in the presence of ethylene. This is discussed further in **4.1**.

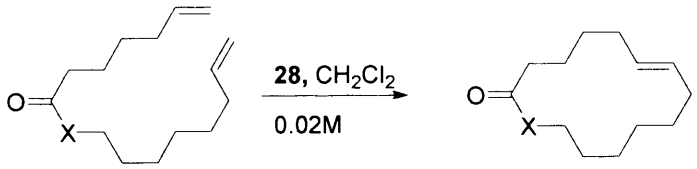

X = O **191**
X = NH **192**
X = NBOC **193**

X = O **194**
X = NH **195**
X = NBOC **196**

Scheme 66 Weiler's macrocycle synthesis

Reiser optimised the synthesis of a range of seven-membered rings such as **198** and **201** *via* RCM, during syntheses of several natural products, using Grubbs' second generation catalyst **29** at relatively high pre-catalyst loading (10 mole %) (**Scheme 67**).[74] Initially, syntheses were carried out under an atmosphere of nitrogen but yields of the cyclic products were typically around 35%. The group used an atmosphere of ethylene, since this has proved beneficial to some enyne metatheses. However, in this case, no cyclisation of the starting diene was effected under the ethylene atmosphere. The reactions were sparged with nitrogen instead, which removed any ethylene released in the reaction from the system, and under these conditions, 66% of the desired cyclic product was obtained. These results suggest that release of ethylene in the system, if not allowed, can seriously affect the reaction outcome, since it either suppresses the consumption of diene, or favours the formation of the thermodynamic product rather than the kinetic (cyclic) product which is a medium ring. However, the conditions of the two experiments are not completely comparable, since one system was sitting under N_2 and the other was constantly sparged with N_2. However, the difference in product yield between these two systems was less than 2-fold, which is not a dramatic difference.

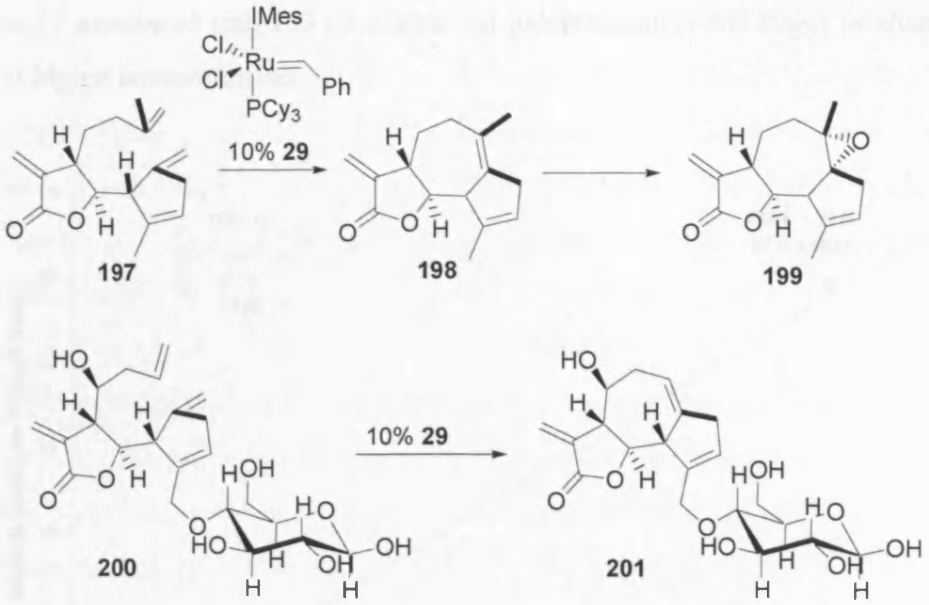

Scheme 67

From the published synthesis of **23** from **22** (**Scheme 68**) we noted that the synthesis of **23** by RCM was carried out at 10 mM in contrast to the 1 mM for the synthesis of the corresponding CH_2 8-ring **3**. This suggested that the presence of the *gem*-dimethyl groups has an effect on the cyclisation efficiency and therefore the effective molarity.

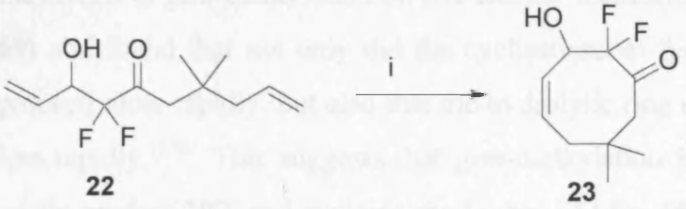

i) 5% Grubbs' II **29**, 0.01 M, CH_2Cl_2, $Ti(OiPr)_4$

Scheme 68 RCM of alcohol 23

The experiment was carried out in the same way, using substrate **150** at varying concentrations from 20 mM up to 250 mM, with 5% catalyst **29** and titanium(IV) co-catalyst in refluxing CH_2Cl_2. The $\{^1H\}^{19}F$ NMR spectra were recorded at 218 K due to the fluxional nature of the cyclooctenone products at ambient temperature. Again, the NMR spectra showed good dispersion between both conformers of

eight-membered ring **153** (characterised independently) and larger products formed at higher concentrations.

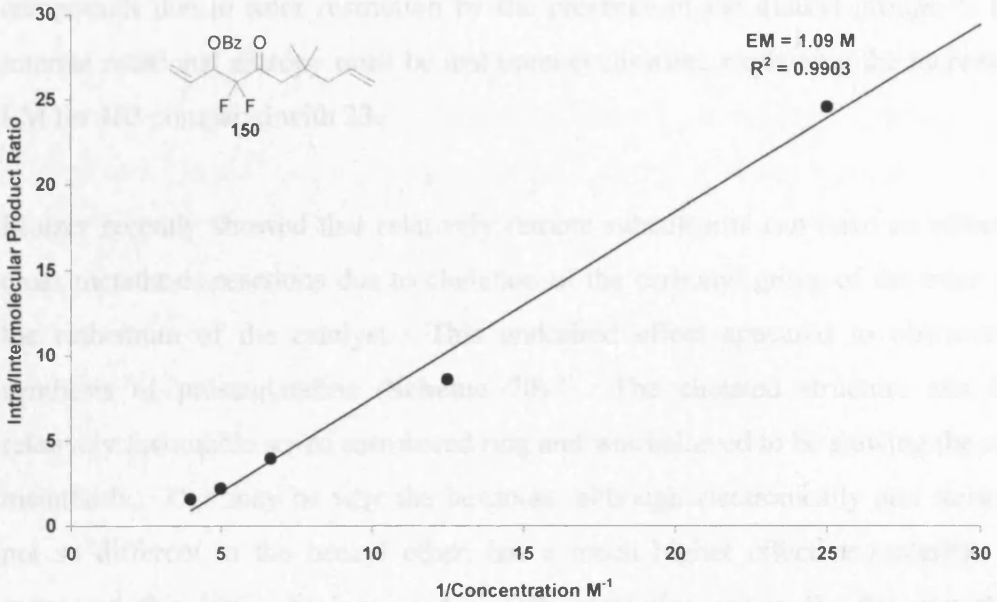

Figure 52 Calculation of EM for the RCM of benzoate 150 (Section 10, p96)

Figure 52 was used to calculate the EM for **150** of 1.09 M, approximately 4.5 times higher than that of the corresponding CH_2 substrate, which shows that *gem*-dialkylation increases the efficiency of cyclisation in these systems. Bruice studied the effects of *gem*-dialkylation on five and six-membered ring cyclisations (**Scheme 69)** and found that not only did the cyclisations of the dialkylated substrates **203** proceed more rapidly, but also that the hydrolytic ring opening reactions proceeded less rapidly.[75,76] This suggests that *gem*-dialkylation increases the stability of the cyclic product **207**, and explains the higher EM for **150**, since for ring opening of the corresponding cyclooctenone **153** to occur rapidly, the substrate concentration would have to be greatly increased.

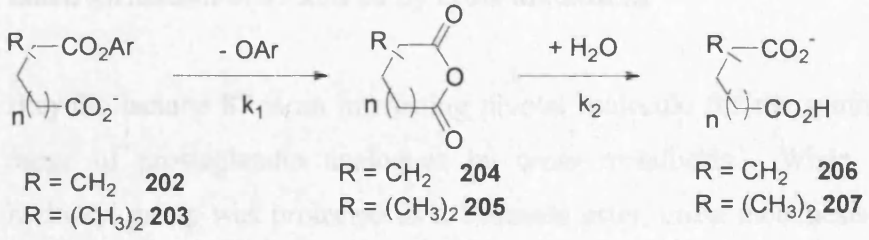

Scheme 69

Allinger and Zalkow studied the effects of *gem*-dialkylation on cyclisation rates, and concluded that entropy loss in cyclisation is reduced with dialkyl substituted compounds due to rotor restriction by the presence of the dialkyl groups.[54] Less internal rotational entropy must be lost upon cyclisation, explaining the increase in EM for **153** compared with **33**.

Mulzer recently showed that relatively remote substituents can have an effect on cross metathesis reactions due to chelation of the carbonyl group of the ester with the ruthenium of the catalyst. This undesired effect appeared to obstruct the synthesis of prostaglandins (**Scheme 70**).[32] The chelated structure sits in a relatively favourable seven membered ring and was believed to be slowing the cross metathesis. This may be why the benzoate, although electronically and sterically not so different to the benzyl ether, has a much higher effective molarity. To overcome this issue, Mulzer used a TBS protecting group for the metathesis substrates.

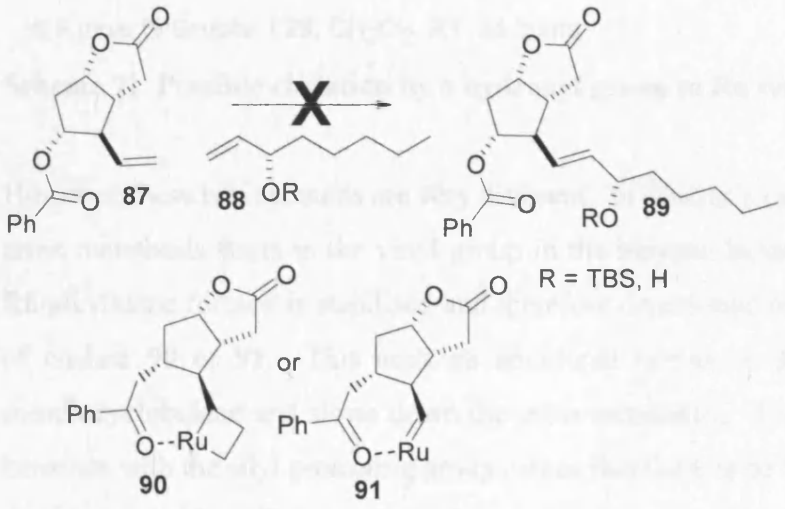

Scheme 70 Possible chelates formed by a benzoate protecting group in the failed formation of 87 and 88 by cross metathesis

Bicyclic lactone **87** is an interesting pivotal molecule for the synthesis of a wide range of prostaglandin analogues by cross metathesis. When the secondary hydroxyl group was protected as a benzoate ester, cross metathesis was slow and low yielding. Replacing the benzoate ester with TBS protection improved the yield

considerably. Mulzer attributed this to chelate formation in the benzoate. The chelate is seven-membered and the stability of such species is not well documented.

However, Ghosh suggested that chelation between an allylic alcohol functionality and the ruthenium of the catalyst is also possible, and retards the RCM process.[30] The group believed this was the reason that dienol **83** did not undergo RCM to give 5-membered ring **85**, as complexation of the hydroxyl group to the ruthenium was strong (**Scheme 71**). Although our substrates have an allylic alcohol, rather than the group shown in **Scheme 71**, a similar, favourable five-membered ring conformation may be accessible from the metallocyclobutane. However, since the calculated effective molarity for **4** is so low, it seems unlikely that there is any slowing down of the RCM and cross metathesis pathways due to chelation, so it is unlikely that we are seeing this particular chelation effect.

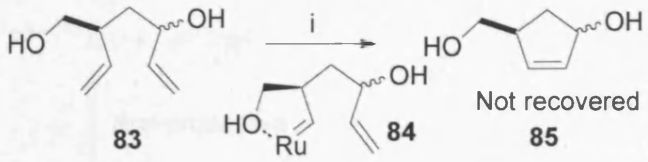

i) 6 mole % Grubbs' I **28**, CH_2Cl_2, RT, 24 hours

Scheme 71 Possible chelation by a hydroxyl group to Ru centre during RCM

However, these two accounts are very different. In Mulzer's case, it is assumed that cross metathesis starts in the vinyl group in the bicyclic lactone, and that the new Ru-alkylidene formed is stabilised and therefore deactivated through the formation of chelate **90** or **91**. This adds an additional barrier to the formation of the metallocyclobutane and slows down the cross metathesis. The replacement of the benzoate with the silyl protecting group means that there is no Lewis basic carbonyl oxygen available. The oxygen of the silyl group could potentially form a 5-membered ring chelate but these oxygens are generally considered to be weak Lewis bases because the oxygen donates into the d-orbitals of the silicon. In the case of the Ghosh system, a five-membered ring chelate can form, but the oxygen is not silicon-bound so its lone pairs are more Lewis basic and able to interact with the ruthenium. A comparison of the Mulzer and Ghosh systems and our system is shown in **Figure 53**. In our RCM system, however, we expect that the cross

metathesis does not start on the allylic double bond, so the formation of similar chelates could only arise by crossing to the non-productive metathesis pathway (**Scheme 72**).

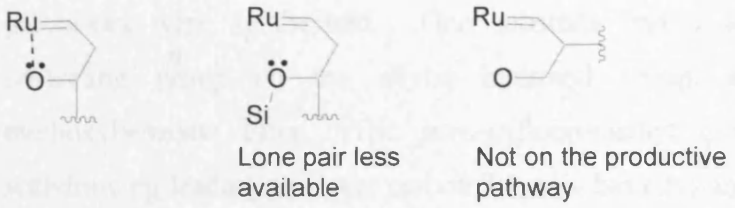

Figure 53 Comparison of Ru-chelates in Mulzer, Ghosh and our systems

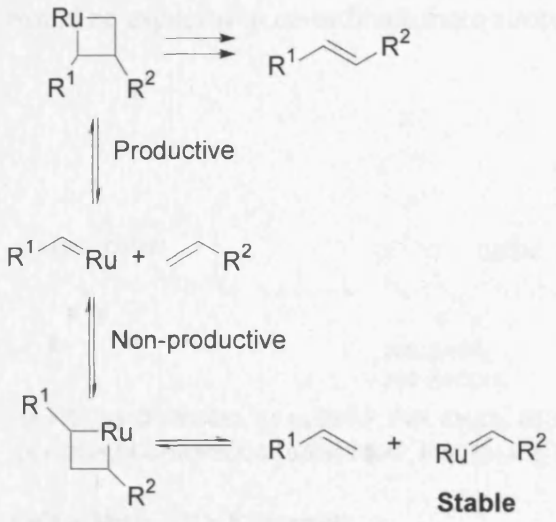

Scheme 72 Productive and non-productive metathesis pathways

Grubbs recently published findings on alkylidene exchange. If 1,2-addition (the productive pathway) is slower than 1,3-addition (the non-productive pathway) and the alkylidenes exchanged, the resulting alkylidene formed is highly stable and would detain the cross metathesis sequence.[77] If this is the case, a chelating feature on either alkene becomes relevant. The productive route would be detained directly if the chelating feature is in R^1, and indirectly if the chelating feature is in R^2. Since it is the 14 electron alkylidenes which are likely to form chelates, this model applies to our RCM systems. Benzoate **31** may be exchanging alkylidenes in this way, and forming a six-membered chelate, the formation of which retards the cross metathesis pathway. Alcohol **4** and benzyl ether **30** are not able to form especially stable exchange products, so the cross metathesis occurs readily between the

productive and non-productive pathways until the thermodynamic product (oligomer) is formed.

In order to begin to test the benzoate chelation theory further, two further RCM precursors were synthesised. One substrate had a 4-trifluoromethylbenzoate protecting group on the allylic hydroxyl group, and the second a 4-methoxybenzoate ester. The *para*-trifluoromethyl group is highly electron-withdrawing leading to lower carbonyl Lewis basicity, and therefore the substrate would be expected to chelate less to the ruthenium centre of the catalyst, hence lowering the EM. The 4-methoxy group is strongly electron-donating and therefore would be expected to co-ordinate more strongly, resulting in a higher EM value.

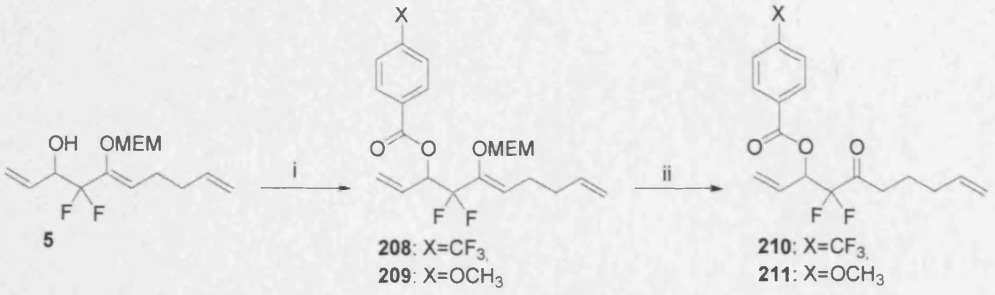

i (X = CF_3) 4-CF_3PhCOCl, 0.5 eq DMAP, PVP, CH_2Cl_2, RT, shake, 72 hours
(X = OCH_3) 4-CH_3OPhCOCl, 0.5 eq DMAP, PVP, CH_2Cl2, RT, shake, 72 hours

ii $SOCl_2$, MeOH, 0°C to RT, overnight

Scheme 73 Syntheses of 210 and 211

The effective molarities were determined in the same way as for the previous substrates, with concentrations varied from 20-200 mM in dichloromethane, using the same synthetic conditions as used previously (0.3 equivalents Ti(O*i*Pr)$_4$, 5% Grubbs' II). $\{^1H\}^{19}F$ NMRs were integrated as before and intra/intermolecular products plotted as before. Larger cyclic products and oligomers were identified by analogy with the δ_F for the characterised benzoates **173** and **174**. Results are shown in **Figures 54** and **55**.

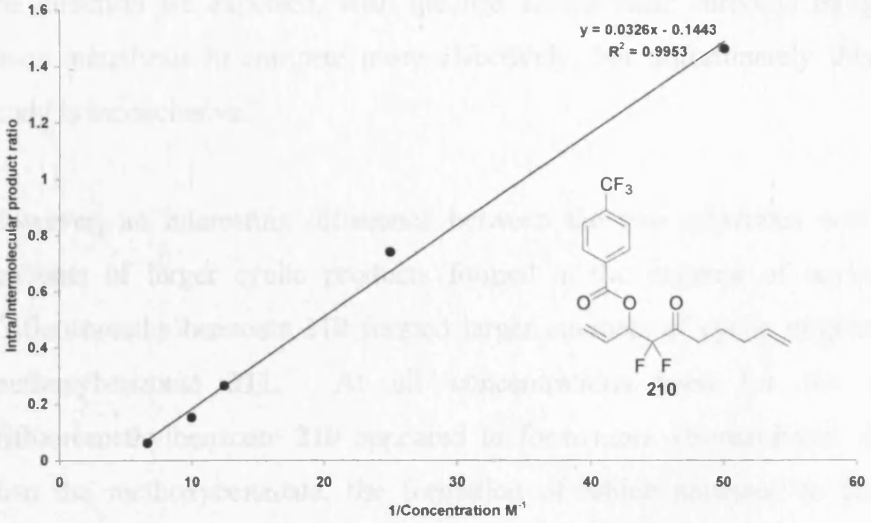

Figure 54 Calculation of the EM for the RCM of 210 (Section 10, p6)

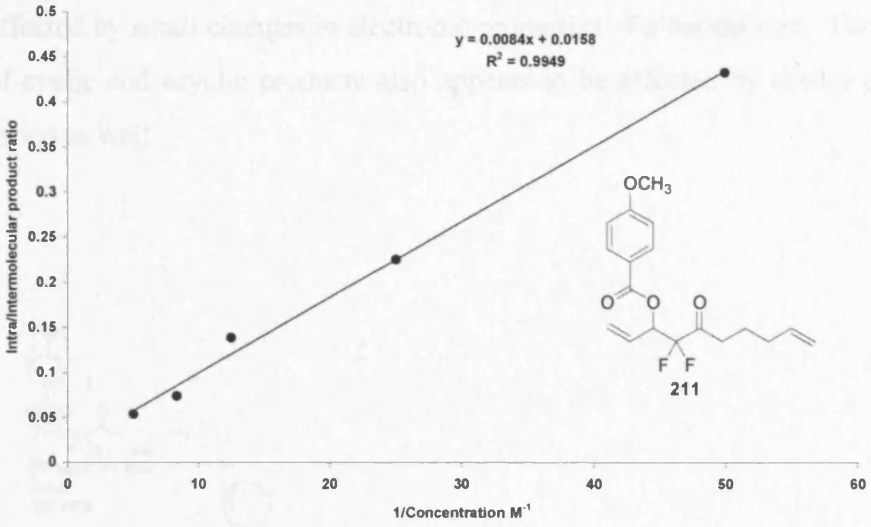

Figure 55 Calculation of the EM for the RCM of 211 (Section 10, p8)

As shown in **Figures 54** and **55**, the CF_3-substituted benzoate **210** has a higher EM (0.031 M) than the 4-methoxy benzoate **211** (0.0084 M). The calculated EMs for **210** and **211** are both lower than that of **31** (8-fold and 30-fold for **210** and **211** respectively), and **211** has a lower EM than **210** which would not be expected if chelation with the Ru centre was the explanation for the high EM of benzoate **31**.

We expected that the *p*-methoxybenzoyl ester would be more Lewis basic than the benzoate ester, and that the EM would rise as the cross metathesis pathway was slowed further. We observed the opposite effect. The effect of the CF_3 group is in

the direction we expected, with the less Lewis basic carbonyl oxygen allowing cross metathesis to compete more effectively, but unfortunately this part of the study is inconclusive.

However, an interesting difference between the two substrates was apparent in amounts of larger cyclic products formed at the expense of acylic oligomers. Trifluoromethylbenzoate **210** formed larger amounts of cyclic oligomers than did methoxybenzoate **211**. At all concentrations used for the studies, the trifluoromethylbenzoate **210** appeared to form more 16-membered ring products than the methoxybenzoate, the formation of which appeared to favour acyclic oligomers (**Figures 56-58**). These EM calculations have shown that the choice of protecting group for an RCM substrate is critical, and the efficiency can be greatly affected by small changes in electronic properties of a substituent. The distribution of cyclic and acyclic products also appears to be affected by choice of protecting group as well.

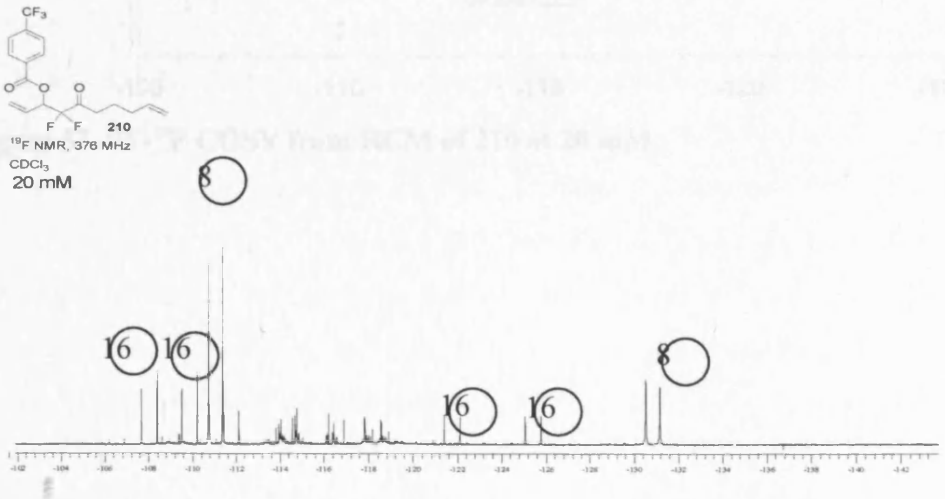

Figure 56 $\{^1H\}^{19}F$ NMR spectrum for RCM of 210 at 20 mM

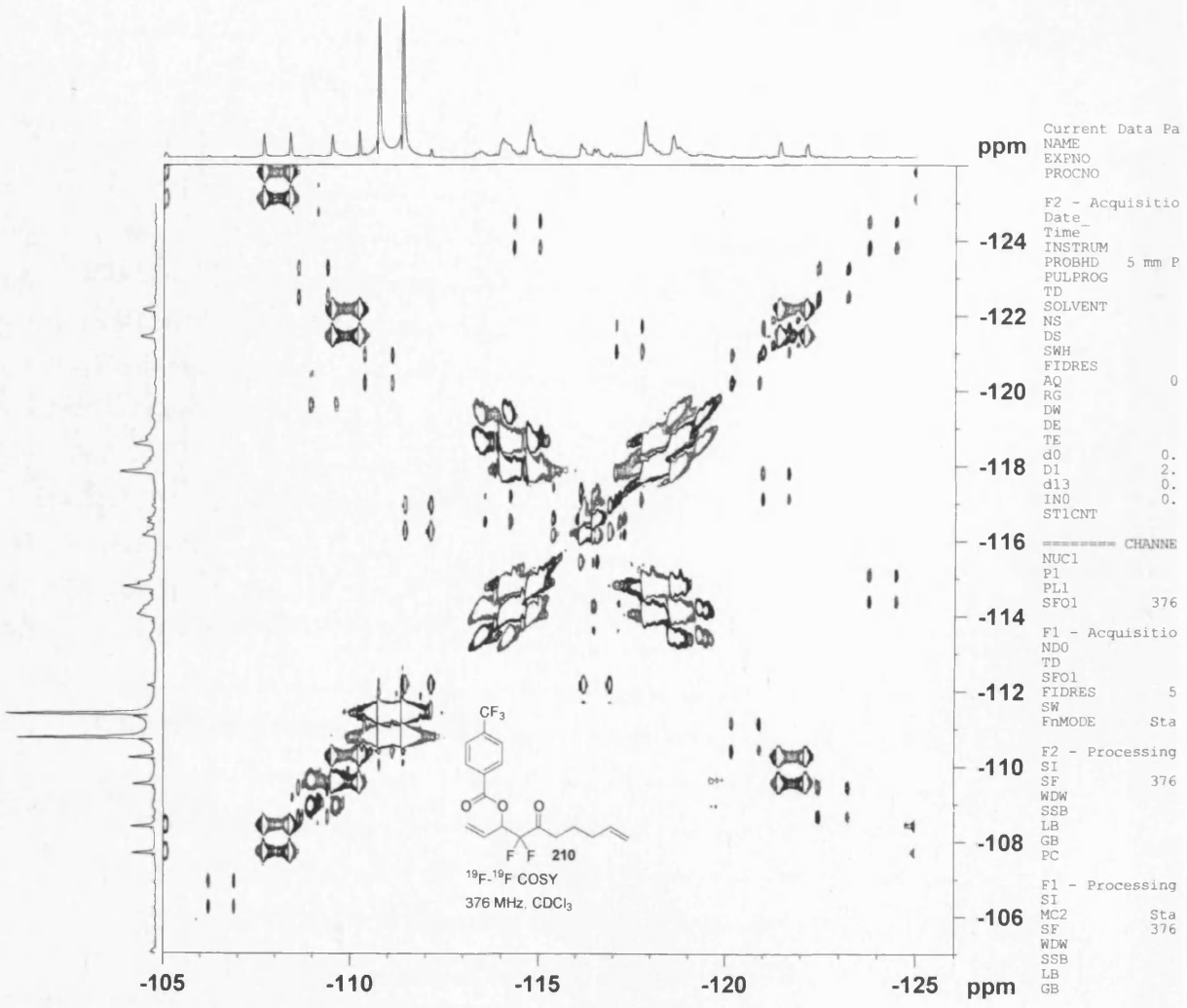

Figure 57 ^{19}F-^{19}F COSY from RCM of 210 at 20 mM

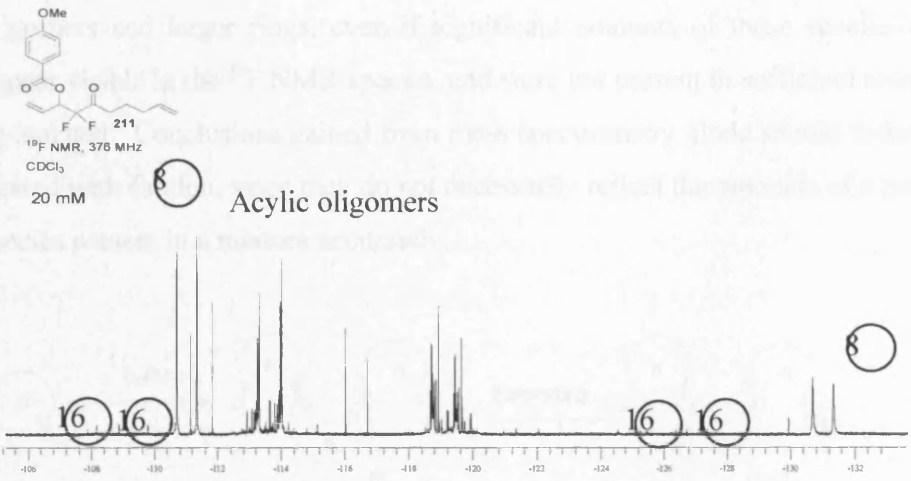

Figure 58 {^{1}H}^{19}F NMR spectrum for RCM of 211 at 20 mM

3.2 Back-biting of Oligomers and RCM

Fogg recently claimed that high dilution conditions may not always offer the best solution to the synthesis of difficult rings by RCM. *'While submillimolar substrate concentrations might be used to minimise oligomerisations and enforce direct RCM, this would retard the bimolecular reaction between substrate and catalyst. The opposite approach greatly improved RCM efficiency...By mixing* ***55*** *and* ***29*** *at 100 mM, and diluting to 5 mM to promote backbiting, we obtained* ***57*** *in 1 h (cf 9 h for the Ziegler method).'* [21] Instead, the desired products can be formed *via* the backbiting process. In this case, the syntheses would be carried out at high concentrations, resulting in the formation of oligomers. Upon dilution of the reaction, these oligomers can bite back to form the desired cyclic product, achieving a significant saving in reaction time (**Scheme 74**). However, the group's characterisation of oligomers was minimal, and their conclusions about the nature and extent oligmerisation were drawn solely from a pentamer ion identified by MALDI. Mass spectrometers are highly sensitive and can pick up small amounts of species which ionise well using specific techniques, and unless coupled with chromatography, are not quantitative.

ES-MS was used to examine the product mixtures for the RCM of **4**. Even at relatively low concentrations (2 mM), ions were present in ES^- for a series of oligomers and larger rings, even if significant amounts of these species did not appear visible in the ^{19}F NMR spectra, and were not present in sufficient amounts to be isolated. Conclusions gained from mass spectrometry alone should therefore be treated with caution, since they do not necessarily reflect the amounts of a particular species present in a mixture accurately.

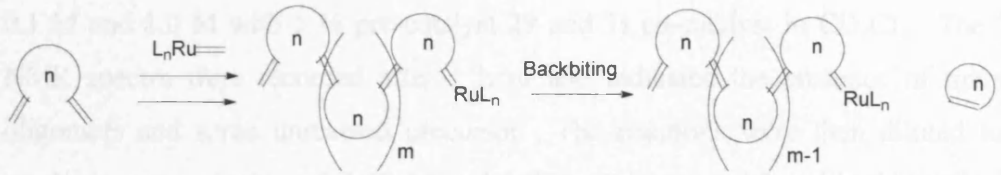

Scheme 74 Formation of cyclic monomers *via* oligomerisation followed by backbiting

Fogg used this approach in an attempt to synthesise eight-membered ring **57** with Grubbs' second generation catalyst **29** (**Scheme 75**). However, for this system, even at low concentrations of diene **55** in dichloromethane (5 mM), rapid formation of oligomers occurred (41% after 15 minutes) and the procedure did not result in a good yield of the desired cyclic product **57** at the end of the reaction (44%). When the concentration of **55** in solution was reduced to 0.5 mM, the yield of **57** at the end of the reaction was 85%, but the yield of oligomers after 15 minutes was very low (7%) compared to the previous attempt, which suggests that the majority of the cyclised product was likely to have formed directly from the acyclic diene monomer, rather than through the backbiting of oligomers. Fogg also quotes an EM for this cyclisation of 750 mM. This EM value was estimated for the synthesis of **57** but not for its synthesis *via* RCM. The value was taken from figures calculated by Mandolini for the synthesis of the same eight-membered ring *via* an etherification reaction.[8] Since good yields of cyclic product were only obtained by RCM at a substrate concentration of 0.5 mM, it appears unlikely that the EM for the synthesis of **57** by RCM is even close to 750 mM.

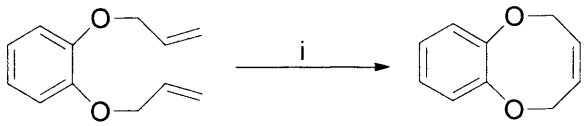

55 **57**

i) Grubbs' II, CH_2Cl_2 (5-100 mM), reflux

Scheme 75

However, we found that in our systems, oligomers do not act as intermediates for the clean synthesis of cyclic molecules by RCM. RCMs of benzoate **31** were run at 0.1 M and 1.0 M with 5 % pre-catalyst **29** and Ti co-catalyst in CD_2Cl_2. The ^{19}F NMR spectra were recorded after 1 hour and indicated the presence of mainly oligomers and some unreacted precursor. The reactions were then diluted to a synthetic concentration of 0.02 M and left for 8 hours. After this time, the ^{19}F NMRs (**Figures 59** and **60**) showed that the dominant product was not cyclooctenone **33** in either case. The reaction initially carried out at 0.1 M showed a higher proportion of cyclooctenone **33**, as well as some 16-membered ring and some remaining oligomers. The reaction carried out initially at 1.0 M still showed predominantly oligomers, with only a small amount of 8 ring **33**, and some 16-membered ring. These studies therefore appear to contradict Fogg's claim that difficult RCM targets can by synthesised more effectively by exploiting backbiting to effect a de-oligomerisation. Whereas formation of oligomers, and then backbiting affords a relatively complex mixture of products after dilution to 20 mM, the RCM of **31** at 20 mM affords clean cyclooctenone product exclusively. This suggests strongly that oligomer formation is not fully reversible, and that cyclooctenone **33** is not a thermodynamic product.

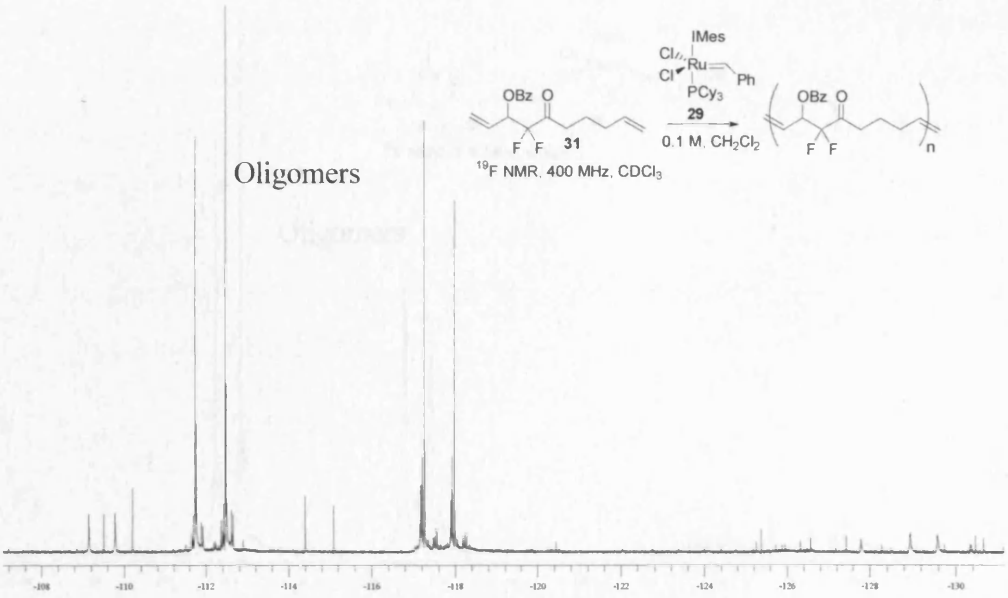

Figure 59 Oligomerisation of 31 at 0.1 M (Section 10, p

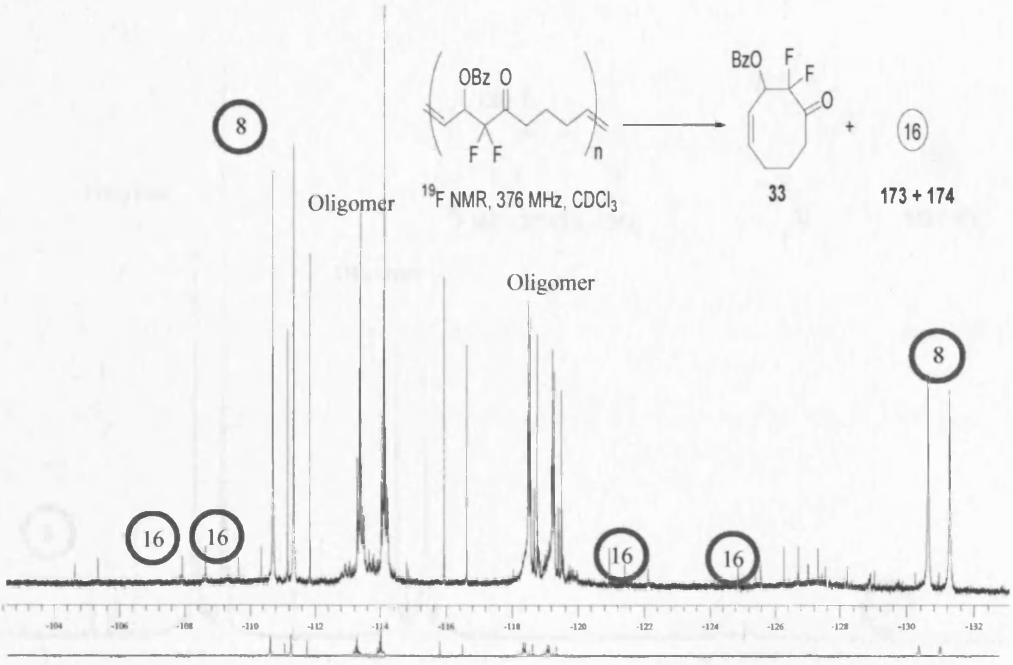

Figure 60 Oligomerisation at 0.1 M followed by back-biting at 0.02 M

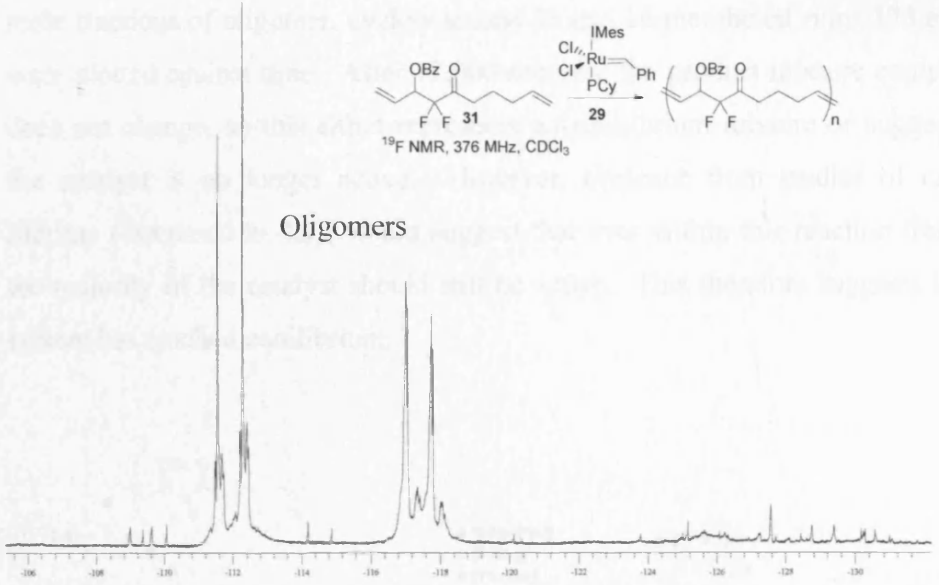

Figure 61 Oligomerisation of 31 at 1.0 M

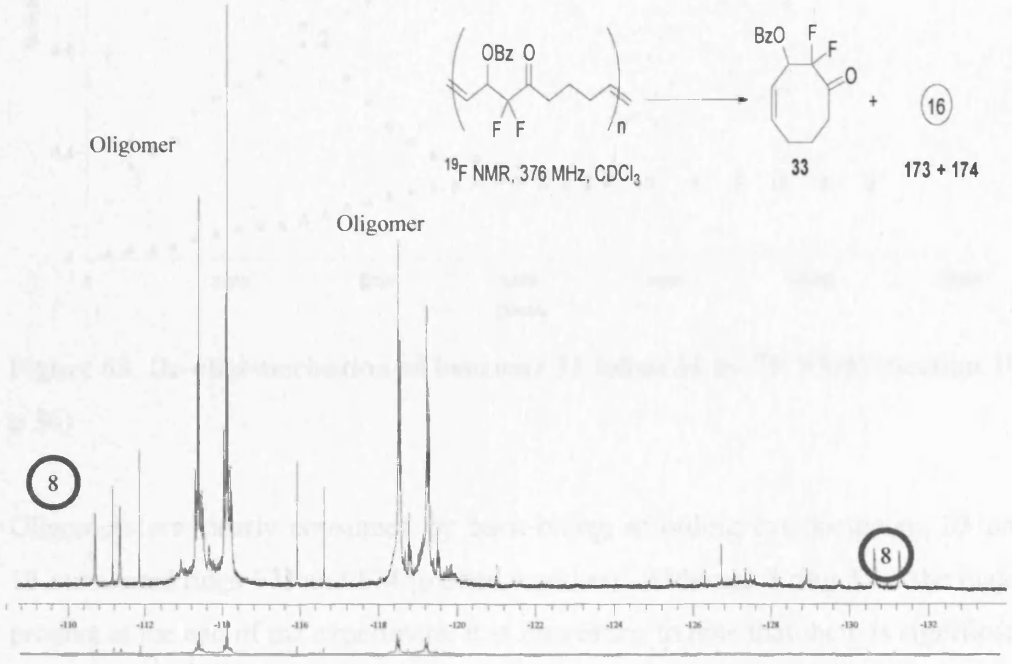

Figure 62 Oligomerisation of 31 at 1.0 M followed by back-biting at 0.02 M

We also attempted to follow the back-biting reaction by ^{19}F NMR (376 MHz). Benzoate **31** was allowed to form oligomers at 0.1 M in $CDCl_3$, with 5% catalyst **29**. After one hour, an aliquot was removed from the reaction and placed in a dry NMR tube and diluted to a substrate concentration of 0.02 M with dry $CDCl_3$. The reaction was then followed by NMR at 318 K over 4.5 hours. The results shown in **Figure 63** were obtained through integration of the ^{19}F NMR spectra obtained. The

mole fractions of oligomer, cyclooctenone **33** and 16-membered rings **173** and **174** were plotted against time. After 12,000 seconds, the product mixture composition does not change, so this either represents an equilibrium mixture or suggests that the catalyst is no longer active. However, evidence from studies of catalytic lifetime (discussed in **4.1**), would suggest that over within this reaction timescale, the majority of the catalyst should still be active. This therefore suggests that the system has reached equilibrium.

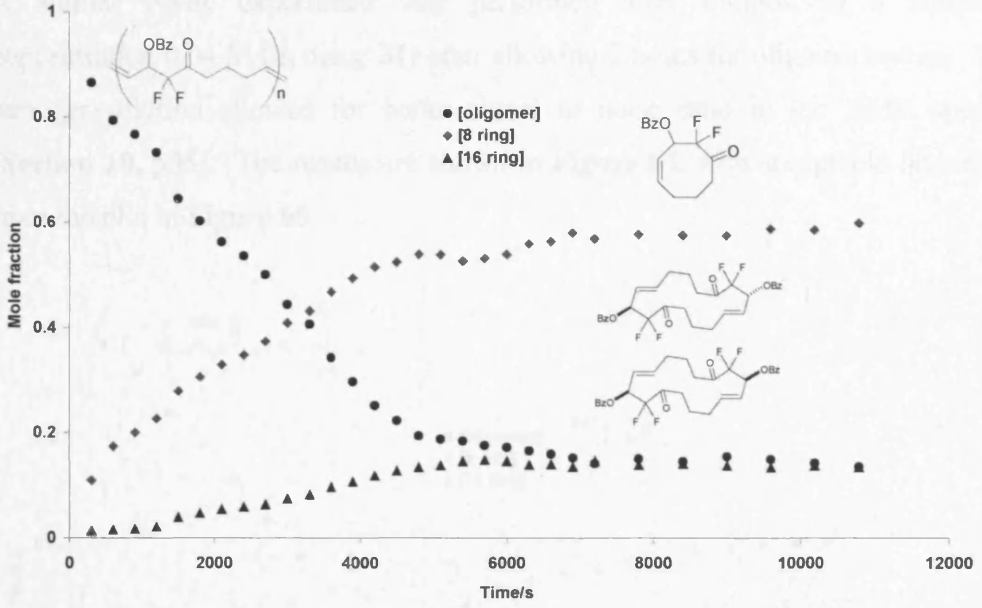

Figure 63 De-oligomerisation of benzoate 31 followed by ^{19}F NMR (Section 10, p 36)

Oligomers are clearly consumed by back-biting, affording cyclooctenone **33** and 16-membered rings **173** and **174** (plotted together). Although 8 ring **33** is the major product at the end of the experiment, it is interesting to note that there is significant formation of 16 ring, whereas normally at 0.02 M we do not observe any formation of these products. Under normal synthetic conditions, the formation of 16 rings is suppressed as the concentration is not sufficiently high. However, when the major starting species is ruthenium-bound oligomer, which bites back at 0.02 M to form smaller products, the possibility of forming larger rings is increased, depending on the number of repeating units in the oligomer. The 16-membered ring products should be less strained than the cyclooctenones, so it is unlikely that the latter represents a thermodynamic product. **Figure 63** shows that the consumption of the

oligomer is not linear (zero order) but it also does not fit a simple first order decay, suggesting that a complex process is occurring at this concentration.

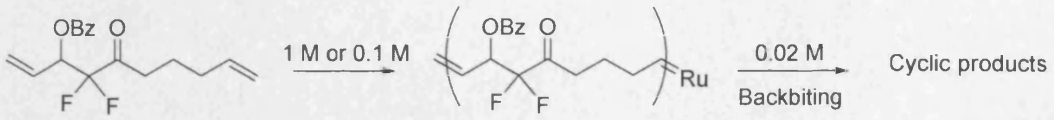

Scheme 76

A similar NMR experiment was performed after dilution to a substrate concentration 0.04 M (in diene **31**) after allowing 2 hours for oligomerisation. The stronger solution allowed for better signal to noise ratio in the NMR spectra (**Section 10, p35**). The results are shown in **Figure 64**, with acceptable linear fits from the plot in **Figure 65**.

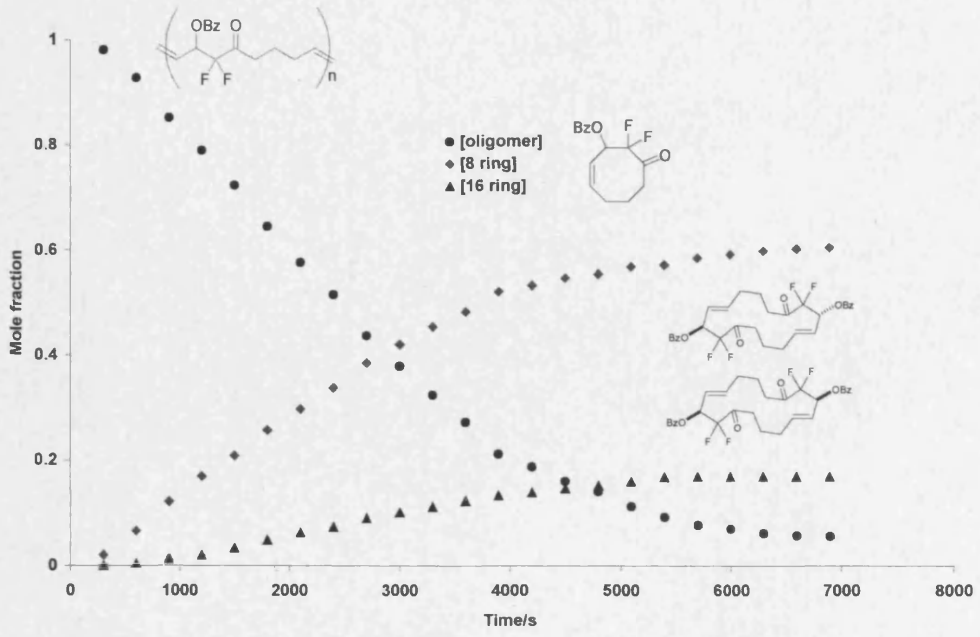

Figure 64 De-oligomerisation of benzoate 31 followed by ^{19}F NMR

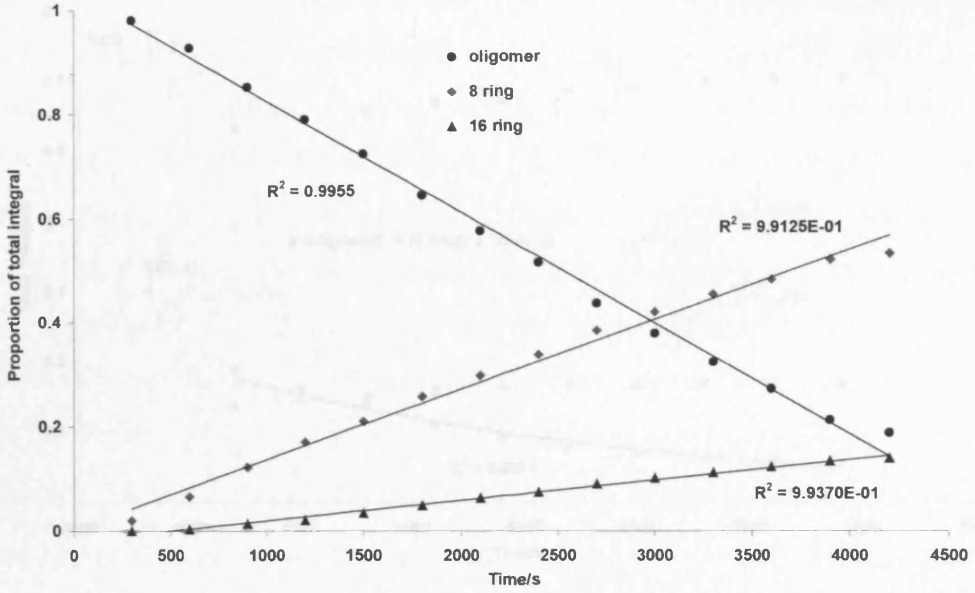

Figure 65 Linear portion of the deoligomerisation of 31 into cyclooctenone 33 and 16-membered rings 173 and 174

Figures 64 and **65** show that the mole fraction of oligomer appears to decrease linearly with time up to approximately 4000 seconds (75% of oligomer consumption), and that the concentrations of cyclooctenone **33** and 16-membered rings **173** and **174** increase linearly with time. The linearity suggests that the rate of back-biting of the oligomers to smaller products is independent of oligomer concentration and is dependent only on the concentration of the ruthenium-bound species, which is at saturation due to the large excess of oligomer to catalyst **29**. The rate of deoligomerisation is therefore only dependent on the rate at which the ruthenium catalyst can turn over. The loss of linearity in the decay of the oligomer after 75% of it has been consumed is due to the much reduced concentration of oligomer in solution relative to catalyst **29**, resulting in the reaction becoming first order in oligomer. **Figure 66** shows the later stages of the reaction (3900-6900 seconds), and includes a first order exponential fit for the consumption of the remaining oligomer. The R^2 value obtained for this is 0.98, which suggests that the reaction does become first order in oligomer once oligomer concentrations in the system become low.

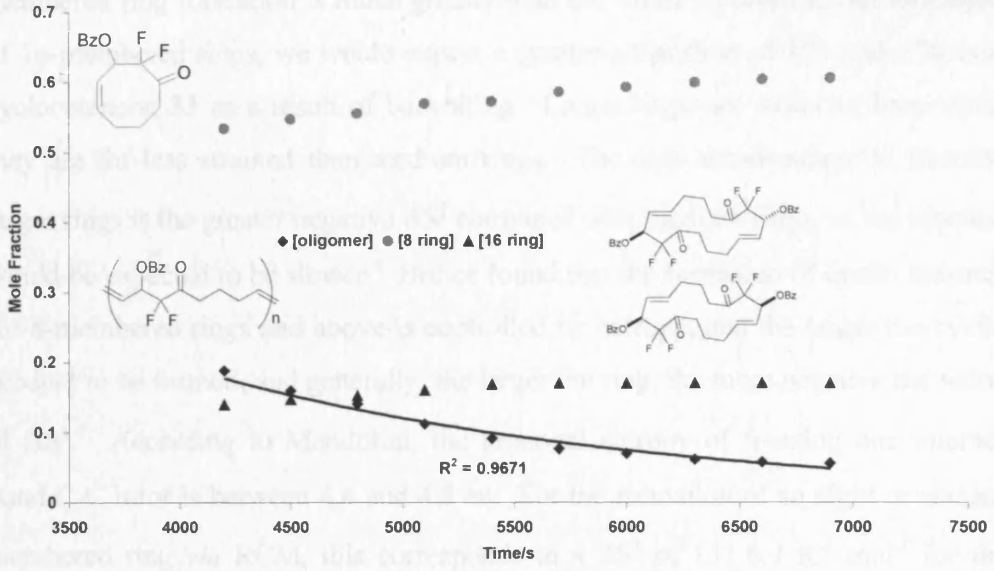

Figure 66 Latter portion of the deoligomerisation of benzoate 31 into cyclooctenone 33 and 16-membered rings 173 and 174, with exponential fit

The linear rates of formation of cyclooctenone **33** and 16-membered rings can be compared, and give an indication as to the relative effective molarities of the two species under these conditions (**Table 16**). The EM ratio under these conditions is 1.72, which suggests, surprisingly that cyclooctenone **33** formation is favoured over 16-membered ring formation. This corresponds to the earlier comparison of EM values calculated for cyclooctenone **33** and the two sixteen-membered rings, where $EM_8/EM_{16} = 2$. The relatively high EM value for benzoate **31** may imply that there is less strain than expected developed in the rate-determining step, or that there is a different rate-determining step for this substrate. This is discussed in greater detail in **4.3**.

Ring species	k_n	k_8/k_{16}
8	$1.35 \times 10^{-4}\ s^{-1}$	3.40
16	3.97×10^{-5}	

Table 16

The formation of greater amounts of cyclooctenone **33** relative to the two 16-membered rings **173** and **174** is surprising. Since the strain involved in 8-

membered ring formation is much greater than the strain involved in the formation of 16-membered rings, we would expect a greater proportion of **173** and **174** over cyclooctenone **33** as a result of backbiting. Larger rings are easier to form since they are far less strained than medium rings. The only disadvantage to forming larger rings is the greater negative $\Delta S^{\ddagger}$ compared with medium rings, so the reaction would be expected to be slower.[8] Bruice found that the formation of cyclic lactones for 8-membered rings and above is controlled by entropy, and the larger the cyclic product to be formed, and generally, the larger the ring, the more negative the value of $\Delta S^{\ddagger}$.[9] According to Mandolini, the torsional entropy of freezing one internal bond C-C rotor is between 4.4 and 4.8 eu. For the formation of an eight or sixteen membered ring *via* RCM, this corresponds to a $\Delta S^{\ddagger}$ of 131.6 J K^{-1} mol^{-1} for the eight-membered ring and 282 J K^{-1} mol^{-1} for the sixteen membered ring, assuming both systems are fully flexible, giving a $\Delta\Delta S^{\ddagger}$ of 150.4.[7] However, this may not take into account the extra flexibility of the sixteen-membered rings over the eight-membered ring, since larger rings have greater flexibility and can behave in a similar way to acyclic molecules.

This result, coupled with the relatively high effective molarity for the RCM of **31** may suggest that strain is not developed in the rate determining step as expected. However, these experiments were carried out using benzoate **31**, which exhibited an unusually high EM for cyclisation compared with other protecting groups, and this may affect the result. Further structural effects on reactivity and in-depth analysis are discussed in **4.3**.

Due to the method used for the calculations of the EMs for **4, 30, 31, 150, 210** and **211** we are unable to identify the mechanism *via* which the larger cyclic molecules are formed. They can form through cyclisation of acyclic oligomer, *via* backbiting of oligomers, or *via* ring opening of smaller rings and cyclisation of the resulting oligomers. At higher reaction concentrations, all of these pathways are possible routes of formation for larger cyclic species, and also oligomers.

Earlier studies on the cyclooctenone products suggested that their formation was irreversible, but the cyclic products had been re-exposed to metathesis catalyst **29**

only at those concentrations used for synthesis, so no ring opening was observed. Fogg's paper suggested the eight-membered rings should form larger products upon re-exposure to catalyst **29** at higher substrate concentrations.[21] Cyclooctenones **33** and **153** (CMe_2) were re-exposed to Grubbs' second generation catalyst **29** (5 mole %) at relatively high concentrations (0.1 M) overnight. After this time, the ^{19}F NMR spectra were recorded, at 300 K and 218 K respectively for the two substrates. After re-exposure of **33** to catalyst **29,** only a small amount of the cyclooctenone was visible, and the remainder of the product mixture contained some 16-membered ring and oligomer. Upon re-exposure of **153**, the major product in the mixture was still 8-membered ring, along with small amounts of 16-membered ring, which suggests that the dimethyl group stabilises the 8-ring, or slows down the addition of the Ru-alkylidene to the alkene, which results in lower reversibility at this concentration. This result indicates that the reaction is subject to a positive Thorpe-Ingold effect, since *gem*-dimethylation at the position homoallylic to the Type I double bond increases the effective molarity and stabilises the final 8-ring product. This observation is in agreement with Bruice's findings, that the rate of ring opening is reduced for the dialkylated substrates.[9]

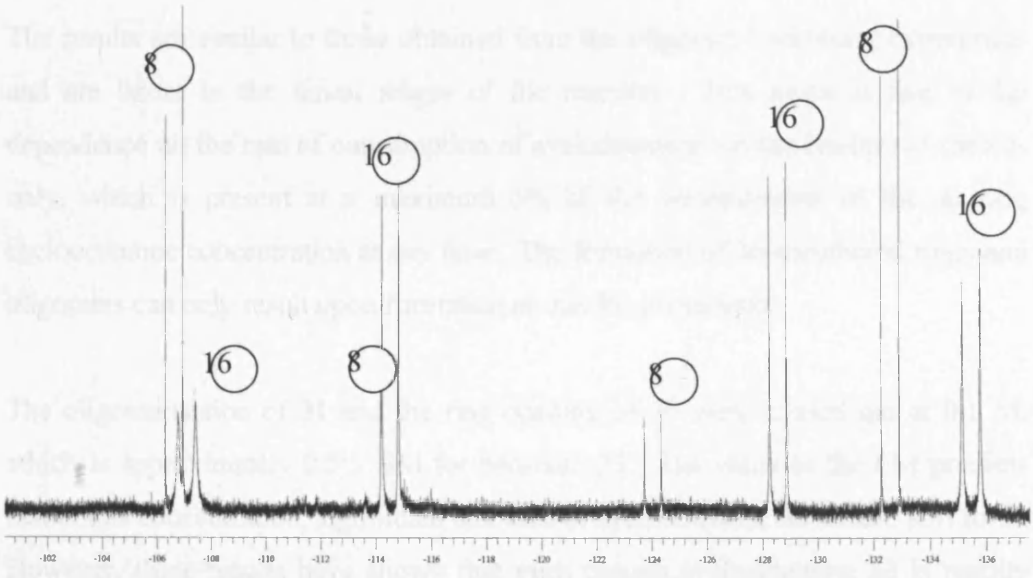

Figure 67 ^{19}F NMR spectrum at 218 K for ring opening of 153 with 5% 29, 0.1 M

^{19}F NMR was also used to investigate the rate of ring opening of cycloctenone **33** at 313K in $CDCl_3$. The reaction was carried out at 0.1 M, with 5% Grubbs' second

generation catalyst. The resulting spectra were integrated to yield the results shown in **Figure 68**.

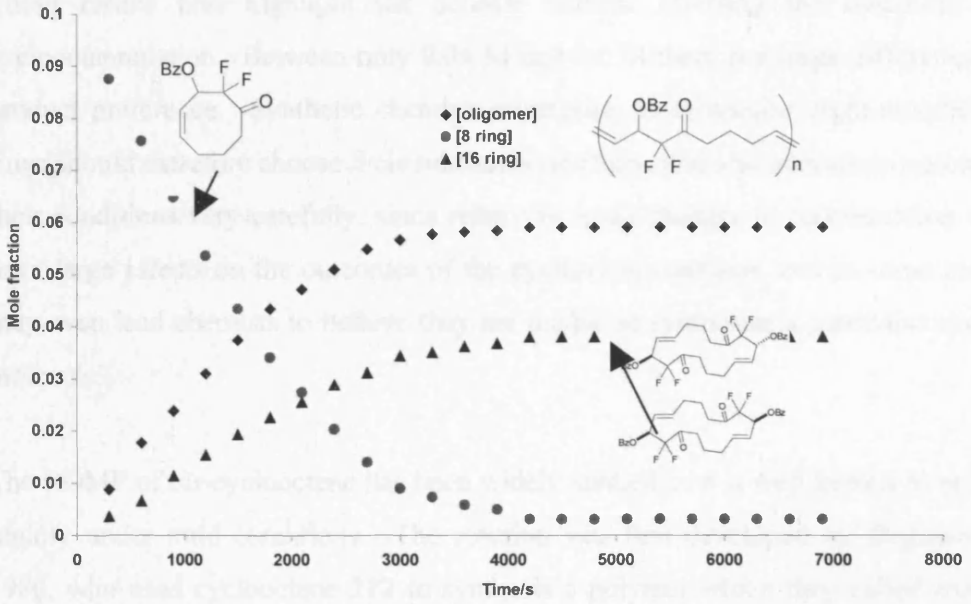

Figure 68 Ring opening of 33 with 5% 29 at 0.1 M in $CDCl_3$ at 313 K (Section 10, p33)

The results are similar to those obtained from the oligomer backbiting experiment and are linear in the initial stages of the reaction. This again is due to the dependence on the rate of consumption of cyclooctenone on the Ru-bound species only, which is present at a maximum 5% of the concentration of the starting cyclooctenone concentration at any time. The formation of 16-membered rings and oligomers can only result upon formation of this Ru-alkylidene.

The oligomerisation of **31** and the ring opening of **33** were carried out at 0.1 M, which is approximately 0.5 x EM for benzoate **31**. The value of the EM predicts that at this concentration, significant amounts of cyclooctenone **33** should still form. However, these results have shown that even though cyclooctenone **33** is readily formed at 0.1 M, it is also readily ring opened to larger rings and oligomers.

The results from the oligomer backbiting experiments show us that there is very little oligomer present at lower concentrations (0.02 and 0.04 M), and that the

dominant products are eight-membered ring, and to a lesser extent 16-membered rings.

These results also highlight the delicate balance affecting the outcomes of cyclooctannulation. Between only 0.04 M and 0.1 M there is a large difference in product preference. Synthetic chemists attempting to synthesise eight-membered rings should therefore choose their substrates carefully, and also attempt to optimise their conditions very carefully, since relatively small changes in concentration can have large effects on the outcomes of the cyclisation reactions, and in some cases may even lead chemists to believe they are unable to synthesise a particular cyclic molecule.

The ROMP of *cis*-cyclooctene has been widely studied as it is well known to occur rapidly under mild conditions. The reaction was first developed by Degussa in 1980, who used cyclooctene **212** to synthesis a polymer which they called *trans*-polyoctenamer (TOR) in the presence of a WCl_6-based catalyst.[x] They found that the product mixture contained two major products – a high molecular weight polymer (around 10^5 Da) and cyclic oligomers, which are likely to have formed *via* backbiting of larger oligomers. Castarlenas studied the rapid ROMP of cyclooctene at 20°C. The group observed complete solidification of the sample, despite only 63% recovery of the resulting polymer.[78] Very little study of the actual kinetics of *cis*-cyclooctene polymerisation has been undertaken, probably because the reaction is so rapid that it may be considered almost impossible to follow at meaningful concentrations.

More recently Kress used ^1H and ^{13}C NMR to identify the products of tungsten-carbene catalysed ring opening of *cis*-cyclooctene.[19,69,79] The cycloalkene was completely consumed within one hour at -23°C. It appeared that the major product of the ring opening reaction consisted of a range products with of long polymer chains, since substantial formation of a white precipitate was observed. In contrast to the observation of the ring opening reaction of cycloheptene and cyclohexene, significant amounts of cyclic dimer were not observed, and it was concluded that this was present although only in statistical amounts. The group also found that the

polymers arising from the ring opening of cylooctenone do not undergo depolymerisation back to the monomer at or below room temperature.

We made an attempt to follow the ROMP of **212**, using ^{1}H NMR (400 MHz), following the proton signals in the alkene region to track changes. The experiment was run in CD_2Cl_2 (0.02M, the minimum concentration at which the experiment could be run due to the small amount of cyclic olefin used) at room temperature, with 1% Grubbs' second generation catalyst **29**. Although the reaction is rapid, and much of the cyclic olefin had been consumed before the first spectrum could be acquired, we were able to follow conversion in the latter 20% of the reaction (**Figure 69**).

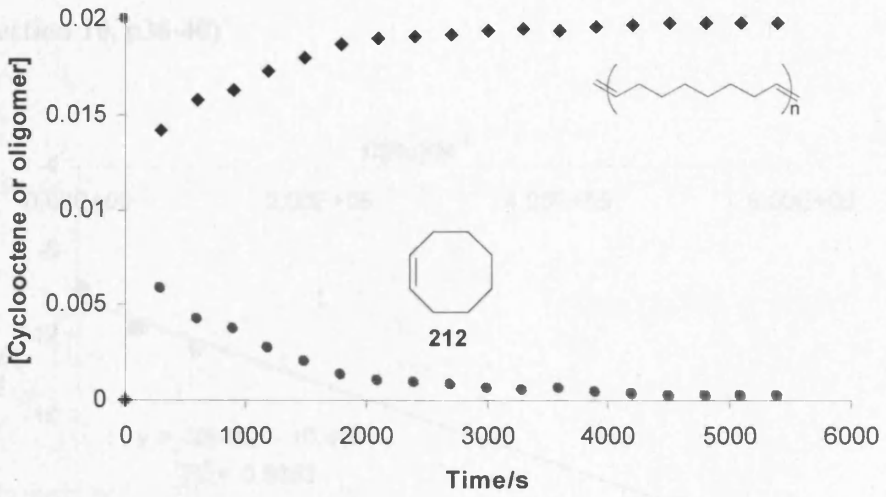

Figure 69 Ring opening of cyclooctene 212 with 1% Grubbs' II, followed by ^{1}H NMR at 25°C (Section 10, p37)

Figure 69 clearly shows that the ring opening of cyclooctene is very rapid even with a low loading of catalyst. The reaction was followed using the same NMR conditions with 0.1, 0.05 and 0.01% loadings of catalyst **29** (overlay **Figure 70**), in order to generate the plot shown in **Figure 71** and enable the closest comparison possible to the ring opening of cyclooctenone **33** by using the line of best fit to extrapolate back to the same concentration of ruthenium in the two ring opening reactions. In the case of the ring opening of **212** with 0.01% **29**, an end point was taken after 16 hours). The calculation of k_{cat} is given in **Table 17**.

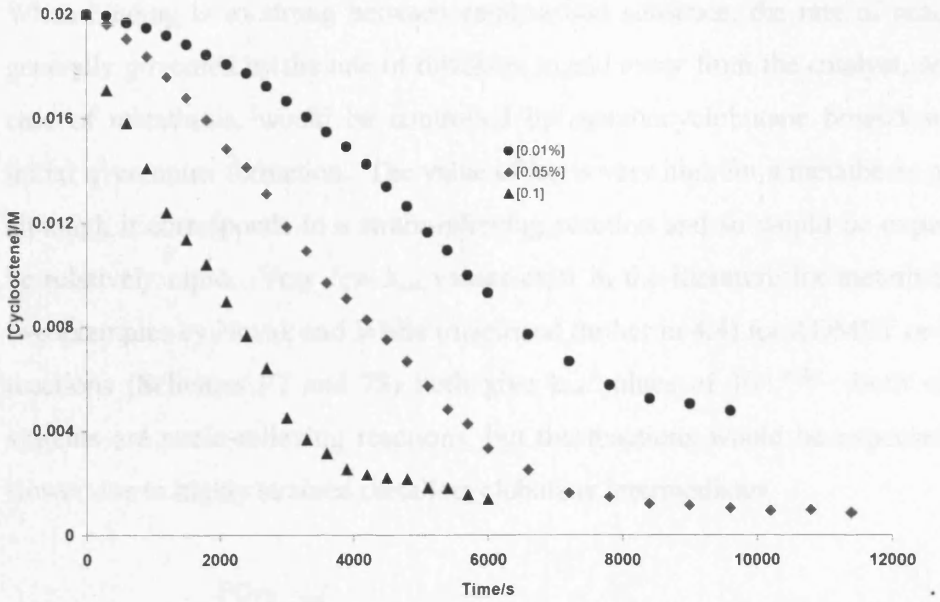

Figure 70 Overlays for cyclooctene ring opening with 0.1, 0.05 and 0.01% 29 (Section 10, p38-40)

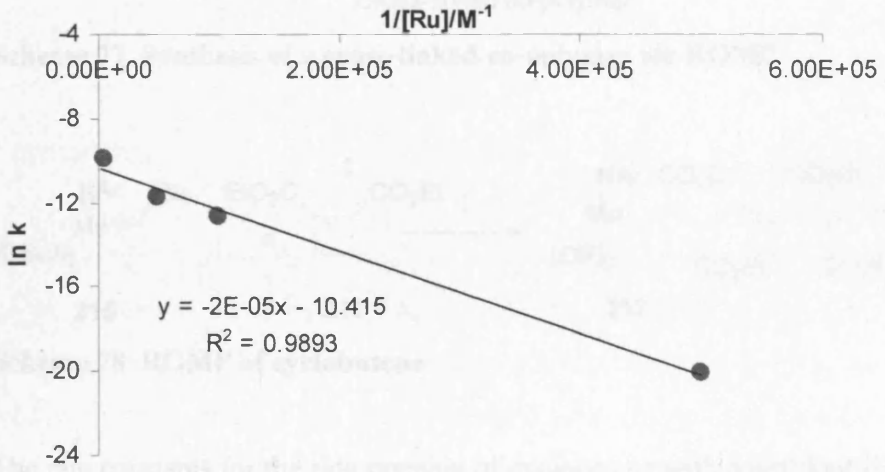

Figure 71 Lineweaver Burk plot for ring opening of *cis*-cyclooctene

V_{max}	9.60×10^{-2} s^{-1}
K_M	1.92×10^{-6} M
k_{cat}	96.0 s^{-1}

Table 17 Calculation of k_{cat}

The values obtained from the Lineweaver-Burk plot show a very small (10^{-6}) K_M, which suggests a very strong binding between the ruthenium catalyst and diene.

When binding is so strong between catalyst and substrate, the rate of reaction is generally governed by the rate of diffusion to and away from the catalyst, so in the case of metathesis, would be controlled by metallocyclobutane breakdown, and initial η^2 complex formation. The value of k_{cat} is very high for a metathesis process, although it corresponds to a strain-relieving reaction and so would be expected to be relatively rapid. Very few k_{cat} values exist in the literature for metathesis, but two examples by Novak and White (discussed further in **4.4**) for ADMET or ROMP reactions (**Schemes 77** and **78**) both give k_{cat} values of 10^{-1}.[80,81] Both of these systems are strain-relieving reactions, but the reactions would be expected to be slower due to highly strained metallocyclobutane intermediates.

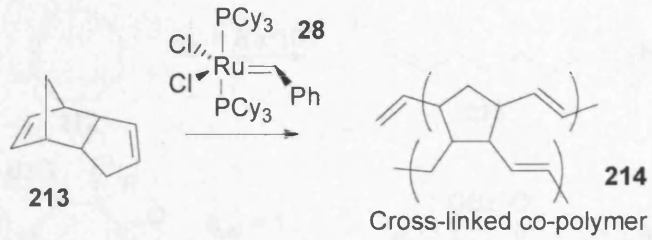

Scheme 77 Synthesis of a cross-linked co-polymer *via* ROMP

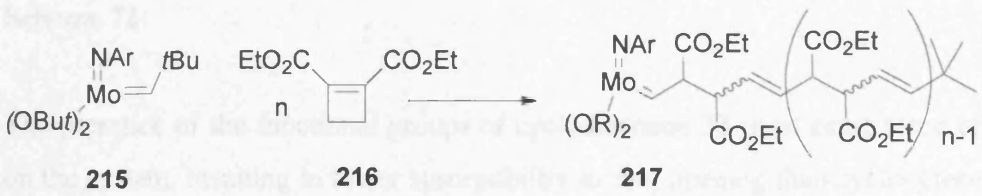

Scheme 78 ROMP of cyclobutene

The rate constants for the ring opening of cyclooctene with equivalent [Ru] for the two ring opening reactions are shown in **Table 18**.

	Rate of Ring Opening, k/s^{-1}
Cyclooctene	2.34
33	3×10^{-5}

Table 18

The results shown in **Table 18** show a 78,000-fold difference between the two rates of ring opening (**Scheme 72**). Unfortunately, a closer comparison between the two

reactions was not possible, since the ring opening of *cis*-cyclooctene would have been too rapid to follow at 0.1M, and the maximum concentration at which the reaction could be followed was 0.02M. In contrast, the formation of cyclooctenone **33** takes place at 0.02M, and the ring opening does not occur at this concentration. The ring opening was followed at higher concentrations (0.1 M). The above dataset generates the closest possible comparison between the two eight-membered rings, and may also give an idea of the concentrations at which *cis*-cyclooctene **212** is formed by RCM. This result gives us an indication of the relative susceptibilities of the two cyclooctenes to ring opening by Grubbs' second generation catalyst, as well as their relative stabilities.

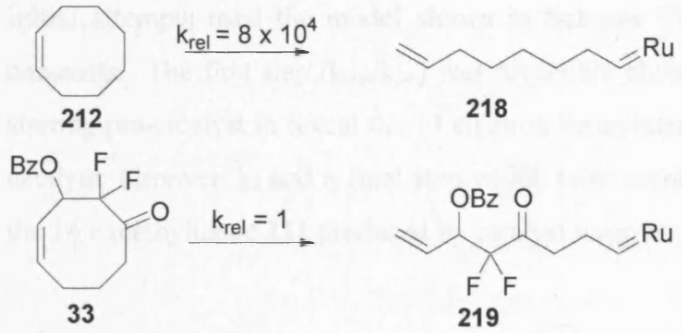

Scheme 72

The presence of the functional groups of cyclooctenone **33** must exert some effect on the system, resulting in lower susceptibility to ring opening than cyclooctene. It also appears that the benzoate protecting group adds some stability to the eight-membered ring, since it can be synthesised at relatively high concentrations (20 mM) compared with alcohol **4** (1 mM). The reason for this may be the formation of a chelate, as described my Mulzer, which blocks either the ring opening event, or the subsequent formation of cross metathesis products.[32]

4 Analysis of Kinetic Data

4.1 NMR Kinetics on Catalyst

The analysis of the data from the initial competition experiments using the double exponential expression in **Equation 2** showed that this treatment of the data was not sufficient to take into account the multi-step mechanism of RCM. Using data simulation in Excel would require extremely complex sets of kinetic expressions, so a kinetic modelling package, Berkeley Madonna was used to simulate the reaction, to generate the best possible fit for all data generated from the kinetic studies.

Initial attempts used the model shown in **Scheme 79** which is based on 5 rate constants. The first step (k_{diss}/k_{ass}) was reversible phosphane dissociation from the starting pre-catalyst to reveal the 14 electron benzylidene catalyst **220**, followed by catalytic turnover, k_1 and a final step which took account of the decomposition of the 14 e methylidene **221** produced by catalyst turnover, k_d.

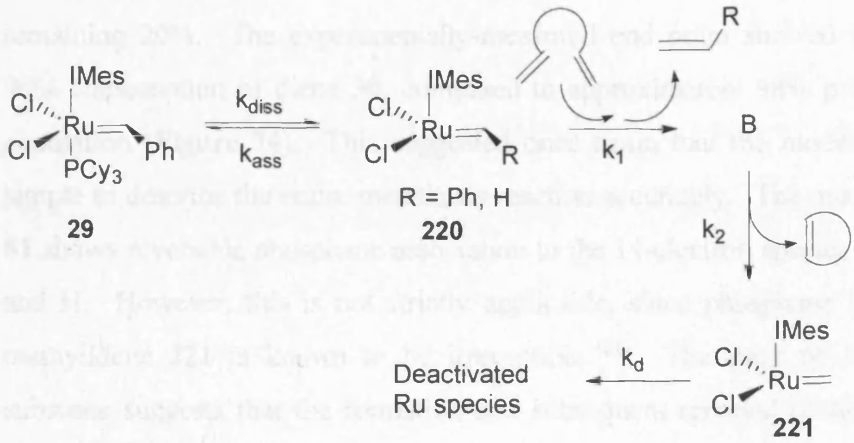

Scheme 79 Initial Model for RCM

This model neglects reversible homodimerisation and heterodimerisation on the basis that the conditions under which the reaction kinetics were followed deliver the eight-membered ring product cleanly. Reversible homodimerisation is known to be a first step in most alkene metatheses, but at low substrate concentration, it should not account for significant quantities of material.[22] ^{19}F NMR analyses at the end of the kinetic reactions (218 K) did not reveal the presence of any species other than

the cyclooctenones, unless dienes were incompletely consumed, in which case, the starting diene remained unabiguously visible.[83]

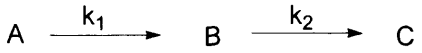

Scheme 80

The k_1 step in which the intermediate B forms in **Scheme 80** is a combination of several steps in the metathesis mechanism, and the use of only one rate constant assumes that the step shown occurs without significant build up of intermediates and with one step which determines the rate. The 'rate constants' derived from the simulation experiments combine several steps in one, and this raises issues with the interpretation of any data derived from fitting experimental data to these models. This will be discussed in greater depth in this chapter.

Encouragingly, the model fitted the data for the RCM of **149** in the Thorpe-Ingold competition experiment perfectly (**Figure 73**), but problems arose in the case of the slower substrate. The model fitted the initial 80% of the reaction well, but not the remaining 20%. The experimentally-measured end point showed approximately 90% consumption of diene **30**, compared to approximately 98% predicted by the simulation (**Figure 74**). This suggested once again that the model was still too simple to describe the entire metathesis reaction accurately. The model in **Scheme 81** shows reversible phosphane association to the 14-electron species where R = Ph and H. However, this is not strictly applicable, since phosphane binding to the methylidene **221** is known to be irreversible.[42,43] The poor fit for the slower substrate suggests that the formation and subsequent removal of the methylidene **221** should be taken into account by the model.

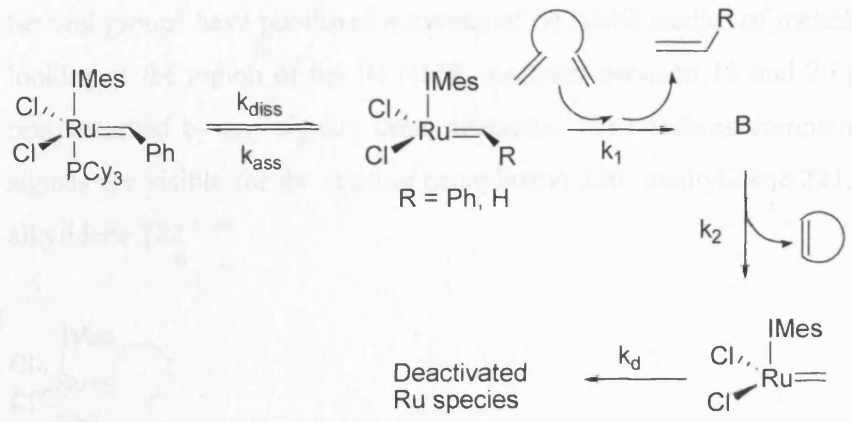

Scheme 81

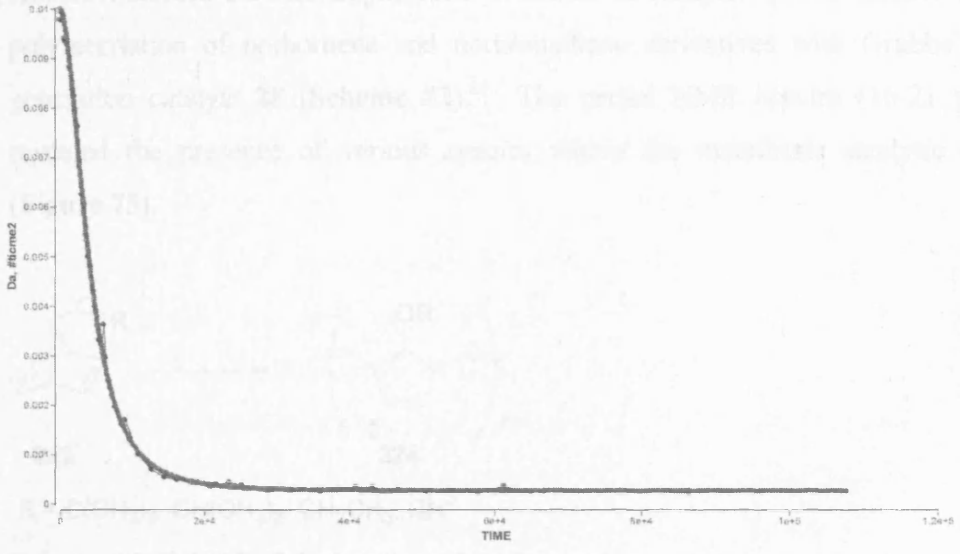

Figure 73 Fit obtained from Berkeley Madonna for RCM of 149

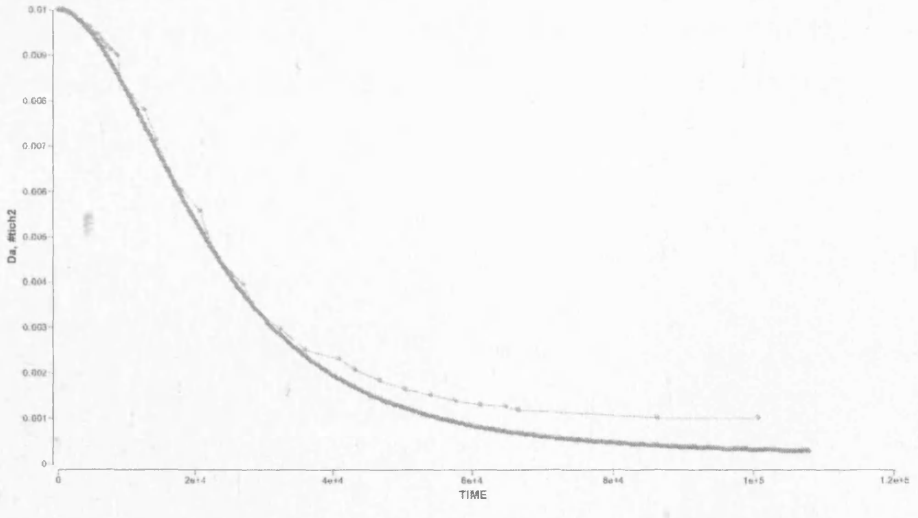

Figure 74 Fit obtained from Berkeley Madonna for RCM of 30

Several groups have published accounts of ^{1}H NMR studies of metathesis catalysts, looking at the region of the ^{1}H NMR spectrum between 15 and 20 ppm, which is not perturbed by any signals from substrates. The authors comment that discrete signals are visible for the starting benzylidene **220**, methylidene **221**, and substrate alkylidene **222**.[79,84]

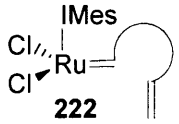

222

Khosravi studied the consumption and evolution of catalytic species formed in the polymerisation of norbornene and norbornadiene derivatives with Grubbs' first generation catalyst **28** (**Scheme 82**).[84] The partial NMR spectra (16-21 ppm), revealed the presence of various species within the metathesis catalytic cycle (**Figure 75**).

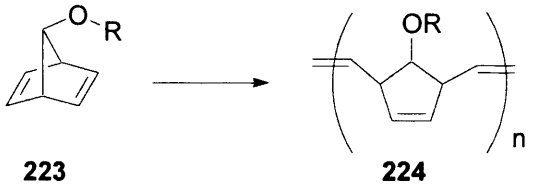

223 **224**

R = $C(CH_3)_3$, $CH(CH_3)_2$, CH_2CH_3, CH^3

Scheme 82 ROMP of derivatives of norbornadiene

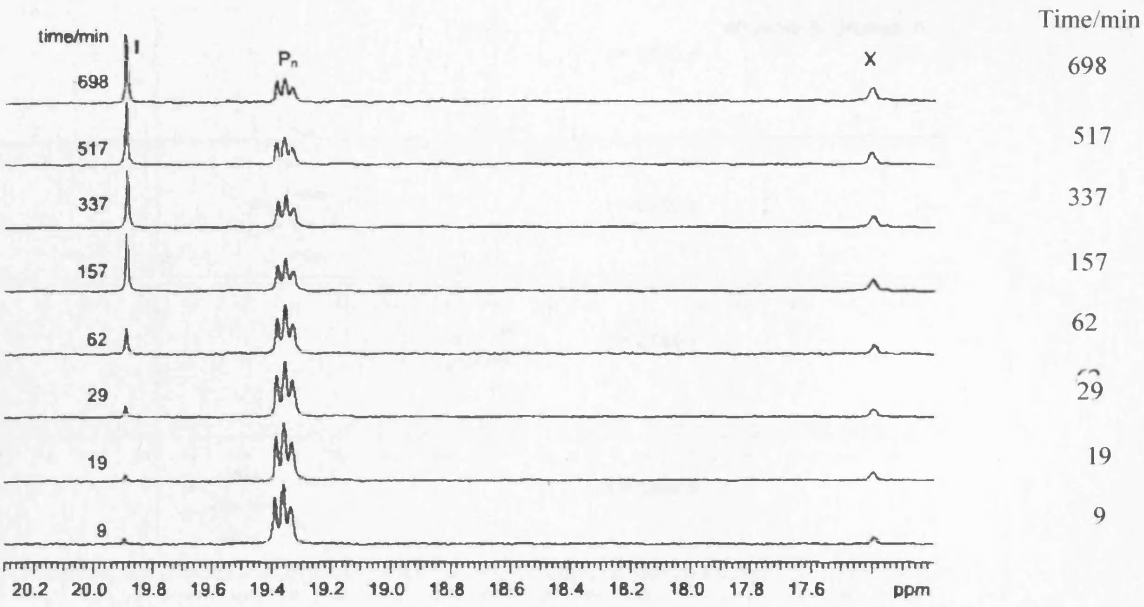

Figure 75 Stack plot showing the alkylidene region of the ^{1}H NMR spectra for the first 12 hours of the ROMP reaction of 223 in $CDCl_3$ (from Ref. 84)

We decided to adopt this approach in order to identify important mechanistic processes which may need to be accounted for when modelling the reaction accurately. Using substrate **31** in CD_2Cl_2 and varying loadings of catalyst **29** (5-60%), we followed the decay and formation of various catalyst species in the Grubbs' second generation catalytic cycle at 25°C at 400 MHz from 11-20 ppm. Luckily, all of the species observed have discrete signals in the ^{1}H NMR spectrum allowing easy identification and integration. ^{1}H NMR spectra were also acquired at 600 MHz to allow better resolution and separation in more complex signals appearing throughout the experiments. **Figure 76** shows some NMR spectra generated from these experiments over time, with 40% Grubbs' second generation catalyst **29**.

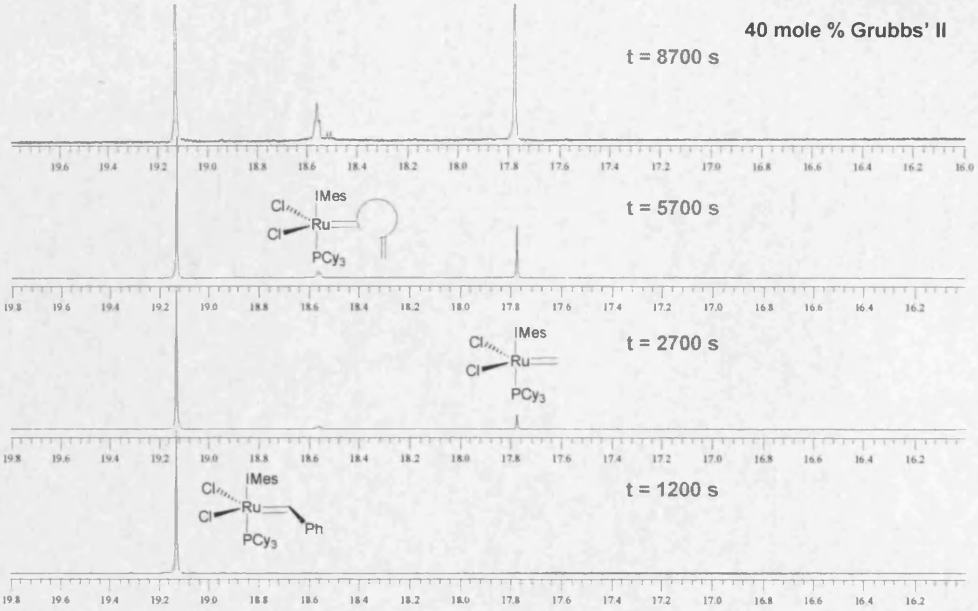

Figure 76 ^{1}H NMR (400 MHz) stack plot for RCM of 31 with Grubbs' second generation catalyst 29 in CD_2Cl_2 at 300 K

Figure 79 shows a plot for the NMR experiment carried out using 30% catalyst **29**, which clearly shows consumption of starting benzylidene **29** and subsequent formation of intermediate alkylidene **222** and methylidene **221** (**Scheme 83**). Upon formation of the methylidene **221** the catalyst has turned over once and the propagating species is now the methylidene. ^{1}H NMR allowed five distinct Ru-alkylidene species to be followed through the time window of the experiment.

^{1}H-^{1}H COSY analysis of the full spectral region between 0-20 ppm was carried out to support the hypothesis that the triplet appearing at 18.6 ppm was indeed the substrate alkylidene. If this triplet was the substrate alkylidene, a cross peak between the triplet and alkyl region of the NMR spectrum should be observed. This cross peak was indeed observed, with some apparent shielding of the alkyl protons since they had shifted slightly upfield, and broadened (**Figures 77** and **78**).

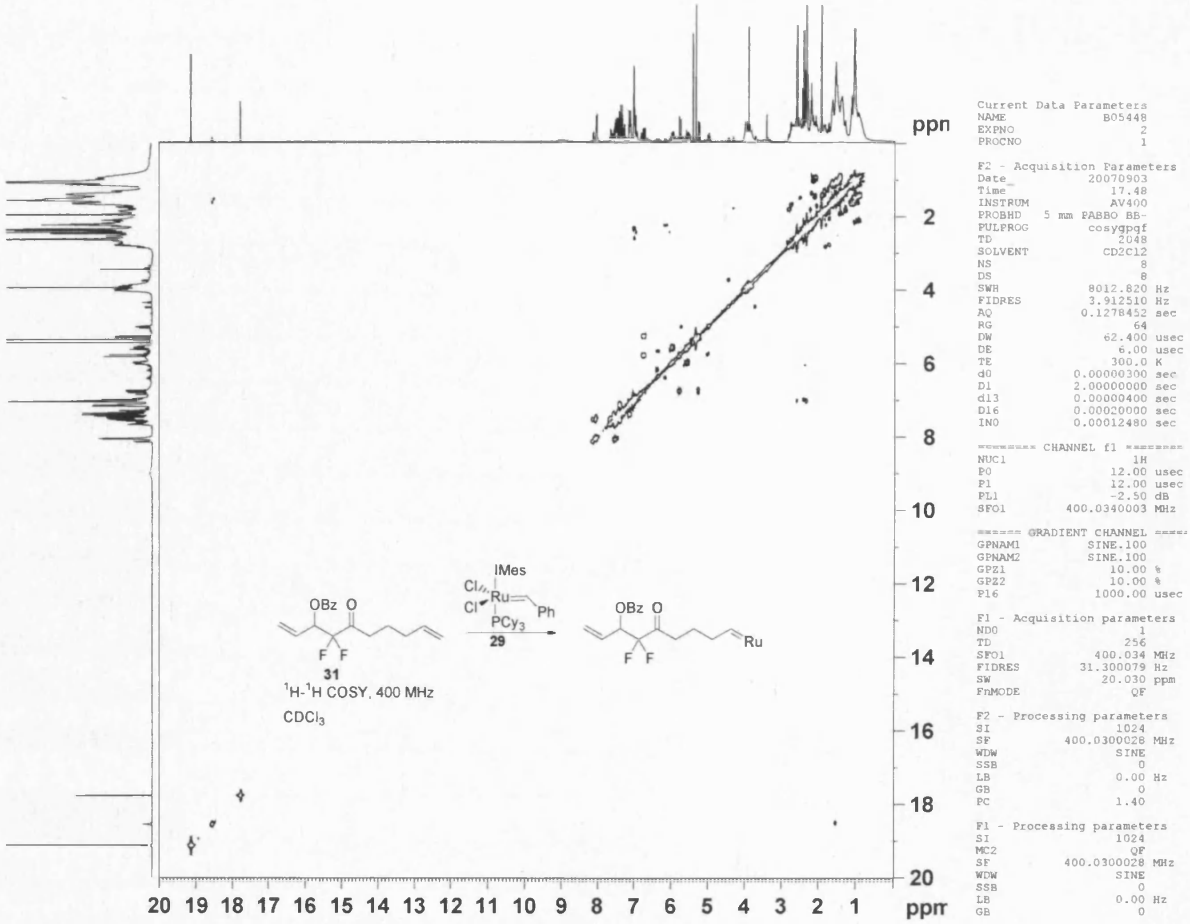

Figure 77 ^{1}H-^{1}H COSY showing full spectral region 0-20 ppm

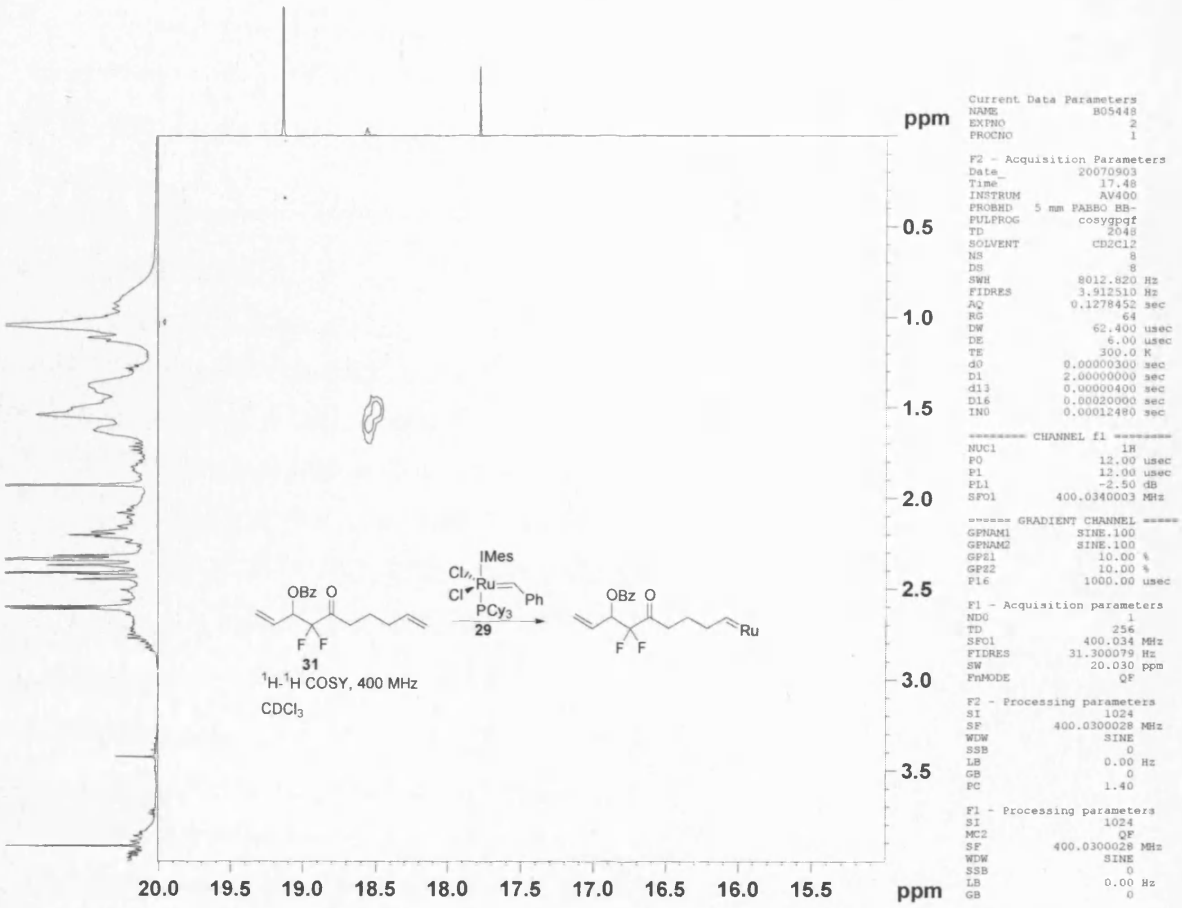

Figure 78 Partial ^{1}H-^{1}H COSY showing clear crosspeak between substrate alkylidene 222 and methylene region.

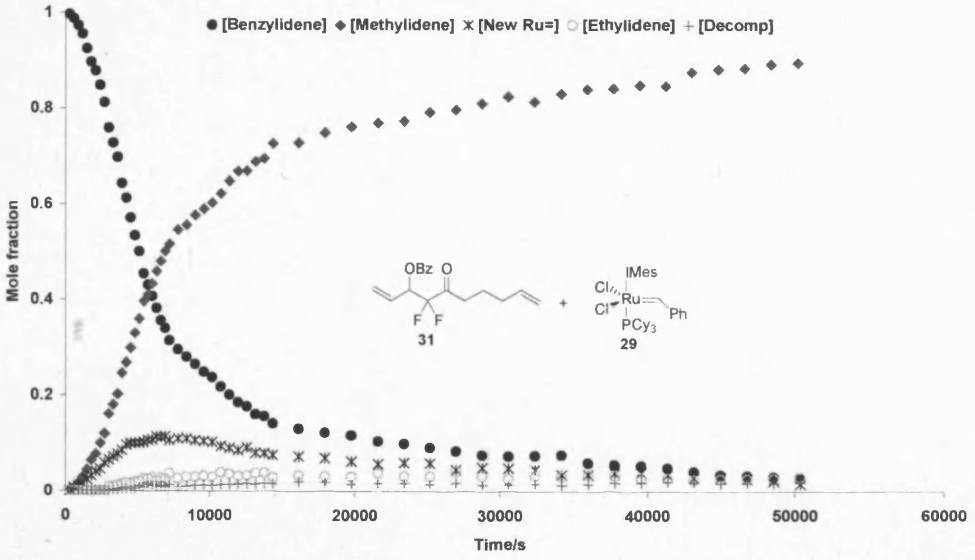

Figure 79 ^{1}H NMR results from RCM of 31 with 30% 29 in CD_2Cl_2 at 300 K (Section 10, p17)

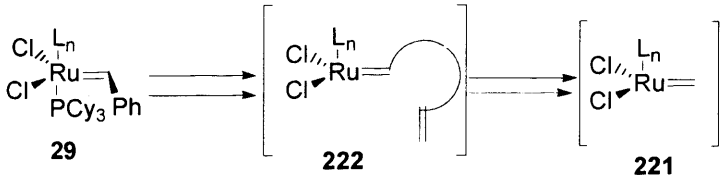

Scheme 83 Formation of substrate alkylidene 222 and methylidene 221 from ruthenium pre-catalyst 29

Other unknown species also appeared in the NMR spectra, suggesting that catalytic decomposition pathways are kinetically significant within the timescale of the reactions we are interested in, and are perhaps the cause of several of the substrates not reaching completion. Once the methylidene has formed, catalytic deactivation pathways become possible. The most well-documented decomposition pathway for the methylidene is the irreversible capture of the phosphane ligand.[42,43] Unlike phosphane capture by the benzylidene, phosphane capture by the methylidene is not reversible, and leads to the formation of decomposition products, a by-product of which can be identified in the ^{31}P NMR spectrum. In order to identify if our kinetic experiments were subject to significant catalyst deactivation over the reaction timescale, the relatively fast RCM of alcohol **22** was followed using 2 mole % **29** at 25°C. The reaction was followed for one hour and left to stir for a further two hours, before adding a further portion of alcohol **22** and following the consumption of diene for a further hour. This was repeated once more and results are shown in **Figure 80**.

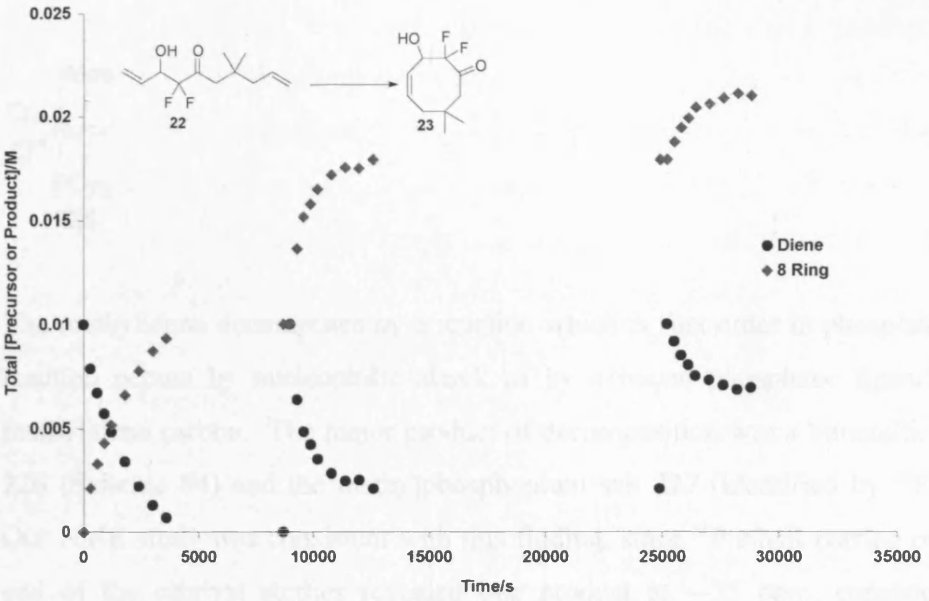

Figure 80 Investigation of lifetime of catalyst 29 in the RCM of 22 (Section 10, p70)

The results shown in **Figure 80** show that even at 25°C, after only three hours, the catalyst is significantly less effective than the initial charge, and upon addition of a third charge of alcohol **22**, catalytic activity is approximately 70% lower than the initial charge, after only seven hours. This result has implications for metathesis reactions as it highlights the finite lifetime of the catalyst, even at 25°C. For reactions which are generally carried out at reflux, the catalyst lifetime may be even shorter, as catalytic decomposition pathways are accelerated with higher temperature. This suggests that leaving reactions under reflux for long periods of time is not productive, as the majority of the catalyst will already be deactivated. Pursuing challenging reactions to completion would therefore require a further addition of pre-catalyst.

Few accounts or studies of the catalytic decomposition pathways have been carried out. Grubbs studied the degradation of a variety of ruthenium metathesis catalysts, identifing the major pathway of decomposition of the methylidene species, and found that all methylidene-phosphane complexes decompose to generate methyl phosphonium salts.[42] The phosphane-bound ruthenium methylidene is the least stable ruthenium alkylidene in the metathesis reaction. The half life of the Ru-IMes complex **225** was found to be approximately 5 hours 40 minutes.

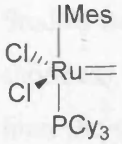

225

The methylidene decomposes by a reaction which is first order in phosphane. The reaction occurs by nucleophilic attack of by a bound phosphane ligand on the methylidene carbon. The major product of decomposition was a bimetallic species **226** (**Scheme 84**) and the methylphosphonium salt **227** (identified by ^{31}P NMR). Our NMR study was consistent with this finding, since ^{31}P NMR carried out at the end of the catalyst studies revealed one product at ~-35 ppm, consistent with Grubbs' observations. Further evidence for decomposition of the catalyst was found in the ^{1}H NMR spectrum in the alkylidene region, where after approximately 20 hours, no signals were visible in this region.

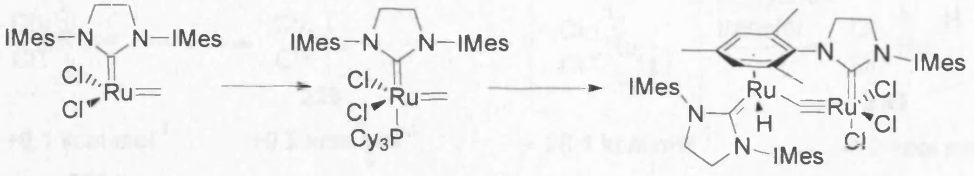

221 Active **225** Inactive **226** Deactivated

Scheme 84 Deactivation of methylidene

A further signal which appeared in the spectrum in the latter stages of the experiment was a quartet. This signal can only arise from ethylidene **228** (**Figure 81**). Grubbs suggested that a further possible route for deactivation of the catalyst was C-H abstraction from the L-type ligand (the NHC ligand in the case of Grubbs' second generation catalyst).

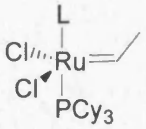

228

The ligands play a key role in enabling, or disabling the deactivation pathways. Studies have found a general correlation between higher catalyst activity and the shortness of catalyst lifetime.[50] To a certain extent, catalyst design strategies can limit the occurrence, or rates of these pathways. However, van Rensburg recently published some findings on substrate-mediated catalyst deactivation and degenerate ethylene metathesis, and produced experimental and theoretical evidence for β-hydride transfer within the metallocyclobutane.[50,85] This results in the formation of an allyl-ruthenium hydride, in a process which competes with productive metathesis. The group's computational analysis showed that the hydride transfer pathway was easily accessible, and that this pathway would result in the formation of π-allyl species **230** (**Scheme 85**). The calculated barrier for the formation of these species from the second generation catalysts with NHC-type ligands, was lower than that for the first generation catalysts, with phosphane ligands, which may account for the known isomerisation activity of second generation-type catalysts.

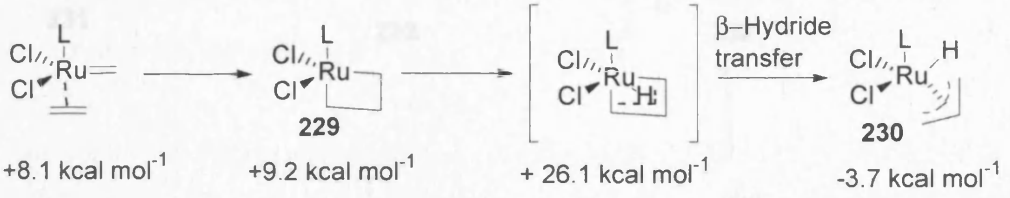

Scheme 85 Hydride transfer pathway upon degenerative ethylene metathesis by methylidene

Experimental evidence for this was found by Wagener who described the formation of a quartet in the Ru-alkylidene region of the ^{1}H NMR spectrum when studying the ADMET of 3-methyl pentene with catalyst **29** (**Figure 82**).[86] The mechanism described by Van Rensburg can explain formation of to the isomerised alkene, and can give result in the formation of the ethylidene (**Scheme 86**).

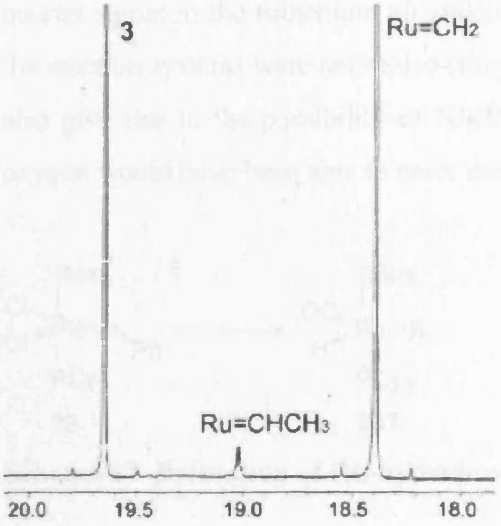

Figure 82 ^{1}H NMR of alkylidene region for reaction of 3-methyl pentene with Grubbs' second generation catalyst 29 (from Ref. 86)

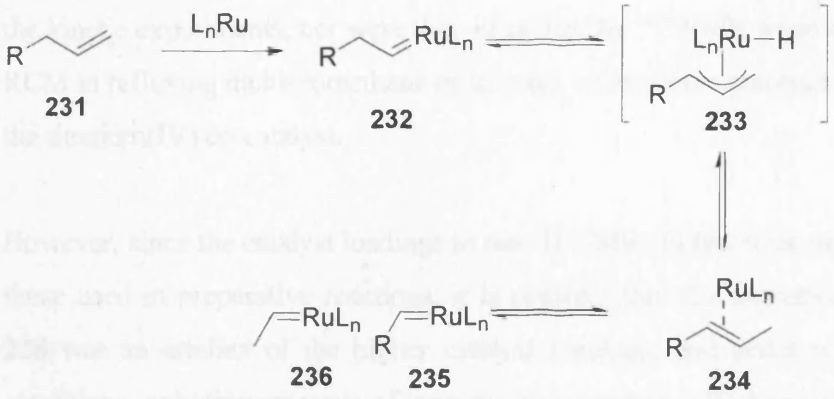

Scheme 86 Possible route of formation of ethylidene *via* double bond isomerisation

The authors attribute the formation of the $L_nRu{=}CHCH_3$ species to double bond migration along the alkene, which is known to occur readily with ruthenium-NHC metathesis catalysts. Mol found that the formation of the ruthenium hydride species formed readily from the second generation-type metathesis catalysts (**Scheme 87**), even at low temperatures, in the presence of oxygen or primary alcohols.[87] Complex **237** was found to be able to perform metathesis reactions, but also effected double bond isomerisation of 1-octene. It is possible that within the system studied by NMR, the presence of oxygen in the system allowed for the formation of complex **237**, which resulted in the isomerisation product, and the appearance of the

quartet signal in the ruthenium alkylidene region of the ^{1}H NMR spectrum. Since the reaction systems were not sealed (this would affect the reaction equilibrium, and also give rise to the possibility of NMR tube lids coming off within the magnet) oxygen would have been able to enter the system easily.

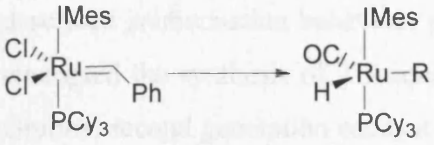

29 237

Scheme 87 Formation of Ru-hydride species from catalyst 29

However, as described in **3.1**, we did not observe any such isomerisation in our system, since this would lead to the formation of the corresponding seven membered ring (**Scheme 88**), and no traces of this were detected by GC-MS during the kinetic experiments, nor were they identified by ^{19}F NMR when carrying out the RCM in refluxing dichloromethane or toluene, either in the presence and absence of the titanium(IV) co-catalyst.

However, since the catalyst loadings in our ^{1}H NMR studies were much higher than those used in preparative reactions, it is possible that the formation of ethylidene **228** was an artefact of the higher catalyst loadings, and under normal synthetic conditions, only tiny amounts of isomerisation product, which would be difficult to detect, are formed.

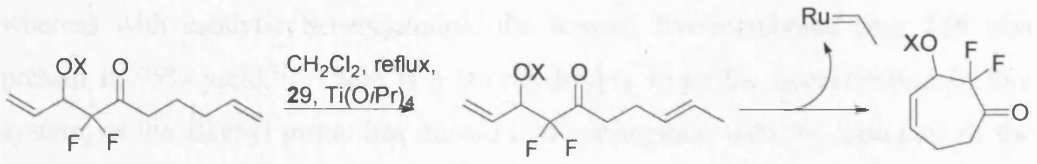

238 239 240

Scheme 88 Isomerisation of a diene followed by RCM to a seven-membered ring

The formation of isomerisation product, although never observed with our diene systems, is often an issue in the synthesis of cyclic olefins. The higher likelihood of the double bond migration occurring in the presence of the second generation-type

ruthenium catalysts suggests that groups which observe this undesired migration should attempt to synthesise their cyclic olefins with a first generation-type catalyst such as **28**, with which isomerisation is much less likely to occur.

Wagener reported isomerisation behaviour in second generation-type catalysts and described isomerisation behaviour previously reported by Kinderman.[88] The group attempted the synthesis of 21-membered cyclic lactone **242** from diene **241** using Grubbs' second generation catalyst **29**. The major product was the desired lactone, however between 2-12% of the isomerisation product **243**, the 20-membered cyclic lactone was also isolated.

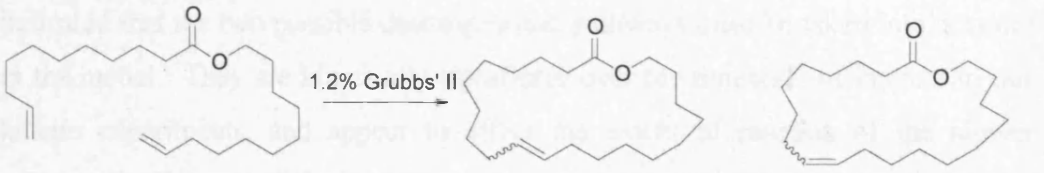

241 **242** 21-membered lactone **243** 20-membered lactone 2-12%

Scheme 89 Double bond migration in the synthesis of macrocyclic lactones *via* RCM

Grubbs, and more recently Rutjes have reported the use of a catalytic amount of benzoquinone in RCM reactions, which has been shown to inhibit double bond isomerisation.[89,90] Grubbs carried out the cyclisation of diallyl ether **244** (**Scheme 90**) in CD_2Cl_2 and followed the reaction by ^1H NMR, and found that in the absence of benzoquinone, the major product was the isomerisation product **246** (95%), whereas with catalytic benzoquinone, the desired five-membered ring **245** was present in 95% yield.[91] There is a strong driving force for isomerisation in this system, as the alkenyl group has moved into conjugation with the lone pair of the oxygen.

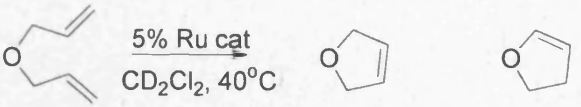

244	**245**	**246**
Without benzoquinone:	5%	95%
10 mol % benzoquinone	95%	5%

Scheme 90 Inhibition of double bond isomerisation with benzoquinone

If in our eight-membered ring syntheses, this double bond isomerisation was occurring, the resulting diene **239** would be expected to undergo slower cyclisation, despite formation of the less strained seven-membered ring **240**. The metathesis would be expected to start on the less substituted alkene terminus, but would be expected to encounter some degree of steric hindrance from the terminal methyl group. However, the evolution of gaseous propene from the reaction would still be expected to provide an entropic driving force for the cyclisation reaction.

The NMR studies showed that catalyst stability is a key issue in these reactions, and indicated that the two possible decomposition pathways must be taken into account in the model. They are kinetically significant over the timescale of interest in our kinetic experiments, and appear to affect the extent of reaction of the slower substrates. The use of Grubbs' second generation catalyst **29** also means that the formation of the ethylidene species must be taken into consideration, since this is clearly kinetically significant for these catalysts, since the quartet signal in the ^{1}H NMR spectra of the Ru-alkylidene region is present in significant levels on the reaction timescale. The new model in Berkeley Madonna was generated using the mechanism and rate constants shown in **Scheme 91**. This model appeared to give a good fit, not only for the catalytst species data obtained from the ^{1}H NMR experiments, but also from all of the substrate data obtained in the kinetic experiments followed by GC.

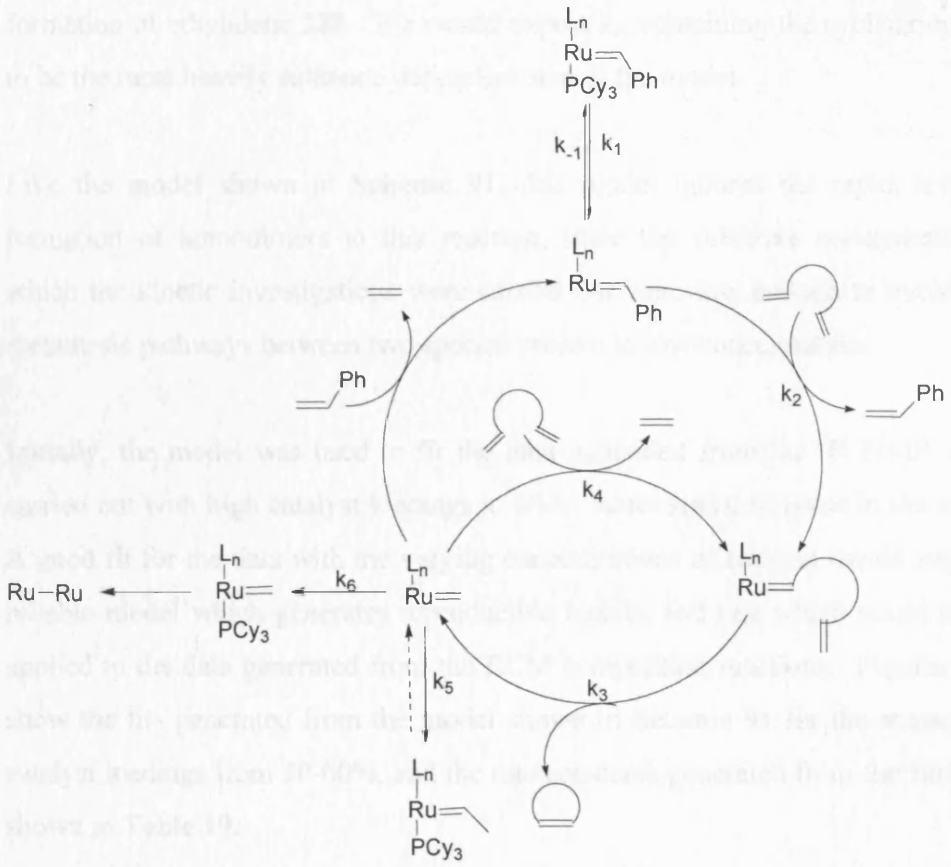

Scheme 91 Model of RCM input into Berkeley Madonna (Section 10, p62)

The initial step which controls the rate is the dissociation of the phosphane from the benzylidene pre-catalyst **29**, which is known to be relatively slow in Grubbs' second generation catalyst. Phosphane dissociation is reversible and re-association of the phosphane to the 14-electron species **220** regenerates the starting pre-catalyst. The second step is the initial catalytic binding to the substrate to generate the substrate alkylidene **222**, with the loss of styrene. The third step is generation of the methylidene **221** from substrate alkylidene **222**, with the loss of product. The k_3 step quantifies the overall rate of diene to cyclooalkene conversion, and is a combination of several mechanistic steps in the metathesis sequence. The k_3 step of the model contains the formation of both cyclic intermediates. The fourth step is the regeneration of substrate alkylidene **222** from methylidene **221**, with the loss of ethylene. The fifth and sixth steps account for the two possible decomposition pathways of methylidene **221**: irreversible phosphane capture by the methylidene, leading to formation of the bimetallic species **226**, and the pathway resulting in the

formation of ethylidene **228**. We would expect k_3, containing the cyclisation event to be the most heavily substrate dependent step in the model.

Like the model shown in **Scheme 91**, this model ignores the rapid reversible formation of homodimers in this reaction, since the substrate concentrations at which the kinetic investigations were carried out were low enough to avoid cross metathesis pathways between two species present in low concentration.

Initially, the model was used to fit the data generated from the ^{1}H NMR studies carried out with high catalyst loadings to allow better signal to noise in the spectra. A good fit for the data with the varying concentrations of catalyst would suggest a reliable model which generates reproducible results, and one which could then be applied to the data generated from the RCM competition reactions. Figures **83-87** show the fits generated from the model shown in **Scheme 91** for the studies with catalyst loadings from 20-60%, and the rate constants generated from the fitting are shown in **Table 19.**

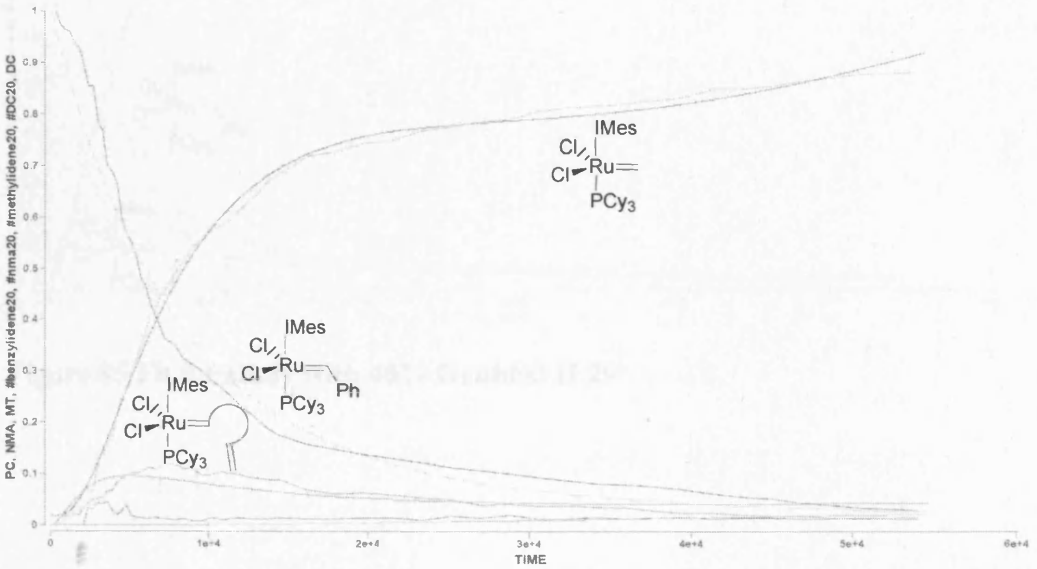

Figure 83 Fit for study with 20% Grubbs' II 29

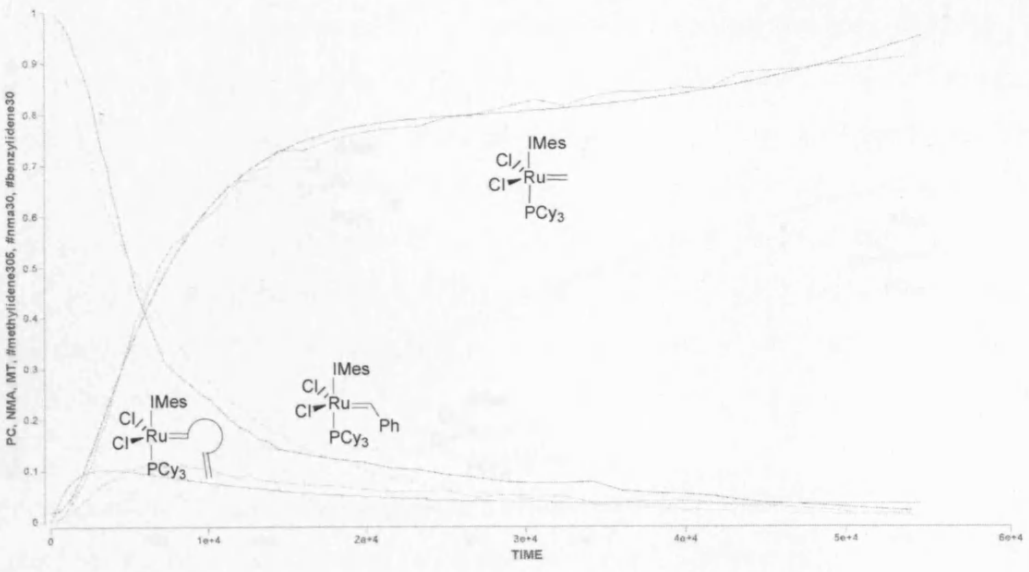

Figure 84 Fit for Study with 30% Grubbs' II 29 (Section 10, 63)

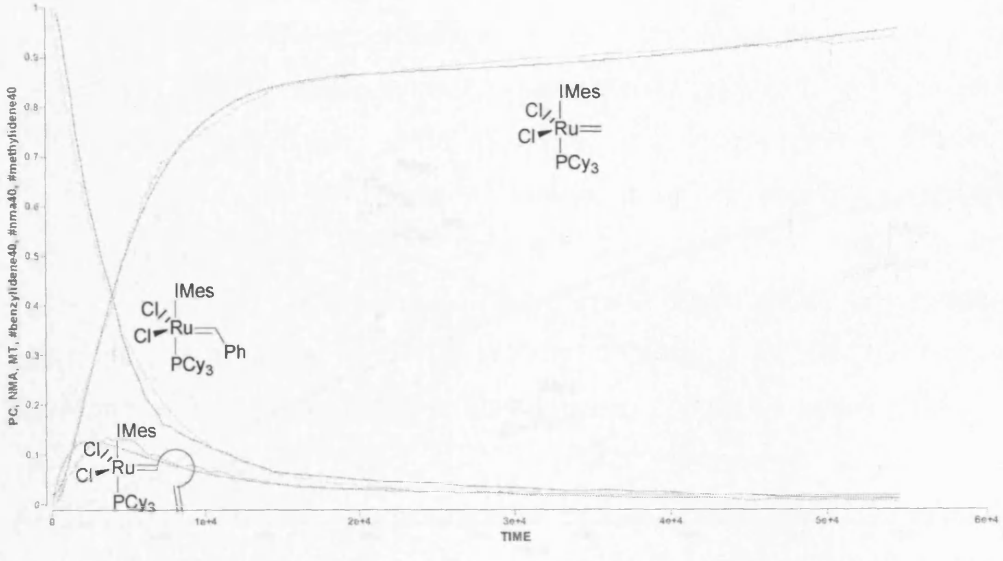

Figure 85 Fit for study with 40% Grubbs' II 29

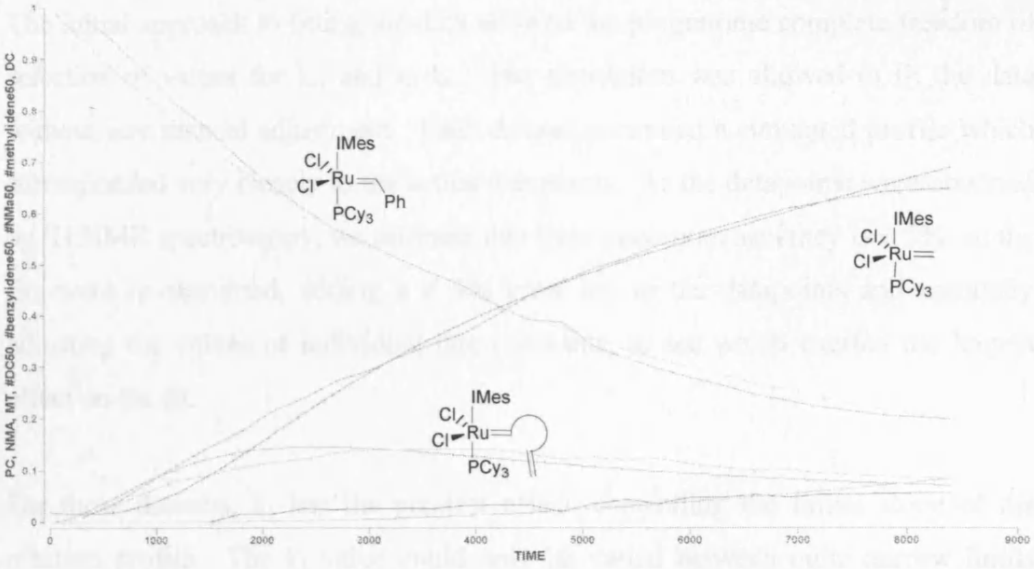

Figure 86 Fit with 50% Grubbs' II 29 (Section 10, p64)

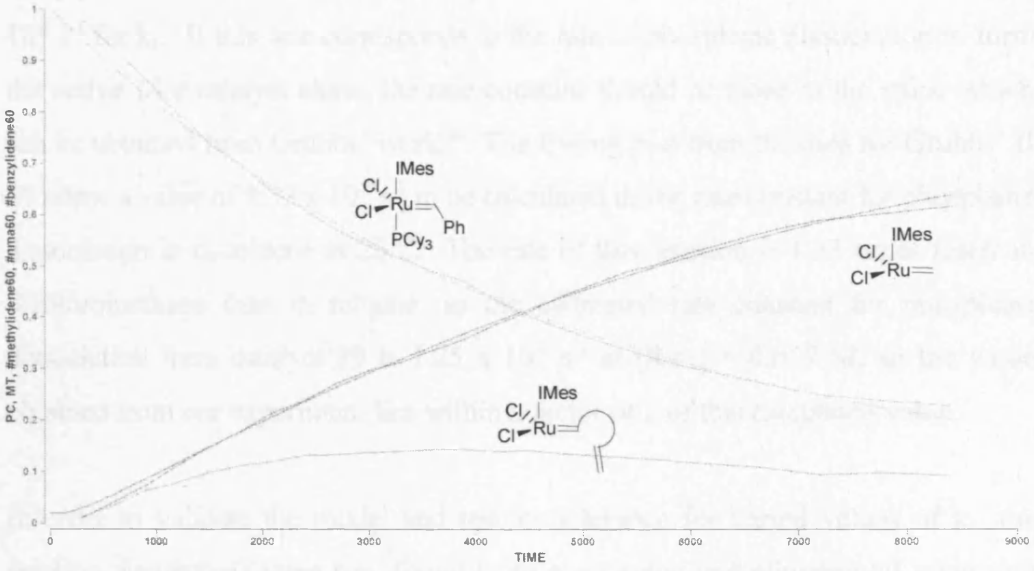

Figure 87 Fit with 60% Grubbs' II 29 (Section 10, p64)

Cat loading	[Ru]/M	k_1 x 10^4 s^{-1}	k_{-1} x 10^6 M^{-1} s^{-1}	k_2 x 10^3 M^{-1} s^{-1}	k_3 x 10^2 s^{-1}	k_4 x 10^4 M^{-1} s^{-1}	k_5 x 10^4 M^{-1} s^{-1}	k_6 x 10^4 M^{-1} s^{-1}
5%	0.002	0.55	1.84	0.77	0.44	2.47	0.82	0.31
12.50%	0.005	1.06	2.39	3.16	0.65	4.13	9.03	0.43
30%	0.012	1.50	4.17	5.11	0.88	5.53	23.1	0.89
40%	0.016	2.14	4.98	7.01	1.35	7.49	34.6	1.40
50%	0.02	2.90	6.11	7.47	1.71	8.71	40.3	1.76
60%	0.024	3.20	6.70	8.56	2.12	9.36	46.9	2.37

Table 19 Rate constants generated by Berkeley Madonna for RCM of 31 with 5-60% 29

The initial approach to fitting the data allowed the programme complete freedom of selection of values for k_{-1} and k_1-k_6. The simulation was allowed to fit the data without any manual adjustment. Each dataset generated a simulated profile which corresponded very closely to the actual datapoints. As the datapoints were obtained by ^{1}H NMR spectroscopy, we estimate that their maximum accuracy is ± 5%, so the fits were re-examined, adding a ± 5% error bar to the datapoints and manually adjusting the values of individual rate constants, to see which exerted the largest effect on the fit.

For these datasets, k_1 has the greatest effect, controlling the initial slope of the reaction profile. The k_1 value could only be varied between quite narrow limits before the simulated and experimentally measured profiles began to diverge quite sharply. For the run with [Ru=] = 0.016 M, we obtained a value of (2.1 ± 0.1) x 10^{-4} s^{-1} for k_1. If this rate corresponds to the rate of phosphane dissociation to form the active 14 e catalyst alone, the rate constant should be close to the value which can be obtained from Grubbs' work.[40] The Eyring plot from the data for Grubbs' II **29** allow a value of 9.37 x 10^{-5} s^{-1} to be calculated as the rate constant for phosphane dissociation in d_8-toluene at 25°C. The rate of this reaction is 1.33 times faster in dichloromethane than in toluene, so the estimated rate constant for phosphane dissociation from catalyst **29** is 1.25 x 10^{-4} s^{-1} at [Ru=] = 0.017 M, so the value obtained from our experiment lies within a factor of 2 of this calculated value.

In order to validate the model and test its tolerance for varied values of k_1, the reaction simulations were run, fixing k_1 to a set value and allowing all other rate constants to be changed. Data were plotted against the experimental data (which are shown with ± 5% error bars (**Figure 88**) in order to identify the limits for k_1 variation within the datasets.

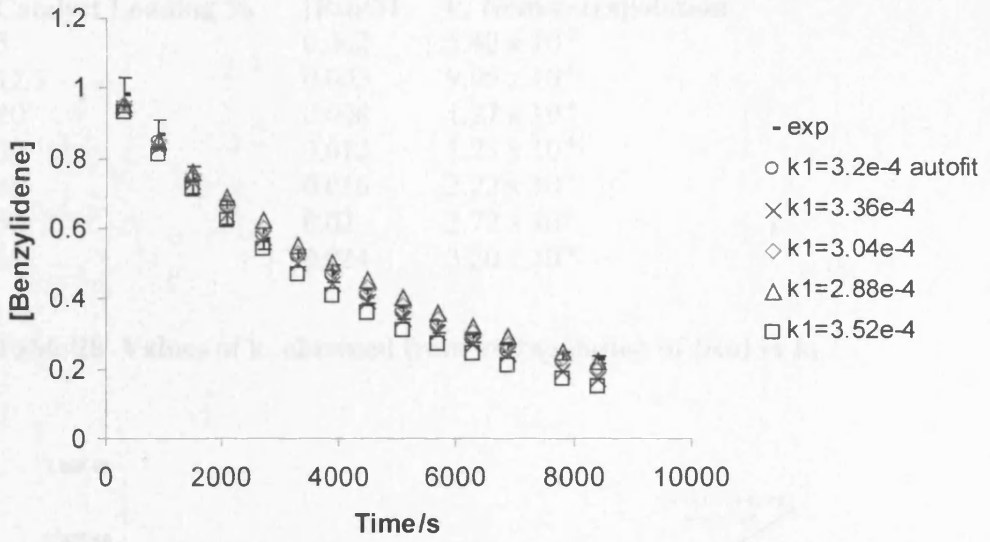

Figure 88 Testing k_1 tolerance with 60% 29

Grubbs identified k_1 as the rate constant for phosphane dissociation from the benzylidene pre-catalyst. Since this step in the mechanism involves only catalyst, the rate constant for this process should not change when the concentration of catalyst in solution is changed. However, we did not observe this in carrying out the reaction simulations. Maintaining the same values of k_1 at all concentrations of ruthenium did not give good fits. This suggests that the k_1 involves a substrate binding event, in which case k_1 would be affected by the concentration of catalyst in solution.

The fits shown in figures **83-87** were especially good for the experiments run with higher catalyst loadings, where NMR line shapes were smoother due to reduced signal to noise, and good fits were obtained for the benzylidene, methylidene and substrate alkylidene concentrations in all cases. Since the consumption and formation profiles of these catalytic species were well simulated, the model was considered useful for the simulation of the kinetic data generated from the competition experiments.

The values of [Ru] were plotted against k_n, and for all rate constants, a linear relationship was observed (**Figures 89-95**). These plots were used to back extrapolate rate constants for k_1 for experimentally-obtained RCM kinetic data, since this event is substrate independent (**Table 20**).

Catalyst Loading %	[Ru]/M	k_1 from extrapolation
5	0.002	5.42×10^{-5}
12.5	0.005	9.05×10^{-5}
20	0.008	1.27×10^{-4}
30	0.012	1.75×10^{-4}
40	0.016	2.22×10^{-4}
50	0.02	2.72×10^{-4}
60	0.024	3.20×10^{-4}

Table 20 Values of k_1 obtained from extrapolation of [Ru] *vs* k_1

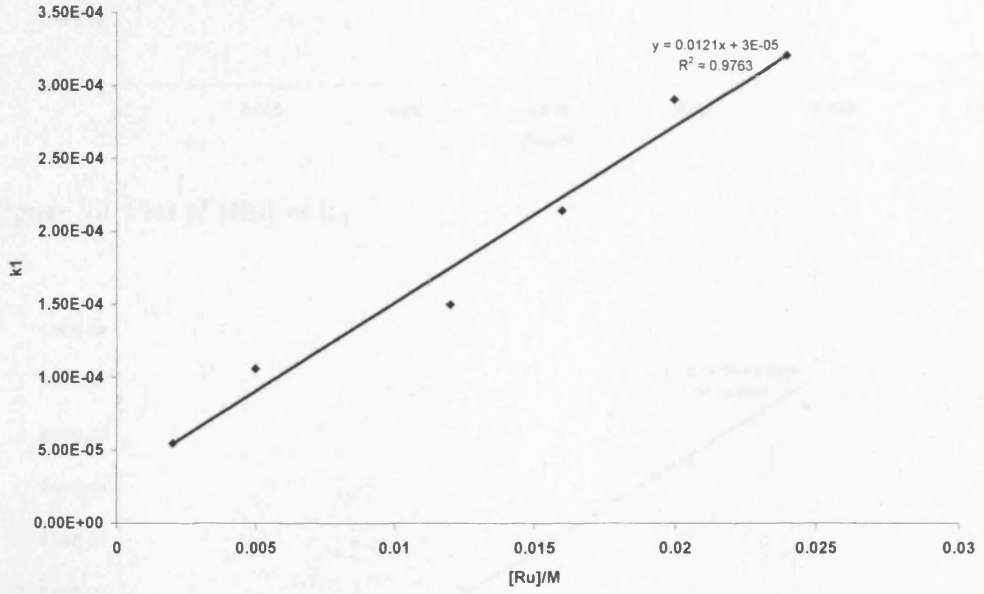

Figure 89 Plot of [Ru] *vs* k_1

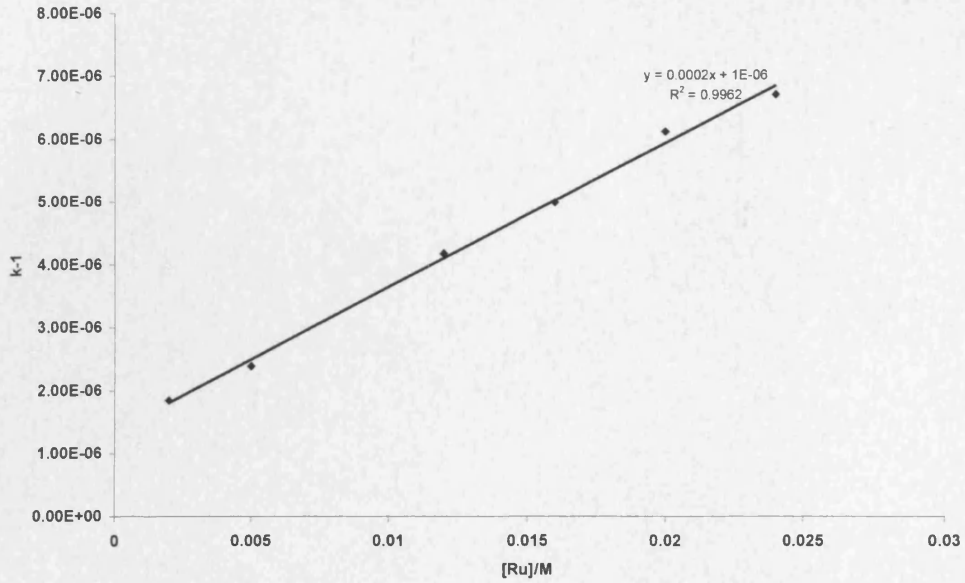

Figure 90 Plot of [Ru] *vs* k_{-1}

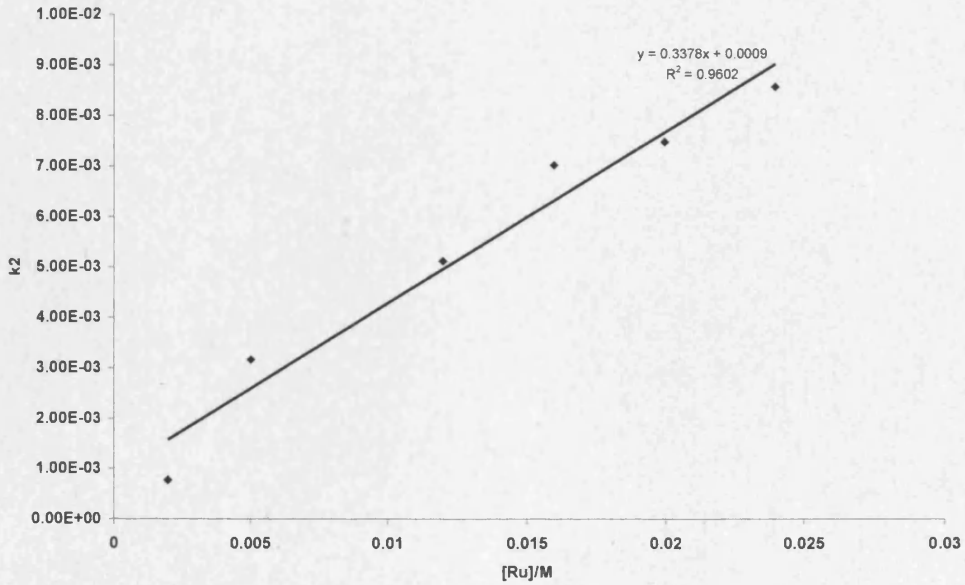

Figure 91 Plot of [Ru] *vs* k_2

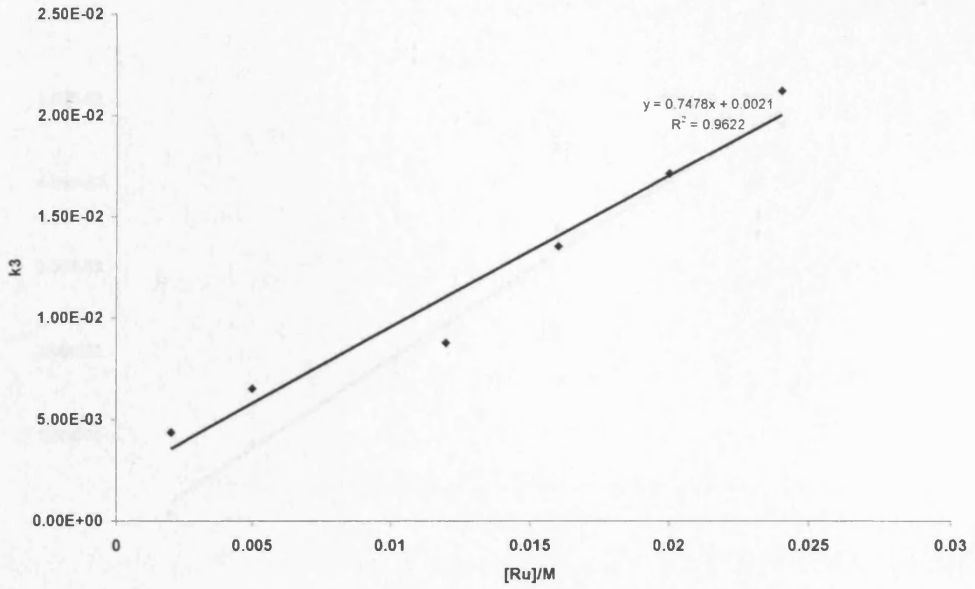

Figure 92 Plot of [Ru] *vs* k_3

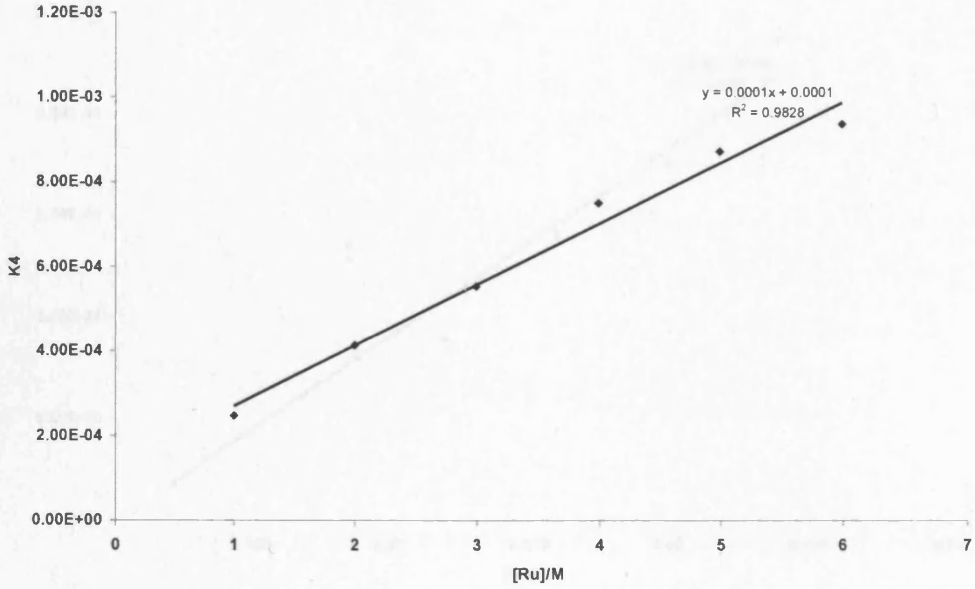

Figure 93 Plot of [Ru] *vs* k_4

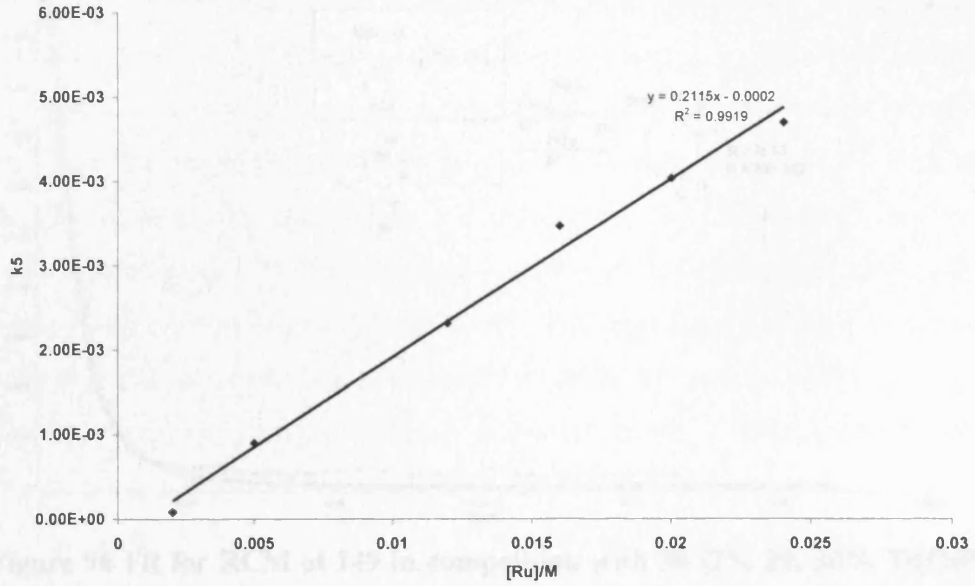

Figure 94 Plot of [Ru] *vs* k_5

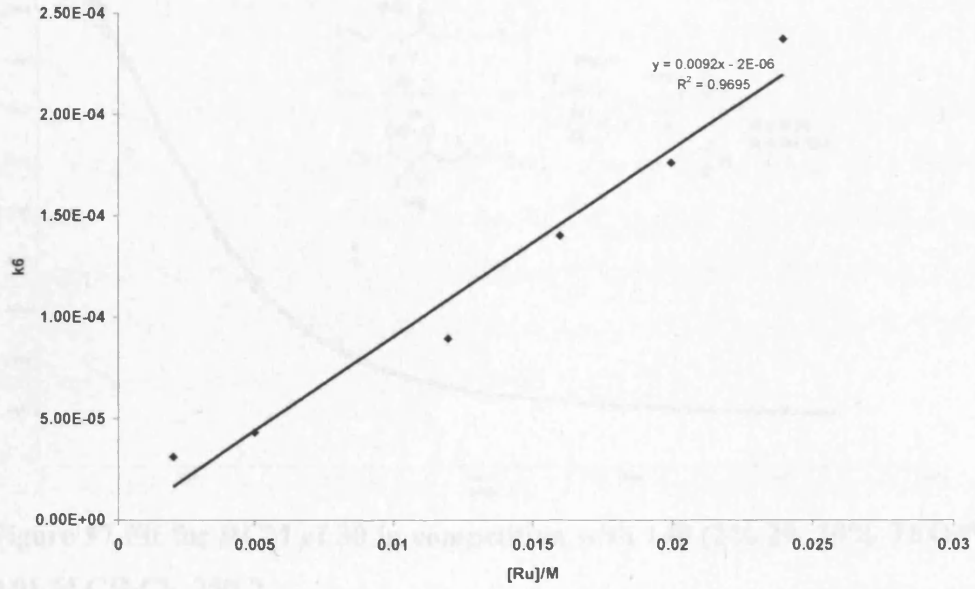

Figure 95 Plot of [Ru] *vs* k_6

The model was used to fit the experimental data from the Thorpe-Ingold experiment. There was a good fit for faster substrate **149**, as before (**Figure 96**) but also a perfect fit for the slower substrate **30** (**Figure 97**), which we had not previously achieved. Rate constants k_1-k_6 generated by the simulations are shown in **Table 21**.

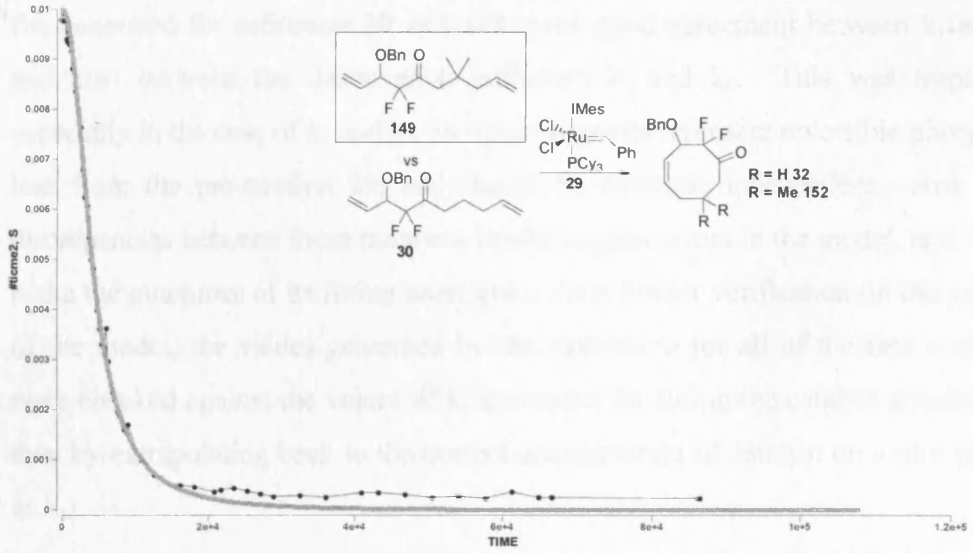

Figure 96 Fit for RCM of 149 in competition with 30 (2% 29, 30% Ti(O*i*Pr)$_4$, 0.01 M CH_2Cl_2, 25°C)

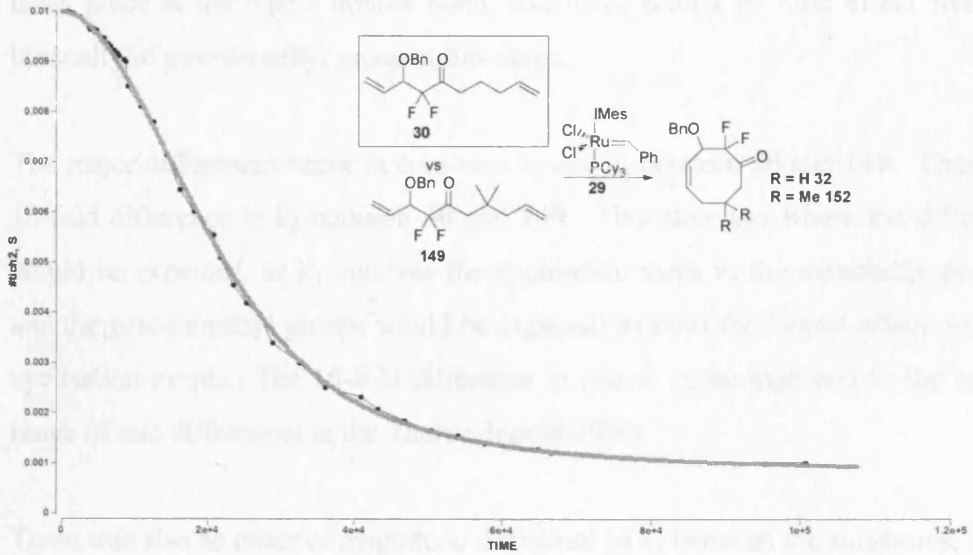

Figure 97 Fit for RCM of 30 in competition with 149 (2% 29, 30% Ti(O*i*Pr)$_4$, 0.01 M CH_2Cl_2, 25°C)

	$k_1 \times 10^4$ s^{-1}	$k_{-1} \times 10^6$ M^{-1} s^{-1}	$k_2 \times 10^3$ M^{-1} s^{-1}	$k_3 \times 10^4$ s^{-1}	$k_4 \times 10^4$ M^{-1} s^{-1}	$k_5 \times 10^5$ M^{-1} s^{-1}	$k_6 \times 10^5$ M^{-1} s^{-1}
CH_2	2.50	2.0	7.50	1.90	1.30	8.70	4.60
CMe_2	2.10	2.0	4.0	17	33	16	1.50

Table 21

The programme was allowed to fit the data automatically initially, before defining upper and lower limits on the values of k_1 and k_{-1} depending on [**29**]. The automatic

fits generated for substrates **30** and **149** show good agreement between k_1 and k_{-1} and also between the deactivation pathways k_5 and k_6. This was important, especially in the case of k_1 and k_{-1}, as these constants represent reversible phosphane loss from the pre-catalyst **29**, and should be substrate independent. Any large discrepancies between these numbers would suggest errors in the model, and would make the outcomes of its fitting unreliable. As a further verification on the validity of the model, the values generated by the simulation for all of the rate constants were checked against the values of k_x generated for fitting the catalyst species, and then by extrapolating back to the correct concentration of catalyst on a plot of [**29**] *vs* k_x.

There is only a small difference in the rates constant k_2 between **30** and **149**, and this is to be expected, since the initial cross metathesis event with the substrate takes place at the type I double bond, and there should be little effect from the homoallylic *gem*-dimethyl group at this stage.

The major differences occur in constants k_3 and k_4 between **30** and **149**. There is a 10-fold difference in k_3 between **30** and **149**. This step was where the difference would be expected, as k_3 involves the cyclisation steps in the metathesis process, and the *gem*-dimethyl groups would be expected to exert the largest effect on these cyclisation events. The 10-fold difference in rate is at the high end of the normal range of rate differences in the Thorpe-Ingold effect.[57]

There was also an order of magnitude difference in k_4 between the substrates, which suggests that the propagation step, which involves turnover of the methylidene **221** is more substrate dependent than the initital cross metathesis step of benzylidene catalyst **220**. This suggests that methylidene **221** is more selective or substrate sensitive than benzylidene **220.**

Although this model fits all the data obtained in kinetic experiments, all of the ^{1}H NMR studies on catalytic species **220-222** had been carried out without the titanium isopropoxide co-catalyst. It is interesting that the model did not including a substrate-titanium binding events, yet fitted data generated for systems including the co-catalyst. A kinetic study was carried out using alcohol **22**, with 2% Grubbs'

second generation catalyst **29**, 0.01 M in CH_2Cl_2, but without the Ti(IV) co-catalyst, to identify any effects of the co-catalyst on the rate of cyclisation. Samples withdrawn from the reaction were treated using the SPE protocol, and analysed by GC. Results are shown in **Figure 98**, overlaid with a kinetic RCM experiment of **22** run with the co-catalyst for direct comparison.

Earlier qualitative reports from Percy in the synthesis of the carbamate series of cyclooctenones reported that without the presence of the co-catalyst, and with the less active Grubbs' first generation catalyst **28**, the reaction does not proceed.[x] In the presence of Grubbs' second generation catalyst **29**, the reaction was still found to proceed in the absence of the Ti(IV) co-catalyst, but longer reaction times were required than when the co-catalyst was used.

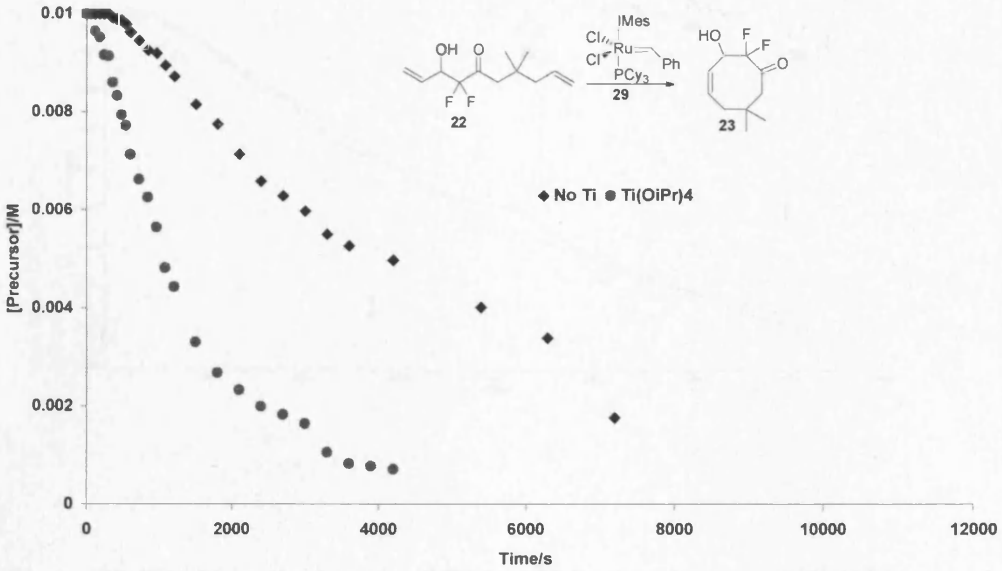

Figure 98 RCM of 22 in the presence and absence of Ti(O*i*Pr)$_4$ with catalyst 29 (Section 10, p83)

Alcohol **22** is a highly reactive RCM substrate and undergoes cyclisation under the normal optimised conditions very rapidly. In contrast to the observations made with the carbamate substrates, the cyclisation does proceed in the absence of the Ti(IV) co-catalyst but is slower. The approximate half lives for the runs with and without Ti(O*i*Pr)$_4$ were 1050 s and 4100 s respectively, suggesting the presence of the co-catalyst accounts for an almost 3-fold difference in cyclisation rate.

It appeared from these observations that the Ti(IV) co-catalyst has a significant effect on the rate of cyclisation but does not need to be accounted for in the model, since the decay curve of the precursor could be simulated using the same model to fit all other data (**Figure 99**). The comparative rate constants for the RCM of **22** in the presence and absence of the co-catalyst are shown in **Table 22**. To verify this, further ^{1}H NMR studies were carried out, recording signals between 11-20 ppm, in the presence of the titanium co-catalyst. Catalyst loadings were kept high (40-50%) to give good signal to noise ratio in the spectra. The RCM of **31** was interrogated once again, in CD_2Cl_2 at 298 K for ease of comparison with previously generated data. Results are shown in **Figure 100** for the run with 50% catalyst loading.

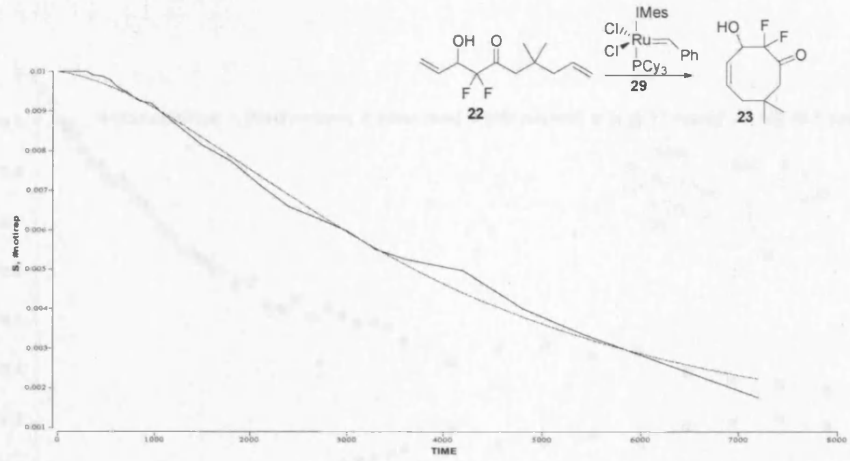

Figure 99 Fit of kinetic data for RCM of 22 in the absence of Ti(O*i*Pr)$_4$

Co-cat	k_1 x 10^4 s^{-1}	k_1 x 10^5 $M^{-1}s^{-1}$	k_2 x 10^3 $M^{-1}s^{-1}$	k_3 x 10^2 s^{-1}	k_4 x 10^3 $M^{-1}s^{-1}$	k_5 x 10^4 $M^{-1}s^{-1}$	k_6 x 10^5 $M^{-1}s^{-1}$
Present	2.81	2.14	15.2	1.87	10.5	7.52	4.53
Absent	1.07	2.72	7.89	1.46	1.93	2.39	1.48

Table 22 Rate constants for RCM of 22 in the presence and absence of Ti(O*i*Pr)$_4$

The rate constants shown in **Table 22** show some interesting differences between the two runs depending the presence or absence of the Ti(IV) co-catalyst.

Importantly, the presence of the co-catalyst does not appear to affect the two substrate-independent steps associated with k_1 and k_{-1}, and this should be expected since the phosphane loss or recapture from the benzylidene does not involve substrate. In the absence of the co-catalyst, the initial cross-metathesis step corresponding to k_2 is approximately half that generated in the presence of Ti(IV). Interestingly, the k_3 (cyclisation step) values are very similar, suggesting that the co-catalyst does not affect the rate of the cyclisation step. There is almost a 10-fold difference in the rate of the propagation cross metathesis event k_4, suggesting the presence of the Ti(IV) strongly affects the reactivity of the propagating species. It is therefore possible that either the presence of the Ti(O*i*Pr)$_4$ directly affects the rate at which propagation can occur, or that a more effective catalytic species is generated in the presence of this reagent.

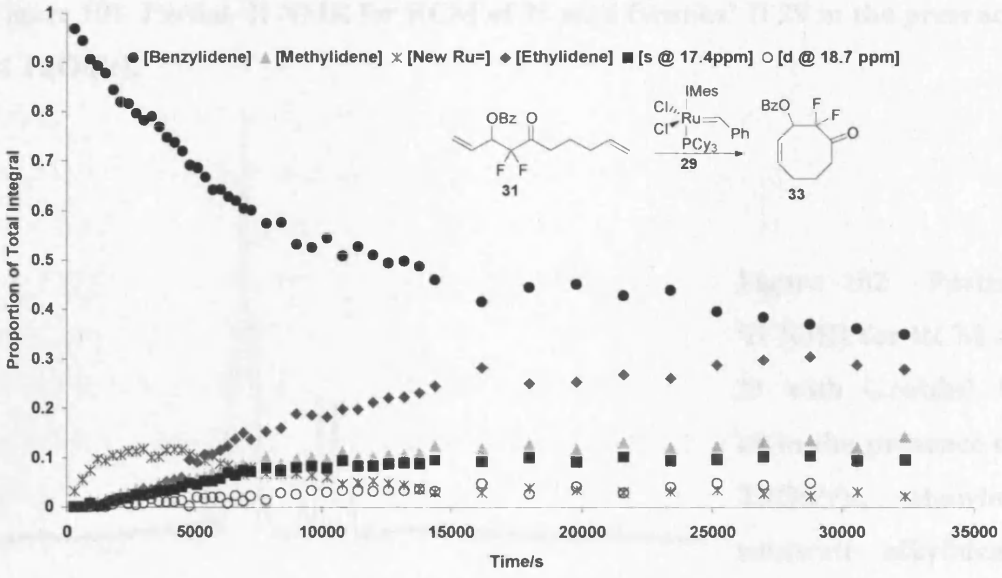

Figure 100 Results from ^{1}H NMR of alkylidene region, for RCM of 31 with Grubbs' II 29 and Ti(O*i*Pr)$_4$ at 298 K (Section 10, p26)

The spectra evolving over the timescale of the experiment were significantly different to those observed in previous studies. The benzylidene **220**, methylidene **221** and substrate alkylidene **222** were all observed as before. However, benzylidene loss appears to be much slower than previously observed, and a species with a chemical shift similar to the methylidene (a singlet at 17.4 ppm compared with the methylidene singlet at 17.7 ppm) appeared to grow in at a similar rate to

that of methylidene **221**. The quartet resulting from ethylidene **228** grew in much more rapidly, becoming the second major species, after from the benzylidene pre-catalyst **29** within the timescale of the experiment. Benzylidene consumption also appears to level off, as does the formation of the ethylidene. The methylidene is not the major species in this case, and reaching only 15%, compared with the ethylidene which accounts for 28% of the population.

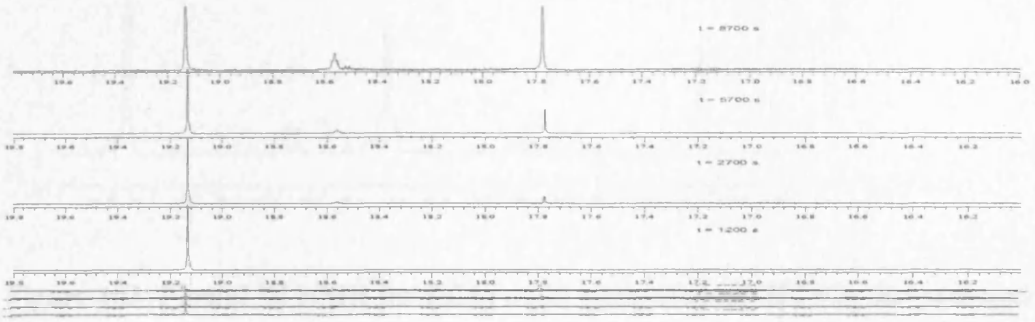

Figure 101 Partial ^{1}H NMR for RCM of 31 with Grubbs' II 29 in the presence of Ti(O*i*Pr)$_4$

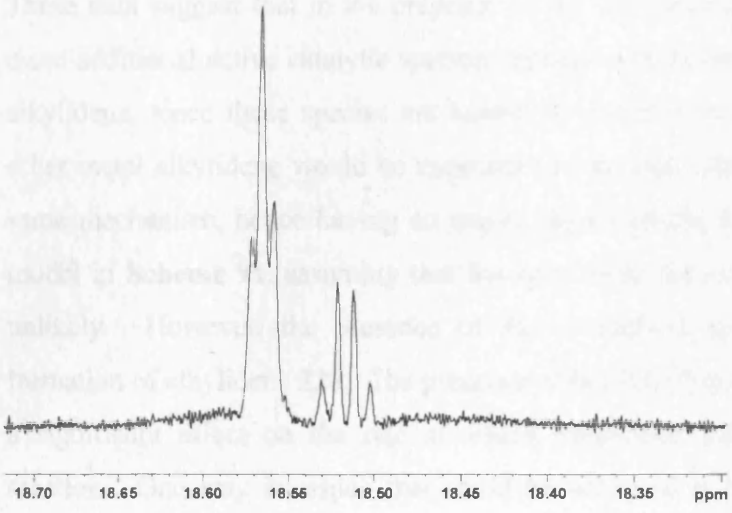

Figure 102 Partial ^{1}H NMR for RCM of 31 with Grubbs' II 29 in the presence of Ti(O*i*Pr)$_4$, showing substrate alkylidene 222 and ethylidene 228

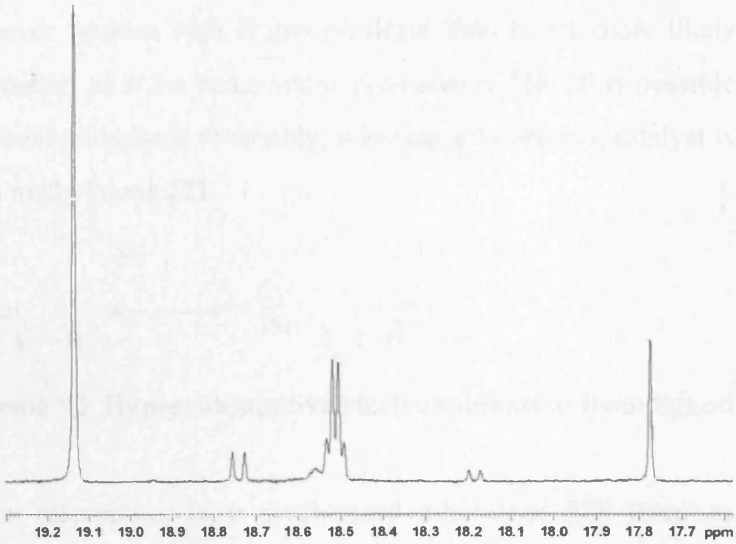

Figure 103 Partial ^{1}H NMR for RCM of 31 with Grubbs' II 29 in the presence of Ti(O*i*Pr)$_4$

These data suggest that in the presence of the Ti(IV) co-catalyst there are one or more additional active catalytic species, perhaps with bound titanium, or a titanium alkylidene, since these species are known to perform metathesis reactions. Any other metal alkylidene would be expected to turn over substrate molecules *via* the same mechanism, hence having no major impact on the propagation stages of the model in **Scheme 91**, assuming that the rates were the same, although this seems unlikely. However, the presence of the co-catalyst appears to accelerate the formation of ethylidene **228**. The presence of the Ti(IV) co-catalyst appears to have a significant effect on the rate at which ethylidene **228** is formed within the reaction. One way in which this could be achieved is by Ti(O*i*Pr)$_4$ acting as a source of propene, with which **221** could react to form **228**. This will be discussed further in this chapter.

The structural similarity of ethylidene **228** to methylidene **221** and other ruthenium alkylidenes does not give any indication that this species would be catalytically inactive in metathesis. Grubbs stated that for ruthenium alkylidene catalysts Ru=CHR, larger R groups are better at mobilising the phosphane ligand due to a combination of steric effects and inductive or hyperconjugative electron donation.[42]

The propagating methylidene **221** is known to be unable to dissociate phosphane; however, species with R groups larger than H are more likely to bind phosphane reversibly, as is the benzylidene pre-catalyst **220**. It is possible that ethylidene **228** can bind phosphane reversibly, allowing it to act as a catalyst with a longer lifetime than methylidene **221**.

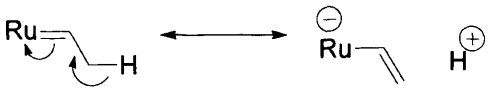

Scheme 92 Hyperconjugative electron donation from ligand

Some researchers have synthesised ethylidene **228** intentionally for metathesis reactions, using Grubbs' second generation catalyst **29** and but-2-ene. Wagener used this strategy, with different alkenes to generate new Ru olefin metathesis catalysts with linear alkyl carbene complexes (**Scheme 93**). These new catalysts were useful for ROMP reactions, to install a primary alkyl end group in the polymers.[92]

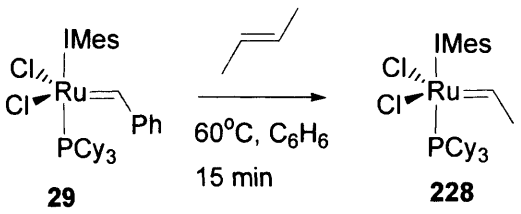

Scheme 93

The new Ru metathesis catalysts were used for the ROMP of cyclooctene **212**. At 0.05% loading, ethylidene complex **228** effected complete conversion of cyclooctene to polymerised material after stirring overnight at room temperature. Ethylidene **228** was also relatively air stable and did not decompose visibly in air overnight. The group also monitored the decomposition behaviour of solutions of the complex in C_6D_6 and observed a large difference depending on how the solution was prepared. Bench preparation of the solution gave a half life of 2.8 hours, whereas careful preparation of the solution in a glove box, in the absence of oxygen and moisture gave a complex with a much longer half life of approximately 100 hours at ambient temperature.

Encouragingly, there are also further examples in which groups have exploited the catalytically active **228** for metathesis reactions. Jackson purposely synthesised the ethylidene complex of Grubbs' second generation catalyst **29** *via* butenolysis (**Scheme 94**).[93] The ethylidene complex **247** was used for the cross metathesis of unsaturated natural oils (**Scheme 95**).[94] The group had observed low yields and turnovers with methylidene complex **221**. The cross metathesis reactions were carried out at -5°C in liquid but-2-ene to enable the formation of the ethylidene. This procedure for cross metathesis gave much higher yields of cross metathesised materials at much lower catalyst loadings (0.003 mole %). The presence of the terminal olefinic products gave rise to the methylidene, and this was believed to be detrimental in the ethenolysis reactions. The Ru-ethylidene complexes were therefore considered to be much more stable than the methylidene, and also showed greater efficiency since lower catalyst loadings were required.

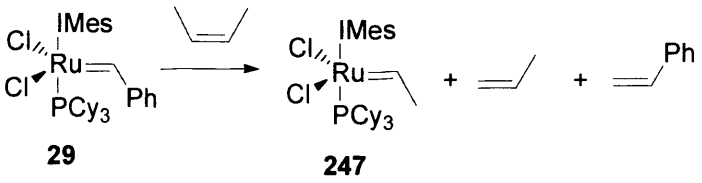

Scheme 94 Formation of 228 from 29 by butenolysis

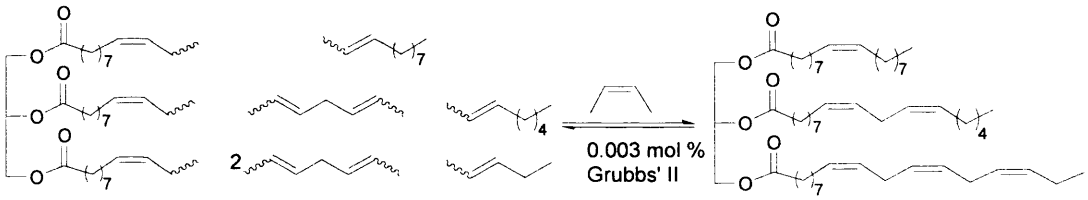

Scheme 95 Synthesis of unsaturated natural oils by cross metathesis with 247

Tulchinsky studied the synthesis of propene from ethylene and *cis*-2-butene by cross metathesis with Grubbs' first generation catalyst **28** in a continuous flow reactor.[95] The catalyst was pretreated with ethylene resulting in formation of methylidene **120** and catalytic deactivation, with a large reduction in catalyst TON. The catalyst pretreated with *cis*-2-butene (resulting in the ethylidene) did not appear to undergo any deactivation and instead gave high TONs for a longer period of time. These findings suggest that the ruthenium-ethylidene is more stable and has a longer lifetime than the methylidene **120**. As shown by Grubbs, the first generation

methylidene **120** has a very short half life, so pre-treatment of the catalyst with ethylene is likely to have resulted in rapid degradation of the catalyst through capture by the phosphane ligand.

These literature accounts suggest that although ethylidene **228** may arise as the result of a side reaction of the Ru-alkylidene, it *can* carry out metathesis reactions, and may, in fact, be a more effective catalyst than propagating methylidene **221** itself. The higher conversion to ethylidene **228** in the presence of the titanium co-catalyst may work in favour of the cyclisation if the ethylidene is a more reactive metathesis catalyst. This would explain the more rapid cyclisation in the presence of the co-catalyst.

Since ethylidene **228** was made intentionally from benzylidene **220**, it is likely that phosphane association to ethylidene **228** is reversible, unlike with methylidene **221**. This also extends the lifetime of the catalyst and is probably why the Jackson group observed fewer catalytic turnovers when generating methylidene **221**. However, the lifetime of ethylidene **228**, as with most Ru alkylidene catalysts is finite and decomposition occurs but *via* different pathways to those taken by methylidene **221**.

It is also possible that the addition of the Ti(IV) co-catalyst leads to the formation of a Ti-alkylidene species, which itself can carry out metathesis. Several groups have published accounts of metathesis by titanium alkylidenes.[96,97] One of the earliest observations of metathesis catalysed by titanium complexes was by Tebbe.[96] In 1979, he observed that the methylenetitanium complex **249** (**Scheme 96**) catalysed a metathesis process in which the methylene groups of isobutene and methylenecyclohexane exchanged.

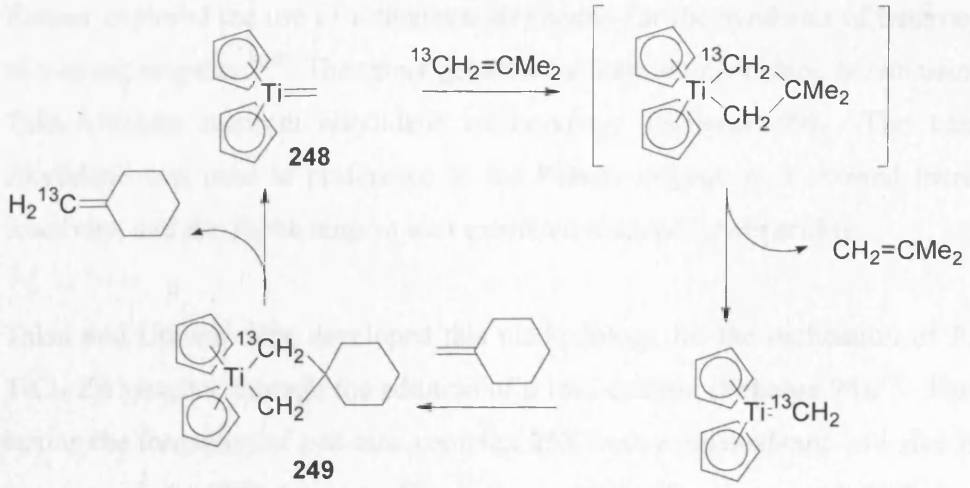

Scheme 96 Metathesis by Tebbe reagent 248

Petasis observed that when norbornene **250** was heated with catalytic amounts of dimethyltitanocene **251**, cyclopentadienyltrimethyl titanium(IV), and *bis*[trimethylsilyl] methyl titanocene, ROMP occurred (**Scheme 97**).[97] A titanium alkylidene **252** was first formed *in situ*, and then performed ROMP of norbornene.

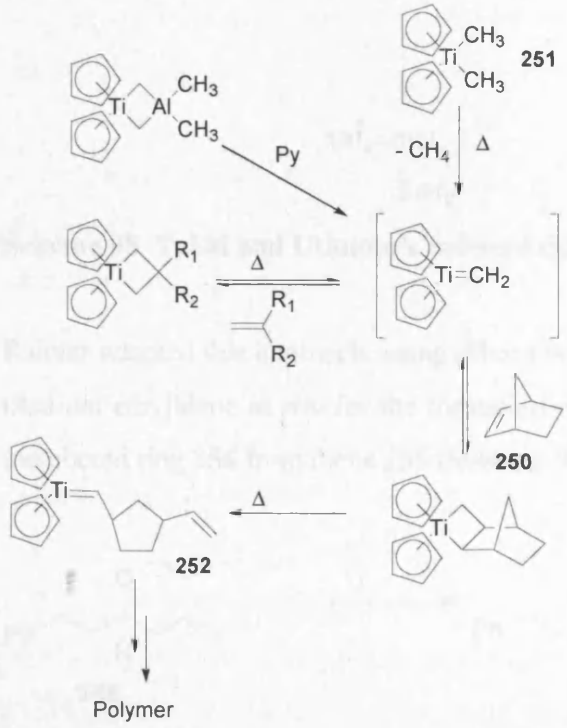

Scheme 97 *In situ* formation of a titanium alkylidene for metathesis

Rainier explored the use of a titanium alkylidene for the synthesis of heterocycles of varying ring size.[98,99] The group generated a titanium alkylidene *in situ* using the Takai-Utimoto titanium alkylidene methodology (**Scheme 99**). The titanium alkylidene was used in preference to the Petasis reagent as it showed increased reactivity, and the Tebbe reagent as it exhibited reduced Lewis acidity.

Takai and Utimoto first developed this methodology for the olefination of RCH_x-$TiCl_4$-Zn systems, through the addition of a lead catalyst (**Scheme 98**).[100] The first step is the formation of a di-zinc complex **253** from a dihaloalkane and zinc in the presence of of a PbX_2 catalyst. The di-zinc complex then reacts with $TiCl_4$ to form the reduced titanium alkylidene **254**.

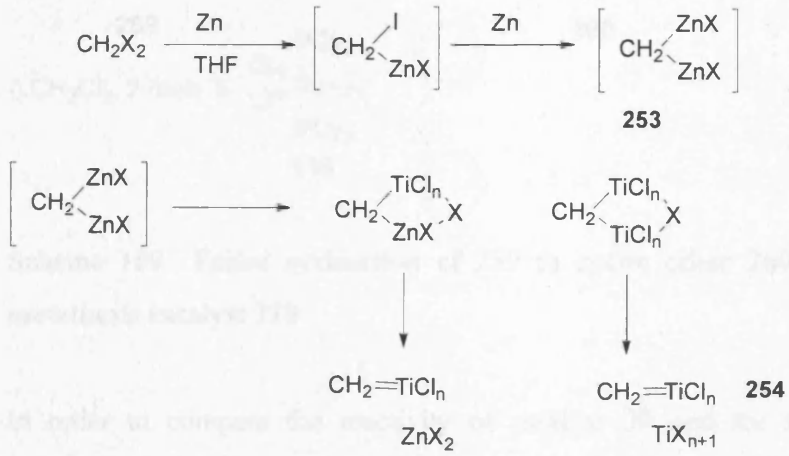

Scheme 98 Takai and Utimoto's reduced titanium alkylidene methodology

Rainier adopted this approach, using dibromoethane as the dihalide, to synthesise a titanium ethylidene *in situ* for the formation of cyclic enol ethers, including eight-membered ring **256** from diene **255** (**Scheme 99**).

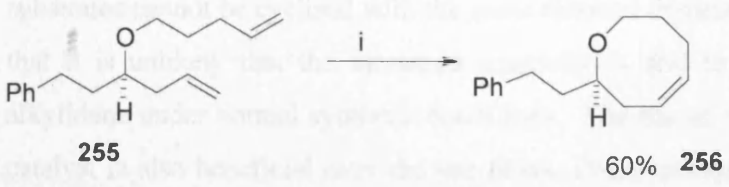

255 60% **256**

i $TiCl_4$, Zn, $PbCl_2$, CH_3CHBr_2, TMEDA, THF, 65°C

Scheme 99 Synthesis of cyclic ether 256 usig a reduced titanium alkylidene

The reduced titanium alkylidene was found to tolerate a wide variety of functionality, and also had the benefit of being relatively inexpensive compared to the conventional metathesis catalysts.

In contrast to this, Hoveyda attempted the synthesis of eight-membered ring **260** *via* RCM from diene **259** using catalyst **119** (**Scheme 100**), but could not isolate the desired product, and found a mixture of products at the end of the reaction.[101] This may suggest that the use of a reduced titanium alkylidene such as that demonstrated by Rainier may be more useful for the cyclisation diene substrates such as **259**

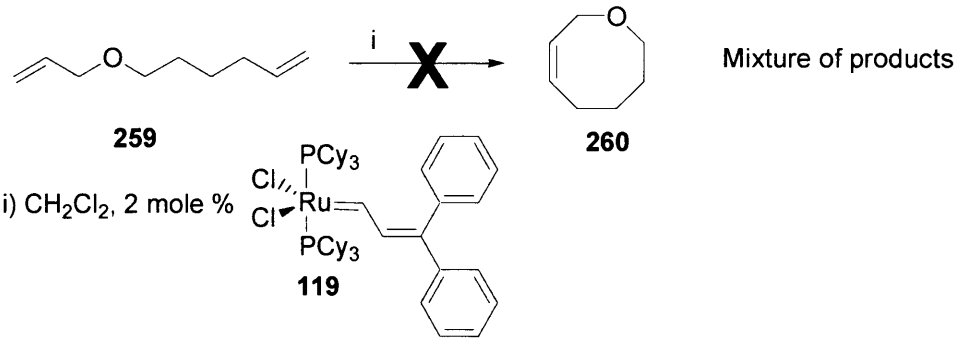

Scheme 100 Failed cyclisation of 259 to cyclic ether 260 using ruthenium metathesis catalyst 119

In order to compare the reactivity of catalyst **29** and the titanium alkylidene described by Petasis, the RCM of **31** was attempted with under the same conditions, with the overall concentration of diene in the reaction solvents at 0.01 M. The Petasis procedure in the literature achieved ring closure reaction in two hours, but in our case the reaction was checked by TLC after 4 hours and only starting material was identified. The reaction was then left to reflux overnight but after this time, cyclooctenone **33** was not observed in the ^{19}F NMR spectrum. It appears that our substrates cannot be cyclised with the same reduced titanium alkylidene, suggesting that it is unlikely that the increased reactivity is due to the formation of a Ti-alkylidene under normal synthetic conditions. The use of ruthenium and the Ti co-catalyst is also beneficial over the use of the $PbCl_2$ catalyst used by Petasis, since this reagent is toxic, whereas the Ru residues from metathesis are non-toxic. There is also a large amount of activated zinc required in this procedure, and although the

reagent is cheaper than Grubbs' catalyst **29**, a large amount of zinc would be required to synthesise a useful quantity of the cyclic product.

From the results generated from the ^{1}H NMR study (**Figure 100**) it is clear that the Ti co-catalyst slows the rate of benzylidene consumption and increases the rate and extent of ethylidene formation. It is unlikely that in our systems we are observing the formation of a titanium-alkylidene, since there appears to be no pathway through which one could form. The literature in which the Ti-alkylidenes are formed use a dihalide to generate the Ti-alkylidene species, and this is not present in our synthetic systems.

It appears more likely that the presence of *iso*propoxy ligands on the Ti co-catalyst assists the formation of ethylidene **228**, and form a catalyst with higher reactivity, longer lifetime, and greater ability to turn over substrate. Since the Ti co-catalyst is present in large excess compared to the Ru-catalyst, this seems a plausible explanation. A possible mechanism is shown in **Scheme 101**. This proposal would be consistent with the increased value of k_4 for the RCM of **22** in the presence of the co-catalyst, suggesting the formation of a more efficient catalytic species. The driving force for the reaction could be the formation of **264**, since the Ti=O double bond is very strong, and the formation of formation of a doubly bonded Ti species is the driving force for the Tebbe and Petasis reactions.

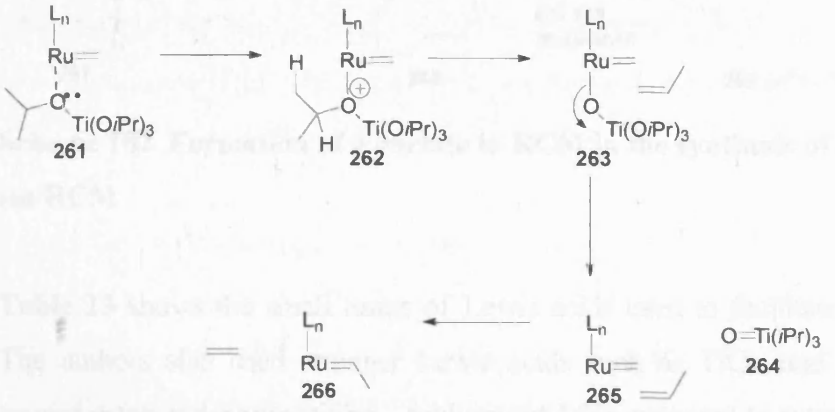

Scheme 101 Speculative generation of propene from Ti(O*i*Pr)$_4$

Sanchez used EXAFS analyses to determine the structures of a range of titanium(IV) alkoxides in and out of solution, and found that titanium(IV)

*iso*propoxide is monomeric in solution, so the behaviour shown in **Scheme 101** is feasible. Titanium(IV) ethoxide was found to be trimeric in solution so may not exhibit the same behaviour because the alkoxides may be less available to act as donor ligands.[102] This is discussed further in **4.2.**

4.2 The Effect of Ti Lewis Acid on RCM

We explored the role of the Ti(IV) co-catalyst further by looking at the effect of varying the alkoxide ligand.

Fűrstner first observed the acceleration of an RCM by $Ti(O\textit{i}Pr)_4$ in the total synthesis (-)-gloesporone **267**, a fungal germination inhibitor, using RCM for the macrocyclisation step.[64] Fűrstner used a Lewis acid co-catalyst in the RCM of 4-pentenoate (**Scheme 102**) to destabilise an unproductive alkylidene of type **270,** , which was assumed to compete with the ruthenium carbene for chelation with the carbonyl group on the diene. Chelation of the carbonyl to the ruthenium would result in the formation of a species such as **270**, which may inhibit further metathesis.

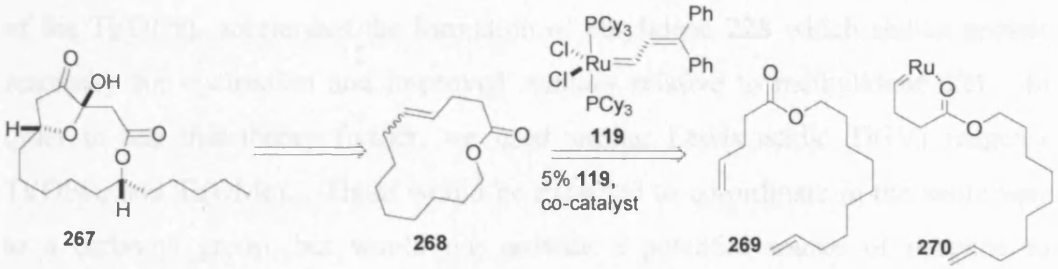

Scheme 102 Formation of a chelate in RCM in the synthesis of macrocycle 267 *via* RCM

Table 23 shows the small range of Lewis acids used to facilitate the cyclisation. The authors also used stronger Lewis acids such as $TiCl_4$ and $SnCl_4$ but these caused catalyst decomposition. Addition of LiBr appeared to retard the cyclisation reaction rather than promote it.

Temperature °C	Additive	Yield 267 %
25	None	22

25	LiBr (5 equiv)	14
25	$Ti(OiPr)_4$ (2 equiv)	40
40	$Ti(OiPr)_4$ (5 mol %)	55

Table 23 Range of Lewis acids used by Furstner as RCM co-catalysts

When using titanium(IV) *iso*propoxide, even in catalytic amounts (5 mole %), the yield of cyclic product is much higher than with the other Lewis acids screened. The authors comment that esters are well known to co-ordinate weakly *trans* to alkoxides on a Ti(IV) template, and this lability ensures that the Ru-catalyst does not coordinate to the carbonyl group and is able to perform the desired cyclisation.

However, Fürstner does not rationalise how a catalytic amount of $Ti(OiPr)_4$ is sufficient to protect the catalyst from chelation with the carbonyl group on the diene. Since the concentration of diene is in a large excess over the concentrations of both catalyst **29** and the Ti(IV) co-catalyst (and the loadings of these reagents are the same), chelation between the diene and Ru-catalyst would be less probable than chelation between diene and Ti(IV) co-catalyst.

From our ^1H NMR investigations described previously, it appears that the presence of the $Ti(OiPr)_4$ accelerates the formation of ethylidene **228** which shows greater reactivity for cyclisation and improved stability relative to methylidene **221**. In order to test this theory further, we used similar Lewis acidic Ti(IV) reagents $Ti(OEt)_4$ and $Ti(OMe)_4$. These would be expected to co-ordinate in the same way to a carbonyl group, but would not provide a potential source of propene to facilitate formation of ethylidene **228** can form.

The RCM of **22** (**Scheme 103**) was followed by GC, to allow direct comparison with previous results (in the presence and absence of $Ti(OiPr)_4$). A 30 mole % loading of either $Ti(OEt)_4$ or $Ti(OMe)_4$, a 2 mole % loading of catalyst **29**, and a substrate concentration of 0.01 M in dichloromethane were used for these reactions. Results overlaid with those obtained using $Ti(OiPr)_4$ and in the absence of a co-catalyst are shown in **Figure 105**.

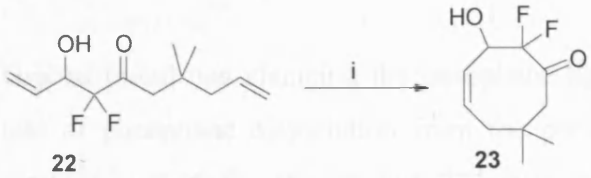

i) 0.01 M, CH_2Cl_2, 0.3 eq $Ti(OR)_4$, 2% 29, 25°C
R = Et, Me

Scheme 103

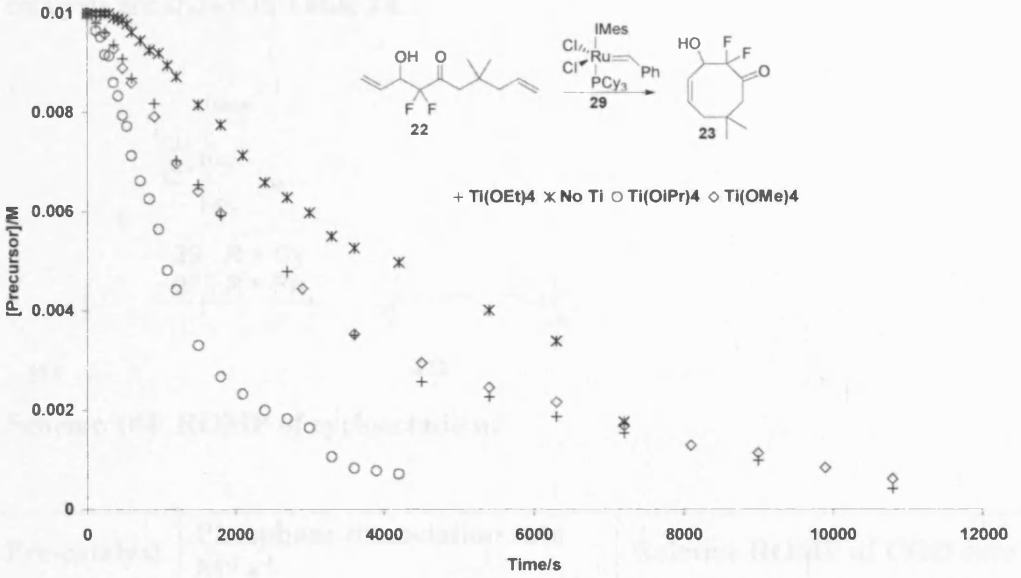

Figure 105 Overlaid results for RCM of 22 with Ti(O*i*Pr)$_4$, Ti(OMe)$_4$, Ti(OEt)$_4$ and in the absence of co-catalyst (Section 10, p83-85)

The results in **Figure 105** clearly show that there is a significant rate difference when the Ti(IV) co-catalyst is changed, suggesting that careful choice of Lewis acid is also important for RCM. The cyclisation with Ti(O*i*Pr)$_4$ is the most rapid, and the RCM in the absence of any co-catalyst is the slowest. The RCM of **22** carried out with Ti(OEt)$_4$ and Ti(OMe)$_4$ appear to fall inbetween the two previous results. The close agreement between the Ti(OEt)$_4$ and Ti(OMe)$_4$ runs is unlikely to be coincidental and suggests that the degree of scatter in the experimental points is relatively low. The results suggest that the presence of the Ti(O*i*Pr)$_4$ co-catalyst may accelerate the RCM through the generation of a more efficient catalytic species **228**, but also that there is a further effect on the cyclisation due to the presence of the Ti(IV) species, which appears to have a significant effect on the initial stages of the reaction in particular.

Grubbs found that changing the phosphane ligand had a significant effect on the rate of phosphane dissociation from the pre-catalyst, as well as on the rate of catalytic activity.[40] Pre-catalyst **273** was synthesised to compare the relative activity with Grubbs' second generation catalyst **29**. The rates of phosphane dissociation and rate of ROMP of cyclooctadiene (COD) **271** (**Scheme 104**) were compared. Rates of phosphane dissociation and ROMP of COD for the two catalysts are shown in **Table 24**.

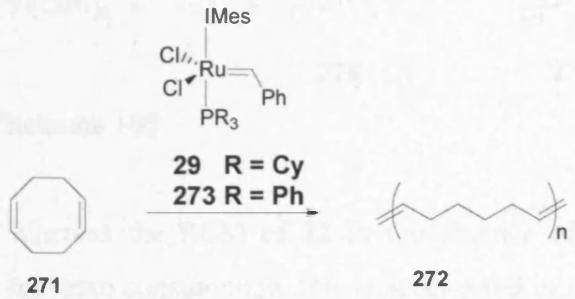

271 272

Scheme 104 ROMP of cyclooctadiene

Pre-catalyst	Phosphane dissociation rate $M^{-1} s^{-1}$	Relative ROMP of COD rate
29	4.6×10^{-4}	1[a]
273	3.3×10^{-3}	0.5[b]

[a] 5% catalyst loading; [b] 0.05% catalyst loading

Table 24

Catalyst **273** exhibited phosphane dissociation an order of magnitude greater than that of commercially available **29**, and also greater activity in the ROMP of **271**, so lower catalyst loadings were required. The greater rate of phosphane dissociation by **273** was attributed to the reduced Lewis basicity of PPh_3 relative to PCy_3. Increased acidity of the ligand increases its lability, hence resulting in more rapid dissociation. It is possible, in our systems containing the Lewis acidic Ti(IV) co-catalysts that there is a rapid substitution of the PCy_3 ligand for co-ordination with $Ti(OR)_4$, which is Lewis acidic (**Scheme 105**). The Lewis acidity of the $Ti(OR)_4$ ligand results in rapid dissociation allowing subsequent reaction of the 14-electron species with the diene substrate. This would account for the observed increased in reaction rate in the presence of all three titanium(IV) reagents compared with the

reaction in the absence of any co-catalyst. The formation of titanium-bound complex **274** is driven by the formation of the strong Ti=O double bond.

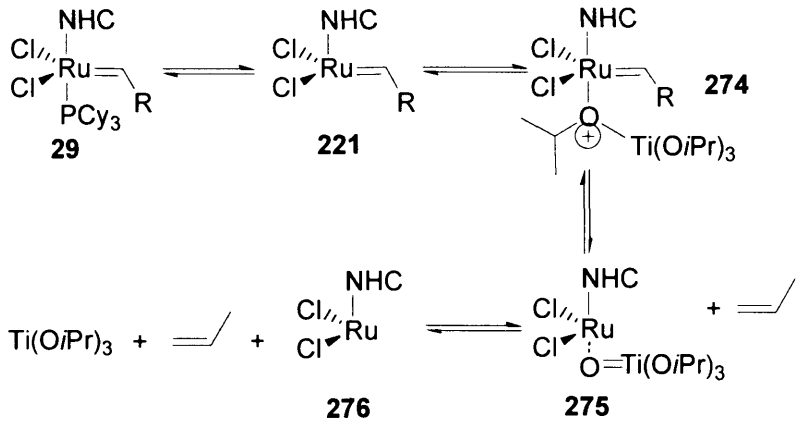

Scheme 105

Whereas the RCM of **22** in the absence of the co-catalyst exhibits slow initial substrate consumption, this is accelerated in the presence of co-catalyst. However, the gradient of the substrate decay appears to be steeper with $Ti(OiPr)_4$ than with $Ti(OEt)_4$ and $Ti(OMe)_4$. In the latter cases, the slope appears to bear a closer resemblance to that of the RCM in the absence of any co-catalyst. This suggests that the presence of the co-catalyst has an effect on the initial stages of the RCM, as well as on the nature of the propagating catalyst, or on the fate of the propagating species.

Percy carried out computational studies on the RCM of alcohol **4** catalysed by **29**, using DFT (B3LYP 6-31G*, with LACVP pseudopotential for Ru, in Spartan06) and found that the presence of the Ti(IV) co-catalysts is likely to have an effect on the rate of metathesis due to the possible formation of a chelate between the Ru and carbonyl of the diene substrate **4** (**Figure 106**).[103] The chelated structure was found to exist at a deep minimum, making its formation highly favourable. The formation of this chelate would be expected to retard both the forward cyclisation reaction, and back reaction to oligomeric products. It is highly plausible that the Ti(IV) co-catalyst in the RCM systems prevents the formation of these chelates, thus speeding up the overall reaction. However, from the results from experiments with alternative titanium(IV) alkoxides, it appears that the co-catalyst has more than one effect on the cyclisation reaction.

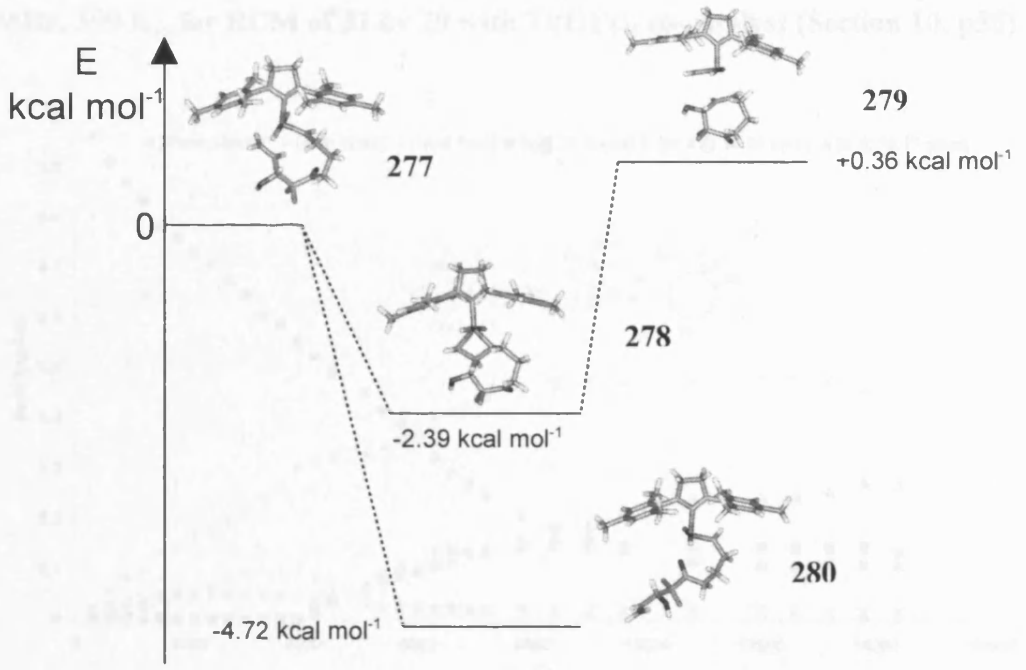

Figure 106 Electronic energy calculations using DFT for initial η^2 complex 277, product metallocyclobutane 278, product η^2 complex 279 and C=O chelated species 280

To study this further, the alkylidene region of the ^{1}H NMR spectrum was followed, using either $Ti(OEt)_4$ or $Ti(OMe)_4$ as the co-catalysts with diene **22** in CD_2Cl_2 (0.04 M), and 40% Grubbs' II **29**. The results are shown in **Figures 107** and **108**.

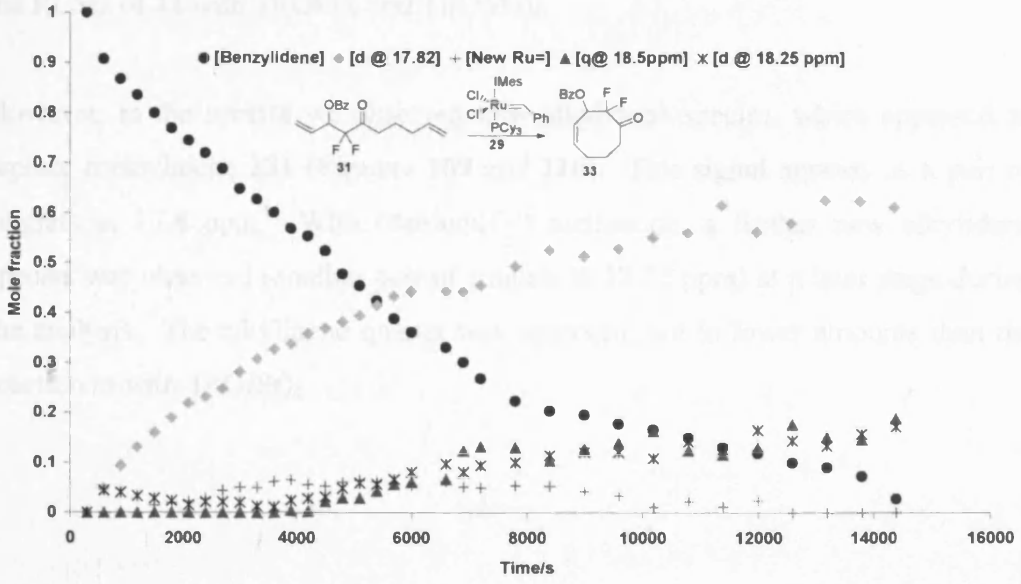

Figure 107 Plot showing Ru-alkylidene species as observed by ^{1}H NMR (400 MHz, 300 K), for RCM of 31 by 29 with Ti(OEt)$_4$ co-catalyst (Section 10, p58)

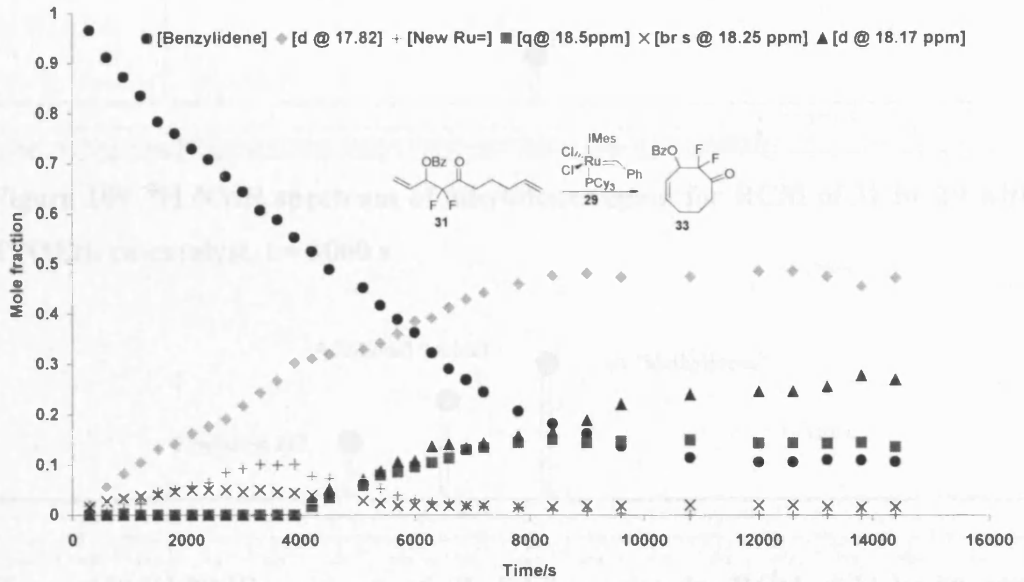

Figure 108 Plot showing Ru-alkylidene species as observed by ^{1}H NMR (400 MHz, 300 K), for RCM of 31 by 29 with Ti(OMe)$_4$ co-catalyst (Section 10, p60)

In both cases, benzylidene **220** is consumed to a much greater extent than in the presence of Ti(O*i*Pr)$_4$, and there is much less extensive formation of ethylidene **228**. This supports the theory that the *iso*propoxy ligands facilitate propene release, which leads to the formation of **228**. This also explains the slower cyclisation of the RCMs of **22** with Ti(OEt)$_4$ and Ti(OMe)$_4$.

However, in the spectra we observed new alkylidene species, which appeared to replace methylidene **221 (Figures 109** and **110)**. This signal appears as a pair of singlets at 17.8 ppm. With titanium(IV) methoxide, a further new alkylidene species was observed (another pair of singlets at 18.25 ppm) at a later stage during the analysis. The ethylidene quartet was observed, but in lower amounts than the reaction in with Ti(O*i*Pr)$_4$.

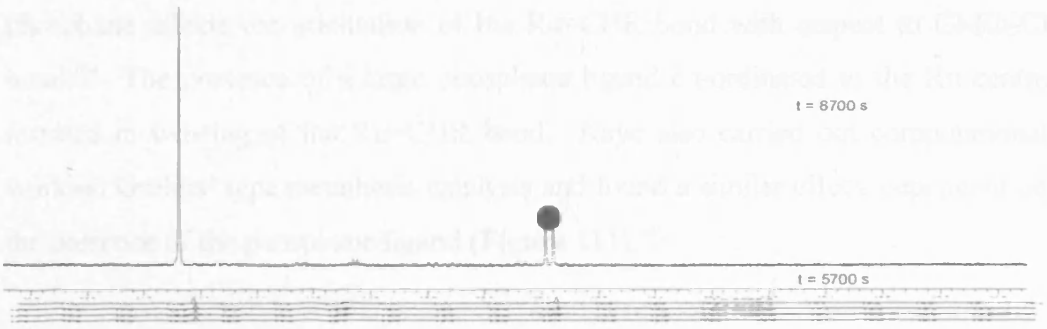

Figure 109 ^{1}H NMR spectrum of alkylidene region for RCM of 31 by 29 with Ti(OEt)$_4$ co-catalyst, t = 3000 s

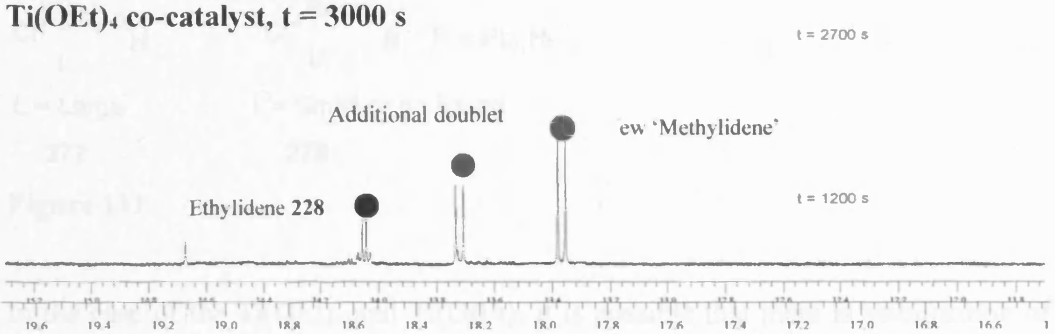

Figure 110 ^{1}H NMR spectrum of alkylidene region for RCM of 31 by 29 with Ti(OMe)$_4$ co-catalyst, t = 25,200 s

Since the two new signals were separated by 10.7 Hz, it was also possible that these signals were actually a doublet, with a coupling into the alkyl region of the ^{1}H NMR spectrum. A ^{1}H-^{1}H COSY was run between 0-20 ppm to search for coupling between the Ru-alkylidene region and alkyl region. No cross peaks were observed between these regions, suggesting that these signals were two singlets. Since the signals had very similar shifts to methylidene **221**, it seemed likely that the protons were two methylidene protons which are non-equivalent. It is possible that the size and nature of the ligand affects the geometry of the Ru=CH_2 bond, and the equivalence or non-equivalence of the two methylidene protons depends on the size of the ligands co-ordinating to the metal centre. The study by Sanchez on a range of Ti(IV) alkoxides suggested that Ti(OEt)$_4$ and Ti(O*i*Pr)$_4$ have different behaviours in solution, since titanium(IV) ethoxide is trimeric in solution. This may also be the case for Ti(OMe)$_4$, and would explain the similar behaviour observed with the two titanium reagents.

Harvey *et al.* carried out computational studies on Grubbs' type ruthenium metathesis catalysts **28** and **29** and found that the size (and presence) of the

phosphane affects the orientation of the Ru=CHR bond with respect to Cl-Ru-Cl bond.[104] The presence of a large phosphane ligand co-ordinated to the Ru centre resulted in twisting of the Ru=CHR bond. Kaye also carried out computational work on Grubbs' type metathesis catalysts and found a similar effect, dependent on the presence of the phosphane ligand (**Figure 111**).[68]

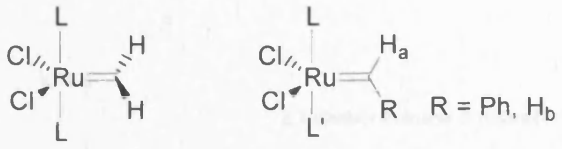

Figure 111

In the case of the $Ti(OEt)_4$ and $Ti(O\textit{i}Et)_4$ it is possible that there is stabilisation of the 14 electron ruthenium species by the Ti(IV) co-catalyst, which accelerates phosphane dissociation; the relatively small size of the co-ordinated titanium species results in a geometry of Ru=CHR such as **278**, where the two protons are non-equivalent and therefore give two separate signals in the ^1H NMR. $Ti(O^iPr)_4$ is bulkier, so the Ru alkylidene adopts a geometry like **277**, in which the methylidene protons are equivalent. The energy differences between the two orthogonal arrangements are also relatively small, giving easy access to both geometries.

These results suggest that the addition of the titanium(IV) co-catalysts changes the catalytic species which are carrying out the cyclisation reaction, and this gives rise to the observed difference in the rate of RCM. These results also challenge those presented by Fűrstner, since they imply that the addition of the co-catalyst to the reaction has a more complex effect than co-ordination with the carbonyl group of the diene. This may be occurring, but it appears that this effect is occurring in conjunction with a change in the catalytic species toward a more efficient one.

The theory that the $Ti(O\textit{i}Pr)_4$ provides a source of propene *via* which ethylidene **228** can form was tested further using $Ti(OEt)_4$ and $Ti(OMe)_4$ in the RCM of **22**. Solutions of **22** in dichloromethane (0.01), with Ti(IV) reagent were sparged with propene for 15 minutes each before adding Grubbs' II **29**. Aliquots were removed

from the reactions over a period of two hours, treating samples with the SPE procedure as described in **2.2.2**. After removing an aliquot, the reaction was quickly sparged with propene once more. Samples were analysed by GC, and the end points were checked by ^{1}H NMR to ensure that the final product was cyclooctenone **23**. Results overlaid with those obtained previously using $Ti(OMe)_4$, $Ti(OEt)_4$ and $Ti(OiPr)_4$ are shown in **Figure 112.**

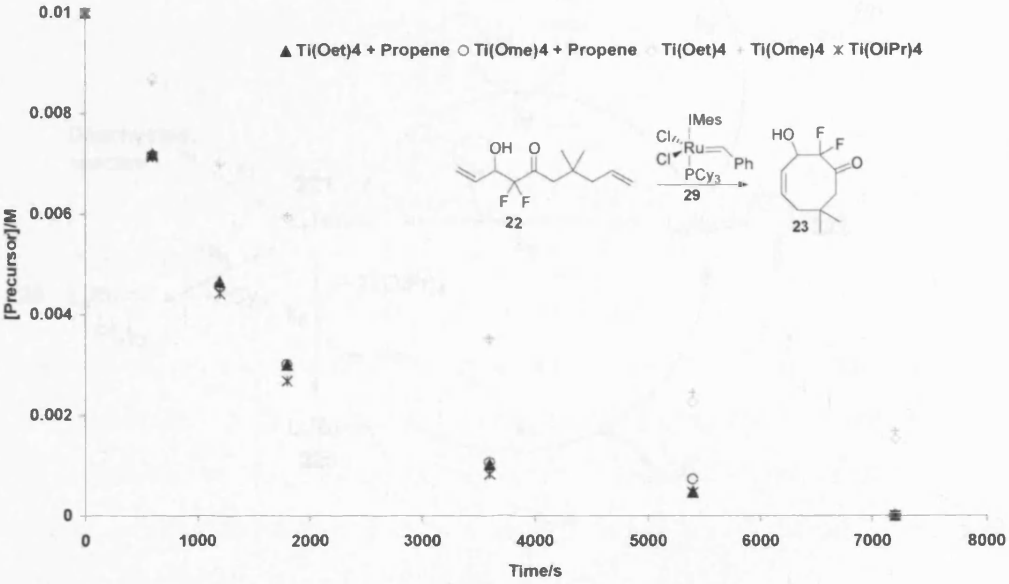

Figure 112 Overlaid results for the RCM of 22 by 29 with $Ti(OMe)_4$ or $Ti(OEt)_4$ in the presence and absence of propene (Section 10, p85)

The results in **Figure 112** support the theory that $Ti(OiPr)_4$ acts as a source of propene through which to generate ethylidene **228**, since the provision of propene with $Ti(OEt)_4$ and $Ti(OMe)_4$ results in acceleration of the RCM over the presence of these Ti(IV) reagents alone, with the cyclisation rate almost equal to that observed in the presence of $Ti(OiPr)_4$. This result was highly useful, and the observation was used to generate a new model.

A new model was generated, in order to take into account the formation of the ethylidene with $Ti(OiPr)_4$ (**Scheme 106**). The model includes two further steps. The rate constant k_5 corresponds to the reaction of methylidene **221** with $Ti(OiPr)_4$ to generate ethylidene **228**, and k_8 corresponds to cross metathesis between ethylidene **228** and substrate, releasing propene.

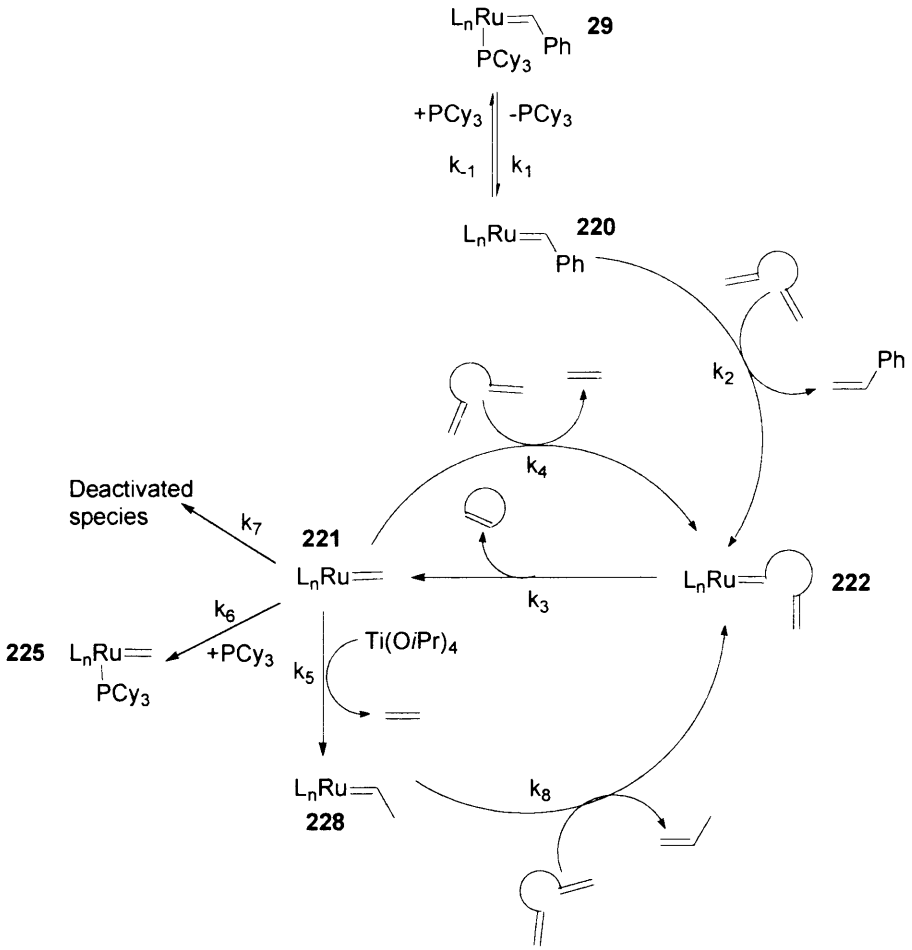

Scheme 106 Metathesis model including generation of ethylidene 228 from Ti(O*i*Pr)$_4$

This model was used to fit all further kinetic data, since the Ti(IV) co-catalyst was used in all cases.

4.3 Analysis of all Kinetic Data

The model shown in **Scheme 106** was input into Berkeley Madonna, and used to generate good fits for all of the data generated from the kinetic experiments carried out using the sampling protocol and GC analysis. The first data to be kinetically simulated were those of substrates **22, 149** and **150** run individually. Initially, the software was allowed complete freedom when fitting the data. However, since the steps in the mechanism corresponding to k_1, k_{-1}, k_5 and k_6 are not substrate dependent, and involve only catalyst species, the values of these rate constants were

fixed by extrapolating the value for the correct [Ru] from the plots obtained from varying the catalyst loadings. The software was then given freedom to vary k_2, k_3, k_4 and k_8 during the fitting process, since these steps in the model are expected to be affected by substrate. Even after fixing the values of k_1, k_{-1}, k_5 and k_6, good fits were still obtained. Rate constants obtained after fixing these rate constants are shown in **Table 25**. Fits overlaid with experimental data are shown in **Figures 114-116**.

X	$k_1 \times 10^5$ s^{-1}	$k_{-1} \times 10^6$ $M^{-1} s^{-1}$	$k_2 \times 10^3$ $M^{-1} s^{-1}$	$k_3 \times 10^2$ s^{-1}	$k_4 \times 10^2$ $M^{-1} s^{-1}$	$k_5 \times 10^4$ $M^{-1} s^{-1}$	$k_6 \times 10^6$ $M^{-1} s^{-1}$	$k_7 \times 10$ s^{-14}	$k_8 \times 10^2$ $M^{-1} s^{-1}$
H	3.24	1.04	5.60	70	1.69	2.89	1.49	2.00	14.4
Bn	3.24	3.00	1.20	3.00	1.22	2.89	1.49	2.00	6.40
Bz	3.24	3.00	0.82	17.0	0.37	2.89	1.49	2.00	0.66

Table 25 Rate constants generated by Berkeley Madonna for individual substrate kinetics

Table 25 shows that the values of k_2, k_3, k_4 and k_8 vary significantly between the three substrates. Initially, we would only expect to observe variation in k_3, since this step in the model contains the cyclisation event, and since we assume that the catalyst initially binds at the Type I alkene, the effect of the allylic substituent should not be felt at this point in the mechanism.[x]

The ethylidene alkylidene **228** appears to show both the largest rates through this part of the cycle, and the highest degree of discrimination between the three substrates. The benzylidene **220** is the least reactive, and next most discriminating, with the methylidene **221** an order of magnitude less reactive than the ethylidene, and less selective than the benzylidene **(Table 26, Figure 113)**. The substrates used in our study are strongly expected to begin to react on the less substituted alkenyl group; this makes it very hard to see how alkylidene transfer rates can be affected so strongly.

X	k_2 $M^{-1} s^{-1}$	k_4 $M^{-1} s^{-1}$	k_8 $M^{-1} s^{-1}$	k_3 s^{-1}
H	5.6×10^{-3}	1.7×10^{-2}	14.4×10^{-2}	70×10^{-2}
Bn	1.2×10^{-3}	1.2×10^{-2}	6.4×10^{-2}	3.0×10^{-2}
Bz	0.8×10^{-3}	0.4×10^{-2}	0.7×10^{-2}	17×10^{-2}

Table 26

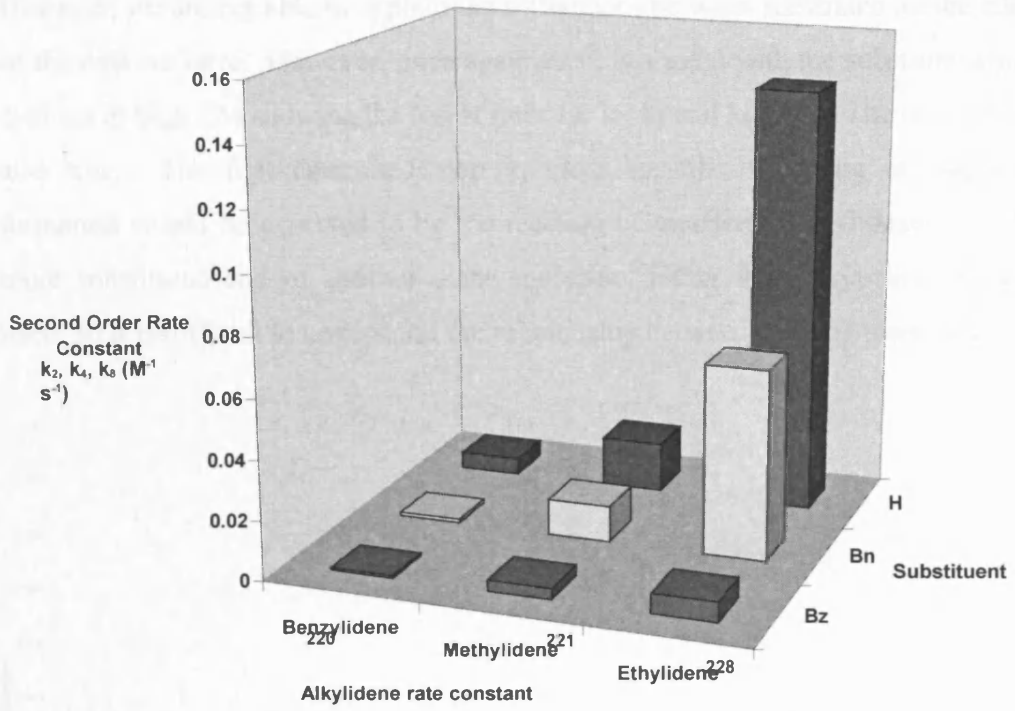

Figure 113

The values obtained for k_3 describe the cyclisation event and follow the trend observed from the crude concentration/time profiles for the RCMs of **22, 149** and **150**. These results confirm that alkylidene cyclisation is rate determining, because none of the other variable rate constants (k_2, k_4, k_8) would predict the correct rank order of substrate reactivity. There are striking, though surprising remote substituent effects on cross metathesis events; the alcohol is the most reactive substrate in each case, and the benzoate the least. **Figure 113** summarises these date graphically and shows clearly the higher reactivity and selectivity of the ethylidene catalyst **228**.

The k_2 step represents alkylidene transfer and extrusion of styrene, whereas k_4 is driven by ethylene release. The observed outcome potentially represents a balance between the high benzylidene reactivity and the lower methylidene reactivity, compensated by loss of volatile ethylene from the reaction. The ethylidene presumably combines release of volatile co-product with extended lifetime, resulting in increase effectiveness.

However, we are not able to explain the differences between substrates on the basis of the data we have. However, once again there is a trend with the substrate which cyclises at high EM showing the losest rates for k_2, k_4 and k_8 steps. The converse is also true. The first commited step in cross metathesis leading to oligomer formation would be expected to be the reaction of transferred alkylidene with the more substituted end of another diene molecule, rather than alkylidene transfer itself, so it is difficult to understand the relationship between EM and these data.

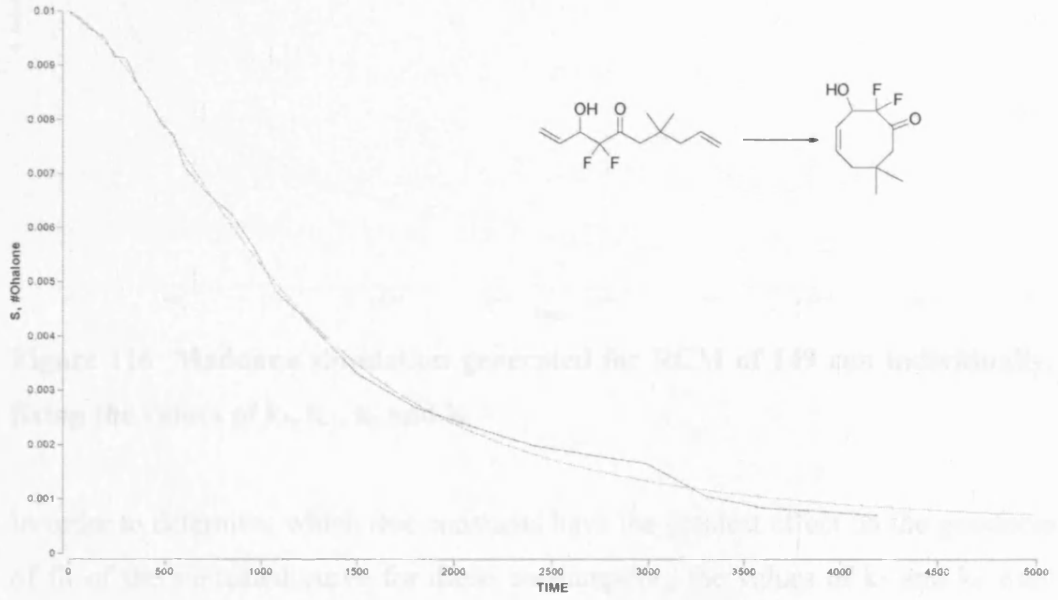

Figure 114 Madonna simulation generated for RCM of 22 run individually, fixing the values of k_1, k_{-1}, k_5 and k_6

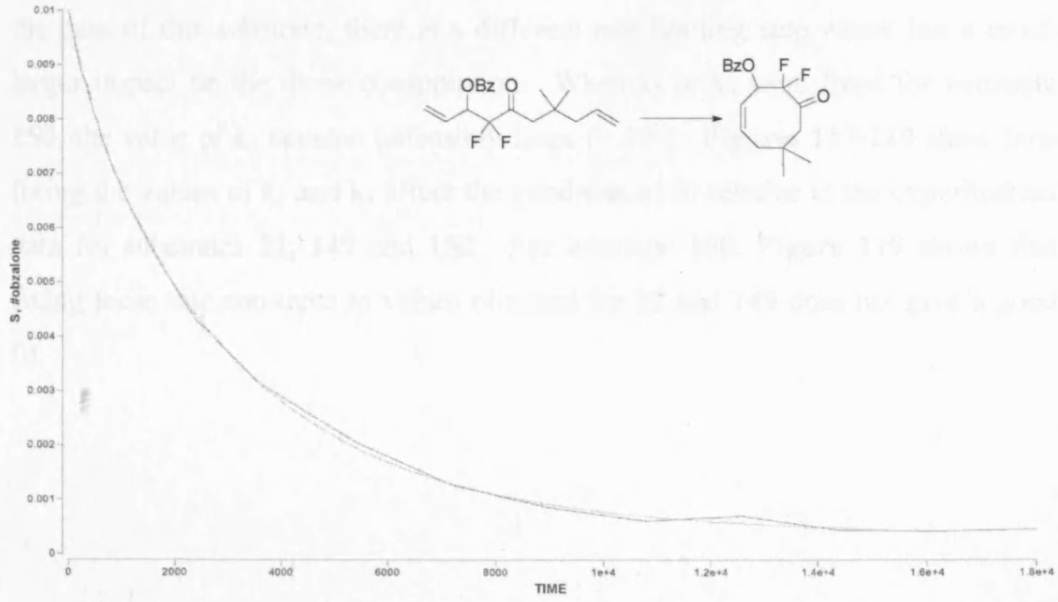

Figure 115 Madonna simulation generated for RCM of 150 run individually, fixing the values of k_1, k_{-1}, k_5 and k_6

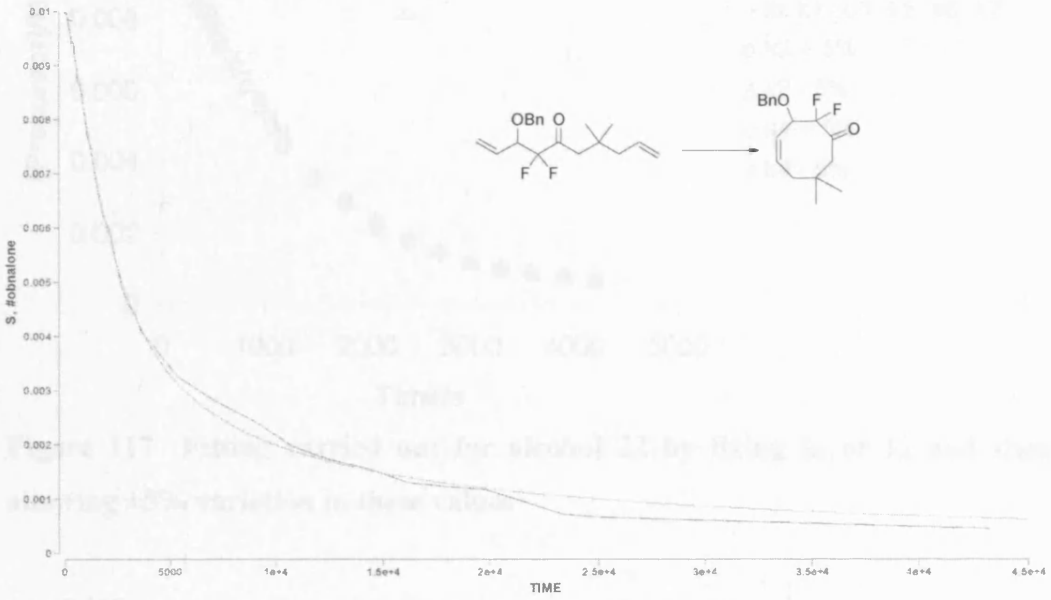

Figure 116 Madonna simulation generated for RCM of 149 run individually, fixing the values of k_1, k_{-1}, k_5 and k_6

In order to determine which rate constants have the greatest effect on the goodness of fit of the simulated curve for diene consumption, the values of k_2 and k_4 were fixed to those obtained for alcohol **22**. The fits obtained for benzyl ether **149** were reasonable, but the fits obtained for benzoate **150** were very poor, suggesting that in the case of this substrate, there is a different rate-limiting step which has a much larger impact on the diene consumption. When k_2 or k_4 were fixed for benzoate **150**, the value of k_3 became unfeasibly large ($\sim 10^1$). **Figures 117-119** show how fixing the values of k_2 and k_4 affect the goodness of fit relative to the experimental data for substrates **22, 149** and **150**. For benzoate **150**, **Figure 119** shows that fixing these rate constants to values obtained for **22** and **149** does not give a good fit.

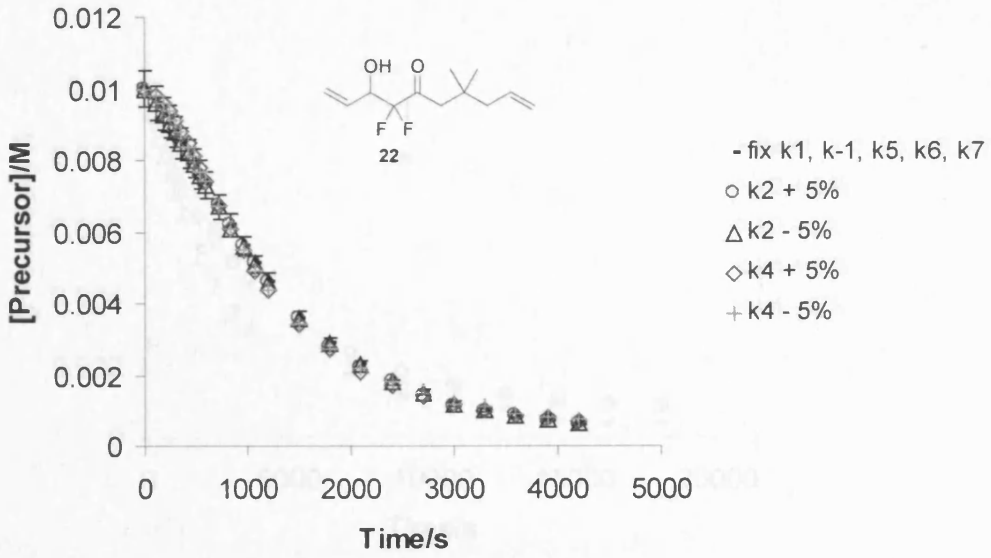

Figure 117 Fitting carried out for alcohol 22 by fixing k_2 or k_4 and then allowing ±5% variation in these values

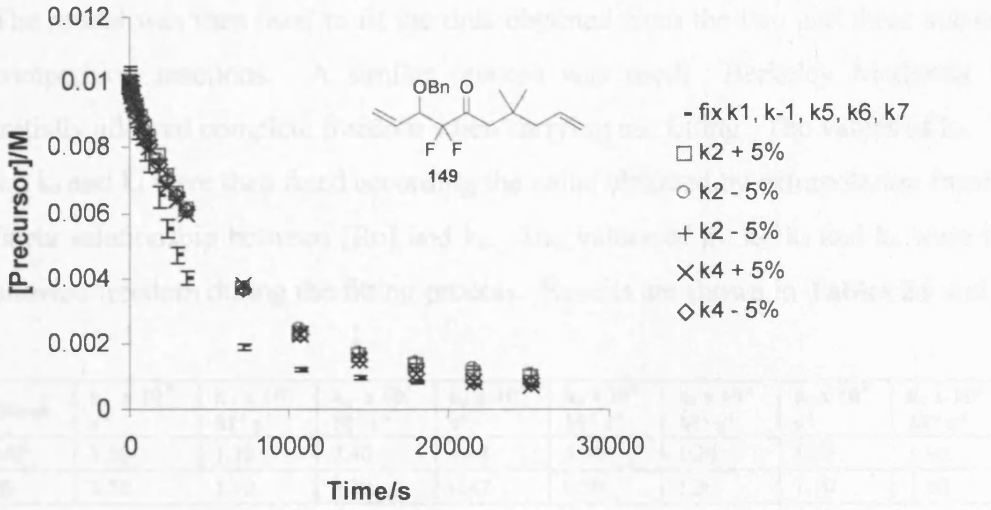

Figure 118 Fitting carried out for benzyl ether 149 by fixing k_2 or k_4 and then allowing ±5% variation in these values

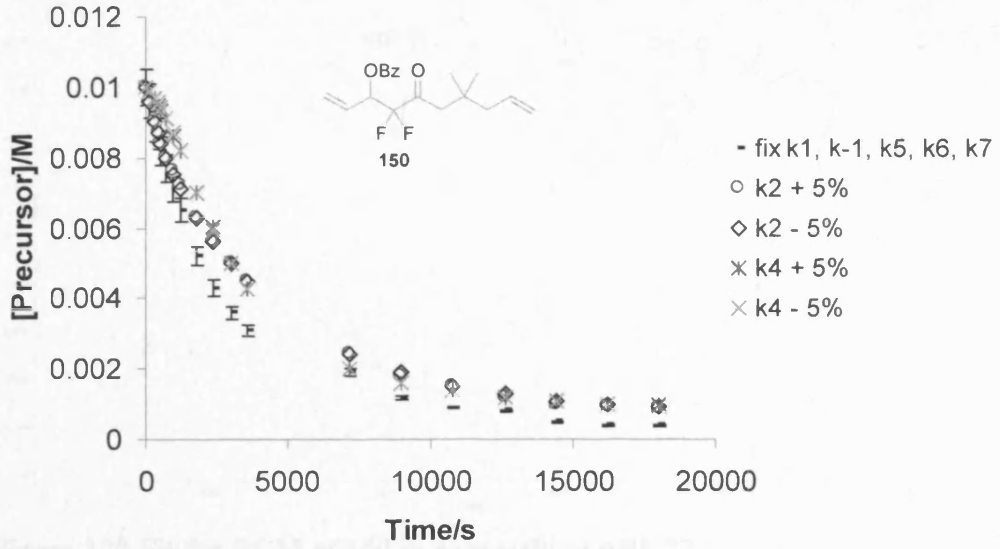

Figure 119 Fitting carried out for benzoate 150 by fixing k_2 or k_4 and then allowing ±5% variation in these values

The model was then used to fit the data obtained from the two and three substrate competition reactions. A similar process was used. Berkeley Madonna was initially allowed complete freedom when carrying out fitting. The values of k_1, k_{-1}, k_5 and k_6 were then fixed according the value obtained by extrapolation from the linear relationship between [Ru] and k_n. The values of k_2, k_3, k_4 and k_8 were then allowed freedom during the fitting process. Results are shown in **Tables 26** and **27**.

Diene	k_1 x 10^{-5} s^{-1}	k_{-1} x 10^6 M^{-1} s^{-1}	k_2 x 10^3 M^{-1} s^{-1}	k_3 x 10^4 s^{-1}	k_4 x 10^3 M^{-1} s^{-1}	k_5 x 10^{-4} M^{-1} s^{-1}	k_6 x 10^6 s^{-1}	k_7 x 10^4 M^{-1} s^{-1}	K_8 x 10^3 M^{-1} s^{-1}
149	3.50	1.10	7.40	16.4	3.70	1.20	1.70	1.90	3.63
30	3.50	1.10	3.30	0.47	0.50	1.20	1.70	1.90	0.62

Table 26 Madonna fitting results from competition reaction between 149 and 30

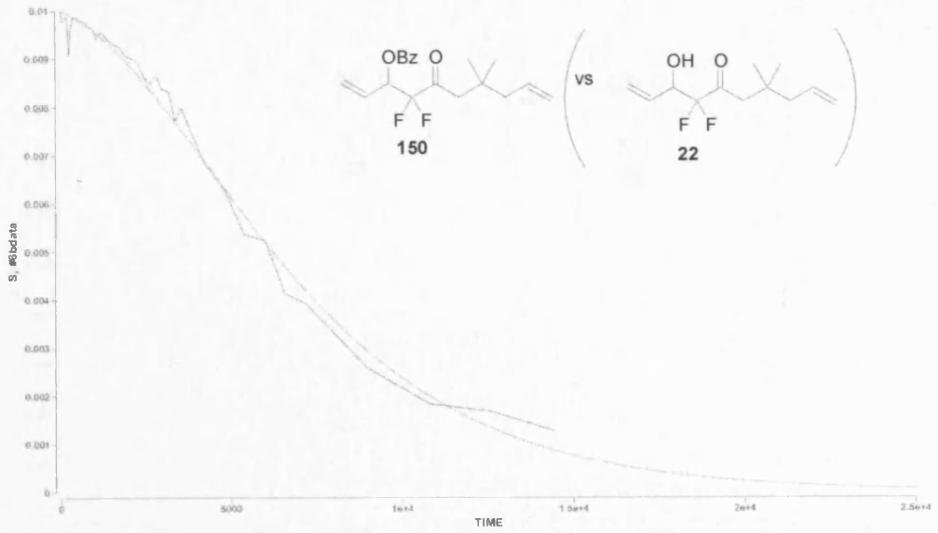

Figure 120 Fit for RCM of 150 in competition with 22

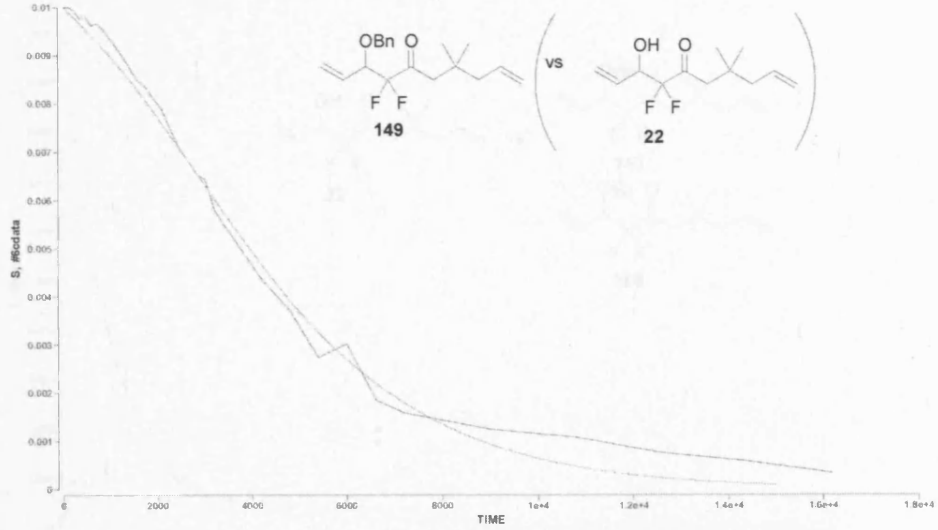

Figure 121 Fit for RCM of 149 in competition with 22

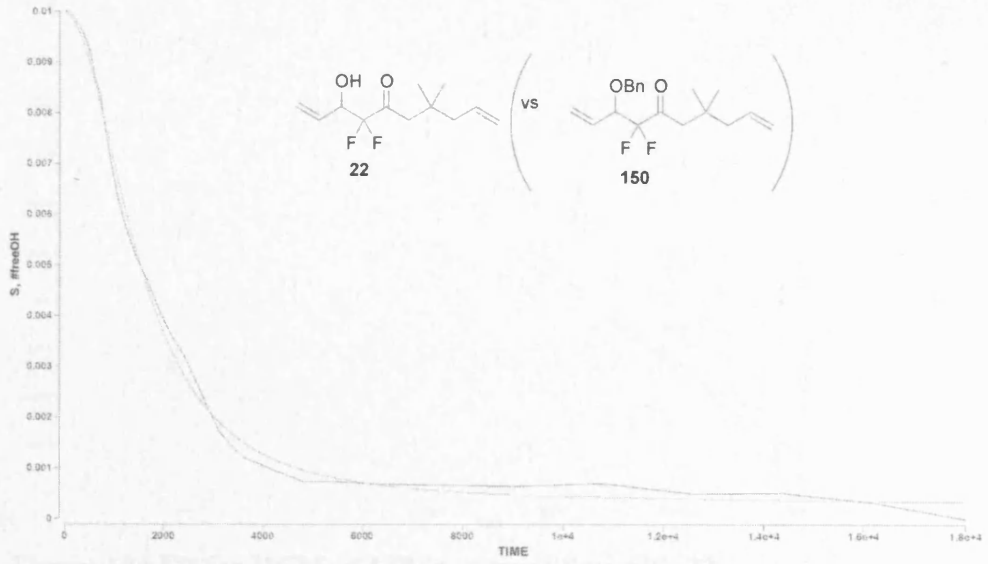

Figure 122 Fit for RCM of 22 in competition with 149

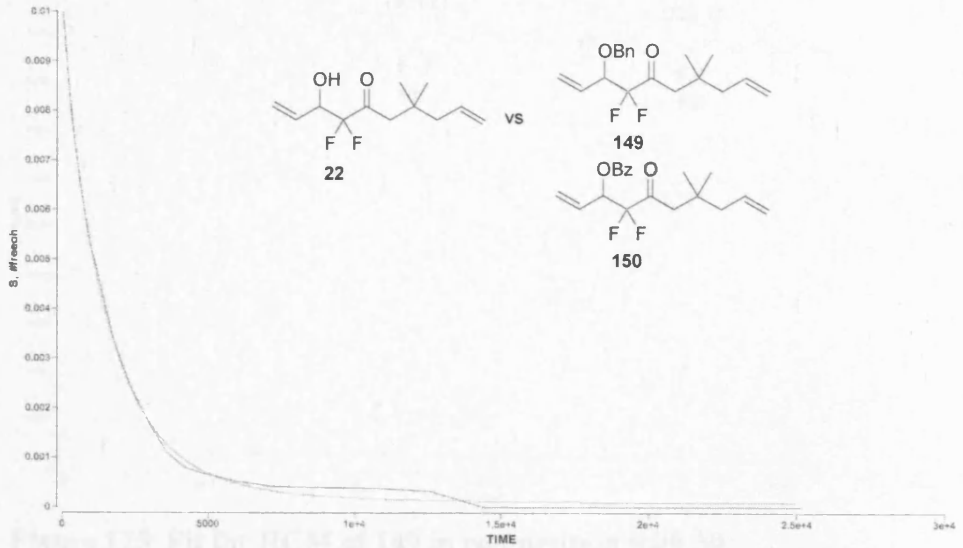

Figure 123 Fit for RCM of 22 in competition with 149 and 150

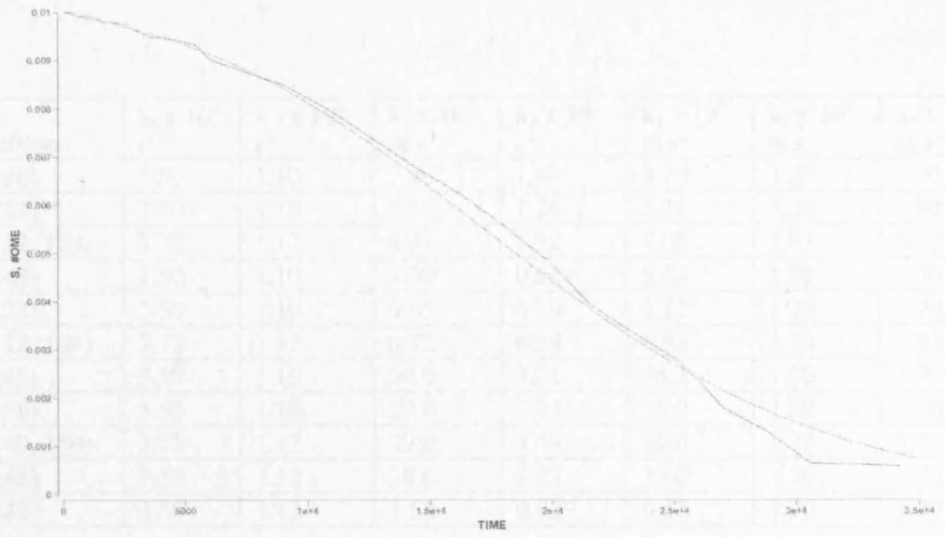

Figure 124 Fit for RCM of 148 in competition with 22

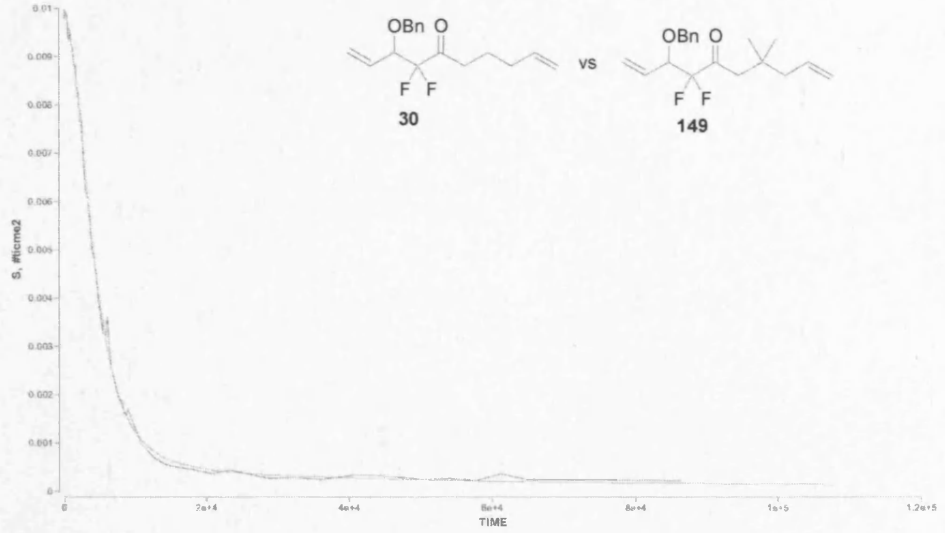

Figure 125 Fit for RCM of 149 in competition with 30

Use of the model on substrates **22, 30, 148-150** allowed a more in-depth analysis of the data generated, and a more direct comparison between the four substrates, and allowed us to identify the steps in the RCM mechanism which are most affected by the allylic protecting group. **Table 27** shows results obtained for each substrate, run either in competition with other substrates or alone.

Competition	$k_1 \times 10^5$ s^{-1}	$k_{-1} \times 10^6$ s^{-1}	$k_2 \times 10^3$ $M\ s^{-1}$	$k_3 \times 10^3$ s^{-1}	$k_4 \times 10^3$ $M\ s^{-1}$	$k_5 \times 10^4$ $M\ s^{-1}$	$k_6 \times 10^6$ $M\ s^{-1}$	$k_7 \times 10^4$ s^{-1}	$k_8 \times 10^3$ $M\ s^{-1}$
149 (*vs* 30)	3.50	1.10	7.40	1.64	3.70	1.20	1.70	1.90	3.63
149 (*vs* 22)	3.50	1.10	7.30	1.26	3.75	1.20	1.70	1.95	3.60
149 (*vs* 22, 150)	3.72	1.12	8.31	1.32	7.08	1.73	3.52	2.05	7.09
30 (*vs* 149)	3.50	1.10	3.30	0.047	0.50	1.20	1.70	1.90	0.62
150 (*vs* 22)	3.50	1.10	0.65	57.9	0.72	1.20	1.70	2.15	0.33
150 (*vs* 22, 149)	3.72	1.12	0.72	62.4	0.83	1.70	3.32	2.05	0.42
22 (*vs* 149)	3.50	1.10	29.0	3.21	36.3	1.20	1.70	1.90	42.0
22 (*vs* 150)	3.50	1.10	27.0	3.24	35.9	1.20	1.70	1.90	42.8
22 (*vs* 149, 150)	3.73	1.12	29.2	4.19	41.0	1.70	3.32	2.05	44.8
22 (*vs* 148)	3.50	1.12	28.0	3.22	36.0	1.20	1.70	1.90	42.4
148 (*vs* 22)	3.50	1.12	1.56	0.029	0.52	1.20	1.70	1.90	0.65

Table 27 Rate constants for competition reactions calculated by Berkeley Madonna, fixing k_1, k_{-1}, k_5 and

SPECIAL NOTE

PAGES 186 TO ___ ARE BLANK AND HAVE NOT BEEN SCANNED

All the data in **Table 27** were obtained from runs in which the simulation was allowed complete freedom. However, this raises a range of problems. For example, the k_1 and k_{-1} values obtained from single substrate runs differ considerably between substrates, and from the values for the same substrate in the threefold competition. In our model, k_1 refers to a step from which the substrate is absent so we would expect the same value of k_1 for each reaction under the same set of conditions. Clearly then, the rate constants obtained from the free simulation must be treated with considerable caution.

We therefore investifated the effect of fixing k_1 and k_{-1} and all other substrate independent step-related rate constants on these fits, using the single substrate runs in the first instance.

Table 27 shows some interesting results. All of the k_1 and k_{-1} values fall close to each other for all substrates **22, 30, 148-150** run as two substrate competition reactions, three substrate competition reactions, and individually. The values of k_5 and k_6 generated by the model are also within a factor of two between substrates run under the conditions. The interesting differences lie in constants k_2-k_4 and may account for the differences in cyclisation efficiency as well as the differences in cyclisation rate.

Chen carried out DFT computational studies on metathesis reactions, and identified three possible rate-limiting steps within the process: phosphane dissociation, metallocyclobutane formation, or metallocyclobutane breakdown, although Chen stated that different substrates may affect which process becomes the rate-limiting step.[105,106] Chen's calculations also revealed that the rate limiting step can depend on the choice of catalyst. In the case of first generation Grubbs' catalyst, the rate limiting step was calculated to be metallocyclobutane formation, whereas the rate-limiting step was calculated to be phosphane dissociation in the case of second generation Grubbs' catalyst. The results in table are in agreement with these findings, since k_1, which relates to the phosphane dissociation step, appears to be the rate-limiting step in the majority of cases, with the only exception being benzoate **150**, where the value of the constant is very close in value to k_4 which appears to be the rate limiting step in this case.

After phosphane dissociation, the smallest calculated rate constant for substrates **22, 30, 148, 149** (but not benzoate **150**) is k_3, which incorporates the cyclisation events within the RCM mechanism. This is not surprising, since any strain in the system is accrued at this stage.

The exception to this rule is benzoate **150**, where the rate limiting steps are the cross metathesis events of substrate with active catalyst, in particular with the propagating species. This may explain the high effective molarities for the RCM of the benzoate substrates **31** and **150**, if the cross metathesis events are rate-limiting. The lower rate of cross metathesis with ethylidene **228** (k_8) compared to that of methylidene **221** (k_4) may also explain the higher EM calculated for benzoate **31** in the presence of the Ti(IV) co-catalyst. Absence of the co-catalyst slows the formation of **228**, so cyclisation must be carried out by **221**, which appears to be less efficient at cyclisation than ethylidene **228**. This observation may be in support of Chen's claim that certain substrates may exhibit different rate-limiting steps.

Alcohol **22** is consumed most rapidly in RCM of all the substrates investigated. This substrate has rate-limiting cyclisation (k_3), although this process is still relatively rapid for **22**. However, the most important observations may lie in k_2 and k_4 and k_8, which represent the initial cross-metathesis event of the active catalytic species with the substrate. The values of these rate constants are all large, and are the largest of all the substrates studied. This observation is important and may help to explain the extremely low EM value for the RCM of **4** (see **3.1**). The EM values calculated for **4**, **30**, and **31** (in the presence and absence of Ti(O*i*Pr)$_4$ are shown in **Table 28.**

Substrate	EM/M
4	0.008
30	0.018
31[a]	0.24
31[b]	0.049

[a] In the presence of Ti(O*i*Pr)$_4$; [b] In the absence of Ti(O*i*Pr)$_4$

Table 28 Comparison of effective molarities calculated for 4, 30 and 31

Since cross metathesis appears to be such a favourable pathway for **22** it is possible that CM occurs between the substrate alkylidene and a further substrate molecule more readily than cyclisation. The large values of k_2, k_4 and k_8 and hence rapid CM reactions may explain the low EM for **4** and the low yields of cyclooctenone **3** even at high dilution.

Interestingly, the value of k_8 for benzoate **150** is much lower than the value of k_4. This corresponds to the high EM calculated for the benzoates in the presence of the Ti(IV) co-catalyst, and also explains the reduced EM calculated in the absence of the co-catalyst. These results suggest that the presence of ethylidene **228** increases the efficiency of the cyclisation reaction over the cross metathesis reaction, and also gives us an indication as to the relative selectivities of ethylidene **228** and methylidene **221** towards cyclisation and oligomerisation. These results suggest that ruthenium ethylidene **228** shows a 5-fold preference towards cyclisation over oligomerisation compared to the methylidene **221**. This observation has important implications for synthetic chemists who wish to synthesise potentially difficult systems, where high dilution is required. Addition of $Ti(O\textit{i}Pr)_4$ may reduce the volume of solvent required by providing access to a catalytic species which exhibits a greater preference for cyclisation over CM.

4.4 Use of Kinetic Model to Generate k_{cat}

Equation **5** refers to a general reaction catalysed by enzyme E, with substrate S, forming product P *via* enzyme-substrate complex ES. The terms k_1, k_{-1} and k_2 are rate constants for the association of the enzyme to the substrate, dissociation of enzyme and substrate back to the starting substrate, and progression of the bound substrate to product which then dissociates from the enzyme.

$$E + S \underset{k_{-1}}{\overset{k_1}{\rightleftharpoons}} ES \overset{k_2}{\rightleftharpoons} E + P$$

Equation 5

The overall rate of the reaction is limited by the formation of E + P and this rate depends on k_2 and the concentration of ES. This is written as

$$v = k_2[ES]$$

Equation 6

It is assumed that that [S]>>[E] since E is present in catalytic amounts. It is also assumed that the concentration of ES is constant (the steady state assumption). This means that its rate of formation and rate of consumption are the same, so [ES] stays constant. The formation of ES depends on k_1 and also on [E] and [S], and its breakdown can occur either *via* the k_{-1} or k_2 pathways:

$$k_1[E][S] = k_{-1}[ES] + k_2[ES]$$

Equation 7

Rearranging this equation to make it equal to [ES] gives:

$$[ES] = \frac{k_1[E][S]}{k_{-1} + k_2}$$

Equation 8

The three rate constant terms can be combined into one, to form the Michaelis constant K_M:

$$\frac{k_{-1} + k_2}{k_1} = K_M$$

Equation 9

Substitution for K_M into **Equation 9** gives:

$$\frac{[E][S]}{K_M} = [ES]$$

Equation 10

The total amount of enzyme must stay the same through the reaction but it is present as free enzyme E, or as ES complex. The total enzyme concentration $[E_0]$ can be expressed as:

$$[E_0] = [E] + [ES]$$

Rearrangement gives: $[E] = [E_0] - [ES]$

Equation 11

Substituting this term back into **Equation 10** gives

$$\frac{([E_0] - [ES])[S]}{K_M} = [ES]$$

Equation 12

The maximum rate, v_{max} is achieved when all of the enzyme is bound as ES complex. When [S]>>[E], it can be assumed that all enzyme will be in the ES form, therefore $[E_0] = [ES]$. Replacing v with v_{max}, gives:

$$v_{max} = k_2 [E_0]$$

Equation 13

Replacing $k_2 [E_0]$ with v_{max} gives

$$v = \frac{v_{max}[S]}{K_M + [S]}$$

Equation 14

This equation is the Michaelis-Menten equation. In practical terms, this equation is used to quantify the rate of enzyme catalysis and identify the strength of binding (K_M), and in the calculation of k_{cat}. When the substrate concentration is equal to K_M, 50% of the catalyst molecules are bound to substrate.

For true catalysts, the rate of reaction increases with increasing substrate concentration. In simple cases, the substrate is consumed exponentially, allowing simple analysis and calculate of k_{cat}. However, in the case of our systems, an

accurate v_{max} and subsequent calculations are difficult since the end point is never truly reached. Instead, k_{cat} can be calculated from the double reciprocal Lineweaver Burke plot of 1/[S] *vs* $1/V_0$, where V_0 is the rate k_n, as calculated from the simulation data for each concentration. The substrate concentration in DCM was varied between 6 mM and 15 mM, maintaining the titanium(IV) co-catalyst loading at 30 mole %, catalyst **29** loading at 2%, and using the method for sample treatment described previously (**p53**).

The generation of the successful model in Berkeley Madonna, and its application to all of the kinetic data obtained allowed the calculation of a series of k_{cat} values for each step accounted for in the RCM process. The calculation of k_{cat} gives high quality insight into catalyst efficiency, and allow direct comparison between different enzymes or catalysts for a particular process. Calculation of this rate constant is generated from the study of the kinetics of the reaction of interest at varying concentrations. Catalytic reactions are known to proceed more rapidly when the substrate concentration is higher. A double reciprocal plot, known as a Lineweaver Burke plot (1/Concentration *vs* $1/k_x$) allows the calculation of k_{cat}, as well as K_M, the Michaelis-Menten binding constant, and V_{max}, which is the maximum rate of cyclisation.

The model shown in **Scheme 106** was used to fit the substrate decay curves for the RCM of benzyl ether **149**, run as a single substrate between 0.006 M and 0.015 M (**Scheme 107**). All aliquots removed from the reaction were treated using the SPE procedure prior to GC analysis. Some overlaid substrate decay curves are shown in **Figure 125** (at substrates concentrations of 0.006 M, 0.008 M and 0.015M).

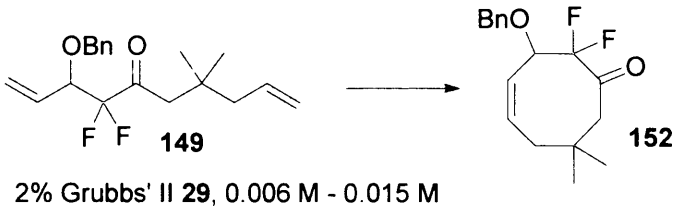

2% Grubbs' II **29**, 0.006 M - 0.015 M
30% $Ti(OiPr)_4$, CH_2Cl_2, 25°C
Followed by GC

Scheme 107

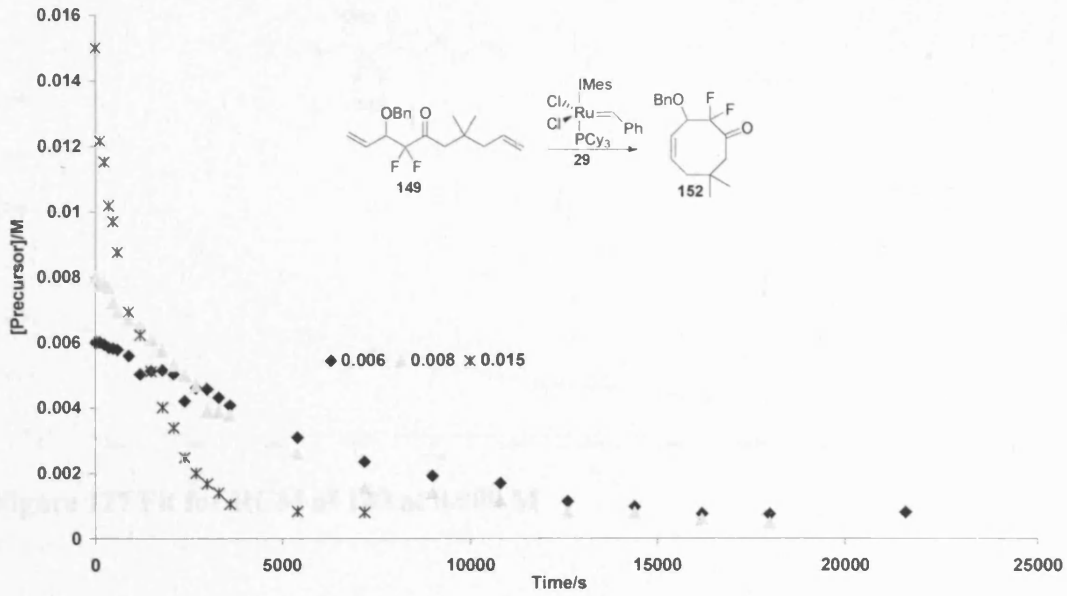

Figure 125 Overlays of RCM of 149 by 29 at 0.006 M, 0.008 M and 0.015 M (Section 10, p77-82)

Due to the complex nature of the RCM reactions, one single k_{cat} value cannot be generated for these data. The kinetic modelling software was applied to these datasets to generate good fits for the 7 RCM steps at varying concentrations (**Figures 126-130**) and the rate constants generated from the automatic fitting (**Tables 29** and **30**) were used to generate K_M, V_{max} and k_{cat} values for each forward reaction (**Figures 131-137**).

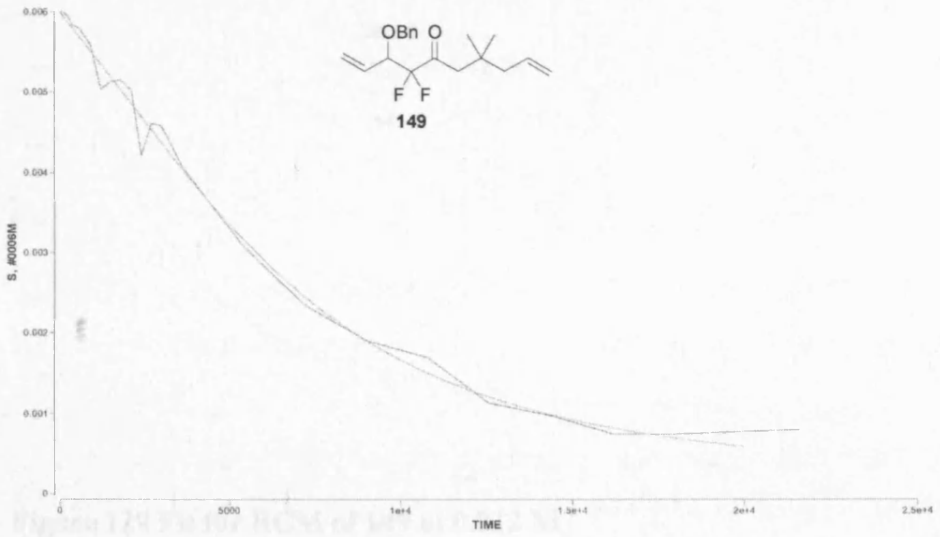

Figure 126 Fit for RCM of 149 at 0.006 M

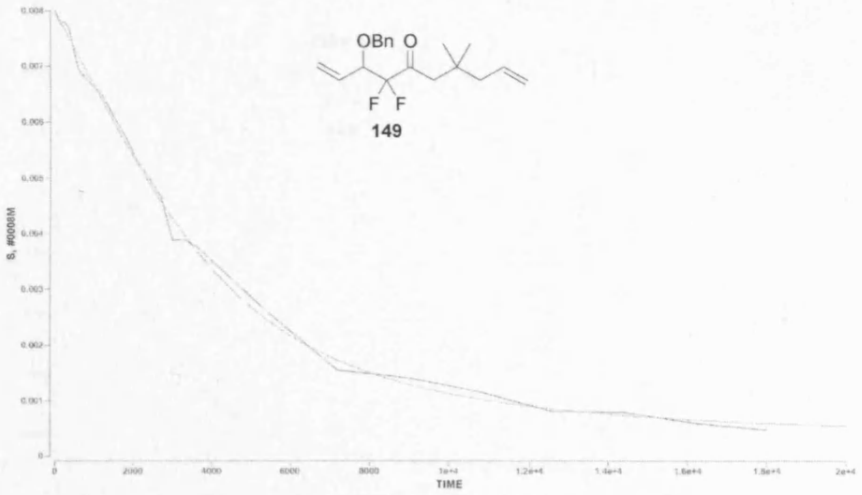

Figure 127 Fit for RCM of 149 at 0.008 M

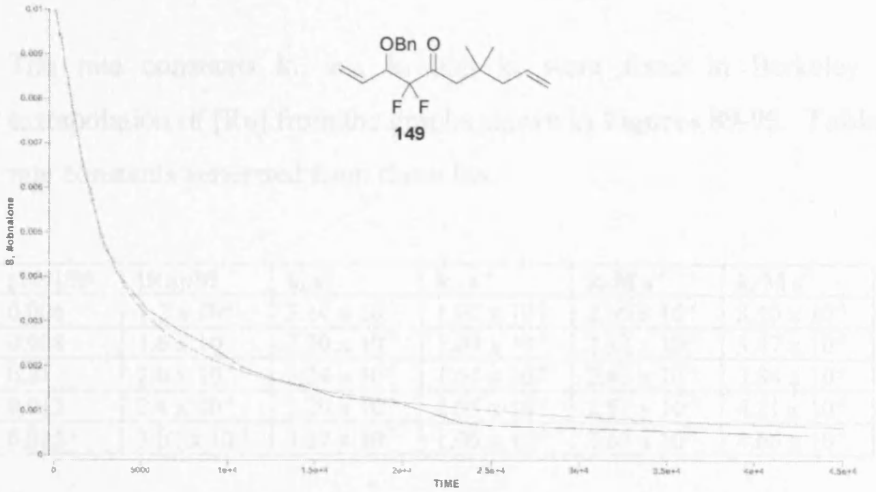

Figure 128 Fit for RCM of 149 at 0.01 M

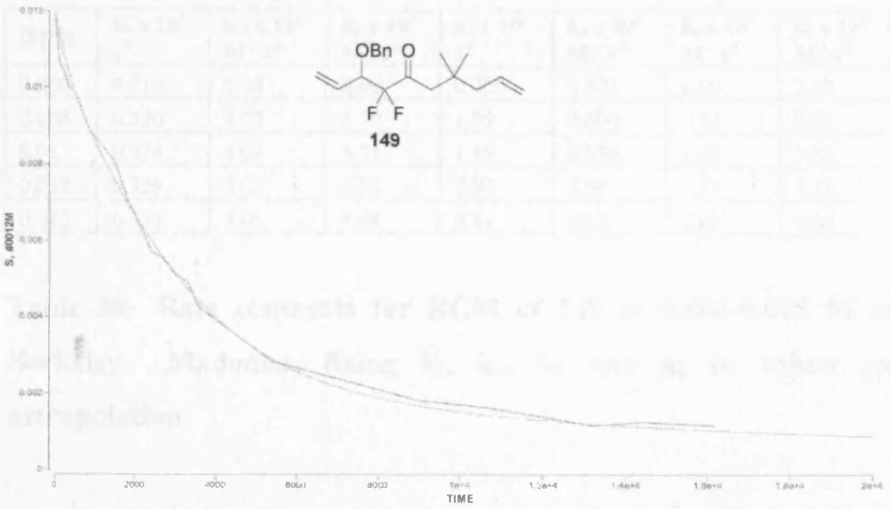

Figure 129 Fit for RCM of 149 at 0.012 M

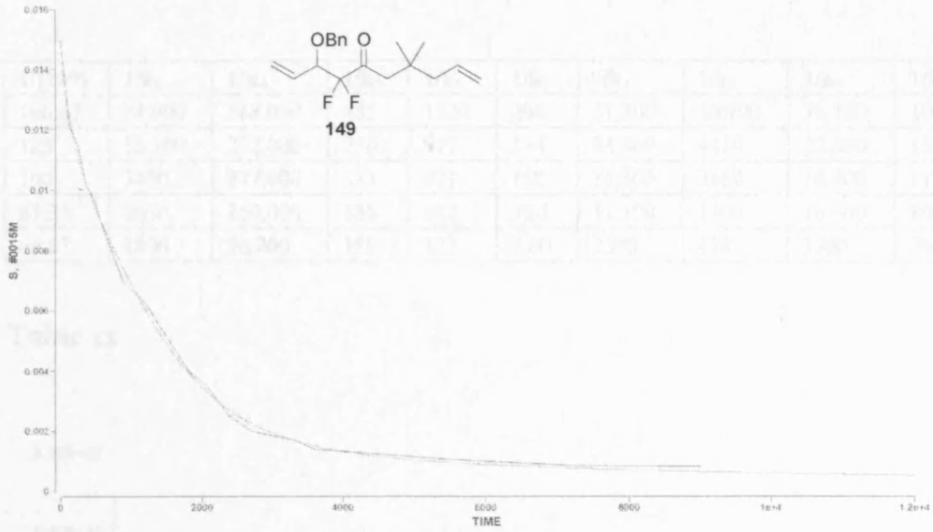

Figure 130 Fit for RCM of 149 at 0.015 M

The rate constants k_1, k_{-1}, k_5 and k_6 were fixed in Berkeley Madonna by extrapolation of [Ru] from the graphs shown in **Figures 89-95**. **Table 29** shows the rate constants generated from these fits.

[149]/M	[Ru]/M	k_1 s^{-1}	k_{-1} s^{-1}	k_5 M s^{-1}	k_6 M s^{-1}
0.006	1.2×10^{-4}	3.14×10^{-5}	1.02×10^{-6}	2.00×10^{-4}	3.10×10^{-6}
0.008	1.6×10^{-4}	3.20×10^{-5}	1.03×10^{-6}	2.33×10^{-4}	3.47×10^{-6}
0.01	2.0×10^{-4}	3.24×10^{-5}	1.04×10^{-6}	2.42×10^{-4}	3.84×10^{-6}
0.012	2.4×10^{-4}	3.29×10^{-5}	1.05×10^{-6}	2.51×10^{-4}	4.21×10^{-6}
0.015	3.02×10^{-4}	3.37×10^{-5}	1.06×10^{-6}	2.63×10^{-4}	4.66×10^{-6}

Table 29 Extrapolated values of k_1, k_{-1}, k_5, k_6

[S]/M	$k_1 \times 10^4$ s^{-1}	$k_{-1} \times 10^6$ M^{-1} s^{-1}	$k_2 \times 10^3$ M^{-1} s^{-1}	$k_3 \times 10^3$ s^{-1}	$k_4 \times 10^2$ M^{-1} s^{-1}	$k_5 \times 10^4$ M^{-1} s^{-1}	$k_6 \times 10^6$ M^{-1} s^{-1}	$k_7 \times 10^5$ s^{-1}	$k_8 \times 10^3$ s^{-1}
0.006	0.314	1.02	2.06	0.755	0.501	2.00	3.10	2.77	5.06
0.008	0.320	1.03	3.70	1.09	0.694	2.33	3.47	6.39	7.36
0.01	0.324	1.04	5.51	1.49	0.756	2.42	3.84	5.44	8.53
0.012	0.329	1.05	6.32	2.92	2.56	2.51	4.21	9.41	9.84
0.015	0.337	1.06	8.64	8.14	10.2	2.63	4.66	29.6	14.1

Table 30 Rate constants for RCM of 149 at 0.006-0.015 M calculated by Berkeley Madonna, fixing k_1, k_{-1}, k_5 and k_6 to values calculated by extrapolation

Reciprocal concentrations of **149** and $1/k_x$ are shown in **Table 31**, followed by plots of 1/[**xx**] *vs* $1/k_x$ for k_2 to k_8 in **Figures 131-137**.

1/[149]	$1/k_1$	$1/k_{-1}$	$1/k_2$	$1/k_3$	$1/k_4$	$1/k_5$	$1/k_6$	$1/k_7$	$1/k_8$
166.67	54,900	568,000	485	1320	200	31,200	10,100	36,100	198
125	16,100	272,000	270	917	144	24,400	4410	22,800	136
100	3450	217,000	181	671	112	15,500	2460	18,400	117
83.33	2630	150,000	158	342	39.1	11,100	1400	10,600	102
66.67	1890	96,200	116	123	9.80	2390	474	3380	70.9

Table xx

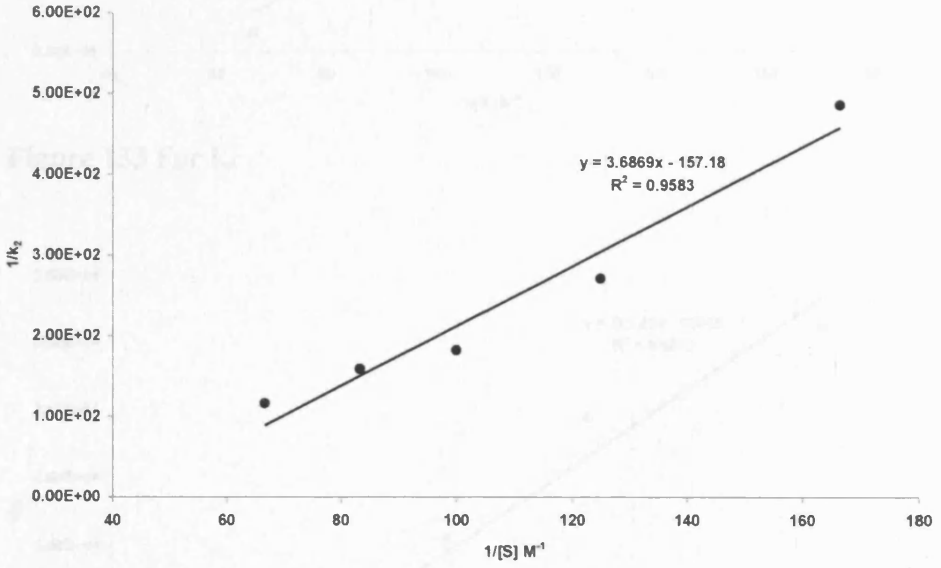

Figure 131 For k_2

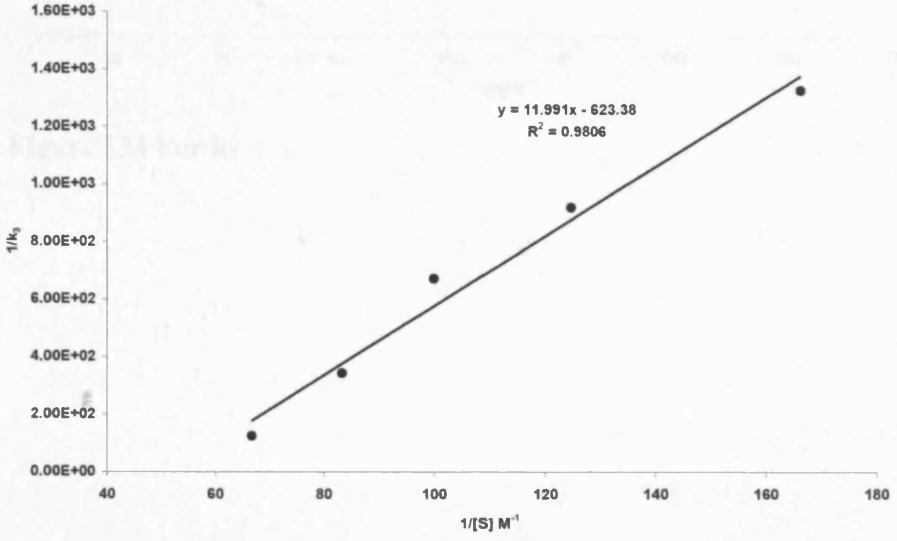

Figure 132 For k_3

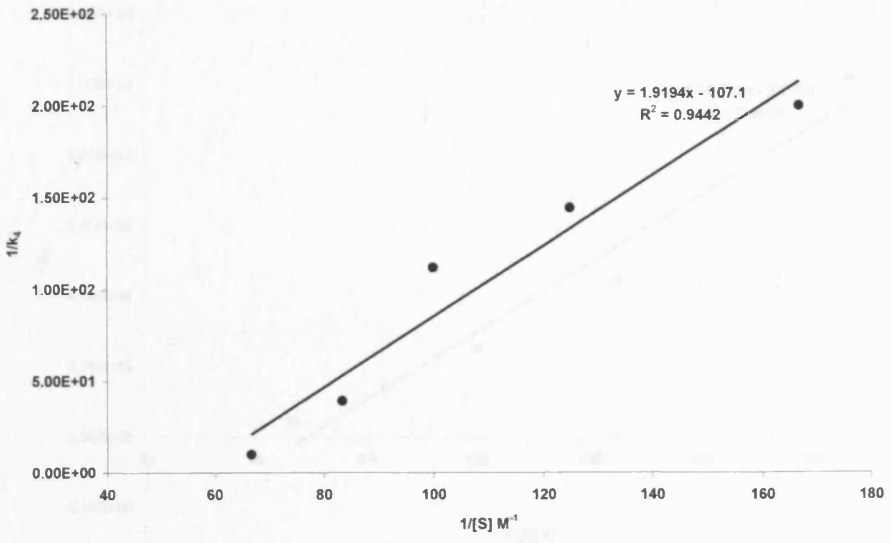

Figure 133 For k_4

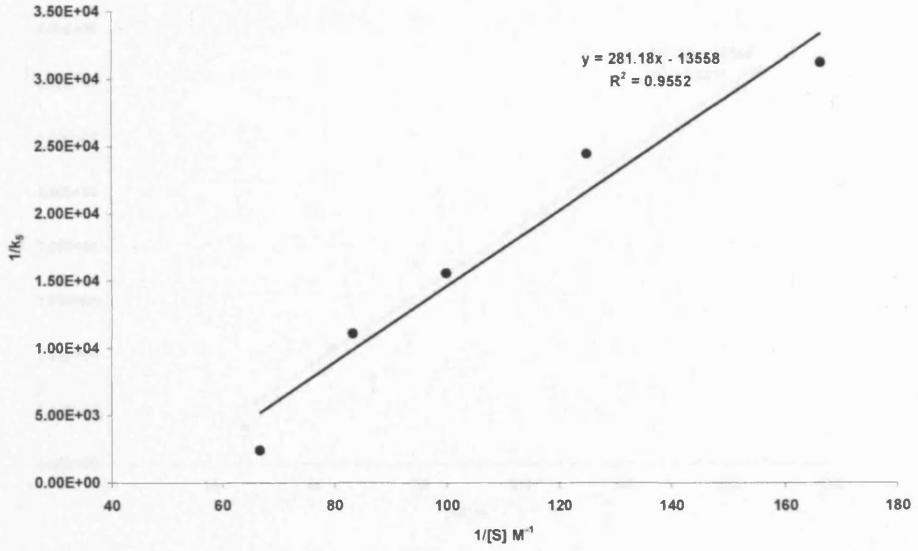

Figure 134 For k_5

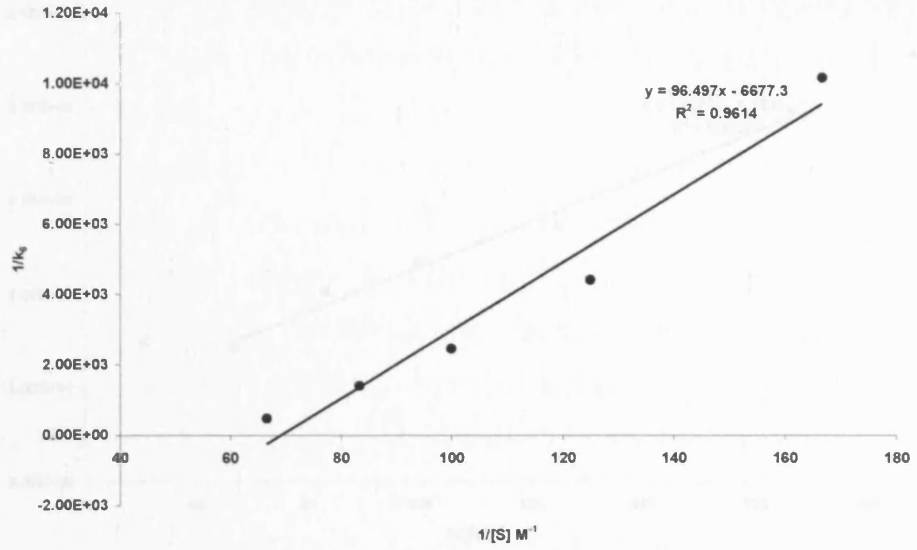

Figure 135 For k_6

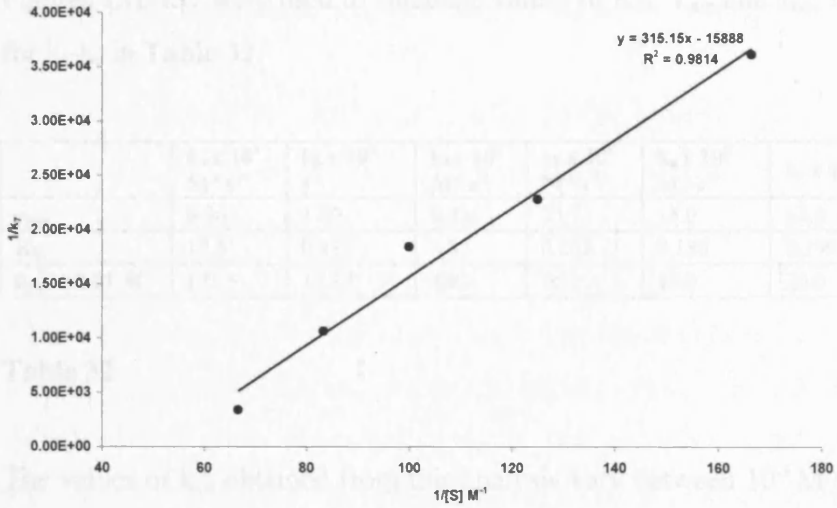

Figure 136 For k_7

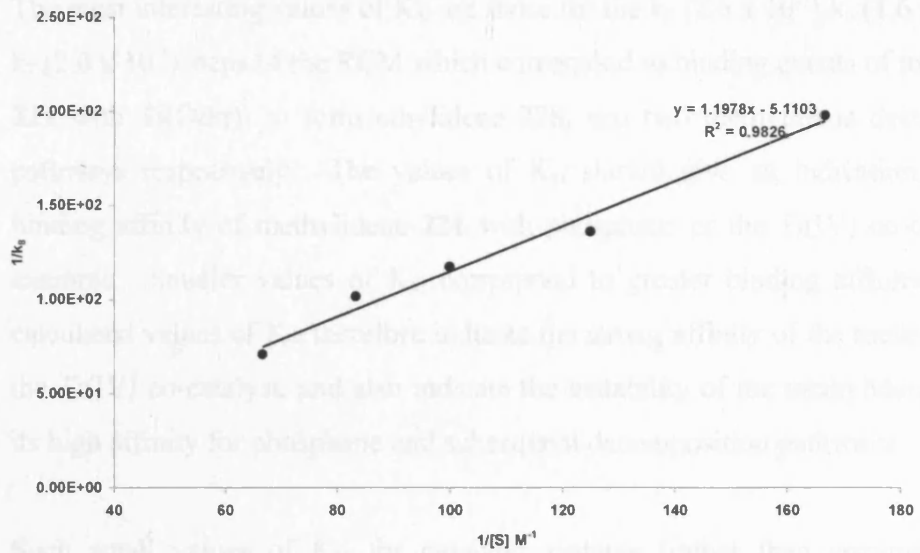

Figure 137 For k_8

Figures **131-137** were used to calculate values of K_M, V_{max} and k_{cat}, which are shown for k_1-k_6 in **Table 32**.

	$k_2 \times 10^3$ $M^{-1} s^{-1}$	$k_3 \times 10^3$ s^{-1}	$k_4 \times 10^3$ $M^{-1} s^{-1}$	$k_5 \times 10^6$ $M^{-1} s^{-1}$	$k_6 \times 10^5$ $M^{-1} s^{-1}$	$k_7 \times 10^6$ s^{-1}	k_8 $M^{-1} s^{-1}$
V_{max}	6.36	1.60	9.34	73.7	15.0	62.9	0.196
K_M	17.3	0.133	4.87	0.262	0.158	0.199	0.163
k_{cat} at 0.01 M	172.5	13.38	486	26.3	15.9	20.0	16.34

Table 32

The values of k_{cat} obtained from this analysis vary between 10^{-5} M s^{-1} for the k_7 step (methylidene decomposition) and 10^1 M s^{-1} for k_8 (cross metathesis between ethylidene **228** and substrate). However, the calculation of k_{cat} may be difficult using this model, since the rate constant must be calculated with [catalyst]. This may correspond to the concentration of pre-catalyst **29** initially added, or may correspond to the concentration of the active catalytic species **220, 221** or **228**, or intermediate relevant to a particular stage of the model. If the latter is the case, then the calculation of k_{cat} becomes difficult since we do not know the concentration of these species in solution at any given time. The values of k_{cat} generated in this case must therefore be regarded with some degree of caution, but perhaps are useful for direct comparison between individual steps within the model.

The most interesting values of K_M are those for the k_5 (2.6×10^{-7}), k_6 (1.6×10^{-6}) and k_7 (2.0×10^{-7}) steps of the RCM which correspond to binding events of methylidene **221** with Ti(O*i*Pr)$_4$ to form ethylidene **228**, and two methylidene decomposition pathways respectively. The values of K_M should give an indication as to the binding affinity of methylidene **221** with phosphane or the Ti(IV) co-catalyst for example. Smaller values of K_M correspond to greater binding affinities. These calculated values of K_M therefore indicate the strong affinity of the methylidene for the Ti(IV) co-catalyst, and also indicate the instability of the methylidene, through its high affinity for phosphane and subsequent decomposition pathways.

Such small values of K_M for catalytic systems (rather than enzyme-catalysed systems) are unusual, since small values of K_M usually indicate high specificity for a particular substrate. For catalytic systems, larger values of K_M are expected, allowing their application to a wide range of substrates and reactions.

The calculation of k_{cat} allows us to evaluate the relative efficiency of the three catalytic species in the RCM: benzylidene **220**, methylidene **221** and ethylidene **228**. **Table 32** shows that ethylidene **228** performs cross metathesis with the substrate **149** much more rapidly than both methylidene **221** and benzylidene **220** since the values obtained for k_8 are larger than those obtained for k_4 and k_2. This finding supports the observed drop in cyclisation rate of dienes in the absence of the Ti(IV) co-catalyst, and shows ethylidene **228** to be the more reactive catalytic species compared to the methylidene and benzylidene. Methylidene **221** is slightly more reactive towards cross metathesis with the substrate than benzylidene **220**.

The majority of kinetic work that has been carried out on RCM substrates has explored a limited range of substrates which usually result in the formation of five-membered rings.[107-110] Most groups studying RCM prefer to calculate turnover numbers (TONs), which are often used to compare new and existing catalysts. However, the calculation of TON appears to be based solely on the conversion of diene to cyclic product after a fixed time period, and the catalyst loading, rather than the rate at which the catalysts are able to perform metathesis reactions. The TON calculations do not take into account possible slower conversion of diene to cyclic product depending on the nature of the diene, or even the catalyst.

A small amount of literature exists, with groups calculating k_{cat} for ROMP and ADMET processes. Novak followed the kinetics of a 'living' ring-opening metathesis polymerisation of 3,4-difunctional cyclobutene **281** (**Scheme 108**) using the Schrock molybdenum catalyst **40**.[81] The value of k_{cat} was calculated to be 1.40 x 10^{-1} M^{-1} s^{-1}.

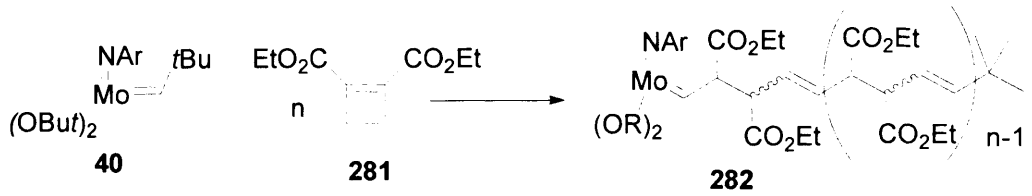

Scheme 108 ROMP of 3,4-difunctional cyclobutene with Schrock catalyst

Kessler and White published a k_{cat} value for the acyclic diene metathesis (ADMET) of dicyclopentadiene **213** with Grubbs' first generation catalyst **28** (**Scheme 109**).[80] The value of k_{cat} was calculated to be 3.65 x 10^{-1} M^{-1} s^{-1}.

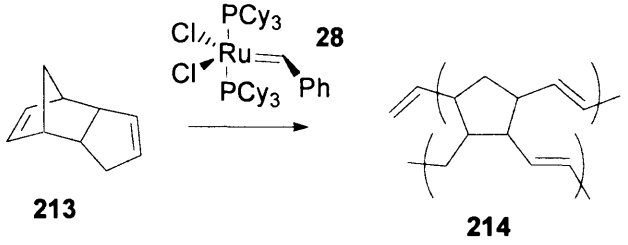

Scheme 109 ADMET of dicyclopentadiene

Whereas these are the only calculated values of k_{cat} to our knowledge which have been published for olefin metathesis, many other groups have published k_{cat} values for other metal-catalysed processes. Banerjee published a k_{cat} value of 41 M^{-1} s^{-1} for the oxidation of hydrogen peroxide using an [ethylenebis(biguanide)] silver(III) ion (**283**) as the catalyst.[111]

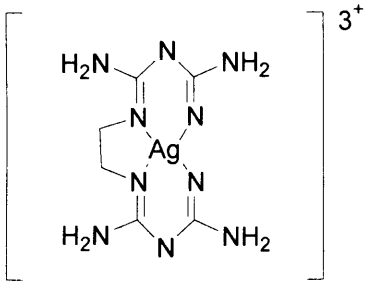

283

Sanchez-Delgado calculated a k_{cat} of 50 M^{-1} s^{-1} for the regioselective homogeneous hydrogenation of quinoline **284** **(Scheme 110)** using $[Rh(COD)(PPh_3)_2]PF_6$ as the catalyst precursor.[112]

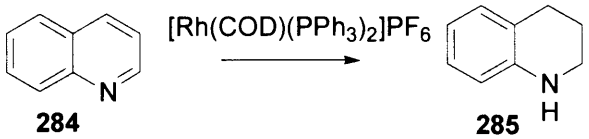

284 285

Scheme 110 Homogeneous hydrogenation of quinoline

Author	k_{cat}
Novak	1.40×10^{-1} M^{-1} s^{-1}
White	3.65×10^{-1} M^{-1} s^{-1}
Banerjee	41 M^{-1} s^{-1}
Sanchez-Delgado	50 M^{-1} s^{-1}

Table 33 Compiled values of k_{cat}

The values given by Novak and White are a k_{cat} for the overall reaction, which unfortunately we are unable to calculate due to the complexity of this reaction and the kinetics we have observed. This makes a direct comparison of our k_{cat} values with the literature values difficult. In comparison with the values shown in **Table 33**, our values of k_{cat} for the k_2, k_4 and k_8 steps in the model compare reasonably well, as they are within the same orders of magnitude. The value of k_{cat} for the k_3 step in the model is an order of magnitude less than those calculated by Novak and White, however this is only a relatively small difference considering the reactions studied by Novak and White are strain-relieving reactions, whereas the k_3 step involves cyclisation processes, which would be expected to be the most negatively entropic stage of the cyclisation reaction.

The value of k_{cat} calculated for the reaction of ethylidene **228** with substrate (k_8 in the model) compares well with the large k_{cat} values calculated for the rapid catalysed hydrogenation and oxidation reactions published by Sanchez-Delgado and Banerjee respectively, suggesting that the reaction of **149** with **228** is a relatively efficient process which occurs readily, suggesting that the use of Grubbs' II and the Ti(IV) co-catalyst system is a relatively efficient catalyst for carrying out RCM reactions.

5.1 Simplification of RCM Kinetics

The kinetic experiments described in **2.2.4**, and subsequent profiling of the reaction using modelling software, showed us that these reactions are complex, and made analyses difficult. The use of nine rate constants for comparison in the model raises problems associated with the number of numerical solutions which may be found and places too much reliance on the software's curve fitting routine.

The formation of methylidene **221** complicates the analysis further, as there are two known catalyst deactivation pathways from this species.[42,43] The recapture of the phosphane by the methylidene is the main deactivation pathway; this is irreversible for the methylidene, unlike benzylidene **220**, for which phosphane binding is reversible. In order to remove these steps from the mechanism, giving us a simpler model to understand and evaluate, a new substrate was designed which would regenerate the benzylidene catalyst rather than the methylidene, resulting in longer catalyst lifetime and simplifying the analysis.

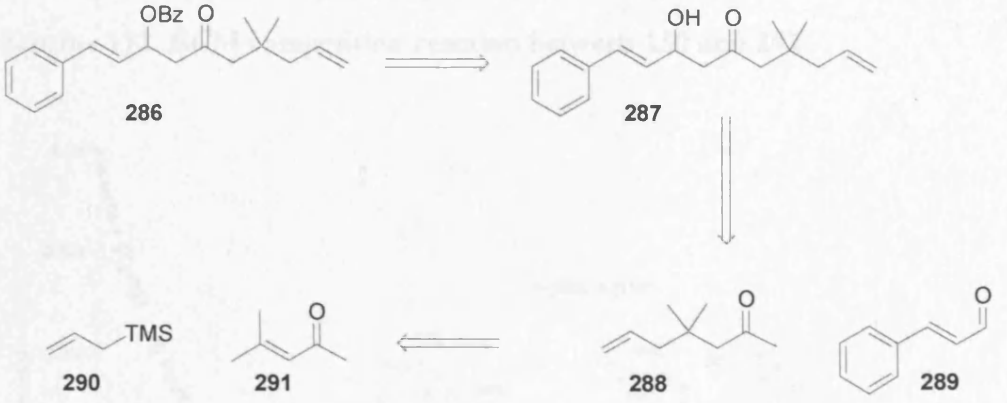

Scheme 111 Retrosynthetic analysis

Scheme 111 shows the retrosynthetic analysis from the desired substrate **286**. As shown in **3.1**, the benzoate group allows reactions of higher concentration to be followed by NMR, affording higher signal-to-noise with fewer scans, without compromising rate significantly.

As shown by R. Webster, who carried out an RCM competition reaction between **150** and **292** (**Scheme 112**) using the protocol described in **2.2.2**, the *gem*-difluoro

group does not affect the rate of cyclisation in these reactions, although it appears to have a small effect on the extent of completion of the reactions.[113] Although the difference in the extent to which the reactions complete is relatively small (~6%), it is not likely that this is due to differences in detection limits by GC, since control experiments were carried out to calculate the response factors for a range of substrates, and the differences in response factors were a maximum of 1.5%. The results are shown in **Figure 131**.

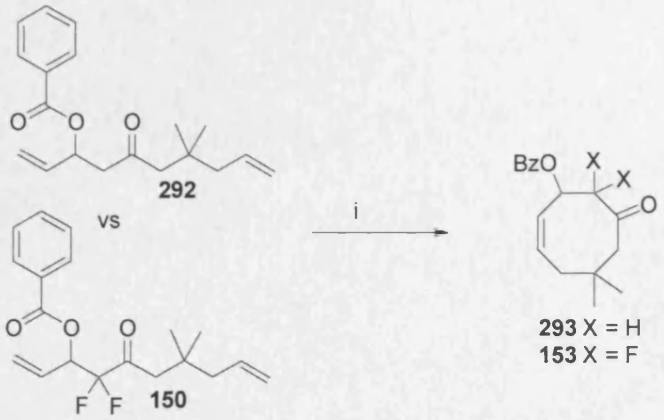

i) 2% **29**, $Ti(OiPr)_4$, 0.01 M CH_2Cl_2, 35°C, follow by GC

Scheme 112 RCM competition reaction between 150 and 292

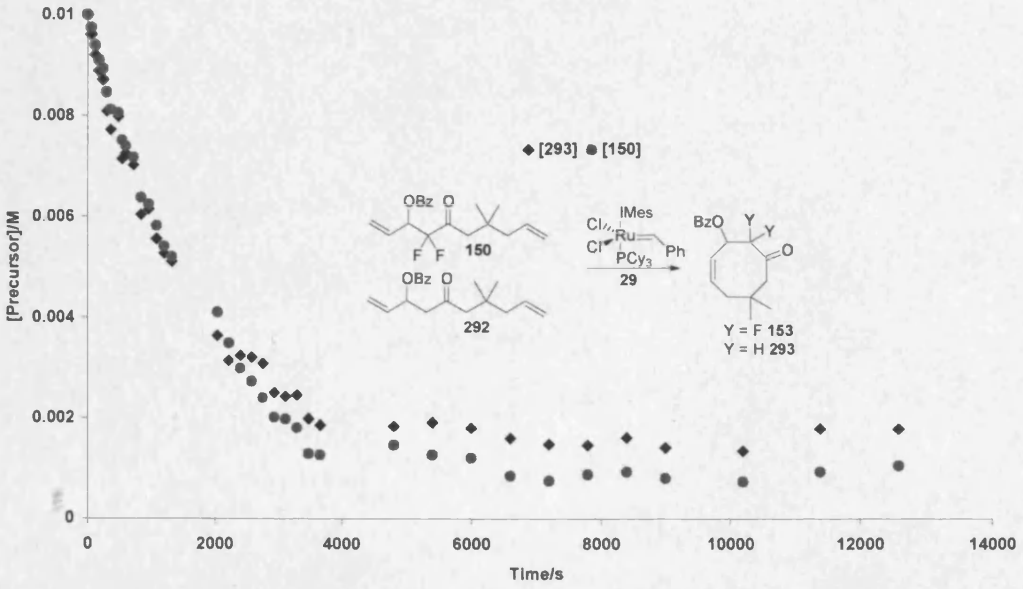

Figure 131 Experimental results obtained from the RCM competition reaction between 150 and 293

The cinnamyl alcohol can be formed from an aldol reaction between commercial *trans*-cinnamaldehyde **289** and 4,4-dimethyl hept-6-en-2-one **288**. This ketone can be easily synthesised from commercially-available mesityl oxide **291** and allyltrimethyl silane **290**.

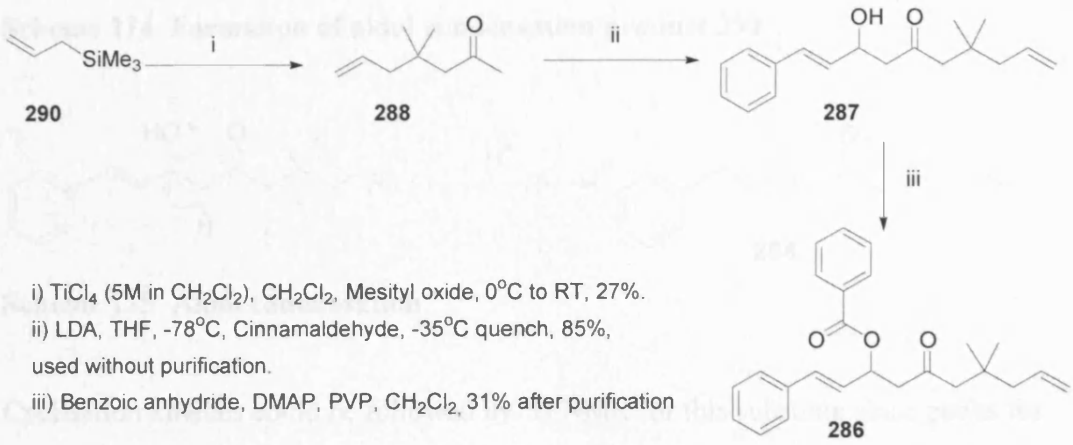

Scheme 113 Synthesis of RCM precursor 286

The first step was the synthesis of ketone **288** from mesityl oxide **291** and allyltrimethylsilane **290** with titanium(IV) chloride.[114] The resulting ketone was obtained in only 27% yield after Kugelrohr distillation at reduced pressure but sufficient amounts were obtained for further synthesis. Alcohol **287** was formed *via* an aldol reaction using LDA, and adding 0.8 equivalents cinnamaldehyde **289** at -78°C. The resulting alcohol still contained some residual cinnamaldehyde but was used to synthesise the benzoate **286** using benzoic anhydride and polymer-supported pyridine as before, without purification. After esterification, benzoate **286** was obtained through column chromatography as a crystalline solid. Recrystallisation from hot pentane ensured the material was of good purity, although elemental analysis for **286** could not be obtained.

Initial attempts at the aldol reaction which was quenched at -15°C led to the condensation and formation of triene **294** which was obtained as a yellow solid after column chromatography in 43% yield. This product forms as a result of the elimination of water from the molecule (**Scheme 114**), the driving force for which is the formation of the highly conjugated system in **294**, which has conjugation of the double bonds into the aromatic ring.

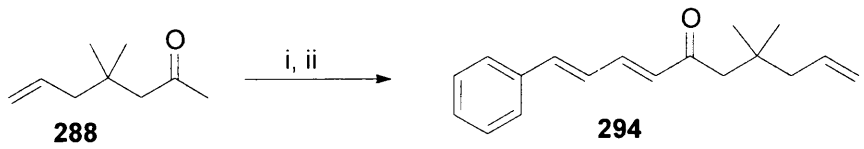

288 294

i) LDA, -78°C, cinnamldehyde

ii) -15°C, NH_4Cl aq quench

Scheme 114 Formation of aldol condensation product 294

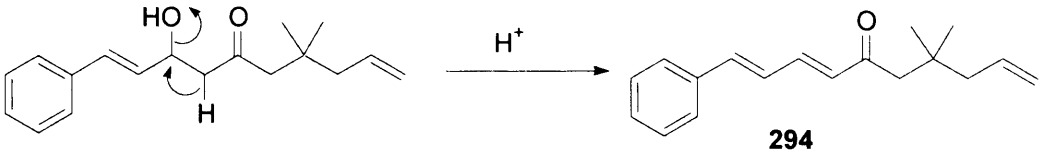

294

Scheme 115 Aldol condensation

Cyclisation kinetics could be followed by ^1H NMR for this substrate since peaks for substrate **286** and eight-membered ring **293** were sharp, unlike with the difluoro dimethyl cyclooctenones **23, 151-153**. The ^1H NMR spectrum (400 MHz, 298 K) in the alkene region was used to track the formation of eight-membered ring **293** from **286**, by monitoring the disappearance of internal and external alkene signals, and the appearance of cyclic alkene signals (**Figure 132**). The results are shown plotted in **Figure 133**.

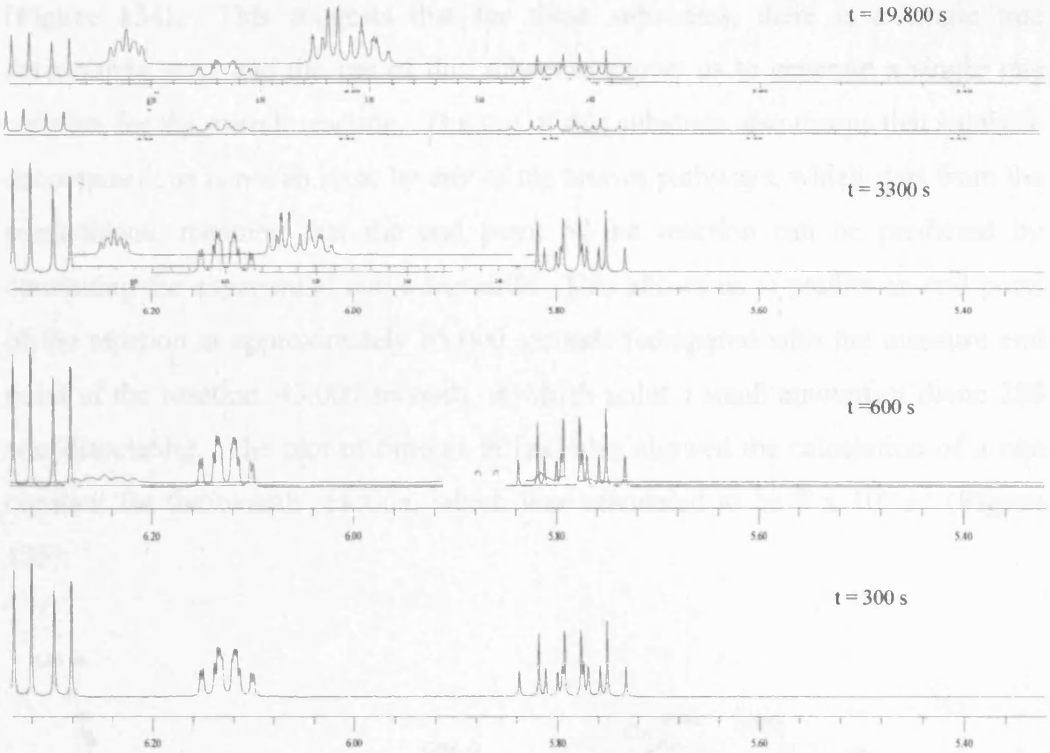

Figure 132 ^{1}**H NMR spectra from the alkene region for cyclisation kinetics of 286**

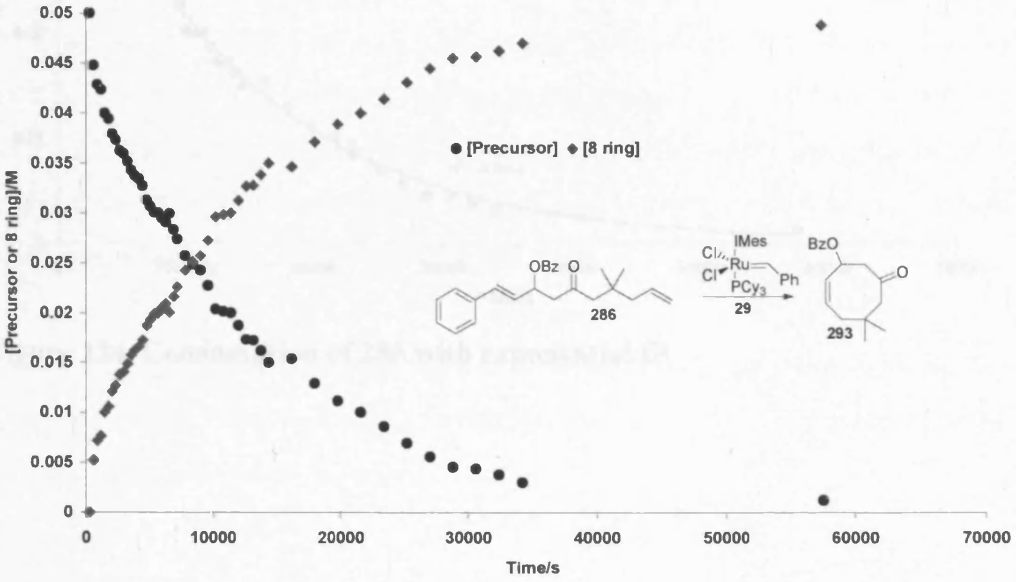

Figure 133 Experimental results from cyclisation kinetics of 286 (Section 10, p40)

Figure 133 shows a much more simple decay profile than observed with previous substrates, with the decay curve of precursor **286** fitting an exponential curve well

(**Figure 134**). This suggests that for these substrates, there is a single rate determining step, and the use of this substrate allows us to generate a single rate constant for the overall reaction. The use of this substrate also means that catalytic decompositions is not an issue by any of the known pathways, which start from the methylidene, meaning that the end point of the reaction can be predicted by continuing the exponential curve forwards. This allows us to predict an end point of the reaction at approximately 65,000 seconds (compared with the measure end point of the reaction, 43,000 seconds, at which point a small amount of diene **286** was detectable). The plot of time *vs* ln [**xx**] also allowed the calculation of a rate constant for the overall reaction, which was calculated to be 8 x 10^{-5} s^{-1} (**Figure 135**).

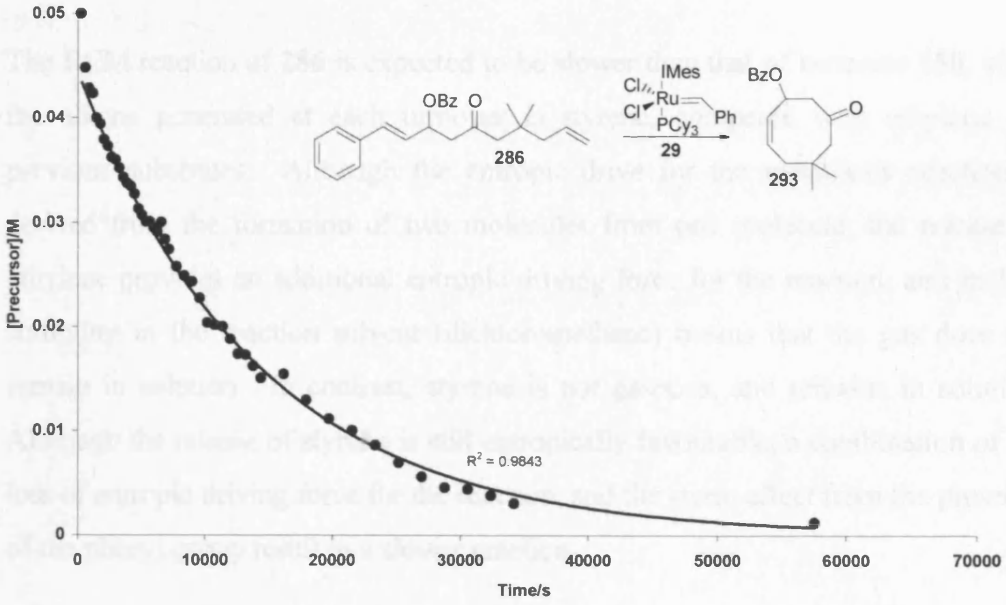

Figure 134 Consumption of 286 with exponential fit

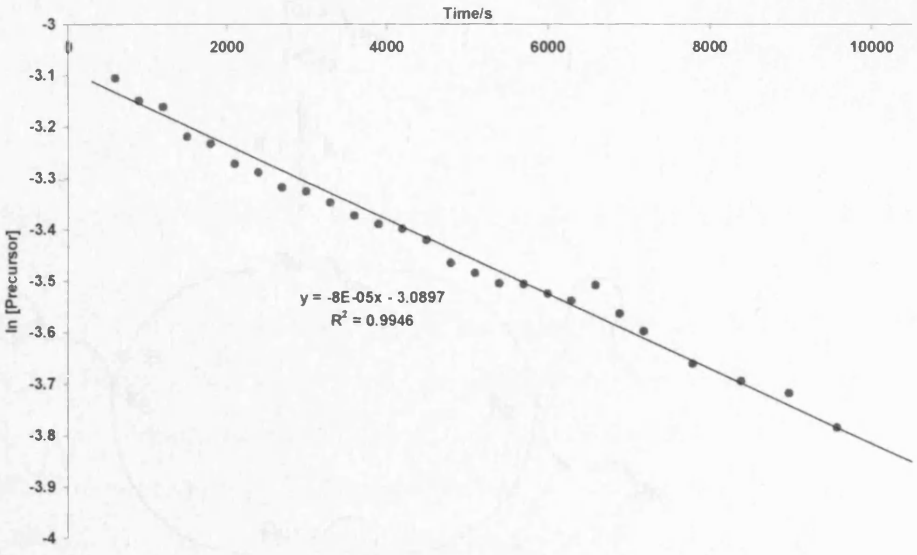

Figure 135 Plot of time *vs* ln [286]

The RCM reaction of **286** is expected to be slower than that of benzoate **150**, since the alkene generated at each turnover is styrene, compared with ethylene for previous substrates. Although the entropic drive for the metathesis reaction is derived from the formation of two molecules from one molecule, the release of ethylene provides an additional entropic driving force for the reaction, and its low solubility in the reaction solvent (dichloromethane) means that the gas does not remain in solution. In contrast, styrene is not gaseous, and remains in solution. Although the release of styrene is still entropically favourable, a combination of the loss of entropic driving force for the reaction, and the steric effect from the presence of the phenyl group result in a slower reaction.

The decay curve of this reaction also fit a simplified model input into Berkeley Madonna, containing only 4 rate constants (k_1, k_{-1}, k_2 and k_3). A general schematic for the model is shown in **Scheme 116**.

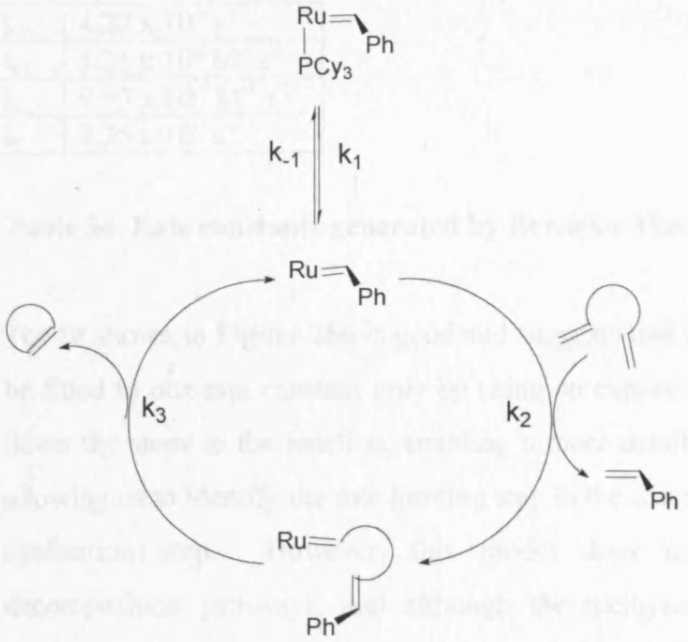

Scheme 116 Simplified model for cyclisation of 286

The model can be simplified because the methylidene is not formed, therefore the propagating catalyst is the same as the initial active catalyst, reducing the number of steps and rate constants required for the model. The fit generated for the decay curve of **286** is shown in **Figure 136**. Rate constants generated by the fit are shown in **Table 34**.

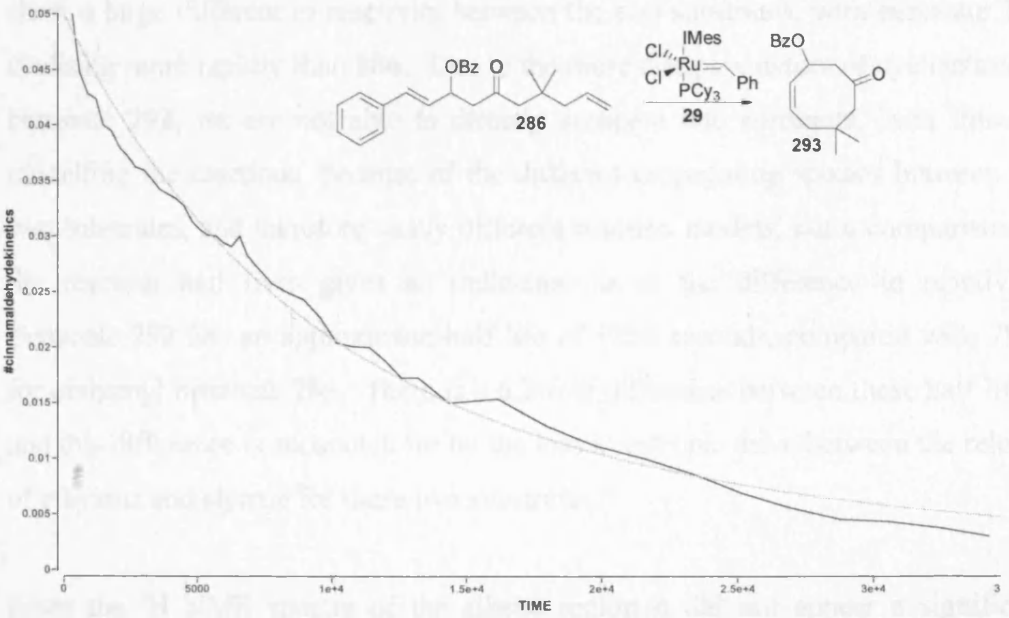

Figure 136 Fit generated by Berkeley Madonna for cyclisation of 286

k_1	$4.20 \times 10^{-5} s^{-1}$
k_{-1}	$1.21 \times 10^{-6} M^{-1} s^{-1}$
k_2	$9.93 \times 10^{-5} M^{-1} s^{-1}$
k_3	$2.25 \times 10^{-5} s^{-1}$

Table 34 Rate constants generated by Berkeley Madonna for cyclisation of 286

The fit shown in **Figure 286** is good and suggests that the although the kinetics can be fitted to one rate constant only by using an exponential fit, it is useful to break down the steps in the reaction, enabling a more detailed look at the reaction, and allowing us to identify the rate limiting step in the reaction, which appears to be the cyclisation step. However, this model does not take into account any decomposition pathways, and although the methylidene is not formed, which removes the possibility of the formation of the methylidene-derived decomposition pathways, the lifetime of the catalyst is unlikely to be infinite, and therefore other, slower deactivation pathways must arise over a longer timescale.

To give a direct comparison between **286** and benzoate **292** (prepared by R. Webster), benzoate **292** was run at 0.05 mM in CD_2Cl_2 with 2% Grubbs' second generation catalyst at 298 K and followed by ^1H NMR, again following the alkene region.[113] The overlay of the two substrates is shown in **Figure 137**. The results show a large different in reactivity between the two substrates, with benzoate **292** cyclising more rapidly than **286**. Due to the more complex nature of cyclisation of benzoate **292**, we are not able to directly compare rate constants, even through modelling the reactions, because of the different propagating species between the two substrates, and therefore vastly different reaction models; but a comparison of the reaction half lives gives an indication as to the difference in reactivity. Benzoate **292** has an approximate half life of 1250 seconds, compared with 7800 for cinnamyl benzoate **286**. There is a 6.2-fold difference between these half lives, and this difference is accounted for by the loss in entropic drive between the release of ethylene and styrene for these two substrates.[12]

From the ^1H NMR spectra of the alkene region it did not appear a significant amount of homodimer was forming during the reaction, as no triplet corresponding to this species was observed. This is interesting considering the steric hindrance of

the phenyl group on the Type II alkene, and suggests that although relatively slow, the cyclisation is favoured over homodimerisation under these conditions.

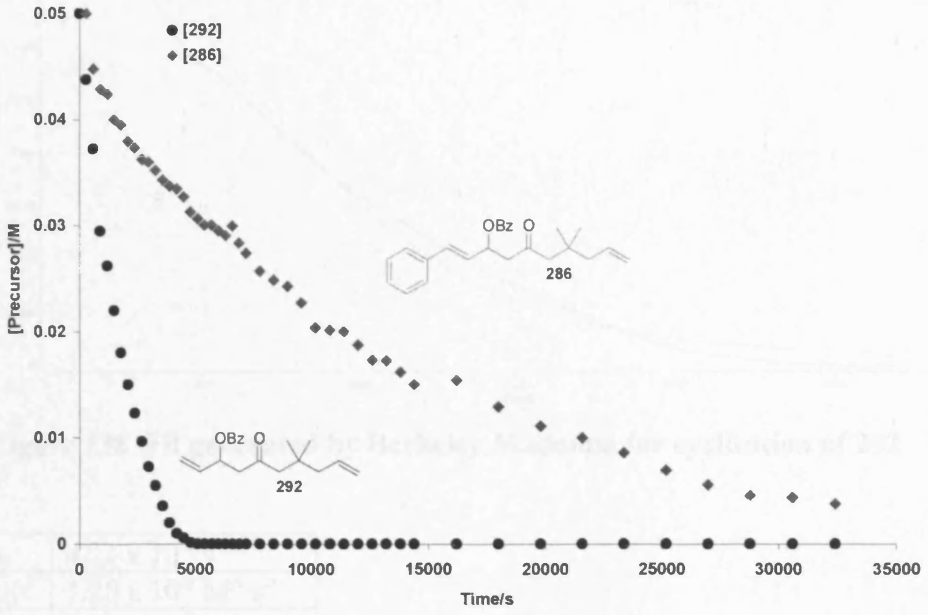

Figure 137 Overlays of cyclisation kinetics of 286 and 292 (Section 10 p40-43)

Benzoate **292** reacted so rapidly that the initiation and catalyst decomposition pathways are insignificant on this timescale. Modelling was used to carry out a more in-depth analysis of the rate constants. The k_3 values for **286** and **292** were compared in order to identify the effect of the terminal phenyl group on the cyclisation step, and the values of k_2 for **286** and k_4 for **292** were compared, which gives an indication as to the effect of the change from generation of ethylene to the generation of styrene on the reaction.

The reaction profile was fitted once again using the model employed for the more complex substrate kinetics. The fit in shown in **Figure 138**and the rate constants generated in **Table 35**.

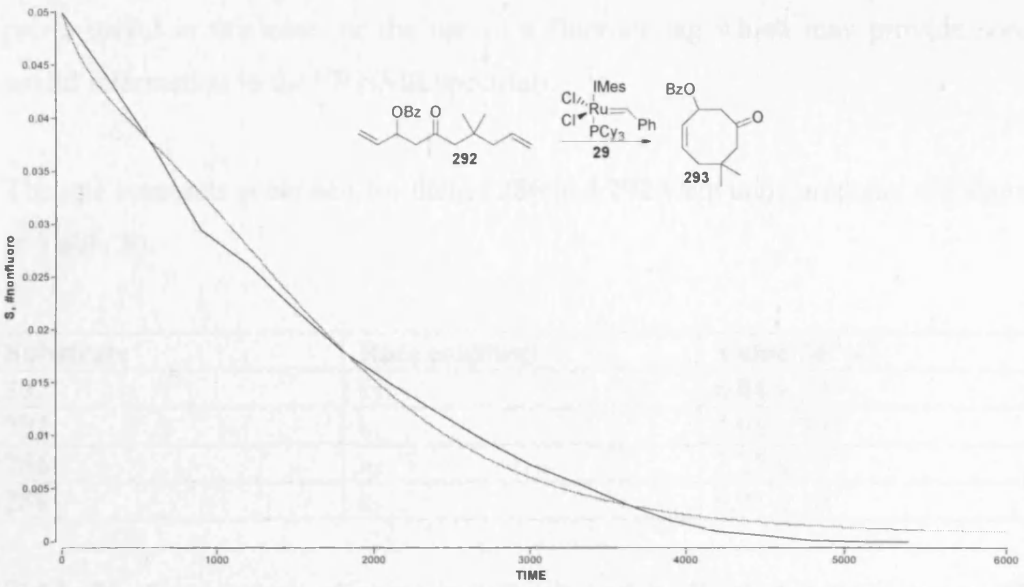

Figure 138 Fit generated by Berkeley Madonna for cyclisation of 292

k_1	4.21×10^{-5} s^{-1}
k_{-1}	1.20×10^{-6} M^{-1} s^{-1}
k_2	1.89×10^{-3} M s^{-1}
k_3	6.84×10^{-3} s^{-1}
k_4	4.95×10^{-3} M^{-1} s^{-1}
k_5	1.15×10^{-5} M^{-1} s^{-1}
k_6	3.20×10^{-6} M^{-1} s^{-1}
k_7	2.01×10^{-4} s^{-1}
k_8	6.70×10^{-3} M^{-1} s^{-1}

Table 35 Rate constants generated from Berkeley Madonna fit

The rate constants generated are consistent with those generated for the fluorinated substrates in **4.3**, with phosphane dissociation being the rate limiting step once again, and then k_2, which corresponds to the cross metathesis by the benzylidene catalyst **220**.[40] Compared to fluorinated benzoate **150**, **292** has a larger value of k_2. The values of k_4 and k_8 are slightly higher for non-fluorinated benzoate **292** than for its *gem*-difluorinated analogue **150**. This may suggest a slightly lower EM for **292**, suggesting that the *gem*-difluoro group has an effect on the cyclisation efficiency. However, although there was good dispersion in the ^{1}H NMR spectrum, an EM may be difficult to calculate if signals for cyclic oligomers have similar chemical shifts to those of cyclooctenone **293**. However, the use of ^{1}H-^{1}H COSY experiments may

prove useful in this case, or the use of a fluorous tag which may provide some useful information in the ^{19}F NMR spectrum.

The rate constants generated for dienes **286** and **292** were compared and are shown in **Table 36.**

Substrate	Rate constant	Value/M^{-1} s^{-1}
292	k_3	6.84×10^{-3}
292	k_4	4.95×10^{-3}
286	k_3	2.25×10^{-5}
286	k_2	9.93×10^{-5}

Table 36 Comparison of cross metathesis and cyclisation rates between 286 and 292

From the values give in **Table 36**, it appears that the presence of the phenyl group on **286** has a large effect on the cyclisation step of the reaction (k_3), of approximately 300-fold. There is a moderate difference (55-fold) in the propagation cross metathesis step rate constant, k_2 (k_4 in the case of **292**), which corresponds to the formation of the intermediate alkylidene from the 14 electron ruthenium species. This step is likely to be affected by the generation of styrene rather than ethylidene, and is likely to be the most affected due to loss of entropic driving force for the reaction. The large difference in cyclisation rate constants, k_3, suggests that the steric bulk of the terminal phenyl substituent causes a vast slow down in the cyclisation.

^1H NMR was used once again to observe the alkylidene region of the spectrum, following the benzylidene **220**, and other signals over time. A 40% catalyst loading in CD_2Cl_2 (and no Ti(IV) co-catalyst) was used to give good signal to noise in the spectrum. The results are shown in **Figure 139**.

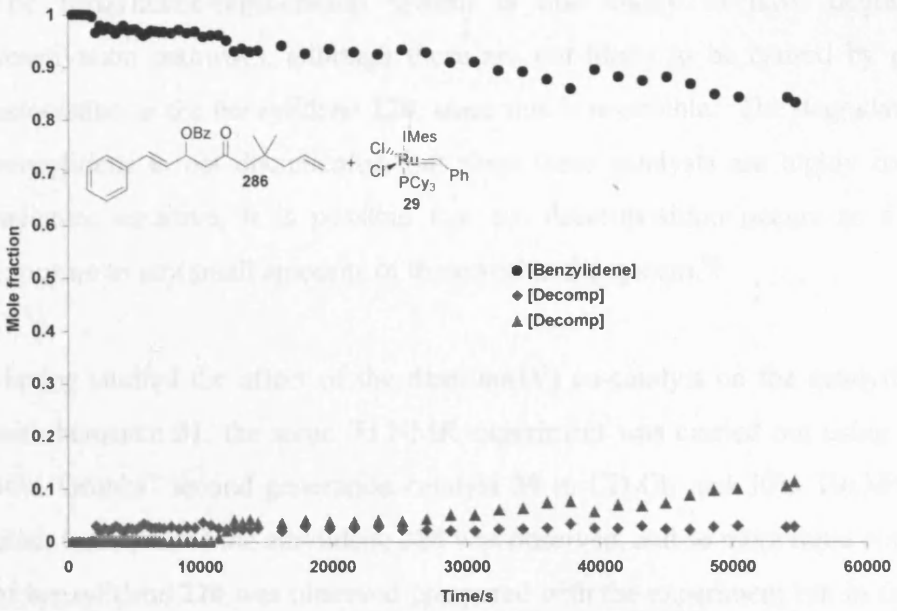

Figure 139 Ruthenium alkylidene region kinetics with diene 286

These results clearly show that on the same timescale as for the previously studied substrates, the concentration of benzylidene **220** remaining in solution is much greater in this case. At the end of the reaction, approximately 15% of the benzylidene has been consumed, and other small peaks start to appear in the spectrum, but the concentration of degradation products is reduced by far on this timescale due to regeneration of the benzylidene over formation of the methylidene. **Figure 140** shows an overlaid plot which shows the formation of decomposition products from benzylidene **220** and methylidene **221**.

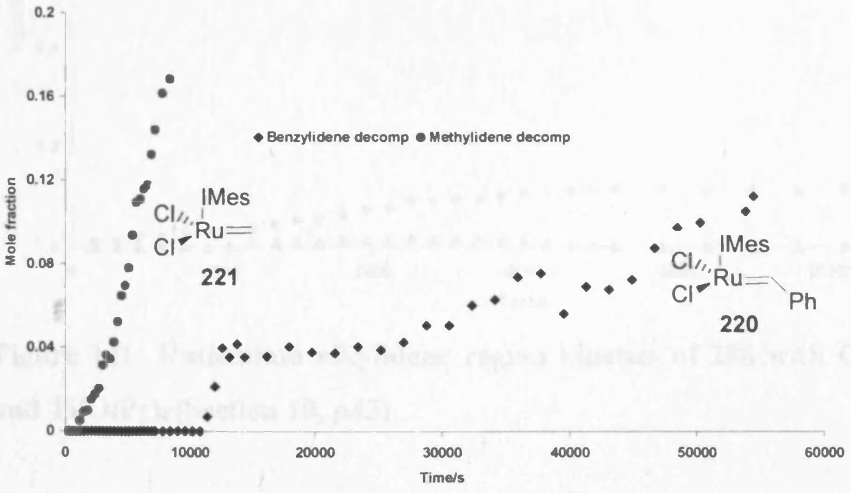

Figure 140 Overlays of methylidene 221 and benzylidene 220 decomposition

The benzylidene-regenerating system is also likely to have degradation or deactivation pathways, although these are not likely to be caused by phosphane association to the benzylidene **220**, since this is reversible. The degradation of the benzylidene is not documented, but since these catalysts are highly oxygen and moisture sensitive, it is possible that the decomposition occurs as a result of exposure to any small amounts of these within the system.[92]

Having studied the effect of the titanium(IV) co-catalyst on the catalytic species, with benzoate **31**, the same ^{1}H NMR experiment was carried out using **286**, with 40% Grubbs' second generation catalyst **29** in CD_2Cl_2 and 30% Ti(O*i*Pr)$_4$. Over time, formation of the ethylidene **228** was observed, and so more rapid consumption of benzylidene **220** was observed compared with the experiment run in the absence of the Ti(IV) co-catalyst. The Ti(IV) co-catalyst therefore appears able to form the ethylidene **228** from the 14-electron benzylidene species **220**, and this accounts for the greater consumption of the benzylidene over this timescale. An overlay of the formation of ethylidene **228** in this system, and in the methylidene-generating system is shown in **Figure 141**.

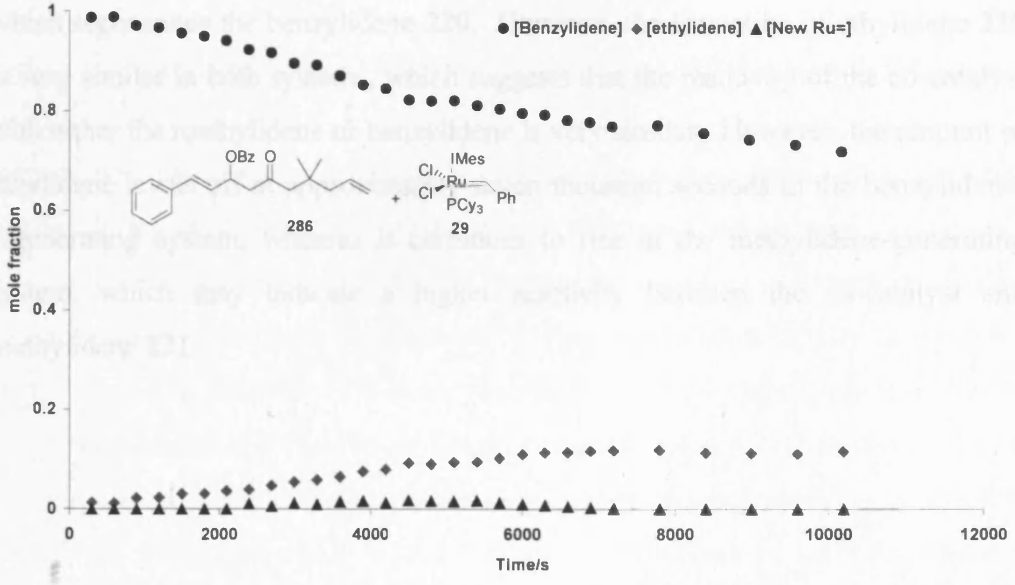

Figure 141 Ruthenium alkylidene region kinetics of 286 with Grubbs' II 29 and Ti(O*i*Pr)$_4$ (Section 10, p43)

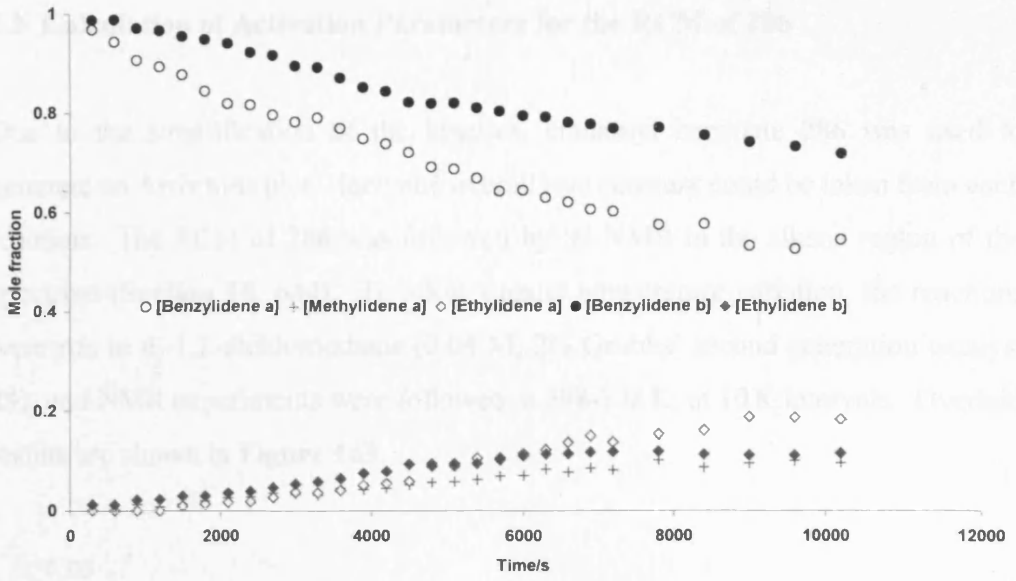

[a] Methylidene-generating system with 40% **31**, Ti(O*i*Pr)$_4$, CD_2Cl_2. [b] Benzylidene-regenerating system with 40% **286**, Ti(O*i*Pr)$_4$, CD_2Cl_2

Figure 142 Overlays of benzylidene consumption and ethylidene formation for 31 and 286 in the presence of Ti(O*i*Pr)$_4$

Figure 142 appears to show that in these two systems, consumption of benzylidene **220** is more rapid in the methylidene-generating systems compared with the system which regenerates the benzylidene **220**. However, the formation of ethylidene **228** is very similar in both systems, which suggests that the reactivity of the co-catalyst with either the methylidene or benzylidene is very similar. However, the amount of ethylidene levels off at approximately seven thousand seconds in the benzylidene-regenerating system, whereas it continues to rise in the methylidene-generating system, which may indicate a higher reactivity between the co-catalyst and methylidene **221**

5.2 Calculation of Activation Parameters for the RCM of 286

Due to the simplification of the kinetics, cinnamyl benzoate **286** was used to generate an Arrhenius plot, since one overall rate constant could be taken from each reaction. The RCM of **286** was followed by ^{1}H NMR in the alkene region of the spectrum (**Section 10, p44**). To allow greater temperature variation, the reactions were run in d_4-1,2-dichloroethane (0.04 M, 2% Grubbs' second generation catalyst **29**), and NMR experiments were followed at 298-338 K, at 10 K intervals. Overlaid results are shown in **Figure 143**.

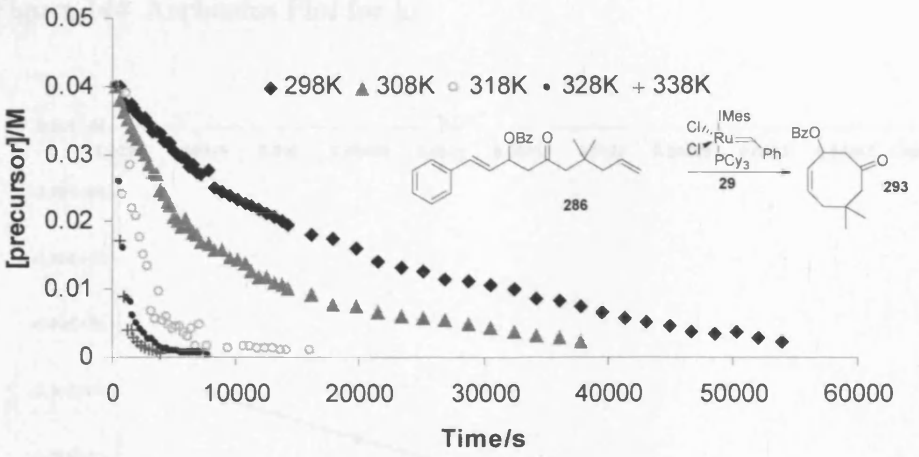

Figure 143 Overlays of cyclisation kinetics of 286 at 298-338 K in d_4-DCE

Figure 143 shows a clear dependence of rate on temperature, as would be expected, although even at 338 K, the cyclisations are still much slower than those of the previously-used substrates **22, 149** and **150** due to reduction in the entropic driving force (ethylene release) for the reaction. The experimental data were fitted to the model shown in **Scheme 116** since the substrate consumption curves at higher temperatures did not fit exponential decay curves with greater than 95% confidence. This enabled separate Arrhenius plots to be drawn for each step in the reaction model, and give an indication as to the activation parameters for different stages of the reaction (**Figure 144-147**).

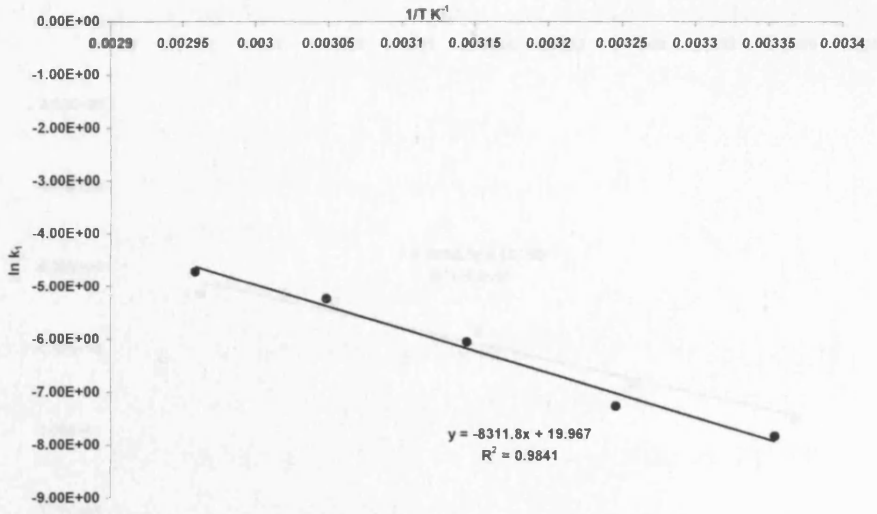

Figure 144 Arrhenius Plot for k_1

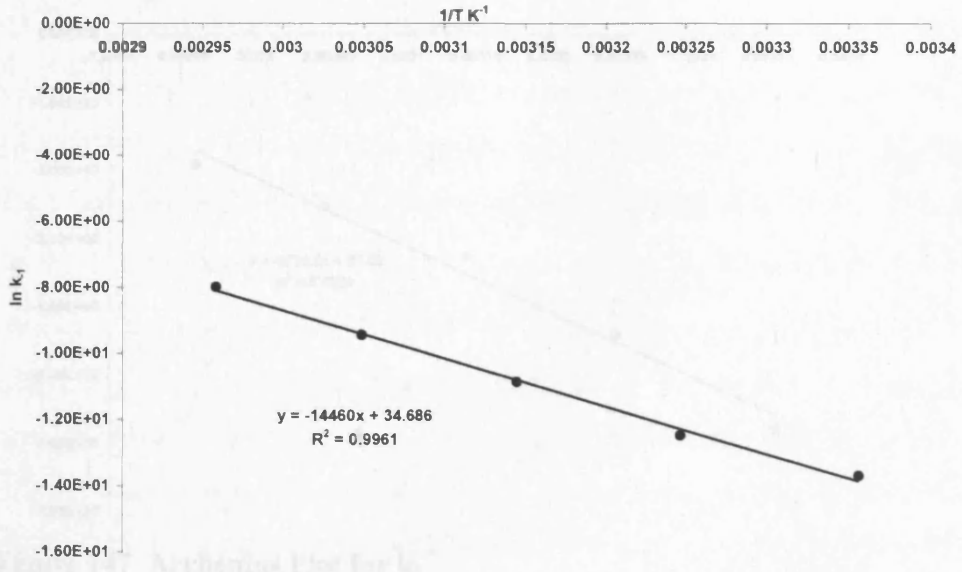

Figure 145 Arrhenius Plot for k_{-1}

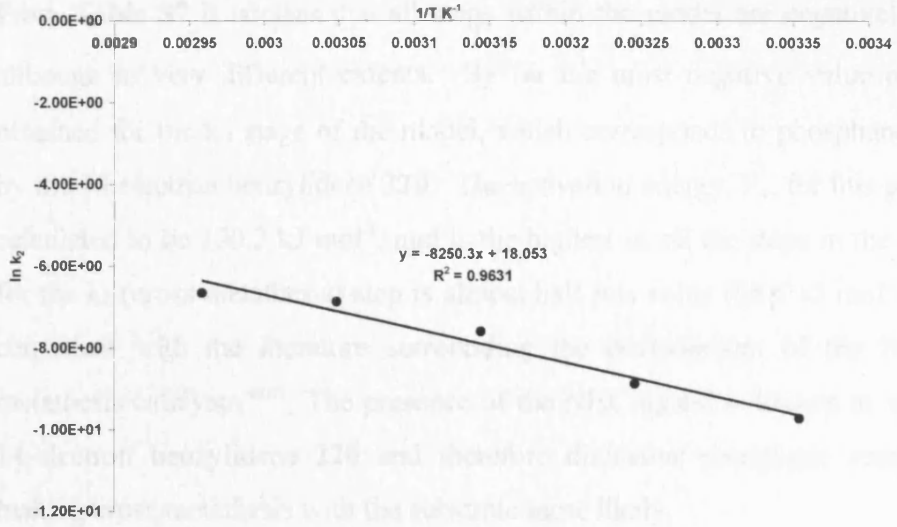

Figure 146 Arrhenius Plot for k_2

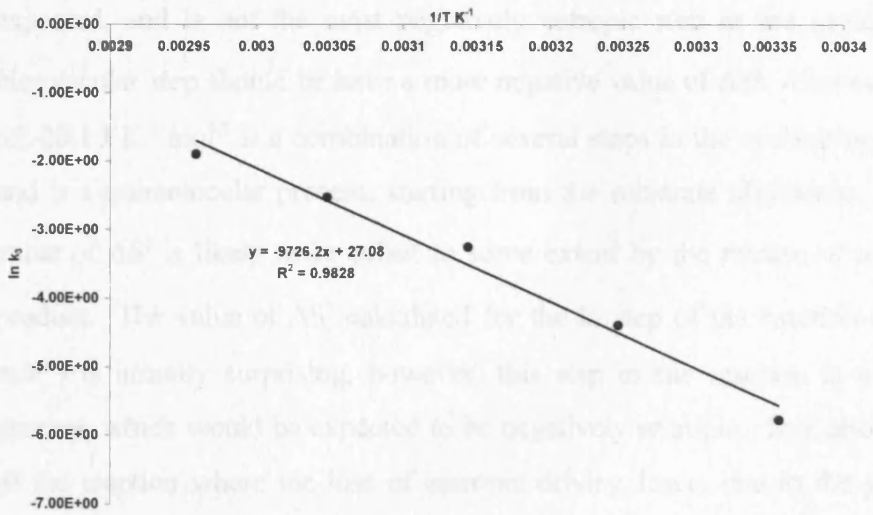

Figure 147 Arrhenius Plot for k_3

	k_1	k_{-1}	k_2	k_3
A	4.69×10^8	1.16×10^{15}	6.92×10^7	5.76×10^{11}
Ea/ kJ mol^{-1}	69.1	120.2	68.6	80.7
$\Delta H^{\ddagger}$ (298 K) kJ mol^{-1}	66.6	117.7	66.12	78.4
$\Delta S^{\ddagger}$ (298 K) J K^{-1} mol^{-1}	-87.2	-467.9	-103.1	-28.1
$\Delta G^{\ddagger}$ (298 K) kJ mol^{-1}	92.6	257.2	96.9	86.8

Table 37 Calculation of activation parameters from Arrhenius plots (Section 10, p50)

From **Table 37** it is clear that all steps within the model are negatively entropic, although to very different extents. By far the most negative value of $\Delta S^{\ddagger}$ was obtained for the k_{-1} stage of the model, which corresponds to phosphane recapture by the 14 electron benzylidene **220**. The activation energy, E_a, for this process was calculated to be 120.2 kJ mol^{-1}, and is the highest of all the steps in the model. E_a for the k_2 (cross metathesis) step is almost half this value (68.6 kJ mol^{-1}), which is consistent with the literature surrounding the development of the NHC-ligand metathesis catalysts.[40,45] The presence of the NHC ligand is known to stabilise the 14-electron benzylidene **220** and therefore disfavour phosphane recapture, and making cross metathesis with the substrate more likely.

The $\Delta S^{\ddagger}$ calculated for the cyclisation step (k_3) is less negative than initially expected, and is not the most negatively entropic step in the model, since any bimolecular step should be have a more negative value of $\Delta S^{\ddagger}$. However, the value of -28.1 J K^{-1} mol^{-1} is a combination of several steps in the cyclisation mechanism, and is a unimolecular process, starting from the substrate alkylidene. The overall value of $\Delta S^{\ddagger}$ is likely to be offset to some extent by the release of a molecule of product. The value of $\Delta S^{\ddagger}$ calculated for the k_2 step of the reaction (-103.1 J K^{-1} mol^{-1}) is initially surprising, however, this step in the reaction is a bimolecular process, which would be expected to be negatively entropic. It is also at this stage of the reaction where the loss of entropic driving force, due to the generation of styrene rather than ethylene, would be felt. It is also important to remember that studies were carried out on a benzoate substrate, and as shown in **4.3** the benzoates exhibit slow rates of cross metathesis relative to the free alcohol and benzyl ethers, so there may be further entropically and enthapically unfavourable processes due to the choice of protecting group which give rise to the large negative value of $\Delta S^{\ddagger}$ in this case. These results are therefore consistent with previously obtained results from modelling, which suggest that cross metathesis for benzoates is unfavourable, and this is what leads to the relatively high EM value.

Very few activation parameters have been calculated for eight-membered ring syntheses, and even fewer of these relate to RCM. The values in **Table 37** compare reasonably well with those presented by Mandolini for typical cyclooctannulations

which are $\Delta H^{\ddagger}$ = 90.0 kJ mol^{-1} and $\Delta S^{\ddagger}$ = -37.7 J K^{-1} mol^{-1}.[8,11] The values of $\Delta H^{\ddagger}$ and $\Delta S^{\ddagger}$ calculated for the k_3 step of the model, which includes the cyclisation steps are 78.4 kJ mol^{-1} and -28.1 J K^{-1} mol^{-1} respectively. These values are similar to those quoted by Mandolini, especially when the large error in Arrhenius plots is taken into account.

Buszek synthesised octalactin A and oxocenes **298-300** *via* a lactonisation from their corresponding *seco* acids (**Scheme 117**). For the same synthesis, some computational work using molecular mechanics (MM2) was also carried out to calculate some activation parameters for the reaction. Although 8-membered rings typically present a large challenge, the values obtained appear to be surprisingly small (**Table 38**).[115]

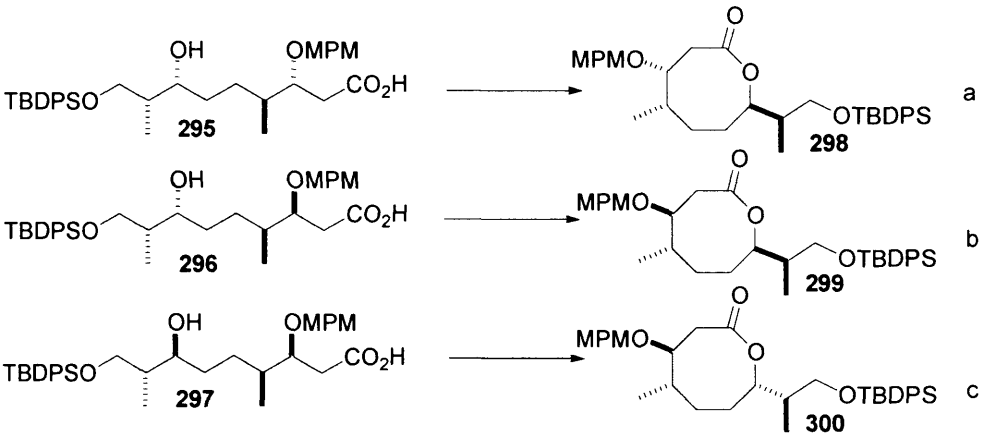

i 2,2'-Dipyridyl disulfide, Ph_3P, CH_2Cl_2
ii $AgBF_4$, PhMe, 100°C, 48hr

Scheme 117 Oxocene synthesis from *seco*-acids

Epimer	$\Delta H^{\ddagger}$ (kJ mol^{-1})	$\Delta S^{\ddagger}$ (J K^{-1} mol^{-1})	k (sec^{-1}, 115°C)
A	89.5	-112.9	1.33x 10^{-5}
B	85.4	-125.5	1.48x 10^{-5}
C	117.9	-46.0	7.52x 10^{-6}

Table 38 Activation parameters for oxocene syntheses calculated by molecular mechanics

The values published by Buszek suggest that the entropic barrier can be lowered through the presence of substituents in the chain, which may reduce the internal

rotational freedom. Our system lies between the values given by Buszek, and has several substituents present on the cyclisation precursor, including a *gem*-dimethyl group, which is known to reduce rotational freedom.[54] $\Delta S^{\ddagger}$ may therefore be higher for the non-dimethylated substrate, but these reactions were not followed as they would be expected to be very slow in dichloroethane at lower temperatures.

Buszek's results are not supported by any detailed description of how they were obtained, and must therefore be regarded with some degree of caution. The MM2 calculations used, and assumptions made in their generation, or in the generation of the Arrhenius plot were not made clear in the paper. No further work has since been published by the author relating to this subject, and he declined to respond to emails requesting further details regarding this article.

The synthesis of **286** has allowed us to avoid the formation of methylidene **221** in the RCM sequence, instead regenerating benzylidene **220**. This appears to extend the catalytic lifetime of the system, and may have implications for chemists if they are able to carefully synthesise precursors of this nature, towards continuous flow metathesis reactions, due to the extent of the active catalyst lifetime. The reactions for these substrates are slower because of the loss of an entropic driving force for the reaction, but the release of less volatile styrene appears to provide enough entropic drive for the reaction to still proceed. Using these substrates would allow us to compare substituent effects more easily.

5.3 Synthesis of an Ethylidene-Generating Substrate

The results discussed above showed that careful design of the RCM substrate can not only simplify the kinetics of RCM, but also potentially extend the lifetime of the catalyst by avoiding methylidene formation, and therefore its associated decomposition pathways. However, with benzylidene-regenerating substrates such as **286**, the rate of cyclisation is drastically reduced due to steric and entropic factors. The formation of styrene is a weaker entropic driving force than the formation of a gaseous alkene such as ethylene.

The literature described in **4.2**, and the results obtained from the study of the effect of the Ti(IV) co-catalyst on the reaction appear to indicate that the reactivity of ethylidene **228** is higher than that of methylidene **221**.[92,93,94] Using the approach adopted in the synthesis of **286**, the synthesis of a new diene, **302**, which would generate the ruthenium-ethylidene **228** upon subsequent catalytic turnovers was carried out. The RCM of this substrate would be potentially beneficial compared with the RCM of **286**, since each catalytic turnover would generate propene as a by-product, which is gaseous, so the entropic driving force for the reaction is maintained. **302** was synthesised as shown in **Scheme 118.**

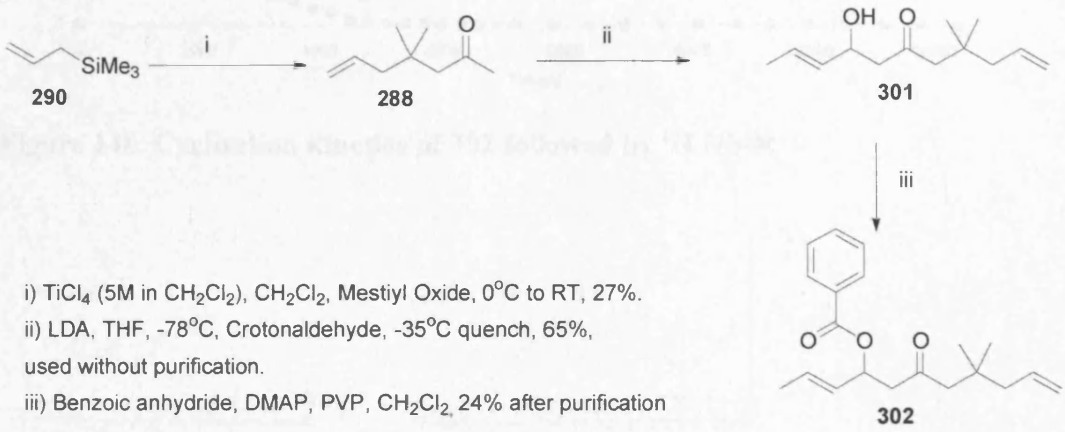

290 288 301 302

i) $TiCl_4$ (5M in CH_2Cl_2), CH_2Cl_2, Mestiyl Oxide, 0°C to RT, 27%.
ii) LDA, THF, -78°C, Crotonaldehyde, -35°C quench, 65%, used without purification.
iii) Benzoic anhydride, DMAP, PVP, CH_2Cl_2, 24% after purification

Scheme 118 Synthesis of 302

The RCM of **302** was followed once again by ^1H NMR, with the spectra centred on the alkene region (3-6 ppm) in CD_2Cl_2, with 2% Grubbs' II **29** at 0.05 M, to allow exact comparison with the RCMs of **286** and **292**. The results were quite different to those observed with previous substrates and are shown in **Figure 148**. **Figure 148** shows some interesting behaviour within this system. There is a rapid, intitial burst of dimer formation, and slow formation of the eight-membered ring **293**, up to approximately 2700 s, at which point there is discontinuity within the system, and the amount of dimer decreases slowly, and the amount of eight-membered ring **293** increases slowly. This appears to coincide with a relatively low concentration of starting diene **302** remaining in the solution, which means that formation of dimer becomes increasingly less likely. Further cyclic product can then form *via* the back-biting process. Some ^1H NMR spectra are shown in **Figure 149 (Section 10, p50)**.

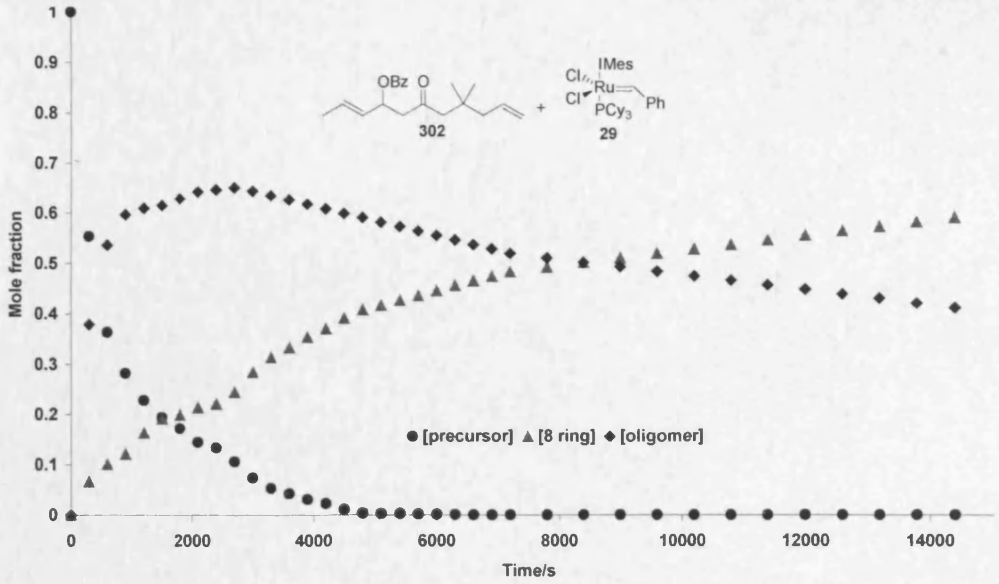

Figure 148 Cyclisation kinetics of 302 followed by ^{1}H NMR

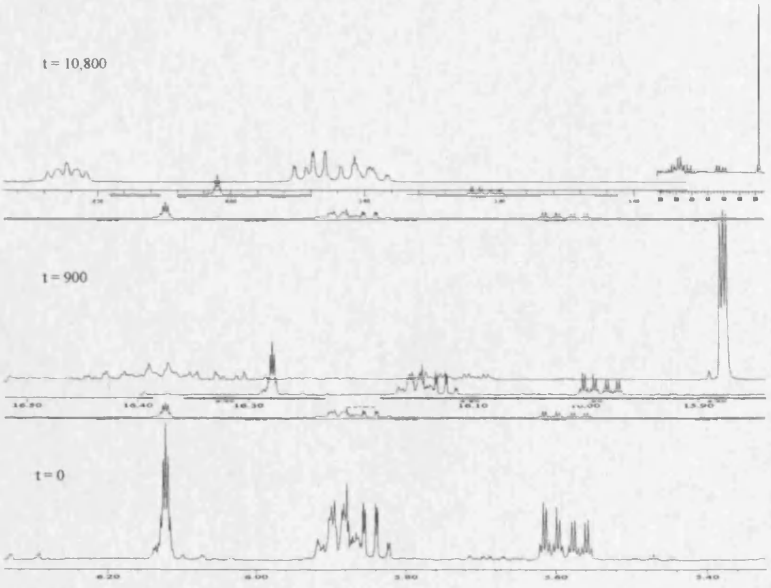

Figure 149 Selected spectra from cyclisation kinetics of 302

The kinetics studies of previous substrates had not revealed the formation of acyclic oligomers prior to the formation of the cyclooctenone **293**. The acyclic homodimer was characterised by a triplet in the alkene region, similar to that observed by J. Miles for **30**.[2,55] The homodimer appears then to have undergone backbiting into cyclic product. The behaviour of **302** was unexpected and previously unobserved for these systems.

The reaction was also followed by ^{1}H NMR between 10-20 ppm, using 40% Grubbs II, with [**302**] at 0.04 M in CD_2Cl_2. The titanium(IV) co-catalyst was omitted for comparison with the other substrates, and also so that any formation of the Ru-ethylidene could be attributed solely to the use of substrate **302**, rather than due to the presence of the co-catalyst. Results and some representative spectra are shown in **Figures 150** and **151-152**.

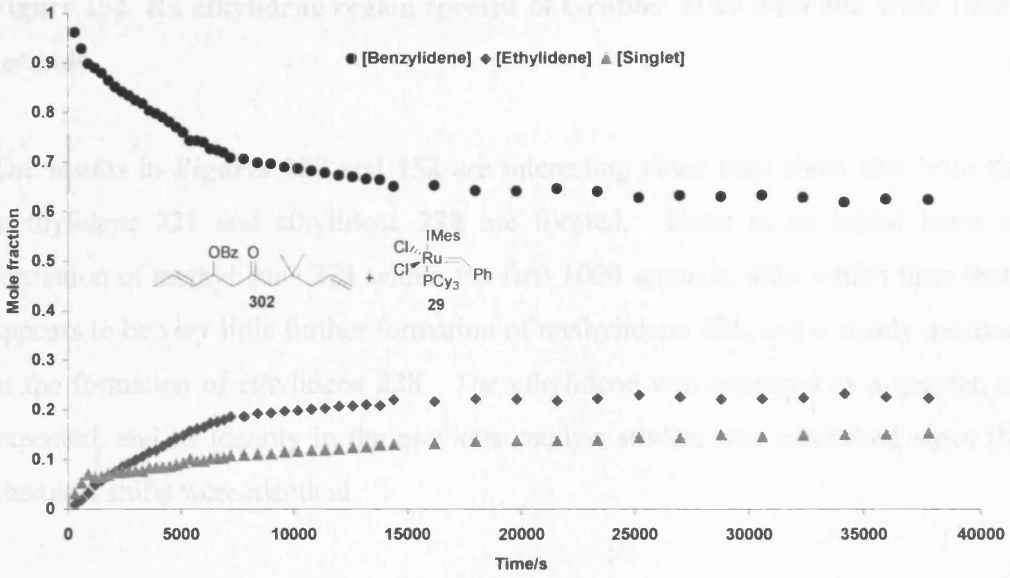

Figure 150 Ruthenium alkylidene region kinetics of Grubbs' II 29 with 302 (Section 10, p52)

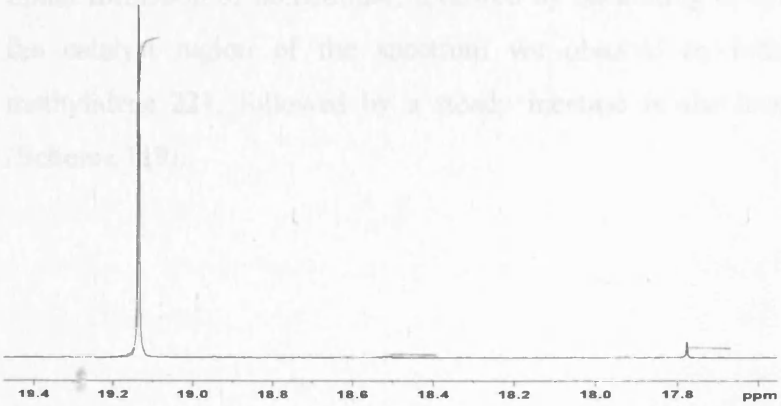

Figure 151 Ru alkylidene region spectra of Grubbs' II 29 with 302 after 300 seconds

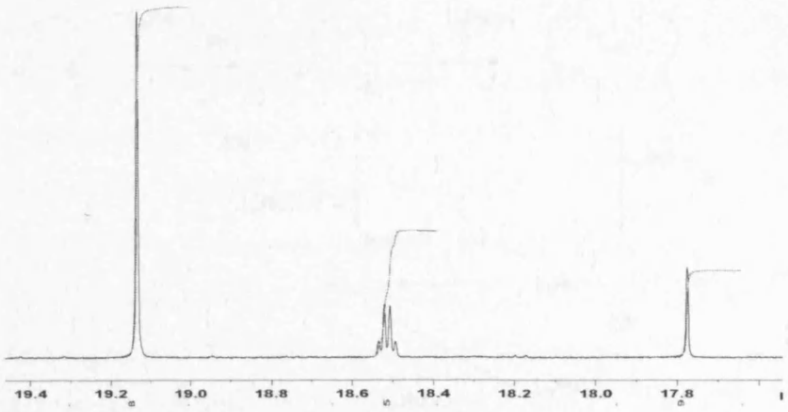

Figure 152 Ru alkylidene region spectra of Grubbs' II 29 with 302 after 18000 seconds

The results in **Figures 150** and **152** are interesting since they show that both the methylidene **221** and ethylidene **228** are formed. There is an initial burst of formation of methylidene **221** within the first 1000 seconds, after which time there appears to be very little further formation of methylidene **221**, and a steady increase in the formation of ethylidene **228**. The ethylidene was appeared as a quartet, as expected, and its identity in the previous catalyst studies was confirmed since the chemical shifts were identical.

There appears to be a link between **Figures 148** and **150** although the two profiles cannot be exactly compared since both the substrate concentrations and catalyst loadings are different. However, upon following the RCM **302**, there was a rapid initial formation of homodimer, followed by backbiting to cyclooctenone **293**. In the catalyst region of the spectrum we observe an intial formation of the methylidene **221**, followed by a steady increase in the level of ethylidene **228** (**Scheme 119**).

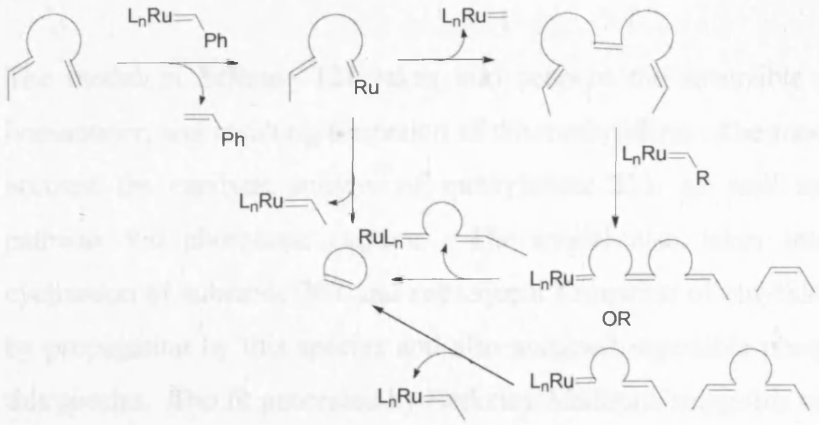

Scheme 119 Possible metathesis scenario for 302

The formation of a homodimer is consistent with the presence of the methylidene, since joining two Type I double bonds is the only route through which the methylidene could form. Backbiting of the homodimer to the cyclic product would liberate the ethylidene. Once cyclooctenone **293** has formed, it cannot be reversed on the timescale of the experiment as the concentration for ROMP is too low.

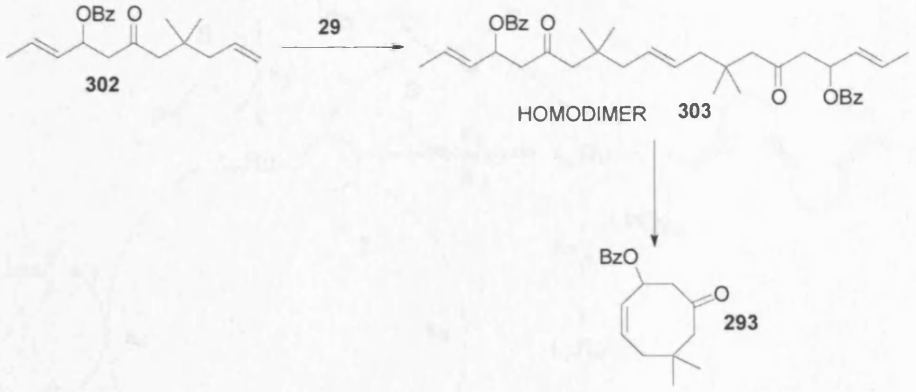

Scheme 120 Homodimerisation of 302 followed by cyclisation

Multiple attempts at modelling the cyclisation kinetics of **302** using Berkeley Madonna were unsuccessful, even when accounting for reversible homodimerisation. The fit for the consumption of diene **302** was generally good, but it was not possible to obtain good fits for both the dimer and cyclooctenone **293**. The best fit was obtained with the model shown in **Scheme 121**, but even this did not simulate the observed behaviour accurately. Diene **302** did not behave as expected and clearly requires much more in depth analysis than was possible at this stage to fully understand the kinetics of cyclisation.

The model in **Scheme 121** takes into account the reversible formation of the homodimer, and resulting formation of the methylidene. The model also takes into account the catalytic activity of methylidene **221**, as well as its deactivation pathway *via* phosphane capture. The model also takes into account direct cyclisation of substrate **302** and subsequent formation of ethylidene **228**, followed by propagation by this species and also assumed reversible phosphane capture by this species. The fit generated by Berkeley Madonna using this model gave a good simulation of consumption of diene **302** and formation of cyclooctenone **293** but did not correctly predict the concentration/time profile for the dimer.

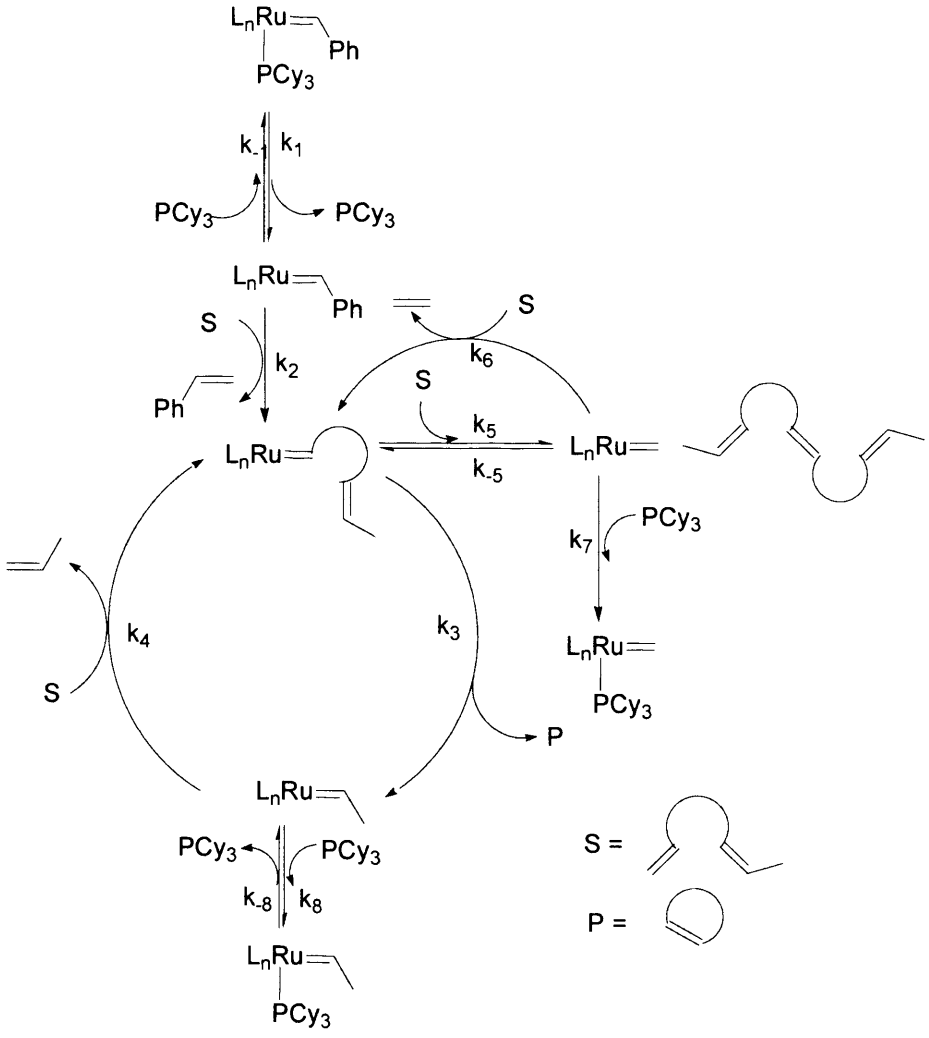

Scheme 121 Model for Metathesis of 302

The syntheses of **286** and **302** have shown us that by designing RCM substrates we are able to generate a more active catalyst, which appears to bind phosphane

reversibly, like the benzylidene **220**, hence increasing catalyst lifetime, and potentially reducing the catalyst loading required. This could be investigated as further work in this area. This result has useful implications for the overall cost of a reaction, since metathesis catalysts are expensive, and also makes purification of cyclisation products easier, since catalyst residues are often difficult to remove. The use of substrate **302** has shown that an extra CH_3 on the allylic double bond slows the RCM somewhat, but formation of the desired cyclic product still occurs on a reasonable timescale, since it still benefits from the entropic drive of releasing the gaseous alkene propene on each catalytic turnover.

6.1 Optimisation of the Cyclooctannulation

The EM studies had already allowed us to identify maximum concentration useful for synthesis for dienes **4, 30** and **31**, and had shown that **150** had the most efficient cyclisation of the four substrates **22, 148-150**. Optimisation of the formation of cyclooctenones *via* RCM required an understanding of the effects of several variables on the reaction, including catalyst loading, substrate concentration, solvent, presence of co-catalyst, and temperature.

Metathesis reactions have been carried out in a range of solvents such as dichloromethane, diethyl ether, toluene and THF, although the effect of the solvent has only been quantified for initiation (phosphane dissociation) of the reaction.[40] In order to understand and quantify the solvent effects on the rate of cyclisation, we compared cyclisations in chloroform and 1,2-dichloroethane with the results already obtained for reactions carried out dichloromethane. The RCM of alcohol **22** was followed using the SPE sample treatment procedure and GC analysis as before. The study in chloroform was carried out at 0.014 M at 30°C and 60°C and the RCMs in 1,2-dichloroethane were carried out at 0.01 M at 25°C and 80°C. Results are shown in **Figures 153** and **154**.

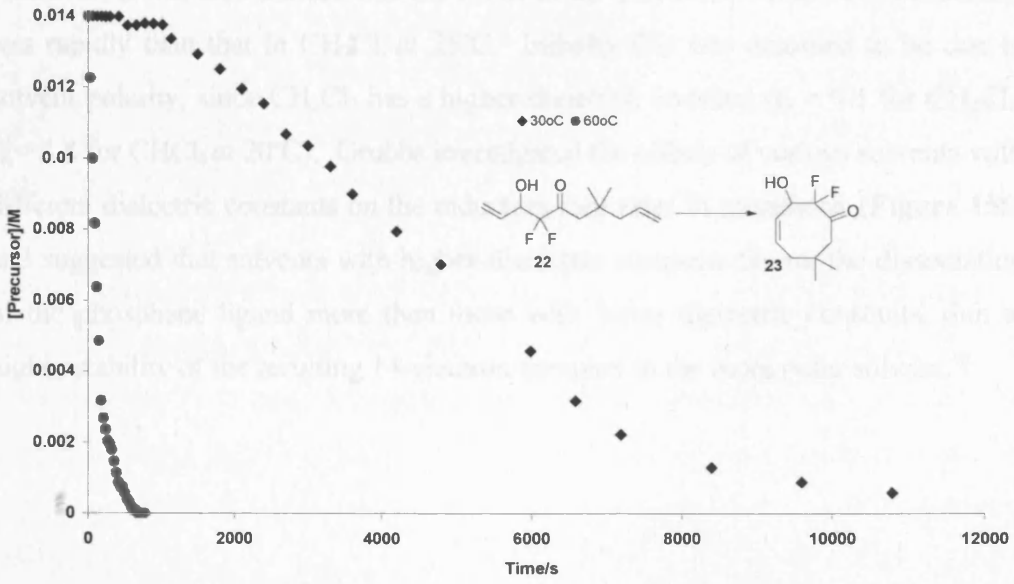

Figure 153 Overlaid concentration/time profiles for the RCM of 22 in $CHCl_3$ at 30°C and 60°C (Section 10, p87)

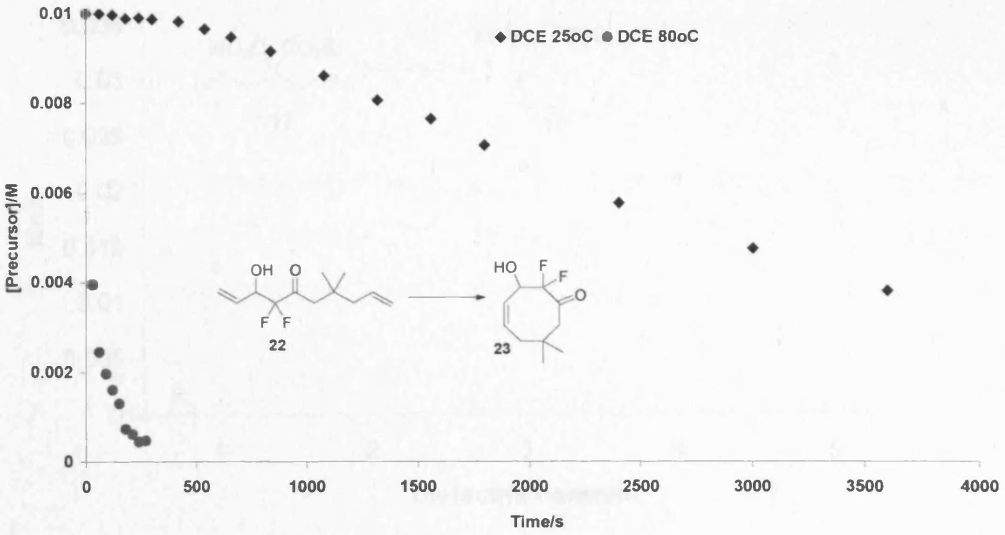

Figure 154 Concentration/time profiles for RCM of 22 in DCE at 25°C and 80°C (Section 10, p89)

Figures 153 and **154** clearly show there is a large temperature dependence of the reaction, and in higher boiling solvents, the reaction half life is much shorter (approx $t_{1/2}$ = 140 s and <25 s for chloroform at 60°C and DCE at 80°C respectively). This shows us that eight-membered ring formation can actually proceed very rapidly under the right conditions.

However, it was also noticed that the RCM of **22** in chloroform at 30°C proceeded less rapidly than that in CH_2Cl_2 at 25°C. Initially this was assumed to be due to solvent polarity, since CH_2Cl_2 has a higher dielectric constant (ε_r = 9.1 for CH_2Cl_2, ε_r = 4.8 for $CHCl_3$ at 20°C). Grubbs investigated the effects of various solvents with different dielectric constants on the induction step rates in metathesis (**Figure 155**) and suggested that solvents with higher dielectric constants favour the dissociation of the phosphane ligand more than those with lower dielectric constants, due to higher stability of the resulting 14-electron complex in the more polar solvent.[40]

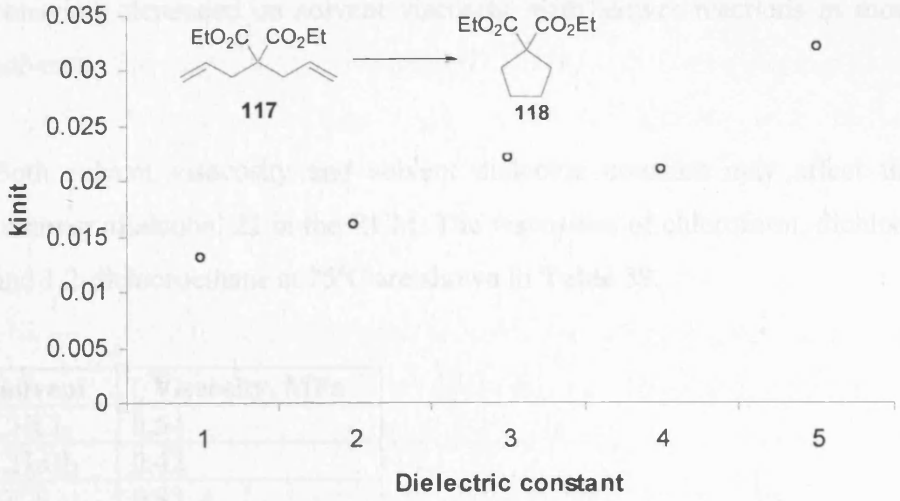

Figure 155 Plot of solvent dielectric constant *vs* k_{init}

The data obtained for the RCM of **22** in chloroform were consistent with Grubbs' data, and suggested that using a solvent with a very high dielectric constant would accelerate the reaction even more. However, Grubbs described the plot in **Figure 155** as linear and whereas there appears to be a general trend, the relationship cannot be described as a linear one. 1,2-Dichloroethane has a dielectric constant of 16.7 at 20°C, so the RCM of **22** would be expected to proceed even more rapidly than the reaction in CH_2Cl_2. However, as **Figure 154** shows, this was not the case, the consumption of starting diene was very slow, especially in the early stages of the reaction. This result suggests that the dielectric constant of a solvent alone is neither an adequate predictor of the rate of phosphane dissociation nor of subsequent substrate consumption in a metathesis reaction, and that other factors must affect the reaction.

Parker reviewed the effects of solvent on reaction rates and concluded that solvent dielectric constants can give very little insight into protic or dipolar aprotic solvent effects on rate.[116] In many instances reactions which take place in DMF (a dipolar aprotic solvent) occur around 10^6 times more rapidly than those in water or methanol (protic solvents) even though all three have very similar dielectric constants.

Nikowa studied the effects of solvent viscosity, ζ, on the low barrier photoisomerisation of *cis*-stilbene by changing the solvents.[117] The observed

behaviour depended on solvent viscosity, with slower reactions in more viscous solvents.

Both solvent visocosity and solvent dielectric constant may affect the rate of turnover of alcohol **22** in the RCM The viscosities of chloroform, dichloromethane and 1,2-dichloroethane at 25°C are shown in **Table 39**.

Solvent	**ζ Viscosity, MPa**
$CHCl_3$	0.54
CH_2Cl_2	0.42
DCE	0.83

Table 39

Solvent viscosity is likely to affect the rate of phosphane dissociation, as this depends on the ease of diffusion of dissociated phosphane ligand away from the active catalyst. The subsequent turnover of the catalyst also depends on the rate of diffusion of substrate to the catalyst and product away from the catalyst. All of these events are likely to be slowed down by a high viscosity solvent: this may explain the slow rate of consumption of **22** in DCE at 25°C.

The advantage of using higher-boiling solvents is that the running temperature of the reaction can be increased. For example Qing attempted the cyclisation of **304** (**Scheme 122**) *via* RCM and achieved best results using high boiling chlorobenzene at reflux. The reaction failed in more volatile solvents.

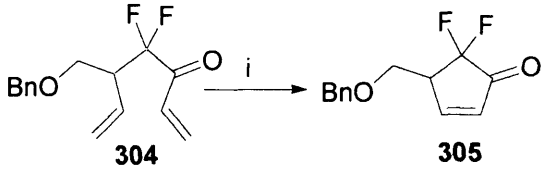

304 **305**

i) Grubbs' I **28**, chlorobenzene, reflux

Scheme 122

The results from **Figures 153** and **154** show that the use of higher reaction temperatures *via* higher boiling solvents for the RCM of **22**is also beneficial, and

could be useful for optimising RCM processes for the synthesis of challenging systems. The only drawback to using DCE however, is that it is highly toxic and a possible carcinogen, although there are risks associated with all halogenated solvents. These can however be minimised with careful handling on the laboratory scale, though their use in industry is now being minimised.

The next stage of the optimisation process was minimising the loading of catalyst **29** in the reactions. Our kinetic investigations had already shown us that the RCMs could be carried out at room temperature with a low (2%) loading of pre-catalyst **29**. Reducing the catalyst loading further would have two benefits. The first of these would be cost, since commercially-available metathesis catalysts are not cheap, and the Grubbs' catalysts **28** and **29** cannot be reused. Reducing the catalyst loading would also make purification easier, since often catalytic residues (Ru or traces of ligands) can be difficult to remove, resulting in multiple purifications. The purity issue has much more important implications for the pharmaceutical industry since the production of pharmaceutical products is stringently regulated and even tiny amount of impurities are unacceptable.

The RCM of **22** was followed, with minimal datapoints, over 40 minutes, in CH_2Cl_2 (0.01 M) at 25°C, and the catalyst loading varied from 2-0.05%. Results are shown in **Figure 156**.

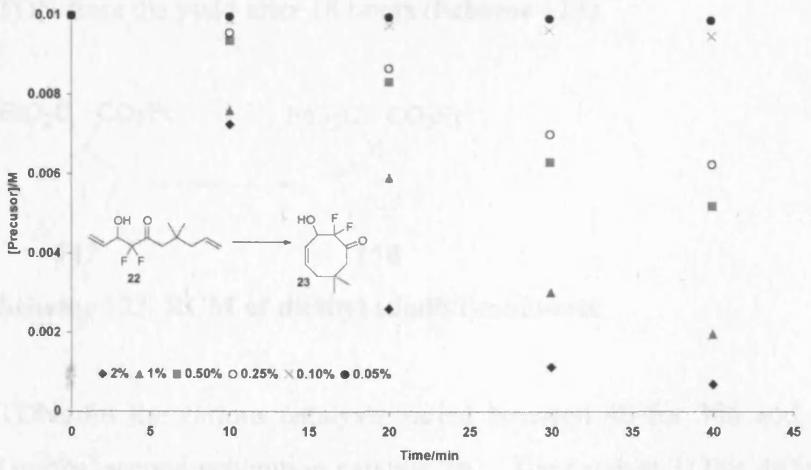

Figure 156 Overlays of concentration/time plots for the RCM of 22 with precatalyst 29 loadings of 2-0.05% (Section 10, p86)

The RCM of **22** with 1 and 2% catalyst proceed to almost end point within the time frame of following the reaction. It appears that catalyst loadings of 0.1 and 0.05% are too low, and will not result in any significant product formation under these conditions. However, in these cases, the catalyst was added from a stock solution since the required amounts of catalyst were too small to accurately weight out. Although not left to stand for a long time, it is possible that some deactivation of the catalyst occurred in this time, although at room temperature very little would be expected.

The catalyst loadings of 0.25-0.5% appear to consume a significant amount of **22** in the time followed, suggesting that these catalyst loadings may be useable in an optimised RCM reaction.

Catalyst loadings and the resulting conversion to the desired product can be used to calculate catalyst turnover numbers (TONs). These are often useful in the design of new catalysts, for comparison against existing catalysts.

Blechert used this methodology in the design of ruthenium-based metathesis catalysts containing electron-withdrawing ligands **306-307**.[118] Grubbs' first and second generation catalysts **28** and **29**, Grubbs-Hoveyda first and second generation catalysts **187** and **308** and novel catalysts were used for RCM of diethyl (diallyl)malonate **117** in refluxing DCM, varying the loading and calculating the TON from the yield after 18 hours (**Scheme 123**).

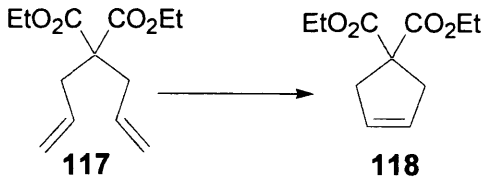

117 **118**

Scheme 123 RCM of diethyl (diallyl)malonate

TONs for the various catalysts varied between 40 for **306** and **307** and 6100 for Grubbs' second generation catalyst **29**. The catalyst TONs differ greatly from the calculated k_{cat}, also known as the turnover number.

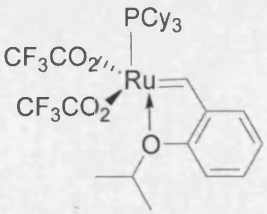

306

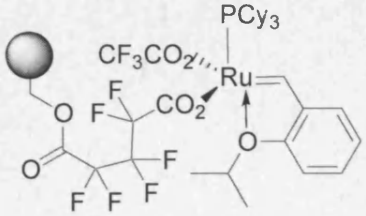

307

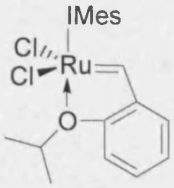

308

To enable a direct comparison, the catalyst loading study data were used to calculate a TON for each loading and compare with the values given by Blechert. The calculated values (**Table 40**) varied between 27 and 150 compared with 720 (for the RCM of diethyl allyl(2-methylallyl)malonate **309**, **Scheme 124**) and 6100 from Blechert's data for the same catalyst. Considering eight-membered rings present a much greater challenge synthetically, the turnover numbers calculated in this way are reasonable but the results indicate that for this system, low catalyst loadings will not lead to high conversion to product. However, considering the large differences in EM values for five and eight-membered rings, the modest difference in catalytic efficiency of 30-fold shows that the ring size does not have a greatly detrimental effect on RCM, but obviously has a larger effect on the concentration at which the reaction can be run synthetically.

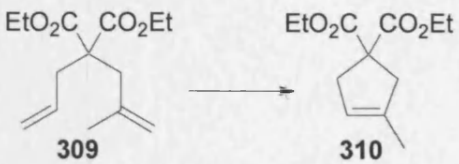

309 310

Scheme 124 RCM of diethyl allyl(2-methylallyl)malonate

In the case of the RCM of **22** with the varied loadings of catalyst, the calculated TONs are shown in **Table 41**.

Catalyst Loading	TON
2%	47
1%	80
0.50%	96
0.25%	150
0.10%	53
0.05%	27

Table 41

The results shown in **Table 41** may be a little misleading since the calculated TON values contain an artefact; the high TON for the catalyst loading of 0.25% is derived from a reasonable (approximately 40%) conversion and low catalyst loading. The method of calculation the TON results in a large TON for the small catalyst loading. Even though this reaction may reach completion with sufficient time in refluxing DCM, this may not necessarily be the ideal catalyst loading. For such a challenging system, on a synthetic scale, the minimum catalyst loading possible may be closer to 1-2% dependent on the allylic protecting group.

Grubbs examined the effect of varying the catalyst concentration on k_{obs} and observed a linear relationship (**Figure 157**).[40] As would be expected, with increasing catalyst concentration, the rate k_{obs} increases proportionately. A similar plot was made with the data obtained in this study as a comparison (**Figure 158**). The gradient in the plot compared well with Grubbs' data. The data shown in **Figure 158** were used to calculate an approximate k_{obs} for each catalyst loading.

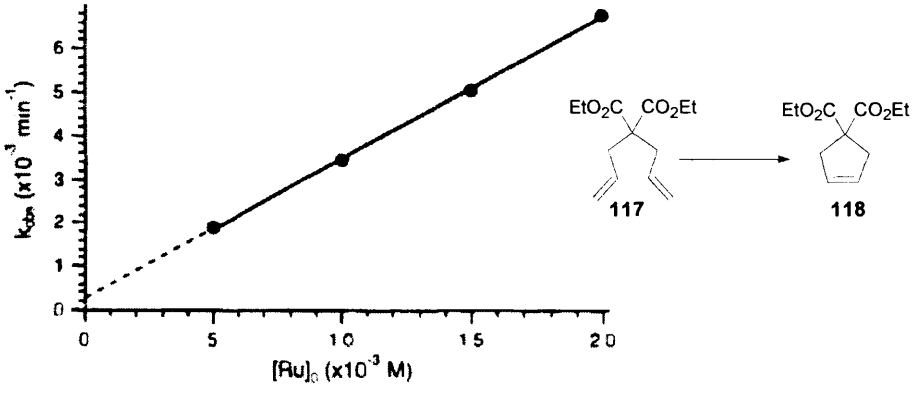

Figure 157 Grubbs' data for [Ru] *vs* k_{obs}

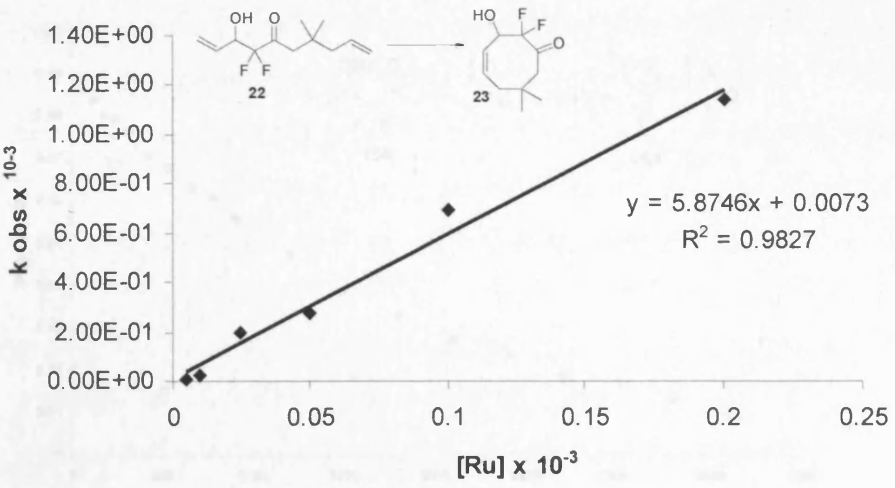

Figure 158 Experimentally-obtained data for [Ru] *vs* k_{obs} for RCM of 22

The two charts both show a linear relationship between ruthenium concentration and observed rate. This suggests that the 'catalyst' is not a catalyst at all and is in fact a reagent, required only in small quantities. Grubbs' kinetic studies found a roughly square root dependence of catalyst concentration on rate. By definition, a true catalyst's concentration in a reaction would not affect the rate of reaction. **Figures 157** and **158** show that this is not true, therefore showing that the ruthenium catalyst is a reagent in the reaction. The ruthenium catalyst is also not strictly a catalyst since, by definition a catalyst should finish unchanged in a reaction. Even prior to catalyst decomposition and/or phosphane recapture, the product of one cycle of reaction is not the same as the 'pre-catalyst' initially added to the reaction.

As shown in **4.2**, the presence of the titanium has an effect on the rate of cyclisation, so especially for slower substrates, it is important to add the co-catalyst to the reaction in order to increase the rate of the reaction. Using the data gathered from these experiments, and from the EM experiments, we aimed to optimise the RCM of **150**, which has the most efficient RCM of all the 4 substrates **4, 30, 31, 150** studied. The EM study showed that even at 0.1 M there was little evidence of cross metathesis. The RCM of **150** was carried out at this concentration in DCE at 80°C using 0.25% Grubbs' second generation catalyst, and 30% Ti (IV) co-catalyst. Results are shown in **Figure 159**.

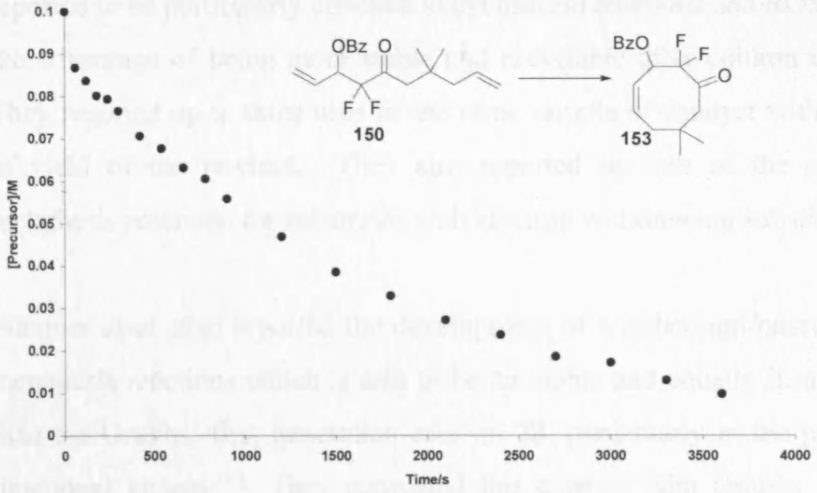

Figure 159 RCM of benzoate 150 with 0.25% 29, 0.1 M in DCE at 80°C (Section 10, p91)

Figure 159 shows that this reaction has a half life of approximately 900 s. Considering the low catalyst loading this is a rapid reaction, and the lower catalyst loading would mean a simpler purification, and a greater chance of elementally pure cyclooctenone **153**.

6.2 Comparison of Metathesis Catalysts

Since the development the highly active molybdenum and ruthenium metathesis catalysts, many new metathesis catalysts have developed for RCM and ROMP reactions by various groups, claiming greater efficiency than existing catalysts or recyclability. It was of interest to compare the reactivity and efficiency of various metathesis catalysts in the synthesis of the eight-membered ring, especially since some of these alternative catalysts were claimed to be air stable and/or recyclable, with obvious cost advantages. To investigate this, and to be able to identify dimeric products, benzoate **31** was used as the metathesis substrate and cyclisation was attempted with a variety of catalysts. Grubbs' first generation catalyst **28** is known to be able to catalyse the formation of eight-membered ring **33** but less efficiently than the second generation catalyst. Hoveyda *et al.* reported the synthesis of additional ruthenium catalysts for olefin metathesis; these were named Hoveyda-Grubbs' first and second generation catalysts **187** and **308**.[119] These catalysts were

reported to be particularly efficient in cyclisation reactions and ROMP, and also had the advantage of being more stable and recyclable after column chromatography. They reported up to three uses of the same sample of catalyst with little or no loss of yield of the product. They also reported the use of the catalyst in cross metathesis reactions for substrates with electron withdrawing substituents.

Fürstner *et al.* also reported the development of a ruthenium-based catalyst **47** for metathesis reactions which is said to be air stable and equally if not more efficient than the Grubbs' first generation catalyst **28**, particularly in the presence of polar functional groups.[120] They compared this catalyst with Grubbs' first generation catalyst **28** for cyclisations already reported in the literature and they also employed their catalyst in the total synthesis of a natural product **114**, which included a cyclooctannulation (**Scheme 125**). They reported a good yield for this system although the RCM precursor is more conformationally rigid than the olefin used in synthesising our cyclic species. They also carried out the metathesis at 2 mM concentration, 10 times lower than the running concentration for our benzoate-protected system.

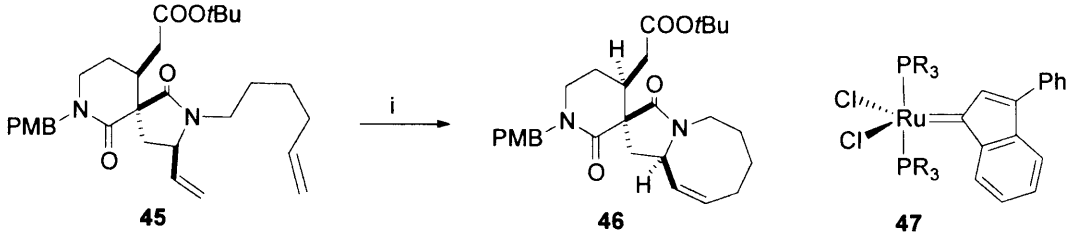

i) 5% **47**, 0.002 M CH_2Cl_2, reflux

Scheme 125 Synthesis of the eight-membered ring of Nakadomarin *viai* RCM with catalyst 47

We carried out the RCM of benzoate **31** under the synthetic conditions (**Scheme 126**) developed using Grubbs' second generation catalyst **29**, and compared several ruthenium metathesis catalysts using the same conditions, checking the conversion after overnight reflux. The results are shown in **Table 42**.

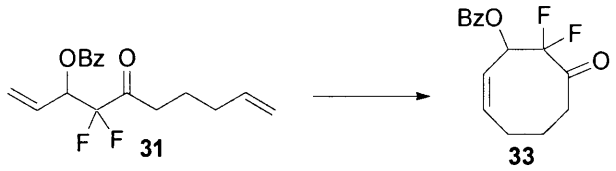

5% Catalyst, 30% Ti(O*i*Pr)$_4$, CH_2Cl_2, 0.02 M, reflux, overnight

Scheme 126 RCM of benzoate 31

Catalyst	% conversion to 33	Concentration / mM	TON
Grubbs' 2nd generation **29**	100%	20mM	20
Grubbs' 2nd Generation **29**	84%	40mM	20*
Grubbs' 2nd generation **29**	77%[c]	60mM	20*
Grubbs' polymer supported	No reaction	20mM	0
Hoveyda-Grubbs' I **187**	No reaction	20mM	0
Hoveyda-Grubbs' II **308**	100%	20mM	20
Hoveyda-Grubbs' II **308**	64%	50mM	20*
Neolyst **47**	Homodimer	20 mM	0

* TONs are 20 due to complete consumption of starting diene

Table 42

Hoveyda-Grubbs' first generation catalyst **187** showed no conversion of the starting material after 24 hours although the second generation analogue went almost completely to the eight-membered ring product. Neolyst **47** did not catalyse conversion of the starting either material after 24 hours after 48 hours. A limited investigation into the limits of catalysis by the Hoveyda-Grubbs' second generation catalyst **308,** of the eight-membered ring formation involved carrying these reactions out at higher concentrations. At 50 mM concentration the main product with this catalyst was eight-membered ring (64%), with the presence of some 16-membered ring and some remaining starting material. Compared to the data obtained from the concentration study with Grubbs' second generation catalyst **29**, where cyclooctenone **33** yield was 84% and 77% for 40 mM and 60 mM respectively, Hoveyda-Grubbs' second generation catalyst **308** is still not as efficient as Grubbs' second generation catalyst **29** but perhaps has an advantage over Grubbs' catalyst in that it can be recycled, although this is yet to be tried. These data also suggest that the choice of catalyst also affects the EM of the reaction, and confirms the literature reports that the Grubbs-Hoveyda type catalysts are particularly useful for ROMP experiments.

The results from this optimisation study have shown us that the syntheses of highly functionalised cyclooctenones, although not trivial, can be relatively rapid and facile if effects of allylic protecting groups on cyclisation rate and efficiency, and the effects of *gem*-dialkyl groups are taken into account. Higher boiling solvents can also be useful to accelerate the rate of reaction, although the more rapid catalytic decomposition pathways at higher temperatures must also be taken into consideration, as well as the possibility of isomerisation pathways, which are known to occur at elevated temperatures (although this was not observed when carrying out the RCM of **31** in refluxing toluene). We have identified a minimum useful catalyst loading (0.25%), which is 20 times lower than the loading of Grubbs' second generation catalyst **29** used in our synthetic reactions, which gives rise not only to more simple purifications, but reduces the overall cost of the reaction as well.

Choice of catalyst is also important for these reactions. It appears from **Table 42** that the best choice of catalyst for these cyclisations is Grubbs' second generation catalyst **29**, although the second generation Grubbs-Hoveyda catalyst **308** also formed cyclooctenone **31**. However, the reaction was less efficient, with larger amounts of cross metathesis products forming at 40 and 60 mM than with Grubbs' second generation catalyst.

7 Conclusions

We have carried out the optimisation of the route towards a small range of cyclooctenones *via* RCM and have identified and quantified some important differences in reaction efficiency between substrates. The use of *gem*-difluorinated substrates has allowed us to exploit highly sensitive $\{^1H\}^{19}F$ NMR to enable calculation of effective molarities for six RCM substrates.

The calculation of EMs has shown us that choice of allylic hydroxyl protecting group has a large effect on cyclisation efficiency, although our kinetic studies have shown that there is only a modest effect on cyclisation rate (less than one order of magnitude between the fastest and slowest substrates). We have also been able to unambiguously identify some products of cross metathesis, either by isolation, or by independent synthesis. Prior to this, literature accounts identify cross metathesis solely by ions found in the mass spectra, which do not give any indication of product stereochemistry.

The use of ^{19}F NMR kinetics has allowed us to follow the backbiting of acyclic oligomers into smaller, cyclic products, and to follow the ring opening of cyclooctenone **33**. These experiments highlight the delicate balance between cyclisation, cross metathesis and ring opening, and concentrations at which each of these reactions dominate.

We have also shown that under normal synthetic conditions of the cyclooctenones, our system is under kinetic control. Closing the system and preventing the escape of ethylene puts the system under thermodynamic control, and changes the distribution of products from eight-membered ring to predominantly oligomeric products.

These results highlight how carefully synthetic chemists must choose their reaction conditions when planning to execute an RCM reaction, particularly of a challenging system, in order to achieve maximum reaction efficiency.

The development of a protocol to follow RCM kinetics by GC has proved very useful and reproducible, and has allowed us to identify some structural effects on reactivity. The cyclisation is accelerated by the presence of *gem*-dimethyl groups, and there is a modest effect on cyclisation depending on the choice of allylic hydroxyl protecting group.

Analysis of the kinetic data showed that the reactions are complex and require multi-step analysis to give an in-depth insight into the reaction kinetics. The model developed and used to analyse kinetic data appears to deal well with the results of competition experiments, and so allows a direct comparison of the substrates studied.

Upon examination of the data obtained from comparing the reactivity of substrates with different allylic hydroxyl protecting groups, there are clear differences in mechanism for benzoate **150** in the rates of cross metathesis and cyclisation. Although benzoate **150** propagates more slowly through cross metathesis (with all catalytic species), the resulting alkylidene undergoes more rapid cyclisation. This outcome may also tie in with the higher EM value calculated for benzoate **150**, and provides good support for the use of this modelling approach in the analysis of our kinetic data.

However, there are some issues with the model, which are likely to require further analysis in the future. The k_1 step of the reaction refers to the catalyst, and the rate *constant* obtained from all of these fittings should not change, although the rate would obviously change. The same is true of rate constant k_{-1}.

Since k_1 corresponds to (in our model) only the dissociation of the phosphane ligand, as defined, this value should be constant and independent of the substrate concentration. However, we some some variation with [S], which suggests that k_1 and k_{-1} are more complex than simple phosphane dissociation/recapture, and may be concealing more complex processes. For example, the effect of the Ti(IV) co-catalyst on rate appears to be quite significant in the initial stages of the reaction. Although this was not accounted for in the model, the k_1 and k_{-1} steps may include the Ti(IV) co-catalyst in some way. The concentration of the $Ti(O\textit{i}Pr)_4$ in solution

depends on the concentration of the substrate, so in this case, k_1 and k_{-1} would be affected by [S].

The uncertainty in k_1 and k_{-1} within the model means that although it appears a useful tool for the in-depth analysis of the propagation steps in RCM between substrates, there appear to be some steps which are inaccurately represented in the initiation stages of the model, and this limits the usefulness of the model as a tool to describe these RCM systems with absolute confidence.

The design and synthesis of substrates with a phenyl-substituted double bond has allowed simplification of the reaction kinetics, by avoiding formation of the methylidene, and its subsequent decomposition pathways. This has allowed calculation of activation parameters for the reaction. However, experimentally obtained data still do not perfectly fit simple first order decay, meaning a new model was used to analyse these data. This raises further issues though, in that the same uncertainty in the k_1 and k_{-1} steps arises. However, the calculation of activation parameters for the propagation and cyclisation steps gives an interesting insight into where entropic and enthalpic penalties arise within the reaction.

The synthesis of **302** provided extra synthetic confirmation to the studies of the Ru-alkylidene region, as characterisation of the ruthenium ethylidene. However, the substrate did not behave as expected, and appears too complex to successfully model. Further work is required to understand the nature of this substrate's behaviour.

8 Further Work

Some of the work described in this thesis has raised further questions which it would be interesting to address in future work. The work into effective molarity and the large effect of allylic hydroxyl protecting group required further exploration to gain greater understanding as to how the protecting group affects the cyclisation efficiency *via* RCM. The effect exerted by the allylic protecting group is clearly not a simple one, and it would be interesting to synthesise further substrates to attempt to rationalise this effect further (**Scheme 127**).

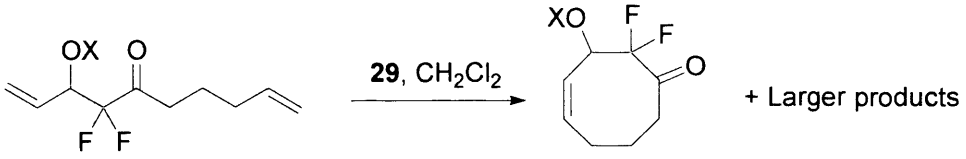

X = Me, OAc, $COPhSO_3$

Scheme 127

Synthesis of a range of different esters would be interesting, to identify any electronic effects on cyclisation, and identify if, as a general rule, substrates with allylic ester protecting groups exhibit greater cyclisation efficiency. In-depth analysis of the kinetics of cyclisation of methyl ether **148** also suggested that this substrate may exhibit a relatively high EM, since the rates of cross metathesis were low. However, the use of this substrate is less practical, due to long reaction times and product volatility, and we would be faced with the same difficulty in sample concentration as with alcohol **22**.

Further identification of the oligomeric series formed at higher RCM concentrations would also be useful. These products were extremely difficult to separate under normal chromatographic conditions, and their identification was limited by the mass range of electrospray, since MALDI analyses proved unsuccessful. The use of fluorous esters such as **309** may help to overcome this problem, using the non-fluorinated dienes, since these can be synthesised more rapidly. The ^{19}F NMR spectrum could be analysed to identify any oligomeric series, and highly fluorinated species could possibly be separated by fluorous phase chromatography methods

(flash chromatography or HPLC) for mass spectral analyses. This would give us an indication as to the range of sizes of oligomer which are formed in these reactions at higher concentrations.

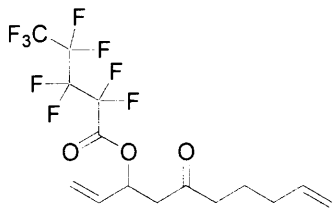

309

The development of new substrates which allow simplification of the complex kinetics of cyclisation *via* ring closing metathesis requires further study. The use of **286**, which avoids the formation of methylidene **221**, and instead regenerates benzylidene **220**, has shown that kinetics can be vastly simplified, although the reaction is slowed significantly due to a combination of steric effects by the terminal phenyl group, and the loss of entropic driving force upon the formation of styrene rather than ethylene. It would be interesting to use this substrate for further analyses, to gain an overall k_{cat} for the cyclisation process. The k_{cat} data generated for diene **149** is interesting, but cannot be compared directly with existing literature values.

The cyclisation kinetics of **302** did not behave as expected when studied, and appeared to show a rapid formation of homodimer, followed by a slower cyclisation. The behaviour within this system was more complex than could be understood with the models input into Berkeley Madonna, and this system therefore needs further study to understand why it should undergo dimerisation/oligomerisation prior to cyclisation when the other systems synthesised do not.

The syntheses of **286** and **302** have shown us that use of these substrates can change the propagating species, and avoid the formation of the methylidene **221**, *via* which decomposition pathways occur due to its relative instability. Synthesis of further substrates, which would give access to new 'catalytic leaving groups' and lead to the formation of new Ru-alkylidene species which can act as the propagating

species in cyclisation reactions would be interesting (**Scheme 128**). This would allow a comparison of relative activity and stability of these species, and also allow determination of the importance of the entropic driving force, arising due to the release of alkene, in these reactions. The choice of alkene R groups would allow us to draw conclusions about how the level of substitution on the terminal double bond affects the rate of reaction, and also give an idea about the relative stabilities and lifetimes of the resulting ruthenium alkylidenes.

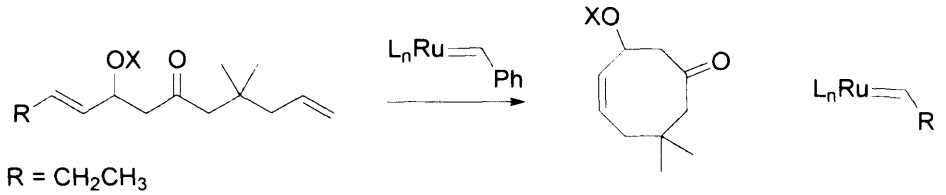

R = CH_2CH_3
$CH(CH_3)_2$
Ph-R

Scheme 128

Study of these systems would allow identification of an efficient system, which potentially allows for reduced catalyst loadings and easier purification of products as a result, thus reducing the overall cost of these reactions, since metathesis catalysts are expensive.

The synthesis and subsequent study of **302** gave some interesting results. The use of ^{1}H NMR in the alkene region of the spectrum to follow cyclisation kinetics showed us that this substrate appeared to form a dimeric or oligomeric structure before backbiting to the cyclic product. Further investigation of this would be interesting, to understand why this substrate forms eight-membered ring **293** after the formation of dimeric/oligomeric products. Headspace monitoring of the reaction would be useful, determine if propene is released during the reaction, since this would result if the ethylidene was present as the propagating species. The amount of propene released would also give an indication as to whether or not the ethylidene was forming as a result of the substrate, or if it was forming as a result of methylidene decomposition.

9 Experimental

NMR spectra were recorded on Bruker DPX-300, Bruker DRX-400, Bruker AV400, or Bruker DPX-600 spectrometers. Routine NMR analyses were carried out on DPX-300, DPX-400 and AV-400 instruments. Routine ^{1}H NMR analyses were carried out at 300, 400 and 600 MHz, ^{13}C NMR analyses at 75 and 100 MHz, and ^{19}F analyses at 282 and 376 MHz. Kinetic experiments were carried out on an AV-400 (^{1}H and ^{19}F) and DPX-600 (^{1}H only). ^{1}H and ^{13}C NMR spectra were recorded using the deuterated solvent as the internal reference. The spectroscopic data are presented as follows: s = singlet, d = doublet, t = triplet, q = quartet, br = broad, m = multiplet. Unless otherwise stated, couplings, *J*, refer to $^{3}J_{H\text{-}H}$ couplings and are given in Hertz. NMR data are presented with chemical shift in ppm, followed by relative integrals, coupling constant (in Hertz), and assignment.

Thin layer chromatography(TLC) was performed on precoated aluminium silica gel plated supplised by E. Merck, A. G. Darmstadt, Germany (silica gel 60 F254, thickness 0.2 mm, art. 1.05554) and compounds were visualised with UV light or a potassium permanganate stain. THF was dried by refluxing with benzophenone over sodium wire until a deep purple colour developed and persisted, then distilled and collected by dry syringe as required, or obtained using a Pure Solv apparatus. Chloroform and 1,2-dichloroethane were dried by distillation over calcium hydride chips. Other solvents were dried using a Pure Solv apparatus (Innovate Technologies Inc). All other chemicals were used as received without any further purification. Where required, solvents were degassed by sparging with argon or oxygen-free nitrogen for at least 30 minutes.

Kinetic GC analyses were carried out using a Perkin Elmer Autosystem XL machine, using a standard PE-5 column. The injector temperature was set to 250°C, and the starting temperature of the oven to 40°C. The temperature was increased at a rate of 10°C/min, up to 280°C and maintained at this temperature for 5 minutes. GC-MS analyses of kinetic samples were carried out using a Finnegan Pro GC-MS system, using the same temperature ramping programme, up to 320°C

Kinetic experiments followed by NMR were monitored using a Bruker AV400 system, using a pseudo 2D programme (either ^{1}H or ^{19}F at either 400 MHz, or 376 MHz respectively) with a variable delay between recording spectra, at 298 K unless otherwise specified. At the end of each experiment, 2D data were unpacked into multiple 1D spectra, which were then integrated either manually or using a macro run by Bruker TopSpin. The sweep width (sw) and centering (o1p) were changed according to the nature of the experiment, to follow different spectral regions as required. The deuterated solvent was used as the internal reference in all cases.

Low resolution mass spectral data were collected either on a Finnegan Pro GC-MS system, using electron impact ionisation; or on a Finnegan Pro electrospray system (by manual injection), using methanol or acetonitrile as solvents. High resolution mass spectra were recorded by the EPSRC National Mass Spectrometry Service at Swansea by either electrospray or chemical ionisation, where polyethyleneimine was used as a reference compound. Attempts at MALDI were carried out on a Shimadzu system, using a range of matrices.

Infra-red analyses were carried out on a Perkin Elmer IR spectrometer, using films in KCl plates. Analysis of solid samples was carried out in a nujol mull. Crystals submitted for X-ray analysis were grown by vapour diffusion. Titration of butyllithium solutions was carried out using the following procedure published by Duhamel: *n*-BuLi (0.5 mL of a 2.5 M solution in hexanes) was added to DIPA (0.28g, excess), and 4-Phenylbenzylidene benzylamine (0.01 g, 0.07 mmol) in dry THF (2 mL) at room temperature.[121] The deep blue color of the azaallylithium anion appeared. The solution was titrated with ^{t}BuOH (as a 1M solution in xylene). The color change on the approach to the endpoint was blue to red, and then on addition of one drop further, the red solution changed to pale yellow. A further portion of *n*-BuLi (0.5 mL) was added to the solution, which returned to dark blue, and the titration was repeated in triplicate.

Preparation of 4,4-Difluoro-3-hydroxy-deca-1,9-diene-5-one [4]

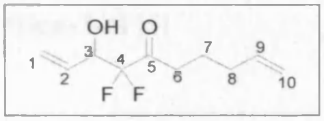

Thionyl chloride (121 μL, 1.4 mmol) was added dropwise over 10 minutes to a solution of alcohol **5** (0.40 g, 1.4 mmol) in methanol (14 mL) at 0°C. The solution was stirred overnight, allowing to warm to room temperature. The mixture was concentrated *in vacuo*, diluted with water (15 mL) and extracted with diethyl ether (3 x 15 mL). The combined organic extracts were washed with brine (10 mL), dried ($MgSO_4$), filtered and concentrated *in vacuo* to yield diene **4** as a brown oil (0.16g, 55%) which was used without purification. δ_H (300 MHz, $CDCl_3$) 5.93 (1H, ddd, *J* 16.9, *J* 10.5, *J* 6.4, H-2), 5.76 (1H, ddt, *J* 16.9, *J* 10.2, *J* 6.7, H-9), 5.50 (1H, dt, *J* 17.2, ^2J 1.5, ^4J 1.5 H-1a), 5.43 (1H, dt, *J* 10.5, ^2J 1.5, ^4J 1.5, H-1b), 5.07-4.98 (2H, m, H-10), 4.63-4.54 (1H, m, H-3), 2.72 (2H, t, *J* 7.3, H-6), 2.37 (1H, br s, OH), 2.12-2.05 (2H, m, H-8), 1.73 (2H, m, H-7), δ_F -113.7 (dd, $^2J_{F\text{-}F}$ 273.0, $^3J_{H\text{-}F}$ 7.1), -123.3 (dd, $^2J_{F\text{-}F}$ 273.0, $^3J_{H\text{-}F}$ 15.2). The data were in agreement with those reported by Roig *et al.*[122].

Preparation of (5*Z*)-4,4-difluoro-5-[(2-methoxyethoxy)methoxy]deca-1,5,9-trien-3-ol [5]

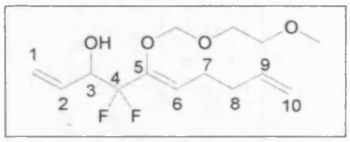

LDA was prepared by the dropwise addition of ^{n}BuLi (10.3 mL, 20.8 mmol of a 2.43 M solution in hexanes) to a solution of DIPA (2.9 mL, 21.8 mmol) in dry THF (20 mL) at -78 °C under nitrogen. The solution was allowed to warm to room temperature before recooling to -100 °C. A solution of difluoroallylic ether **6** (3.0 g, 9.9 mmol) in THF (10 mL) was added dropwise at this temperature before allowing the solution to warm to -70 °C over two hours. The mixture was stirred at this temperature for four hours before quenching at -30 °C with saturated aqueous ammonium chloride solution (25 mL). The reaction mixture was warmed to room temperature over one hour and diluted with water (10 mL). The aqueous layer was extracted with diethyl ether (3 x 30 mL) and the combined organic extracts were washed with brine (25ml), dried over $MgSO_4$, filtered and concentrated *in vacuo* to yield alcohol **5** as a brown oil (2.76 g, 92%) which was used without purification. R_f (20% ethyl acetate in hexane) 0.19; δ_H (300 MHz, $CDCl_3$); 5.90 (1H, ddd, *J* 17.2, 10.5, 5.6, H-2), 5.77 (1H ddt, *J* 16.7, 10.2, 6.4, H-9), 5.54 (1H, td, *J* 7.3, $^4J_{H\text{-}F}$ 1.5, H-6), 5.45 (1H, dd, *J* 17.2, $^4J_{H\text{-}F}$ 1.5, H-1a), 5.30 (1H, dt, *J* 10.5, ^2J 1.5, ^4J 1.5, H-1b), 5.05-4.95 (4H, m, H-10 and OCH_2OCH_2), 4.56-4.40 (1H, m, H-3), 3.88-3.77 (2H, m, $OCH_2CH_2OCH_3$) 3.58 (2H, m, $OCH_2CH_2OCH_3$), 3.36 (3H, s, OCH_3), 2.90 (1H, br s, OH), 2.31-2.22 (2H, m, H-7), 2.17-2.09 (2H, m, H-8); δ_F (300 MHz, $CDCl_3$) -110.0 (dd $^2J_{F\text{-}F}$ 252.5, $^3J_{F\text{-}H}$ 8.3), -115.7 (dd, $^2J_{F\text{-}F}$ 252.5, $^3J_{F\text{-}H}$ 14.3).

Preparation of 3-Allyloxy-1,1-difluoro-2-(methoxyethoxymethoxy)-hepta-1,6-diene [6]

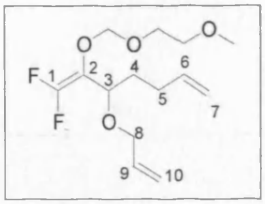

Difluoroallylic alcohol **7** (1.8 g, 7.1 mmol) and allyl bromide (0.60 mL, 7.8 mmol) were mixed with sodium hydroxide (3.6 mL of a 50% aqueous solution, 0.05 mol) at 0°C. Tetrabutylammonium hydrogensulphate, (0.1 g, 0.33 mmol) was added and the solution was stirred vigorously overnight, warming to room temperature. The mixture was diluted with water (25 mL), extracted with diethyl ether (3 x 50 mL) and the combined organic extracts washed with brine (25 mL), dried ($MgSO_4$), filtered and concentrated *in vacuo* to give **6** as a pale yellow/orange oil (4.70g, 94%), which was used without purification. The ^1H NMR spectrum showed good purity and was in agreement with that published by Roig.[122] δ_H (300MHz, $CDCl_3$), 5.96-5.83 (1H, m, H-9) 5.81 (1H, ddt, *J* 16.1, 10.1, 6.6, H-6), 5.25 (1H, ddd, *J* 17.2, ^2J 3.2, ^4J 1.8, H-10a), 5.16 (1H, ddd, *J* 10.2, ^2J 3.2, ^4J 1.2, H-10b), 5.05-4.91 (4H, m, H-7 and OCH_2O), 4.09 (1H, ddt, *J* 12.5, *J* 5.0, ^4J 1.5, H-3), 4.04-3.97 (1H, m, H-8a), 3.91-3.72 (3H, m, H-8b, $CH_2CH_2OCH_3$), 3.56-3.45 (2H, m, $OCH_2CH_2OCH_3$), 3.38 (3H, s, OCH_3), 2.09 (2H, dd, *J* 14.0, *J* 7.3, H-5), 1.95-1.70 (2H, m, H-4); δ_F (282MHz, $CDCl_3$); -97.50 (dd, $^2J_{F-F}$ 63.5, $^4J_{F-H}$ 1.9), -115.7 (dd, $^2J_{F-F}$ 63.5, $^4J_{F-H}$ 3.8); GC purity 98%.

Preparation of 1,1-Difluoro-2-(2-methoxyethoxymethoxy)-hepta-1,6-diene-3-ol [7]

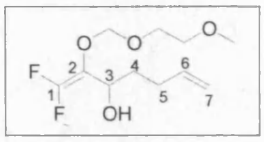

^{n}BuLi (38.1 mL of a 2.23 M solution in hexanes, 70.9 mmol) was added dropwise to a solution of DIPA (12.4 mL, 88.4 mmol) in THF (44 mL) at -78 °C under nitrogen. The solution was allowed to warm to room temperature and was then recooled to -78 °C. MEM-ether **8** (7.7 g, 40.8 mmol) was added to this solution dropwise over forty minutes and the solution stirred for two hours before adding aldehyde **128** (4.0 g, 47.6 mmL) in one portion. The solution was allowed to warm to -30 °C before quenching with an aqueous saturated solution of ammonium chloride (25 mL). The reaction mixture was diluted with water (30 mL) and the organic and aqueous layers separated. The aqueous layer was extracted with diethyl ether (3 x 50 mL) and the combined organic extracts washed with brine (20 mL), dried ($MgSO_4$) and then concentrated *in vacuo*. The resulting red/brown oil was distilled (Kugelrohr, bp 70-80°C, 0.075 mm Hg) to give **7** as a clear, colourless oil (9.5g, 79%). bp 70-80°C, 0.075 mm Hg. δ_H (300MHz, $CDCl_3$) 5.80 (1H, ddt, $^3J_{trans}$ 16.7, 10.2, 6.7, H-6), 5.06-4.85 (4H, m, H-7 and $OCH_2OCH_2OCH_3$), 4.24 (1H, br, OH), 3.96 (1H, dd, ^2J 6.2, J 3.6, $OCH_aH_bCH_2O$), 3.93 (1H, dd, ^2J 6.2, J 4.0, $OCH_aH_bCH_2O$), 3.78 (1H, dd, ^2J 4.9, J 3.2, $OCH_2CH_aH_bO$), 3.75 (1H, dd, ^2J 4.9, J 3.2, $OCH_2CH_aH_bO$), 3.36 (3H, s, OCH_3), 2.14-2.05 (2H, m, H-4), 1.87-1.64 (2H, m, H-5); δ_C (75 MHz, $CDCl_3$) 154.6 (dd, $^1J_{C-F}$ 290.3, 284.3), 137.7, 118.2 (dd, $^2J_{C-F}$ 36.4, 9.8), 115.1, 98.0, 71.4, 68.5, 66.5, 59.0, 33.1, 29.7; δ_F (282 MHz, $CDCl_3$) -100.2 (d, $^2J_{F-F}$ 64.0), -110.0 (dd, $^2J_{F-F}$ 64.0, $^4J_{F-H}$ 3.8). The data are in agreement with those reported by Roig *et al.*[122]

Preparation of 1,1-difluoro-2-(2'-methoxyethoxymethoxy)-4,4-dimethylhepta-1,6-diene [20]

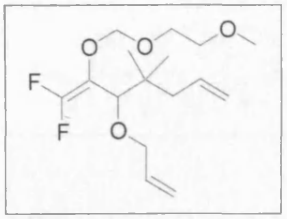

Allylic alcohol **144** (14.1 g, 50.4 mmol) was mixed with allyl bromide (5.0 mL, 60.5 mmol) in aqueous sodium hydroxide solution (28 mL of a 50% w/v solution, 353 mmol). Phase transfer catalyst tetrabutyalammonium hydrogensulPh-Hate (0.35 g, 1.0 mmol) was added at 0°C and the mixture stirred overnight vigorously, allowing to warm to room temperature. The reaction was quenched with a saturated aqueous solution of ammonium chloride (20 mL). The aqueous layer was extracted with diethyl ether (3 x 30 mL). The combined organic extracts were washed with brine (30 mL), dried with $MgSO_4$, and concentrated *in vacuo* to yield ether **20** as an orange oil (14.7 g, 91%). The resulting ether **20** was used without purification. δ_H (300 MHz, $CDCl_3$) 5.93-5.72 (2H, m, H-6 and H-2''), 5.26 (1H, dq, *J* 17.3, ^2J 1.5, ^4J 1.5, H-3''a), 5.15 (1H, dq, *J* 5.1, ^2J 1,5, ^4J 1.5, H-3''b), 5.05-4.97 (2H, m, H-7a and H-7b), 4.99 (1H, d, ^2J 5.9, OCH_aH_bO), 4.88 (1H, d, ^2J 5.9, OCH_aH_bO), 4.13-3.71 (4H, m, $OCH_2CH_2OCH_3$), 3.62 (1H, dd, $^4J_{H\text{-}F}$ 4.1, 2.2, H-3), 3.57-3.51 (2H, m, H-1''), 3.38 (3H, s, OCH_3), 2.16 (1H, dd, ^2J 13.6, ^3J 7.7, H-5a), 2.04 (1H, dd, ^2J 13.6, *J* 7.7, H-5b), 0.99 (3H, s, CH_3), 0.91 (3H, s, CH_3); δ_C (75 MHz, $CDCl_3$) 156.9 (dd, $^1J_{C\text{-}F}$ 293.9, 286.0), 135.0, 134.4, 117.4, 117.0, 112.1(dd, $^2J_{C\text{-}F}$ 33.9, 10.2), 97.2 (dd, $^3J_{C\text{-}F}$ 4.0, 2.8), 80.1 (t, $^4J_{C\text{-}F}$ 2.8), 71.7, 69.8, 68.3, 59.0, 44.0, 38.5 (t, $^4J_{C\text{-}F}$ 1.7), 23.5, 23.1; δ_F (1F, d, $^2J_{F\text{-}F}$ 61.7), -108.2 (1H, d, $^2J_{F\text{-}F}$ 61.7). Spectral data were in agreement with those published by Percy.[2]

Preparation of (5*Z*)-4,4-difluoro-5-[(2-methoxyethoxy)methoxy]-7,7-dimethyldeca-1,5,9-trien-3-ol [21]

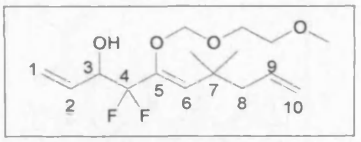

LDA was prepared by the dropwise addition of ^{n}BuLi (10.3 mL of a 2.43 M solution in hexanes) to a solution of DIPA (2.9 mL, 21.8 mmol) in dry THF at -78 °C. The solution was allowed to warm to room temperature before recooling to -78 °C. Difluoroallylic ether, **20** (3.0 g, 9.9 mmol) was added dropwise at this temperature before warming to -30°C and stirring at this temperature overnight. The reaction was quenched with ammonium chloride (25 mL of a saturated aqueous solution) and allowed to warm to room temperature. The aqueous layer was extracted with diethyl ether (3 x 30 mL) and the combined organic extracts washed with brine (20 mL), dried ($MgSO_4$) and concentrated *in vacuo* to yield **21** as a brown oil (92%, 2.91g) which was used without purification. δ_H (300 MHz, $CDCl_3$) 5.95-5.68 (2H, m, H-2 and H-9), 5.46 (1H, d, *J* 17.3, H-1a), 5.40 (1H, s, H-6), 5.33 (1H, d, *J* 10.7, H-1b), 5.04-4.98 (4H, m, H-10a, H-10b and H-OC*H*$_2$O), 4.58-4.50 (1H, m, H-3), 3.85-3.81 (2H, m, OC*H*$_2$CH$_2$O), 3.58-3.55 (2H, m, OCH$_2$C*H*$_2$O), 3.37 (3H, s, OC*H*$_3$), 2.71 (1H, br s, O*H*), 2.15 (2H, d, *J* 6.6, H-8), 1.13 (3H, s, CH_3), 1.12 (3H, s, CH_3); δ_C (75 MHz, $CDCl_3$) 142.3 (t, $^2J_{C\text{-}F}$ 24.9), 135.2, 132.4 (t, $^3J_{C\text{-}F}$ 3.1), 128.4 (t, $^3J_{C\text{-}F}$ 5.4), 118.7, 118.4 (t, $^1J_{C\text{-}F}$ 250.1), 117.1, 98.2, 72.6 (t, $^2J_{C\text{-}F}$ 5.4), 71.4, 68.8, 58.8, 47.4, 35.0, 27.8; δ_F (282 MHz, $CDCl_3$) -109.9 (1H, dd, $^2J_{F\text{-}F}$ 251.8, $^3J_{H\text{-}F}$ 10.1), -112.0 (1F, dd, $^2J_{F\text{-}F}$ 251.8, $^3J_{H\text{-}F}$ 12.7). The spectral data were in agreement with those reported by Percy.[2]

Preparation of 3-Benzyloxy-4,4-difluorodeca-1,9-dien-5-one [31]

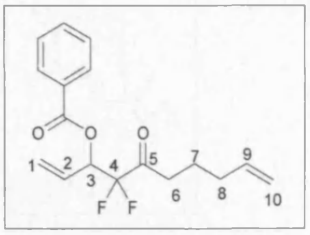

Thionyl chloride (0.31 mL, 4.2 mmol) was added dropwise over 15 minutes to a solution of benzoate ester **133** (1.7 g, 4.2 mmol) in methanol (42 mL), at 0°C. The reaction was stirred overnight, allowing to warm to room temperature. The solution was concentrated *in vacuo* and diluted with water (10 mL) and diethyl ether (20 mL). The aqueous layer was extracted with diethyl ether (2 x 20 mL). The original ether layer and the combined organic extracts were washed with brine (20 mL), dried ($MgSO_4$) and concentrated *in vacuo* to yield **31** as a brown oil (1.1g, 89%) which did not require purification since the NMR spectral data showed good purity. δ_H (300MHz, $CDCl_3$) 7.99-7.94 (2H, m, *ortho* Ph-H), 7.56-7.50 (1H, m, *para* Ph-H), 7.42-7.36 (2H, m, *meta* Ph-H), 5.97-5.81 (2H, m, H-2, H-9), 5.64 (1H, ddd, *J* 16.8, $^3J_{H\text{-}F}$ 14.2, $^3J_{H\text{-}F}$ 9.0, H-3), 5.50 (1H, dd, *J* 16.1, $^4J_{H\text{-}H}$ 0.9, H-1a), 5.43 (1H, dd, *J* 10.2, $^4J_{H\text{-}H}$ 0.9, H-1b), 4.95-4.87 (2H, m, H-10), 2.69-2.64 (2H, m, H-6), 2.01-1.98 (2H, m, H-8), 1.64 (2H, dt, *J* 14.6, 7.3, H-7); δ_F (282MHz, $CDCl_3$), -113.7 (dd, $^2J_{F\text{-}F}$ 273.9, $^3J_{F\text{-}H}$ 9.0), -118.9 (dd, $^2J_{F\text{-}F}$ 273.9, $^3J_{F\text{-}H}$ 14.2). GC retention time 19.55 min.

Preparation of 1-benzoyl-2,2,difluoro-cyclooct-7-en-3-one [33]

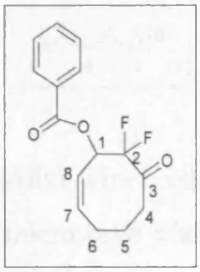

A solution of difluoroketone **31** (1.36 g, 4.5 mmol) and titanium *iso*propoxide (430 µl, 0.15 mmol) in dry, degassed CH_2Cl_2 (297 mL, substrate concentration 0.015M) was refluxed for 30 minutes under nitrogen. A solution of Grubbs' second generation catalyst **29** (180 mg, 5%) in dry, degassed CH_2Cl_2 (1 mL). The mixture was refluxed overnight. The solution was cooled and concentrated *in vacuo* to yield a brown oil which was purified by column chromatograpy (10% Ethyl acetate/hexane) to yield **33** as a white solid (64%, 0.80g). mp 92-94°C. R_f (10% Ethyl acetate/hexane) 0.15. δ_H (300MHz, $CDCl_3$) 8.14-8.10 (2H, m, *ortho* Ph-H), 7.64-7.58 (1H, m, *para* Ph-H), 7.51-7.45 (2H, m, *meta* Ph-H), 6.36 (ddd, 1H, $^3J_{H\text{-}F}$ 21.2, *J* 7.9, ^4J 1.5, H-1), 6.06-5.98 (1H, m, H-7), 5.68-5.60 (1H, m, H-8), 2.82 (1H, dd, ^2J 12.6, *J* 10.2, H-4a), 2.68 (1H, ddt, ^2J 12.6, *J* 10.8, $^4J_{H\text{-}H}$ 3.5, H-4b), 2.44-2.27 (2H, m, H-6), 2.13-2.02 (1H, m, H-5a), 1.89-1.74 (1H, m, H-5b); δ_F (382MHz, $CDCl_3$), -110.0 (d, $^2J_{F\text{-}F}$ 239.8), -130.9 (dd, $^2J_{F\text{-}F}$ 239.8, $^3J_{H\text{-}F}$ 21.2). The NMR data were in agreement with those published by Percy.[2]

Preparation of pent-4-en-1-al [128]

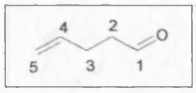

Allyl vinyl ether **129** (3.91 g, 46.5 mmol) was placed in a CEM Discover microwave vial and sealed with a crimp cap. The tube was placed in a CEM Discover Microwave and irradiated with stirring for five hours at 150°C, 300 psi pressure, 300 W power. ^{1}H NMR analysis showed total conversion of the ether to the aldehyde. The material **128** was used without purification since ^{1}H NMR data was in agreement with the literature compound.[xx] δ_H (300MHz, $CDCl_3$) 9.99 (1H, t, *J* 1.5, H-1), 6.13-5.97 (1H, m, H-4), 5.32-5.21 (2H, m, H-5), 2.80-2.73 (2H, m, H-2), 2.65-2.56 (2H, m, H-3); δ_C (63 MHz, $CDCl_3$) 202.1, 136.8, 115.9, 43.0, 26.4. The spectral data were in agreement with those reported by Murphy.[47]

Preparation of allyl vinyl ether [129]

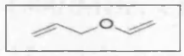

A solution of mercuric trifluoroacetate (0.9 g, 2.1 mmol) in allyl alcohol (23.4 mL, 344.3 mmol) and ethyl vinyl ether (184 mL) was refluxed under nitrogen overnight The solution was cooled and washed with $NaHCO_3$ (75 mL of a saturated solution). The organic layer was distilled; ethyl vinyl ether was removed at 40 °C (760 mm Hg). The NMR analysis of the product agreed well with NMR data reported for commercial allyl vinyl ether. Allyl vinyl ether **129** was distilled as a 3:1 azeotrope with an acetal contaminant. Ether **129** (15.0 g, 51%) could still undergo rearrangement in the presence of the acetal so was not purified further.

Preparation of 3-benzyloxy-4,4-difluoro-5-[(2-methoxyethoxy)methoxy]deca-1,5(Z),9-triene [133]

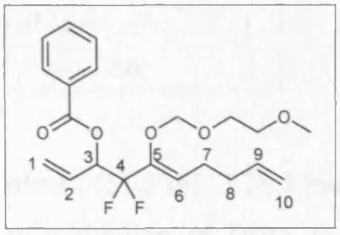

Difluoroalcohol **5** (6.3 g, 21.7 mmol), benzoic anhydride (4.90 g, 21.7 mmol) and DMAP (0.53 g, 4.3 mmol) were dissolved in CH_2Cl_2 (217 mL). PVP (10.6 g, 10.6 mmol, 0.5 equivalents) was added and the reaction mixture swirled gently at room temperature overnight. The resin was collected at the pump and washed with water (50 mL) and saturated aqueous sodium hydrogencarbonate solution (50 mL). The aqueous layer was extracted with diethyl ether (3 x 50 mL) and the combined organic extracts were washed with brine (30 mL) and dried ($MgSO_4$) concentrated *in vacuo* to yield **80** as a brown oil (6.85g, 80%). The PVP was dried after washing for re-use. The crude product **133** was taken on and used without purification. δ_H (300 MHz, $CDCl_3$) 7.99 (2H, dd, *J* 8.5, $^4J_{H\text{-}H}$ 1.3, *ortho* Ph-H), 7.50 (1H, tt, *J* 7.5, $^4J_{H\text{-}H}$ 1.3, *para* Ph-H), 7.37 (2H, dd, *J* 8.5, *J* 7.5, *meta* Ph-H), 5.92-5.86 (1H, m, H-2), 5.65 (2H, dd, *J* 10.2, *J* 6.6, H-10), 5.55 (1H, t, *J* 7.5 H-6), 5.46 (1H, dd, *J* 15.9, $^2J_{H\text{-}H}$ 3.7, H-1a), 5.35 (1H, dd, *J* 10.5, $^2J_{H\text{-}H}$ 3.7, H-1b), 4.92 (2H, s, OCH_2O), 4.85 (1H, dt, *J* 12.4, *J* 10.2, H-9), 3.78 (2H, dd, *J* 8.2, *J* 4.4, $OCH_2CH_2OCH_3$), 3.40 (2H, dd, *J* 8.2, *J* 4.4, $OCH_2CH_2OCH_3$), 3.31 (3H, s, OCH_3), 2.20 (2H, dt, *J* 11.7, *J* 7.5, H-7), 2.01 (2H, dd, *J* 12.4, *J* 11.7, H-8), δ_F (282 MHz, $CDCl_3$) -110.8 (dd, $^3J_{H\text{-}F}$ 10.9, $^2J_{F\text{-}F}$ 253.5), -112.3 (dd, $^2J_{F\text{-}F}$ 253.5, $^3J_{H\text{-}F}$ 12.8; GC purity 99%. NMR data were in agreement with those published by Percy.[2]

Preparation of 1,1-difluoro-2-[(2-methoxyethoxy)methoxy]-4,4-dimethylhepta-1,6-dien-3-ol [144]

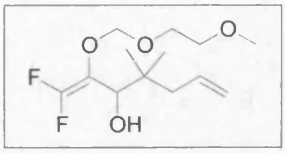

nBuLi (51.3 mL, 128.3 mmol of a 2.5 M solution in hexanes) was added dropwise to a solution of DIPA (18.0 mL, 128.3 mL) in THF (125 mL) at -78°C. On completion, the solution was allowed to warm to room temperature. The solution was then recooled to -78°C and MEM ether **8** (11.5 g, 61.2 mmol) in THF (50 mL) was added dropwise, maintaining this temperature. The reaction was then stirred for 50 minutes at -70°C before adding dimethyl pentenal (6.9 g, 61.2 mmol) in one portion. The mixture was allowed to warm to -30°C over two hours before quenching with a saturated aqueous solution of ammonium chloride (40 mL). The reaction mixture was warmed to room temperature and water (50 mL) was added, followed by diethyl ether (50 mL). The aqueous layer was extracted with diethyl ether (3 x 50 mL). The combined organic extracts were washed with brine (40 mL) and dried with $MgSO_4$ before concentrating *in vacuo* to yield **144** as an orange oil which was used without purification (14.1g, 82%). δ_H (300 MHz, $CDCl_3$) 5.80-5.75 (1H, m, H-6), 5.06-5.02 (2H, m, H-7a and H-7b), 5.02 (1H, d, ^2J 6.3, OCH_aH_bO), 4.83 (1H, d, ^2J 6.3, OCH_aH_bO), 3.96-3.89 (2H, m, $OCH_2CH_2OCH_3$), 3.79-3.72 (1H, m, H-3), 3.57-3.54 (2H, m, $OCH_2CH_2OCH_3$), 3.38 (3H, s, OCH_3), 2.21 (1H, dd, ^2J 13.5, J 7.7, H-5a), 2.14 (1H, dd, ^2J 13.5, J 7.7, H-5b), 0.93 (3H, s, CH_3), 0.88 (3H, s, CH_3); δ_C (75 MHz, $CDCl_3$) 155.0 (dd, $^1J_{C\text{-}F}$ 291.6, 285.4), 135.0, 117.5, 98.5 (dd, $^2J_{C\text{-}F}$ 4.5, 2.8), 72.6 (t, $^3J_{C\text{-}F}$ 2.6), 71.5, 69.0, 59.0, 55.9, 43.5, 39.0 (t, $^4J_{C\text{-}F}$ 2.3), 23.1, 22.9; δ_F (282 MHz, $CDCl_3$) -100.3 (1F, d, $^2J_{F\text{-}F}$ 66.1), -108.1 (1F, dd, $^2J_{F\text{-}F}$ 66.1, $^4J_{H\text{-}F}$ 4.5). Spectral data were in agreement with those published by Percy.[1]

Preparation of 4,4-Difluoro-3-methoxy-5-(2-methoxy-ethoxymethoxy)-7,7-dimethyl-deca-1,5,9-triene [145]

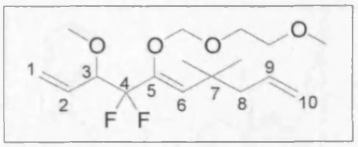

Sodium hydride (0.6 g, 23.4 mmol of a 60% suspension in oil) was washed with petrol (3 x 10 mL) in a flame-dried flask The washings were removed by syringes and the powder was suspended in THF (50 mL). Alcohol **21** (2.5 g, 7.8 mmol) was added to this solution neat at 0°C followed by methyl iodide (0.53 mL, 8.6 mmol). The solution was stirred overnight, warming to room temperature. The reaction was quenched with water (15 mL) and the aqueous layer extracted with diethyl ether (3 x 25 mL). The combined organic extracts were washed with brine (15 mL), dried ($MgSO_4$) and concentrated *in vacuo.* The residual orange oil was purified by flash column chromatography (5% ethyl acetate/hexane) to give **145** as a pale yellow oil (2.0 g, 85 %, 98% pure by GC.). R_f (10% ethyl acetate/hexane) 0.32, δ_H (300MHz, $CDCl_3$) 5.77-5.63 (2H, m, H-2 and H-9), 5.42 (1H, s, H-6), 5.35 (2H, dd, *J* 9.6, *J* 6.0, H-1), 4.98-4.91 (3H, m, H-3 and H-10), 4.05-3.94 (2H, m, OCH_2O), 3.79 (2H, dd, *J* 9.4, *J* 4.8, OCH_2CH_2O), 3.52 (2H, dd, *J* 9.4, *J* 4.8, OCH_2CH_2O), 3.33 (6H, s, 2 x OCH_3), 2.10 (2H, d, *J* 7.31, H-8), 1.07 (3H, s, CH_3), 1.06 (3H, s, CH_3); δ_C (75.5 MHz, $CDCl_3$) 143.6 (t, $^2J_{C\text{-}F}$ 24.9), 135.4, 130.9, 128.3, 121.2, 118.3 (t, $^1J_{C\text{-}F}$ 252.0), 117.2, 98.2 (t, $^2J_{C\text{-}F}$ 32.4), 81.6, 77.1, 71.6, 69.0, 59.0, 57.9, 47.6, 35.1, 27.9; δ_F (282 MHz, $CDCl_3$) –107.8 (dd, $^2J_{F\text{-}F}$ 254.9, $^3J_{H\text{-}F}$ 9.0), -112.5 (dd, $^2J_{F\text{-}F}$ 254.9, $^3J_{H\text{-}F}$ 14.2), [HRMS (ES, $[M]^+$) found: 334.1955. Calc for $C_{17}H_{28}F_2O_4$ 334.1956]; LRMS (ES) *m/z* 352 $[M+NH_4]^+$ (30%), 89 [MEM^+] (100%).

Preparation of 3-(benzyloxy)-4,4-difluoro-5-[(2-methoxyethoxy)methoxy]-7,7-dimethyldeca-1,5Z,9-triene [146]

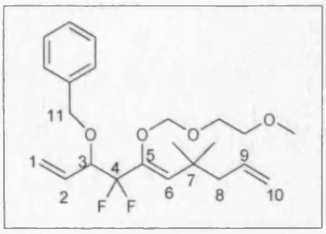

Sodium hydride (0.4 g, 16.3 mmol of a 60% suspension with oil) was washed three times with petroleum ether (3 x 20 mL). Dry THF (30 mL) was added, followed by **21** (1.0 g, 3.3 mmol). Benzyl bromide (1.1 equivalents, 0.40 mL, 3.63 mmol) was added slowly, followed by TBAI (0.15 g, 0.41 mmol) and the mixture stirred at 0°C under nitrogen for 4 hours. The reaction was quenched carefully with water (25 mL) and diluted with diethyl ether (25 mL), and the aqueous solution extracted with diethyl ether (3 x 20 mL). The combined organic extracts and the original organic Phase were washed with brine (25 mL) and dried ($MgSO_4$) and concentrated *in vacuo* to leave **146** as a dark orange oil (89%, 1.2 g) which was purified by flash column chromatographyon silica gel (10% ethyl acetate/hexane). 99% pure by GC; R_f (10% Ethyl acetate/hexane) 0.40; δ_H (300 MHz, $CDCl_3$) 7.37-7.28 (5H, m, Ph-H), 5.93-5.71 (2H, m, H-2 and H-9), 5.49 (1H, br s, H-1a and H-6), 5.44 (1H, dd, *J* 8.7, ^2J 2.5, H-1b), 5.04 (1H, ddt, *J* 10.6, ^2J 2.5, ^4J 1.1, H10a), 5.00-4.95 (3H, m, H-10b and OCH_2O), 4.70 (1H, ½ AB q, ^2J 11.9, OCH_aH_bPh-H), 4.55 (1H, ½ AB q, ^2J 11.9, OCH_aH_bPh-H), 4.29 (1H, ddd, $^3J_{H\text{-}F}$ 14.8, $^3J_{H\text{-}F}$ 8.2, *J* 7.5, H-3), 3.71 (2H, td, *J* 4.5, ^2J 2.5 OCH_2CH_2O), 3.52 (2H, td, *J* 4.5, ^2J 3.2, OCH_2CH_2O), 3.38 (3H, s, OCH_3), 2.18 (2H, dt, *J* 7.5, ^4J 1.1, H-8), 1.16 (6H, s, 2 x CH_3); δ_C (75.5 MHz, $CDCl_3$) 143.6 (t, $^2J_{C\text{-}F}$ 25.1), 137.6, 135.3, 131.2, 128.3, 128.2, 128.1, 127.9, 127.7, 121.5, 118.3 (t, $^1J_{C\text{-}F}$ 253.1), 117.2, 98.2, 78.9 (t, $^2J_{C\text{-}F}$ 31.7), 71.6, 71.3, 68.8, 59.0, 47.7, 35.0, 27.9, 27.8; δ_F (282 MHz, $CDCl_3$) -106.2 (dd, $^2J_{F\text{-}F}$ 255.4, $^3J_{H\text{-}F}$ 8.2), -113.1 (dd, $^2J_{F\text{-}F}$ 255.4, $^3J_{H\text{-}F}$ 14.8; [HRMS (EI, $[M]^+$) found: 410.22691. Calc for $C_{23}H_{32}F_2O_4$ 410.22687]; LRMS (ES) *m/z* 433 $[M+Na]^+$ (5%), 242 (100%).

Preparation of 3-(benzoyloxy)-4,4-difluoro-5-[(2-methoxyethoxy)methoxy]-7,7-dimethyldeca-1,5-(Z),9-triene [147]

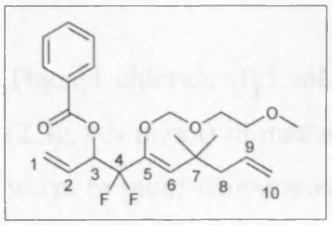

DMAP (0.2 equivalents, 0.10 g, 0.83 mmol), benzoic anhydride (0.74 g, 3.30 mmol) and PVP (1.7 g, 1.70 mmol) were added to a solution of **21** (1.0 g, 3.30 mmol) in CH_2Cl_2 (33 mL), and the mixture swirled at room temperature overnight. The solids were filtered off and washed with a saturated solution of $NaHCO_3$ (20 mL). The aqueous layer was extracted with diethyl ether (3 x 20 mL) and the combined organic extracts washed with brine (20 mL), dried ($MgSO_4$) and concentrated *in vacuo*. The product was purified with flash column chromatographyon silica (10% ethyl acetate/hexane) to yield **147** as a pale yellow oil (98%, 1.4 g). R_f (10% Ethyl acetate/hexane) 0.48; δ_H (75.5 MHz, $CDCl_3$) 6.03-5.83 (2H, m, H-2 and H-9), 5.57 (1H, ddt, $^3J_{H\text{-}F}$ 13.7, $^3J_{H\text{-}F}$ 9.5, *J* 7.5, H-3), 5.46 (1H, dd, *J* 16.1, ^2J 2.0, H-1a), 5.42 (1H, s, H-6), 5.36 (1H, dd, *J* 9.2, ^2J 2.1, H-1b), 4.93 (2H, s, OCH_2O), 4.91-4.81 (2H, m, H-10), 3.53 (2H, t, *J* 4.7, OCH_2CH_2O), 3.32 (3H, s, OCH_3), 2.03 (2H, d, *J* 7.3, H-8), 1.00 (3H, s, CH_3), 0.98 (3H, s, CH_3); δ_C (75.5 MHz, $CDCl_3$) 164.7, 143.1 (t, $^2J_{C\text{-}F}$ 23.9), 135.0, 133.4, 129.9, 129.5, 128.9, 128.4, 128.3, 121.3, 117.5 (t, $^1J_{C\text{-}F}$ 253.1), 117.3, 98.5, 72.8 (t, $^2J_{C\text{-}F}$ 32.3), 71.6, 69.0, 59.0, 47.4, 35.0, 27.8, 27.7; δ_F (282 MHz, $CDCl_3$) -108.1 (dd, $^2J_{F\text{-}F}$ 254.5, $^3J_{H\text{-}F}$ 9.5), -111.3 (dd, $^2J_{F\text{-}F}$ 254.5, $^3J_{H\text{-}F}$ 13.7); [HRMS (ES, $[M+NH_4]^+$) found: 443.2477. Calc for $C_{23}H_{30}F_2O_5NH_4$ 443.2484]; LRMS (ES) *m/z* 443 $[M+NH_4]^+$ (100%), 349 [M-(Ph-HMe)]$^+$ (65%), 89 $[MEM]^+$; 97% pure by GC.

Preparation of 4,4-Difluoro-3-methoxy-7,7-dimethyl-deca-1,9-dien-5-one [148]

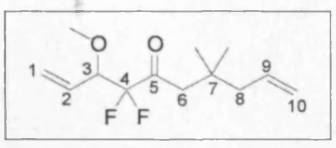

Thionyl chloride (0.5 mL, 6.9 mmol) was added dropwise to a solution of **145** (2.3g, 6.9 mmol) in methanol (70 mL) at 0°C. The stirred solution was allowed to warm to room temperature overnight. The resulting solution was concentrated *in vacuo* to give an orange oil which was diluted with water (20 mL) and diethyl ether (25 mL). The aqueous layer was extracted with diethyl ether (3 x 25 mL). The combined organic extracts were washed with brine (15 mL) and dried ($MgSO_4$) and concentrated *in vacuo* to yield an orange oil which was purified by flash column chromatography(10% ethyl acetate hexane) to yield **148** as a pale orange oil (1.6 g, 94 %, 99% pure by GC). R_f (10% ethyl acetate/hexane) 0.23; δ_H (300 MHz, $CDCl_3$) 5.78-5.64 (2H, m, H-2 and H-9), 5.44 (1H, dd, *J* 9.4, ^2J 2.4, H-1a), 5.34 (1H, dd, *J* 15.8, ^2J 2.4, H-1b), 4.97 (2H, dd, *J* 10.2, ^4J 2.3, H-10), 3.95 (1H, ddd, $^3J_{H-F}$ 24.4, $^3J_{H-F}$ 17.1, *J* 12.8, H-3), 3.23 (3H, s, OMe), 2.51 (2H, s, H-6), 2.07 (2H, d, *J* 7.6, H-8), 0.96 (6H, s, 2 x Me); δ_F (282 MHz, $CDCl_3$) –111.4 (d, $^2J_{F-F}$ 263.9), -124.5 (dd, $^2J_{F-F}$ 263.9, $^3J_{H-F}$ 17.1); δ_C (75.4 MHz $CDCl_3$) 201.0 (t, $^2J_{C-F}$ 30.5), 134.7, 129.4, 122.9, 117.3, 114.5, 111.0 (t, $^1J_{C-F}$ 254.9), 81.6 (t, $^2J_{C-F}$ 30.5), 57.4, 47.4, 46.0, 33.4, 26.9; LRMS (EI^+) m/z 231 [$M-CH_3^+$] (10%), 141 (100).

Preparation of 3-(benzyloxy)-4,4-difluoro-7,7-dimethyldeca-1,9-dien-5-one [149]

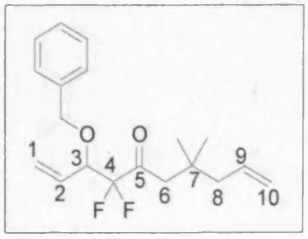

146 (1.2 g, 2.9 mmol) was dissolved in methanol (29 mL) and thionyl chloride (0.21 mL, 2.9 mmol) was added dropwise at 0°C. The solution was stirred overnight, and allowed to warm to room temperature. The solution was concentrated *in vacuo* and the residue taken up in water (20mL). This suspension was extracted with diethyl ether (3 x 20 mL) and the combined organic extracts were washed with brine (10 mL) and dried ($MgSO_4$) and the solvent removed *in vacuo*. The resulting brown oil **149** (0.84g, 89%, 99% pure by GC), was used without further purification. R_f (10% Ethyl acetate/hexane) 0.33; δ_H (300 MHz, $CDCl_3$) 7.28-7.15 (5H, m, Ph-H), 5.82-5.57 (2H, m, H-2 and H-9), 5.45-5.35 (2H, m, H-1), 4.96 (1H, ddt, *J* 16.2, ^2J 2.3, ^4J 1.4, H-10a), 4.89 (1H, ddt, *J* 10.5, ^2J 2.3, ^4J 0.9, H-10b), 4.53 (1H, ½ AB q, ^2J 11.4, OCH_aH_bPh-H), 4.30 (1H, ½ AB q, ^2J 11.4, OCH_aH_bPh-H), 4.18 (1H, ddd, $^3J_{H\text{-}F}$ 16.1, *J* 14.1, $^3J_{H\text{-}F}$ 7.6, H-3), 2.50 (1H, d, ^2J 2.0, H-6a), 2.48 (1H, d, ^2J 2.0, H-6b), 2.02 (2H, ddd, *J* 7.5, ^4J 1.4, ^4J 0.9, H-8), 1.02 (3H, s, CH_3), 0.96 (3H, s, CH_3); δ_C (75.5 MHz, $CDCl_3$) 198.9 (t, $^2J_{C\text{-}F}$ 29.3), 164.3, 134.4, 133.7, 129.9, 129.6, 128.9, 128.6, 122.7, 117.8, 113.8 (t, $^1J_{C\text{-}F}$ 262.7), 72.2 (t, $^2J_{C\text{-}F}$ 30.5), 46.7, 46.0, 33.5, 26.9, 26.8; δ_F (282 MHz, $CDCl_3$) -110.7 (d, $^2J_{F\text{-}F}$ 262.5), -123.6 (dd, $^2J_{F\text{-}F}$ 262.5, $^3J_{H\text{-}F}$16.1); [HRMS (ES, $[M+NH_4]^+$) found: 340.2082. Calc for $C_{19}H_{24}F_2O_2NH_4$ 340.2088]. LRMS (ES) *m/z* 340 $[M+NH_4]^+$ (100%), 216 (30).

Preparation of 3-Benzyloxy-4,4-difluoro-7,7-dimethyl-deca-1,9-dien-5-one [150]

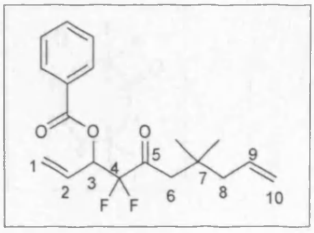

Thionyl chloride (0.27 mL, 3.6 mmol) was added dropwise to a solution of **147** (1.4 g, 3.3 mmol), in methanol (33 mL) at 0°C and stirred overnight, allowing to warm to room temperature. The solution was concentrated *in vacuo* and diluted with water (15 mL), then the solution was extracted with diethyl ether (3 x 20 mL) and the combined organic extracts washed with brine (15 mL), dried ($MgSO_4$) and concentrated *in vacuo* to yield **150** as a brown oil (0.90g, 82%); 99% pure by GC; R_f (10% Ethyl acetate/hexane) 0.41; Found: C, 67.68; H, 6.57. $C_{19}H_{22}F_2O_3$ requires C, 67.84; H, 6.59; δ_H (300 MHz, $CDCl_3$) 7.97 (2H, dd, *J* 8.5, ^4J 2.0, *ortho*-Ph-H), 7.52 (1H, tt, *J* 7.5, ^4J 2.0, *para*-Ph-H), 7.38 (td, *J* 8.5, *J* 7.5, *meta*-Ph-H), 5.96-5.80 (2H, m, H-2 and H-9), 5.63 (1H, ddt, $^3J_{H\text{-}F}$ 14.2, $^3J_{H\text{-}F}$ 10.4, *J* 7.5, H-3), 5.49 (1H, dd, *J* 16.2, ^2J 1.0, H-1a), 5.42 (1H, dd, *J* 9.4, ^2J 1.0, H-1b), 4.94-4.85 (2H, m, H-10), 2.53 (2H, s, H-6), 2.03 (2H, d, *J* 7.6, H-8), 0.91 (6H, s, 2 x CH_3); δ_C (75.5 MHz, $CDCl_3$) 198.6 (t, $^2J_{C\text{-}F}$ 29.3), 164.3, 134.4, 133.7, 129.9, 129.6, 128.9, 128.6, 122.7, 117.8, 113.8 ($^1J_{C\text{-}F}$ 256.7), 72.2 (t, $^2J_{C\text{-}F}$ 30.5), 47.0, 46.0, 33.5, 26.9, 26.8; δ_F (282 MHz, $CDCl_3$) -113.5 (dd, $^2J_{F\text{-}F}$ 273.9, $^3J_{H\text{-}F}$ 9.0), -118.9 (dd, $^2J_{F\text{-}F}$ 273.9, $^3J_{H\text{-}F}$ 14.2); [HRMS (ES, $[M+NH_4]^+$) found: 354.1877. Calc for $C_{19}H_{22}F_2O_3NH_4$ 354.1881]; LRMS (ES) 354 $[M+NH_4^+]$ 354 (100%), 214 (30%).

Synthesis of 2,2-Difluoro-3-methoxy-7,7-dimethyl-cyclooct-4-enone [151]

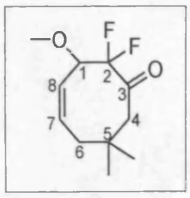

Titanium isopropoxide (88 μL, 0.3 mmol) was added to a solution of diene **148** (0.25 g, 1.0 mmol) in dry, degassed CH_2Cl_2 (100 mL, 0.01 M), and the solution refluxed for thirty minutes under nitrogen. Grubbs' second generation catalyst (17 mg, 0.02 mmol, 2 mol %) was added to this solution, and the solution refluxed under nitrogen overnight. After cooling, the solution was concentrated *in vacuo* and purified using a Polymer Labs Evalution Thiol SPE cartridge preconditioned with methanol (1mL), eluting with methanol (1 mL). The resulting solution was concentrated *in vacuo* to yield **151** as a white solid (0.15 g, 69 %). R_f (10% Ethyl acetate/hexane) 0.10. mp 89-93 °C. δ_H (400 MHz, 218 K, $CDCl_3$) major conformer 6.01 (1H, br d, *J* 8.9, H-7), 5.56-5.48 (1H, br m, H-8), 4.78 (1H, br d, $^3J_{H-F}$ 19.7, H-1), 3.51 (3H, s, OMe), 2.85 (1H, br d, *J* 12.1, H-4a), 2.33 (1H, br d, *J* 20.9, H-6a), 2.15 (1H, br d, *J* 12.1, H-4b), 2.06 (br d, *J* 20.9, H-6b), 1.13 (3H, s, CH_3), 0.98 (3H, s, CH_3), minor conformer 6.11-6.03 (1H, br m, H-7), 5.66-5.59 (1H, br m, H-8), 4.11-4.01 (br m, H-1), 3.74 (3H, s, OMe), 2.93 (1H, br d, *J* 8.9, H-4a), 1.90 (1H, br d, *J* 12.3, H-6a), 1.87-1.81 (1H, br m, H-4b), 1.67 (1H, br d, 12.3, H-6b), 1.19 (3H, s, CH_3); δ_C (100.6 MHz, 218 K, $CDCl_3$) major conformer 196.8 (t, $^2J_{C-F}$ 27.1), 136.4, 128.2, 116.4 (dd $^1J_{C-F}$ 260.4, $^1J_{C-F}$ 262.0), 74.6 (dd, $^2J_{C-F}$ 22.4, $^2J_{C-F}$ 23.2), 58.4, 49.6, 41.6 (d, $^1J_{C-H}$ 54.3), 33.5, 25.7, 24.1, minor conformer 201.1, 131.5, 129.2, 123.3 (dd $^1J_{C-F}$ 260.4, $^1J_{C-F}$ 247.5), 76.3 (dd, $^2J_{C-F}$ 24.0, $^2J_{C-F}$ 22.4), 66.3, 59.7, 45.7, 39.2, 29.4, 28.5; δ_F (376.5 MHz, 218 K, $CDCl_3$) major conformer –106.6 (d, $^2J_{F-F}$ 240.2), -134.3 (dd, $^2J_{F-F}$ 240.2, $^3J_{H-F}$ 19.7), minor conformer –115.9 (d, $^2J_{F-F}$ 228.7), -126.2 (dd, $^2J_{F-F}$ 228.7, $^3J_{H-F}$ 26.4). No mass spectral data could be obtained for this compound.

Preparation of (7Z)-1-(benzyloxy)-2,2-difluoro-5,5-dimethylcyclooct-7-en-3-one [152]

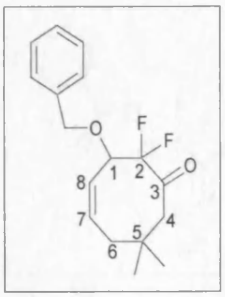

Titanium *iso*propoxide (55 μl, 0.19 mmol) was added to a solution of **152** (0.2 g, 0.62 mmol) in dry, freshly degassed CH_2Cl_2 (62 mL) under an atmosphere of nitrogen and the mixture refluxed for 30 minute before adding a solution of Grubbs' second generation catalyst **29** (11 mg, 31 μmol) in CH_2Cl_2 (0.5 mL), thenrefluxed overnight. The solution was concentrated *in vacuo* and the resulting brown oil purified by elution with methanol (1mL) through a Polymer Labs Evalution Thiol SPE cartridge, preconditioned with methanol (1mL), to yield **152** as a white solid (0.11 g, 60%, 99% pure by GC.). mp 52-55 °C. R_f (10% Ethyl acetate/hexane) 0.25; Found: C, 69.43; H, 6.74. $C_{17}H_{20}F_2O_2$ requires C, 69.37; H, 6.85; δ_H (300 MHz, $CDCl_3$, 300 K) 7.30-7.27 (5H, m, Ph-H), 5.88 (1H, ddd, *J* 19.0, *J* 10.8, *J* 9.4 , H-7), 5.60 (1H, br dd, *J* 10.8, *J* 7.7, H-8), 4.67 (1H, ½ AB a, ^2J 12.0, OCH_2H_bPh-H), 4.63 (1H, ½ AB q, ^2J 12.0, OCH_aH_bPh-H), 4.51 (1H, br dd, $^3J_{H\text{-}F}$ 24.7, *J* 7.7, H-1), 4.39 (1H br ½ AB q, ^2J 12.2, H-4a), 4.30 (1H, br ½ AB q, ^2J 12.2, H-4b), 1.91 (2H, dd, *J* 19.0, *J* 7.7, H-6), 1.02 (3H, s, CH_3), 0.96 (3H, s, CH_3); δ_C (75.5 MHz, $CDCl_3$, 300 K) 200.8 (t, $^2J_{C\text{-}F}$ 25.7), 137.0, 134.8, 130.7, 128.5, 128.4, 128.0, 127.9, 127.8, 117.7, 117.3 (t, $^1J_{C\text{-}F}$ 260.9), 73.2 (t, $^2J_{C\text{-}F}$ 20.3), 72.2, 40.2, 20.6, 20.1; δ_F (376 MHz, $CDCl_3$, 218 K) major conformer -106.5 (d, $^2J_{F\text{-}F}$ 241.5), -134.0 (dd, $^2J_{F\text{-}F}$ 241.6, $^3J_{H\text{-}F}$ 20.1), minor conformer -115.3 (d, $^2J_{F\text{-}F}$ 230.2), -125.7 (dd, $^2J_{F\text{-}F}$ 230.2, $^3J_{H\text{-}F}$ 27.0); [HRMS (ES, $[M+NH_4]^+$) found: 312.1771. Calc for $C_{17}H_{20}F_2O_2NH_4$ 312.1775]; LRMS (ES) *m/z* 295 $[M+H]^+$ (10%), 307 (100).

Preparation of 1-benzoyl-2,2,difluoro-5,5-dimethyl-cyclooct-7-en-3-one [153]

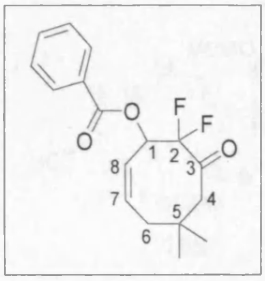

Titanium isopropoxide (52.8 μL, 0.2 mmol) was added to a solution of **150** (0.2 g, 0.6 mmol) in dry degassed CH_2Cl_2 (60 mL, 0.01 M) under nitrogen. Then the solution refluxed under nitrogen for 30 minutes. Grubbs' second generation catalyst **29** (25 mg, 0.03 mmol, 5% mol) was added in 0.5 mL dry CH_2Cl_2 and the solution refluxed under nitrogen overnight. After this time, the solution was concentrated *in vacuo* to yield a brown oil which was purified by flash column chromatographyon silica (10% EtOAc/hexane) to yield **153** as an off-white solid, (0.14 g, 76%) mp 80-82°C. An elementally pure sample was obtained by eluting the columned product with 1 mL methanol through Polymer Labs MP-Thiol SPE tubes preconditioned with methanol. R_f (5% EtOAc/hexane) 0.22. Found; C, 66.15; H, 5.89. $C_{17}H_{18}F_2O_3$ requires C, 66.22; H, 5.88. δ_H (400 MHz, $CDCl_3$, 323 K) 8.14 (2H, dd, *J* 8.4, ^4J 1.3, *ortho*-Ph-H), 7.62 (1H, tt, *J* 7.6, ^4J 1.3, *para*-Ph-H), 7.49 (2h, tt, *J* 8.4, *J* 7.6, *meta*-Ph-H), 6.29 (1H, br dd, $^3J_{H\text{-}F}$ 24.3, *J* 7.1, H-1), 6.03 (1H, ddd, *J* 9.6, *J* 9.4, *J* 7.8, H-7), 5.73 (1H, apparent dt, *J* 9.4, *J* 7.1, H-8), 2.67 (1H, br d, *J* 11.8, H-4a), 2.50 (1H, br d, *J* 11.8, H-4b), 2.32 (1H, br dd, ^2J 13.6, *J* 9.6, H-6a), 2.15 (1H, dd, ^2J 13.6, *J* 7.8, H-6b), 1.22 (3H, s, CH_3), 1.11 (3H, s, CH_3); δ_C (100 MHz, $CDCl_3$, 212 K) 209.2, 168.5 (t, $^2J_{C\text{-}F}$ 23.5), 134.8, 134.2, 130.6, 129.6, 129.0, 126.5, 113.2 (t, $^1J_{C\text{-}F}$ 234.4), 79.6 (t, $^2J_{C\text{-}F}$ 29.4), 68.7, 48.8, 41.0, 26.8, 26.7; δ_F (376 MHz, $CDCl_3$, 212 K) major conformer -106.7 (d, $^2J_{F\text{-}F}$ 242.2), -132.6 (dd, $^2J_{F\text{-}F}$ 242.2, $^3J_{H\text{-}F}$ 21.1), minor conformer -114.5 (d, $^2J_{F\text{-}F}$ 230.2), -124.0 (dd, $^2J_{F\text{-}F}$ 230.2, $^3J_{H\text{-}F}$ 27.1); [HRMS (ES, $[M+NH_4]^+$) found: 326.156. Calc for $C_{17}H_{18}F_2O_3NH_4$ 326.156]; LRMS (ES) *m/z* 326 $[M+NH_4^+]$ (15%), 297 (100)

Crystallographic data for **153** are located on CD in section **10**.

Preparation of (3*Z*,11*Z*,7*E*,15*E*)-2,2,10,10-tetrafluoro-3,11-di(methoxyethoxymethoxy)cyclohexadeca-3,7,11,15-tetraene-1,9-diols [169] and [170]

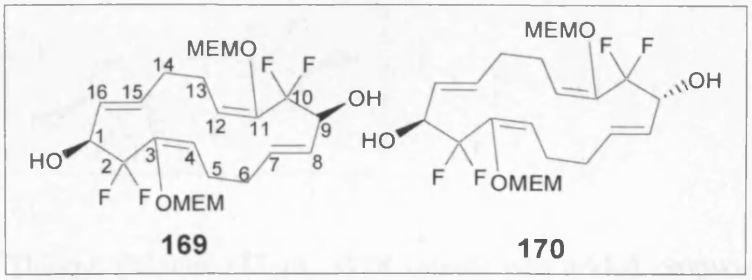

Grubbs' second generation catalyst **29** (29 mg, 5%) was added to a solution of alcohol **5** (0.2 g, 0.68 mmol) in dry, degassed CH_2Cl_2 (68 mL) under nitrogen, and the solution refluxed for 24 hours before adding a further portion of the catalyst (29 mg, 5%) and stirring at reflux for a further 24 hours. The solution was concentrated *in vacuo* and purified by column chromatography (80% ethyl acetate/hexane) to give **169** and **170** as white solids (total 98 mg, 55 %). C_2 symmetric 16 ring **169**: R_f (80% Ethyl acetate/hexane) 0.45; δ_H (400 MHz, 300K, $CDCl_3$) 5.85 (2H, ddd, *J* 15.3, *J* 7.8, *J* 6.3, H-7 and H-15), 5.53 (2H, t, *J* 7.0, H-4 and H-12), 5.43 (2H, dd, *J* 15.3, *J* 5.7, H-8 and H-16), 5.02 (4H, s, OCH_2O), 4.51 (2H, br d, $^3J_{H\text{-}F}$ 18.9, H-1 and H-9), 3.93-3.83 (4H, m, OCH_2CH_2O), 3.60 (4H, t, *J* 4.7, OCH_2CH_2O), 3.41 (6H, s, OCH_3), 2.48-2.30 (10H, m, H-5 and H-13, H-6 and H-14 and 2 x OH); δ_C (100 MHz, 300K, $CDCl_3$) 144.7 (t, $^2J_{C\text{-}F}$ 24.8), 133.3, 126.2, 119.9, 118.0 (t, $^1J_{C\text{-}F}$ 243.7), 98.4, 73.0 (t, $^2J_{C\text{-}F}$ 35.1), 71.6, 69.0, 59.1, 31.6, 23.2; δ_F (282 MHz, 300K, $CDCl_3$) -108.1 (d, $^2J_{F\text{-}F}$ 245.5), -117.7 (br d, $^2J_{F\text{-}F}$ 245.5); [HRMS ES $[M+NH_4]^+$ found 546.2685 calc for $C_{24}H_{36}O_8F_4$ 528.23.

Achiral/*meso* 16 ring **170**: R_f (80% ethyl acetate/hexane) 0.42; δ_H (300 MHz, $CDCl_3$); 5.75 (2H, dd, *J* 15.5, *J* 8.2, *J* 7.0, H-7 and H-15), 5.44 (2H, t, *J* 7.0, H-4 and H-12), 5.33 (2H, ddd, *J* 15.5, *J* 7.0, ^4J 1.2, H-8 and H-16), 4.93 (4H, s, OCH_2O), 4.41 (2H, br dd, $^3J_{H\text{-}F}$ 19.5, *J* 7.0, H-1 and H-9), 3.80 (4H, dd, ^2J 7.7, *J* 4.3, OCH_2CH_2O), 3.51 (4H, t, *J* 4.3, OCH_2CH_2O), 3.32 (6H, s, OCH_3), 2.34-2.19 (4H, br m, H-6 and H-14), 2.14 (4H, t, *J* 6.14, H-5 and H-13), 1.80 (2H, br s, 2 x OH); δ_C (100 MHz, 300K, $CDCl_3$) 140.6, 133.9, 126.2, 119.7, 98.6, 73.6 (t, $^3J_{C\text{-}F}$ 32.8), 71.8, 69.1, 59.1, 31.9, 23.2; δ_F (282 MHz, 300K, $CDCl_3$)-107.1 (d, $^2J_{F\text{-}F}$ 246.9), -116.4 (br d, $^2J_{F\text{-}F}$ 246.9);

Preparation of (1*S*,7*E*,9*S*,15*E*)-2,2,10,10-tetrafluoro-1,9- dihydroxy-cyclohexadeca-7,15-diene-3,11-dione [171]

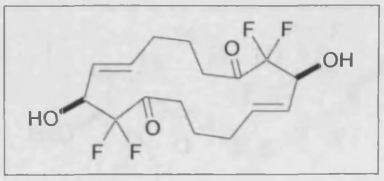

Thionyl chloride (12 μL, 0.18 mmol) was added dropwise over ten minutes to a solution of **169** (48 mg, 0.09 mmol) in methanol (1 mL) at 0°C and the solution was stirred overnight and allowed to warm to room temperature. The solution was concentrated *in vacuo* and diluted with water (15 mL) and extracted with diethyl ether (3 x 15 mL). The combined organic extracts were washed with brine (10 mL), dried ($MgSO_4$) and concentrated *in vacuo* to yield **171** as an oily yellow solid (17 mg, 53 %). R_f (20% Petroleum ether/CH_2Cl_2) 0.13; δ_F (282 MHz, $CDCl_3$) -107.8 (br d, $^2J_{F\text{-}F}$ 253.0), -126.2 (br d, $^2J_{F\text{-}F}$ 253.0). The material was used without purification and further characterisation.

Preparation of (1*R*,7*E*,9*S*,15*E*)-2,2,10,10-tetrafluoro-1,9-dihydroxy-cyclohexadeca-7,15-diene-3,11-dione [172]

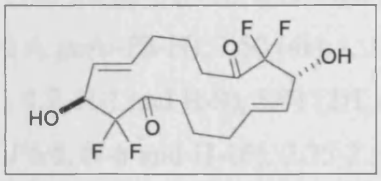

Thionyl chloride (15 μL, 0.2 mmol) was added dropwise over ten minutes to a solution of **170** (50 mg, 0.10 mmol) in methanol (2 mL) at 0°C and the solution stirred overnight, warming to room temperature. The solution was concentrated *in vacuo* and diluted with water (15 mL) and extracted with diethyl ether (3 x 15 mL). The combined organic extracts were washed with brine (10 mL), dried ($MgSO_4$) and concentrated *in vacuo* to yield **172** as an off white oily solid (20 mg, 61%). R_f 60% Ethyl acetate/hexane 0.33; δ_F (376 MHz, $CDCl_3$) -111.9 (dd, $^2J_{F\text{-}F}$ 265.0, $^3J_{H\text{-}F}$ 5.2), -122.1 (dd, $^2J_{F\text{-}F}$ 265.0, $^3J_{H\text{-}F}$ 17.8). The material was used without purification and further characterisation.

Preparation of (1*S*,7*E*,9*S*,15*E*)-2,2,10,10-tetrafluoro-1,9- dibenzoyloxy-cyclohexadeca-7,15-diene-3,11-dione [173]

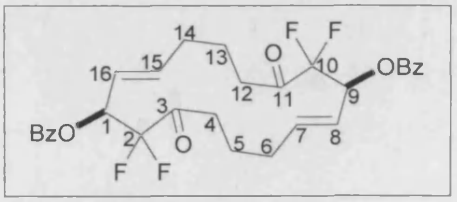

Benzoic anhydride (41mg, 0.18 mmol) and DMAP (3.0 mg, 0.036 mmol, 0.2 equivalents) were added to a solution of **171** (60 mg, 0.18 mmol) in CH_2Cl_2 (1.8 mL). PVP (0.18 g, 0.18 mmol) was added and the solutions swirled gently at room temperature overnight. After this time the solids were filtered off and washed with aqueous sodium hydrogencarbonate (20 mL of a saturated solution) and CH_2Cl_2 (20 mL). The aqueous layer was extracted with CH_2Cl_2 (3 x 20 mL). Combined organic extracts were washed with brine (15 mL) and dried ($MgSO_4$) before concentrating in vacuo to give a pale brown solid. Residual benzoic acid was removed by passing a solution of **173** in CH_2Cl_2 (1 mL) through a Supelco DSC-NH_2 SPE tube preconditioned with CH_2Cl_2 (3 mL), eluting with CH_2Cl_2 (1 mL), to obtain **173** as a white solid (59 mg, 49%). Crystals of **173** were grown by vapour diffusion (ethyl acetate/hexane). R_f (10% DCM/hexane) 0.19; mp 137-139°C; δ_H (400 MHz, $CDCl_3$) 8.12 (4H, dd, *J* 8.6, ^4J 1.4, *ortho*-Ph-H), 7.63 (2H, tt, *J* 7.7, ^4J 1.4, *para*-Ph-H), 7.50 (4H, t, *J* 7.7, *meta*-Ph-H), 6.09 (2H, ddd, $^3J_{H\text{-}F}$ 20.1, *J* 6.8, $^3J_{H\text{-}F}$ 4.7, H-1 and H-9), 5.91 (2H, dt, *J* 15.7, *J* 7.2, H-7 and H-15), 5.46 (2H, dd, *J* 15.7, *J* 6.8, H-8 and H-16), 2.75-2.56 (4H, m, H-6 and H-14), 2.34 (2H, dt, 15.4, ^2J 6.7, H-4a and H-12a), 2.15 (2H, dt, *J* 14.1, ^2J 6.7, H-4b and H-12b), 1.78 (2H, dt, *J* 14.1, *J* 7.1, H-5 and H-13); δ_C (100 MHz, $CDCl_3$) 200.0 (t, $^2J_{C\text{-}F}$ 32.8), 164.8, 137.9, 133.6, 129.9, 129.2, 128.5, 127.9, 121.9, 114.6 (t, $^1J_{C\text{-}F}$ 262.0), 71.6 (t, $^2J_{C\text{-}F}$ 24.8), 35.8, 30.2; δ_F (282 MHz, $CDCl_3$) -108.9 (dd, $^2J_{F\text{-}F}$ 264.9, $^3J_{H\text{-}F}$ 4.7), -125.0 (dd, $^2J_{F\text{-}F}$ 264.9, $^3J_{H\text{-}F}$ 20.1); [HRMS (CI, $[M+NH_4]^+$) found 578.2162. Calc for $C_{30}H_{28}F_4O_6NH_4$: 578.2160].

Crystallographic data are located on CD in **10**.

Preparation of (1*R*,7*E*,9*S*,15*E*)-2,2,10,10-tetrafluoro-1,9-dibenzoyloxy-cyclohexadeca-7,15-diene-3,11-dione [174]

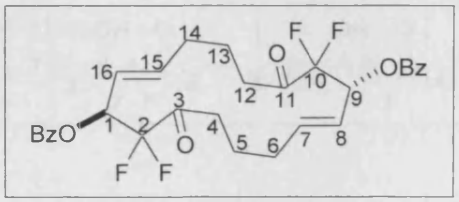

Benzoic anhydride (27 mg, 0.12 mmol) and DMAP (1.5 mg, 0.024 mmol, 0.2 equivalents) were added to a solution of **172** (40 mg, 0.12 mmol) in CH_2Cl_2 (2.5 mL). PVP (0.12 g, 0.12 mmol) was added and the solutions swirled gently at room temperature overnight. After this time the solids were filtered off and washed with aqueous sodium hydrogencarbonate (20 mL of a saturated solution) and CH_2Cl_2 (20 mL). The aqueous layer was extracted with CH_2Cl_2 (3 x 20 mL). Combined organic extracts were washed with brine (15 mL) and dried ($MgSO_4$) before concentrating in vacuo to give a pale brown solid. Residual benzoic acid was removed by passing a solution of **174** in CH_2Cl_2 (1 mL) through a Supelco DSC-NH_2 SPE tube preconditioned with CH_2Cl_2 (3 mL), eluting with CH_2Cl_2 (1 mL), to obtain **174** as an off-white solid (42 mg, 63%). R_f (10% CH_2Cl_2/hexane) 0.26. mp 133-136°C. δ_H (400 MHz, $CDCl_3$) 8.11 (4H, dd, *J* 7.3, ^4J 1.4, *ortho*-Ph-H), 7.63 (2H, t, *J* 7.3, *para*-Ph-H), 7.51 (4H, t, *J* 7.3, *meta*-Ph-H), 6.05-5.92 (4H, m, H-7 and H-15, H-1 and H-9), 5.52 (2H, dd, *J* 15.9, *J* 7.4, H-8 and H-16), 2.66 (4H, dd, *J* 12.1, *J* 7.3, H-4 and H-12), 2.27 (4H, dd, *J* 13.5, *J* 7.3, H-6 and H-14), 1.87-1.72 (4H, m, H-5 and H-13); δ_C (100 MHz, $CDCl_3$) 199.9 (t, $^2J_{C\text{-}F}$ 29.5), 164.5, 137.5, 133.9, 130.7, 130.0, 129.1, 128.8, 122.9, 114.3 (t, $^1J_{C\text{-}F}$ 260.9), 72.6 (t, $^2J_{C\text{-}F}$ 29.5), 36.9, 32.8, 21.7; δ_F (376 MHz, $CDCl_3$) –109.9 (dd, $^2J_{F\text{-}F}$ 265.0, $^3J_{H\text{-}F}$ 4.6), -121.7 (dd, $^2J_{F\text{-}F}$ 265.0, $^3J_{H\text{-}F}$ 18.4) [HRMS (CI, $[M+NH_4]^+$) found 578.2162. Calc for $C_{30}H_{28}F_4O_6NH_4$: 578.2160].

Preparation of (9*E*)-4,4,12,12-tetrafluoro-3,11-dihydroxyoctadeca-1,9,17-triene-5,13-dione [175]

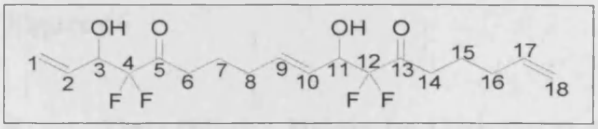

Alcohol **4** (0.15 g, 0.72 mmol) and titanium isopropoxide (59 μL, 0.22 mmol) were dissolved in a dry, degassed CH_2Cl_2 (18.3 mL, 0.04 M) and refluxed for 30 minutes under nitrogen before adding Grubbs' II **29** (31.2 mg, 5 mole %) and refluxing overnight. After this time, the solution was concentrated *in vacuo* and dried under high vacuum to remove any traces of **4**. **175** was isolated as two isomers, one major and one minor, which were inseparable by column chromatography, but evidence for which was obtained through separation by reverse phase HPLC. R_f (5% MeOH/ CH_2Cl_2) 0.34; δ_H (400 MHz, $CDCl_3$) 5.99-5.72 (3H, m, H-2, H-9 and H-17), 5.52 (1H, dd, *J* 17.4, *J* 2.8, H-10), 5.45 (2H, dd, *J* 17.4, *J* 10.6, H-18), 5.07-4.99 (2H, m, H-1), 4.64-4.44 (2H, br m, H-3 and H-11), 2.72 (4H, dd, *J* 15.2, *J* 7.6, H-6 and H-14), 2.21-1.98 (4H, m, H-8 and H-16), 1.81-1.69 (4H, m, H-7 and H-15), 1.61 (2H, br s, 2 x OH); δ_F (376 MHz, $CDCl_3$) -113.8 (d, $^2J_{F\text{-}F}$ 263.2), -123.2 (dd, $^2J_{F\text{-}F}$ 263.2, $^3J_{H\text{-}F}$ 11.3); LRMS (ES^-) *m/z* 379 (90%) $[M\text{-}H]^-$.

HPLC analysis was carried out using a Varian C-18 reverse Phase column, with a 100 Å pore size, with 0.5 mL/min flow rate, and using a mobile Phase of THF/water, and UV detection A mobile Phase gradient was used starting from 65% THF/water up to 85% THF/water over 35 minutes.

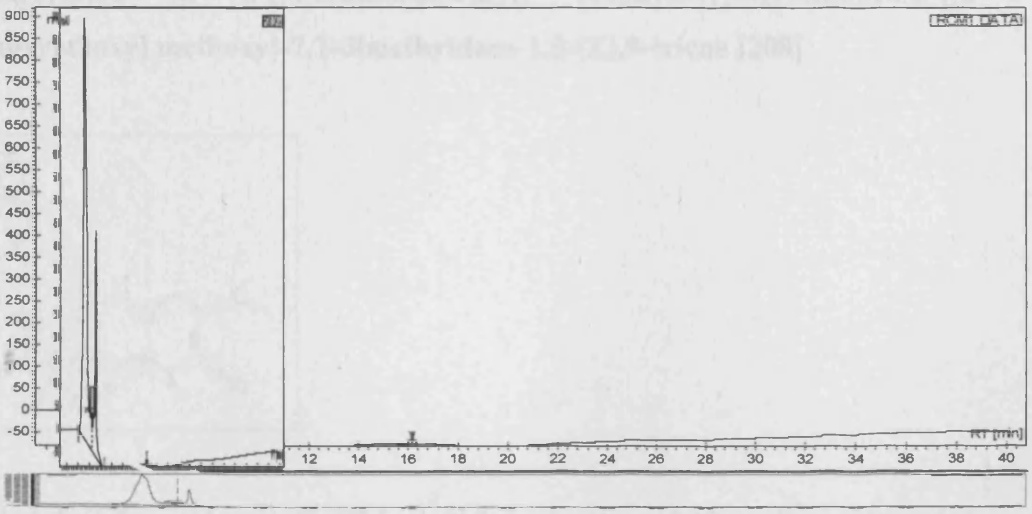

Figure 46

#	Time [Min]	Height [mAU]	Area % [%]
1	5.16	921.6	80.383
2	6.51	68.4	0.218

Prepararation of 3-((4-trifluoromethyl) benzoyloxy)-4,4-difluoro-5-[(2-methoxyethoxy) methoxy]-7,7-dimethyldeca-1,5-(Z),9-triene [208]

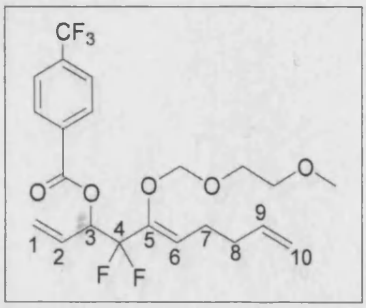

Alcohol **5** (1.5 g, 5.1 mmol), DMAP (0.2 equivalents, 0.12 g, 1 mmol) and 4-

(trifluoromethyl)benzoyl chloride (0.76 mL, 5.1 mmol) were combined in dichloromethane (50 mL). PVP (5.1 g, 5.1 mmol) was added and the mixture swirled gently for three days at room temperature. After this time the resin was collected by filtration and washed with CH_2Cl_2 (50 mL) and a saturated aqueous solution of sodium hydrogencarbonate (30 mL). The aqueous layer was extracted with CH_2Cl_2 (3 x 30 mL). Combined organic extracts and the original washing was washed with brine (30 mL), dried ($MgSO_4$) and concentrated *in vacuo.* The residual brown oil was purified by flash column chromatography (10% Et_2O/Petroleum ether) to afford **208** as a pale yellow oil (1.64 g, 69%). R_f (10% Et_2O/Pet ether) 0.06; υ_{max} (film) cm^{-1} 3000-2850s, 1710m (C=O), 1685m, 1610-1600w, 1600-1550w, 1500-1400m, 700m; δ_H (400 MHz, $CDCl_3$) 8.11 (2H, d, *J* 8.2, *ortho*-Ph-H), 7.65 (2H, d, *J* 8.2, *meta*-Ph-H), 5.94-5.82 (2H, m, H-2 and H-3), 5.66 (1H, ddt, *J* 17.0, *J* 10.2, *J* 6.8, H-9), 5.55 (1H, t, *J* 7.3, H-6), 5.47 (1H, dd, *J* 17.0, ^2J 1.3, H-10a), 5.38 (1H, dd, *J* 10.2, ^2J 1.3,H-10b), 4.94-4.88 (1H, m, H-1a), 4.93 (1H, s, OCH_2O), 4.85 (1H, ddd, *J* 10.1, ^4J 2.0, ^2J 1.0, H-1b), 3.84-3.75 (2H, m, OCH_2CH_2O), 3.51 (2H, t, *J* 5.1, OCH_2CH_2O), 3.31 (OCH_3), 2.25-2.17 (2H, m, H-8), 2.02 (2H, q, *J* 6.7, H-7); δ_C (100 MHz, $CDCl_3$) 163.7, 144.7 (t, $^2J_{C\text{-}F}$ 24.9), 137.2, 130.3, 128.5, 125.5, 121.9, 120.4, 119.5 (dd, $^1J_{C\text{-}F}$ 260.5, $^1J_{C\text{-}F}$ 250.3), 115.4, 98.3, 73.4 (t, $^2J_{C\text{-}F}$ 29.2), 71.6, 68.9, 59.0, 41.3, 29.0, 22.6, 20.4, 14.3; δ_F (376 MHz, $CDCl_3$) -63.2 (3F, t, $^1J_{C\text{-}F}$ 84.4, CF_3), -111.6 (dd, $^2J_{F\text{-}F}$ 253.0, $^3J_{H\text{-}F}$ 11.5), 112.0 (dd, $^2J_{F\text{-}F}$ 253.0, $^3J_{H\text{-}F}$ 11.5); [HRMS (CI, $[M+NH_4]^+$) found 482.1962 Calc for $C_{22}H_{29}F_2O_6N$: 482.1960]; LRMS (EI) *m/z* 463.3 $[M-H]^+$ (2%).

Preparation of 3-((4-methoxy) benzoyloxy)-4,4-difluoro-5-[(2-methoxyethoxy) methoxy]-7,7-dimethyldeca-1,5-(Z),9-triene [209]

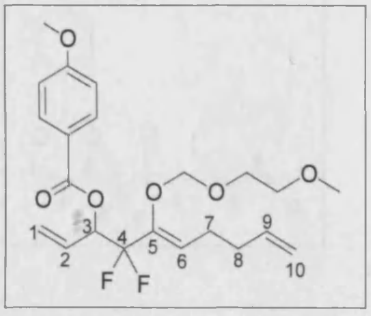

PVP (5.1 g, 5.1 mmol) was added to a solution of alcohol **5** (1.5 g, 5.1 mmol),

DMAP (0.2 equivalents, 0.12 g, 1 mmol) and 4-(methoxy)benzoyl chloride (0.70 mL, 5.1 mmol) in dichloromethane (50 mL). The mixture was swirled gently for three days at room temperature. The resin was filtered off and washed with CH_2Cl_2 (50 mL) and a saturated aqueous solution of sodium hydrogencarbonate (30 mL). The aqueous layer was extracted with CH_2Cl_2 (3 x 30 mL). Combined organic extracts were washed with brine (30 mL), dried ($MgSO_4$) and concentrated *in vacuo*. The residual brown oil was purified by flash column chromatography (10% Et_2O/Petroleum ether) to afford **209** as a pale yellow oil (1.49 g, 69%). R_f (10% EtOAc/hexane) 0.11; υ_{max} (film) cm^{-1} 3000-2850s, 1725m (C=O), 1606m, 1606-1512w, 1318-1200w, 1115-1055m, 734m; δ_H (400 MHz, $CDCl_3$) 8.03 (2H, d, *J* 8.9, *ortho*-Ph-H), 6.93 (2H, d, *J* 8.9, *meta*-Ph-H), 5.99-5.89 (2H, m, H-2 and H-3), 5.74 (1H, ddt, *J* 17.0, *J* 10.5, *J* 6.6, H-9), 5.62 (1H, t, *J* 7.3, H-6), 5.52 (1H, dd, *J* 17.0, ^2J 1.3, H-10a), 5.42 (1H, dd, *J* 10.5, ^2J 1.3, H-10b), 5.02-4.92 (2H, m, H-1), 5.00 (2H, s, OCH_2O), 3.87-3.85 (5H, m, OCH_2CH_2O and Ph-$HOCH_3$), 3.58 (2H, t, *J* 5.1, OCH_2CH_2O), 3.39 (3H, s, OCH_3), 2.27 (2H, q, *J* 7.1, H-8), 2.09 (2H, q, *J* 7.1, H-7); δ_C (100 MHz, $CDCl_3$) 164.6, 163.7, 144.8 (t, $^2J_{C\text{-}F}$ 24.9), 137.3, 131.9, 129.1, 121.8, 121.2, 120.2, 117.3 (dd, $^1J_{C\text{-}F}$ 251.6, $^1J_{C\text{-}F}$ 251.8), 115.3, 113.7, 98.2, 72.4 (dd, $^2J_{C\text{-}F}$ 30.7, $^2J_{C\text{-}F}$ 32.2), 71.6, 68.9, 59.1, 55.5, 33.0, 24.5; δ_F (376 MHz, $CDCl_3$); -110.9 (dd, $^2J_{F\text{-}F}$ 253.5, $^3J_{H\text{-}F}$ 10.3), -112.3 (dd, $^2J_{F\text{-}F}$ 253.5, $^3J_{H\text{-}F}$ 12.6); [HRMS (CI, $[M+NH_4]^+$) found 444.2189. Calc for $C_{22}H_{32}F_2O_6N$: 444.2192].

Preparation of 3-((4-Trifluoromethyl) benzoyloxy)-4,4-difluorodeca-1,9-dien-5-one [210]

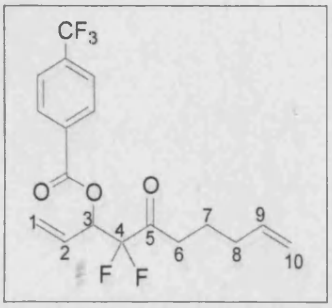

Thionyl chloride (0.25 mL, 3.4 mmol) was added dropwise to a solution of ester **208** (1.58 g, 3.4 mmol) in methanol (34 mL) at 0°C. The solution was stirred

overnight, allowing to warm to room temperature. After this time, the solution was concentrated *in vacuo* to give a yellow oil which was partitioned between diethyl ether (20 mL) and water (20 mL). The aqueous layer was extracted with diethyl ether (3 x 20 mL). Combined organic extracts were washed with brine (20 mL), dried ($MgSO_4$) and concentrated *in vacuo*. Ketone **208** was obtained as a yellow oil (0.91 g, 71%). R_f (10% EtOAc/hexane) 0.51; δ_H (400 MHz, $CDCl_3$) 8.16 (2H, d, *J* 8.2, *ortho*-Ph-H), 7.73 (2H, d, *J* 8.2, *meta*-Ph-H), 6.06-5.91 (2H, m, H-2 and H-3), 5.72 (1H, ddt, *J* 16.9, *J* 10.3, *J* 6.6, H-9), 5.60 (1H, dd, *J* 16.9, ^2J 1.7, H-10a), 5.54 (1H, dd, *J* 10.3, ^2J 1.7, H-10b), 5.03-4.96 (2H, m, H-1), 2.74 (2H, t, *J* 7.3, H-6), 2.07 (2H, dt, *J* 6.8, ^4J 1.3, H-8), 1.73 (2H, quin, *J* 7.3, H-7); δ_C (100 MHz, $CDCl_3$) 198.5 (t, $^2J_{C\text{-}F}$ 29.3), 162.2, 136.2, 134.3, 131.1, 129.2, 126.3, 124.6, 123.8, 122.4, 114.7, 112.8 (dd, $^1J_{C\text{-}F}$ 262.0, $^1J_{C\text{-}F}$ 260.5), 71.7 (dd, $^2J_{C\text{-}F}$ 29.3, $^2J_{C\text{-}F}$ 29.3), 35.6, 31.6, 20.4; δ_F (376 MHz, $CDCl_3$) -63.2 (s), -114.3 (dd, $^2J_{F\text{-}F}$ 278.2, $^3J_{H\text{-}F}$ 9.2), -118.2 (dd, $^2J_{F\text{-}F}$ 278.2, $^3J_{H\text{-}F}$ 13.2); [HRMS (CI, $[M+NH_4]^+$) found 394.1436 Calc for $C_{18}H_{21}F_5O_3N$: 394.1436];]; LRMS (ES) *m/z* 375 (15%) $[M\text{-}H]^-$, 189 (60%) $[CO_2Ph\text{-}HCF_3]^-$.

Preparation of 3-((4-Methoxy) benzoyloxy)-4,4-difluorodeca-1,9-dien-5-one [211]

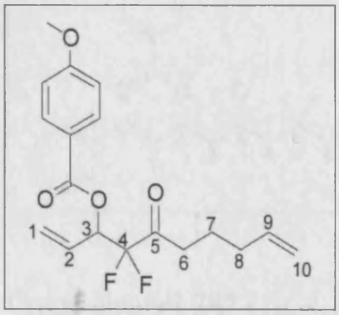

Thionyl chloride (0.27 mL, 3.66 mmol) was added dropwise to a solution of ester **209** (1.55 g, 3.66 mmol) in methanol (37 mL) at 0°C. The solution was stirred

overnight, allowing to warm to room temperature. After this time, the solution was concentrated *in vacuo* to give a yellow oil which was diluted with diethyl ether (20 mL) and water (20 mL). The aqueous layer was extracted with diethyl ether (3 x 20 mL). Combined organic extracts were washed with brine (x mL), dried ($MgSO_4$) and concentrated *in vacuo*. Ketone **211** was obtained as a yellow oil (0.79 g, 62%). R_f (10% EtOAc/hexane) 0.38; υ_{max} (film), cm^{-1} 3100-2830s, 1732m (C=O), 1606m, 1620-1580w, 1513m, 1410-1360w, 773m; δ_H (400 MHz, $CDCl_3$) 7.99 (2H, d, *J* 9.0, *ortho*-Ph-H), 6.93 (2H, d, *J* 9.0, *meta*-Ph-H), 6.00-5.90 (2H, m, H-2 and H-3), 5.71 (1H, ddt, *J* 16.9, *J* 10.1, *J* 6.6, H-9), 5.56 (1H, dd, *J* 16.9, ^2J 1.0, H-10a), 5.49 (1H, dd, *J* 10.1, ^2J 1.0, H-10b), 5.02-4.95 (2H, m, H-1), 2.73 (2H, t, *J* 7.3, H-6), 2.05 (2H, q, *J* 7.1, H-8), 1.71 (2H, quin, *J* 7.3, H-7); ; δ_C (100 MHz, $CDCl_3$) 198.7 (t, $^2J_{C\text{-}F}$ 29.3), 162.9, 136.3, 130.9, 126.7, 121.5, 120.1, 114.6, 113.2 (dd, $^1J_{C\text{-}F}$ 260.5, $^1J_{C\text{-}F}$ 260.5), 112.8, 71.0 (dd, $^2J_{C\text{-}F}$ 30.7, $^2J_{C\text{-}F}$ 30.7), 54.5, 35.8, 31.6, 29.9, 20.5; δ_F (376 MHz, $CDCl_3$) -113.6 (dd, $^2J_{F\text{-}F}$ 272.5, $^3J_{H\text{-}F}$ 9.2), -119.1 (dd, $^2J_{F\text{-}F}$ 272.5, $^3J_{H\text{-}F}$ 14.9); [HRMS (CI), $[M+NH_4]^+$) found 356.1667 Calc for $C_{18}H_{24}O_4F_2N$: 356.1668]; LRMS (CI) *m/z* 356.2 (20%) $[M+NH_4]^+$, 328.2 (100%), 135.0 (25) $[C_6H_9F_2O]^+$.

Preparation of (1*E*)-3-benzoyloxy-7,7-dimethyl-1-phenyldeca-1,9-dien-5-one [286]

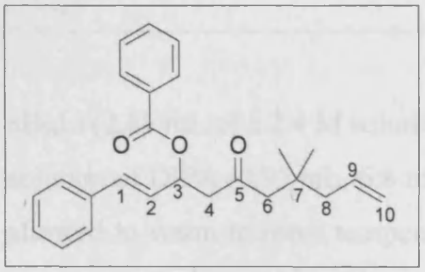

Crude alcohol **287** (1g, 4.1 mmol), DMAP (0.1 g, 0.82 mmol, 0.2 equivalents) and benzoic anhydride were combined in CH_2Cl_2 (41 mL). PVP (4.1 g, 4.1 mmol) was added and the solution swirled gently overnight at room temperature. After this

time, the solids were filtered off and washed with CH_2Cl_2 (20 mL) and a saturated solution of sodium hydrogencarbonate (20 mL). The aqueous layer was extracted with dichloromethane (3 x 25 mL). The combined organic extracts were washed with brine (20 mL), dried ($MgSO_4$) and concentrated *in vacuo* to give **286** as a yellow oil (1.1 g, 72%) which was purified by flash column chromatography(10% diethyl ether/petroleum ether) to give **286** as a pale yellow solid, which was recrystallised in hot hexane to recover **286** as white needles (0.34 g, 23%). R_f (10% diethyl ether/petroleum ether) 0.15; mp 65-69°C. δ_H (400 MHz, $CDCl_3$) 8.07 (2H, dd, *J* 8.6, ^4J 1.5, *ortho*-Ph-H (ester)), 7.57 (1H, td, *J* 7.6, ^4J 1.5, *para*-Ph-H (ester)), 7.47-7.23 (7H, m, Ph-H-H), 7.66 (1H, d, *J* 15.7, H-1), 6.31 (1H, dd, *J* 15.7, *J* 7.1, H-2), 6.12 (1H, ddd, *J* 12.4, *J* 7.6, *J* 5.6, H-3), 5.78 (1H, ddt, *J* 16.7, *J* 7.6, *J* 10.3, H-9), 5.04-4.97 (2H, m, H-10), 3.09 (1H, dd, ^2J 16.6, *J* 7.6, H-4a), 2.86 (1H, dd, ^2J 16.6, *J* 5.6, H-4b), 2.40 (1/2 AB q, ^2J 15.4, H-6a), 2.37 (1H, ½ AB q, ^2J 15.4, H-6b), 2.11 (2H, d, *J* 7.6, H-8), 1.02 (3H, s, CH_3), 1.02 (3H, s, CH_3); δ_C (100 MHz, $CDCl_3$) 206.5, 165.5, 136.1, 134.9, 133.1, 132.9, 129.7, 128.6, 128.5, 128.4, 128.1, 126.7, 126.5, 117.7, 71.1, 53.1, 49.4, 46.3, 33.8, 27.3; [HRMS (ES), $[M+NH_4]^+$) found 394.2375 Calc for $C_{25}H_{32}O_3N$: 394.2377]; LRMS (ES) *m/z* 770.3 (80%) $[2M+NH_4]^+$, 394.2 (65%) $[M+NH_4]^+$, 255 (100%) $[M-OBz]^+$.

Preparation of (E)-3-hydroxy-1-phenyldeca-1,9-dien-5-one [287]

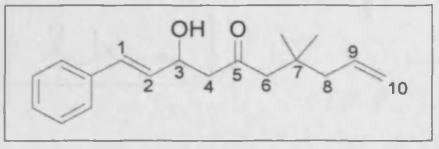

nBuLi (2.85 mL of a 2.4 M solution in hexanes, 6.8 mmol) was added dropwise to a solution of DIPA (0.95 mL, 6.8 mmol) in THF (30 mL) at -78°C. The solution was allowed to warm to room temperature before recooling to -78°C. Ketone **288** (0.8 g, 5.7 mmol) in THF (10 mL) was added dropwise *via* a cannula at this temperature and the pale yellow solution stirred for one hour. Cinnamaldehyde (0.57 mL, 4.6 mmol) was then added in one portion and the solution was allowed to warm to -30°C over two hours, quenched with a saturated solution of ammonium chloride (30 mL) and warmed to room temperature. The aqueous layer was extracted with

diethyl ether (3 x 25 mL). Combined organic extracts were washed with brine (25 mL) and dried ($MgSO_4$) and concentrated *in vacuo* to give **287** as a yellow oil (1.1 g, 76%) which was esterified without purification.

Preparation of 4,4-dimethyl hep-1-tenone [288]

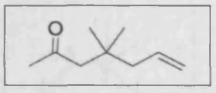

Titanium (IV) chloride (69 mL of a 1 M solution in CH_2Cl_2, 69 mmol) was added dropwise *via* a cannula to a solution of mesityl oxide (7.9 mL, 69 mmol) in dry, degassed dichloromethane (250 mL) at 0°C. The solution was stirred for 30 minutes, then a solution of allyltrimethylsilane (10 mL, 62.7 mmol) in dichloromethane (75 mL) was added dropwise *via* a cannula over 40 minutes. The mixture was stirred at room temperature for three hours. The stirred mixture was quenched with a saturated solution of sodium hydrogencarbonate (200 mL) and the mixture filtered through a plug of Celite. The aqueous layer was extracted with dichloromethane (3 x 50 mL) and the combined organic extracts were washed with

brine (50 mL), dried ($MgSO_4$) and concentrated *in vacuo*. The residual orange oil was purified by reduced pressure distillation (70°C 75 mm Hg). Ketone **288** was obtained as a pale yellow liquid (2.4 g, 29%). R_f (10% diethyl ether/pentane) 0.31. The spectra obtained upon purification were in agreement with those published by Sakurai.[114]

Preparation of 1-benzoyl-5,5-dimethyl -cyclooct-7-en-3-one [293]

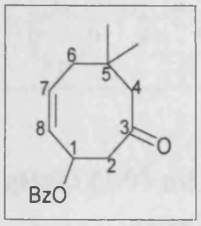

Titanium *iso*propoxide (0.2 mmol, 0.06 mL) was added to a solution of **286** (0.7 mmol, 0.26 g) or **302** (0.7 mmol, 0.23 g) in dry, degassed CH_2Cl_2 (133 mL) at room temperature. The reaction mixture was refluxed for 30 minutes under nitrogen, then a solution of **3** (0.035 mmol, 5 mole %, 0.03 g) in dry degassed CH_2Cl_2 (1 mL) was added. The solution was refluxed overnight at 40 °C under nitrogen. The crude mixture was concentrated *in vacuo* to leave a light brown oil which was purified by

column chromatography(15 % ethyl acetate in pentane) to afford **293** (1.16 g, 68%, 97% by GC, t_r 19.66 min). A purer sample was obtained upon eluting the product through a Polymer Labs MP-thiol SPE tube, preconditioned with methanol (1 mL), with methanol (1 mL) to afford the product as a colourless cubes; R_f (15 % ethyl acetate in pentane) 0.5; mp 78-80 °C; υ_{max}(mull)/cm^{-1} 3000-2850s, 1710m (C=O), 1685m, 1610-1600w, 1600-1550w, 1500-1400m, 700m; δ_H (400 MHz, $CDCl_3$) 7.97 (2H, dd, *J* 8.4, ^4J 1.3, *ortho* Ph-H), 7.51 (1H, tt, *J* 7.6, ^4J 1.3, *para* Ph-H), 7.38 (2H , t, *J* 7.6, *meta* Ph-H), 6.16 (1H, br ddd, *J* 11.9, *J* 6.8, *J* 6.3, H-1), 5.82-5.68 (2H, m, H-7 and H-8), 3.00 (1H, dd, ^2J 12.9, *J* 6.8, H-2a), 2.71 (1H, dd, ^2J 12.9, *J* 11.6, H-2b), 2.52 (1H, d, ^2J 11.6, H-4a), 2.31 (1H, dd, ^2J 13.6, *J* 8.9, H-6a), 2.24 (1H, d, ^2J 11.6, H-4b), 1.93 (1H, dd, ^2J 13.6, *J* 7.6, H-6b), 1.04 (3H, s, CH_3), 0.94 (3H, s, CH_3); δ_c (100 MHz, $CDCl_3$) 206.9, 165.6 (C-3), 133.2 (C-1 *para*), 132.2 (C-8), 130.0 (C-8), 129.8 (C-1 *ipso*) 129.6 (C-7), 128.4 (C-1 *meta*), 67.2 (C-1), 53.7 (C-6), 52.8 (C-2), 40.5 (C-4), 36.5 (C-5), 31.9 (C-9_A), 26.3 (C-9_B); (CI^+) 312 (100%, $[M+NH_4]^+$), 294 (4), 216 (33), 186 (20), 170 (9), 126 (8), 108 (11), 84 (8); HRMS (CI^+, $[M+H]^+$) Calc for **293**: found: 273.1485. The data were in agreement with those reported by R. Webster.[113]

Preparation of (1*E*,3*E*)-7,7-dimethyl-1-phenyldeca-1,3,9-trien-5-one [294]

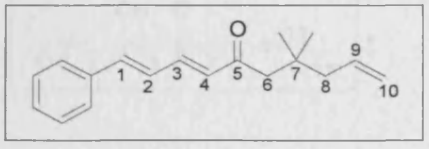

nBuLi (1.95 mL of a 2.2 M solution in hexanes, 4.3 mmol) was added dropwise to a solution of DIPA (0.60 mL, 4.3 mmol) in THF (25 mL) at -78°C. The solution was allowed to warm to room temperature before recooling to -78°C. Ketone **288** (0.5 g, 3.6 mmol) in THF (5 mL) was added dropwise *via* a cannula and the solution warmed to -30°C over two hours. Cinnamaldehyde (0.49 mL, 0.51 mmol) was added in one portion and the solution warmed to -10°C and quenched with a saturated aqueous solution of ammonium chloride (50 mL) before warming to room temperature. The aqueous layer was extracted with diethyl ether (3 x 30 mL). combined organic extracts were washed with brine (30 mL), dried ($MgSO_4$) and

concentrated *in vacuo* to give **294** as a yellow oil which was purified by flash column chromatography(10% diethyl ether/petroleum ether) to give **294** as a yellow oil (0.43 g, 45%). R_f (5% diethyl ether/petroleum ether) 0.17; δ_H (400 MHz, $CDCl_3$) 7.50 (2H, dd, *J* 8.1, ^4J 1.5, *ortho*-Ph-H), 7.51-7.32 (4H, m, *meta* and *para*-Ph-H and H-2), 7.00-6.86 (2H, m, H-3 and H-4), 6.31 (1H, d, *J* 15.4, H-1), 5.88 (1H, ddt, *J* 17.9, *J* 10.3, *J* 7.5, H-9), 5.13-5.06 (2H, m, H-10), 2.50 (2H, s, H-6), 2.15 (2H, d, *J* 7.5, H-8), 1.07 (6H, s, 2 x CH_3); δ_C (100 MHz, $CDCl_3$) 200.3, 142.4, 141.2, 138.1, 129.7, 129.1, 128.8, 127.2, 126.7, 115.2, 39.9, 33.2, 23.4, 22.3. 14.0; [HRMS (CI, $[M+H]^+$) found 255.3751 Calc for $C_{18}H_{23}O$: 255.3787]; LRMS (CI) *m/z* 255.3 $[M+H]^+$ (100%).

Preparation of (2*E*)-4-hydroxy-8,8-dimethylundeca-2,10-dien-6-one [301]

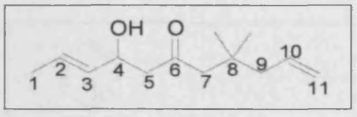

nBuLi (2.48 mL of a 2.5 M solution in hexanes, 6.1 mmol) was added dropwise to a solution of DIPA (0.86 mL, 6.1 mmol) in THF (30 mL) at -78°C under nitrogen. The solution was warmed to room temperature to allow complete formation of LDA before re-cooling to -78°C. Ketone **288** (0.7 g, 5.0 mmol) in THF (10 mL) was added dropwise over 20 minutes at this temperature and the solution was stirred at -78°C for 40 minutes then freshly distilled crotonaldehyde (0.35 g, 0.41 mL, 5 mmol) was added in one portion. The solution was warmed to -40°C over 3 hours and quenched with a saturated aqueous solution of ammonium chloride (25 mL). After warming to room temperature, the aqueous layer was diluted with water (20 mL) and extracted with diethyl ether (3 x 20 mL). The combined organic layers

were washed with brine (25 mL), dried ($MgSO_4$) and concentrated at reduced pressure (150 mbar), resulting in a yellow oil. ^1H NMR revealed a complex mixture which proved difficult to separate at the first attempt, so the mixture was benzoylated directly, without purification.

Preparation of (2*E*)-4-benzoyloxy-8,8-dimethylundeca-2,10-dien-6-one [302]

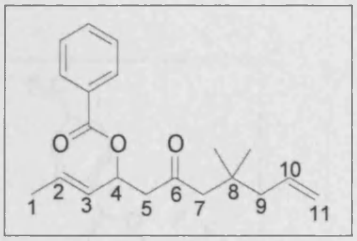

Benzoic anhydride (0.67 g, 2.96 mmol) and DMAP (72 mg, 0.59 mmol) were added to a solution of crude **301** (0.62g, 2.96 mmol) in dichloromethane (30 mL). PVP (2.96 g, 2.96 mmol) was added and the suspension swirled gently overnight at room temperature. The solids were filtered off and washed with dichloromethane (20 mL) and a saturated aqueous solution of sodium hydrogencarbonate (20 mL). The aqueous layer was extracted with dichloromethane (3 x 20 mL). Combined organic extracts were washed with brine (20 mL), dried ($MgSO_4$) and concentrated *in*

vacuo. The residual orange oil was purified by flash column chromatography(5% Et_2O/pentane), which afforded **302** as a yellow oil (0.29 g, 31%). R_f (10% Et_2O/petroleum ether) 0.38. υ_{max} (film), cm^{-1} 2916s, 1715m (C=O), 1621 (C=O), 1450-1378w, 1270m, 1139m; δ_H (400 MHz, $CDCl_3$) 8.01 (2H, dd, *J* 8.6, ^4J 1.5, *ortho*-Ph-H), 7.55 (1H, tt, *J* 7.3, ^4J 1.5, *para*-Ph-H), 7.43 (2H, tt, *J* 8.6, *J* 7.3, *meta*-Ph-H), 6.12 (1H, s, H-2), 5.91-5.82 (4H, m, H-3, H-10 and H-11), 5.59 (1H, ddd, *J* 15.4, *J* 7.6, *J* 5.6, H-4), 2.96 (1H, dd, ^2J 15.4, *J* 7.6, H-5a), 2.76 (1H, dd, ^2J 15.4, *J* 5.6, H-5b), 2.10 (2H, s, H-7), 1.87 (3H, s, H-1), 1.22 (3H, s, CH_3), 1.21 (3H, s, CH_3); δ_C (100 MHz, $CDCl_3$) 205.7, 164.4, 133.9, 131.9, 128.8, 128.6, 127.4, 127.2, 116.6, 114.3, 70.2, 52.0, 48.4, 45.3, 32.7, 26.2, 16.7; [HRMS (CI), $[M+NH_4]^+$) found 332.2223, Calc for $C_{20}H_{30}O_3N$: 332.2220]; LRMS (ES) *m/z* 337 $[M+Na]^+$ (100%).

Preparation of 1-((4-Trifluoromethyl) benzoyl)-2,2,difluoro-cyclooct-7-en-3-one [310]

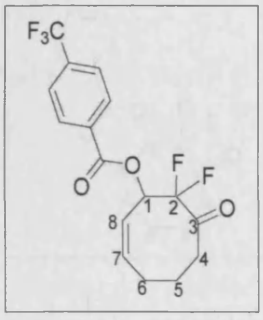

Diene **210** (0.1 g, 0.27 mmol) and titanium *iso*propoxide (24 μL, 0.1 mmol) were combined in dry, degassed dichloromethane (26.5 mL, 0.01 M) and refluxed under nitrogen for 30 minutes. A solution of Grubbs' second generation catalyst **29** (11.5 mg, 0.01 mmol, 5 mole %) in dichloromethane (1 mL) was added and the mixture was refluxed under nitrogen overnight. The solution was cooled and concentrated

in vacuo. The residual brown oil was purified by flash column chromatography(10% ethyl acetate/hexane) to give **310** as a white solid (64 mg, 68%). R_f (10% ethyl acetate/hexane) 0.25; mp 104-106°C; δ_H (400 MHz, $CDCl_3$) 8.25 (2H, d, *J* 8.2, *ortho* Ph-H), 7.76 (2H, d, *J* 8.2, *meta* Ph-H), 6.37 (1H, dddd, $^3J_{H\text{-}F}$ 21.2, $^3J_{H\text{-}F}$ 11.6, *J* 8.1, ^4J 1.5, H-1), 6.04 (1H, dd, *J* 18.7, *J* 9.2, H-7), 5.66 (1H, ddd, *J* 9.2, *J* 8.1, ^4J 1.5, H-8), 2.81 (1H, ddd, *J* 14.1, *J* 10.3, ^2J 3.7, H-4a), 2.75-2.68 (1H, m, H-4b), 2.47-2.31 (2H, m, H-6), 2.15-2.07 (1H, m, H-5a), 1.90-1.79 (1H, m, H-5b); δ_C (100 MHz, $CDCl_3$) 198.3 (t, $^2J_{C\text{-}F}$ 24.9), 163.1, 134.9, 134.0, 131.2, 129.4, 124.6, 123.8, 121.1, 118.1 (t, $^1J_{C\text{-}F}$ 260.5), 67.7 (dd, $^2J_{C\text{-}F}$ 24.9, $^2J_{C\text{-}F}$ 23.4), 35.7, 26.5, 26.0; δ_F (282 MHz, $CDCl_3$) -63.3 (t, $^1J_{C\text{-}F}$ 68.4, CF_3), -111.0 (d, $^2J_{F\text{-}F}$ 240.1), -130.8 (br d, $^2J_{F\text{-}F}$ 240.1); [HRMS (CI), $[M+NH_4]^+$) found 366.1121 Calc for $C_{16}H_{17}O_3F_5N$: 366.1123]; LRMS (EI) *m/z* 348.2 (2%) $[M]^+$, 329.1 (100%) $[M\text{-}HF]^+$, 190 (20%) $[COOPh\text{-}HCF_3]^+$.

Preparation of 1-((4-methoxy)-benzoyl)-2,2,difluoro-cyclooct-7-en-3-one [311]

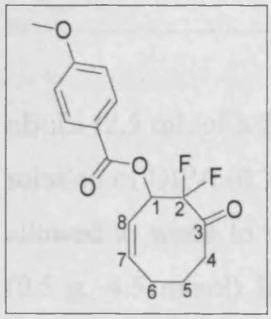

A solution of **211** (0.1 g, 0.30 mmol) and titanium isopropoxide (27 μL, 0.1 mmol) in dry, degassed dichloromethane (30 mL, 0.01 M) was refluxed under nitrogen for 30 minutes. A solution of Grubbs' second generation catalyst **29** (12.7 mg, 0.015 mmol, 5 mole %) in dichloromethane (1 mL) and the mixture refluxed under nitrogen overnight. The solution was cooled and concentrated *in vacuo.* The residual brown oil was purified by flash column chromatography(10% ethyl acetate/

hexane) to give **311** as a white solid (67 g, 72%). R_f (10% ethyl acetate/hexane) 0.15; mp 111-114°C. δ_H (400 MHz, $CDCl_3$) 8.08 (2H, d, *J* 9.1, *ortho*-Ph-H), 6.96 (2H, d, *J* 9.1, *meta*-Ph-H), 6.34 (1H, dddd, $^3J_{H\text{-}F}$ 22.4, $^3J_{H\text{-}F}$ 11.6, *J* 8.0, ^4J 3.8, H-1), 6.01 (1H, dd, *J* 19.5, *J* 9.1, H-7), 5.64 (1H, ddd, *J* 9.1, *J* 8.0, ^4J 2.5, H-8), 3.89 (3H, s, OCH_3), 2.83 (tdd, *J* 14.7, *J* 10.6, ^2J 3.7,H-4a), 2.72-2.65 (1H, m, H-4b), 2.44-2.32 (2H, m, H-6), 2.13-2.05 (1H, m, H-5a), 1.89-1.79 (1H, m, H-5b); δ_C (100 MHz, $CDCl_3$) 198.6 (t, $^2J_{C\text{-}F}$ 24.9), 162.9, 134.4, 131.2, 124.5, 124.4, 120.3, 115.6 (dd, $^1J_{C\text{-}F}$ 263.5, $^1J_{C\text{-}F}$ 259.1), 112.8, 66.9 (dd, $^2J_{C\text{-}F}$ 24.9, $^2J_{C\text{-}F}$24.9), 54.5, 35.9, 26.5, 26.2; δ_F (376 MHz, $CDCl_3$) -111.0 (d, $^2J_{F\text{-}F}$ 239.8), -131.0 (dd, $^2J_{F\text{-}F}$ 239.8, $^3J_{H\text{-}F}$ 22.4); [HRMS (CI), $[M+NH_4]^+$) found 328.1358, Calc for $C_{16}H_{20}F_2O_4N$: 328.1355]; LRMS (CI) *m/z* 328.2 (90%) $[M+NH_4]^+$, 158.1 (100%) $[M\text{-}COOPh\text{-}HOMe]^+$.

Preparation of (1E,3E)-1-Phenyldeca-1,3,9-trien-5-one [312]

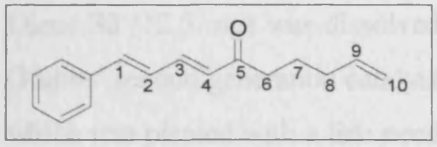

nBuLi (2.5 mL of a 2.2 M solution in hexanes, 5.4 mmol) was added dropwise to a solution of DIPA (0.76 mL, 5.4 mmol) in THF (20 mL) at -78°C. The solution was allowed to warm to room temperature before recooling to -78°C. Hept-1-en-6-one (0.5 g, 4.5 mmol) in THF (5 mL) was added dropwise *via* a cannula and the solution warmed to -30°C over two hours. Cinnamaldehyde (0.59 mL, 0.58 mmol) was added in one portion and the solution warmed to -10°C and quenched with a saturated aqueous solution of ammonium chloride (50 mL) before warming to room temperature. The aqueous layer was extracted with diethyl ether (3 x 30 mL). combined organic extracts were washed with brine (30 mL), dried ($MgSO_4$) and concentrated *in vacuo* to give **312** as a yellow oil which was purified by flash column chromatography(10% diethyl ether/petroleum ether) to give **312** as a white

solid (0.52 g, 51%). R_f (10% diethyl ether/pentane) 0.31, mp 145-148°C; δ_H (400 MHz, $CDCl_3$) 7.40 (2H, dd, *J* 7.8, ^4J 1.8, *ortho*-Ph-H), 7.34-7.22 (4H, m, Ph-H-H and H-2), 6.90-6.77 (2H, m, H-3 and H-4), 6.21 (1H, d, *J* 15.4, H-1), 5.73 (1H, ddt, *J* 16.9, *J* 10.1, *J* 6.7, H-9), 4.99-4.89 (2H, m, H-10), 2.54 (2H, t, *J* 7.5, H-6), 2.04 (2H, dd, *J* 14.1, *J* 6.7, H-8), 1.69 (2H, quintet, *J* 7.5, H-7); δ_C (100 MHz, $CDCl_3$) 200.3, 142.4, 141.2, 129.7, 129.1, 128.8, 127.2, 126.7, 115.2, 39.9, 33.2, 23.4, 22.3, 14.0; [HRMS (CI, $[M+H]^+$) found 227.1437. Calc for $C_{16}H_{19}O$: 227.2351]; LRMS (CI) *m/z* 227.3 $[M+H]^+$ (100%).

General Protocol for ^{1}H NMR Kinetics (p128)

Diene **30** (12.5 mg) was dissolved in CD_2Cl_2 (1 mL) in an oven dried NMR tube. Grubbs' second generation catalyst **29** was added and the tube topped with parafilm which was pierced with a fine needle to allow any evolving ethylene to escape. The sample was analysed using 400 MHz ^{1}H NMR (Bruker AV400) using a pseudo 2D programme with variable delay over 4.5 to 15 hours (dependent on catalyst loading –see **Table 53**). Analyses were carried out between 11-20 ppm at 298 K in CD_2Cl_2 unless otherwise specified.

12 References

JOC Article

Selected Substituent Effects on the Rate and Efficiency of Formation of an Eight-Membered Ring by RCM

Lisa Mitchell,[†,‡] John A. Parkinson,[‡] Jonathan M. Percy,*[,‡] and Kuldip Singh[†]

Department of Chemistry, University of Leicester, University Road, Leicester LE1 7RH, United Kingdom, and Department of Pure and Applied Chemistry, WestCHEM, University of Strathclyde, Thomas Graham Building, 295 Cathedral Street, Glasgow G1 1XL, United Kingdom

jonathan.percy@strath.ac.uk

Received December 21, 2007

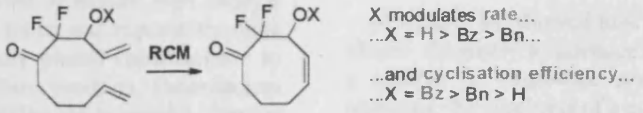

Studies of a range of reactions forming cyclooctenones highlight a discrepancy between cyclization rate and cyclization efficiency. Cyclization rates change modestly as the oxygen function at the allylic position is varied, and increase upon *gem*-dimethylation. Cyclization efficiency has also been quantified for four substrates, revealing a range of effective molarities (EMs) of 2 orders of magnitude that are substituent dependent. The most efficient cyclization appears to result from suppression of the cross-metathesis pathway through which oligomerization begins, rather than from a particularly rapid cyclization reaction. In the presence of a Ti(IV) cocatalyst, diene monomers transform smoothly to eight-membered-ring products without the intermediacy of dimers or other oligomers, indicating that the cyclizations are kinetically and not thermodynamically controlled. The *gem*-dialkyl effect is also shown to be kinetic.

Introduction

The ring closing metathesis (RCM) reaction has changed the way we think about the synthesis of cyclic molecules, leading to the award of the Nobel Prize to the three chemists most responsible for the major strategic advances in the area.[1] The direct synthetic connection of an α,ω-diene to a cyclic alkene or unsaturated heterocycle in the presence of numerous functional groups of a wide range of types and at high density can be achieved routinely by using commercially available and easy-to-handle Ru catalysts. Total syntheses of many complex natural products[2] have been planned and executed by using the RCM as a strategic event.[3] The tolerance of the reaction to variations in ring size is remarkable, with even rings that are usually difficult to make, like medium rings,[4] being formed in high yield (if appropriate substitution patterns are present). Though Fürstner[5] inter alia has outlined a number of extremely useful general ideas that explain the success of RCM reactions, our detailed knowledge of the interplay of structure and efficiency in the RCM is limited.[6] Some detailed computational studies of very simple prototypical reactions[7] and of relatively complex cyclization systems[8] have been carried out, but there seem to be relatively few general computational insights concerning cyclization.

† University of Leicester.

‡ University of Strathclyde.

(1) For the award lectures from the three Laureates, see: (a) Chauvin, Y. *Angew. Chem., Int. Edit.* **2006**, *45*, 3740. (b) Schrock, R. R. *Angew. Chem.-Int. Ed.* **2006**, *45*, 3748. (c) Grubbs, R. H. *Angew. Chem., Int. Ed.* **2006**, *45*, 3760. For a recent overview, see: *Chem. Eng. News* **2007**, *85*, 37. For a recent review, see: Hoveyda, A. H.; Zhugralin, A. R. *Nature* **2007**, *450*, 243.

(2) For recent examples, see: (a) Klar, U.; Buchmann, B.; Schwede, W.; Skuballa, W.; Hoffmann, J.; Lichtner, R. B. *Angew. Chem., Int. Ed.* **2006**, *45*, 7942. (b) Hong, Z. Y.; Liu, L.; Hsu, C. C.; Wong, C. H. *Angew. Chem., Int. Ed.* **2006**, *45*, 7417. (c) Gradillas, A.; Perez-Castells, J. *Angew. Chem., Int. Ed.* **2006**, *45*, 6086. (d) Furstner, A.; Nevado, C.; Tremblay, M.; Chevrier, C.; Teply, F.; Aissa, C.; Waser, M. *Angew. Chem., Int. Ed.* **2006**, *45*, 5837. (e) Deiters, A.; Pettersson, M.; Martin, S. F. *J. Org. Chem.* **2006**, *71*, 6547. (f) Inoue, M.; Sato, T.; Hirama, M. *Angew. Chem., Int. Ed.* **2006**, *45*, 4843. (g) Hoye, T. R.; Eklov, B. M.; Jeon, J.; Khoroosi, M. *Org. Lett.* **2006**, *8*, 3383. (h) Hong, S. W.; Yang, J. H.; Weinreb, S. M. *J. Org. Chem.* **2006**, *71*, 2078. (i) Bohrsch, V.; Neidhofer, J.; Blechert, S. *Angew. Chem., Int. Ed.* **2006**, *45*, 1302.

(3) For an elegant and comprehensive recent review, see: Nicolaou, K. C.; Bulger, P. G.; Sarlah, D. *Angew. Chem., Int. Ed.* **2005**, *44*, 4490.

(4) (a) Maier, M. E. *Angew. Chem., Int. Ed.* **2000**, *39*, 2073. (b) Deiters, A.; Martin, S. F. *Chem. Rev.* **2004**, *104*, 2199.

(5) Furstner, A. *Angew. Chem., Int. Ed.* **2000**, *39*, 3013.

(6) (a) For an excellent overview, see: Conrad, J. C.; Fogg, D. E. *Curr. Org. Chem.* **2006**, *10*, 185. Enyne metathesis has received much more detailed scrutiny; see: (b) Villar, H.; Frings, M.; Bolm, C. *Chem. Soc. Rev.* **2007**, *36*, 55. (c) Lloyd-Jones, G. C.; Margue, R. G.; de Vries, J. G. *Angew. Chem., Int. Ed.* **2005**, *44*, 7442.

(7) (a) Cavallo, L. *J. Am. Chem. Soc.* **2002**, *124*, 8965. (b) Tsipis, A. C.; Orpen, A. G.; Harvey, J. N. *Dalton Trans.* **2005**, 2849. (c) Adlhart, C.; Chen, P. *J. Am. Chem. Soc.* **2004**, *126*, 3496. (d) Fomine, S.; Vargas, S. M.; Tlenkopatchev, M. A. *Organometallics* **2003**, *22*, 93.

10.1021/jo702726b CCC: $40.75
Published on Web 02/14/2008

Two classic reviews by Mandolini[9] summarized a large set of data derived from lactonizations, intramolecular etherifications, and C−C bond-forming reactions, and reported the relationship between cyclization efficiency and ring size. Medium rings represent some of the most difficult challenges for cyclization strategies; the combination of developing ring strain and the requirement to restrict rotations around 7−9 flexible bonds ensures unfavorable enthalpic and entropic[10] contributions to $\Delta G^{\ddagger}$; cyclization reactions that form medium rings are therefore often relatively slow. High dilution (or Ziegler) conditions are often employed to reduce the rate of competing oligomerization pathways, because relatively inefficient cyclization is anticipated.

The RCM reaction converts a diene precursor to two alkene molecules, one of which is volatile ethylene in most synthetic sequences, allowing the unfavorable $\Delta S^{\ddagger}$ (and $\Delta H^{\ddagger}$) associated with cyclization to be compensated for entropically. Nevertheless, RCM reactions that form medium rings, for example, cyclooctannulation,[11] which is severely enthalpically and entropically disadvantaged, are reported to require high catalyst loading, high dilution, long reaction times, and importantly some degree of "gearing" of appropriately placed substituents[12] to deliver acceptable yields of cycloalkene products. These factors combine to severely restrict scaleability (in principle). Almost all our insights concerning RCM efficiency come from yield measurements; there are very few kinetic studies of the RCM reactions and those that are published involve the formation of five-membered rings and cyclization is not rate-determining.[13] There are no *measured* effective molarities in the literature; Fogg has presented a number of *expected* values of RCM EMs based on ring size but we are unaware of any experimental determinations of EM for RCM reactions.[14]

In the absence of quantitative information about a wide range of systems, the optimization of RCM reactions remains a matter of trial and error rather than one of rational design based on a *detailed* understanding of the underlying principles.

SCHEME 1

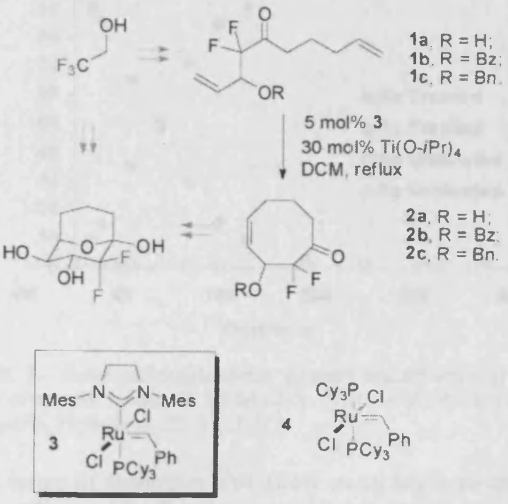

Recently, we showed how we could use metalated difluoroalkene chemistry to advance trifluoroethanol rapidly to deliver a number of sugar-like systems and a glycosyl phosphate analogue; the synthesis of a cyclooctenone template **1** by RCM[15] was a key step (Scheme 1).[16]

We wished to optimize the RCM reaction by varying the reaction solvent and temperature and the loading of the Ruthenium catalyst and by the correct choice of protection (R in **1**) for an allylic hydroxyl group, reporting the results of qualitative studies in our full synthetic paper. We now wish to report the results of a study in which substituent effects on RCM are quantified for the first time, with the two fluorine atoms acting as reporter groups for the various constituents within complex reaction mixtures.

A number of authors have reported that allylic substituents can exert large effects on RCM reaction yield[17] and regiochemical outcome.[18] In the most cited paper in the area, Hoye and

(8) (a) Vyboishchikov, S. E.; Thiel, W. *Chem.-Eur. J.* **2005**, *11*, 3921. (b) Castoldi, D.; Caggiano, L.; Panigada, L.; Sharon, O.; Costa, A. M.; Gennari, C. *Chem.- Eur. J.* **2005**, *12*, 51.

(9) (a) Illuminati, G.; Mandolini, L. *Acc. Chem. Res.* **1981**, *14*, 95. (b) Galli, C.; Mandolini, L. *Eur. J. Org. Chem.* **2000**, 3117.

(10) Buszek and co-workers have measured very small $\Delta S^{\ddagger}$ values for a series of lactonisations forming eight-membered rings; see: Buszek, K. R.; Jeong, Y.; Sato, N.; Still, P. C.; Muino, P. L.; Ghosh, I. *Synth. Commun.* **2001**, *31*, 1781.

(11) For a recent review, see: Michaut, A.; Rodriguez, J. *Angew. Chem., Int. Ed.* **2006**, *45*, 5740.

(12) The literature describes a number of failed attempts to cyclize simple (often geminally disubstituted) cyclooctene precursors; however, Taylor and Crimmins found that precursors with appropriately placed vicinal substituents could be cyclized successfully. For successful examples demonstrating the importance of substituent patterns or gearing, see: (a) Crimmins, M. T.; Choy, A. L. *J. Org. Chem.* **1997**, *62*, 7548. (b) Crimmins, M. T.; Tabet, E. A. *J. Am. Chem. Soc.* **2000**, *122*, 5473. (c) Edwards, S. D.; Lewis, T.; Taylor, R. J. K. *Tetrahedron Lett.* **1999**, *40*, 4267. For unsuccessful attempts to cyclize less substituted systems, see: (d) Kirkland, T. A.; Grubbs, R. H. *J. Org. Chem.* **1997**, *62*, 7310. (e) Hammer, K.; Undheim, K. *Tetrahedron* **1997**, *53*, 2309. For the ROMP of cyclooctene with tungsten alkylidene catalysis, see: (f) Kress, J. *J. Mol. Catal. A* **1995**, *102*, 7. The copious ROMP literature for cyclooctenes is well reviewed by Ivin; see: (g) Ivin, K. J. *Olefin Metathesis*; Academic Press: New York, 1983.

(13) Most of the quantitative studies deal with simple 5- and 6-ring-forming reactions: (a) Dias, E. L.; Nguyen, S. T.; Grubbs, R. H. *J. Am. Chem. Soc.* **1997**, *119*, 3887. (b) Bassetti, M.; Centola, F.; Semeril, D.; Bruneau, C.; Dixneuf, P. H. *Organometallics* **2003**, *22*, 4459. See also: (c) Basu, K.; Cabral, J. A.; Paquette, L. A. *Tetrahedron Lett.* **2002**, *43*, 5453. (d) Guo, X.; Basu, K.; Cabral, J. A.; Paquette, L. A. *Org. Lett.* **2003**, *5*, 789. (e) Paquette, L. A.; Basu, K.; Eppich, J. C.; Hofferberth, J. E. *Helv. Chim. Acta* **2002**, *85*, 3033.

(14) For a study that begins to examine a much wider range of systems and discusses cyclization efficiency, see: Conrad, J. C.; Eelman, M. D.; Duarte Silva, J. A.; Monfette, S.; Pamas, H. H.; Snelgrove, J. L.; Fogg, D. E. *J. Am. Chem. Soc.* **2007**, *129*, 1024.

(15) (a) Miles, J. A. L.; Mitchell, L.; Percy, J. M.; Singh, K.; Uneyama, E. *J. Org. Chem.*, **2007**, *72*, 1575−1587. (b) For a related system, see: Griffith, G. A.; Percy, J. M.; Pintat, S.; Smith, C. A.; Spencer, N.; Uneyama, E. *Org. Biomol. Chem.* **2005**, *3*, 2701.

(16) For examples of RCM-based syntheses of selectively fluorinated molecules, see: (a) Butt, A. H.; Percy, J. M.; Spencer, N. S. *Chem. Commun.* **2000**, 1691. (b) Audouard, C.; Fawcett, J.; Griffiths, G. A.; Percy, J. M.; Pintat, S.; Smith, C. A. *Org. Biomol. Chem.* **2004**, *2*, 528. (c) Audouard, C.; Fawcett, J.; Griffith, G. A.; Kerouredan, E.; Miah, A.; Percy, J. M.; Yang, H. L. *Org. Lett.* **2004**, *6*, 4269. (d) Fustero, S.; Catalan, S.; Piera, J.; Sanz-Cervera, J. F.; Fernandez, B.; Acena, J. L. *J. Org. Chem.* **2006**, *71*, 4010. (e) Fustero, S.; Sanchez-Rosello, M.; Jimenez, D.; Sanz-Cervera, J. F.; del Pozo, C.; Acena, J. L. *J. Org. Chem.* **2006**, *71*, 2706. (f) Fustero, S.; Bartolome, A.; Sanz-Cervera, J. F.; Sanchez-Rosello, M.; Soler, J. G.; de Arellano, C. R.; Fuentes, A. S. *Org. Lett.* **2003**, *5*, 2523. (g) De Matteis, V.; van Delft, F. L.; Jakobi, H.; Lindell, S.; Tiebes, J.; Rutjes, F. *J. Org. Chem.* **2006**, *71*, 7527. (h) De Matteis, V.; van Delft, F. L.; Tiebes, J.; Rutjes, F. *Eur. J. Org. Chem.* **2006**, 1166. (i) Yang, Y. Y.; Meng, W. D.; Qing, F. L. *Org. Lett.* **2004**, *6*, 4257. (j) You, Z. W.; Wu, Y. Y.; Qing, F. L. *Tetrahedron Lett.* **2004**, *45*, 9479.

(17) For reports of significant substitutent effects on RCM outcomes, see: (a) Castoldi, D.; Caggiano, L.; Bayon, P.; Costa, A. M.; Cappella, P.; Sharon, O.; Gennari, C. *Tetrahedron* **2005**, *61*, 2123. (b) Caggiano, L.; Castoldi, D.; Beumer, R.; Bayon, P.; Tesler, J.; Gennari, C. *Tetrahedron Lett.* **2003**, *44*, 7913. (c) Kaliappan, K. P.; Kumar, N. *Tetrahedron* **2005**, *61*, 7461. (d) Maishal, T. K.; Sinha-Mahapatra, D. K.; Paranjape, K.; Sarkar, A. *Tetrahedron Lett.* **2002**, *43*, 2263. (e) Hyldtoft, L.; Madsen, R. *J. Am. Chem. Soc.* **2000**, *122*, 8444.

SCHEME 2

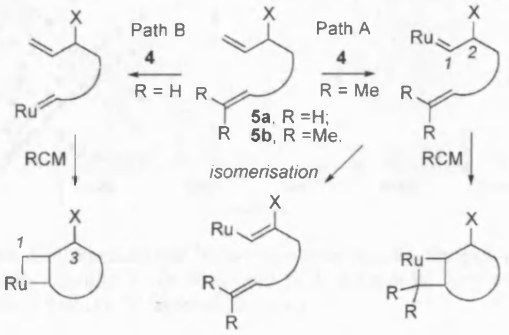

CHART 1

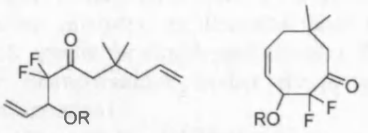

6a, R = H;
6b, R = Bz;
6c, R = Bn.

7a, R = H;
7b, R = Bz;
7c, R = Bn.

Zhao[19] studied the effect of allylic substitutents on the rate ofcyclopentannulation (Scheme 2, path A) using Grubbs' first generation catalyst **4** and concluded that "free allylic hydroxyl groups exerted a large *activating* effect upon the initial carbene exchange reaction with an adjacent vinyl group...". They also observed that "secondary hydroxyl groups are a liability in RCM reactions because of a net fragmentation reaction that consumes ruthenium alkylidene species" (this arises via the isomerization pathway shown in the scheme). Hoye's system (**5b**) sterically commits the active catalyst to react at the allylic alcohol terminus (Path A).[20] The published papers that cite Hoye and Zhao usually refer to another order of events which is path B (substrate **5a** would react by this pathway).

The large effects in Hoye's system presumably arise because of the orientation of the addition of the starting alkylidene across the alkenyl group of the allylic fragment. To start the reaction, the metal must add close to the substituent (the fragmentation reaction can then proceed from this pathway) and significant steric effects would be expected because the coordination sphere around ruthenium is compressed by bulky ligands. Hoye concludes that the large effect observed arises from a difference in the rate of alkylidene transfer, rather than cyclization (a conclusion overlooked by most of the authors citing the paper). In the case of **1a**−**c** and **6a**−**c** (Chart 1), reaction would be expected to initiate at the terminal Type I alkenyl group. Though *gem*-dimethylation at the homoallylic position is likely to reduce the rate of initiation in the more substituted species slightly,[21] we would expect the rate retarding effect of an allylic oxygen function to be bigger than the more remote steric effect.

(18) Allylic substituents appear to modulate the competition between RCM reactions that form 5- and 6-membered rings; see: (a) Schmidt, B.; Nave, S. *Chem. Commun.* **2006**, 2489. (b) Quinn, K. J.; Isaacs, A. K.; Arvary, R. A. *Org. Lett.* **2004**, *6*, 4143.

(19) Hoye, T. R.; Zhao, H. *Org. Lett.* **1999**, *1*, 1123.

(20) Chatterjee, A. K.; Choi, T. L.; Sanders, D. P.; Grubbs, R. H. *J. Am. Chem. Soc.* **2003**, *125*, 11360.

(21) (a) Homoallylic methylation lowers the rate of alkylidene transfer by ca. 50%; see: Ulman, M.; Grubbs, R. H. *Organometallics* **1998**, *17*, 2484. (b) For a recent investigation of related effects, see: Courchay, F. C.; Baughman, T. W.; Wagener, K. B. *J. Organomet. Chem.* **2006**, *691*, 585.

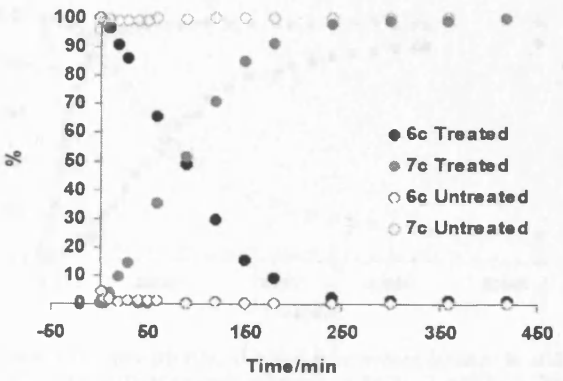

FIGURE 1. Substrate consumption appears instantaneously in the absence of sample treatment. RCM of **6c** (0.01 M in DCM, 1 mol % **3**, 30 mol % Ti(O-*i*Pr)$_4$, 25 ± 0.1 °C).

This range of substrates will allow us to begin to quantify both the effects of the free hydroxyl group and commonly used protected forms at the allylic position in path B and the *gem*-dialkyl effect on the rate and efficiency of the cyclization reaction.

Results and Discussion

Development of a Sampling Protocol for RCM Reactions. We developed a protocol to follow RCM directly (2% precatalyst **3**, 30% Ti(O*i*-Pr)$_4$ cocatalyst, 10 mM in substrate in dry degassed CH_2Cl_2 at room temperature or above), in which aliquots were withdrawn by syringe and passed through C-18 silanized solid-phase extraction (SPE) tubes that had been preconditioned with wet acetonitrile. Each sample was eluted with acetonitrile into a GC vial. This protocol ensured that the alkylidene catalyst was destroyed very close to the time of sampling and gave reproducible results for all substrates. Figure 1 shows the effects of aliquot treatment on the cyclization of **6c**; in the untreated experiment, the consumption of precursor appears to be instantaneous. Samples removed from reactions which were transferred straight to GC vials for analysis without treatment and the queued for GC analysis gave unreproducible and misleading results as the RCM continued in the GC vial, despite addition of wet CH_2Cl_2.[22]

The apparent rapid consumption of starting material can be shown to be an experimental artifact by ^{19}F NMR analysis, in which starting material can be seen to be the major species present in untreated aliquots taken close to the beginning of the reaction. The profiles arising from the treated samples show the smooth conversion of diene monomer into eight-membered-ring product, without the formation of other products (detectable by GC-MS or ^{19}F NMR). The product formation curve mirrors precursor consumption; response factors were determined for all precursors and products. We also checked the composition of product mixtures before and after passage through the SPE media; there was no perturbation of the composition, indicating that there was no selective retention of products or precursors

(22) A landmark paper describes the scale-up of a synthetic campaign in which RCM delivers a macrocycle. Analysis is secured by using a sulfur nucleophile to sequester and deactivate the Ru-catalyst: Yee, N. K.; Farina, V.; Houpis, I. N.; Haddad, N.; Frutos, R. P.; Gallou, F.; Wang, X. J.; Wei, X. D.; Simpson, R. D.; Feng, X. W.; Fuchs, V.; Xu, Y. B.; Tan, J.; Zhang, L.; Xu, J. H.; Smith-Keenan, L. L.; Vitous, J.; Ridges, M. D.; Spinelli, E. M.; Johnson, M.; Donsbach, K.; Nicola, T.; Brenner, M.; Winter, E.; Kreye, P.; Samstag, W. *J. Org. Chem.* **2006**, *71*, 7133.

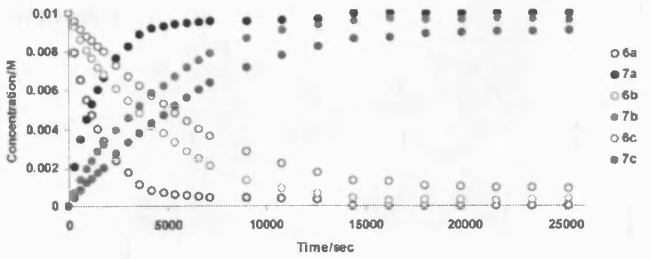

FIGURE 2. Competitive RCM between substrates **6a**, **6b**, and **6c** (0.01 M in each substrate in DCM, 2 mol % **3**, 30 mol % Ti(O-*i*Pr)$_4$ per substrate, 25 ± 0.1 °C, treated aliquots).

(see the Supporting Information for details). Carrying out the reactions at higher concentration leads to the formation of more complex reaction mixtures, as discussed later in the paper ($\{^1H\}^{19}F$ NMR spectra for simple and complex RCM product mixtures and characterization studies are presented in the Supporting Information).

Kinetic Profiling of the RCM Reactions. A competition experiment was carried with **6a**−**c** in the same reactor to investigate the relationship between cyclization reactivity and allylic functional group. The reactions were run in degassed CH_2Cl_2 at 298 K with **3** at 2 mM (2 mol %) and Ti(O-*i*Pr)$_4$ (30 mol %) per substrate (each substrate present at 10 mM) to maintain a constant ratio of catalyst to total substrate.

Data showed a relatively low degree of scatter suggesting that the sampling and preparation routine was reliable and reproducible. None of the reactions could be fitted to first-order kinetic plots.[23] The nature of the allylic substituent exerted a decisive effect on the rate of consumption of precursor as shown in Figure 2 (and on product formation which mirrors the precursor consumption profile in each case); the order of reactivity is **6a** > **6b** > **6c**.[24] The approximate half-lives of the three substrates are 1200, 3500, and 5400 s. There is no obvious explanation for this difference in reactivity but a number of authors have commented on remote substituent effects on RCM reactions.[25,26] The steric sizes of −OH, −OBn, and −OBz substituents as measured by their *A*-values are all rather similar so significant steric effects seem unlikely.

The reactions continue to different extents, with **6a** reaching 100% conversion, **6b** ca. 97%, and **6c** 90%. Diene and cycloalkene concentration can be measured reproducibly to ±4% so the slower reaction has clearly failed to reach completion.[27]

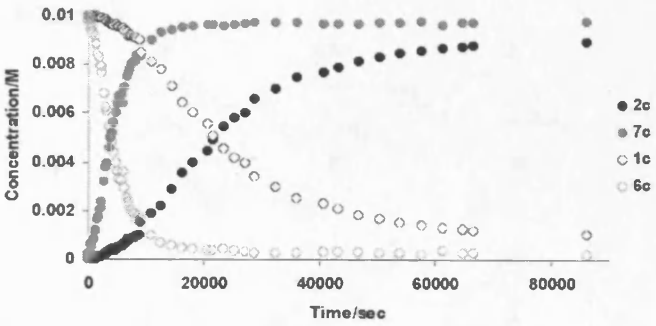

FIGURE 3. Competitive RCM between *gem*-dimethylated **6c** and less substituted **1c** (0.01 M in each substrate in DCM, 2 mol % **3**, 30 mol % Ti(O-*i*Pr)$_4$ per substrate, 25 ± 0.1 °C, treated aliquots).

We cannot explain these data by postulating the existence of an equilibrium reaction between diene and a mixture of cycloalkene and ethylene, because ethylene has very low solubility in the reaction solvent and is free to depart the open system.[9f] As cyclooctenol formation accurately mirrored diene consumption, we are not observing an equilibrium reaction between oligomers and cyclooctenol (several aliquots were concentrated after analysis to look for oligomers by ^{19}F NMR, and none were found). Synthetic reactions run at higher initial concentrations reach completion indicating that inhibition by reaction product is not responsible for the establishment of an equilibrium reaction under these conditions. Instead, it appears that the loss of activity of **3** appears to be significant at room temperature in CH_2Cl_2 even on the relatively short time scale of 10 h, with major implications for the conduct of slow RCM reactions with **3** (see the Supporting Information for the procedure used to establish this and the experimental data). To our knowledge, the rates of decomposition of **3**, the active benzylidene, or the methylidene formed upon turnover have not been reported under *synthetic* conditions,[28] though some computational studies have been carried out.[29]

The *gem*-Dialkyl Effect on the RCM. Figure 3 shows the competition between **1c** and **6c** in CH_2Cl_2 at 298 K under the usual conditions and with the same sampling protocol as described previously. The reaction of **6c** is dominated by the rapid cyclization with no visible induction period. The reaction end-point lies within experimental error of 100% completion. The failure of the slower reaction of **1c** to complete is believed to be due to the decomposition of catalyst on this time scale; this reaction also appears to have a distinct induction period, where relatively little substrate is turned over.

The exaggerated induction phase in the decay curve is presumably due to competition between the two substrates. The consumption of **1c** speeds up significantly once most of **6c** has been consumed; this would be consistent with intermediate alkylidene exiting more rapidly through cyclization in the *gem*-dialkylated case. The approximate half-lives of the reactions are 3900 and 21600 s, corresponding to an approximate rate

(23) Bassetti and co-workers (ref 9b) followed the formation of a 5-membered ring by RCM and noted that precursor consumption was not first order in some circumstances. The kinetic regime can include catalyst formation from precatalyst and a number of other events in addition to cyclization. We have established that the range and order of reactivity is correct by repeating the experiments with only a single substrate present. The detailed kinetic analysis will be reported elsewhere.

(24) A referee suggested that the competition between the three substrates may lead to perturbation of the profiles for the slower substrates. However, the purpose of the experiment is to show the rank order of reactivity, and the approximate range from highest to lowest, that the profiles from the competition reaction do successfully. The order of reactivity is not changed from single substrate experiments.

(25) (a) Aissa, C.; Riveiros, R.; Ragot, J.; Furstner, A. *J. Am. Chem. Soc.* **2003**, *125*, 15512. (b) Meng, D. F.; Su, D. S.; Balog, A.; Bertinato, P.; Sorensen, E. J.; Danishefsky, S. J.; Zheng, Y. H.; Chou, T. C.; He, L. F.; Horwitz, S. B. *J. Am. Chem. Soc.* **1997**, *119*, 2733.

(26) For effects due to hydrogen bond formation, see: (a) Vassilikogiannakis, G.; Margaros, L.; Tofi, M. *Org. Lett.* **2004**, *6*, 205. Furstner, A.; Thiel, O. R.; Blanda, G. *Org. Lett.* **2000**, *2*, 3731.

(27) Detection limits were estimated based on response factor measurements and we estimate that ±4% is a reasonable estimate of the accuray of individual concentration measurements at 10 mM starting concentration.

(28) Ulman and Grubbs studied the lifetimes of a range of precatalyst systems; the imidazolidinylidene-based precatalyst related to **3** was studied but no data were reported for **3** (the dihydroimidazolidinylidene-based precatalyst). See: Ulman, M.; Grubbs, R. H. *J. Org. Chem.* **1999**, *64*, 7202. Grubbs and co-workers recently examined the decomposition of the relevant phosphine complexes in the presence of ethene: Hong, S. H.; Wenzel, A. G.; Salguero, T. T.; Day, M. W.; Grubbs, R. H. *J. Am. Chem. Soc.* **2007**, *129*, 7961.

(29) (a) van Rensburg, W. J.; Steynberg, P. J.; Kirk, M. M.; Meyer, W. H.; Forman, G. S. *J. Organomet. Chem.* **2006**, *691*, 5312. (b)

SCHEME 3

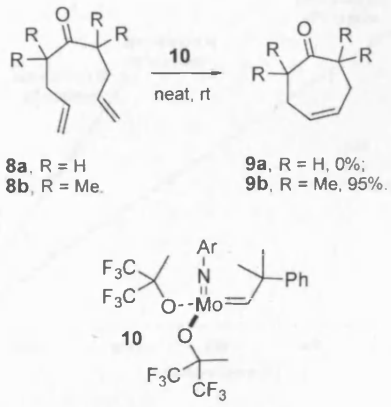

SCHEME 4

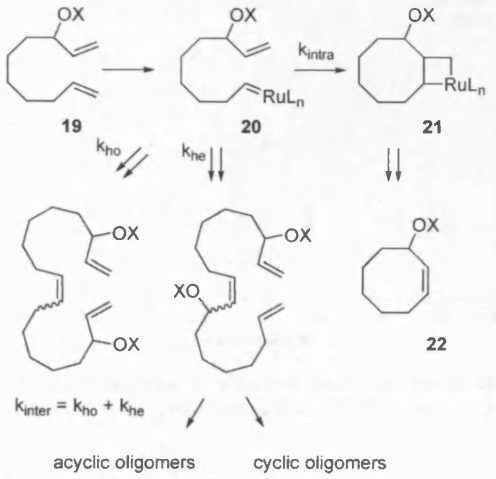

difference of less than an order of magnitude, which is a typical *gem*-dialkyl effect. The *gem*-dialkyl effect has been studied extensively but the acceleration of medium ring formation has not been quantified. The recent review by Jung and Piizzi[30] includes a single example of an RCM subject to a *gem*-dialkyl effect; *gem*-dimethylation on both sides of a midchain ketonic carbonyl group (a major structural perturbation) changes the outcome of a solvent-free metathesis reaction catalyzed by **10** completely from oligomerization to cycloheptannulation (Scheme 3).[31]

Forbes[31] attributed the outcome to significant thermodynamic destabilization of the acyclic ketone **8b** relative to **9b** caused by the mutual proximity of two quaternary centers.[32] As the reactive Schrock catalyst is capable of catalyzing the ROMP of neat **9b**, the outcome would appear to be under thermodynamic control. Our observed rate increase represents the only observation of a *kinetic gem*-dialkyl effect on an RCM to our knowledge; the origin of the effect will be explored elsewhere.

Measurement of Effective Molarities for Cyclooctannulations. Scale-up requires reactions that can be run at concentrations approaching 0.01 M or higher, or the volumes of solvent required become prohibitive for normal laboratory equipment.[22] We therefore sought to explore the effects of concentration upon the metathesis outcomes quantitatively.[33] In synthetic work, we found that the RCM of benzoate **1b** could be carried out successfully up to 20 mM concentration (100% conversion, 46% isolated purified yield, losses being incurred during removal of ruthenium residues) with catalyst **3** (5 mol %) and a Ti(IV) cocatalyst, with products resulting from cross metathesis forming at higher concentrations. Discrete oligomer signals cannot be identified by $\{^1H\}^{19}F$ NMR under these conditions, as the fluorine environments are too similar, resulting in overlapping signals with a chemical shift similar to that of the starting diene, indicating an acyclic species. The synthetic concentration for RCM of **1b** is a relatively high concentration compared to most of those used in the literature for 8-membered-ring RCM. Higher dilution was required for benzyl ether **1c** (2.5 mM) and alcohol **1a** (1 mM); significant quantities of cross metathesis products were formed at 20 mM with these substrates, suggesting that the allylic substituent modulates cyclization *efficiency* significantly. We also noted that the synthesis of **6a** could be carried out at 10 mM without formation of other products, suggesting that *gem*-dialkylation increases cyclization efficiency over cross metathesis.

The effective molarity[10,34] (EM, k_{intra}/k_{inter}) measures the relative efficiency of the cyclization rate (k_{intra}) compared to the most chemically congruent dimerization (k_{inter}). Scheme 4 shows how the total yields of cyclized and oligomerized products were used to estimate k_{intra} and k_{inter}.

This mechanism assumes that the RCM of **19** will always initiate most rapidly on the Type I alkene leading to the formation of new alkylidene **20**, which closes affording metallocyclobutane **21**. Varying the diene concentration and exploiting the *gem*-difluoro group in the system by integrating the $\{^1H\}^{19}F$ NMR spectra should allow the EM to be determined from a linear plot between the intramolecular:total intermolecular product ratio and the reciprocal diene concentration, assuming that this ratio accurately represents the partitioning of **20** between oligomerization and cyclization pathways, because

$$\%_{intra}\text{ (yield of cyclic product }\mathbf{22}) = k_{intra}[\mathbf{20}]$$

and

$$\%_{inter}\text{ (total yield of other products)} = k_{inter}[\text{diene }\mathbf{19}][\mathbf{20}]$$

so

$$\%_{intra}/\%_{inter} = k_{intra}[\mathbf{20}]/k_{inter}[\text{diene }\mathbf{19}][\mathbf{20}] = \text{EM}(1/[\text{diene }\mathbf{19}])$$

The analysis assumes that ROMP (or ring opening then ADMET) of the cycloalkene product **22** is slow under these conditions. We have re-exposed **2b** and **7b** to **3** under *synthetic* conditions (0.02 M) and failed to observe any change in the ^{19}F NMR spectrum of the mixture after 24 h, vide supra. However, under *more concentrated* conditions (1 M), we can observe slow ring opening and oligomerization for **2b** and **7b**. Alkenes within large rings are known to isomerize under

(30) Jung, M. E.; Piizzi, G. *Chem. Rev.* **2005**, *105*, 1735.

(31) (a) Forbes, M. D. E.; Patton, J. T.; Myers, T. L.; Maynard, H. D.; Smith, D. W.; Schulz, G. R.; Wagener, K. B. *J. Am. Chem. Soc.* **1992**, *114*, 10978. (b) Murphy has suggested that a single methyl substituent facilitates a macrocyclization by RCM; to our knowledge, these represent the sole examples and neither has been quantified; see: Commeureuc, A. G. J.; Murphy, J. A.; Dewis, M. L. *Org. Lett.* **2003**, *5*, 2785.

(32) Alder, R. W.; Allen, P. R.; Anderson, K. R.; Butts, C. P.; Khosravi, E.; Martin, A.; Maunder, C. M.; Orpen, A. G.; St Pourcain, C. B. *J. Chem. Soc., Perkin Trans. 2* **1998**, 2083.

(33) An interesting qualitative study is described by: Yamamoto, K.; Biswas, K.; Gaul, C.; Danishefsky, S. J. *Tetrahedron Lett.* **2003**, *44*, 3297.

(34) Kirby, A. J. *Adv. Phys. Org. Chem.* **1980**, *17*, 183.

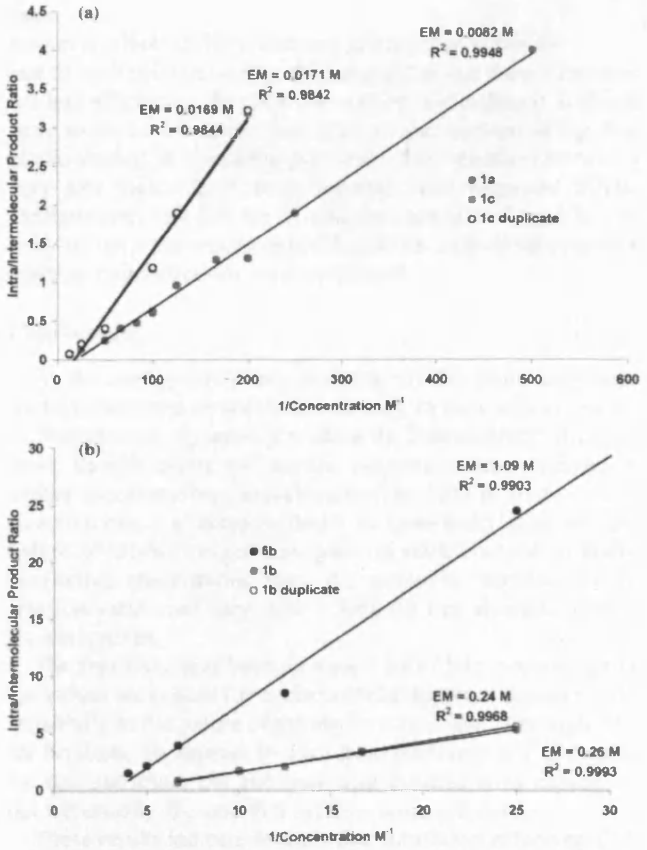

FIGURE 4. Determination of effective molarities for the RCMs of (a) **1a** and **1c** and (b) **1b** and **6b** (DCM, 5 mol % **3**, 30 mol % Ti(O-iPr)$_4$, reflux, 18 h).

thermodynamic control[35] in the presence of **3** but our cyclizations appear to be under kinetic control. These results will be discussed more fully elsewhere.

Fortunately we observed excellent dispersion between **2b** and other products in the $\{^1H\}^{19}F$ NMR spectra of product mixtures from **1b**, with the majority of the which, larger products (other than oligomers) being formed having discrete signals, that could be paired up using $^2J_{F-F}$ coupling constants and via correlation spectra ($^{19}F-^{19}F$ COSY).[36] Spectra were determined initially with a default relaxation delay, then re-recorded (duplicate determinations) with a relaxation delay (D_1) equal to $5T_1$ (T_1 values were measured) to ensure reliable integration. Full sweep width (0 to −300 ppm) spectra were also recorded to exclude the possibility of peaks wrapped or folded into the window used for integration.

In some cases, we were able to observe oligomers as distinct ions in the electrospray mass spectra. We also synthesized an acyclic heterodimer from **1a**, and (16-membered) cyclic dimers of **1a** and **1b**; these results are described fully in the Supporting Information.

The correlation between intramolecular:intermolecular product ratio and the reciprocal concentration is excellent (Figure 4) affording an EM of 0.25 M, which is high for the formation of an eight-membered ring from a highly flexible system. Since

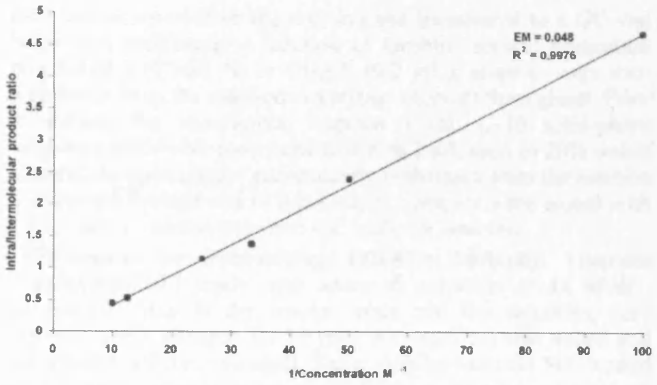

FIGURE 5. Determination of effective molarities for the RCMs of **1b** in the absence of the Ti(IV) cocatalyst (DCM, 5 mol % **3**, reflux, 18 h).

the synthesis of **7a** can be carried out at higher concentration than that for **2a**, we also determined an EM for **6b**. The $\{^1H\}^{19}F$ NMR spectra at 218 K (the cyclooctenones are fluxional at 300 K) again showed good dispersion between an eight-membered ring and side products, affording an EM of 1.09 M, which is high for a reaction forming an eight-membered ring.

EMs of 0.017 and 0.008 M were obtained for the cyclizations of **1c** and **1a**, respectively, using this method. These EM values are more typical of reactions forming eight-membered rings.[10a,34,37]

EMs for the formation of eight-membered rings range from 0.001 to 0.1 M with the larger values obtaining for heteroannelations of systems that have one or more rotors removed.[38] The nature of the allylic functional group clearly exerts a significant effect on the *relative efficiencies* of the cyclization and competing oligomerization.[39]

We also determined the EM of the cyclization of **1b** in the absence of the Ti(IV) cocatalyst (Figure 5). The cyclization is five times less efficient in the absence of the cocatalyst, but is still more efficient than any of the cocatalyzed cyclizations of the other substrates. Exploration of the role of the Ti(IV) cocatalyst falls outside of the scope of this paper and will be reported elsewhere.[40]

Most other discussions of substituent effects on RCM outcomes derive exclusively from measurements of yields or percent conversions that are assumed to correlate with reaction

(35) Lee, C. W.; Grubbs, R. H. *Org. Lett.* **2000**, *2*, 2145.

(36) The possibility of alkene (positional) isomerization before cyclization was also examined explicitly; we found no evidence for the formation of seven-membered-ring products under conditions that might promote isomerization (see the Supporting Information for details).

(37) Fogg and co-workers (ref 14) quote EMs for the formation of rings of a range of sizes which are for etherifications and C−C bond forming reactions of various types, rather than RCMs.[9f] While it is true to say that EMs for a given ring size fall within a particular band, some of those bands are quite wide. There are a number of significant changes in geometry on the pathway from acyclic diene to cycloalkene that may be represented well or poorly by the enthalpic and entropic properties of the product cycloalkene. We would argue that the EMs for non-RCM reactions are at absolute best a guideline, rather than a reliable predictor of cyclization efficiency.

(38) For a remarkably effective RCM forming an 8-membered ring, see: Chavan, S. P.; Thakkar, M.; Jogdand, G. F.; Kalkote, U. R. *J. Org. Chem.* **2006**, *71*, 8986.

(39) The relative effect of ether and ester allylic functionality on cross-metathesis rate has not been quantified but there are a number of publications that claim that chelation between ester carbonyl oxygen and Ru disables cross-metathesis events. For example, see: (a) McNaughton, B. R.; Bucholtz, K. M.; Camaano-Moure, A.; Miller, B. L. *Org. Lett.* **2005**, *7*, 733. (b) Michaelis, S.; Blechert, S. *Org. Lett.* **2005**, *7*, 5513. (c) Sheddan, N. A.; Arion, V. B.; Mulzer, J. *Tetrahedron Lett.* **2006**, *47*, 6689.

(40) Lewis acids are known to facilitate RCM; see: (a) Marsella, M. J.; Maynard, H. D.; Grubbs, R. H. *Angew. Chem., Int. Ed. Engl.* **1997**, *36*, 1101. (b) Furstner, A.; Langemann, K. *J. Am. Chem. Soc.* **1997**, *119*, 9130. The two papers describe quite different scenarios. In the former, a crown ether is synthesized efficiently via a Group I metal-templated RCM. The

rates.

However, since allylic protecting groups slow down the rate of cyclization modestly, the assumption that these substrates are less efficient or do not work may be misleading if analyses were made on the same time scale as the reaction of the free allylic alcohol. It is possible that many of the reactions for which very low yields have been reported with protected allylic alcohols were not left for an adequate amount of time before carrying out a conversion or yield analysis, or that inappropriate reaction concentrations were employed.

Conclusions

At the appropriate concentrations, all the diene substrates studied converted smoothly and directly to their corresponding cyclooctenones, apparently without the intermediacy of oligomers, though cyclic and acyclic oligomers were detected at higher concentrations (and characterized fully in some cases). Reaction rate is affected modestly by *gem*-dialkylation and the nature of allylic oxygen functions, in stark contrast to many qualitative observations from the synthetic literature where reaction yields can vary from >50% for free alcohols to zero for derivatives.

The first EMs have been *measured* for RCM reactions; while the values are typical for cyclooctannelation, there is remarkable sensitivity to the nature of the allylic substituent. The high EM for benzoate **1b** appears to arise from relatively low CM rates for this substrate; *the substrate that cyclizes most rapidly* is not necessarily the one that *cyclizes most efficiently*.

These results indicate strongly that substituent effects on CM must be considered in addition to the likely rate of cyclization when planning or evaluating an RCM reaction or outcomes. Quantification of the interplay of structure and reactivity will aid rational activity and efficiency-based design of RCM substrates, especially for challenging synthetic targets. The overall equilibrium constant for the process is important, but the reaction outcome is determined by a wider range of subtle factors, which we hope to understand more fully through electronic structure calculations and detailed study of reaction kinetics.

Experimental Section

Full preparative and characterization details for all compounds are reported in the Supporting Information.

Procedure for Determining Reaction Concentration/Time Profiles. Titanium(IV) isopropoxide (30 mol %) was added to a 0.01 M solution of dienes **1a**–**c** and **6a**–**c** in dry, degassed dichloromethane and the solution was stirred in a jacketed flask connected to a circulating chiller to maintain constant temperature (25.0 ± 0.1 °C) under an atmosphere of nitrogen. An aliquot (0.2 mL) was removed from the reaction and transferred to a GC vial before the addition of a solution of Grubbs' second generation precatalyst **3** (2 mol %) in CH_2Cl_2 (0.2 mL); aliquots were then withdrawn from the reaction at varying intervals throughout. Prior to starting the experiment, Supelco 1 mL C-18 solid-phase extraction tubes were preconditioned with 1 mL each of 20% water/acetonitrile. Each aliquot subsequently withdrawn from the reaction was passed through one of these tubes. Samples were eluted with 1 mL each of acetonitrile into GC vials for analysis.

latter paper describes the facilitation by a Ti(IV) cocatalyst of an RCM catalyzed by **4**. However, the lower Lewis acidity of **3** is expected to diminish the effect of chelate formation on RCM; see: Furstner, A.; Thiel, O. R.; Lehmann, C. W. *Organometallics* **2002**, *21*, 331.

Procedure for Determining Effective Molarity. Titanium isopropoxide (0.3 equiv) was added to solutions of **1a** in dry, degassed CH_2Cl_2 in dry reactor tubes and the solutions were refluxed under nitrogen for 30 min: **3** (5 mol %) was added and the solution refluxed overnight. These samples were not SPE treated on the basis that catalyst activity is likely to be minimal after $>6 \times 10^4$ s at reflux in CH_2Cl_2 so there is no issue arising from further reaction during sample concentration.

All spectra for the experiment upon repetition were run with $D_1 = 5$ s ($5T_1$, longest T_1 measured at 1 s) to ensure no slow relaxing signals were unresolved within the spectral time scale. The spectral window was set to 40 ppm (between −100 and −140 ppm, centered at −120 ppm), and 1024 scans were recorded. Folding/wrapping was interrogated recording the full spectral window (0 to −300 ppm) in 100 ppm increments ($D_1 = 5$ s, 256 scans per experiment). No folding or wrapping was observed into the product spectral window.

Each solution was cooled and the solvent carefully distilled off at atmospheric pressure to prevent loss of volatile **2a**. The crude products were analyzed by $\{^1H\}^{19}F$ NMR and ES-MS. Larger products were not characterized from these mixtures but a series of larger rings were identified in the ES^- mass spectrum; 16-membered-ring species were synthesized by another route (vide infra).

Duplicate EM Determination for 1a with Modified Product Isolation. Experiments were run between 5 and 40 mM, this time leaving weaker solutions (5−10 mM) to evaporate at room temperature at atmospheric pressure. ^{19}F NMR spectra were obtained directly from the stronger solutions (15−40 mM) to confirm that **2a** was not lost during slow evaporation. All spectra for these experiments were run with $D_1 = 5$ s (vide infra) to ensure no slow relaxing signals were unresolved within the spectral time scale.

Acknowledgment. We thank the EPSRC and the University of Leicester (DTG studentship for L.M.), and the University of Strathclyde for affording visitor status to L.M. We also wish to acknowledge the use of the EPSRC's (Engineering and Physical Sciences Research Council) National Mass Spectrometry Service Centre, University of Wales Swansea.

Supporting Information Available: Synthetic procedures and characterization data for kinetic substrates, kinetic data and details of EM determination, oligomer characterization, and synthesis of 16-membered products. This material is available free of charge via the Internet at http://pubs.acs.org.

JO702726B

JOC Article

Total Syntheses of Conformationally Locked Difluorinated Pentopyranose Analogues and a Pentopyranosyl Phosphate Mimetic

Jonathan A. L. Miles,[†] Lisa Mitchell,[†,‡] Jonathan M. Percy,*[,‡] Kuldip Singh,[†] and E. Uneyama[†]

Department of Chemistry, University of Leicester, University Road, Leicester LE1 7RH, U.K., and Department of Pure and Applied Chemistry, WestCHEM, University of Strathclyde, Thomas Graham Building, 295 Cathedral Street, Glasgow G1 1XL, U.K.

jonathan.percy@strath.ac.uk

Received September 30, 2006

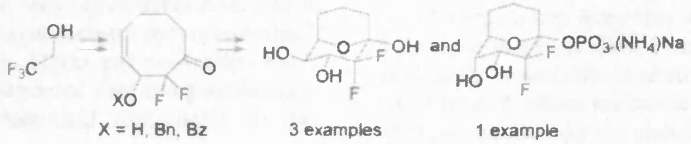

Trifluoroethanol has been elaborated, via a telescoped sequence involving a metalated difluoroenol, a difluoroallylic alcohol, [2,3]-Wittig rearrangement, and ultimately an RCM reaction and requiring minimal intermediate purification, to a number of cyclooctenone intermediates. Epoxidation of these intermediates followed by transannular ring opening or dihydroxylation, then transannular hemiacetalization delivers novel bicyclic analogues of pentopyranoses, which were elaborated (in one case) to an analogue of a glycosyl phosphate.

Introduction

Saccharide recognition is a key event in a wide range of biological processes. Sugars present arrays of hydroxyl groups in a spatially defined manner, and proteins bind to and distinguish between different saccharides by forming complex networks of hydrogen bonds to them.[1] The core six-membered oxacycle in pyranose sugars also exerts a significant effect on a range of conformational properties via the anomeric effect.[2] The linkages between sugars in di- and higher saccharides are acetals, and a wide range of glycosyltransferases and glycosidases exist to synthesize and cleave those linkages, respectively. Saccharide mimetics,[3] which present hydroxyl groups in a useful manner but cannot be cleaved from their sites of attachment by glycosidases, could be useful probes of sugar-processing enzymes. If the mimetics lack the pyranose oxygen and therefore the anomeric effect, different conformers could become available.

Many groups have described the synthesis of five-, six-, and seven-membered carbocyclic analogues of saccharides. More recently, highly functionalized cyclooctane derivatives have attracted attention as ring-expanded analogues (Chart 1). The Sinaÿ group combined the ideas of the stability of carbasugars with the potential for occupying uncharted conformational space, synthesizing **1**, which was shown by NOE to occupy a boat-chair conformation related to that of the corresponding galac-

[†] University of Leicester.
[‡] University of Strathclyde.

(1) (a) Loganathan, D.; Aich, U. *Glycobiology* **2006**, *16*, 343. (b) Laederach, A.; Reilly, P. J. *Proteins: Struct., Funct., Bioinf.* **2005**, *60*, 591. (c) Carcabal, P.; Jockusch, R. A.; Hunig, I.; Snoek, L. C.; Kroemer, R. T.; Davis, B. G.; Gamblin, D. P.; Compagnon, I.; Oomens, J.; Simons, J. P. *J. Am. Chem. Soc.* **2005**, *127*, 11414. (d) Flint, J.; Bolam, D. N.; Nurizzo, D.; Taylor, E. J.; Williamson, M. P.; Walters, C.; Davies, G. J.; Gilbert, H. J. *J. Biol. Chem.* **2005**, *280*, 23718. (e) Fernandez, M. D.; Canada, F. J.; Jimenez-Barbero, J.; Cuevas, G. *J. Am. Chem. Soc.* **2005**, *127*, 7379. (f) Mitchell, E. P.; Sabin, C.; Snajdrova, L.; Pokorna, M.; Perret, S.; Gautier, C.; Hofr, C.; Gilboa-Garber, N.; Koca, J.; Wimmerova, M.; Imberty, A. *Proteins: Struct., Funct., Bioinf.* **2005**, *58*, 735. (g) Loris, R.; Imberty, A.; Beeckmans, S.; Van, Driessche, E.; Read, J. S.; Bouckaertt, J.; De Greve, H.; Buts, L.; Wyns, L. *J. Biol. Chem.* **2003**, *278*, 16297. (h) Vyas, N. K.; Vyas, M. N.; Chervenak, M. C.; Bundle, D. R.; Pinto, B. M.; Quiocho, F. A. *Proc. Natl. Acad. Sci. U.S.A.* **2003**, *100*, 15023. (i) Pathiaseril, A.; Woods, R. J. *J. Am. Chem. Soc.* **2000**, *122*, 331. (j) Zacharias, M.; Straatsma, T. P.; McCammon, J. A.; Quiocho, F. A. *Biochemistry* **1993**, *32*, 7428. (k) Quiocho, F. A. *Biochem. Soc. Trans.* **1993**, *21*, 442. (l) Jimenez-Barbero, J.; Canada, F. J.; Cuevas, G.; Asensio, J. L.; Aboitiz, N.; Canales, A.; Chavez, M. I.; Fernandez-Alonso, M. C.; Garcia-Herrero, A.; Mari, S.; Vidal, P. *NMR Spectroscopy and Computer Modeling of Carbohydrates: Recent Advances*; ACS Symposium Series 930; American Chemical Society: Washington, DC, 2006; p 60. (m) Bryce, R. A.; Hillier, I. H.; Naismith, J. H. *Biophys. J.* **2001**, *81*, 1373.

(2) (a) Kirby, A. *The Anomeric Effect and Related Stereoelectronic Effects at Oxygen*; Springer-Verlag: Berlin, 1983. (b) For recent mechanistic studies, see: Bennet, A. J.; Kitos, T. E. *J. Chem. Soc., Perkin Trans.* **2002**, *2*, 1207. (c) For a computational examination of the mechanism, see: Dimelow, R. J.; Bryce, R. A.; Masters, A. J.; Hillier, I. H.; Burton, N. A. *J. Chem. Phys.* **2006**, 124. (d) Mohr, M.; Bryce, R. A.; Hillier, I. H. *J. Phys. Chem. A* **2001**, *105*, 8216.

10.1021/jo0620258 CCC: $37.00
Published on Web 02/01/2007

CHART 1

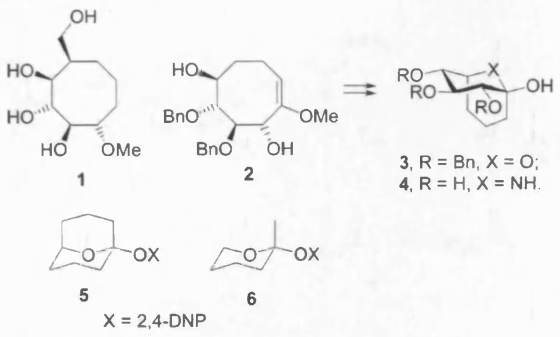

topyranose.[4] The synthesis used carbohydrate starting materials to provide most of the functionality in the products and ensure stereocontrol, exploiting a Lewis acid mediated ring-expanding Claisen rearrangement (described originally by Paquette) as the key step. More recently, Paquette has shown that zirconocene-promoted ring contraction can be used to convert vinylfuranosides to cyclooctane polyols via vinyl cyclobutanones, and a [3,3]-sigmatropic rearrangement again secures the carbocycles.[5] Using a quite different approach, Mehta and co-workers have shown that unsaturated eight-membered ring compounds such as cyclooctatetraene can be elaborated controllably to the corresponding polyols.[6]

The ring-expanding Claisen rearrangement also allows the synthesis of masked cyclooctanones **2**. Van Boom and the Leiden group exploited transannular strain-relieving nucleophilic attack upon a ketone carbonyl group to close a number of bicyclic systems, which provide conformationally locked analogues of sugars **3** and azasugars **4**.[7] The bicyclic array is very interesting because of the extremely low reactivity of the pseudoglycosidic bond. Kirby and co-workers showed that **5** was 10^{13} times less reactive than **6** because of the way the bicyclic architecture opposes stabilization of developing positive charge at the pseudoanomeric carbon through oxacarbenium ion formation as the pseudoglycosidic bond stretches toward cleavage.[8] The idea of using conformational locking to allow mimicry

SCHEME 1. Outline of Sequence Showing the Development of NDP Sugar Analogues

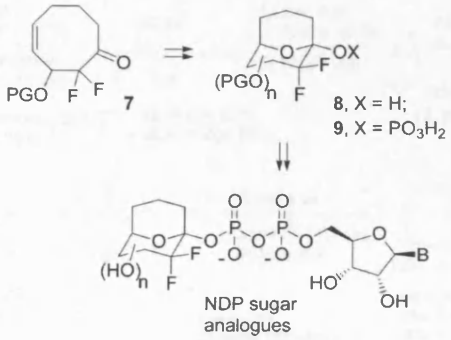

of conformations traversed at transition states has also been explored extensively.[9]

We[10] and others[11] have developed a number of approaches for the synthesis of fluorinated analogues of the molecules of nature from commercial fluorinated starting materials, in which RCM forms a key step. One of our projects aimed to develop a de novo route via difluorinated cyclooctenones **7** to conformationally locked difluorinated analogues **8** of pentoses and their phosphates **9**, which we would advance ultimately to analogues of NDP sugars, with the global aim of the development of new chemical tools for the study of glycosyltransferase enzymes. The syntheses would start from sustainable fluorinated starting materials, avoiding the use of materials banned under the Montreal and Kyoto Protocols (Scheme 1). Although these protocols deal with large-scale production, they affect the availability and supply of materials for use on the laboratory scale; the development of a new methodology based on banned substances would therefore seem like nugatory effort.

The fluorine atoms would allow location of the compounds in vitro or in vivo by ^{19}F NMR, and they could report conformational changes in the hydroxyl-bearing ring through $^{3}J_{H-F}$ coupling constants.[12] In our preliminary publications, we showed how we could use metalated difluoroalkene chemistry to advance trifluoroethanol rapidly to precursors to eight-membered rings and then close them via RCM[13] to afford difluorinated cyclooctenones, templates for stereoselective oxidation (dihydroxylation[14] or epoxidation[15]), and transannular reactions. These preliminary findings delivered a number of model polyol systems which contain the distinctly unnatural *gem*-dimethyl and *N,N*-diethylcarbamoyloxy groups, which we now wished to delete. We wished to explore a route, which would avoid the use of strong base/low-temperature conditions

(3) (a) Haneda, T.; Goekjian, P. G.; Kim, S. H.; Kishi, Y. *J. Org. Chem.* **1992**, *57*, 490. (b) Goekjian, P. G.; Wu, T. C.; Kang, H. Y.; Kishi, Y. *J. Org. Chem.* **1991**, *56*, 6422. (c) Kuntz, D. A.; Ghavami, A.; Johnston, B. D.; Pinto, B. M.; Rose, D. R. *Tetrahedron: Asymmetry* **2005**, *16*, 25. (d) Yang, G. L.; Schmieg, J.; Tsuji, M.; Franck, R. W. *Angew. Chem., Int. Ed.* **2004**, *43*, 3818. (e) Mikkelsen, L. M.; Hernaiz, M. J.; Martin-Pastor, M.; Skrydstrup, T.; Jimenez-Barbero, J. *J. Am. Chem. Soc.* **2002**, *124*, 14940. For reviews, see: (f) Sears, P.; Wong, C. H. *Angew. Chem., Int. Ed.* **1999**, *38*, 2301. (g) Wong, C. H. *Acc. Chem. Res.* **1999**, *32*, 376.

(4) (a) Wang, W.; Zhang, Y. M.; Sollogoub, M.; Sinay, P. *Angew. Chem., Int. Ed.* **2000**, *39*, 2466. (b) Wang, W.; Zhang, Y. M.; Zhou, H. H.; Bleriot, Y.; Sinay, P. *Eur. J. Org. Chem.* **2001**, 1053.

(5) Paquette, L. A.; Zhang, Y. L. *J. Org. Chem.* **2006**, *71*, 4353.

(6) (a) Mehta, G.; Pallavi, K. *Tetrahedron Lett.* **2004**, *45*, 3865. (b) Mehta, G.; Pallavi, K. *Chem. Commun.* **2002**, 2828. (c) For a review of earlier work, see: Mehta, G.; Singh, V. *Chem. Rev.* **1999**, *99*, 881.

(7) van Hooft, P. A. V.; Litjens, R.; van der Marel, G. A.; van Boeckel, C. A. A.; van Boom, J. H. *Org. Lett.* **2001**, *3*, 731.

(8) Briggs, A. J.; Evans, C. M.; Glenn, R.; Kirby, A. J. *J. Chem. Soc., Perkin Trans. 2* **1983**, 1637.

(9) For recent examples, see: (a) Bleriot, Y.; Vadivel, S. K.; Herrera, A. J.; Greig, I. R.; Kirby, A. J.; Sinay, P. *Tetrahedron* **2004**, *60*, 6813. (b) Lorthiois, E.; Meyyappan, M.; Vasella, A. *Chem. Commun.* **2000**, 1829.

(10) (a) Audouard, C.; Fawcett, J.; Griffiths, G. A.; Percy, J. M.; Pintat, S.; Smith, C. A. *Org. Biomol. Chem.* **2004**, *2*, 528. (b) Audouard, C.; Fawcett, J.; Griffith, G. A.; Kerouredan, E.; Miah, A.; Percy, J. M.; Yang, H. L. *Org. Lett.* **2004**, *6*, 4269. (c) Kariuki, B. M.; Owton, W. M.; Percy, J. M.; Pintat, S.; Smith, C. A.; Spencer, N. S.; Thomas, A. C.; Watson, M. *Chem. Commun.* **2002**, 228. (d) Butt, A. H.; Percy, J. M.; Spencer, N. S. *Chem. Commun.* **2000**, 1691.

(11) (a) Fustero, S.; Catalan, S.; Piera, J.; Sanz-Cervera, J. F.; Fernandez, B.; Acena, J. L. *J. Org. Chem.* **2006**, *71*, 4010. (b) Fustero, S.; Sanchez-Rosello, M.; Jimenez, D.; Sanz-Cervera, J. F.; del Pozo, C.; Acena, J. L. *J. Org. Chem.* **2006**, *71*, 2706. (c) Fustero, S.; Bartolome, A.; Sanz-Cervera, J. F.; Sanchez-Rosello, M.; Soler, J. G.; de Arellano, C. R.; Fuentes, A. S. *Org. Lett.* **2003**, *5*, 2523. (d) Yang, Y. Y.; Meng, W. D.; Qing, F. L. *Org. Lett.* **2004**, *6*, 4257. (e) You, Z. W.; Wu, Y. Y.; Qing, F. L. *Tetrahedron Lett.* **2004**, *45*, 9479. (f) De Matteis, V.; van Delft, F. L.; de Gelder, R.; Tiebes, J.; Rutjes, F. *Tetrahedron Lett.* **2004**, *45*, 959. (g) Marhold, M.; Buer, A.; Hiemstra, H.; van Maarseveen, J. H.; Haufe, G. *Tetrahedron Lett.* **2004**, *45*, 57.

(12) Thibaudeau, C.; Plavec, J.; Chattopadhyaya, J. *J. Org. Chem.* **1998**, *63*, 4967.

(13) Griffith, G. A.; Percy, J. M.; Pintat, S.; Smith, C. A.; Spencer, N.; Uneyama, E. *Org. Biomol. Chem.* **2005**, *3*, 2701.

(14) Fawcett, J.; Griffiths, G. A.; Percy, J. M.; Pintat, S.; Smith, C. A.; Spencer, N.; Uneyama, E. *Chem. Commun.* **2004**, 302.

(15) Fawcett, J.; Griffith, G. A.; Percy, J. M.; Uneyama, E. *Org. Lett.* **2004**, *6*, 1277.

SCHEME 2. Retrosynthetic Analysis of Key Cyclooctenone 14

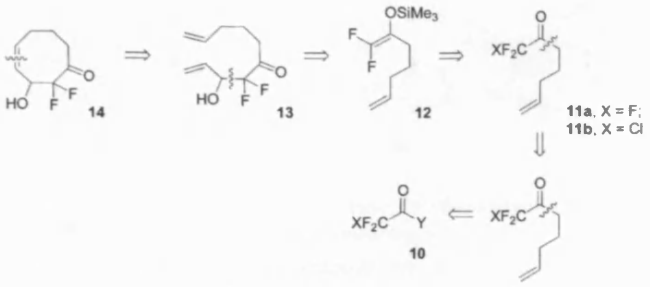

SCHEME 3. Attempted Halodifluoromethyl Ketone Syntheses

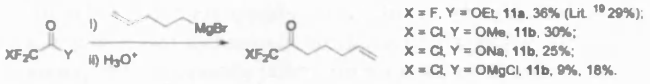

if possible and minimize the number of purifications in the sequences, to complete syntheses of a number of analogues of sugar-like and an illustrative phosphate monoester through stereoselective oxidation reactions and the development of an effective phosphorylation strategy. We report the results of these studies in this manuscript.

Results and Discussion

Attempted Development of a Scaleable Route Based on Reductive Dehalogenation. Scheme 2 shows the retrosynthetic analysis carried out for **14** from key intermediate α,α-difluoro-β-hydroxy ketone **13**. The literature describes a number of methods for the generation of difluorinated silyl enol ether **12**, which could make **13** available through aldol chemistry under potentially scaleable conditions (Scheme 2).

Ishihara[16] and Uneyama[17] have described methods for the synthesis of difluoroenol silyl ethers such as **12** from chlorodifluoromethyl and trifluoromethyl ketones, respectively, so we prepared **11a** and **11b** from commercial 1-bromopent-4-ene via reaction of the Grignard reagent with electrophiles **10** derived from chlorodifluoroacetic or trifluoroacetic acids (Scheme 3).[18] These starting materials are available at low cost and appear to be sustainable.

Typical reaction conditions for this type of perhalomethylketone synthesis use ester electrophiles or, alternatively, an excess of Grignard reagent and the free acid.[18] The latter procedure would waste a moderately expensive bromide, so we preformed the sodium or magnesium salts using NaH or *i*-PrMgCl.

A large number of unsuccessful experiments are summarized in the Scheme. The ketones were isolated by distillation after careful extraction of the product into pentane/diethyl ether, and hydration of the ketones was a distinct problem during these procedures. The poor yield of the trifluoromethyl ketone was comparable to that obtained by Laurent and co-workers.[19] We were unable to synthesize **12** in more than trace amounts from either **11a** or **11b** under published (Zn, Me_3SiCl, MeCN, Δ or excess Mg/Me_3SiCl, DMF) conditions. Uneyama[17] has reported

SCHEME 4. Cyclooctenone Syntheses Based on Metalated Difluoroenol Acetal Chemistry

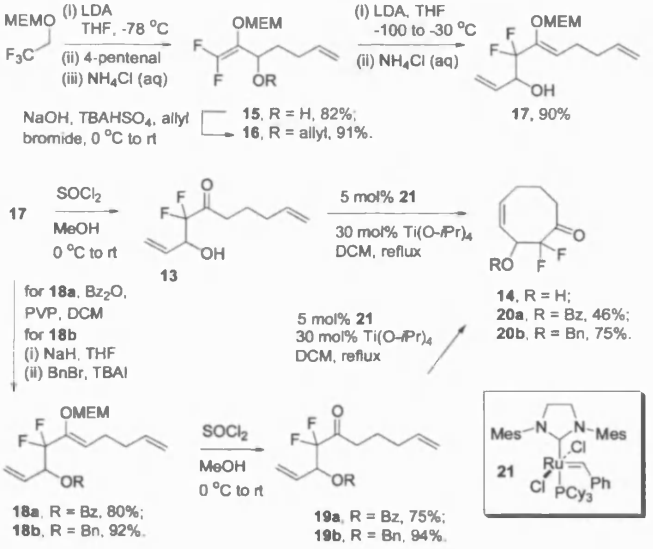

that aliphatic trifluoromethyl ketones undergo slow reductive defluorination under the latter conditions; for **11a**, the reaction was prohibitively slow. We also attempted to use the conditions described by Ishihara[18] for direct aldol reaction between **11b** and acrolein or cinnamaldehyde. The best result (ca. 10% conversion) was obtained with the latter electrophile despite considerable efforts to optimize the reactions, which stopped at very low conversion, and we were not able to isolate any of **13**. We therefore decided to use our metalated difluoroenol chemistry to develop a working strategy to the target aldol.

Successful Dehydrofluorination/Metalation Route. Known[20] difluoroallylic alcohol **15** was synthesized in good yield (82%, 20 g scale) using our published procedure from the MEM-ether of trifluoroethanol and 4-pentenal (Scheme 4).[21] The Kugelrohr-distilled alcohol was allylated under phase-transfer conditions[22] to ether **16** (91%) and progressed without further purification (Scheme 4).

The rearrangement of **16** took place over 4 h on warming from −100 to −30 °C, and chromatography of the product returned a disappointing yield of pure **17** (ca. 30%) initially. We were able to purify hydroxyketone **13** (following enol ether cleavage[23]) by Kugelrohr distillation improving the yield to 50% over the two steps and removing two chromatographic purifications from the sequence if the enol ether was cleaved directly from crude [2,3]-Wittig product. In the RCM reaction (5 mol % of **21**, 30 mol % of Ti(O-*i*Pr)$_4$, 5 mM in DCM), starting material appeared to be consumed completely within 2 h but the volatile cyclooctenone product **14** was difficult to isolate. Careful removal of the dichloromethane solvent by distillation at atmospheric pressure and then eluting the residue through a polymer-bound thiol SPE tube with methanol afforded the product in modest (estimated 60%) yield. This first-generation synthesis provides proof of concept but delivered a rather

(16) Yamana, M.; Ishihara, T.; Ando, T. *Tetrahedron Lett.* **1983**, *24*, 507.
(17) (a) Amii, H.; Kobayashi, T.; Hatamoto, Y.; Uneyama, K. *Chem. Commun.* **1999**, 1323. (b) For a review, see: Uneyama, K.; Amii, H. *J. Fluorine Chem.* **2002**, *114*, 127.
(18) Kuroboshi, M.; Ishihara, T. *Bull. Chem. Soc. Jpn.* **1990**, *63*, 428.
(19) Felix, C.; Laurent, A.; Mison, P. *J. Fluorine Chem.* **1995**, *70*, 71.
(20) Griffith, G. A.; Hillier, I. H.; Percy, J. M.; Roig, R.; Vincent, M. A. *J. Org. Chem.* **2006**, *71*, 8250.
(21) Patel, S. T.; Percy, J. M.; Wilkes, R. D. *Tetrahedron* **1995**, *51*, 9201.
(22) Patel, S. T.; Percy, J. M.; Wilkes, R. D. *J. Org. Chem.* **1996**, *61*, 166.
(23) Broadhurst, M. J.; Brown, S. J.; Percy, J. M.; Prime, M. E. *J. Chem. Soc., Perkin Trans. 1* **2000**, 3217.

CHART 2

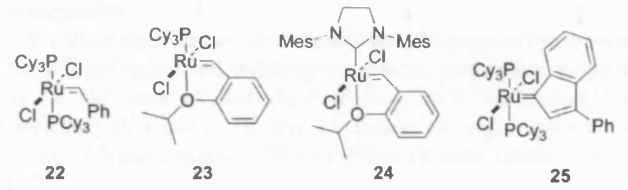

22 23 24 25

volatile product, which was not easy to characterize fully, in ca. 20% overall yield from trifluoroethanol.

We therefore sought to optimize the sequence. The [2,3]-Wittig step afforded good estimated yields (ca. 90%) of up to 24 mmol of homoallylic alcohol **17** which was sufficiently pure by ^{1}H and ^{19}F NMR spectra and GC-MS to take on directly. Material of the same quality could also be obtained by taking crude undistilled difluoroallylic alcohol through the allylation/rearrangement sequence (after checking the purity from the ^{1}H and ^{19}F NMR spectra). We esterified **17** by shaking with benzoic anhydride and polymer-supported base poly(4-vinylpyridine) in dichloromethane to afford **18a** and then cleaved the MEM group directly from the crude material. Benzoate **19a** was purified before RCM in the first round of reactions and underwent RCM (second-generation Grubbs' catalyst **21**, Ti(O*i*-Pr)$_4$ cocatalyst) to afford **20a** in acceptable (46%) yield after chromatography. We subsequently found that the unpurified precursor also underwent RCM in good yield. Trace contaminants of Ru could be removed by eluting the columned material through thiol SPE tubes with MeOH. The entire sequence from the starting trifluoroethyl acetal therefore finally involves only a single purification, which is a column after RCM, and the overall yield of **20a** is ca. 30% from trifluoroethanol. Rearrangement product **17** was also benzylated (92%, using an excess of sodium hydride to ensure complete alkoxide formation), subjected to enol ether methanolysis (94%), and taken through the RCM without purification to afford **20b** in good (75%) yield.

Though superficially less attractive than the Ishihara and Uneyama aldol syntheses because it contains two low-temperature steps, our route delivers gram-scale quantities of the RCM product reproducibly with 30 mmol of material coming through the [2,3]-Wittig rearrangement (the most demanding step) and with minimal purification.

Developing Conditions for the RCM Reaction. Many of the RCM reactions[24] which form medium rings[25] use relatively high loadings of ruthenium catalysts, suggesting that either catalytic efficiency is low or cyclizations are very slow,[26] or both. We screened commercial precatalysts **21**−**25** (Chart 2) for the cyclization of **19a** and **19b** at an initial loading of 5 mol %.

SCHEME 5. Attempted RCM with the Neolyst Catalyst

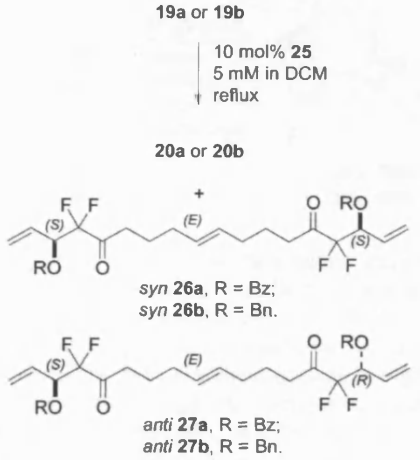

The reaction with Neolyst catalyst **25**[27] (10 mol %) returned significant quantities of homodimeric cross-metathesis products from **19a** as a mixture of C_2-symmetric racemic *syn* and achiral and *meso anti* diastereoisomers **26a** and **27a**, respectively, in moderate (34% isolated from a possible 50%) yield, along with recovered starting material (42%) and traces of RCM product **20a** (Scheme 5).

A similar result was observed from benzyl ether **19b** with the isolation of **26b** and **27b** (38% combined) along with recovered starting material (36%) and a small amount of **20b** (4%). The reaction was started with a lower loading (5%) of catalyst, followed by the addition of a further portion (5%) when the reaction did not appear to proceed. The homodimerization was observed with and without the Ti(IV) cocatalyst.

The *isolation* of terminal alkene open-chain homodimers from an RCM reaction run at high dilution is relatively unusual.[28] The ^{1}H NMR spectra obtained for the mixtures of **26** and **27** are relatively simple and highly symmetrical, consistent only with the formation of these dimers. The COSYs show the relationship between the vinylic proton of the symmetrical internal alkene and the allylic methylene protons clearly. The connectivity between the terminal alkene and the allylic methine is also established unambiguously. The 1D ^{1}H and ^{13}C NMR spectra fail to show the presence of the different stereoisomers clearly, though some of the methylene carbon signals are doubled. The 1D {^{1}H}^{19}F NMR spectrum appears to show the only difference between the diastereoisomers; formally, there are four ^{19}F environments arising from two pairs of enantiotopic fluorines (two environments) in the achiral and *meso* stereoisomers and two pairs of homotopic fluorines (two environments) in the C_2-symmetric species (similar considerations apply to various protons, but the higher chemical shift range of fluorine nucleii reveals more subtle differences in environment). Though we observed four environments for **26b**/**27b**, there were seven for **26a**/**27a**; given the rather flexible nature of these extended

(24) For general reviews of RCM issues, see: (a) Conrad, J. C.; Fogg, D. E. *Curr. Org. Chem.* **2006**, *10*, 185. (b) Nicolaou, K. C.; Bulger, P. G.; Sarlah, D. *Angew. Chem., Int. Ed.* **2005**, *44*, 4490. (c) Furstner, A. *Angew. Chem., Int. Ed.* **2000**, *39*, 3013.

(25) For reviews of medium ring forming RCM, see: (a) Deiters, A.; Martin, S. F. *Chem. Rev.* **2004**, *104*, 2199. (b) Maier, M. E. *Angew. Chem., Int. Ed.* **2000**, *39*, 2073. (c) Yet, L. *Chem. Rev.* **2000**, *100*, 2963. (d) Michaut, A.; Rodriguez, J. *Angew. Chem., Int. Ed.* **2006**, *45*, 5740. For recent examples, see: (e) Bleriot, Y.; Giroult, A.; Mallet, J. M.; Rodriguez, E.; Vogel, P.; Sinay, P. *Tetrahedron: Asymmetry* **2002**, *13*, 2553. (f) Bourgeois, D.; Mahuteau, J.; Pancrazi, A.; Nolan, S. P.; Prunet, J. *Synthesis* **2000**, 869. (g) Boyer, F. D.; Hanna, I.; Nolan, S. P. *J. Org. Chem.* **2001**, *66*, 4094. (h) Buono, F.; Tenaglia, A. *J. Org. Chem.* **2000**, *65*, 3869. (i) Furstner, A.; Langemann, K. *J. Org. Chem.* **1996**, *61*, 8746. (j) Buszek, K. R.; Sato, N.; Jeong, Y. *Tetrahedron Lett.* **2002**, *43*, 181.

(26) Illuminati, G.; Mandolini, L. *Acc. Chem. Res.* **1981**, *14*, 95.

(27) Furstner, A.; Guth, O.; Duffels, A.; Seidel, G.; Liebl, M.; Gabor, B.; Mynott, R. *Chem.−Eur. J.* **2001**, *7*, 4811.

(28) (a) Creighton and co-workers identified an open-chain dimer by LC-MS from a mixture of products generated during a cyclooctannulation reaction: Creighton, C. J.; Du, Y. M.; Reitz, A. B. *Bioorg. Med. Chem.* **2004**, *12*, 4375. For recent applications, see: (b) Creighton, C. J.; Du, Y. M.; Santulli, R. J.; Tounge, B. A.; Reitz, A. B. *Bioorg. Med. Chem. Lett.* **2006**, *16*, 3971. (c) Abell, A. D.; Brown, K. M.; Coxon, J. M.; Jones, M. A.; Miyamoto, S.; Neffe, A. T.; Nikkel, J. M.; Stuart, B. G. *Peptides* **2005**, *26*, 251.

molecules, conformational erosion of symmetry is perhaps unsurprising.

We were surprised by the homodimerization given the reports that this ruthenium indenylidene complex is particularly suitable for the formation of medium-sized rings by RCM. Indeed this (pre)catalyst is more effective at closing the eight-membered E-ring of Nakadomarin A **28** than either Grubbs' catalyst **21** or **22**.[27]

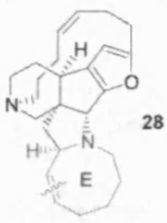

The effectiveness of Neolyst **25** for slow RCM reactions is attributed to higher stability in solution, though it is not clear if this refers to slow initial dissociation of phosphane, slow recapture of the catalytically active 14e complex, or slow second-order decomposition of the latter reactive species.[29] It appears that the RCM is slow for **19a** and **19b** with this precatalyst and that **26** and **27**, once formed, either are too unreactive to form η^2-complexes with the methylidene 14e complex which must now carry the chain or cannot progress to metallocyclobutanes from the η^2-complexes. The presence of phosphane, rather than the NHC ligand, is known to make metallocyclobutane formation less favorable. Relatively rapid consumption and recycling of **26** and **27** would be expected under these conditions. The internal alkene derives from cross metathesis between type I alkenes,[30] which is normally fast, so we have observed an interruption of the normally rapid retro-cross metathesis. Exposure of a purified **26b/27b** mixture to 5 mol % of **21** in the presence of the Ti(IV) cocatalyst resulted in 50% conversion to **20b** after 18 h as the sole product by ^{19}F NMR (the remainder was unreacted starting material). Mixing the crude product with a sample of authentic **20b** and running the GC of the mixture resulted in a single peak being observed. Clearly, the retro-cross metathesis is not rapid under these conditions, even with the more reactive precatalyst **21**.

Catalyst **22** alone will not catalyze RCM of any of our substrates; the presence of the Ti(IV) cocatalyst is required to achieve slow cyclization. Second-generation catalyst **21** is the most effective catalyst explored for the cyclooctannulation reaction, and despite the generally lower Lewis acidity of the alkylidene when the NHC ligand replaces phosphane, the Ti(IV) cocatalyst still exerted a small positive qualitative effect on the reaction outcome. Second-generation Grubbs−Hoveyda catalyst[31] **24** showed comparable reactivity to **21** (in terms of apparent rate of consumption of **19a**) but afforded a lower yield of eight-membered cyclic products under any given conditions due to oligomer formation, whereas the corresponding first-generation catalyst **23** was ineffective.

Scale-up requires reactions that can be run at concentrations approaching 0.01 M or better, or the volumes of solvent required become prohibitive for normal laboratory equipment. We therefore sought to explore the effects of concentration upon the metathesis outcomes qualitatively. The RCM of benzoate **19a** could be carried out successfully up to 20 mM, with dimerization and other side reactions starting at higher concentrations. This is a relatively high concentration compared to most of those used in the literature, and its use has allowed the preparation of gram quantities of material. Higher dilution was required for benzyl ether **19b** (2.5 mM) and alcohol **13** (1 mM); significant quantities of side products were formed at 20 mM in these cases. Quantitative aspects of these investigations will be presented elsewhere.

SCHEME 6. Dioxirane Oxidations

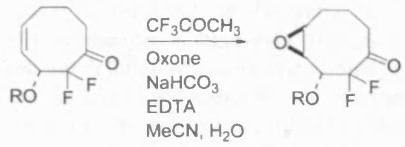

20a, R = Bz; **29a**, 75%;
20b, R = Bn. **29b**, 50%.

Elaboration of RCM Products to Protected Pentopyranose Analogues via Oxidation Transformations. Epoxides **29a** and **29b** were made using the dioxirane method of Yang[32] which was diastereofacially selective (Scheme 6). In the case of benzyl ether **20b**, a trace of benzoate **29a** was observed in the product consistent with oxidation at the benzylic methylene by the reactive dioxirane.[33] The sharp ^{19}F NMR spectra of the crude products showed the formation of a single diastereoisomer in each case with yield loss occurring on purification and removal of the hydrate of the trifluoroacetone. Neither product formed crystals of sufficient quality for the sense of stereoselection to be confirmed directly, but the size of J between H-1 and H-2 provides a strong indication; at ca. 9 Hz, it is more likely to arise from a *trans* pseudodiaxial relationship between these protons in electron-deficient environments, consistent with a *trans* relationship between the benzoyloxy (or benzyloxy) and epoxide C−O bonds rather than a *cis* arrangement. This conclusion is supported strongly by precedent from previous systems which crystallized well[14] and the outcome of epoxide-opening reactions (vide infra).

The results also appear to be consistent with the sense of diastereofacial selection reported by Curci and co-workers[34] during the acetone/potassium caroate epoxidation of cyclooctenol and in our preliminary studies; dioxirane attack occurs on the more sterically open face of the alkene (assuming the solution conformer type or population is not modified significantly by the presence of the protecting group).[13] Hydrogen bond formation to a hydroxyl group clearly cannot play a part in controlling this reaction because the outcome is the same when the hydroxyl group is protected.

Epoxide hydrolysis was carried out under microwave conditions in most cases. We used *N*-methylimidazole as a base

(29) Sanford, M. S.; Love, J. A.; Grubbs, R. H. *J. Am. Chem. Soc.* **2001**, *123*, 6543.

(30) Chatterjee, A. K.; Choi, T. L.; Sanders, D. P.; Grubbs, R. H. *J. Am. Chem. Soc.* **2003**, *125*, 11360.

(31) (a) Kingsbury, J. S.; Harrity, J. P. A.; Bonitatebus, P. J.; Hoveyda, A. H. *J. Am. Chem. Soc.* **1999**, *121*, 791. (b) For a review, see: Hoveyda, A. H.; Gillingham, D. G.; Van Veldhuizen, J. J.; Kataoka, O.; Garber, S. B.; Kingsbury, J. S.; Harrity, J. P. A. *Org. Biomol. Chem.* **2004**, *2*, 8.

(32) Yang, D.; Wong, M.-K.; Yip, Y.-C. *J. Org. Chem.* **1995**, *60*, 3887.

(33) For examples of related oxidations, see: (a) Csuk, R.; Dorr, P. *Tetrahedron* **1994**, *50*, 9983. (b) Angibeaud, P.; Defaye, J.; Gadelle, A.; Utille, J. P. *Synthesis* **1985**, 1123. (c) Hayes, C. J.; Sherlock, A. E.; Selby, M. D. *Org. Biomol. Chem.* **2006**, *4*, 193. (d) Ochiai, M.; Ito, T.; Takahashi, H.; Nakanishi, A.; Toyonari, M.; Sueda, T.; Goto, S.; Shiro, M. *J. Am. Chem. Soc.* **1996**, *118*, 7716. (e) Arnone, A.; Bernardi, R.; Cavicchioli, M.; Resnati, G. *J. Org. Chem.* **1995**, *60*, 2314.

(34) Cicala, G.; Curci, R.; Fiorentino, M.; Laricchiuta, O. *J. Org. Chem.* **1982**, *47*, 2670.

SCHEME 7. Epoxide-Opening Reactions

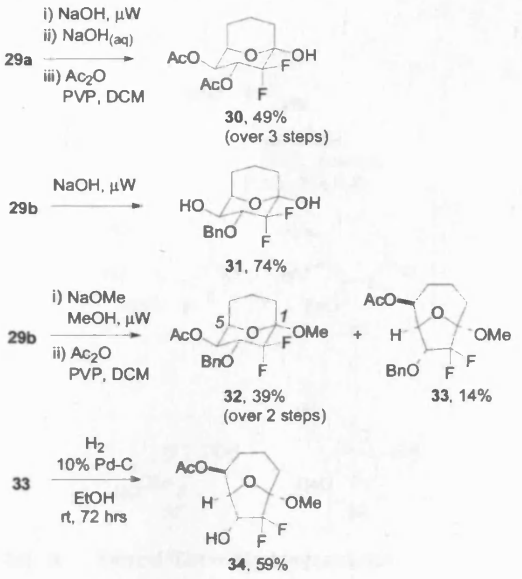

catalyst in our preliminary study[14] but found subsequently that sodium hydroxide works just as well. In the case of **29a**, microwave irradiation in water alone consumed starting material to afford a mixture of products, which was saponified to afford a single crude triol. The crude product was then treated with an excess (5 equiv) of acetic anhydride in DCM containing poly(vinylpyridine) to afford bisacetate **30** (49% over three steps), for which a crystal structure was obtained, confirming the stereochemistry of the ring-opened product. The pseudoanomeric hydroxyl group is expected to be the least nucleophilic in the triol and was unaffected under these neutral acetylation conditions (Scheme 7).

The hydrolysis of epoxy benzyl ether **29b** was more straightforward. Treatment with a dilute (5%) aqueous solution of NaOH in the microwave resulted in the formation of **31** in good (74%) yield. The structure and stereochemistry of this educt also was confirmed by X-ray crystallography. We note that although the two $^3J_{H-F}$ couplings visible in the ^{19}F NMR spectrum are consistent with the presence of a pseudoaxial proton next to the CF_2 center (and therefore a chair-type conformation for this ring) one of the couplings is smaller than the values reported for H−C−C−F dihedrals approaching the antiperiplanar angle. These species are now highly oxygenated, which will lower $^3J_{H-F}$ values generally.

The hydrolytic ring opening of the epoxide is believed to take place via initial reversible attack on the carbonyl followed by irreversible transannular epoxide opening[35] with strain relief. Though the addition of nucleophiles to the carbonyl group of cyclooctanone is opposed by the development of additional transannular strain (an *I*-strain effect), the equilibrium constant for cyanohydrin formation from cyclooctanone is still as high as 1.2.[36] Fluorination next to a ketonic carbonyl group favors the addition of nucleophiles,[37] so there seems to be no difficulty in postulating enough of the hydroxide adduct to trigger a subsequent strain-relieving reaction,[38] if we assume that hydroxide addition is at least as favorable as cyanohydrin formation. The mechanism is supported strongly by the methanolysis of **29b** carried out with catalytic sodium methoxide in methanol under microwave conditions. An inseparable mixture containing two products and starting material (ratio 39:10:1 by ^{19}F NMR) was obtained, but acetylation allowed separation, to afford **32** and **33** (obtained as a mixture with **32**). The presence of the methoxy group at the pseudoanomeric position in **32** is easily detectable in the HMBC spectrum by the presence of a strong $^3J_{C-H}$ cross-peak between the methoxy protons and C-1. The structure of this major product was also confirmed by the elucidation of the molecular structure in the crystal. The only credible route to major product **32** from **29b** involves methoxide attack at the ketone carbonyl of **29b** followed by transannular ring opening which confirms the sense of diastereofacial selection assigned in Scheme 6.

The formation of **33** was unexpected. We detected a similar $^3J_{C-H}$ cross-peak between the methoxy protons and C-1 in the HMBC spectrum, which proves that direct epoxide opening by methoxide does not account for the formation of this second product. The 1D NMR spectra showed smaller $^3J_{H-F}$ coupling constants than usual (the biggest one visible was 9.9 Hz, compared to 17.5 Hz for **32**) suggesting a nonchairlike conformation. One of the ^{19}F NMR signals was very highly split, indicating extended or through-space couplings involving the methoxy group which appears as a doublet in the coupled spectrum and simplifies to a singlet in the $\{^{19}F\}^1H$ spectrum. The structure **33** is assigned on the basis of this evidence; it must be formed by transannular nucleophilic ring opening of the epoxide from C-8 rather than from C-7. We were unable to grow suitable crystals of this material. Unfortunately, hydrogenolysis of the benzyl ether to afford **34** failed to deliver crystalline material, but the HMBC spectrum showed a much stronger CH_3O/C-1 cross-peak. The full scope of this reaction and its mechanism will be discussed elsewhere.

Dihydroxylation of benzyl ether **20b** under UpJohn conditions[39] afforded a mixture of separable diols; both afforded crystals of suitable quality for X-ray crystallographic analysis allowing the identification of the major and minor products as **37** and **38** (3:1), arising from diols **35** and **36** which undergo transannular collapse with relief of strain (Scheme 8).

We were surprised to note that the major product **37** arose from oxidant attack *cis* to the benzyloxy group. In our communication of related work, we advanced an explanation which involved delivery of the osmium reagent to the less accessible concave face of a boat-chair conformer by coordination to the Lewis basic carbonyl group oxygen. In the preliminary case,[13] we were confident of the identity of the major conformer in solution; however, the ^{19}F NMR spectra of **20a** and **20b** merely broaden at temperatures as low as 213 K preventing conformational insight.

This product is still formed under the conditions developed by Donohoe[40] which involve the stoichiometric OsO_4·TMEDA

(35) White, J. D.; Hrnciar, P. *J. Org. Chem.* **2000**, *65*, 9129.
(36) Eliel, E. L.; Wilen, S. H.; Mander, L. N. *Stereochemistry of Organic Compounds*; Wiley-Interscience: New York, 1994; p 769.
(37) Gelb, M. H.; Svaren, J. P.; Abeles, R. H. *Biochemistry* **1985**, *24*, 1813.
(38) (a) For a computational study of the prototypical transannular reaction, see: Parveen; Singh, H.; Singh, T. V.; Bharatam, P. V.; Venugopalan, P. *Theochem: J. Mol. Struct.* **2004**, *685*, 139. For a recent elegant synthetic application of a transannular reaction, see: (b) Nicolaou, K. C.; Carenzi, G. E. A.; Jeso, V. *Angew. Chem., Int. Ed.* **2005**, *44*, 3895. (c) Park, C. M. *J. Org. Chem.* **2006**, *71*, 413.
(39) VanRheenen, V.; Kelly, R. C.; Cha, D. Y. *Tetrahedron Lett.* **1976**, 1973.
(40) Donohoe, T. J. *Synlett* **2002**, 1223.

SCHEME 8. Dihydroxylation and Transannular Collapse

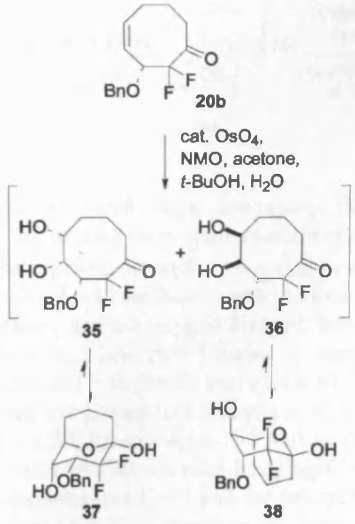

SCHEME 9. Benzyl Ether Hydrogenolyses

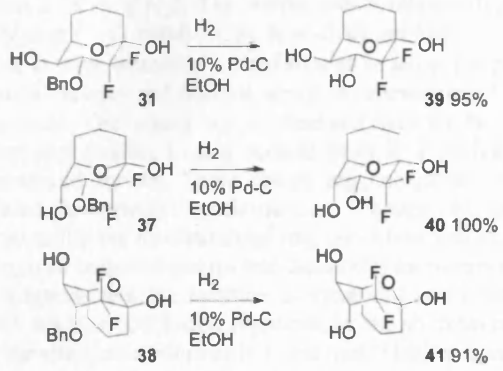

SCHEME 10. Attempted Selective Phosphorylation

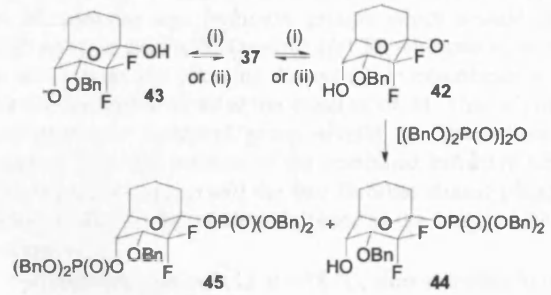

(i) *n*-BuLi, THF, -78 to 0 °C; or,
(ii) NaHMDS, 15-crown-5, THF, -78 to 0 °C.

complex. In an NMR experiment, we observed an ca. 1:1 mixture of osmate esters[41] before acidic methanolysis and a 1:1 mixture of **37** and **38** after workup. The presence of the chelating TMEDA ligand appears to have made the unexpected pathway less favorable but has not prevented its operation. Donohoe and co-workers have suggested that the diamine and the metal oxide appear to stay bound together under the dihydroxylation conditions, so control via coordination to the carbonyl group seems extremely unlikely under these conditions.

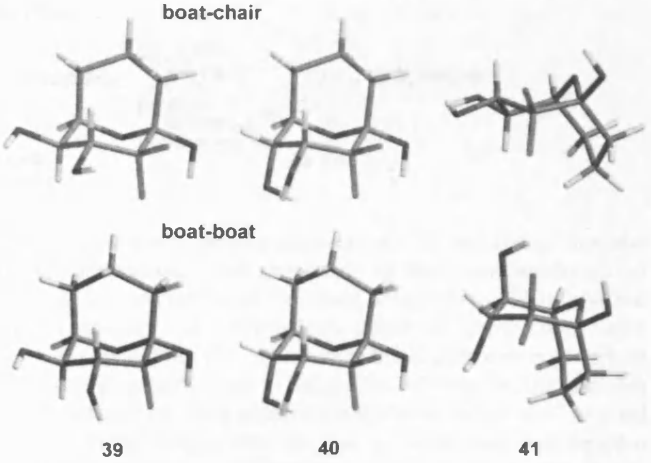

FIGURE 1. Calculated lowest-energy conformations for **39**−**41**. The conformational descriptors refer to the carbon skeleton.

TABLE 1. Energies for RHF 6-31G* Optimized Structures and Calculated Energies (RHF 6-31+G) for the Lowest-Energy Conformers of 39−41**

triol	conformer	E_{rel}/kcal mol^{-1} (6-31G*)	E_{rel} /kcal mol^{-1} (6-311+G**)
39	boat-boat	0.594	0.000
39	boat-chair	3.028	2.310
40	boat-boat	0.000	0.276
40	boat-chair	2.118	2.397
41	boat-boat	2.742	3.150
41	boat-chair	4.774	4.126

We also examined the ruthenium-based dihydroxylation described recently by Tiwari and Misra[42] and found it most effective with rapid conversion of **29b** to the bicyclic products after a short reaction time, though with lower stereoselectivity (**37**/**38** 1.7:1) than under the UpJohn conditions. The elucidation of the controlling factors in these oxidations will require electronic structure calculations which lie outside the scope of this manuscript.

Unprotected Pentopyranose Analogues and Conformational Analysis. Diols **31**, **37**, and **38** were debenzylated smoothly under conventional conditions to afford triols **39**−**41** completing the syntheses of the first three examples of this new class of difluorinated and conformationally locked sugar analogues (Scheme 9). As drawn, **39** represents a locked 2-deoxy-2,2-difluoro analogue of the β-L-lyxo- or β-L-xylopyranoside in the $^1C_4$ conformation whereas **41** is the α-anomer in the $^4C_1$ conformation. As drawn, triol **40** is the locked 2-deoxy-2,2-difluoro analogue of β-D-arabino- or ribopyranoside.

The line formula representations of **39**−**41** conceal a number of close contacts between atoms which will result in Van der Waals strain, notably between **40** and **41** where there are pseudo-1,3-diaxial heavy atoms.

The consequences were explored by carrying out a Monte Carlo conformational search (MMFF94 force field) in Spartan 04.[43] The geometries of all the conformers generated in this way were optimized by ab initio calculations (RHF 6-31G*), and energies were calculated using the 6-311+G** basis set. Table 1 shows the relative energies of the lowest-energy

(41) Donohoe, T. J.; Johnson, P. D.; Pye, R. J.; Keenan, M. *Org. Lett.* **2005**, *7*, 1275. This paper describes a well-characterized cyclic osmate ester complexed to TMEDA.

(42) Tiwari, P.; Misra, A. K. *J. Org. Chem.* **2006**, *71*, 2911.

(43) *Spartan 04*, version 1.0.3, Wavefunction Inc.: 18401 Von Karman Avenue, Suite 370, Irvine, CA 92612, 2005.

SCHEME 11. Phosphorylation Following Secondary Hydroxyl Protection

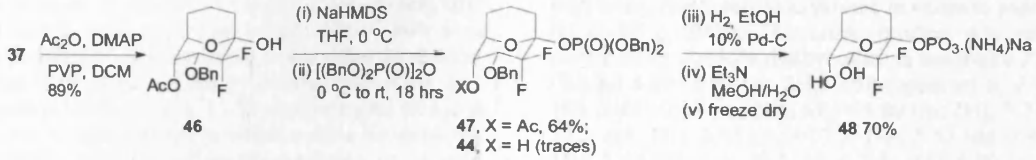

conformers; for all three sugar analogues, these have the functionalized pyran ring in a chair conformation (Figure 1).

Formally, the eight-membered *carbon* skeleta of the bicycles occupy oxygen-bridged boat-boat conformations in the lowest-energy conformers, and the oxygen-bridged boat-chair conformations are both ca. 2 kcal mol^{-1} higher in energy for **39** and **40** and ca. 1 kcal mol^{-1} higher in energy for **41**. The boat-boat conformer brings two groups (substituents on C-3 and C-7) very close together. In **39**, for example, H-3 and an H-7 proton are within 2.1 Å, but it also allows each bridging C−O bond to be close to antiperiplanar to a C−H and the exocyclic C−O bond to be antiperiplanar to a C−C bond. In the boat-chair, H-2 and an H-7 proton are within 2.25 Å, and one of the fluorine atoms is within 2.25 Å of H-2. The antiperiplanar relationships with the bridging C−O bonds in the boat-chair are lost.

There is some distortion of structure **40** to allow the pseudo-1,3-diaxial oxygen and fluorine atoms to relieve some Van der Waals strain. The largest $^3J_{H-F's}$ observed were for **40** and the intermediates leading to and derived from it; a similar value was observed for **39**. These values are consistent with the calculated low-energy conformations. Though **41** has the potential to flip the functionalized ring into a boat and exchange the two axial hydroxyl groups into equatorial environments, the $^3J_{H-F}$ suggests that the methine is equatorial and bisects the F−C−F angle, a conclusion supported by the ab initio calculations (the alternate conformer is 1 kcal mol^{-1} higher in energy).

Synthesis of a Pentopyranosyl Phosphate Analogue. Initially, phosphorylation was attempted without further protection steps. Diol **37** contains two hydroxyl groups which should differ significantly in acidity.[44] Treating diol **31** with one equivalent of a strong base and allowing the system to equilibrate should favor the formation of **42** at the expense of **43**. The pK_a of the pseudoanomeric hydroxyl group should be lower than the secondary hydroxyl because of the combined inductive effects of the bridging oxygen and the two fluorine atoms; phosphorylation of **42** was therefore anticipated as the kinetic pathway (Scheme 10).[45]

Deprotonation with *n*-BuLi at −78 °C, slow warming to room temperature, and equilibration overnight, followed by the addition of tetrabenzyl pyrophosphate, afforded a mixture of **44** (14%), **45** (3%), and recovered **37** (35%). A higher yield (43%) of the monophosphate **44** could be achieved by changing the base to NaHMDS and adding Na-selective 15-crown-5, consistent with the formation of a more ionic and dissociated Na salt. However, the poor conversion of **37** and loss of material in **45** directed us toward protection of the secondary hydroxyl group. Acetylation to **46** occurred selectively (89%), and the regiochemistry was confirmed by an HMBC experiment which shows a cross-peak ($^3J_{C-H}$) between the acetate carbonyl carbon and H-4. Exposure of **46** to NaHMDS followed by the addition of tetrabenzyl pyrophosphate allowed the isolation of **47** in good yield, though deacetylated **44** was an occasional contaminant after chromatography. Hydrogenolysis of the benzyl groups was followed by deacetylation, lyophilization, and column chromatography allowing the isolation of deprotected material (Scheme 11). No intermediates were purified during this sequence, but we did check for ^{19}F and ^{31}P NMR spectral changes, obtaining accurate ion masses of the crude materials at each stage. Particularly broad (and rather uninformative) ^{31}P NMR spectra were obtained for the free phosphomonoester diacid intermediates.

The final structure **48** is assigned as the ammonium sodium salt on the basis of the presence of ammonia in the chromatographic eluent; chromatography over silica can lead to the formation of monosodium salts, consistent with the results of combustion analysis.

The successful development of a phosphorylation and deprotection strategy sets the stage for the preparation of a wider range of analogues and the chemical or enzymatic synthesis of the NDP sugar analogues themselves.

Conclusions

Telescoped syntheses of locked difluorinated analogues of pentopyranosides have been achieved using metalated difluoroenol acetal chemistry and RCM as key steps in high-yielding multistep sequences which contain minimal purifications. Dihydroxylation allows triol synthesis though with modest stereoselectivity in the case of the all-*cis* triol and subsequent bicyclic hemiacetal. The toxic osmium(VIII) reagent can be replaced by Ru when stereoselectivity is not an issue. Epoxidation and hydrolysis provide a highly stereoselective route to a stereocomplementary class of analogue. A viable phosphorylation strategy involving blocking of the secondary hydroxyl group followed alkoxide formation from the pseudoanomeric hydroxyl group, and subsequent phosphorylation has been developed. Conversion of the sensitive triester to the more robust monoester then allows base-catalyzed deacetylation-completing syntheses of a representative example of a new class of analogue of important biomolecules.

Experimental Section

Representative procedures only are described in this section. Full preparative and characterization details for all other compounds are in the electronic Supporting Information (SI). 2-(2′-Methoxyethoxymethoxy)-1,1,1-trifluoroethane[21] and 1,1-difluoro-2-(2′-methoxy-ethoxymethoxy)-4,4-dimethyl-hepta-1,6-dien-3-ol **15**[20] were prepared according to published procedures.

(44) (a) For calculations of hemiacetal pK_a (the values are only ca. 2−3 pK_a units lower than those of the analogous alcohols), see: Guthrie, J. P.; Pitchko, V. *J. Am. Chem. Soc.* **2000**, *122*, 5520. (b) An estimate used by Jencks suggests a larger difference of 5 pK_a units: Jencks, W. P. *Catalysis in Chemistry and Enzymology*; McGraw-Hill: New York, 1969; p 522.

(45) The rates of nucleophilic oxyanion attack at phosphotriesters were shown to depend linearly on nucleophile pK_a with a Brönsted coefficient (β_N) of 0.3−0.48 (the size depends on the leaving group). See: Khan, S. A.; Kirby, A. J. *J. Chem. Soc. (B)* **1970**, 1172. We therefore anticipated a competition. Though **42** sould be the major species present, **43** could be as much as 2.5 log units more nucleophilic than **42** (assuming a maximum β_N of 0.5). This may explain the relatively low selectivity.

3-Allyloxy-1,1-difluoro-2-(2′-methoxy-ethoxymethoxy)-hepta-1,6-diene 16. A mixture of **15** (68.24 mmol, 17.40 g) and allyl bromide (81.90 mmol, 6.87 mL) was added over 1 min to a vigorously stirred solution of tetra-*n*-butylammonium hydrogensulfate (3.45 mmol, 1.16 g) and sodium hydroxide (488 mmol, 24.3 mL of a 50% aqueous solution) at 0 °C. The mixture was stirred at this temperature for 30 min, allowed to warm to room temperature, and stirred for a further 16 h. The yellow white solution was diluted with water (40 mL), and the layers were separated. The aqueous phase was extracted with diethyl ether (4 × 100 mL). The combined organic extracts were washed with brine (2 × 30 mL), dried ($MgSO_4$), filtered, and concentrated under reduced pressure to afford **16** as a pale yellow oil (18.24 g, 91%, 100% by GC), which was used without any further purification: R_f (10% diethyl ether in hexane) 0.42; δ_H (300 MHz, $CDCl_3$) 5.96−5.83 (m, 1H), 5.81 (ddt, J = 16.1, 10.1, 6.6, 1H), 5.28 (ddd, J = 17.2, ^2J = 3.0, ^4J = 1.8, 1H), 5.19 (ddd, J = 10.2, ^2J = 3.0, ^4J = 1.2, 1H), 5.09−4.94 (env., 4H), 4.10 (ddt, J = 12.7, 5.1, 1.5, 1H), 4.06−4.00 (m, 1H), 3.94−3.74 (m, 3H), 3.61−3.57 (m, 2H), 3.41 (s, 3H), 2.13−2.06 (m, 2H), 1.95−1.70 (m, 2H); δ_C (75 MHz, $CDCl_3$) 156.0 (dd, $^1J_{C-F}$ = 291.8, 282.8), 137.7, 134.3, 117.3, 115.1, 112.4 (dd, $^2J_{C-F}$ = 36.8, 9.8), 97.1, 73.8, 71.6, 69.3, 68.3, 59.0, 31.0, 29.6; δ_F (282 MHz, $CDCl_3$) −97.7 (dd, $^2J_{F-F}$ = 63.5, $^4J_{F-H}$ = 1.9, 1F), −109.5 (dd, $^2J_{F-F}$ = 63.5, $^4J_{F-H}$ = 3.8, 1F); ν_{max}(film)/cm^{-1} 2880s, 1748m, 1642w; *m/z* (FAB) 293 (20%, [M + H]$^+$) 215 (24), 165 (74), 137 (90), 89 (100), 59 (84); HRMS (FAB, [M + H]$^+$) calcd for $C_{14}H_{23}F_2O_4$ 293.15634, found 293.15634.

4,4-Difluoro-5-(2-methoxy-ethoxymethoxy)-deca-1,5,9-trien-3-ol 17. A solution of ether **16** (34.25 mmol, 10.00 g) in THF (60 mL) was added dropwise over 15 min to a stirred solution of LDA (prepared from *n*BuLi (68.50 mmol, 28.30 mL of a 2.42 M solution in hexane) and diisopropylamine (75.30 mmol, 10.58 mL) in THF (342 mL)) at −100 °C under a nitrogen atmosphere. The pale pink solution was stirred at this temperature for 30 min before being allowed to warm to −30 °C over 4 h and stirred for a further 3 h at this temperature. The solution changed color during warming, from yellow through orange to brown and finally black. The reaction was quenched with ammonium chloride (10 mL of a saturated aqueous solution), whereupon the black color disappeared and an orange/red solution was observed. The layers were separated, and the aqueous phase was extracted with diethyl ether (3 × 150 mL). The combined organic extracts were washed with brine (2 × 50 mL), dried ($MgSO_4$), and concentrated under reduced pressure to give the homoallylic alcohol **17** (8.71 g, 95% conversion by NMR and GC) as a red−brown oil, which was used without further purification: R_f (30% ether in hexane) 0.12; δ_H (300 MHz, $CDCl_3$) 5.93 (ddd, J = 17.2, 10.5, 5.6, 1H), 5.80 (ddt, J = 17.1, 10.1, 6.4, 1H), 5.57 (td, J = 7.3, 1.3, 1H), 5.47 (dt, J = 17.2, ^2J = 1.5, 1H), 5.35 (dt, J = 10.5, ^2J = 1.5, 1H), 5.07−4.95 (m, 4H), 4.50 (broad s, 1H), 3.86 (t, J = 4.6, 1H), 3.85 (t, J = 4.6, 1H), 3.58 (t, J = 4.6, 2H), 3.38 (s, 3H), 2.92 (1H, broad s), 2.35−2.25 (m, 2H), 2.20−2.08 (m, 2H); δ_C (75 MHz, $CDCl_3$) 145.4 (dd, $^2J_{C-F}$ = 27.5, $^2J_{C-F}$ = 25.2), 135.5, 131.5, 119.8 (t, J_{C-F} = 5.4), 118.8, 118.2 (dd, $^1J_{C-F}$ = 250.1, $^1J_{C-F}$ = 247.1), 115.4, 97.2, 72.4 (dd, $^2J_{C-F}$ = 30.5, $^2J_{C-F}$ = 27.5), 70.5, 67.9, 58.0, 32.0, 23.6; δ_F (282 MHz, $CDCl_3$) −109.5 (dd, $^2J_{F-F}$ = 253.2, J_{H-F} = 8.3, 1F), −115.9 (dd, $^2J_{F-F}$ = 253.5, J_{H-F} = 14.7, 1F); ν_{max}(film)/cm^{-1} 3434br, 2928w, 1682w, 1641w, 1452w, 1252w, 1170s, 1112s, 1006s, 933s; *m/z* (FAB) 293 (44%, [M + H]$^+$), 137 (100), 89 (90), 59 (100); HRMS (FAB, MH$^+$) calcd for $C_{14}H_{23}F_2O_4$ 293.15648, found 293.15648.

3-Benzoyloxy-4,4-difluoro-5-(2′-methoxy-ethoxymethoxy)-deca-1,5*Z*,9-triene 18a. Alcohol **17** (6.3 g, 21.7 mmol), benzoic anhydride (4.90 g, 21.7 mmol), and DMAP (0.53 g, 4.3 mmol) were dissolved in DCM (217 mL). Poly(vinylpyridine) (10.6 g, 10.6 mmol, 0.5 equiv) was added, and the reaction mixture was swirled gently at room temperature overnight. The resin was collected at the pump and washed with water (50 mL) and saturated $NaHCO_3$ solution (50 mL). The aqueous layer was extracted with diethyl ether (3 × 50 mL), and the combined organic extracts were washed with brine, dried, and concentrated in vacuo to yield **18a** as a brown oil (6.85 g, 80%). The crude product was taken on without purification: R_f (30% diethyl ether in hexane) 0.27; δ_H (300 MHz, $CDCl_3$) 8.09−8.05 (m, 2H), 7.58 (apparent tt, J = 7.4, ^4J = 1.4, 1H), 7.48−7.42 (m, 2H), 6.01−5.89 (m, 2H), 5.73 (ddt, J = 17.0, 10.2, 6.4, 1H), 5.62 (t, J = 7.5, 1H), 5.53 (dd, J = 16.0, ^2J = 1.3, 1H), 5.43 (dd, J = 10.3, ^2J = 1.3, 1H), 5.00 (s, 2H), 5.00−4.90 (m, 2H), 3.94−3.80 (m, 2H), 3.60−3.55 (m, 2H), 3.38 (s, 3H), 2.33−2.23 (m, 2H), 2.13−2.04 (m, 2H); δ_C (75 MHz, $CDCl_3$) 164.8, 144.8 (t, $^2J_{C-F}$ = 25.7), 137.3, 133.4, 129.9, 129.5, 128.9 (dd, J_{C-F} = 3.6, 1.8), 128.4, 121.4, 120.2 (t, J_{C-F} = 5.1), 117.3 (dd, $^1J_{C-F}$ = 251.2, 247.4), 115.4, 98.3, 72.8 (dd, $^2J_{C-F}$ = 31.7, 26.9), 71.6, 68.9, 59.0, 33.9, 24.5; δ_F (282 MHz, $CDCl_3$) −110.8 (dd, $^2J_{F-F}$ = 253.2, J_{H-F} = 10.9, 1F), −112.4 (dd, $^2J_{F-F}$ = 253.2, J_{H-F} = 12.3, 1F); ν_{max}(film)/cm^{-1} 2887w, 1730s, 1602w, 1452w, 1264s, 1096s, 988s, 709s; *m/z* (EI) 396 (3%, M$^-$) 355 (7), 220 (39), 205 (100), 145 (21), 106 (68); HRMS (EI, M$^+$) calcd for $C_{21}H_{26}F_2O_5$ 396.17473, found 396.17473.

3-Benzoyloxy-4,4-difluoro-deca-1,9-dien-5-one 19a. Thionyl chloride (15.6 mmol, 1.12 mL) was added to a stirred solution of benzoate **18a** (15.6 mmol, 6.16 g) in methanol (156 mL) at 0 °C. The solution was allowed to warm to room temperature and stirred for 18h, and then the solvent was removed in vacuo. The resulting paste was taken up in water (120 mL), and the mixture was extracted with diethyl ether (5 × 100 mL). The combined organic extracts were washed with $NaHCO_3$ (200 mL) and brine (200 mL), dried ($MgSO_4$), filtered, and concentrated in vacuo to give ketone **19a** (100 mg, 75%, 88% by GC) as a brown oil, which could be used crude or purified on silica gel eluted with 10% ethyl acetate in hexane to afford a clear oil (3.60 g, 75%, 97% by GC): R_f (10% diethyl ether in hexane) 0.56; δ_H (300 MHz, $CDCl_3$) 8.06−8.01 (m, 2H), 7.60 (tt, J = 7.5, ^4J = 1.3, 1H), 7.49−7.42 (m, 2H), 6.05−5.88 (m, 2H), 5.71 (ddt, J = 17.0, J = 10.2, J = 6.7, 1H), 5.57 (dd, J = 16.0, ^4J = 0.9, 1H), 5.50 (dd, J = 9.4, ^4J = 0.9, 1H), 5.02−4.94 (m, 2H), 2.74 (t, J = 7.3, 2H), 2.05 (q, J = 7.3, 2H), 1.71 (pentet, J = 7.3, 2H); δ_C (75 MHz, $CDCl_3$) 199.7 (dd, $^2J_{C-F}$ = 28.7, 28.7), 164.4, 137.3, 133.7, 129.9, 128.9, 128.6, 127.7, 122.8, 115.7, 114.1 (dd, $^1J_{C-F}$ = 260.9 256.1), 72.4 (dd, $^2J_{C-F}$ = 29.9, 25.1), 36.7, 32.6, 21.5; δ_F (282 MHz, $CDCl_3$) −113.7 (dd, $^2J_{F-F}$ = 293.9, J_{H-F} = 9.0, 1F), −118.9 (dd, $^2J_{F-F}$ = 273.9, J_{H-F} = 14.2, 1F); ν_{max}(film)/cm^{-1} 3076w, 2937w, 1733s, 1642w; *m/z* (EI) 308 (37%, M$^+$), 105 (85); HRMS (EI, M$^+$) calcd for $C_{17}H_{18}F_2O_3$ 308.12242, found 308.12240.

3-Benzoyloxy-2,2-difluoro-cyclooct-4*Z*-en-1-one 20a. A solution of diene **19a** (4.07 mmol, 1.26 g) and Ti(O^{i}Pr)$_4$ (1.21 mmol, 0.365 mL) in freshly degassed DCM (407 mL) was refluxed under nitrogen for 30 min, and then Grubbs' catalyst **21** (0.203 mmol, 173 mg, 5 mol %) was added via syringe in DCM (5 mL). Reflux was maintained until the ^{19}F NMR spectrum of an aliquot showed that starting material had been consumed completely (after 18 h). The solvent was then removed in vacuo, and the residue was taken up in diethyl ether (30 mL) then filtered and concentrated to give crude cyclooctenone as a brown oil which was purified by flash column chromatography (silica gel, 10% diethyl ether in hexane) to give cyclooctenone **20a** which crystallized (0.531 g, 46%, 96% by GC): R_f (10% diethyl ether in hexane) 0.20; mp 91−90 °C; δ_H (300 MHz, $CDCl_3$) 8.14−8.10 (m, 2H), 7.64−7.58 (m, 1H), 7.52−7.45 (m, 2H), 6.36 (dddd, J_{H-F} = 21.3, 1.5, J = 7.8, ^4J = 3.8, 1H), 6.07−5.96 (m, 1H), 5.65 (ddd, J = 11.0, 7.8, 2.5, 1H), 2.82 (dddd, ^2J = 12.6, J = 10.4, 3.9, 2.0, 1H), 2.68 (ddt, ^2J = 12.6, J = 7.2, ^4J = 3.7, 1H), 2.44−2.27 (m, 2H), 2.13−2.02 (m, 1H), 1.89−1.74 (m, 1H); δ_C (75 MHz, $CDCl_3$) 199.5 (t, $^2J_{C-F}$ = 25.5), 165.2, 135.6, 133.7, 130.0, 129.0, 128.6, 125.3, 116.6 (dd, $^1J_{C-F}$ = 262.6, 260.0), 68.2 (dd, $^2J_{C-F}$ = 24.2, 18.9), 36.8, 27.5, 27.1; δ_F (282 MHz, $CDCl_3$) −111.0 (d, $^2J_{F-F}$ = 239.8, 1F), −130.9 (dd, $^2J_{F-F}$ = 239.8, $^3J_{F-H}$ = 21.3, 1F); ν_{max} (solid)/cm^{-1} 2968m, 2919m, 1725w, 1743w; *m/z* (ES$^+$) 281 (M + H$^+$, 42%) 121 (PhCOO, 100%). Anal. calcd for $C_{15}H_{14}F_2O_3$: C, 64.28; H, 5.03.

Found: C, 64.31; H, 5.16. Colorless or almost colorless material of improved quality for further use can be obtained by taking the crude oil (ca. 0.5 g, 2 mmol) up in a minimum volume of methanol and eluting through a preconditioned (3 mL of MeOH per tube) thiol SPE tube with MeOH (3 mL).

3-Benzyloxy-4,4-difluoro-5-(2′-methoxy-ethoxymethoxy)-deca-1,5*Z*,9-triene 18b. A solution of **17** (20.2 mmol, 5.9 g) in THF (50 mL) was added cautiously to a suspension of NaH (101 mmol, 4.04 g of a 60% suspension in mineral oil, prewashed with hexane 3 × 30 mL) in THF at 0 °C under nitrogen. The mixture was stirred at this temperature for 45 min as hydrogen evolved. TBAI (2.86 mmol, 1.05 g) then benzyl bromide (19.19 mmol, 2.28 mL) were added, and the mixture was allowed to warm to room temperature over 1 h and then stirred for a further 12 h. The reaction was quenched by the cautious addition of water (150 mL), and the layers were separated. The aqueous layer was extracted with ethyl acetate (3 × 150 mL), and the combined organic extracts were washed with brine (100 mL), dried ($MgSO_4$), and concentrated in vacuo to give benzyl ether **18b** as a brown oil (7.10 g, 92%, 97% by GC) which was used without further purification: R_f (30% ether in hexane) 0.38; δ_H (400 MHz, $CDCl_3$) 7.25−7.17 (m, 5H), 5.77 (ddd, J = 17.5, 10.1, 7.4, 1H), 5.72 (ddt, J = 17.1, 10.2, 6.5, 1H), 5.50 (td, J = 7.4, $^4J_{H-F}$ = 1.4, 1H), 5.38−5.36 (m, 1H), 5.35−5.32 (m, 1H), 4.98−4.92 (dq, J = 17.1, ^4J = 1.7, 1H), 4.89−4.87 (dq, J = 10.2, ^4J = 1.9, 1H), 4.87 (d, ^2J = 5.9), 4.86 (d, ^2J = 5.9), 4.58 (d, ^2J = 11.9, 1H), 4.44 (d, ^2J = 11.9, 1H), 4.14 (dddt, J_{H-F} = 14.2, 8.5, J = 7.4, ^4J = 0.9), 3.71 (t, J = 4.8, 1H), 3.69 (t, J = 4.4, 1H), 3.46 (dd, J = 5.1, 4.3, 2H), 3.29 (s, 3H), 2.26−2.18 (m, 2H), 2.09−2.03 (q, J = 7.1, 2H); δ_C (100 MHz, $CDCl_3$) 145.4 (dd, $^2J_{C-F}$ = 27.2, 24.8), 137.6, 137.5, 131.1 (dd, J_{C-F} = 3.6, 1.8), 128.3, 127.8, 127.7, 121.5, 119.7 (t, J_{C-F} = 5.1), 118.1 (dd, $^1J_{C-F}$ = 251.0, 246.0), 115.3, 98.2, 79.0 (dd, $^2J_{C-F}$ = 31.7, 25.7), 71.6, 71.4, 68.8, 59.0, 33.1, 24.6; δ_F (282 MHz, $CDCl_3$) −108.1 (dd, $^2J_{F-F}$ = 254.8, J_{H-F} = 8.5, 1F), −114.7 (dd, $^2J_{F-F}$ = 154.8, J_{H-F} = 14.2, 1F); ν_{max}(film)/cm^{-1} 2923s, 1743w, 1678w, 1637w, 1454s, 1113s, 938s, 850w, 732w, 699s. A satisfactory mass spectrum could not be obtained for this compound (ES-MS, EI, CI, FAB).

3-Benzyloxy-4,4-difluoro-deca-1,9-dien-5-one 19b. Thionyl chloride (18.6 mmol, 1.34 mL) was added to a stirred solution of enol ether **18b** (18.6 mmol, 7.10 g) in methanol (180 mL) at 0 °C. The solution was allowed to warm to room temperature over 1 h and stirred for 15 h. The methanol was removed in vacuo, and the resulting paste was taken up in water (40 mL) and extracted with ethyl acetate (3 × 150 mL). The combined organic extracts were washed with $NaHCO_3$ (70 mL) and brine (2 × 100 mL), dried ($MgSO_4$), and concentrated in vacuo to give ketone **19b** as a yellow oil (5.13 g, 94%, 99% by GC) which was used in the next step without purification. The following data were obtained from a purified sample (flash chromatography, 10% diethyl ether in hexane): R_f (30% ether in hexane) 0.68; δ_H (400 MHz, $CDCl_3$) 7.37−7.21 (m, 5H), 5.85 (ddd, J = 17.2, 10.5, 7.6, 1H), 5.72 (ddt, J = 17.1, 10.2, 6.7, 1H), 5.53 (ddd, J = 10.5, ^2J = 1.4, ^4J = 0.9, 1H), 5.48 (dt, J = 17.2, ^2J = 1.4, 1H), 4.99 (ddd, J = 17.1, ^2J = 3.4, ^4J = 1.6, 1H), 4.96 (dddd, J = 10.2, ^2J = 3.4, ^4J = 2.0, 1.2, 1H), 4.61 (d, ^2J = 11.5, 1H), 4.38 (d, ^2J = 11.5, 1H), 4.26 (dddt, J_{H-F} = 16.6, 6.6, J = 7.5, ^4J = 0.9, 1H), 2.68 (tt, J = 7.3, 1.7, 2H), 2.03 (tdd, J = 7.3, 6.7, ^4J = 1.2, 2H), 1.69 (pentet, J = 7.3, 2H); δ_C (75 MHz, $CDCl_3$) 201.7 (dd, $^2J_{C-F}$ = 31.1, 25.1), 137.6, 136.8, 129.6 (dd, J_{C-F} = 3.6, 1.2), 128.4, 128.1, 128.0, 123.2, 115.4, 115.0 (dd, $^1J_{C-F}$ = 261.5, 253.7), 79.4 (dd, $^2J_{C-F}$ = 30.5, 23.9), 71.4, 37.6, 32.7, 21.5; δ_F (282 MHz, $CDCl_3$) −110.6 (dd, $^2J_{F-F}$ = 263.0, J_{H-F} = 6.6, 1F), −124.1 (dd, $^1J_{F-F}$ = 263.0, J_{H-F} = 16.6, 1F); ν_{max}(film)/cm^{-1} 1941w, 1740s (C=O), 1642w, 1455w, 1372w, 1217s, 1091s, 913s, 736s, 698s; *m/z* (CI$^+$) 312 (100%, $[M + NH_4]^+$) 294 (4), 216 (33), 186 (20), 170 (9), 126 (8), 108 (11), 84 (8); HRMS (CI$^+$, $[M + NH_4]^+$) calcd for $C_{17}H_{24}F_2O_2N$ 312.1770, found 312.1769. Anal. calcd for $C_{17}H_{20}F_2O_2$: C, 69.37; H, 6.85. Found: C, 69.49; H, 6.98.

3-Benzyloxy-2,2-difluoro-cyclooct-4*Z*-en-1-one 20b. A solution of **19b** (2.21 mmol, 0.650 g) and $Ti(O^iPr)_4$ (0.66 mmol, 0.198 mL) in freshly degassed DCM (1000 mL) was refluxed for 30 min under nitrogen, and then a solution of Grubbs' catalyst **21** (0.11 mmol, 94 mg, 5 mol %) in DCM (5 mL) was added via syringe. Reflux was maintained until the ^{19}F NMR spectrum of an aliquot showed that starting material had been consumed completely (after 18h). The solvent was removed in vacuo, and the residue was taken up in diethyl ether (50 mL), then filtered, and concentrated to give crude cyclooctenone **20b** as a brown oil which was purified by flash column chromatography (silica gel, 10% diethyl ether in hexane) to afford cyclooctenone **20b** as a yellow solid (440 mg, 75%, 96% by GC): R_f (30% diethyl ether in hexane) 0.40; mp 32−35 °C; δ_H (300 MHz, $CDCl_3$) 7.40−7.22 (m, 5H), 5.93 (app. q, J = 9.2, 1H), 5.60 (ddd, J = 11.1, 9.2, 1.2, 1H), 4.76 (d, ^2J = 12.0, 1H), 4.66 (d, ^2J = 12.0, 1H), 4.66 (ddd, $^3J_{H-F}$ = 20.0, J = 8.0, 1.3, 1H), 2.60−2.48 (m, 2H), 2.28 (dddd, J = 13.7, 11.1, 5.6, 3.1, 1H), 2.04−1.86 (m, 2H), 1.80−1.46 (m, 1H); δ_C (75 MHz, $CDCl_3$) 200.4 (dd, $^2J_{C-F}$ = 26.6, 24.8), 137.0, 135.4, 128.6, 128.1, 128.0, 127.7 (d, $^3J_{C-F}$ = 6.0), 117.8 (dd, $^1J_{C-F}$ = 263.9, 258.5), 173.0 (dd, $^2J_{C-F}$ = 23.3, 19.7), 72.1, 36.7, 27.4, 27.1; δ_F (376 MHz, 323 K, $CDCl_3$) −110.9 (d, $^2J_{F-F}$ = 240.4, 1F), −130.8 (dd, $^2J_{F-F}$ = 240.4, $^3J_{H-F}$ = 19.5, 1F); ν_{max}(solid)/cm^{-1} 2866s, 1743s, 1648w, 1497w, 1455s, 1185s, 1100s, 1070s, 992w, 845s, 812s, 737s, 698s; *m/z* (CI$^+$) 284 (100%, $[M + NH_4]^+$) 270 (5), 220 (3), 158 (7), 140 (11), 123 (6), 90 (8); HRMS (ES$^+$, $[M + NH_4]^+$) calcd for $C_{15}H_{20}F_2O_2N$ 284.1456, found 284.1457. Anal. calcd for $C_{15}H_{16}F_2O_2$: C, 67.66; H, 6.06. Found: C, 67.59; H, 6.15.

Carrying out the RCM with 7.12 mmol of **19b** at 0.005 M afforded **20b** in 50% yield after purification. The crude material contained significant quantities of higher molecular weight material, so use of the lower concentration is therefore recommended.

2*R-Benzoyloxy-3,3-difluoro-9-oxa-(1*S**,8*S**)-bicyclo[6.1.0]-nonan-4-one 29a.** Disodium EDTA (7.2 mL of a 4 × 10^{-4} M aqueous solution, 2.9 μmol) followed by trifluoroacetone (3.6 mL of a 60% aqueous solution, 25 mmol from a precooled syringe) was added to a solution of **20a** (0.5 g, 1.8 mmol) in acetonitrile (18 mL) at 0 °C. Sodium hydrogen carbonate (2.3 g, 31.9 mmol) and oxone (5.5 g, 8.6 mmol) were added in one portion. The mixture was stirred for 6 h and allowed to warm to room temperature. The solids were removed by filtration and washed at the pump with DCM (25 mL). The aqueous phase was extracted with DCM (3 × 20 mL), and the combined organic extracts and filter washings were washed with brine (20 mL), dried ($MgSO_4$), and concentrated in vacuo to yield **29a** as a white solid (0.40 g, 75%) which was used without purification: R_f (30% ethyl acetate in hexane) 0.22; mp 75−78 °C; δ_H (300 MHz, $CDCl_3$) 8.18−8.13 (m, 2H), 7.62 (dt, J = 7.3, ^4J = 1.5, 1H), 7.49 (t, J = 7.3, 2H), 5.59 (ddd, J_{H-F} = 20.9, J = 8.9, J_{H-F} = 4.4, 1H), 3.24 (ddt, J = 8.9, 4.3, ^4J = 1.2, 1H), 3.05 (dt, J = 10.6, 4.3, 1H), 2.86−2.65 (m, 2H), 2.49 (dddd, ^2J = 14.7, J = 4.5, 4.3, 3.0, 1H), 2.20−2.10 (m, 1H), 2.05−1.90 (m, 1H), 1.37 (dddd, ^2J = 14.7, J = 13.6, 10.6, 3.4, 1H); δ_C NMR (75 MHz, $CDCl_3$) 198.9, 164.0, 132.8, 129.2, 127.6, 127.6, 116.7 (t, $^1J_{C-F}$ = 260.9), 68.9, 53.9, 52.0, 35.0, 27.5, 23.2; δ_F (282 MHz, $CDCl_3$) −113.2 (dd, $^2J_{F-F}$ = 247.4, J_{H-F} = 4.4, 1F), −127.3 (dd, $^2J_{F-F}$ = 247.4, J_{H-F} = 20.9, 1F); ν_{max}(solid)/cm^{-1} 2954w, 1736s, 1275, 1262, 1250 all m, 1081m, 1070m, 707s; *m/z* (EI$^+$) 296 (30%, M^+) 224 (40), 174 (100, M − BzOH); HRMS (EI, M^+) calcd for $C_{15}H_{14}F_2O_4$ 296.08602, found 296.08601. Anal. calcd for $C_{15}H_{14}F_2O_4$: C, 60.8; H, 4.8. Found: C, 60.9; H, 4.8.

2*R-Benzyloxy-3,3-difluoro-9-oxa-(1*S**,8*S**)-bicyclo[6.1.0]-nonan-4-one 29b.** Prepared as for **29a**, from **20b** (0.620 g, 2.33 mmol), Na_2EDTA (9.31 mL of a 4 × 10^{-4} M aqueous solution), acetonitrile (23.30 mL), trifluoroacetone (4.66 mL of a 60% aqueous solution, 25 mmol), $NaHCO_3$ (2.94 g, 34.95 mmol), and oxone (7.16 g, 11.65 mmol) for 6 h at 0 °C. Purification (flash chromatography, silica gel, 20% diethyl ether in hexane) gave epoxide **29b** as a white solid (495 mg, 50%, 98% by GC): R_f (30% diethyl ether in hexane) 0.20; mp 70−73 °C; δ_H (400 MHz, $CDCl_3$) 7.44−7.29 (m, 5H),

4.89 (d, ^2J = 11.9, 1H), 4.85 (d, ^2J = 11.9, 1H), 3.68 (ddd, J_{H-F} = 20.3, J = 8.6, 5.1, 1H), 3.07 (ddt, J = 8.6, 4.3, ^4J = 1.6, 1H), 2.90 (dt, J = 10.7, 4.3, 1H), 2.76−2.68 (m, 1H), 2.48 (dddd, ^2J = 13.4, J = 9.2, 4.1, ^4J = 2.2, 1H), 2.36 (dtd, J = 14.7, 4.5, ^2J = 3.1, 1H), 2.09−1.99 (m, 1H), 1.97−1.85 (m, 1H), 1.02 (dddd, J = 14.5, 13.7, 10.6, 3.3, 1H); δ_C (75 MHz, $CDCl_3$) 201.1 (t, J_{C-F} = 25.7), 136.8, 128.5, 128.2, 128.1, 115.6 (dd, $^1J_{C-F}$ = 161.5, 157.9), 75.3 (dd, $^2J_{C-F}$ = 22.4, 18.7), 73.2 (d, $^4J_{C-F}$ = 1.2), 54.6 (d, J_{C-F} = 10.8), 53.8, 35.8, 28.3, 24.0; δ_F (282 MHz, $CDCl_3$) −113.6 (d, $^2J_{F-F}$ = 245.9, 1F), −128.8 (dd, $^2J_{F-F}$ = 245.9, J_{H-F} = 20.3, 1F); ν_{max}(solid)/cm^{-1} 3465w, 2923w, 1744s, 1499w, 1452s, 1340w, 1236w, 1193s, 1105s, 1083s, 1019s, 1028s, 969s, 862s, 830s, 755s, 702s; *m/z* (CI$^+$) 300 (100%, [M + NH_4]$^+$) 282 (6), 262 (2), 174 (3), 125 (3), 108 (3); HRMS (ES$^+$, [M + NH_4]$^+$) calcd for $C_{15}H_{20}F_2O_3N$ 300.1406, found 300.1409. Anal. calcd for $C_{15}H_{16}F_2O_3$: C, 63.82; H, 5.71. Found: C, 63.77; H, 5.78.

3*R-Benzyloxy-2,2-difluoro-9-oxa-1*S**,5*R**-bicyclo[3.3.1]nona-1*S**,4*R**-diol 31.** Epoxide **29b** (0.44 mmol, 125 mg) and NaOH (2.2 mL of a 0.5% aqueous solution, 0.28 mmol) were sealed in a microwave vial containing a stirrer bead. The solution was irradiated in the cavity of a CEM Discover instrument (30 W power to maintain a temperature of 100 °C for 10 min, with a 10 min heating ramp, no cooling). The vial was vented and opened, and the solution was made just acidic (pH 6 to indicator paper) by the addition of a few drops of HCl (0.3 mL of a 3 M aqueous solution), which caused a white solid to precipitate. The aqueous solution was extracted with ethyl acetate (3 × 20 mL), and the combined organic extracts were washed with $NaHCO_3$ (20 mL) and brine (30 mL), dried ($MgSO_4$), and then filtered. The solvent was removed in vacuo to give a white solid which was purified (flash silica, 50% ethyl acetate in hexane) to give **31** as a white solid (98 mg, 74%): R_f (50% ethyl acetate in hexane) 0.28; mp 127−130 °C; δ_H (300 MHz, $CDCl_3$) 7.45−7.32 (m, 5H), 5.01 (dd, ^2J = 11.3, ^4J = 1.1, 1H), 4.67 (d, ^2J = 11.3, 1H), 4.22 (t, J = 5.1, 1H), 4.06−3.98 (m, 2H), 3.39 (d, J = 5.4, 1H), 2.23 (br. s, 1H), 2.11−2.02 (m, 1H), 1.95−1.52 (m, 5H); δ_C (75 MHz, CD_3OD) 138.0, 127.9, 127.8, 127.4, 118.7 (dd, $^1J_{C-F}$ = 257.6, 252.8), 93.6 (dd, $^2J_{C-F}$ = 26.9, 20.3), 80.2 (dd, $^2J_{C-F}$ = 19.1, 19.1), 74.4 (d, $^4J_{C-F}$ = 2.4), 73.0, 71.4 (d, $^3J_{C-F}$ = 8.4), 28.7 (d, $^3J_{C-F}$ = 2.4), 20.0, 17.9; δ_F (282 MHz, CD_3OD) −115.8 (dd, $^2J_{F-F}$ = 247.8, J_{H-F} = 7.6, 1F), (−128.7)−(−129.8) (m, incl. app. d, $^2J_{F-F}$ = 247.8, 1F); ν_{max}(solid)/cm^{-1} 3364br, 2949w, 1350w, 1213, 1080s, 1022s, 907s, 735s, 695s; *m/z* (CI$^+$) 318 (100%, [M + NH_4]$^+$) 228 (3), 210 (3), 108 (10), 91 (5), 52 (52); HRMS (ES$^+$, [M + NH_4]$^+$) calcd for $C_{15}H_{22}F_2O_4N$ 318.1511, found 318.1510. Anal. calcd for $C_{15}H_{18}F_2O_4$: C, 59.99; H, 6.04. Found: C, 60.13; H, 6.10.

Crystal data: $C_{15}H_{18}F_2O_4$, crystal size 0.19 × 0.10 × 0.04 mm^3, M = 300.29, triclinic, a = 9.9359(15) Å, b = 11.1641(17) Å, c = 13.130(2) Å, α = 78.181(3)°, β = 86.925(3)°, γ = 88.750(3)°, U = 1423.4(4) Å^3, T = 150(2) K, space group $P\bar{1}$, Z = 4, μ(Mo Kα) = 0.117 mm^{-1}, 10 395 reflections measured, 4966 [R(int) = 0.0818] which were used in all calculations. Final R indices [$F^2 > 2\sigma(F^2)$] R1 = 0.0571, wR2 = 0.0924; R indices (all data) R1 = 0.1002, wR2 = 0.1055.

4*R-Acetoxy-3*R**-benzyloxy-2,2-difluoro-1*S**-methoxy-9-oxa-1*S**,5*R**-bicyclo[3.3.1]nonane 32 and 5*S**-Acetoxy-3*R**-benzyloxy-2,2-difluoro-1*S**-methoxy-9-oxa-1*S**,4*R**-bicyclo[4.2.1]nonane 33.** A solution of epoxide **29b** (0.32 mmol, 90 mg) in methanolic sodium methoxide (3.2 mL of a 0.1 M solution in methanol) was irradiated in the microwave as for the hydrolysis of **29b** (30 W, 100 °C for 20 min, 10 min heating ramp, no cooling). The solvent was removed in vacuo, and the residue was taken up in DCM (70 mL) and washed with cold HCl (10 mL of a 1 M solution) and brine (20 mL), dried ($MgSO_4$), then filtered. Poly(vinylpyridine) (340 mg) and acetic anhydride (1.17 mmol, 0.160 mL) were added to the filtrate, and the mixture was swirled at room temperature for 64 h. The poly(vinylpyridine) was removed by filtration and washed with DCM (70 mL). The combined organic extracts and washings were washed with $NaHCO_3$ (10 mL), brine (20 mL), dried ($MgSO_4$), filtered, and concentrated in vacuo to give a gray paste which was purified (flash chromatography, silica, 20% ethyl acetate in hexane) to give (in order of elution) **33** as a gray paste (20 mg, ca. 18%, 83% of a mixture with **32** by ^{19}F NMR) followed by **32**. **33**: R_f (20% ethyl acetate in hexane) 0.30; δ_H (400 MHz, $CDCl_3$) 7.38−7.30 (m, 5H), 5.15 (dd, J = 5.7, 5.3, 1H), 4.84 (d, ^2J = 11.9, 1H), 4.57 (d, ^2J = 11.9, 1H), 4.42−4.38 (m, 1H), 4.33 (ddd, J_{H-F} = 9.9, 8.5, J = 3.7, 1H), 3.49 (d, $^5J_{H-F}$ = 1.8, 3H), 2.11−1.96 (m, 2H), 1.92 (s, 3H), 1.70−1.28 (m, 4H); δ_C (100 MHz, $CDCl_3$) 169.6, 136.9, 128.5, 128.1, 128.1, 123.7 (dd, $^1J_{C-F}$ = 267.2, 261.6), 105.8 (dd, $^2J_{C-F}$ = 29.2, 18.0), 77.9 (d, J_{C-F} = 9.6), 77.3 (dd, $^2J_{C-F}$ = 16.0, 10.4), 72.4 (d, $^4J_{C-F}$ = 2.4), 71.0, 51.8 (d, $^4J_{C-F}$ = 5.6), 34.3, 30.1, 20.9, 18.0; δ_F (376 MHz, $CDCl_3$) −114.3 (dd, $^2J_{F-F}$ = 235.0, J_{H-F} = 9.9, 1F), (−126.0)−(−126.9) (m incl. apparent d, $^2J_{F-F}$ = 235.0, 1F); ν_{max}(film)/cm^{-1} 2948s, 2359s, 1742s, 1454m, 1372m, 1238s, 1062s, 739w, 699w; *m/z* (CI$^+$) 374 (100%, [M + NH_4]$^+$) 284 (5), 208 (6), 106 (9), 77 (18), 52 (79); HRMS (ES$^+$, [M + NH_4]$^+$) calcd for $C_{18}H_{26}F_2O_5N$ 374.1774, found 374.1773. In the {^{19}F}^{1}H NMR spectrum, the signal at 4.42−4.38 simplified to 4.40 (dd, J = 6.5, 4.0, 1H) and the signal at 3.49 simplified to 3.49 (s, 3H). **32** (45 mg, 39%): R_f (20% ethyl acetate in hexane) 0.16; mp 92−93 °C; δ_H (400 MHz, $CDCl_3$) 7.41−7.32 (m, 5H), 5.21 (ddd, J = 9.9, 6.5, 1.2, 1H), 4.96 (d, ^2J = 12.0, 1H), 4.70 (d, ^2J = 12.0, 1H), 4.46−4.42 (m, 1H), 4.16 (ddd, J_{H-F} = 17.4, 7.6, J = 9.9, 1H), 3.51 (d, $^5J_{H-F}$ = 1.5, 3H), 2.02 (s, 3H), 1.96−1.60 (m, 6H); δ_C (100 MHz, $CDCl_3$) 169.5, 137.4, 128.4, 128.4, 128.0, 119.2 (dd, $^1J_{C-F}$ = 259.2, 257.6), 95.8 (dd, $^2J_{C-F}$ = 25.6, 17.6), 77.2 (dd, $^2J_{C-F}$ = 21.6, 19.2), 74.1 (d, $^4J_{C-F}$ = 2.4), 72.5 (d, J_{C-F} = 8.8), 69.6, 50.7 (d, $^4J_{C-F}$ = 4.0), 25.9 (d, J_{C-F} = 2.4), 21.1, 20.7, 18.1; δ_F (376 MHz, $CDCl_3$) −114.8 (dd, $^2J_{F-F}$ = 248.3, J_{H-F} = 7.1), −128.0 (dddq, $^2J_{F-F}$ = 248.3, J_{H-F} = 17.5, J = 3.8, $^5J_{H-F}$ = 1.4, 1F); ν_{max}(solid)/cm^{-1} 2955w, 1737s, 1440w, 1363s, 1239s, 1029s, 892s, 758s; *m/z* (CI$^+$) 374 (100%, [M + NH_4]$^+$) 284 (13), 208 (9), 108 (21), 77 (19); HRMS (ES$^+$, [M + NH_4]$^+$) calcd for $C_{18}H_{26}F_2O_5N$ 374.1774, found 374.1777. Anal. calcd for $C_{18}H_{22}F_2O_5$: C, 60.67; H, 6.22. Found, C, 60.76; H, 6.30. In the {^{19}F}^{1}H NMR spectrum, the signal at 3.51 simplified to 3.51 (s, 3H).

Crystal data: $C_{18}H_{22}F_2O_5$, crystal size 0.35 × 0.24 × 0.20 mm^3, M = 356.36, triclinic, a = 7.240(2) Å, b = 9.607(3) Å, c = 13.226(4) Å, α = 98.732(5)°, β = 102.590(5)°, γ = 100.713(5)°, U = 864.2(4) Å^3, T = 150(2) K, space group $P\bar{1}$, Z = 2, μ(Mo Kα) = 0.113 mm^{-1}, 6306 reflections measured, 3024 [R(int) = 0.0485] which were used in all calculations. Final R indices [$F^2 > 2\sigma(F^2)$] R1 = 0.0455, wR2 = 0.1179; R indices (all data) R1 = 0.0554, wR2 = 0.1240.

5*S-Acetoxy-2,2-difluoro-1*S**-methoxy-9-oxa-1*S**,4*R**-bicyclo[4.2.1]nonan-3*R**-ol 34.** Acetate **33** (0.07 mmol, 25 mg) was dissolved in ethanol (1 mL) containing 10% palladium on activated carbon (10 mg). The atmosphere was removed and replaced with hydrogen from a balloon. The solution was stirred at room temperature for 72 h, and then the hydrogen atmosphere was removed and replaced with air. The solution was filtered through celite, then concentrated in vacuo, and purified by flash chromatography (silica gel, 10−30% ethyl acetate/hexane) to give alcohol **34** as a gray paste (10 mg, 59%): R_f (30% ethyl acetate/hexane) 0.25; ν_{max}(film)/cm^{-1} 3447br, 2952w, 1736s, 1441w, 1374w, 1232s, 1036s, 973w, 787w; δ_H (400 MHz, $CDCl_3$) 5.20−5.15 (m, 1H), 4.54 (ddd, $^3J_{H-F}$ = 11.0, 8.1, J = 3.5, 1H), 4.32 (ddd, J = 6.4, 3.5, $^4J_{H-F}$ = 1.7, 1H), 3.49 (d, $^5J_{H-F}$ = 1.4, 3H), 2.12−1.94 (env., 6H), 1.74−1.60 (m, 3H); δ_C (100 MHz, $CDCl_3$) 170.0, 122.8 (t, $^1J_{C-F}$ = 262.8), 105.5 (dd, $^2J_{C-F}$ = 28.8, 18.4), 80.0 (d, $^3J_{C-F}$ = 9.6), 72.0 (dd, $^2J_{C-F}$ = 28.0, 17.6), 71.2, 51.6 (d, $^4J_{C-F}$ = 4.8), 33.7−33.6 (m), 29.75−29.70 (m), 21.0, 18.1; δ_F (376 MHz, $CDCl_3$) −119.6 (dd, $^2J_{F-F}$ = 236.5, $^3J_{H-F}$ = 11.1, 1F), (−126.6)−(−127.5) (m, incl. app. d, $^2J_{F-F}$ = 236.5, 1F); *m/z* (ES$^+$) 289 (33%, [M + Na]$^+$) 155 (5), 136 (6), 73 (22), 51 (100); HRMS (ES$^+$, [M + NH_4]$^+$) calcd for $C_{11}H_{20}F_2O_5N$ 374.1774, found 374.1778. In the {^{19}F}^{1}H NMR spectrum, the signal at 4.32 collapses to 4.32 (dd,

J = 6.4, 3.5, 1H) and the signal at 3.49−3.49 (s, 3H). The signals reported as multiplets in the ^{13}C NMR spectrum are weak and significantly broadened.

3*R-Benzyloxy-2,2-difluoro-9-oxa-1*S**,5*R**-bicyclo[3.3.1]nona-1*S**,4*S**-diol 37 and 3*R**-Benzyloxy-2,2-difluoro-9-oxa-1*R**,5*S**-bicyclo[3.3.1]nona-1*R**,4*R**-diol 38.** NMO (295 mg, 2.52 mmol) was added to a solution of cyclooctenone **20b** (336 mg, 1.26 mmol) in acetone (3.16 mL) and H_2O (1.58 mL) at 0 °C. Osmium tetroxide (0.790 mL of a 2.5% by wt. solution in *t*-BuOH, 0.063 mmol) was added, and the black solution was stirred at 0 °C for 6 h. Solid Na_2SO_3 (0.4 g) was added, and the suspension was stirred for 1 h, then diluted with water (3 mL) and extracted with ethyl acetate (3 × 30 mL). The combined organic extracts were washed with brine (30 mL), dried ($MgSO_4$), filtered, and concentrated in vacuo. Flash chromatography (silica gel, 50−70% ethyl acetate in hexane) gave (in order of elution) minor diastereoisomer **38** (44 mg, 12%) followed by a mixture of **37** and **38** (106 mg, 28%) and then **37** as a white solid. **38**: R_f (50% ethyl acetate in hexane) 0.24; mp 128−131 °C; δ_H (300 MHz, $CDCl_3$) 7.40−7.29 (m, 5H), 4.89 (d, ^2J = 11.5, 1H), 4.66 (d, ^2J = 11.5, 1H), 4.21 (d, J = 6.7, 1H), 3.97 (dddd, $^3J_{H-F}$ = 13.2, J = 6.4, 4.4, 0.9, 1H), 3.78−3.71 (m, 1H), 3.44 (d, $^4J_{H-F}$ = 6.3, 1H), 2.46 (dd, ^4J = 7.9, 1.2, 1H), 2.24−2.06 (m, 2H), 1.92−1.81 (m, 1H), 1.78−1.68 (m, 3H); δ_C (75 MHz, $CDCl_3$) 137.2, 128.6, 128.2, 127.9, 118.2 (dd, $^1J_{C-F}$ = 268.1, 251.9), 94.7 (dd, $^2J_{C-F}$ = 29.9, 20.3), 80.2 (dd, $^2J_{C-F}$ = 30.4, 18.0), 77.0, 75.0 (d, $^4J_{C-F}$ = 1.8), 71.5 (dd, ^3J = 3.0, 3.0), 29.6, 24.4, 15.9; δ_F (282 MHz, $CDCl_3$) −109.5 (ddd, $^2J_{F-F}$ = 259.6, J_{H-F} = 13.3, 5.5, 1F), (−121.8)−(−122.8) (m incl. app. d, $^2J_{F-F}$ = 259.6, 1F); ν_{max}(solid)/cm^{-1} 3364br, 3166br, 2913s, 1470m, 1351s, 1210s, 1150s, 1072s, 1034s, 943s, 915s, 882m, 819w, 750s, 699s; *m/z* (CI^+) 318 (100%, $[M + NH_4]^+$), 288 (8), 258 (3), 241 (14), 228 (5), 212 (4), 192 (5), 163 (10), 108 (3); HRMS (ES^+, $[M + NH_4]^+$) calcd for $C_{15}H_{22}F_2O_4N$ 318.1511, found 318.1512. Anal. calcd for $C_{15}H_{18}F_2O_4$: C, 59.99; H, 6.04. Found: C, 59.86; H, 5.90.

Crystal data: $C_{15}H_{18}F_2O_4$, crystal size 0.16 × 0.13 × 0.08 mm^3, M = 300.29, monoclinic, a = 10.3624(14) Å, b = 6.6363(9) Å, c = 11.0444(15) Å, α = 90°, β = 112.613(2)°, γ = 90°, U = 701.11(16) Å^3, T = 150(2) K, space group $P2(1)$, Z = 2, μ(Mo Kα) = 0.119 mm^{-1}, 5059 reflections measured, 2397 [R(int) = 0.0672] which were used in all calculations. Final R indices [$F^2 > 2\sigma(F^2)$] R1 = 0.0465, wR2 = 0.0618; R indices (all data) R1 = 0.0684, wR2 = 0.0683.

37 (158 mg, 42%): R_f (50% ethyl acetate in hexane) 0.12; mp 109−112 °C; δ_H (300 MHz, $CDCl_3$) 7.41−7.33 (m, 5H), 4.91 (d, ^2J = 11.7, 1H), 4.78 (d, ^2J = 11.7, 1H), 4.32 (d, ^3J = 6.6, 1H), 4.01 (ddd, J_{H-F} = 20.1, 7.8, J = 4.8, 1H), 3.86−3.80 (m, 1H), 3.64 (d, ^4J = 5.5, 1H), 2.95 (s, 1H), 2.08−2.00 (m, 1H), 1.96−1.70 (m, 3H), 1.50−1.37 (m, 2H); δ_C (75 MHz, $CDCl_3$) 136.6, 128.6, 128.5, 128.2, 118.0 (dd, $^1J_{C-F}$ = 258.8, 254.6), 94.1 (dd, $^2J_{C-F}$ = 26.9, 20.3), 74.8, 74.6 (dd, $^2J_{C-F}$ = 20.0, 17.6), 73.3 (d, $^4J_{C-F}$ = 1.8), 71.0 (dd, $^3J_{C-F}$ = 7.8, 1.2), 27.9 (d, $^3J_{C-F}$ = 1.8), 23.0, 18.3; δ_F (282 MHz, $CDCl_3$) (−114.0)−(−114.9) (m incl. app. d, $^2J_{F-F}$ = 287.8, 1F), −124.1 (dddd, $^2J_{F-F}$ = 287.8, $^3J_{H-F}$ = 20.1, $^4J_{H-F}$ = 5.5, 2.4, 1F); ν_{max}(solid)/cm^{-1} 3364br, 3180br, 2902w, 1737s, 1453w, 1343w, 1155s, 1089s, 933s, 867w, 728s, 693s; *m/z* (CI^+) 318 (100%, $[M + NH_4]^+$) 302 (4), 228 (17), 212 (3), 121 (6), 52 (10); HRMS (ES^+, $[M + NH_4]^+$) calcd for $C_{15}H_{22}F_2O_4N$ 318.1511, found 318.1515. Anal. calcd for $C_{15}H_{18}F_2O_4$: C, 59.99; H, 6.04. Found: C, 59.86; H, 5.95.

Crystal data: $C_{15}H_{18}F_2O_4$, crystal size 0.14 × 0.09 × 0.06 mm^3, M = 300.29, monoclinic, a = 15.5415(19) Å, b = 6.6332(8) Å, c = 13.9404(17) Å, α = 90°, β = 106.126(2)°, γ = 90°, U = 1380.6(3) Å^3, T = 150(2) K, space group $P2(1)/c$, Z = 4, μ(Mo Kα) = 0.121 mm^{-1}, 9657 reflections measured, 2430 [R(int) = 0.0967] which were used in all calculations. Final R indices [$F^2 > 2\sigma(F^2)$] R1 = 0.0514, wR2 = 0.0661; R indices (all data) R1 = 0.1050, wR2 = 0.0785. Crude cyclooctenone **20b** could be used in the dihydroxylation reaction to give diols **37** and **38** in 61% combined yield over two steps from purified RCM precursor **19b**.

2,2-Difluoro-9-oxa-1*S,5*R**-bicyclo[3.3.1]nona-1*S**,3*R**,4*R**-triol 39.** Hemiacetal **31** (0.080 mmol, 24 mg) was dissolved in ethanol (1 mL) containing 10% Pd−C (5 mg). The atmosphere was removed and replaced several times by hydrogen from a double balloon, and then the reaction was stirred at room temperature for 23 h. The hydrogen atmosphere was removed in vacuo and replaced with air, and then the catalyst was removed by filtration through celite. Concentration of the filtrate in vacuo afforded **39** (16 mg, 95%): R_f (100% ethyl acetate) 0.31; mp 156−158 °C; δ_H (300 MHz, CD_3OD) 4.06−3.92 (m, 2H), 3.76 (dd, ^3J = 9.5, 6.4, 1H), 1.92−1.48 (env., 6H); δ_C (100 MHz, CD_3OD) 117.9 (dd, $^1J_{C-F}$ = 156.4, 150.9), 93.5 (dd, $^2J_{C-F}$ = 26.8, 20.4), 73.0, 72.9 (dd, $^2J_{C-F}$ = 20.4, 20.4), 72.0 (d, $^3J_{C-F}$ = 8.0), 28.7 (d, $^3J_{C-F}$ = 2.4), 20.0, 18.9; δ_F (282 MHz, CD_3OD) −118.2 (dd, $^2J_{F-F}$ = 246.7, J_{H-F} = 8.2, 1F), −129.4 (ddd, $^2J_{F-F}$ = 246.7, J_{H-F} = 19.4, $^4J_{H-F}$ = 4.3, 1F); ν_{max}(solid)/cm^{-1} 3296br, 2964w, 1440w, 1345w, 1207m, 1116m, 1034s, 996s, 929s, 823s; *m/z* (CI^-) 209 (30%, $[M - H]^-$) 191 (11), 170 (18), 152 (15), 79 (22); HRMS (CI^-, $[M - H]^-$) calcd for $C_8H_{11}F_2O_4$ 209.0631, found 209.0630. Anal. calcd for $C_8H_{12}F_2O_4$: C, 45.72; H, 5.75. Found: C, 45.68; H, 5.70.

2,2-Difluoro-9-oxa-1*S,5*R**-bicyclo[3.3.1]nona-1*S**,3*R**,4*S**-triol 40.** From **37** (0.077 mmol, 23 mg), 10% Pd−C (5 mg) in ethanol (1 mL) over 72 h. Filtration through celite and concentration afforded triol **40** (36 mg, 100%): R_f (100% ethyl acetate) 0.15; mp 153−155 °C; δ_H (300 MHz, CD_3OD) 4.17−4.04 (env, 2H, containing 4.10 (ddd, J_{H-F} = 21.6, $^3J_{H-F}$ = 8.6, J = 4.8, 1H) and 4.11−4.09 (m, 1H)), 3.72 (broad s, 1H), 1.90 (broad d, J = 9.6, 1H), 1.80−1.44 (m, 5H); δ_C (100 MHz, CD_3OD) 117.9 (dd, $^1J_{C-F}$ = 254.0, 254.0), 93.8 (dd, $^2J_{C-F}$ = 26.8, 20.4), 75.9, 72.0 (dd, $^3J_{C-F}$ = 8.0, 1.6), 68.8 (dd, $^2J_{C-F}$ = 21.6, 19.2), 29.0 (d, $^3J_{C-F}$ = 2.4), 23.0, 17.7; δ_F (282 MHz, CD_3OD) −(−119.3)−(−120.2) (m incl. app. d, $^2J_{F-F}$ =247.4, 1F), −127.3 (ddd, $^2J_{F-F}$ = 247.4, $^3J_{H-F}$ = 21.3, $^4J_{H-F}$ = 3.8, 1F); ν_{max}(solid)/cm^{-1} 3346br, 2951w, 1647w, 1444w, 1353w, 1204s, 1076s, 1037s, 928s; *m/z* (CI^+) 228 (100%, $[M + NH_4]^+$) 123 (6); HRMS (ES^+, $[M + NH_4]^+$) calcd for $C_8H_{16}F_2O_4N$ 228.1042, found 228.1038. Anal. calcd for $C_8H_{12}F_2O_4$: C, 45.72; H, 5.75. Found: C, 45.79; H, 5.80.

2,2-Difluoro-9-oxa-1*R,5*S**-bicyclo[3.3.1]nona-1*R**,3*R**,4*R**-triol 41.** From **38** (0.067 mmol, 20 mg), 10% palladium-on-carbon (5 mg) in ethanol (1 mL) over 23 h. Filtration through celite and concentration in vacuo afforded triol **41** (25 mg, 91%): R_f (100% ethyl acetate) 0.29; mp 57−60 °C; δ_H (300 MHz, CD_3OD) 3.97 (broad s, 1H), 3.86 (ddd, J_{H-F} = 13.4, 12.5, J = 6.9, 1H), 3.53 (dt, J = 6.9, 2.7, 1H), 2.00−1.90 (m, 1H), 1.72−1.38 (m, 5H); δ_C (400 MHz, CD_3OD) 118.1 (dd, $^1J_{C-F}$ = 258.0, 258.0), 94.2 (dd, $^2J_{C-F}$ = 31.2, 20.0), 77.0, 72.2 (dd, $^2J_{C-F}$ = 28.8, 19.2), 70.6 (dd, $^3J_{C-F}$ = 6.0, 2.0), 30.2, 24.8, 15.4; δ_F (282 MHz, CD_3OD) −112.7 (ddd, $^2J_{F-F}$ = 253.5, J =$_{H-F}$ 12.5, $^4J_{H-F}$ = 3.8, 1F), −125.1 (dd, $^2J_{F-F}$ = 253.5, J_{H-F} = 13.4, 1F); ν_{max}(solid)/cm^{-1} 3289br, 2963w, 1351m,1205m, 1092s, 1000s, 958s, 894s; *m/z* (CI^+) 228 (100%, $[M + NH_4]^+$); HRMS (ES^+, $[M + NH_4]^+$) calcd for $C_8H_{16}F_2O_4N$ 228.1042, found 228.1038. Anal. calcd for $C_8H_{12}F_2O_4$: C, 45.72; H, 5.75. Found: C, 45.84; H, 5.88.

4*S-Acetoxy-3*R**-benzyloxy-2,2-difluoro-9-oxa-1*S**,5*R**-bicyclo-[3.3.1]nonan-1*S**-ol 46.** Acetic anhydride (0.214 mL, 2.26 mmol), DMAP (16.5 mg, 0.14 mmol), and poly(vinylpyridine) (0.9 mmol, 450 mg at 2.0 mmol per gram of loading) were added to a solution of diol **37** (136 mg, 0.45 mmol) in DCM (4.5 mL). The suspension was shaken at room temperature for 75 h. TLC analysis showed the reaction was incomplete, so additional acetic anhydride (200 μL, 2.11 mmol), DMAP (20 mg, 0.17 mmol), and poly(vinylpyridine) (320 mg) were added. The reaction was shaken at room temperature for a further 48 h until consumption of starting material was observed by TLC. Workup as before afforded **46** (138 mg, 89%) as a white solid: R_f (50% ethyl acetate in hexane) 0.34; mp 28−30 °C; δ_H (300 MHz, $CDCl_3$) 7.39−7.30 (m, 5H), 5.20 (ddd, J = 4.9, $^4J_{H-F}$ = 3.8, J = 1.5, 1H), 4.76 (d, ^2J = 12.4, 1H), 4.73 (d, ^2J = 12.4, 1H), 4.22 (d, J = 6.7, 1H), 4.04 (ddd, J_{H-F} = 21.8, 7.3, J = 5.0, 1H), 3.61 (d, J = 6.4, 1H), 2.15 (s, 3H), 2.06−1.38

(m, 6H); δ_C (100 MHz, $CDCl_3$) 170.6, 136.7, 128.6, 128.3, 128, 117.4 (dd, $^1J_{C-F}$ = 256.4, 255.6), 94.3 (dd, $^2J_{C-F}$ = 26.8, 20.4), 73.8−73.2 (m), 70.8 (dd, $^3J_{C-F}$ = 9.2, 1.6), 27.8 (d, $^3J_{C-F}$ = 1.6), 23.0, 21.0, 18.2; δ_F (282 MHz, $CDCl_3$) (−116.8)−(−117.8) (m, incl. app. d, $^2J_{F-F}$ = 245.9, 1F), −127.0 (ddt, $^2J_{F-F}$ = 245.8, J_{H-F} = 21.8, $^4J_{H-F}$ = 5.2, 1F); ν_{max}(film)/cm^{-1} 3434br, 2951s, 1730s, 1367s, 1074s, 908s, 733s; *m/z* (EI$^+$) 342 (2%, [M + H]$^+$) 176 (13), 116 (83), 91 (100), 43 (61); HRMS (ES$^+$, [M + H]$^+$) calcd for $C_{17}H_{21}F_2O_5$ 343.1352, found 343.1356. Anal. calcd for $C_{17}H_{20}F_2O_5$: C, 59.64; H, 5.89. Found: C, 59.50; H, 5.73.

The ^{13}C NMR spectrum contained a number of weak signals in the 73.8−73.2 ppm region which could not be resolved well, hence the recording of this signal as a multiplet.

4*R-Acetoxy-3*R**-benzyloxy-1*R**-(dibenzylphosphoryloxy)-2,2-difluoro-9-oxa-1*R**,5*S**-bicyclo[3.3.1]nonane 47 and 3*R**-Benzyloxy-1*R**- (dibenzylphosphoryloxy)-2,2-difluoro-9-oxa-1*R**,5*S**-bicyclo[3.3.1]nonan-4*R**-ol 44.** NaHMDS (0.54 mmol, 317 μL of a 1.7 M solution in THF) was added dropwise to a solution of **46** (0.49 mmol, 168 mg) in THF (10 mL) at 0 °C and stirred at this temperature for 1 h. Tetrabenzyl pyrophosphate (0.54 mmol, 290 mg) was added, and the reaction was allowed to warm to room temperature over 2 h, then stirred for 18 h after which a white precipitate was observed. The reaction was quenched with pH 7 buffer (10 mL) and extracted with ethyl acetate (2 × 50 mL). The combined organic extracts were washed with brine (20 mL), dried ($MgSO_4$), filtered, and concentrated in vacuo to give a gray paste which was purified (flash chromatography, silica, 50% ethyl acetate in hexane) to afford **47** (188 mg, 64%): R_f (ethyl acetate) 0.60; δ_H (300 MHz, $CDCl_3$) 7.38−7.28 (m, 15H), 5.22−5.18 (m, 1H), 5.17−5.05 (m, 4H), 4.75 (s, 2H), 4.35 (d, ^3J = 6.6, 1H), 4.05 (ddd, $^3J_{H-F}$ = 20.5, J = 7.0, 5.0, 1H), 2.56−2.40 (m, 1H), 2.16−1.79 (envelope, 6H), 2.06 (s, 3H), 1.52−1.36 (m, 2H); δ_C (100 MHz, $CDCl_3$) 170.5, 136.6, 136.0 (d, $^3J_{C-P}$ = 8.8), 135.7 (d, $^3J_{C-P}$ = 8.0), 128.6, 128.5, 128.5, 128.4, 128.4, 128.3, 128.1, 128.0, 127.9, 116.0 (ddd, $^2J_{F-F}$ = 264.7, 256.9, $^3J_{C-P}$ = 6.8), 99.8 (ddd, $^2J_{C-F}$ = 27.2, 18.4, $^2J_{C-P}$ = 7.2), 75.8, 73.3, 73.0 (ddd, $^2J_{C-F}$ = 21.6, 17.6, $^4J_{C-P}$ = 1.6), 70.4 (d, $^3J_{C-F}$ = 9.6), 69.7 (dd, $^2J_{C-P}$ = 6.4, $^6J_{C-F}$ = 1.6), 69.4 (d, $^2J_{C-P}$ = 6.4), 27.8, 22.6, 20.9, 18.4; δ_F (282 MHz, $CDCl_3$) (−117.7)−(−118.5) (m, 1F), −124.3 (ddd, $^2J_{F-F}$ = 245.9, J_{H-F} = 20.5, J = 5.2, 1F); δ_P (121 MHz, $CDCl_3$) −8.8 (quintet, $^3J_{H-P}$ = 7.3); ν_{max}(film)/cm^{-1} 3472w, 2955s, 1738s, 1496s, 1455s, 1371s, 1243s, 1017s, 873w, 738s; *m/z* (CI$^+$) 603 (28%, [M + H]$^+$) 513 (5), 360 (7), 125 (13), 108 (51), 106 (100); HRMS (ES$^+$, [M + H]$^+$) calcd for $C_{31}H_{34}F_2O_8P$ 603.1954, found 603.1955. Traces of deprotected **44** (16 mg, 6%) were also produced, as reported previously.

2,2-Difluoro-3*R,4S*-dihydroxy-9-oxa-1*S**,5*R**-bicyclo[3.3.1]-nonanyl-1*S**-phosphate Ammonium Sodium Salt 48. Hydrogenolysis.** 10% Palladium-on-carbon (64 mg) was added to a solution of **47** (0.28 mmol, 170 mg) in ethanol (5.6 mL). The apparatus was pump-purged with hydrogen from a double balloon, and the reaction was stirred under hydrogen at room temperature for 90 h. The solution was filtered through celite, and the filtrate was concentrated in vacuo (98 mg, 100%): {^{1}H}δ_F (282 MHz, CD_3OD) −116.3 (d, $^2J_{F-F}$ = 243.2, 1F), −121.2 (d, $^2J_{F-F}$ = 243.2, 1F); δ_P (121 MHz, CD_3OD) (+8)−(−12) (br, m); *m/z* (ES$^-$) 331 (100%, [M − H]$^-$) 289 (15), 167 (17), 89 (46), 75 (44); HRMS (ES$^-$, [M − H]$^-$) calcd for $C_{10}H_{14}F_2O_8$ 331.0400, found 331.0396.

Acetate Cleavage and Bis(triethylammonium) Salt Formation. The crude acid (0.28 mmol, 98 mg) was taken up in a mixture of methanol, water, and triethylamine (5.9 mL, 5:2:1) and stirred at room temperature for 22 h. The organic solvents were removed in vacuo, then the residue was freeze-dried to afford the crude bis-(triethylammonium) salt: δ_F (282 MHz, CD_3OD) −119.7 (d, $^2J_{F-F}$ = 245.0, 1F), −124.2 (dd, $^2J_{F-F}$ = 245.0, J_{H-F} = 20.8, 1F); δ_P (121 MHz, CD_3OD) −3.9 (s); *m/z* (ES$^+$) 493 (58%, [M + H]$^+$) 392 (97), 242 (5), 102 (100), 74 (35); HRMS (ES$^+$, [M + H]$^+$) calcd for $C_{20}H_{43}F_2N_2O_7P$ 493.2849, found 493.2851.

Purification and Ammonium Sodium Salt Formation. Flash chromatography (silica, ethanol/water/35% aqueous ammonia (5:3:1)) afforded ammonium sodium salt **48** (60 mg, 66%): R_f (ethanol/water/35% aqueous ammonia (5:3:1)) 0.13; mp 137−139 °C; δ_H (400 MHz, D_2O) 4.35 (ddd, J_{H-F} = 21.5, 8.1, J = 4.8, 1H), 4.33−4.31 (m, 1H), 3.98−3.92 (m, 1H), 2.28 (ddd, ^2J = 14.2, J = 14.0, 7.3, 1H), 2.06 (dd, ^2J = 14.2, J = 5.4, 1H), 1.95−1.75 (m, 2H), 1.71−1.60 (m, 1H), 1.57−1.50 (dd, J = 14.0, 5.3, 1H); δ_C (100 MHz, D_2O) 117.4 (dd, $^1J_{C-F}$ = 256.4, 250.1), 97.2 (ddd, $^2J_{C-F}$ = 25.6, 18.4, $^2J_{C-P}$ = 7.2), 76.8, 71.4 (dd, $^3J_{C-F}$ = 8.0, 1.6), 68.4 (dd, $^2J_{C-F}$ = 20.8, 18.4), 27.6, 22.3, 17.5; δ_F (282 MHz, D_2O) (−118.4)−(−119.4) (m, incl. app. d, $^2J_{F-F}$ = 243.1, 1F), −123.7 (ddd, $^2J_{F-F}$ = 243.1, J_{H-F} = 21.5, $^4J_{H-F}$ = 5.9, 1F); δ_P (121 MHz, D_2O) −4.1 (s); ν_{max}(film)/cm^{-1} 2952br, 1444w, 1361w, 1167m, 1078s, 1040s, 910s, 808s, 751s, 685w; *m/z* (ES$^-$) 289 (4%, [M − H]$^-$) 273 (5), 183 (3), 125 (56), 97 (100); HRMS (ES$^-$, [M − H]$^-$) calcd for $C_8H_{12}F_2O_7P$ 289.0294, found 289.0297. Anal. calcd for $C_8H_{15}F_2NO_7NaP$: C, 29.18; H, 4.56; N, 4.26. Found: C, 29.48; H, 4.32; N, 4.27.

Acknowledgment. We thank the EPSRC for studentships (J.A.L.M., L.M.), the EPSRC Mass Spectrometry Service (Swansea) for accurate mass measurements, Dr. Roland Wende (Umicore) for a donation of the Neolyst catalyst, and Dr. A. Caravano (Sanofi-Aventis) and Professor R. A. Field (University of East Anglia) for helpful discussions.

Supporting Information Available: Experimental procedures for **11a**, **11b**, **13**, **14**, **26a**−**27b**, **30**, **44**, and **45**; NMR spectra (^{1}H, ^{13}C, ^{19}F, ^{31}P) for **11a**, **11b**, **13**, **14**, **16**−**19a**, **26a**−**27b**, **33**, **34**, **44**, **45**, and **47**; Cartesian coordinates and energies for RHF 6-31G* optimized structures for lowest-energy conformers of **39**−**41**, and calculated energies (RHF 6-31+G**) for **39**−**41**. This material is available free of charge via the Internet at http://pubs.acs.org.

JO0620258